



# **BEYOND CONVENTIONAL MODELS: EXPANDING EXPERIMENTAL SYSTEMS FOR ANIMAL-MICROBIOME INTERACTION RESEARCH**

EDITED BY: Henning Seedorf, Jean-François Brugère, Wakako Ikeda-Ohtsubo,  
Aram Mikaelyan and David Kamanda Ngugi  
PUBLISHED IN: Frontiers in Microbiology



# frontiers

## Frontiers eBook Copyright Statement

The copyright in the text of individual articles in this eBook is the property of their respective authors or their respective institutions or funders. The copyright in graphics and images within each article may be subject to copyright of other parties. In both cases this is subject to a license granted to Frontiers.

The compilation of articles constituting this eBook is the property of Frontiers.

Each article within this eBook, and the eBook itself, are published under the most recent version of the Creative Commons CC-BY licence.

The version current at the date of publication of this eBook is CC-BY 4.0. If the CC-BY licence is updated, the licence granted by Frontiers is automatically updated to the new version.

When exercising any right under the CC-BY licence, Frontiers must be attributed as the original publisher of the article or eBook, as applicable.

Authors have the responsibility of ensuring that any graphics or other materials which are the property of others may be included in the CC-BY licence, but this should be checked before relying on the CC-BY licence to reproduce those materials. Any copyright notices relating to those materials must be complied with.

Copyright and source acknowledgement notices may not be removed and must be displayed in any copy, derivative work or partial copy which includes the elements in question.

All copyright, and all rights therein, are protected by national and international copyright laws. The above represents a summary only. For further information please read Frontiers' Conditions for Website Use and Copyright Statement, and the applicable CC-BY licence.

ISSN 1664-8714

ISBN 978-2-83250-317-1

DOI 10.3389/978-2-83250-317-1

## About Frontiers

Frontiers is more than just an open-access publisher of scholarly articles: it is a pioneering approach to the world of academia, radically improving the way scholarly research is managed. The grand vision of Frontiers is a world where all people have an equal opportunity to seek, share and generate knowledge. Frontiers provides immediate and permanent online open access to all its publications, but this alone is not enough to realize our grand goals.

## Frontiers Journal Series

The Frontiers Journal Series is a multi-tier and interdisciplinary set of open-access, online journals, promising a paradigm shift from the current review, selection and dissemination processes in academic publishing. All Frontiers journals are driven by researchers for researchers; therefore, they constitute a service to the scholarly community. At the same time, the Frontiers Journal Series operates on a revolutionary invention, the tiered publishing system, initially addressing specific communities of scholars, and gradually climbing up to broader public understanding, thus serving the interests of the lay society, too.

## Dedication to Quality

Each Frontiers article is a landmark of the highest quality, thanks to genuinely collaborative interactions between authors and review editors, who include some of the world's best academicians. Research must be certified by peers before entering a stream of knowledge that may eventually reach the public - and shape society; therefore, Frontiers only applies the most rigorous and unbiased reviews.

Frontiers revolutionizes research publishing by freely delivering the most outstanding research, evaluated with no bias from both the academic and social point of view. By applying the most advanced information technologies, Frontiers is catapulting scholarly publishing into a new generation.

## What are Frontiers Research Topics?

Frontiers Research Topics are very popular trademarks of the Frontiers Journals Series: they are collections of at least ten articles, all centered on a particular subject. With their unique mix of varied contributions from Original Research to Review Articles, Frontiers Research Topics unify the most influential researchers, the latest key findings and historical advances in a hot research area! Find out more on how to host your own Frontiers Research Topic or contribute to one as an author by contacting the Frontiers Editorial Office: [frontiersin.org/about/contact](https://frontiersin.org/about/contact)



# BEYOND CONVENTIONAL MODELS: EXPANDING EXPERIMENTAL SYSTEMS FOR ANIMAL-MICROBIOME INTERACTION RESEARCH

Topic Editors:

**Henning Seedorf**, Temasek Life Sciences Laboratory, Singapore

**Jean-François Brugère**, Université Clermont Auvergne, France

**Wakako Ikeda-Ohtsubo**, Tohoku University, Japan

**Aram Mikaelyan**, North Carolina State University, United States

**David Kamanda Ngugi**, German Collection of Microorganisms and Cell Cultures GmbH (DSMZ), Germany

**Citation:** Seedorf, H., Brugère, J.-F., Ikeda-Ohtsubo, W., Mikaelyan, A., Ngugi, D. K., eds. (2022). Beyond Conventional Models: Expanding Experimental Systems for Animal-Microbiome Interaction Research. Lausanne: Frontiers Media SA. doi: 10.3389/978-2-83250-317-1

# Table of Contents

- 05** *A Model System for Feralizing Laboratory Mice in Large Farmyard-Like Pens*  
Henriette Arnesen, Linn Emilie Knutsen, Bente Wabakken Hognestad, Grethe Marie Johansen, Mats Bemark, Oliver Pabst, Anne Kristine Storset and Preben Boysen
- 21** *Microbiome and Metabolome Analyses Reveal Novel Interplay Between the Skin Microbiota and Plasma Metabolites in Psoriasis*  
Dongmei Chen, Jingquan He, Jinping Li, Qian Zou, Jiawei Si, Yatao Guo, Jiayu Yu, Cheng Li, Fang Wang, Tianlong Chan and Huijuan Shi
- 31** *Surface Topography, Bacterial Carrying Capacity, and the Prospect of Microbiome Manipulation in the Sea Anemone Coral Model Aiptasia*  
Rúben M. Costa, Anny Cárdenas, Céline Loussert-Fonta, Gaëlle Toullec, Anders Meibom and Christian R. Voolstra
- 47** *Sex-Dependent Effects of the Microbiome on Foraging and Locomotion in Drosophila suzukii*  
Runhang Shu, Daniel A. Hahn, Edouard Jurkevitch, Oscar E. Liburd, Boaz Yuval and Adam Chun-Nin Wong
- 57** *Effects of Microplastics Exposure on the Acropora sp. Antioxidant, Immunization and Energy Metabolism Enzyme Activities*  
Baohua Xiao, Dongdong Li, Baolin Liao, Huina Zheng, Xiaodong Yang, Yongqi Xie, Ziqiang Xie and Chengyong Li
- 69** *Disentangling the Complexity of the Rumen Microbial Diversity Through Fractionation Using a Sucrose Density Gradient*  
Ruth Hernández, Hugo Jimenez, Cesar Vargas-Garcia, Alejandro Caro-Quintero and Alejandro Reyes
- 85** *The Axenic and Gnotobiotic Mosquito: Emerging Models for Microbiome Host Interactions*  
Blair Steven, Josephine Hyde, Jacquelyn C. LaReau and Doug E. Brackney
- 100** *Pathogen Challenge and Dietary Shift Alter Microbiota Composition and Activity in a Mucin-Associated in vitro Model of the Piglet Colon (MPigut-IVM) Simulating Weaning Transition*  
Raphaële Gresse, Frédérique Chaucheyras-Durand, Juan J. Garrido, Sylvain Denis, Angeles Jiménez-Marín, Martin Beaumont, Tom Van de Wiele, Evelyne Forano and Stéphanie Blanquet-Diot
- 120** *New Insights From Transcriptomic Data Reveal Differential Effects of CO<sub>2</sub> Acidification Stress on Photosynthesis of an Endosymbiotic Dinoflagellate in hospite*  
Marcela Herrera, Yi Jin Liew, Alexander Venn, Eric Tambutté, Didier Zoccola, Sylvie Tambutté, Guoxin Cui and Manuel Aranda
- 132** *Differences in Gut Microbiome Composition Between Sympatric Wild and Allopatric Laboratory Populations of Omnivorous Cockroaches*  
Kara A. Tinker and Elizabeth A. Ottesen



- 144** *Decisive Effects of Life Stage on the Gut Microbiota Discrepancy Between Two Wild Populations of Hibernating Asiatic Toads (Bufo gargarizans)*  
Xiaowei Song, Jingwei Zhang, Jinghan Song and Yuanyuan Zhai
- 158** *The Effect of Ryegrass Silage Feeding on Equine Fecal Microbiota and Blood Metabolite Profile*  
Yiping Zhu, Xuefan Wang, Bo Liu, Ziwen Yi, Yufei Zhao, Liang Deng, Reed Holyoak and Jing Li
- 169** *Controlled Complexity: Optimized Systems to Study the Role of the Gut Microbiome in Host Physiology*  
Robert W. P. Glowacki, Morgan J. Engelhart and Philip P. Ahern
- 185** *Microbiome Heritability and Its Role in Adaptation of Hosts to Novel Resources*  
Karen Bisschop, Hylke H. Kortenbosch, Timo J. B. van Eldijk, Cyrus A. Mallon, Joana F. Salles, Dries Bonte and Rampal S. Etienne



# A Model System for Feralizing Laboratory Mice in Large Farmyard-Like Pens

Henriette Arnesen<sup>1,2</sup>, Linn Emilie Knutsen<sup>1</sup>, Bente Wabakken Hognestad<sup>1</sup>, Grethe Marie Johansen<sup>1</sup>, Mats Bemark<sup>3,4</sup>, Oliver Pabst<sup>5</sup>, Anne Kristine Storset<sup>1</sup> and Preben Boysen<sup>1\*</sup>

<sup>1</sup> Faculty of Veterinary Medicine, Norwegian University of Life Sciences, Oslo, Norway, <sup>2</sup> Faculty of Chemistry, Biotechnology and Food Science, Norwegian University of Life Sciences, Aas, Norway, <sup>3</sup> Department of Microbiology and Immunology, Institute of Biomedicine, Sahlgrenska Academy, University of Gothenburg, Gothenburg, Sweden, <sup>4</sup> Region Västra Götaland, Sahlgrenska University Hospital, Department of Clinical Immunology and Transfusion Medicine, Gothenburg, Sweden, <sup>5</sup> Institute of Molecular Medicine, RWTH Aachen University, Aachen, Germany

## OPEN ACCESS

### Edited by:

Jean-François Brugère,  
Université Clermont Auvergne, France

### Reviewed by:

Henning Seedorf,  
Temasek Life Sciences Laboratory,  
Singapore  
Stephan Rosshart,  
University of Freiburg Medical Center,  
Germany

### \*Correspondence:

Preben Boysen  
preben.boysen@nmbu.no

### Specialty section:

This article was submitted to  
Microbial Symbioses,  
a section of the journal  
Frontiers in Microbiology

**Received:** 09 October 2020

**Accepted:** 09 December 2020

**Published:** 11 January 2021

### Citation:

Arnesen H, Knutsen LE,  
Hognestad BW, Johansen GM,  
Bemark M, Pabst O, Storset AK and  
Boysen P (2021) A Model System  
for Feralizing Laboratory Mice in Large  
Farmyard-Like Pens.  
Front. Microbiol. 11:615661.  
doi: 10.3389/fmicb.2020.615661

Laboratory mice are typically housed under extremely clean laboratory conditions, far removed from the natural lifestyle of a free-living mouse. There is a risk that this isolation from real-life conditions may lead to poor translatability and misinterpretation of results. We and others have shown that feral mice as well as laboratory mice exposed to naturalistic environments harbor a more diverse gut microbiota and display an activated immunological phenotype compared to hygienic laboratory mice. We here describe a naturalistic indoors housing system for mice, representing a farmyard-type habitat typical for house mice. Large open pens were installed with soil and domestic animal feces, creating a highly diverse microbial environment and providing space and complexity allowing for natural behavior. Laboratory C57BL/6 mice were co-housed in this system together with wild-caught feral mice, included as a source of murine microbionts. We found that mice feralized in this manner displayed a gut microbiota structure similar to their feral cohabitants, such as higher relative content of Firmicutes and enrichment of Proteobacteria. Furthermore, the immunophenotype of feralized mice approached that of feral mice, with elevated levels of memory T-cells and late-stage NK cells compared to laboratory-housed control mice, indicating antigenic experience and immune training. The dietary elements presented in the mouse pens could only moderately explain changes in microbial colonization, and none of the immunological changes. In conclusion, this system enables various types of studies using genetically controlled mice on the background of adaptation to a high diversity microbial environment and a lifestyle natural for the species.

**Keywords:** animal model, mice, feral mice, feralized mice, trained immunity, immune experience, gut microbiota, naturalistic environment

## INTRODUCTION

The common habitat for the house mouse (*Mus musculus*) is on the ground, typically close to larger animals like humans and their livestock, and the genetic basis for all research mice evolved in such environments (Boursot et al., 1993). Colonization by a host-specific microbiota is necessary to develop essential parts of the mucosal immune system in mice (Cebra, 1999; Chung et al., 2012),



and expression of effector- as well as tolerance-associated immune genes are upregulated following microbial colonization (El Aidy et al., 2012). Nevertheless, mice are usually studied under strictly hygienic laboratory conditions. Hence, concerns have been raised whether hygienically raised laboratory (lab) mice will reach a level of immune maturation that fully recapitulates the immune response in a mammal (Tao and Reese, 2017). Large variations in microbiota and cellular composition of the gut mucosa have been observed between animal facilities, accompanied by different immune phenotypes and experimental performance (Ivanov et al., 2009; Kriegl et al., 2011; Jakobsson et al., 2015; Rausch et al., 2016; Franklin and Ericsson, 2017). Thus, an artificial between-lab variability may have replaced natural variability in the course of comprehensible efforts to standardize the world's most used animal model.

Theories have postulated that a modernized lifestyle has led to a loss of proximity to a diverse range of microbes and parasites, thus removing balancing factors in the immune homeostasis, which may explain an increase of inflammatory diseases and cancer (Hunter, 2020). A major current research field addresses how colonizing microbes, including bacteria, parasites and even viruses, may affect the immune system to generate a lasting and general protection from various diseases. Beyond specific immunity, recent evidence shows how innate immune cells may undergo long-lasting reprogramming following microbial challenges, sometimes referred to as trained immunity (Oh et al., 2014; Honda and Littman, 2016; Netea et al., 2020). Adaptive immune cells may also be primed in a similar manner (Muraille and Goriely, 2017). The concept of immune training has been associated with enhancement of immune responses to vaccines and infections as well as to anti-inflammatory actions (Quinn et al., 2019). The outcome of immune training for a particular disease may thus point in either direction and needs to be explored empirically in organisms exposed to diverse microbial cues.

This background gives a rationale to develop animal models reflecting more realistic ecological contexts (Flies and Wild Comparative Immunology Consortium, 2020). In contrast to the widespread use of hygienically raised inbred mice, studies investigating the microbiota and immunity of mice under more naturalistic conditions have only recently emerged. We and others have demonstrated that feral (wild-caught) mice had an immunological steady state different from lab mice (Devalapalli et al., 2006; Abolins et al., 2011, 2017, 2018), as well as a thicker mucus layer in the gut (Jakobsson et al., 2015). In an effort to decipher the impact of environment, one study found profound changes in the immune system of inbred mice following co-housing with “dirty” pet store mice, approaching

phenotypes found in feral mouse as well as adult humans (Beura et al., 2016). In another, pre-infection of inbred mice with selected common mouse pathogens resulted in stronger vaccine responses (Reese et al., 2016). Furthermore, by transplanting feral mouse feces (Rosshart et al., 2017) or by transferring microbiota vertically from feral surrogate mothers (Rosshart et al., 2019), “wildling” lab mice were shown to develop a trained immune system and increased protection against disease. The latter study demonstrated the translational gain by using naturalized mice, as wildling mice behaved immunologically human-like in two clinical settings where conventional lab mice had failed to predict the response. Another study showed that the provision of soil heaps in mice cages modified the gut microbiota and repressed Th2-driven inflammation, in support of the “hygiene hypothesis” (Ottman et al., 2019). However, in all the studies mentioned above, lab mice remained in conventional cages, with limitations of space and behavioral opportunities relative to a wild house mouse lifestyle. A recently described model where mice were kept in large outdoor enclosures, showed altered microbiota, a shift toward Th1-type immunity and an increased susceptibility to helminth infection (Leung et al., 2018; Lin et al., 2020; Yeung et al., 2020). While offering a habitat clearly representing wild conditions, this setup allows limited surveillance of the animals and may prove inaccessible for most researchers.

We present a naturalistic environment housing system for mice consisting of large indoor enclosures (pens) containing farmyard-like elements such as fecal content from farm animals, soil and plant materials, with spatial living conditions reflecting a natural habitat. In a set of experiments, C57BL/6 mice were feralized under these conditions in the presence of feral house mice, serving as a natural source of mouse microbes, including pathogens and parasites. We show that feralization lead to a significant conversion of the gut microbiota composition, and to immunological parameters associated with antigenic experience and immune training.

## MATERIALS AND METHODS

### Animals and Experimental Design

A mouse pen housing system was designed at The Norwegian University of Life Sciences (NMBU) by escape-proofing pig pens with sheets of galvanized steel, each pen measuring 2.0 × 2.5 × 1.25 m (WxDxH) on concrete floor (**Figures 1A–E** and **Supplementary Video S1**). Pens were enriched with wood shavings, organic garden soil, compost, twigs, hay and fecal content from pigs, cows and horses. Oat and carrot sprouts were planted occasionally to provide fresh plants as would be encountered in a farmyard. Wooden pallets were used as stepping platforms for personnel to avoid disturbing the habitats or crushing animals, also contributing to environmental complexity and shelter. Standard nipples drinking bottles provided water. Small wooden boxes were provided for nesting and sheltering. In Experiment (Exp.) 1, surveillance cameras with infrared sensors were used for continuous monitoring.

**Abbreviations:** B6, C57BL/6 inbred mouse strain; CM T-cell, Central memory T-cell; EM T-cell, Effector memory T-cell; Exp. 1/Exp. 2, Experiment 1/Experiment 2; Fzd, Feralized (here: female) B6 mice; Fzd<sup>F</sup>, B6 females feralized in the presence of female feral mice; Fzd<sup>M</sup>, B6 females feralized in the presence of male feral mice; Ig, Immunoglobulin; IL, Interleukin; IVC, Individually ventilated cage; KLRG1, Killer cell lectin-like receptor subfamily G member 1; NRP-1, Neuropilin-1; OTU, Operational taxonomic unit; PCA, Principal component analysis; PLN, Peripheral lymph node; pTreg, Peripherally induced regulatory T-cell; Rm1, Rat and Mouse No.1 diet (<sup>TM</sup>of Special Diet Services); SPF, Specific pathogen-free; Treg, Regulatory T-cell.

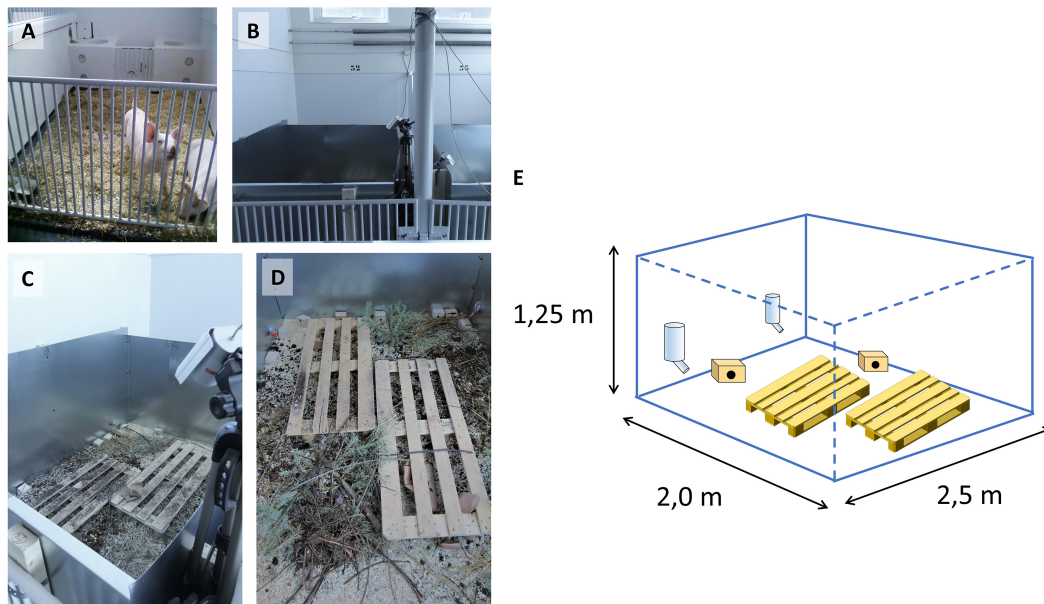


**FIGURE 1 |** Construction of mouse pens. Original pig pens in the large animal clinic at NMBU shown in (A) were modified with steel sheets (B,C) and equipped with surveillance cameras (B,C). (D) Contents of mouse pens as outlined in section “Materials and Methods.” (E) Schematic representation of pen construction, showing pallets, wooden houses and drinking bottles (pallet graphics from <https://publicdomainvectors.org/>).

Following purchase, C57BL/6N (B6) specific pathogen-free (SPF) mice (Charles River/Scanbur, Norway) were acclimatized for 1 week in individually ventilated cages (IVCs) under SPF conditions at NMBU. Feral house mice were captured in domestic animal farms in south-eastern Norway by overnight deployment of Ugglan Special No1 live traps (Grahnb, Gnosjö, Sweden), equipped with wood shavings, fresh fruit and peanut butter as bait, as previously described (Boysen et al., 2011). Representatives of these catches were subtyped as *Mus musculus* ssp. *musculus*, with a minor contribution of ssp. *domesticus* as reported previously (Knutsen et al., 2019). The ages of feral mice could not be determined, but only visibly adult individuals were included. Mice were individually marked using ear punch or microchip injected subcutaneously (Nonatec Lutronic, Rodange, Luxembourg). Feral and B6 mice were released simultaneously into pens.

Experiments and housing design were approved by the National Animal Research Authority in Norway (FOTS 4788, 6801, and 8080). Feral mice capture was approved by The Norwegian Directorate for Nature Management (2012/693 and 2014/7215).

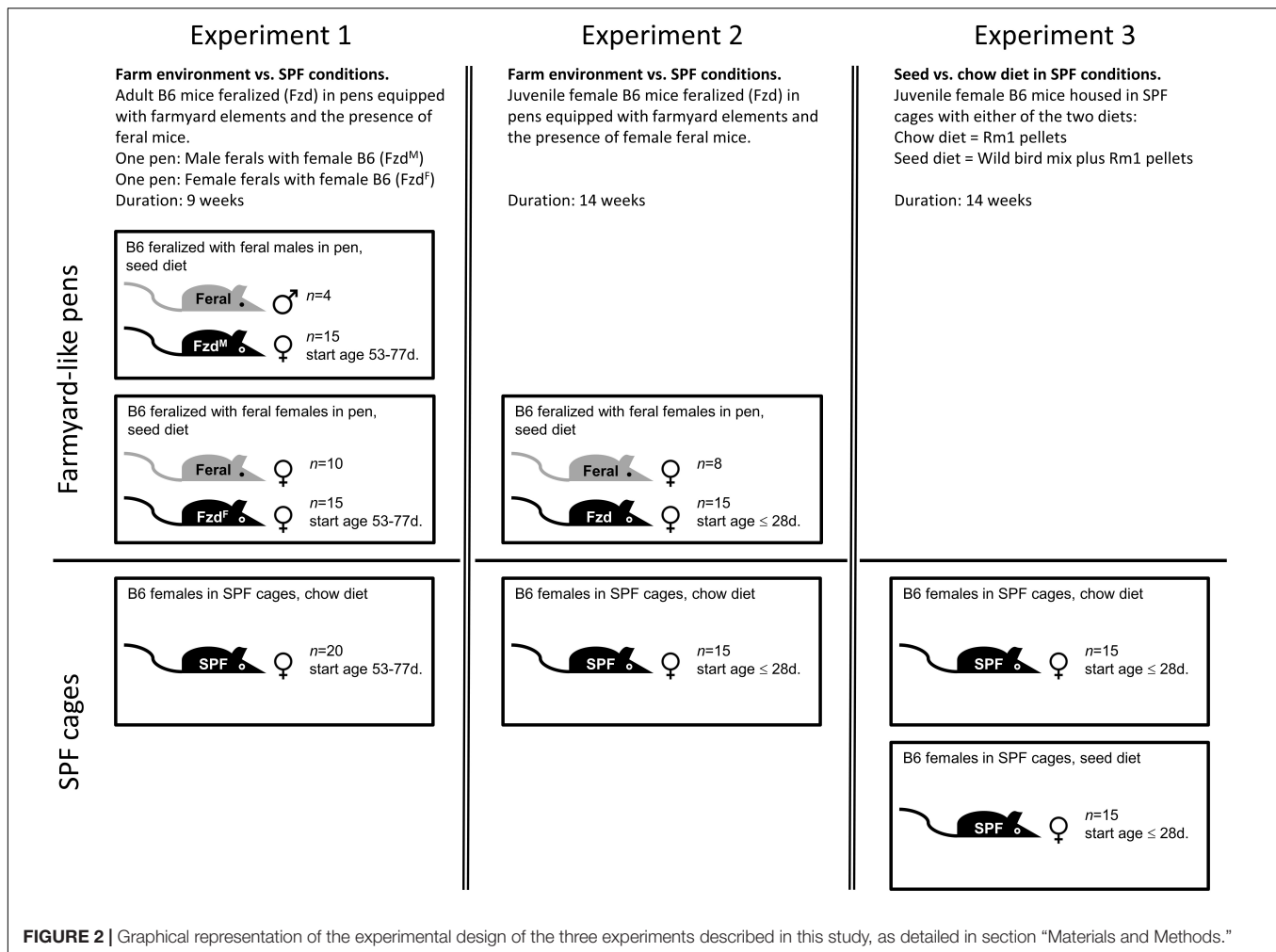
In Exp. 1 (Figure 2), female B6 mice aged 53–77 days were feralized by housing in pens together with feral mice for 9 weeks, divided into two subgroups: In one pen, 15 female B6 mice were co-housed with 10 female feral mice (Fzd<sup>F</sup>; feralized with feral females). In a second pen, 15 female B6 mice were co-housed with 4 male feral mice (Fzd<sup>M</sup>; feralized with feral males). Fzd<sup>M</sup> mice produced several litters of hybrid offspring excluded from the study. To provide a diet reflecting food sources in a natural setting, we provided an unprocessed wild bird seed mix consisting of sunflower seeds (25%), sorghum

(25%), oat (25%), and wheat (25%) (Wild bird mix, Plantasjen, Köping, Sweden), mixed with standard “chow” pellets (Rm1, Special Diet Services, United Kingdom/Scanbur, Norway) *ad lib* on the ground (see **Supplementary Table S1** for nutrient composition.) In addition, pen mice had access to a variation of plant material, including dried hay, spruce twigs collected outdoors, and occasional fresh lettuce, carrots and fruits. 20 female B6 mice of the same cohort were housed in cages under SPF conditions as controls, receiving standard chow diet only, to maintain typical lab conditions.

In Exp. 2 (Figure 2), 15 female B6 mice aged 28 days were feralized in mouse pens with 8 female adult feral mice for 14 weeks (Fzd), while 15 B6 females were kept in cages as SPF controls. Feeding regimen as described above. As the feralized mice were fed a natural diet in the previous experiments, we designed Exp. 3 (Figure 2) to assess the effects of the major dietary sources of the previous two experiments, carried out in IVCs under conventional lab conditions. 30 female B6 mice (source, age and gender as in Exp. 2) were housed for 14 weeks in cages of 5 mice per cage. The animals were randomized into two groups receiving either chow or a combinatory diet of chow and seed mix (the latter hereafter referred to as seed group for simplicity).

The mice were exposed to human caretakers in the pens on a daily basis, but direct handling was minimized, and mice were not re-captured until termination of the experiment. Only mice that were clinically healthy condition at termination were included in the studies. All mice were euthanized by neck dislocation, followed by immediate exsanguination by cardiac puncture, weighing and measuring, and dissection of sample tissues.





## Isolation of Cells and Serum

Cells harvested from tissues using a GentleMACS dissociator and mouse Spleen Dissociation Kit (Miltenyi Biotech, Bergisch Gladbach, Germany) according to the manufacturer's instructions. Splenic suspensions were briefly treated with NH<sub>4</sub>Cl solution to lyse erythrocytes. Single-cell suspensions were prepared using a 70 μm cell strainer (BD Biosciences) and concentrations standardized after counting using a Countess automated cell counter (Thermo Fisher Scientific). Serum was isolated from blood following centrifugation of clotted whole blood at 3,000 g for 5 min.

## Microbial Community Analyses

For microbial community analyses, fecal pellets were flash frozen in liquid N<sub>2</sub> after collection and stored at -80°C. DNA extraction, library preparation and 16S rDNA 454 pyrosequencing were conducted as described previously (Lindner et al., 2015). Briefly, DNA was isolated and purified with QIAamp DNA Stool Mini Kit (Qiagen) according to manufacturer's manual. Libraries were generated with a primer set covering the V1–V3 regions of the 16S rRNA gene (8F/541R). 16S rRNA gene amplicons were purified by gel electrophoresis followed by gel

extraction (QIAquick Gel Extraction kit, Qiagen). Amplicons were prepared with the GS FLX Titanium SV emPCR kit (Lib-A) for 454 pyrosequencing on the Genome Sequencer FLX system (Roche) according to manufacturer's instructions. In Exp. 2 and 3, feces was collected from all individuals at baseline (t0) and termination following 14 weeks of feralization (t1).

Raw reads were processed using the Integrated Microbial Next Generation Sequencing (IMNGS) pipeline (Lagkouvardos et al., 2016) based on the UPARSE approach. Briefly, sequences were demultiplexed, trimmed to the first base with a quality score > 3 and paired. Sequences with > 1000 nucleotides and assembled reads with expected error of > 3 were excluded from the analyses (Exp. 2, USEARCH 8.0; Exp. 3, USEARCH 8.1) (Edgar, 2010). Remaining reads were trimmed by 10 nucleotides at forward and reverse end. The presence of chimeras was tested with UCHIME (Edgar et al., 2011). Operational taxonomic units (OTUs) were clustered at 97% sequence similarity (Edgar, 2010) (Exp. 2, USEARCH 8.0; Exp. 3, USEARCH 8.1), and only those with a relative abundance of > 0.50% (Exp. 2) or > 0.25% (Exp. 3) in at least one sample were kept. Taxonomies were assigned at 80% confidence level with the RDP classifier (Wang et al., 2007) (version 2.11, training set 15). Sequences were aligned with

MUSCLE (Edgar, 2004) and trees were generated with Fasttree (Price et al., 2010). In Exp. 2 the analyzed dataset included 1,207,683 quality- and chimera-checked sequences ranging from 6,527 to 48,172 per sample, representing a total of 338 OTUs. One individual in the Fzd group was excluded from analyses due to abnormally high sequence depth (152,009). In Exp. 3 the analyzed dataset included 3,481,304 quality- and chimera-checked sequences ranging from 39,504 to 131,663 per sample, representing a total of 220 OTUs. Sequencing files from Exp. 2 and Exp. 3 are deposited to the Sequence Read Archive and are available under the accession number PRJNA668303.

## Flow Cytometry and *in vitro* T-Cell Stimulation

Immunophenotyping was carried out by incubating single-cell suspensions in phosphate-buffered saline (PBS) with 0.5% bovine serum albumin and 10 mM NaN<sub>3</sub> on ice. After FcR-blocking with anti-CD32/16 antibody (eBioscience), cells were stained with Live/Dead Fixable Yellow Dead Cell Stain Kit (Thermo Fisher Scientific) followed by incubation with combinations of monoclonal antibodies as listed in **Supplementary Table S2**. For intracytoplasmic staining, cells were treated with Intracellular Fixation and Permeabilization Buffer Set, or with Foxp3/Transcription Factor Staining Buffer Set for intranuclear antigens (both eBioscience), according to the manufacturer's instructions. Fluorescence levels were measured using a Gallios 3-laser flow cytometer and analyzed using Kaluza 1.2 software (Beckman Coulter). Cells were gated as shown in **Supplementary Figure S1**, using single cell staining, omission of antibodies and matched isotypes as controls. For stimulation assays, splenocytes were cultured at concentration of  $2 \times 10^6$  cells/ml together with Dynabeads Mouse T-Activator CD3/CD28 (Thermo Fisher Scientific) at a 1:1 ratio, in RPMI (Gibco) l-glutamine supplemented with 60 µg/ml penicillin, 100 µg/ml streptomycin, 1 mM sodium pyruvate, 50 µM 2-mercaptoethanol, non-essential amino acids (all Gibco/Invitrogen), 10% fetal calf serum (PAA) and 30 U/ml recombinant murine (rm)IL-2 (eBioscience) for 48 h. Brefeldin A (10 µg/ml; Sigma) was added 4 h before harvesting, followed by immunophenotyping.

## Multiplex Assays

Cytokines were measured in serum using the following multiplex assays: Bio-Plex Pro Mouse Cytokine 8-plex panel (#M60000007A) supplemented with IL-6 and IL-17A singleplex, Bio-Plex Pro™ TGF-β 3-plex Assay (#171W4001M) (Bio-Rad), or ProcartaPlex Th1/Th2/Th9/Th17/Th22/Treg Cytokine 17-Plex Mouse Panel (EPX170-26087-901) (Thermo Fisher Scientific). Antibody subclasses were measured using ProcartaPlex Mouse Antibody Isotyping 7-plex panel (EPX070-20815-901). In all cases the analyses were carried out following the manufacturers' instructions, using a Luminex 200 reader and BioPlex Manager 6.0 software (BioRad). Analysis was performed on fluorescence index (FI) values minus background, while figures show concentrations calculated from standard curve. Analytes with more than 40% data points

below limit of detection (Antweiler, 2015) were excluded from statistical evaluation.

## Statistical Analyses

Microbial profiles and composition were analyzed in the R programming environment (R version 4.0.2) (R\_Core\_Team, 2020) using Rhea (Lagkouvardos et al., 2017)<sup>1</sup>. To account for differences in sequence depth, OTU tables were first normalized by dividing each sample's reads to their total reads, then multiplication by the total reads of the smallest sample. Beta-diversity was calculated based on generalized UniFrac distances (Chen et al., 2012) and the significance of separation between groups was tested by permutational multivariate analysis of variance (PERMANOVA). Alpha-diversity was assessed based on species richness and Shannon effective diversity as described in detail in Rhea. Only taxa with a prevalence of  $\geq 30\%$  (proportion of samples positive for the given taxa) in one given group, and relative abundance  $\geq 0.25\%$  were considered for statistical testing. For analyses of differences in relative abundance between  $> 2$  groups (Exp. 2), Kruskal-Wallis Rank Sum test was performed. A significant Kruskal-Wallis test ( $p < 0.05$ ) was followed by pairwise Wilcoxon Rank Sum tests. *P*-values were corrected for multiple comparisons according to the Benjamini-Hochberg method, and adjusted *p*-values are reported. For comparisons of two groups (Exp. 3), Wilcoxon Rank Sum tests were performed directly. For analyses of differences in prevalence between groups, Fisher's exact tests were performed. Over-time analyses within groups were performed using paired Wilcoxon Signed Rank Sum tests.

In order to identify patterns of differentially abundant and prevalent OTUs in Feral and SPF mice, we conducted an indicator species analysis implemented by the *indicspecies* package (De Cáceres and Legendre, 2009) in R. The significance of the associations was determined by permutation tests followed by Benjamini-Hochberg correction of resulting *p*-values. To identify highly indicative OTUs, we included only OTUs that occurred in  $\geq 70\%$  of the mice in either the Feral or SPF group at each timepoint. For Exp. 3, an indicator species analysis was conducted in the same manner as described for Exp. 2, to identify OTUs indicative of Chow-fed or Seed-fed animals independent of timepoint. For all groups at both timepoints, the relative abundances of the identified indicator-OTUs were plotted with the *heatmap.2* function from the *gplots* package (Warnes et al., 2020) in R. The closest species related to the indicator-OTU sequences were identified with EzBioCloud (Yoon et al., 2017). See **Supplementary Table S3** for a complete list of indicator-OTUs presented in **Figure 3E** and **Supplementary Figure S4E**.

Immunological data was analyzed using log (Ln)-transformed values. Comparisons between groups were performed using the statistical applications JMP v.14 (SAS Institute Inc.) or Prism v.7 (GraphPad Software, Inc.), applying Student's *t*-test for two groups, and Tukey-Kramer's multiple comparison test for  $> 2$  groups, at alpha level 0.05, unless otherwise stated. In figures with letter indications, levels not sharing the same letter were significantly different. Multivariate analyses were

<sup>1</sup><https://github.com/Lagkouvardos/Rhea>



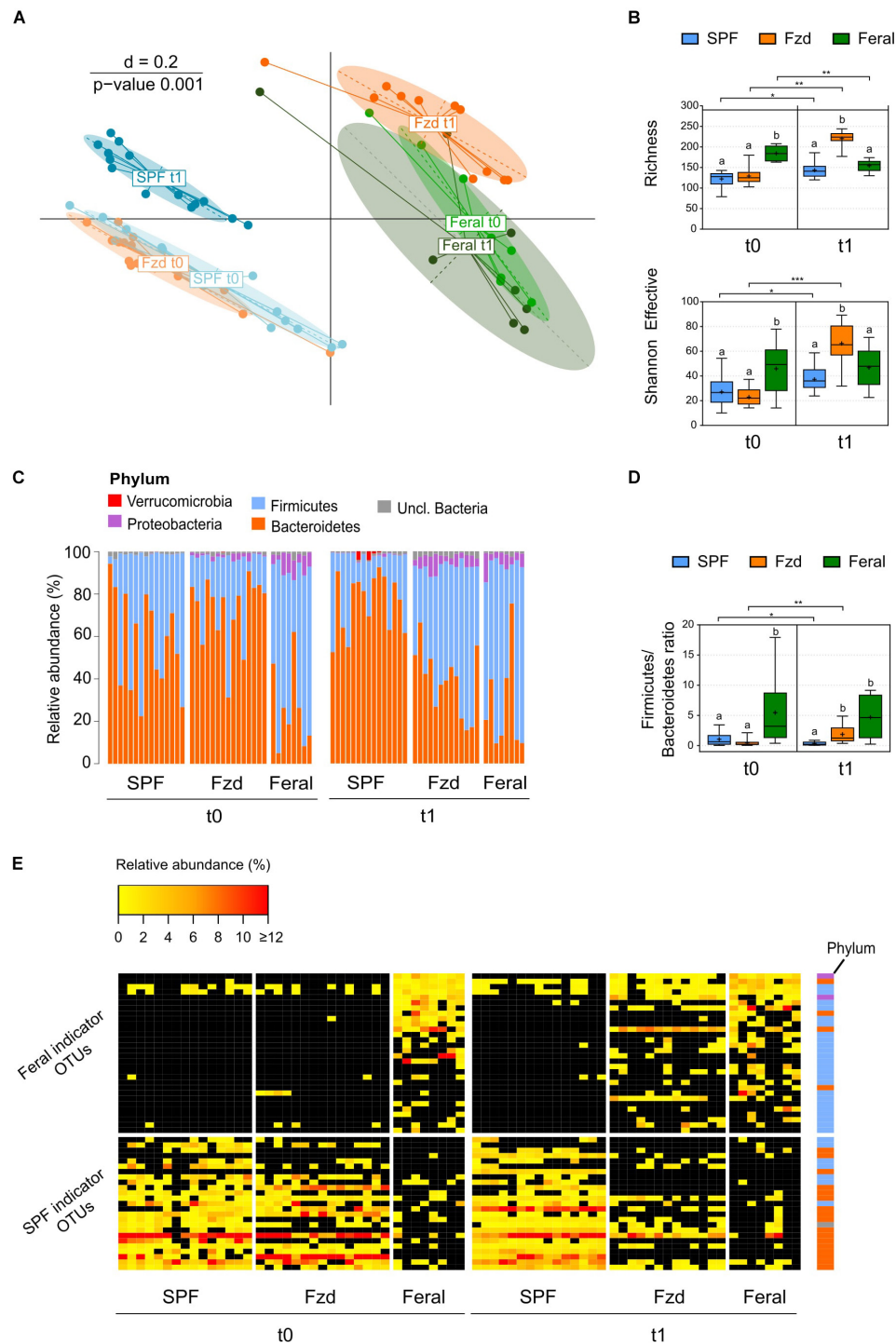


**FIGURE 3 |** Feralization lead to a gut microbiota diversity and composition converging with feral mice. Presented data is from Exp. 2. **(A)** Multi-dimensional scaling (MDS) plot of microbiota profiles for feral, feralized (Fzd) and SPF mice at baseline (t0) and termination (t1). Similarities between profiles were computed using generalized Unifrac distances. The significance of separation between groups was tested by PERMANOVA.  $d$  = dissimilarity scale. **(B)** Richness (observed OTUs) and Shannon effective diversity index. Box plots show median (line), mean (+), IQR (box) and minimum to maximum (whiskers). Asterisks designate over-time differences determined by Wilcoxon Signed-Rank Sum test. Differences between groups at each timepoint were determined by Kruskal-Wallis and Mann-Whitney  $U$ -tests. The Benjamini-Hochberg method was used to correct for multiple testing. Levels not sharing the same letter were significantly different at  $\alpha = 0.05$ .  $*p \leq 0.05$ ,  $**p \leq 0.01$ ,  $***p \leq 0.001$ . **(C)** Taxonomic binning at the rank of phylum, presented as relative abundance for each individual, with groups and timepoints indicated. **(D)** Firmicutes/Bacteroidetes ratio presented as in **(B)**. **(E)** Heatmap of relative abundance of Feral- and SPF-associated OTUs identified by indicator species analysis. Phyla of which the OTUs belong to are designated with colored squares specified in **(C)**. Relative abundances of the OTUs  $< 0.25\%$  were set to NA (black). All plots:  $n = 8$  (feral) or  $n = 13\text{--}15$  (other groups).

performed using the principal component analysis (PCA) on Correlations, and hierarchical clustering using Ward's minimum variance method in JMP on the variables listed in **Supplementary Table S4**, excluding one Fzd mouse with an incomplete data set.

## RESULTS

### Lab Mice Adapted Well to a Farmyard Habitat in the Presence of Feral Mice

Throughout Exp. 1 we closely monitored how animals performed through direct inspection and using surveillance or handheld cameras (**Supplementary Figure S2**). Feral and B6 mice were released simultaneously into the pens to avoid biased territorializing (**Supplementary Video S2**). The mice dug holes in the soil that appeared preferential for nesting rather than using wooden houses provided for this purpose (**Supplementary Video S3**). Feral and B6 mice mingled well, in both the male-female and the female-female setups. Feral mice generally reacted to human presence by hiding, re-emerged within few minutes and approached people (**Supplementary Video S4**), whilst the B6 mice were generally less shy. Feral mice quickly adapted to drinking from water bottles. However, four feral individuals were found dead with no visible signs of injuries and lack of water being a possible cause. No B6 mice died, showed visible bruises or signs of disease, except one slow-moving Fzd<sup>M</sup> female that was excluded from the study. Fzd<sup>M</sup> females mated with feral males and produced litters that were cared for in a shared dirt-hole nursing colony. However, since past or present pregnancy might confound the readouts, we chose to carry out subsequent experiments in an all-female setting. In Exp. 2 the observed behavior was similar to Exp. 1, and all introduced mice were recaptured in healthy condition.

### Feralized Mice Acquired Mouse Pathogens and a Feral-Like Gut Microbiota

Serum samples from four individuals of each mouse group in Exp. 1 were screened for antibodies against a range of pathogens. Feral mice carried antibodies for Minute virus of mice (MVM), Mouse parvovirus (MPV), Mouse Cytomegalovirus (MCMV) and, in one case, *Pasteurella pneumotropica* (*Pp*) (**Supplementary Table S5A**). Fzd<sup>M</sup> mostly seroconverted to mimic the feral mice, while only a single Fzd<sup>F</sup> mouse tested positive for one pathogen (*Pp*). SPF controls were negative for all tested agents. A gross parasitological examination of intestines with fecal content revealed the presence worms or eggs in feral and Fzd<sup>M</sup> mice, but to a less extent in Fzd<sup>F</sup> mice while negative in SPF controls (**Supplementary Table S5B**).

The terminal gut microbiota in stool samples from Fzd<sup>F</sup> mice in Exp. 1 has been reported previous (Lindner et al., 2015). Briefly, the microbiota profile of the feralized mice approached that of feral mice, including a higher relative abundance of Firmicutes and Proteobacteria, while SPF mice stood out with a separate profile. Data from Exp. 2 largely mirrored the findings of Exp. 1. At baseline, *beta*-diversity analysis demonstrated a distinct

clustering of baseline gut microbiota of the B6 mice separate from feral mice (**Figure 3A**), and *alpha*-diversity measures showed a significantly higher number of observed OTUs (richness) in feral mice compared to the Fzd and SPF groups (both  $p \leq 0.001$ ) (**Figure 3B**). At the rank of phylum, a significantly higher relative abundance of Firmicutes and lower relative abundance of Bacteroidetes was detected in feral mice compared to Fzd (both  $p \leq 0.001$ ) and SPF ( $p = 0.035$  and  $p = 0.005$ , respectively), as reflected in a higher Firmicutes/Bacteroidetes ratio (**Figures 3C,D**). Moreover, Proteobacteria abundance above cutoffs were detected in all feral mice and the majority of feralized mice, but only in one SPF individual (**Figure 3C**). In feral mice, the Proteobacteria was mainly accounted for by two OTUs with closest sequence similarity to *Helicobacter* species (*Helicobacter ganmani*, 99.6% similarity; *Helicobacter typhlonius*, 100% similarity), while in Fzd the Proteobacteria was mainly accounted for by one OTU with the closest sequence similarity to *Kiloniella laminariae* (86.3% similarity).

A clear shift in the microbiota profile was seen following feralization, in which the Fzd mice approached a Feral-like profile (**Figure 3A**). Feralization led to a dramatic increase in both richness and Shannon effective ( $p = 0.002$  and  $p \leq 0.001$ , respectively), indicating an elevated number of species representing a higher level of phylogenetic diversity (**Figure 3B**). An increase in relative abundance of Firmicutes and decrease in relative abundance of Bacteroidetes (both  $p = 0.001$ ) was observed following feralization, reflected in an increased Firmicutes/Bacteroidetes ratio ( $p = 0.005$ ) (**Figures 3C,D**). The shift following feralization was further supported by analysis of the terminal gut microbiota, in which the Fzd and feral mice demonstrated significantly higher *alpha*-diversity measures and Firmicutes/Bacteroidetes ratios, and increased relative abundances of Proteobacteria compared to the SPF mice (**Figures 3C,D**). Moreover, we conducted an Indicator Species Analysis to identify OTUs that were most indicative for Feral and SPF mice based on the probability of occurrence and abundance in these groups independent of timepoint. This algorithm was first developed by Dufrene and Legendre (1997) and has been employed previously to track persistence of OTUs in mice following environmental changes (Seedorf et al., 2014) and fecal microbiota transfer from wild to laboratory mice (Rosshart et al., 2017). Generally, the OTUs associated with Feral mice belonged to the Firmicutes phylum, while the SPF-associated OTUs were members of Bacteroidetes, mirroring the detected phylum-level differences (**Figure 3E**). Two OTUs with closest sequence similarities to *Helicobacter* species (*Helicobacter ganmani*, 99.6%; *Helicobacter typhlonius*, 100%) were identified as Feral-associated OTUs (**Figure 3E** and **Supplementary Table S3A**). By plotting the abundances of the indicator OTUs for all samples, we were able to track the Feral-associated and SPF-associated OTUs in the Fzd group over time. Prior to feralization, the Fzd and SPF groups showed overlapping patterns, with high abundance of SPF-associated and generally low abundance of Feral-associated OTUs. Following feralization, a substantial proportion of Feral-associated OTUs was detected, while only a very few SPF-associated OTUs undetected in Feral mice remained in the Fzd group at endpoint (**Figure 3E**).

Taken together, feralization led to a substantial change in gut microbiota structure, approaching the profile and composition seen in feral mice. Seropositivity to viral pathogens was detected in all feral mice, and in female feralized mice co-housed with feral males, but not in those co-housed with feral females.

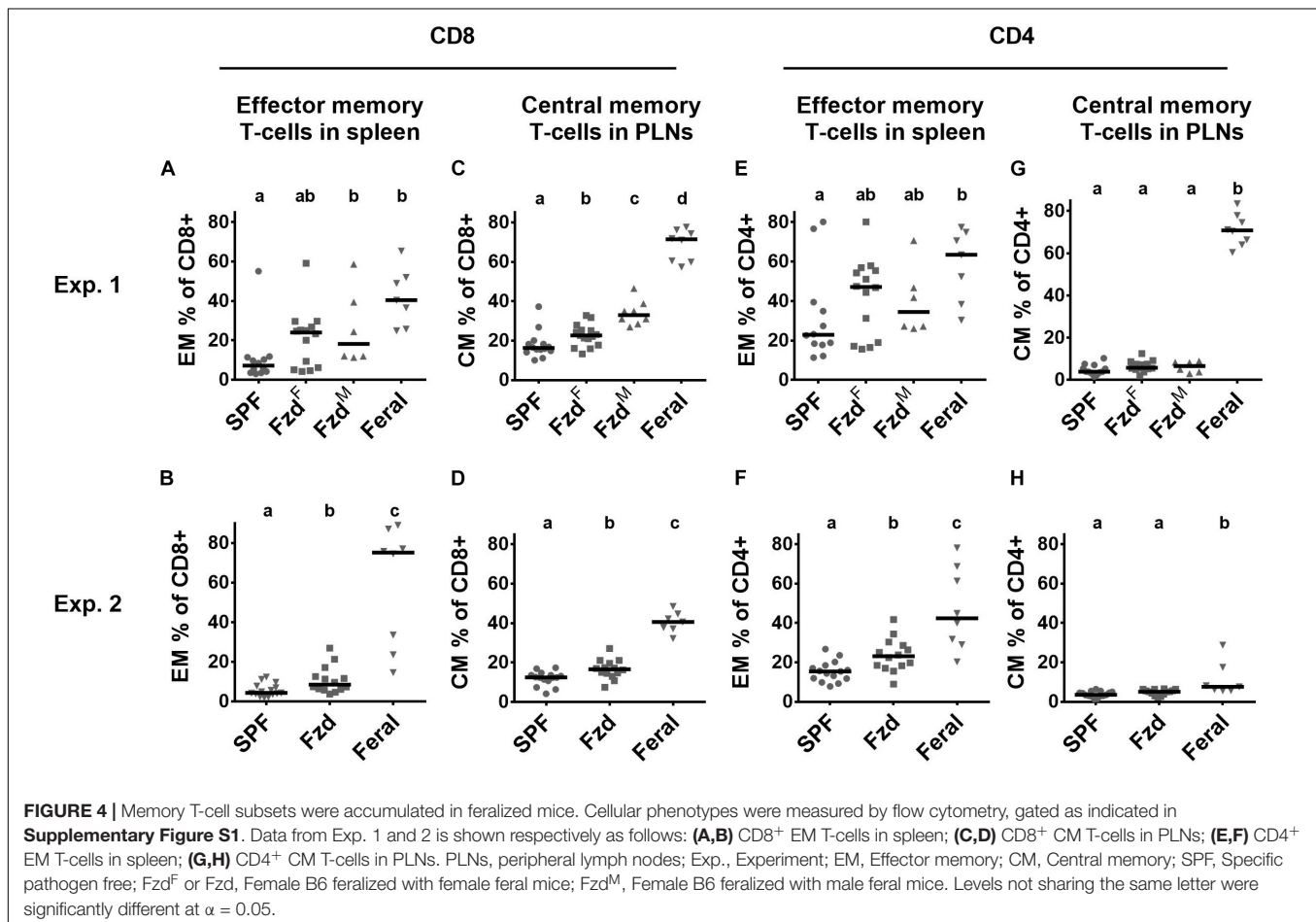
## Feralization Lead to Immunophenotypes Consistent With Antigenic Experience and Immune Training

Cellular phenotypes were measured according to gating strategies shown in **Supplementary Figure S1**. In both Exp. 2 and Exp. 3, the number of T-cells and CD4<sup>+</sup> and CD8<sup>+</sup> subsets were similar in feralized and SPF mice in SPL as well as peripheral lymph nodes (PLNs) (not shown). Memory T-cells, defined as CD44<sup>+</sup>CD62L<sup>+</sup> central memory (CM) cells, or CD44<sup>+</sup>CD62L<sup>-</sup> effector memory (EM) cells were measured in the spleen and PLNs, respectively, according to the most common compartments for these subsets (Wherry et al., 2003; Stockinger et al., 2006). Feralized mice showed increased levels of CD8<sup>+</sup> T cells with an EM phenotype in the spleen (**Figures 4A,B**) as well as CM cells in the PLNs (**Figures 4C,D**). A tendency for increased proportions of EM CD4<sup>+</sup> cells was seen in the spleen of feralized mice (**Figures 4E,F**), but not for CM CD4<sup>+</sup> cells in

the PLNs (**Figures 4G,H**). Feral mice consistently had more cells displaying an EM or CM phenotype within the CD8 as well as the CD4 subsets (**Figures 4A–H**). To assess if T-cells of feralized mice had changed their potency as effector cells, we cultured splenocytes with anti-CD3/CD28 coupled beads for 48 h in the presence of IL-2 in Exp. 2. The frequency of interferon-gamma positive CD8<sup>+</sup> and to a lesser extent CD4<sup>+</sup> T-cell populations was higher in feralized mice compared to SPF mice (**Figures 5A,B**).

Regulatory T-cells (Tregs) (CD3<sup>+</sup>CD4<sup>+</sup>CD25<sup>+</sup>Foxp3<sup>+</sup>) were measured in PLNs. In Exp. 1, feralized mice had similar number of Tregs as SPF mice, while feral mice had a lower proportion (**Figure 6A**). In Exp. 2, slightly elevated Treg numbers were seen in feralized but not in feral mice (**Figure 6B**). We furthermore, assessed neuropilin-1 (NRP-1) dim or negative cells, associated with peripherally induced regulatory T-cells (pTregs), especially induced by gastrointestinal exposure (Bilate and Lafaille, 2012). In both Exp. 1 and 2, the proportion of pTregs was slightly elevated in the feral mice, but insignificantly so in feralized mice (**Figures 6C,D**).

NK cells numbers were elevated in PLNs but not spleens of feral mice (**Figures 7A,B** and **Supplementary Figures S3A,B**), as observed previously (Boysen et al., 2011). In feralized mice NK cells tended to increase, albeit not statistically significant, in the PLNs (**Figures 7A,B**), while no differences were observed



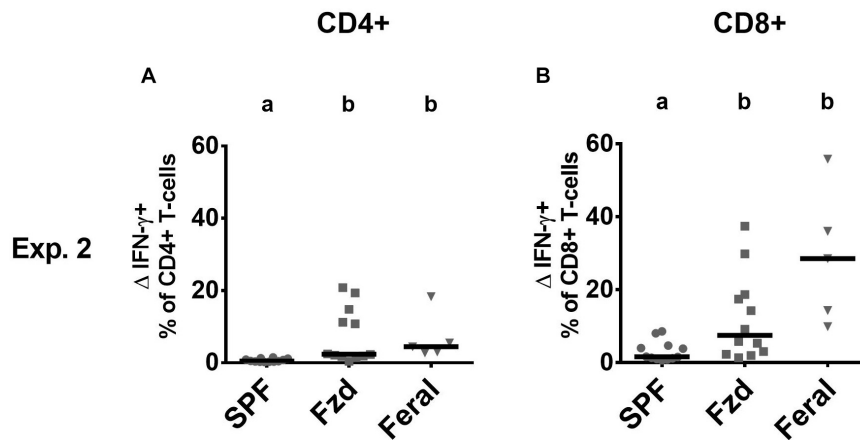


**FIGURE 5 |** T-cells in feralized mice responded to in vitro stimulation with increased interferon gamma (IFN- $\gamma$ ) production. Splenocytes were incubated for 48 h with bead-coupled anti-CD3/CD28 antibodies in the presence of IL-2 and measured for intracellular IFN- $\gamma$  production by flow cytometry.  $\Delta$ IFN- $\gamma$ <sup>+</sup> (IFN- $\gamma$ <sup>+</sup> NK cells in stimulated cultures—ditto in medium control cultures) is shown as per cent of CD4<sup>+</sup> T-cells (A) or of CD8<sup>+</sup> T-cells (B). All data from Exp. 2. Abbreviations and statistics as in **Figure 4**.

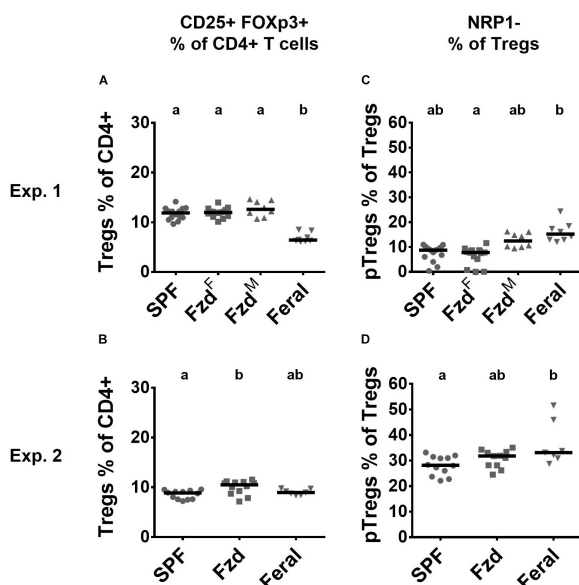


**FIGURE 6 |** Regulatory T-cell numbers and phenotypes in peripheral lymph nodes were largely unaffected by feralization. Data from Exp.1 and 2 is shown respectively as follows: (A,B) Relative numbers of Tregs as per cent of CD4<sup>+</sup> T-cells; (C,D) Proportion of Tregs defined as pTregs according to lack of NRP1 expression. Tregs, Regulatory T-cells; pTregs, peripheral Tregs; NRP1, Neuropilin-1; otherwise abbreviations and statistics as in **Figure 4**.

in the spleen (**Supplementary Figures S3A,B**). Murine NK cells can be phenotypically divided into maturation stages as early (S1) CD27<sup>−</sup>CD11b<sup>−</sup>, mid (S2) CD27<sup>+</sup>CD11b<sup>−</sup>, late (S3) CD27<sup>+</sup>CD11b<sup>+</sup>, and fully mature (S4) CD27<sup>−</sup>CD11b<sup>+</sup> stages (Chiossone et al., 2009; Abolins et al., 2017), most cells normally found within the S2–S4 categories. We found that feral mice had a decreased S4/S2 ratio in both PLNs and in spleen, as

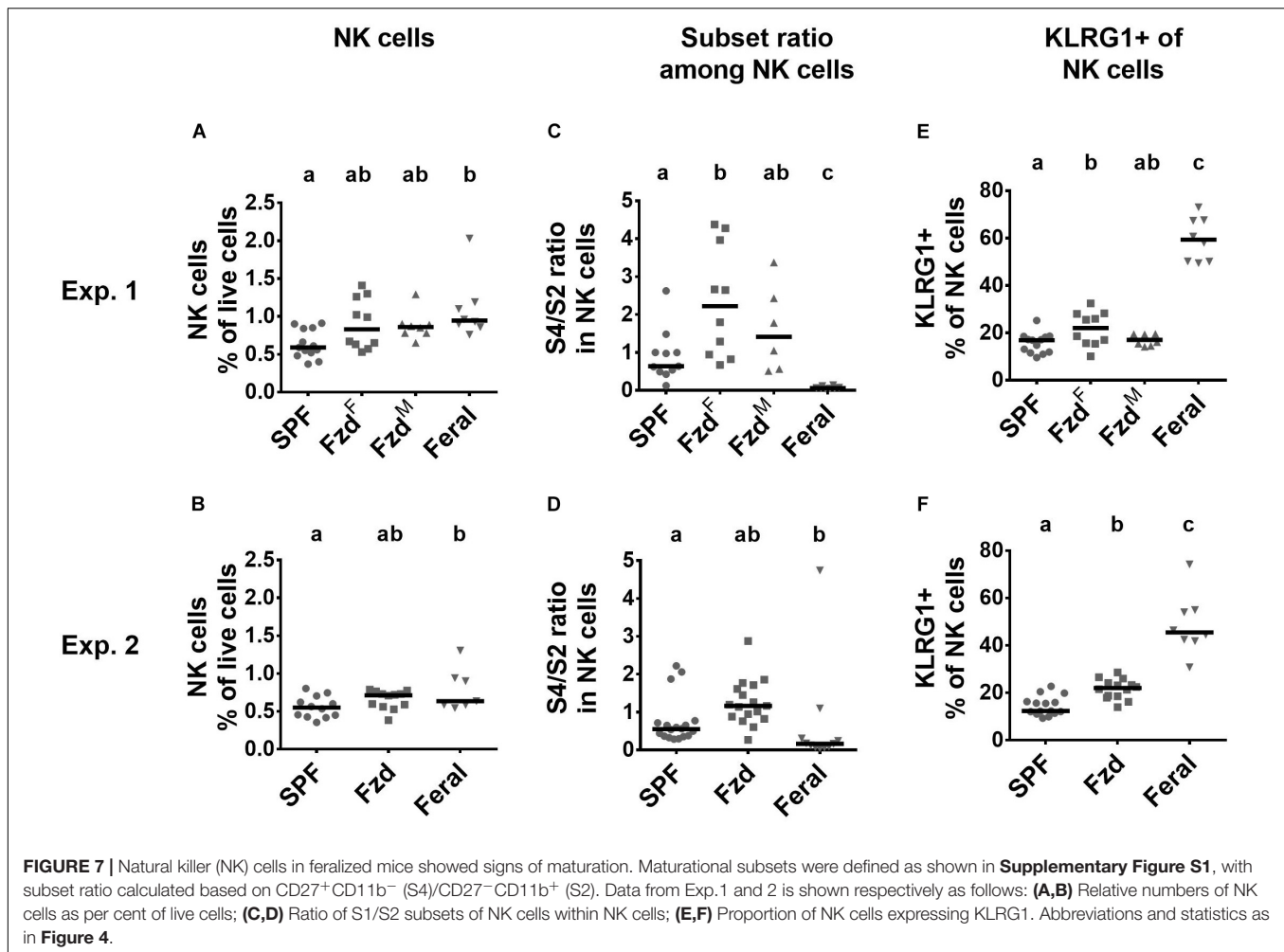
seen previously (Boysen et al., 2011). In contrast, increased S4/S2 ratio was detected in feralized mice, most evident in the PLNs (**Figures 7C,D** and **Supplementary Figures S3C,D**). KLRG1 expression was elevated in NK cells in feral mice in PLN (**Figures 7E,F**) and partly in spleen (**Supplementary Figures S3E,F**), confirming previous observations (Boysen et al., 2011). To a lesser extent, feralized mice also had elevated KLRG1 in PLNs (**Figures 7E,F**), a tendency also evident in spleen (**Supplementary Figures S3E,F**).

Most tested serum cytokines were low and not significantly altered between groups (**Figure 8**). However, IL-18 was lower in the feralized and feral mice (**Figure 8F**). A tendency of increased TGF- $\beta$ 1 in feralized mice was noted but with high variability and not statistically confirmed (**Figures 8G,H**). Some additional cytokines were either not significantly altered or fell below the lower limit of detection (**Supplementary Table S6**).

Increased serum levels of IgE and IgG1 have previously been reported in feral mice (Devalapalli et al., 2006; Abolins et al., 2011), and in Exp. 2 we measured immunoglobulin subclasses using a multiplex assay, demonstrating that feral mice had increased serum IgA, IgE, Ig2a, Ig2b, and IgM (**Figure 9**). Feralized mice showed a tendency of increased IgE and IgG2b, while the remaining subclasses fell within the same range as SPF controls. IgG1 was not detected above background levels (not shown).

The data from Exp. 2 had a completeness that allowed multivariate analysis of immune parameters, in order to explore any co-variation undetected when assessing single parameters. A PCA analysis revealed that feralized mice grouped separately from SPF controls, in the direction of feral mice (**Figure 10A**), significantly different between all groups in first principal component (Prin1) but not Prin2 (**Figure 10B**). Likewise, a cluster analysis grouped mice from each study group separately, except a minor overlap between SPF and feralized mice (**Figure 10C**).

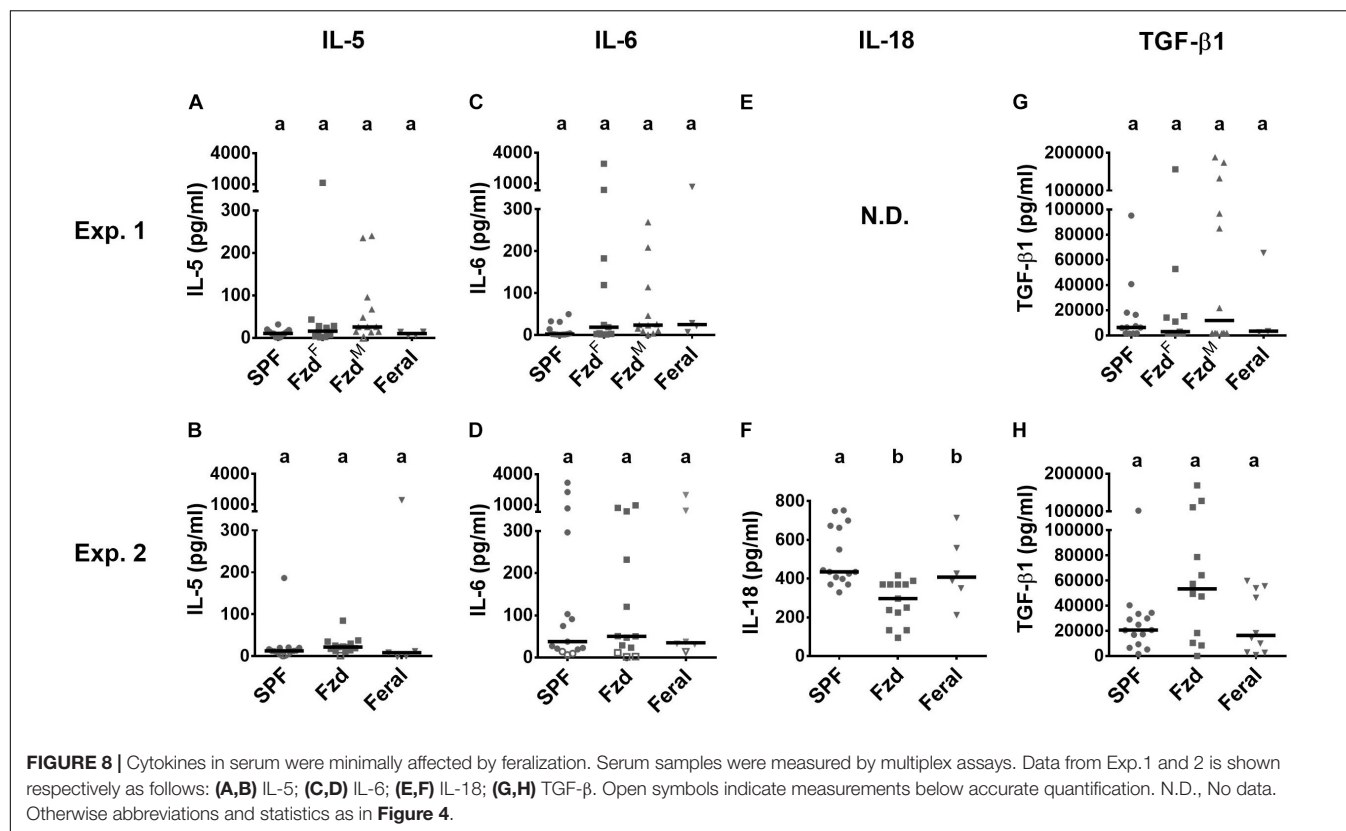




## Diet May Explain Shifts in Gut Microbiota, but Was Not Found to Drive Immunological Changes

To assess the contributions of differing diets between groups in Exp. 1 and 2 to gut microbiota and immunophenotypes, Exp. 3 was designed to incorporate the two diets in a SPF lab cage setting. Microbial profiling of feces showed a shift in microbiota composition and increased *alpha*-diversity measures on both diets, although more prominently in mice fed the seed diet compared to regular chow (**Supplementary Figures S4A,B**). At the rank of phylum, no significant changes were detected in the chow-fed animals. For the seed-fed animals, we detected a significantly decreased relative abundance of Bacteroidetes ( $p = 0.013$ ) and increased relative abundance of Firmicutes ( $p = 0.011$ ), reflected in increased Firmicutes/Bacteroidetes ratio over-time ( $p = 0.048$ ) (**Supplementary Figures S4C,D**). Similar to Exp. 2, the over-time changes were supported by analyses of the terminal gut microbiota, in which seed-fed mice demonstrated significantly higher *alpha*-diversity measures and Firmicutes/Bacteroidetes ratio compared to the chow-fed mice. However, in contrast to the findings from

Exp. 2, relative abundances of Proteobacteria were unchanged following the different diets. In the analysis of data from Exp. 3 we also conducted an indicator species analysis to identify OTUs that were most indicative for the Chow-fed and Seed-fed mice independent of timepoint. Relatively few indicator-OTUs were identified in this analysis, indicating only small differences between Chow- and Seed-fed mice at the OTU-level (**Supplementary Figure S4E** and **Supplementary Table S3B**). At baseline, prior to administration of different diets, the two groups showed overlapping patterns (**Supplementary Figure S4E**). From baseline to endpoint, Seed-fed animals showed an enrichment of several OTUs belonging to the phylum Firmicutes, mirroring the findings at phylum-level. Whilst we found changes in gut microbiota following the two diets, immunophenotyping showed no diet-induced difference in CD44<sup>+</sup> cells in the CD8<sup>+</sup> T-cell compartment. In the CD4<sup>+</sup> T-cell subset, a minor increase of CD44<sup>+</sup> cells was observed in seed-fed mice (**Supplementary Figure S5A**). In *ex vivo* CD3/CD28 stimulated splenocytes, intracellular IFN- $\gamma$  production was similar in the two diet groups in both CD8<sup>+</sup> or CD4<sup>+</sup> T-cells (**Supplementary Figure S5D**). Moreover, we observed no significant effect of diet on Treg



levels or pTreg proportions, NK cells or NK cells subsets (Supplementary Figures S5B,D).

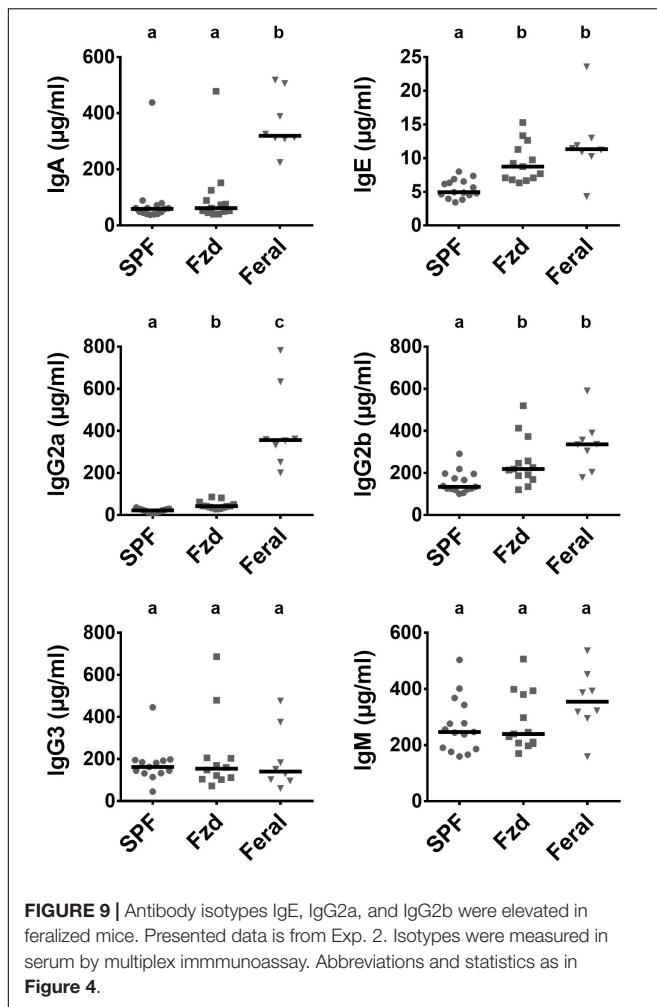
Taken together, the findings from Exp. 3 indicated that a diet similar to that given to feralized mice in Exp. 1 and 2 caused a significant shift in gut microbiota structure, yet provided no evidence for any shift in immunological parameters assignable to the diet.

## DISCUSSION

A spacious and naturalistically enriched environment meets an increasing demand to improve housing conditions to refine the experimental output from mouse models (Balcombe, 2010). Large indoor enclosures have previously been used to study house mouse behavior (Gray et al., 2000; Jensen et al., 2003, 2005; Weissbrod et al., 2013), but to our knowledge, no reports describe the microbiological and immunological phenotypes of mice reared in such enclosures enriched as a naturalistic environment. The tremendous adaptability of the house mouse implies that no single habitat is universally “natural.” Nevertheless, house mice are predominantly found in or near human dwellings, farm buildings, food stores and waste areas, and its dispersal largely follows human movements (Pocock et al., 2005). The house mouse often forms high-density territories as small as a few square meters (Selander, 1970). To set up a well-defined naturalistic scenario we constructed large pens containing essential farmyard elements through domestic animal fecal

material, soil and plants, and with wild-caught mice present as microbial donors. The aim of the current report was to observe the performance of laboratory mice housed in this model system and to observe their resulting fecal microbiota and key elements of their systemic immunity phenotype.

Feralization led to a significant shift in gut microbiota composition and increased *alpha*-diversity measures following feralization, supportive of previous reports of microbially exposed mice (Ottman et al., 2019; Liddicoat et al., 2020). We observed an enrichment of Proteobacteria in feral and feralized mice, in agreement with findings in “wildling” B6 mice born to feral mothers (Rosshart et al., 2019) as well as B6 mice co-housed with pet store mice (Huggins et al., 2019). Two OTUs associated with feral mice microbiota showed the closest similarity to *Helicobacter* species and were enriched in feralized mice. In a recent paper, *Helicobacter* species have been suggested to trigger colonic T cell responses in a context-dependent manner (Chai et al., 2017). Moreover, the higher Firmicutes/Bacteroidetes ratios in feralized and feral mice corresponds to a previous report of feral mice (Kreisinger et al., 2014), but contrasts the lower relative abundance of Firmicutes seen in fecal samples from wildlings (Rosshart et al., 2019), from B6 mice receiving fecal transfer from wild mice (Rosshart et al., 2017), as well as from soil-exposed mice (Ottman et al., 2019). However, care should be taken when interpreting between studies, as geographical factors have been shown to drive the microbiota composition to a larger extent than genotypes, including between *Mus musculus* subspecies (Linnenbrink et al., 2013; Kreisinger et al., 2014).



Notably, feral mice maintained a similar microbiota before and after pen housing in Exp. 2. Their prior microbial environment and diet is unknown, but they were caught at farms distant from the sources used for enrichment, and these findings could either indicate that the conditions we created reflected their feral situation, or that their colonized microbiota was more resilient to change compared to the SPF-derived laboratory mice.

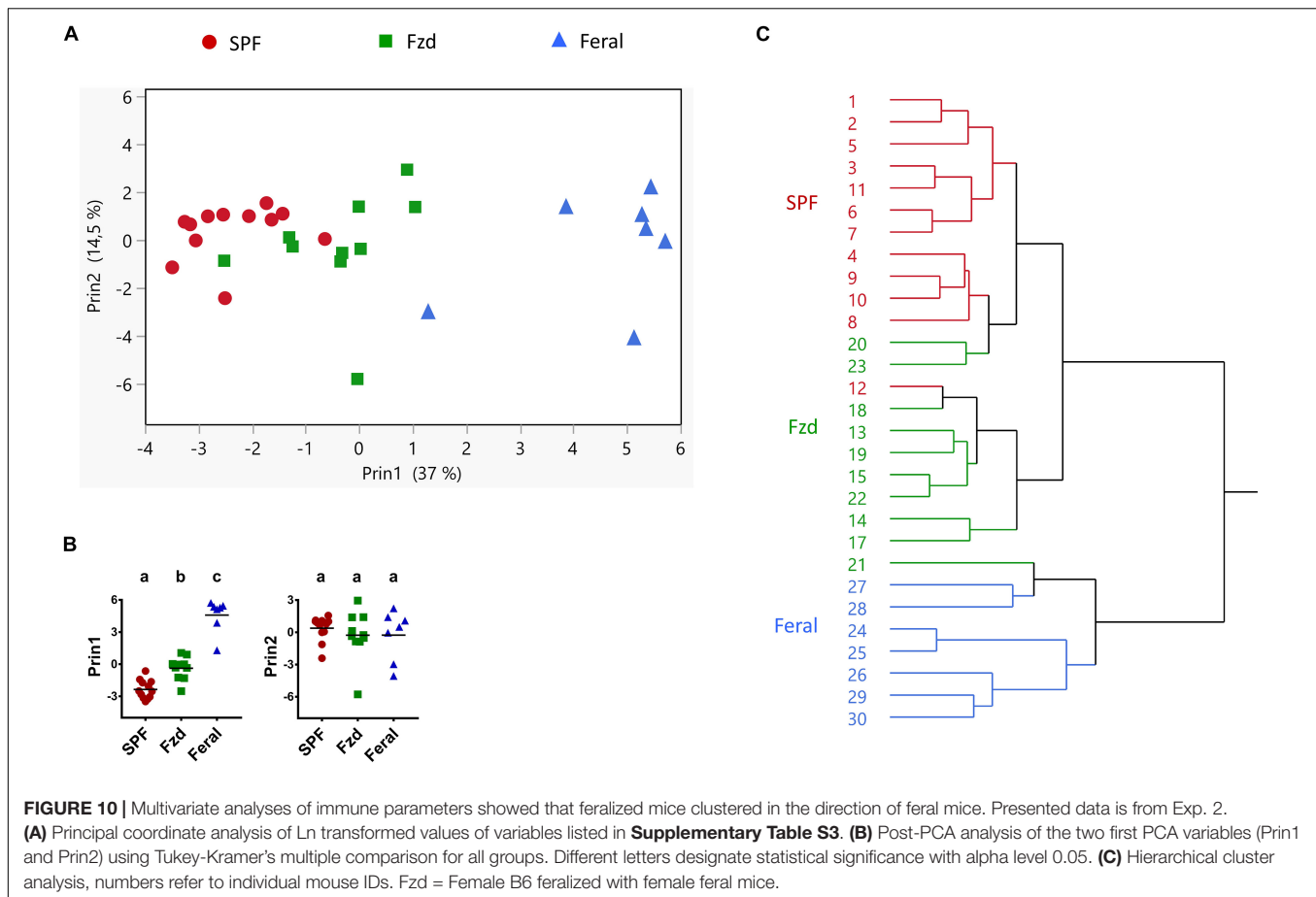
The seed-based diet offered in the naturalistic environment contained higher amounts of fiber and fat compared to the standard chow diet, both of which are groups of dietary components demonstrated to alter gut microbiota composition and influence immunity in a wide range of previous studies (Daniel et al., 2014; Trompette et al., 2014; Desai et al., 2016; Xiao et al., 2017; Las Heras et al., 2019). We therefore set up a third experiment to assess this impact in an otherwise hygienic context. Seed-fed mice had increased *alpha*-diversity and Firmicutes/Bacteroidetes ratio, suggesting a partial explanation for changes seen in the feralized mice. We did not observe differences in the investigated immune parameters following the two diets, suggesting the alterations of immunophenotypes were driven by other stimuli, or other components of the microbiota, than those conferred by diet.

A multivariate analysis showed that the combined systemic immune phenotype of feralized mice clustered distinctly from SPF mice in the direction of feral mice, albeit still closer to SPFs. For cellular measurements we concentrated on NK and T-cell phenotypes associated with maturation and memory. Feralized and feral mice had increased numbers of memory CD8<sup>+</sup> T cells, in line with report of long-lasting expansion following *in vivo* challenge (Vezys et al., 2009). Similar upregulation of memory T cells has been reported in feral and pet-store mice, in lab mice co-housed with pet-store mice and in rewilded mice (Beura et al., 2016; Abolins et al., 2017; Lin et al., 2020). Following *ex vivo* stimulation, we found that T-cells in feralized and feral mice responded more potently with IFN-gamma production compared to lab mice, similar to previous reports in feral and rewilded mice (Abolins et al., 2017; Lin et al., 2020).

We found little effect of feralization on the total Treg cell numbers, while pTregs, defined as NRP-1<sup>+</sup> Tregs (Bilate and Lafaille, 2012), showed a slightly increasing tendency, not significant in feralized but significant in feral mice. A previous study in feral mice found marginal increase in splenic Tregs (Abolins et al., 2017), while two other studies of microbially diversified lab mice found no alteration in Treg cell numbers (Frossard et al., 2017; Rosshart et al., 2019). These findings suggest that Tregs in systemic organs do not respond substantially to these types of environmental triggers.

NK cells may be activated by pathogens or primed by proinflammatory cytokines, transforming the cells into a more mature state, in many cases persisting as memory-like or trained NK cells (Nabekura and Lanier, 2016; Netea et al., 2020). In mice, trained NK cells have been found to display a mature KLRG1<sup>+</sup> and CD27<sup>+</sup>CD11b<sup>+</sup> phenotype (Nabekura and Lanier, 2016). We reproducibly found more CD27<sup>+</sup>CD11b<sup>+</sup> and KLRG1<sup>+</sup> NK cells in feralized B6 mice. Notably, as reported previously (Boysen et al., 2011; Abolins et al., 2017), feral mice had a contrasting overweight of CD27<sup>+</sup>CD11b<sup>+</sup> NK cells, yet with a high KLRG1 expression. Feral and feralized mice underwent the same microbial pressure for 2–3 months, suggesting that the CD27/CD11b discrepancy may be genetic rather than environmental. However, this aberrance is unlikely due to genetic differences amongst subspecies, as while the present mice were *M. m. musculus*-dominated, the same NK cell phenotype have been noted in feral *M. m. domesticus* mice (Abolins et al., 2017), the latter constituting the major genetic background for the B6 mouse (Yang et al., 2011). Regardless of cause, the finding emphasizes the importance of assessing genetically controlled individuals in this type of studies.

Low levels of serum cytokines were detected and these were apparently not sensitive to environmental changes, as also seen in wildlings (Rosshart et al., 2019). The observed elevation of IgE in feral and feralized mice compare with findings from other studies (Devalapalli et al., 2006; Abolins et al., 2011, 2017) and are possibly caused by the presence of parasites as were detected in Exp. 1. Besides parasites, seroconversion for pathobionts were especially evident in the Fzd<sup>M</sup> females, which made frequent intimate contacts with feral males during mating. In the all-female setup, a feral-type feral microbiota was obtained,



yet the serological results indicated that they acquired less of a pathogenic burden. These findings may suggest that relatively strong and/or frequent transmission pressure of pathobionts is needed for a mouse to reach a feral-like immunophenotype.

The scope of the presented studies was to achieve a full-scale naturalistic environment, rather than to explore underlying mechanisms, which would require multiple investigations or a substantial reduction of the very elements that create diversity. Depending on the scope, future studies may add or exclude elements, such as considering the necessity of mouse-specific microbionts obtained through the inclusion of feral mice. While the basis for environmental diversity will inevitably vary between geographical sites (Linnenbrink et al., 2013; Kreisinger et al., 2014), so does the microbiota in highly isolated conventional facilities (Rausch et al., 2016). The strength of genetically controlled model animals remains, and studies on the background of mice feralized in this manner can complement studies in conventional SPF and germ-free lab mice, as demonstrated by us in two reports (Lindner et al., 2015; Monin et al., 2020). By ensuring that environmental materials derive from the same sources throughout the experiment, and preferably between experiments, well-controlled and reproducible experiments can be achieved. A “dirty” environment as described here must in most cases be established separate from clean mouse houses, in our hands

successfully achieved in an experimental large animal facility, and later built as a separate satellite unit.

## CONCLUSION

In conclusion, we have demonstrated how laboratory mice can be feralized in large pens containing feral cohabitant mice, recapitulating a natural mouse habitat. Feralized mice reproducibly carried an altered fecal microbiota and immunophenotype in systemic immune tissues. This model system represents a refinement opportunity for various purposes, such as assessing the performance of infections, drugs or vaccines on the background of “real-world” adapted animals.

## DATA AVAILABILITY STATEMENT

The original contributions presented in the study are publicly available. This data can be found in NCBI, under accession number PRJNA668303.

## ETHICS STATEMENT

The animal study was reviewed and approved by National Animal Research Authority, Norwegian Food Safety Authority.



## AUTHOR CONTRIBUTIONS

PB and AKS designed the research. BWH and PB conducted animal Exp. 1. LEK and PB conducted animal Exp. 2 and 3. BWH, LEK, GMJ, MB, OP, and PB performed the laboratory procedures. HA and PB analyzed the data and wrote the manuscript. All authors contributed to the article and approved the submitted version.

## FUNDING

This research was funded internally at NMBU and the collaborators, microbiota analyses was supported by a grant from The Nansen Fund (Unifor, Norway).

## ACKNOWLEDGMENTS

We are indebted to Jane Hurst (University of Liverpool, United Kingdom) for valuable advice on the design of the mouse pens, the staff at Department of ProdMed at NMBU for assistance with the pen constructions and monitoring of mice (and for keeping the cat out!), the staff at ExBio (NMBU) for housing and tending of control mice, Andrew Janczak (NMBU) for lending of surveillance cameras, Teresa Hagen (NMBU, Parasitology group) for parasitological examinations, Peter O. Hofgaard (University of Oslo, Department of Immunology at Oslo University Hospital), Profs. Jan E. Paulsen and Harald Carlsen (NMBU) for advice on animal dissection and lab methods, Johanna Kabbert, Christina Petrick, Thomas Hitch (RWTH Aachen, Germany), and Anne Mari Herfindal (NMBU) for help and discussions related to the microbiota analyses.

## SUPPLEMENTARY MATERIAL

The Supplementary Material for this article can be found online at: <https://www.frontiersin.org/articles/10.3389/fmicb.2020.615661/full#supplementary-material>

**Supplementary Figure 1** | Flow cytometry gating strategies. (A) Single cell, mononuclear cells (MNC) and live cell gates. (B) NK cells defined as NKp46+CD3- cells, further defined as maturational stages S1–S4 based on CD27

and CD11b expression, or gated for the expression of KLRG1. (C) T-cells gated equivalent to above, gated as CD4<sup>+</sup> or CD8<sup>+</sup> and defined as Central Memory (CM; CD62L<sup>+</sup>CD44<sup>+</sup>) or Effector Memory (EM; CD62L<sup>+</sup>CD44<sup>+</sup>). (D) Regulatory T-cells, gated on CD4<sup>+</sup> T-cells equivalent to above, defined as CD25<sup>+</sup>Foxp3<sup>+</sup>, and further gated for the expression of Neuropilin-1 (NRP1). (E) *In vitro* stimulated T-cells, cultured for 48 h in the presence of CD3/CD28 activator beads and IL-2, gated on T-cells equivalent to above and gated for the expression of interferon gamma (IFNγ).

**Supplementary Figure 2** | Photos from the mouse experiments carried out in the farmyard-like pens. (A) Pallet, soil, large animal feces, twigs, straw, feral mice. (B) Feral mouse peeking from water bottle. (C) Nest with B6 x feral mouse crosses. (D) B6 mice checking box (mostly used as toilets; dirt holes were preferred as nests). (E) Feral mouse. (F) Nighttime grazing on sprouts. (G) Offspring playing in box.

**Supplementary Figure 3** | Natural killer (NK) cell numbers and phenotypes in spleen, equivalent to Figure 7. Abbreviations and statistics as in Figure 4.

**Supplementary Figure 4** | Gut microbiota diversity and composition of SPF mice fed different diets. Presented data is from Exp. 3. (A) Multi-dimensional scaling (MDS) plot of microbiota profiles for seed- and chow-fed animals at baseline (t0) and termination (t1). Similarities between profiles were computed using generalized Unifrac distances. The significance of separation between groups was tested by PERMANOVA.  $d$  = dissimilarity scale. (B) Richness (observed OTUs) and Shannon effective diversity index. Box plots show median (line), mean (+), IQR (box) and minimum to maximum (whiskers). Asterisks designate over-time differences determined by Wilcoxon Signed-Rank Sum test. Letters designate differences between groups at each timepoint determined by Kruskal-Wallis and Mann-Whitney U tests. The Benjamini-Hochberg method was used to correct for multiple testing. Different letters designate statistical significance with corrected  $p \leq 0.05$ . \* $p \leq 0.05$ , \*\* $p \leq 0.01$ , \*\*\* $p \leq 0.001$ . (C) Taxonomic binning at the rank of phylum, presented as relative abundance for each individual, with groups and timepoints indicated. (D) Firmicutes/Bacteroidetes ratio presented as in (B). (E) Heatmap of relative abundances of Chow- and Seed-associated OTUs identified by indicator species analysis. Phyla of which the OTUs belong to are designated with colored squares specified in (C). Relative abundances of the OTUs < 0.25% were set to NA (black). All plots:  $n = 12$  (chow) or  $n = 13$  (seed).

**Supplementary Figure 5** | Cellular immunological phenotypes of mice in Exp. 3, corresponding to measurements in main experiments shown in Figures 4–7. Abbreviations and statistics as in Figure 4.

**Supplementary Video 1** | Mouse pen overview, wooden pallets, soil heaps with fresh domestic animal manure, straw, spruce twigs. / C57BL/6 mice in farm environment.

**Supplementary Video 2** | Release of feral (wild-caught) mouse. / First encounters between C57BL/6 and feral mice.

**Supplementary Video 3** | Feral mouse showing agile behavior, use of available space and resources.

**Supplementary Video 4** | Feral mice showing curiosity, adaptability to B6 mice and people.

## REFERENCES

- Abolins, S., King, E. C., Lazarou, L., Weldon, L., Hughes, L., Drescher, P., et al. (2017). The comparative immunology of wild and laboratory mice, *Mus musculus domesticus*. *Nat. Commun.* 8:14811. doi: 10.1038/ncomms14811
- Abolins, S., Lazarou, L., Weldon, L., Hughes, L., King, E. C., Drescher, P., et al. (2018). The ecology of immune state in a wild mammal, *Mus musculus domesticus*. *PLoS Biol.* 16:e2003538. doi: 10.1371/journal.pbio.2003538
- Abolins, S. R., Pocock, M. J., Hafalla, J. C., Riley, E. M., and Viney, M. E. (2011). Measures of immune function of wild mice, *Mus musculus*. *Mol. Ecol.* 20, 881–892. doi: 10.1111/j.1365-294x.2010.04910.x
- Antweiler, R. C. (2015). Evaluation of statistical treatments of left-censored environmental data using coincident uncensored data sets. II. Group comparisons. *Environ. Sci. Technol.* 49, 13439–13446. doi: 10.1021/acs.est.5b02385
- Balcombe, J. (2010). Laboratory rodent welfare: thinking outside the cage. *J. Appl. Anim. Welf. Sci.* 13, 77–88. doi: 10.1080/10888700903372168
- Beura, L. K., Hamilton, S. E., Bi, K., Schenkel, J. M., Odumade, O. A., Casey, K. A., et al. (2016). Normalizing the environment recapitulates adult human immune traits in laboratory mice. *Nature* 532, 512–516. doi: 10.1038/nature17655
- Bilate, A. M., and Lafaille, J. J. (2012). Induced CD4<sup>+</sup>Foxp3<sup>+</sup> Regulatory T Cells in immune tolerance. *Annu. Rev. Immunol.* 30, 733–758. doi: 10.1146/annurev-immunol-020711-075043
- Boursot, P., Auffray, J. C., Britton-Davidian, J., and Bonhomme, F. (1993). The evolution of house mice. *Annu. Rev. Ecol. Syst.* 24, 119–152. doi: 10.1146/annurev.es.24.110193.001003



- Boysen, P., Eide, D. M., and Storset, A. K. (2011). Natural killer cells in free-living *Mus musculus* have a primed phenotype. *Mol. Ecol.* 20, 5103–5110. doi: 10.1111/j.1365-294X.2011.05269.x
- Cebra, J. J. (1999). Influences of microbiota on intestinal immune system development. *Am. J. Clin. Nutr.* 69, 1046S–1051S.
- Chai, J. N., Peng, Y., Rengarajan, S., Solomon, B. D., Ai, T. L., Shen, Z., et al. (2017). *Helicobacter* species are potent drivers of colonic T cell responses in homeostasis and inflammation. *Sci. Immunol.* 2:eaa15068. doi: 10.1126/sciimmunol.aal5068
- Chen, J., Bittiger, K., Charlson, E. S., Hoffmann, C., Lewis, J., Wu, G. D., et al. (2012). Associating microbiome composition with environmental covariates using generalized UniFrac distances. *Bioinformatics* 28, 2106–2113. doi: 10.1093/bioinformatics/bts342
- Chiossone, L., Chaix, J., Fuseri, N., Roth, C., Vivier, E., and Walzer, T. (2009). Maturation of mouse NK cells is a 4-stage developmental program. *Blood* 113, 5488–5496. doi: 10.1182/blood-2008-10-187179
- Chung, H., Pamp, S. J., Hill, J. A., Surana, N. K., Edelman, S. M., Troy, E. B., et al. (2012). Gut immune maturation depends on colonization with a host-specific microbiota. *Cell* 149, 1578–1593. doi: 10.1016/j.cell.2012.04.037
- Daniel, H., Gholami, A. M., Berry, D., Desmarchelier, C., Hahne, H., Loh, G., et al. (2014). High-fat diet alters gut microbiota physiology in mice. *ISME J.* 8, 295–308. doi: 10.1038/ismej.2013.155
- De Cáceres, M., and Legendre, P. (2009). Associations between species and groups of sites: indices and statistical inference. *Ecology* 90, 3566–3574. doi: 10.1890/08-1823.1
- Desai, M. S., Seekatz, A. M., Koropatkin, N. M., Kamada, N., Hickey, C. A., Wolter, M., et al. (2016). A dietary fiber-deprived gut microbiota degrades the colonic mucus barrier and enhances pathogen susceptibility. *Cell* 167, 1339–1353.e21. doi: 10.1016/j.cell.2016.10.043
- Devalapalli, A. P., Leshner, A., Shieh, K., Solow, J. S., Everett, M. L., Edala, A. S., et al. (2006). Increased levels of IgE and autoreactive, polyreactive IgG in wild rodents: implications for the hygiene hypothesis. *Scand. J. Immunol.* 64, 125–136. doi: 10.1111/j.1365-3083.2006.01785.x
- Dufrene, M., and Legendre, P. (1997). Species assemblages and Indicator species: the need for a flexible asymmetrical approach. *Ecol. Monogr.* 67, 345–366. doi: 10.2307/2963459
- Edgar, R. C. (2004). MUSCLE: multiple sequence alignment with high accuracy and high throughput. *Nucleic Acids Res.* 32, 1792–1797. doi: 10.1093/nar/gkh340
- Edgar, R. C. (2010). Search and clustering orders of magnitude faster than BLAST. *Bioinformatics* 26, 2460–2461. doi: 10.1093/bioinformatics/btq461
- Edgar, R. C., Haas, B. J., Clemente, J. C., Quince, C., and Knight, R. (2011). UCHIME improves sensitivity and speed of chimera detection. *Bioinformatics* 27, 2194–2200. doi: 10.1093/bioinformatics/btr381
- El Aidy, S., van Baarlen, P., Derrien, M., Lindenberg-Kortleve, D. J., Hooiveld, G., Levenez, F., et al. (2012). Temporal and spatial interplay of microbiota and intestinal mucosa drive establishment of immune homeostasis in conventionalized mice. *Mucosal Immunol.* 5, 567–579. doi: 10.1038/mi.2012.32
- Flies, A. S., and Wild Comparative Immunology Consortium (2020). Rewilding immunology. *Science* 369, 37–38. doi: 10.1126/science.abb8664
- Franklin, C. L., and Ericsson, A. C. (2017). Microbiota and reproducibility of rodent models. *Lab Anim.* 46, 114–122. doi: 10.1038/labana.1222
- Frossard, C. P., Lazarevic, V., Gaia, N., Leo, S., Doras, C., Habre, W., et al. (2017). The farming environment protects mice from allergen-induced skin contact hypersensitivity. *Clin. Exp. Allergy* 47, 805–814. doi: 10.1111/cea.12905
- Gray, S. J., Jensen, S. P., and Hurst, J. L. (2000). Structural complexity of territories: preference, use of space and defence in commensal house mice, *Mus domesticus*. *Anim. Behav.* 60, 765–772. doi: 10.1006/anbe.2000.1527
- Honda, K., and Littman, D. R. (2016). The microbiota in adaptive immune homeostasis and disease. *Nature* 535, 75–84. doi: 10.1038/nature18848
- Huggins, M. A., Sjaastad, F. V., Pierson, M., Kucaba, T. A., Swanson, W., Staley, C., et al. (2019). Microbial exposure enhances immunity to pathogens recognized by TLR2 but increases susceptibility to cytokine storm through TLR4 sensitization. *Cell Rep.* 28, 1729. doi: 10.1016/j.celrep.2019.07.028
- Hunter, P. (2020). Public Health struggles to square hygiene with diversity: research on the link between microbiomes and immune function puts the “hygiene hypothesis” to rest. *EMBO Rep.* 21:e51540. doi: 10.15252/embr.202051540
- Ivanov, I. I., Atarashi, K., Manel, N., Brodie, E. L., Shima, T., Karaoz, U., et al. (2009). Induction of intestinal Th17 cells by segmented filamentous bacteria. *Cell* 139, 485–498. doi: 10.1016/j.cell.2009.09.033
- Jakobsson, H. E., Rodriguez-Pineiro, A. M., Schutte, A., Ermund, A., Boysen, P., Bemark, M., et al. (2015). The composition of the gut microbiota shapes the colon mucus barrier. *EMBO Rep.* 16, 164–177. doi: 10.15252/embr.201439263
- Jensen, S. P., Gray, S. J., and Hurst, J. L. (2003). How does habitat structure affect activity and use of space among house mice? *Anim. Behav.* 66, 239–250. doi: 10.1006/anbe.2003.2184
- Jensen, S. P., Gray, S. J., and Hurst, J. L. (2005). Excluding neighbours from territories: effects of habitat structure and resource distribution. *Anim. Behav.* 69, 785–795. doi: 10.1016/j.anbehav.2004.07.008
- Knutsen, L. E., Dissen, E., Saether, P. C., Bjornsen, E. G., Pialek, J., Storset, A. K., et al. (2019). Evidence of functional Cd94 polymorphism in a free-living house mouse population. *Immunogenetics* 71, 321–333. doi: 10.1007/s00251-018-01100-x
- Kreisinger, J., Cizkova, D., Vohanka, J., and Pialek, J. (2014). Gastrointestinal microbiota of wild and inbred individuals of two house mouse subspecies assessed using high-throughput parallel pyrosequencing. *Mol. Ecol.* 23, 5048–5060. doi: 10.1111/mec.12909
- Kriegel, M. A., Sefik, E., Hill, J. A., Wu, H. J., Benoist, C., and Mathis, D. (2011). Naturally transmitted segmented filamentous bacteria segregate with diabetes protection in nonobese diabetic mice. *Proc. Natl. Acad. Sci. U.S.A.* 108, 11548–11553. doi: 10.1073/pnas.1108924108
- Lagkouvardos, I., Fischer, S., Kumar, N., and Clavel, T. (2017). Rhea: a transparent and modular R pipeline for microbial profiling based on 16S rRNA gene amplicons. *PeerJ* 5:e2836. doi: 10.7717/peerj.2836
- Lagkouvardos, I., Joseph, D., Kapfhammer, M., Giritli, S., Horn, M., Haller, D., et al. (2016). IMNGS: a comprehensive open resource of processed 16S rRNA microbial profiles for ecology and diversity studies. *Sci. Rep.* 6:33721. doi: 10.1038/srep33721
- Las Heras, V., Clooney, A. G., Ryan, F. J., Cabrera-Rubio, R., Casey, P. G., Hueston, C. M., et al. (2019). Short-term consumption of a high-fat diet increases host susceptibility to *Listeria monocytogenes* infection. *Microbiome* 7:7. doi: 10.1186/s40168-019-0621-x
- Leung, J. M., Budischak, S. A., The, H. C., Hansen, C., Bowcutt, R., Neill, R., et al. (2018). Rapid environmental effects on gut nematode susceptibility in rewilded mice. *PLoS Biol.* 16:e2004108. doi: 10.1371/journal.pbio.2004108
- Liddicoat, C., Sydnor, H., Cando-Dumancela, C., Dresken, R., Liu, J., Gellie, N. J. C., et al. (2020). Naturally-diverse airborne environmental microbial exposures modulate the gut microbiome and may provide anxiolytic benefits in mice. *Sci. Total Environ.* 701:134684. doi: 10.1016/j.scitotenv.2019.134684
- Lin, J. D., Devlin, J. C., Yeung, F., McCauley, C., Leung, J. M., Chen, Y. H., et al. (2020). Rewilding Nod2 and Atg16l1 mutant mice uncovers genetic and environmental contributions to microbial responses and immune cell composition. *Cell Host Microbe* 27, 830–840.e4. doi: 10.1016/j.chom.2020.03.001
- Lindner, C., Thomsen, I., Wahl, B., Ugur, M., Sethi, M. K., Friedrichsen, M., et al. (2015). Diversification of memory B cells drives the continuous adaptation of secretory antibodies to gut microbiota. *Nat. Immunol.* 16, 880–888. doi: 10.1038/ni.3213
- Linnenbrink, M., Wang, J., Hardouin, E. A., Kunzel, S., Metzler, D., and Baines, J. F. (2013). The role of biogeography in shaping diversity of the intestinal microbiota in house mice. *Mol. Ecol.* 22, 1904–1916. doi: 10.1111/mec.12206
- Monin, L., Ushakov, D. S., Arnesen, H., Bah, N., Jandke, A., Munoz-Ruiz, M., et al. (2020). gamma delta T cells compose a developmentally regulated intrauterine population and protect against vaginal candidiasis. *Mucosal Immunol.* 13, 969–981. doi: 10.1038/s41385-020-0305-7
- Muraille, E., and Goriely, S. (2017). The nonspecific face of adaptive immunity. *Curr. Opin. Immunol.* 48, 38–43. doi: 10.1016/j.coi.2017.08.002
- Nabekura, T., and Lanier, L. L. (2016). Tracking the fate of antigen-specific versus cytokine-activated natural killer cells after cytomegalovirus infection. *J. Exp. Med.* 213, 2745–2758. doi: 10.1084/jem.20160726
- Netea, M. G., Dominguez-Andres, J., Barreiro, L. B., Chavakis, T., Divangahi, M., Fuchs, E., et al. (2020). Defining trained immunity and its role in health and disease. *Nat. Rev. Immunol.* 20, 375–388. doi: 10.1038/s41577-020-0285-6

- Oh, J. Z., Ravindran, R., Chassaing, B., Carvalho, F. A., Maddur, M. S., Bower, M., et al. (2014). TLR5-mediated sensing of gut microbiota is necessary for antibody responses to seasonal influenza vaccination. *Immunity* 41, 478–492. doi: 10.1016/j.immuni.2014.08.009
- Ottman, N., Ruokolainen, L., Suomalainen, A., Sinkko, H., Karisola, P., Lehtimäki, J., et al. (2019). Soil exposure modifies the gut microbiota and supports immune tolerance in a mouse model. *J. Allergy Clin. Immunol.* 143, 1198. doi: 10.1016/j.jaci.2018.06.024
- Pocock, M. J., Hauffe, H., and Searle, J. B. (2005). Dispersal in house mice. *Biol. J. Linn. Soc.* 84, 565–583. doi: 10.1111/j.1095-8312.2005.00455.x
- Price, M. N., Dehal, P. S., and Arkin, A. P. (2010). FastTree 2—approximately maximum-likelihood trees for large alignments. *PLoS One* 5:e9490. doi: 10.1371/journal.pone.0009490
- Quinn, S. M., Cunningham, K., Raverdeau, M., Walsh, R. J., Curham, L., Malara, A., et al. (2019). Anti-inflammatory trained immunity mediated by helminth products attenuates the induction of T cell-mediated autoimmune disease. *Front. Immunol.* 10:1109. doi: 10.3389/fimmu.2019.01109
- Rausch, P., Basic, M., Batra, A., Bischoff, S. C., Blaut, M., Clavel, T., et al. (2016). Analysis of factors contributing to variation in the C57BL/6J fecal microbiota across German animal facilities. *Int. J. Med. Microbiol.* 306, 343–355. doi: 10.1016/j.ijmm.2016.03.004
- Reese, T. A., Bi, K., Kambal, A., Filali-Mouhim, A., Beura, L. K., Burger, M. C., et al. (2016). Sequential infection with common pathogens promotes human-like immune gene expression and altered vaccine response. *Cell Host Microbe* 19, 713–719. doi: 10.1016/j.chom.2016.04.003
- Rosshart, S. P., Herz, J., Vassallo, B. G., Hunter, A., Wall, M. K., Badger, J. H., et al. (2019). Laboratory mice born to wild mice have natural microbiota and model human immune responses. *Science* 365:eaaw4361. doi: 10.1126/science.aaw4361
- Rosshart, S. P., Vassallo, B. G., Angeletti, D., Hutchinson, D. S., Morgan, A. P., Takeda, K., et al. (2017). Wild mouse gut microbiota promotes host fitness and improves disease resistance. *Cell* 171, 1015–1028.e13. doi: 10.1016/j.cell.2017.09.016
- R\_Core\_Team (2020). *R: A Language and Environment for Statistical Computing*. Vienna: R Foundation for Statistical Computing.
- Seedorf, H., Griffin, N. W., Ridaura, V. K., Reyes, A., Cheng, J., Rey, F. E., et al. (2014). Bacteria from diverse habitats colonize and compete in the mouse gut. *Cell* 159, 253–266. doi: 10.1016/j.cell.2014.09.008
- Selander, R. K. (1970). Behavior and genetic variation in natural populations. *Am. Zool.* 10, 53–66. doi: 10.1093/icb/10.1.53
- Stockinger, B., Bourgeois, C., and Kassiotis, G. (2006). CD4+ memory T cells: functional differentiation and homeostasis. *Immunol. Rev.* 211, 39–48. doi: 10.1111/j.0105-2896.2006.00381.x
- Tao, L., and Reese, T. A. (2017). Making mouse models that reflect human immune responses. *Trends Immunol.* 38, 181–193. doi: 10.1016/j.it.2016.12.007
- Trompette, A., Gollwitzer, E. S., Yadava, K., Sichelstiel, A. K., Sprenger, N., Ngom-Bru, C., et al. (2014). Gut microbiota metabolism of dietary fiber influences allergic airway disease and hematopoiesis. *Nat. Med.* 20, 159–166. doi: 10.1038/nm.3444
- Vezys, V., Yates, A., Casey, K. A., Lanier, G., Ahmed, R., Antia, R., et al. (2009). Memory CD8 T-cell compartment grows in size with immunological experience. *Nature* 457, 196–199. doi: 10.1038/nature07486
- Wang, Q., Garrity, G. M., Tiedje, J. M., and Cole, J. R. (2007). Naive Bayesian classifier for rapid assignment of rRNA sequences into the new bacterial taxonomy. *Appl. Environ. Microbiol.* 73, 5261–5267. doi: 10.1128/aem.00062-07
- Warnes, G. R., Bolker, B., Bonebakker, L., Gentleman, R., Huber, W., Liaw, A., et al. (2020). Available online at: <https://CRAN.R-project.org/package=gplots> (accessed December 01, 2020).
- Weissbrod, A., Shapiro, A., Vasserman, G., Edry, L., Dayan, M., Yitzhaky, A., et al. (2013). Automated long-term tracking and social behavioural phenotyping of animal colonies within a semi-natural environment. *Nat. Commun.* 4:2018. doi: 10.1038/ncomms3018
- Wherry, E. J., Teichgräber, V., Becker, T. C., Masopust, D., Kaeck, S. M., Antia, R., et al. (2003). Lineage relationship and protective immunity of memory CD8 T cell subsets. *Nat. Immunol.* 4, 225–234. doi: 10.1038/ni889
- Xiao, L., Sonne, S. B., Feng, Q., Chen, N., Xia, Z., Li, X., et al. (2017). High-fat feeding rather than obesity drives taxonomical and functional changes in the gut microbiota in mice. *Microbiome* 5:43.
- Yang, H., Wang, J. R., Didion, J. P., Buus, R. J., Bell, T. A., Welsh, C. E., et al. (2011). Subspecific origin and haplotype diversity in the laboratory mouse. *Nat. Genet.* 43, 648–655. doi: 10.1038/ng.847
- Yeung, F., Chen, Y. H., Lin, J. D., Leung, J. M., McCauley, C., Devlin, J. C., et al. (2020). Altered immunity of laboratory mice in the natural environment is associated with fungal colonization. *Cell Host Microbe* 27, 809–822.e6. doi: 10.1016/j.chom.2020.02.015
- Yoon, S. H., Ha, S. M., Kwon, S., Lim, J., Kim, Y., Seo, H., et al. (2017). Introducing EzBioCloud: a taxonomically united database of 16S rRNA gene sequences and whole-genome assemblies. *Int. J. Syst. Evol. Microbiol.* 67, 1613–1617. doi: 10.1099/ijsem.0.001755

**Conflict of Interest:** The authors declare that the research was conducted in the absence of any commercial or financial relationships that could be construed as a potential conflict of interest.

Copyright © 2021 Arnesen, Knutsen, Hognestad, Johansen, Bemark, Pabst, Storset and Boysen. This is an open-access article distributed under the terms of the Creative Commons Attribution License (CC BY). The use, distribution or reproduction in other forums is permitted, provided the original author(s) and the copyright owner(s) are credited and that the original publication in this journal is cited, in accordance with accepted academic practice. No use, distribution or reproduction is permitted which does not comply with these terms.



# Microbiome and Metabolome Analyses Reveal Novel Interplay Between the Skin Microbiota and Plasma Metabolites in Psoriasis

Dongmei Chen<sup>1,2†</sup>, Jingquan He<sup>3†</sup>, Jinping Li<sup>4</sup>, Qian Zou<sup>5</sup>, Jiawei Si<sup>5</sup>, Yatao Guo<sup>5</sup>, Jiayu Yu<sup>5</sup>, Cheng Li<sup>5</sup>, Fang Wang<sup>5</sup>, Tianlong Chan<sup>3</sup> and Huijuan Shi<sup>1,6\*</sup>

<sup>1</sup> Innovation Team for Skin Disease Diagnosis and Treatment Technology & Drug Discovery and Development, The General Hospital of Ningxia Medical University, Yinchuan, China, <sup>2</sup> Institute of Human Stem Cell Research, The General Hospital of Ningxia Medical University, Yinchuan, China, <sup>3</sup> Biotree Metabolomics Research Center, Biotree, Shanghai, China, <sup>4</sup> Department of Oncology Surgery, Ningxia Medical University, Yinchuan, China, <sup>5</sup> Clinical Medical School, Ningxia Medical University, Yinchuan, China, <sup>6</sup> Department of Dermatovenereology, The General Hospital of Ningxia Medical University, Yinchuan, China

## OPEN ACCESS

### Edited by:

David Kamanda Ngugi,  
German Collection of Microorganisms  
and Cell Cultures GmbH (DSMZ),  
Germany

### Reviewed by:

Shigefumi Okamoto,  
Kanazawa University, Japan  
Kazuhiro Ogai,  
Kanazawa University, Japan

### \*Correspondence:

Huijuan Shi  
shijym@163.com

<sup>†</sup> These authors have contributed  
equally to this work

### Specialty section:

This article was submitted to  
Microbial Symbioses,  
a section of the journal  
Frontiers in Microbiology

**Received:** 18 December 2020

**Accepted:** 22 February 2021

**Published:** 16 March 2021

### Citation:

Chen D, He J, Li J, Zou Q, Si J,  
Guo Y, Yu J, Li C, Wang F, Chan T  
and Shi H (2021) Microbiome  
and Metabolome Analyses Reveal  
Novel Interplay Between the Skin  
Microbiota and Plasma Metabolites  
in Psoriasis.  
Front. Microbiol. 12:643449.  
doi: 10.3389/fmicb.2021.643449

Psoriasis is a chronic inflammatory skin disease that affects millions of people worldwide. There is still no effective approach for the clinical treatment of psoriasis. This is largely due to the lack of understanding of the pathological mechanism. Here, we comprehensively characterized the skin microbiome and plasma metabolome alterations of psoriasis patients. We observed that some pathogenic bacteria, including *Vibrio*, were significantly increased in psoriasis patients. The metabolomics results showed alterations in some metabolic pathways, especially pathways for lipid metabolism. In addition, microbiome-specific metabolites, including bile acids and kynurenine, were significantly changed. Correlation analysis revealed the interplay between the skin microbiota and plasma metabolites, especially between *Vibrio* and several lipids. Our results provide new evidence for the interplay between the skin microbiome and plasma metabolites, which is dramatically disrupted in psoriasis patients. This study also revealed the mechanism underlying the pathogenesis of psoriasis.

**Keywords:** psoriasis, skin microbiome, plasma metabolome, lipid metabolism, inflammation

## INTRODUCTION

Psoriasis is one of the most common skin disorders worldwide, with approximately 2% of people affected (Boehncke and Schön, 2015). It affects not only the skin but also other organs. The molecular mechanism of psoriasis is not clear, which makes the discovery of new therapeutic drugs difficult. Most patients have to suffer from the disease for their whole life (Dubertret et al., 2006; Nestle et al., 2009).

The causes of psoriasis remain largely unknown but are reported to be related to many factors, including environmental factors, genetic factors, and immunologic factors (Nestle et al., 2009). In addition, the progression and even relapse after clinical treatment are all influenced by these

factors, which act together and form the specific metabolic characteristics of psoriasis. Glucose metabolism, amino acid metabolism, and lipid metabolism have been shown to be significantly changed in psoriasis patients (Zeng et al., 2017; Zhu and Thompson, 2019). The roles of metabolic regulation of cell proliferation and apoptosis are considered to be key to unregulated keratinocyte pathogenesis in psoriasis (Luo et al., 2020; Pohla et al., 2020). In addition, it is well known that the chronic inflammatory features of psoriasis, the associated characteristics of metabolic syndrome with psoriasis, and even the diet-related pathogenesis mechanism of psoriasis all indicate the importance of metabolism in the disease (Wolters, 2005; Gisondi et al., 2018). These reports suggest that alterations in global metabolism may contribute to the specific phenotype of psoriasis patients. However, additional information is still needed to answer these questions.

Microorganisms, which are located in many sites in our body, play very important roles in system homeostasis. Most studies have focused on the gut microbiome. The abundance and composition of the gut microbiome can vary under different conditions and are related to many human diseases (Chávez-Talavera et al., 2017). Increasing evidence has suggested that the activity of the microbiota is critical, especially in modulating tissue metabolism (Liu et al., 2017; He et al., 2020). In recent years, the role of the microbiome in maintaining healthy skin status and regulating skin-related diseases has been reported (Zeeuwen et al., 2013; Dréno et al., 2016; Byrd et al., 2018). For psoriasis, the role of the gut microbiome in disease pathogenesis and progression has been reported. In addition, the gut microbiota can be a potential biomarker of the disease (Thio, 2018; Myers et al., 2019). However, the organization of the skin microbiome and its potential function in regulating global metabolism in psoriasis patients remain unclear.

In this study, we collected skin microbiome samples and plasma samples from patients with severe plaque psoriasis and from healthy controls. We performed 16S sequencing of the skin microbiome and plasma metabolomic analysis. Our results revealed alterations in the skin microbiota in psoriasis patients, including the accumulation of species of *Gammaproteobacteria*. Functional prediction revealed changes in metabolic pathways. In addition, our metabolomic data showed very obvious changes in systemic metabolism in psoriasis patients. Furthermore, we established a novel correlation map of the skin microbiome and plasma metabolites. These results highlighted the role of the skin microbiome in regulating global metabolism and provided new insights regarding the pathological view of psoriasis.

## MATERIALS AND METHODS

### Patient Information

A total of 32 patients diagnosed with severe plaque psoriasis were recruited at the General Hospital of Ningxia Medical University (Ningxia Province, China) for this study from December 2018 to May 2019. At the same time, 29 healthy volunteers were recruited. The average age of the patients was 38.16 years, with a range of 17–74 years. For healthy

controls, the average age was 35.53 years, with a range of 23–54 years. The severity of psoriasis was quantified by using the Psoriasis Area and Severity Index (PASI) score ( $38.96 \pm 2.64$ , mean  $\pm$  SE), the Psoriasis Global Assessment score ( $4.41 \pm 0.13$ , mean  $\pm$  SE), and the body surface area score ( $24.85 \pm 2.82$ , mean  $\pm$  SE). Patients who met the following criteria at the same time were included: patients with severe plaque psoriasis (PASI score  $\geq 12$ ) (Mrowietz et al., 2011), patients with at least half a year of disease duration, and patients who had previously received at least one course of systemic treatment without obvious improvement. The exclusion criteria were as follows: volunteers with severe liver or kidney damage, mental illness, hematopoietic dysfunction, or other serious organic disease; patients who received immunosuppressive treatment or high doses of glucocorticoids or retinoid treatment in the previous 2 months; and all participants, including healthy controls and psoriasis patients, who had used any skin care product or lotion in the previous week. None of the healthy volunteers had a history of any immune diseases, and none of them had any skin disorders. All samples and clinical information were obtained under the condition of informed consent. This study was conducted with the approval of the institutional review board of the General Hospital of Ningxia Medical University and in accordance with the Declaration of Helsinki.

### Sample Collection

Skin microbiome samples were collected according to a previous report (Oh et al., 2014). Briefly, a swab was rinsed with phosphate-buffered saline, and a defined skin area of approximately  $2 \times 2 \text{ cm}^2$  was swabbed at least 20 times to maximize the amount of microbiome DNA collected. All samples were stored at  $-80^\circ\text{C}$  until extraction.

The plasma samples were collected on the same day after overnight fasting with a heparin sodium anticoagulant tube. The samples were then centrifuged at 3,000 rpm for 10 min at room temperature. The supernatants were collected and aliquoted into different tubes and stored at  $-80^\circ\text{C}$ .

### Microbiome DNA Extraction and 16S Sequencing

Genomic DNA from skin microbiome samples was extracted by using the Mobio Powersoil DNA Isolation Kit (Qiagen, Hilden, Germany) according to the manufacturer's instructions. The V3 and V4 regions of the 16S rRNA genes were amplified by using Phusion® High-Fidelity PCR Master Mix with GC Buffer (New England Biolabs, MA, United States) and the primers 341F and 806R. After purification of the polymerase chain reaction product by using AMPure XP magnetic beads (Beckman Coulter, IN, United States), the samples were analyzed by the Illumina NovaSeq 6000 platform (Illumina, CA, United States) through a paired-end sequencing strategy.

### 16S Sequencing Data Analysis

After Illumina sequencing, barcode and primer sequences were removed. Specific tags were generated by FLASH



software<sup>1</sup> according to the overlap information of the reads. Then, we applied Trimmomatic software (v0.33) to remove the low-quality tags and obtained clean tags. Clean tags were further filtered to exclude the chimeric sequences by using UCHIME software (v4.2). Next, the remaining sequences with an identity >97% were classified as operational taxonomic units (OTUs) by using Uparse software<sup>2</sup>. Taxonomic information was annotated by searching against the SSU rRNA database<sup>3</sup>. OTUs were then assigned to different phylogenetic levels (kingdom, phylum, class, order, family, genus, and species). Alpha diversity and beta diversity were analyzed by QIIME software (v1.9.1) based on the effective tags. The relative abundance and the difference in diversity were compared by Student *t*-test and the Wilcoxon rank-sum test. Furthermore, linear discriminant analysis coupled with effect size (LEfSe) was applied to identify microorganisms that can be used to discriminate psoriasis patients from people with no psoriasis.

## Liquid Chromatography–Mass Spectrometry Metabolomic Data Collection

A 100- $\mu$ L plasma sample from each patient was mixed with 300  $\mu$ L of methanol containing 1  $\mu$ g/mL 2-chloro-L-phenylalanine (Hengbai Biotech, Shanghai, China) as the internal standard. After brief sonication in ice water for 10 min, all the samples were placed at  $-40^{\circ}\text{C}$  for 1 h and centrifuged at 10,000 rpm for 15 min at  $4^{\circ}\text{C}$ . Then, the samples were resuspended in 100  $\mu$ L of 50% acetonitrile. For quality control (QC) sample preparation, a mixture containing an equal volume (10  $\mu$ L) of each plasma extract was prepared.

For liquid chromatography–mass spectrometry (LC-MS) metabolomic data collection, all plasma samples were analyzed by a 1290 UHPLC instrument (Agilent Technologies, CA, United States) coupled with a Thermo Q Exactive Focus (Thermo Fisher Scientific, MA, United States) by Biotree Ltd. (Shanghai, China), according to previously reported methods with minor modifications (He et al., 2020). Briefly, mobile phase A in positive ion mode was 0.1% formic acid in water, and in negative ion mode, it was 5 mmol/L ammonium acetate in water. Mobile phase B was acetonitrile. The elution gradient was set as follows: 1% B at 1 min, 99% B at 8 min, 99% B at 10 min, 1% B at 10.1 min, and 1% B at 12 min. The flow rate was set to 0.5 mL/min. The Q Exactive mass spectrometer was run at a spray voltage of 4.0 kV in positive mode and  $-3.6$  kV in negative mode. Other ESI source conditions were as follows: sheath gas flow rate of 45 Arb, Aux gas flow rate of 15 Arb, and capillary temperature of  $400^{\circ}\text{C}$ . All MS1 and MS2 data were obtained under the control of Xcalibur (Thermo Fisher Scientific). A UPLC HSS T3 column (Waters, MA, United States) was used for all analyses. Organic reagents, including methanol, acetonitrile, and formic

acid (HPLC grade), were purchased from CNW Technologies (Dusseldorf, Germany).

## Gas Chromatography–MS Data Collection

The extracted plasma samples were resuspended in 30  $\mu$ L of methoxyamine hydrochloride (20 mg/mL in pyridine) and incubated at  $80^{\circ}\text{C}$  for 30 min. After derivatization with 40  $\mu$ L of N,O-bis(trimethylsilyl)trifluoroacetamide (BSTFA) with 1% trimethylsilyldiethylamine (Sigma, Darmstadt, Germany) at  $70^{\circ}\text{C}$  for 1.5 h, the samples were cooled down gradually to room temperature. For QC sample preparation, a mixture containing an equal volume (10  $\mu$ L) of each plasma extract was prepared. An additional 5  $\mu$ L of saturated fatty acid methyl esters (Dr. Ehrenstorfer GmbH, Augsburg, Germany) dissolved in chloroform was added to the QC samples for gas chromatography (GC)–MS analysis.

Gas chromatography–time of flight (TOF)–MS analysis was carried out by using an Agilent 7890 gas chromatograph (Agilent Technologies) coupled with a Pegasus HT TOF mass spectrometer (LECO, Michigan, United States). In this analysis, a DB-5MS capillary column (30 m  $\times$  250  $\mu\text{m}$   $\times$  0.25  $\mu\text{m}$ , Agilent Technologies) was used. The carrier gas was helium, the front inlet purge flow was set as 3 mL/min, and the gas flow rate was 1 mL/min. The temperature gradient was set as  $50^{\circ}\text{C}$  for 1 min, increased to  $310^{\circ}\text{C}$  at a rate of  $20^{\circ}\text{C}/\text{min}$ , and then maintained for 6 min. The front injection temperature, transfer line temperature, and ion source temperature were 280, 280, and  $250^{\circ}\text{C}$ , respectively. The energy was  $-70$  eV in electron impact mode. The MS data were acquired in full-scan mode with an *m/z* range of 50–500 at a rate of 12.5 spectra per second after a solvent delay of 4.85 min. A 1- $\mu$ L sample was injected for this analysis.

## LC-MS and GC-MS Metabolomic Data Analyses

ProteoWizard software was used to transform the original LC-MS data to mzXML format. The data were processed by XCMS. GC-MS raw data were processed by Chroma TOF software. After peak identification, peak alignment, peak extraction, retention time (RT) correction, and peak integration, a three-dimensional data matrix was obtained. To make the metabolomics data reproducible and reliable, peaks with relative standard deviations greater than 30% in the QC samples were filtered out. The remaining peaks were identified by comparison of RT and mass to charge ratio (*m/z*) indexes in a library containing spectral information from the online database of HMDB<sup>4</sup>, Kyoto Encyclopedia of Genes and Genomes (KEGG)<sup>5</sup>, and the in-house library. The GC-MS data were matched with the LECO-Fiehn Rtx5 database. Peak intensity was quantified by using the area under the curve. The data matrix was further processed by removing the peaks with missing values in more than 50% of the samples and substituting the remaining missing values

<sup>1</sup><http://ccb.jhu.edu/software/FLASH/>, v1.2.7

<sup>2</sup><http://www.drive5.com/uparse/>, v7.0.1001

<sup>3</sup>[www.Arb-silva.de](http://www.Arb-silva.de)

<sup>4</sup>[www.hmdb.ca](http://www.hmdb.ca)

<sup>5</sup>[www.genome.jp/kegg](http://www.genome.jp/kegg)

with half of the minimum value. Then, a new data matrix was generated by normalizing the data to the peak intensity of the internal standard.

## Statistical Analysis

Statistical analysis was performed by using Microsoft Excel (Microsoft Inc., Redmond, WA, United States) and R software version 3.5.1 (R Foundation for Statistical Computing, Vienna, Austria). The differential abundance of bacterial taxa at different levels (phylum, class, order, family, and genus) between psoriasis patients and healthy controls was calculated by the Wilcoxon rank-sum test and Metastat. The differences in alpha diversity indexes were determined by Student *t*-test. The beta diversity difference between psoriasis patients and the control group was analyzed by analysis of similarity (ANOSIM). To understand the difference in the metabolomic profile between psoriasis patients and healthy people, multivariate statistical analyses, including principal component analysis (PCA) and orthogonal projections to latent structure-discriminant analysis (OPLS-DA), were carried out. Small molecules with a VIP (variable importance in projection) >1 in OPLS-DA and  $p < 0.05$  by Student *t*-test were considered significantly altered metabolites. Spearman correlation was carried out to determine the relationship between the skin microbiota and plasma metabolites.

## RESULTS

### Altered Skin Microbiota Composition in Psoriasis Patients

We recruited 32 severe plaque psoriasis patients (PASI > 12) and 29 healthy controls to identify the psoriasis-related microbiota. After QC, the DNA sample amounts from only 26 patients and 10 controls were sufficient for 16S sequencing.

Overall, we obtained 83,998 effective tags and 7,887 OTUs according to 97% similarity. After taxonomic assignment against the Silva132 database, 7,606 OTUs were annotated at different phylogenetic levels (**Supplementary Table 1**). According to the species accumulation curve, the sequencing data and samples were sufficient for taxon identification. However, there were no significant differences between control individuals and psoriasis patients in terms of number of species on skin (**Supplementary Figure 1A**). In addition, the alpha diversity indexes, including the total observed species, Shannon index, ACE index, Simpson index, and Chao1 index, of the skin of psoriasis patients were not significantly different from those of the control group (**Supplementary Figures 1B–F**). To identify the microbes that were altered in psoriasis patients, we then conducted Student *t* test at the genus level (**Figure 1A**). The average abundance of *Lactobacillus*, which is widely distributed in the human gut and skin and plays a role as a lactic acid producer, was increased in psoriasis patients. This may suggest a potential positive role of *Lactobacillus* in regulating skin cell proliferation, which is consistent with a previous report that *Lactobacillus* was capable of enhancing skin repair after UV damage (Im et al., 2018). Moreover, the abundances of *Thermomonas* and *Luteimonas*, which are pathogenic members of Proteobacteria

(phylum)\_Gammaproteobacteria (class), were also increased, suggesting that the skin of psoriasis patients was a pathogenic environment. To further analyze the alterations in the microbiota in psoriasis patients, we applied Metastat, another widely used statistical analysis tool, to screen for significantly changed organisms (**Figure 1B**). Similarly, the change in the *Lactobacillus* abundance was also identified as an important alteration. In addition, another member of Gammaproteobacteria, *Vibrio*, was identified as being significantly elevated in psoriasis patients. Together, these data suggest an elevation in the abundance of pathogenic bacteria, especially Gammaproteobacteria, in psoriasis patients.

To further examine the alterations associated with psoriasis, we conducted LEfSe analysis. The main differences were the increase in abundance of undefined\_Cyanobacteria (class unidentified\_Cyanobacteria and order Cyanobacteria) in psoriasis patients (**Figure 2A**). Some differences were also observed at a lower taxonomic level. Psoriasis patients showed a loss in the abundance of the genus *Citrobacter* (**Figure 2B**). Taken together, these data indicate alterations in the commensal gut microbiome composition in psoriasis patients, suggesting dysregulation of the microbial community.

### Functional Prediction of the Skin Microbiome of Psoriasis Patients

To further determine the functional impact of skin gut microbiota alterations in psoriasis, we predicted the KEGG pathways based on the 16S sequencing data by using PICRUSt software (Langille et al., 2013). Metabolic pathways ranked as the most abundant pathways predicted, accounting for approximately 50% of the pathways (**Figure 3A**). Among these pathways, carbohydrate metabolism and the metabolism of other amino acids were obviously decreased (**Supplementary Figure 2**). In contrast, pyrimidine and purine metabolism (nucleotide metabolism); glycolysis/gluconeogenesis, oxidative phosphorylation, and methane metabolism (energy metabolism); the metabolism of cofactors and vitamins; and the biosynthesis of other secondary metabolites showed an increase in psoriasis patients compared with healthy controls (**Figure 3B** and **Supplementary Figure 2**).

### Plasma Metabolic Profiling of Psoriasis Patients

Microbiota alterations have been reported to be correlated with tissue metabolism in many studies (Liu et al., 2017; Olson et al., 2018). In addition, our data showed that skin microbiota-mediated small molecule metabolism was impacted by psoriasis (**Figure 3**). We thus investigated the metabolic alterations in psoriasis patients by applying GC and ultrahigh-pressure LC coupled with MS. In general, a total of 3,562 features and 716 metabolites were obtained (**Supplementary Table 2**). PCA showed very obvious separation of metabolic profiles between psoriasis patients and healthy controls, demonstrating different metabolic activities (**Figure 4A**). After statistical analysis, we obtained 117 significantly altered metabolites (VIP >1 and  $p < 0.05$ ) (**Figure 4B**). Among them, we found several

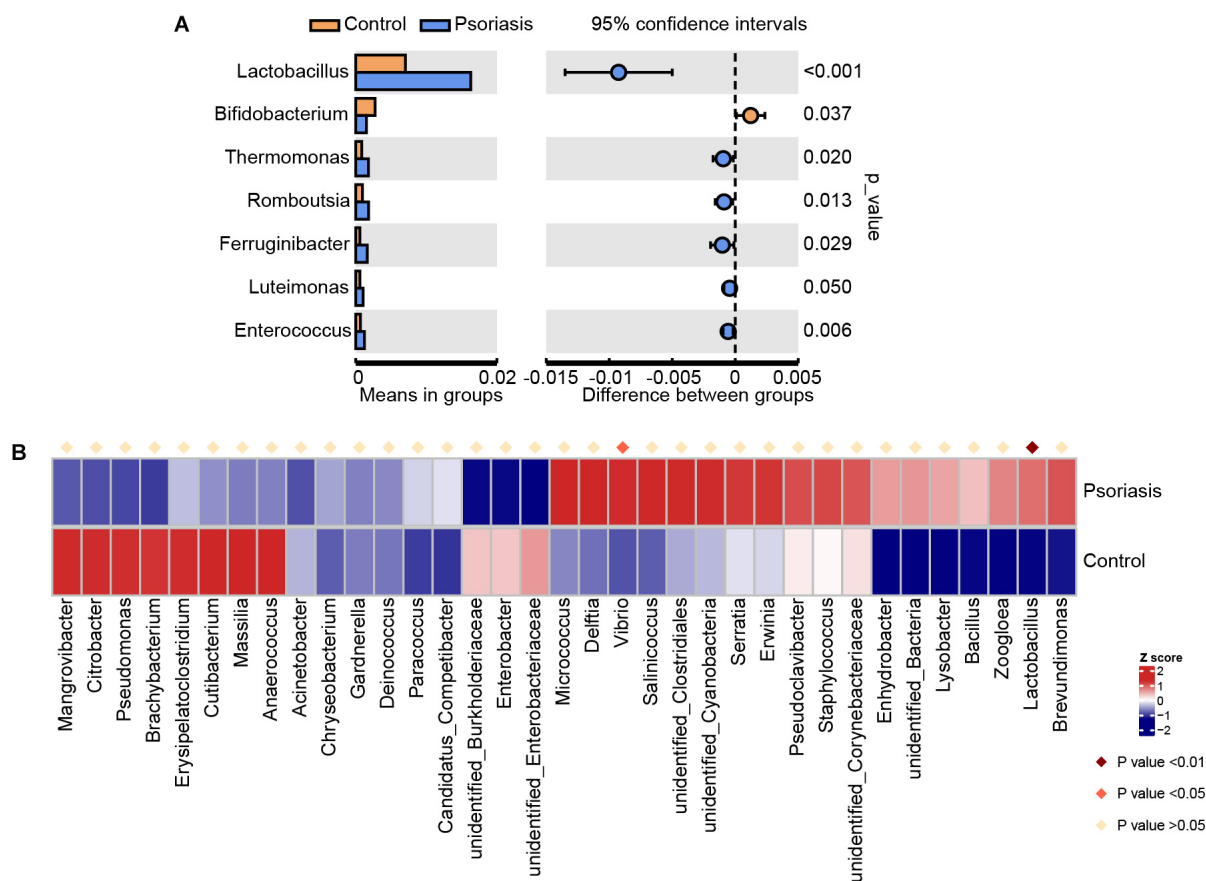


**FIGURE 1 |** Skin microbiota alterations in psoriasis patients. **(A)** Significantly altered skin microbiota in psoriasis patients compared with healthy controls analyzed by Student's *t*-test at the genus level. **(B)** Heatmap shows the significantly altered skin microbiota at the genus level in psoriasis patients compared with healthy controls analyzed by Metastat.

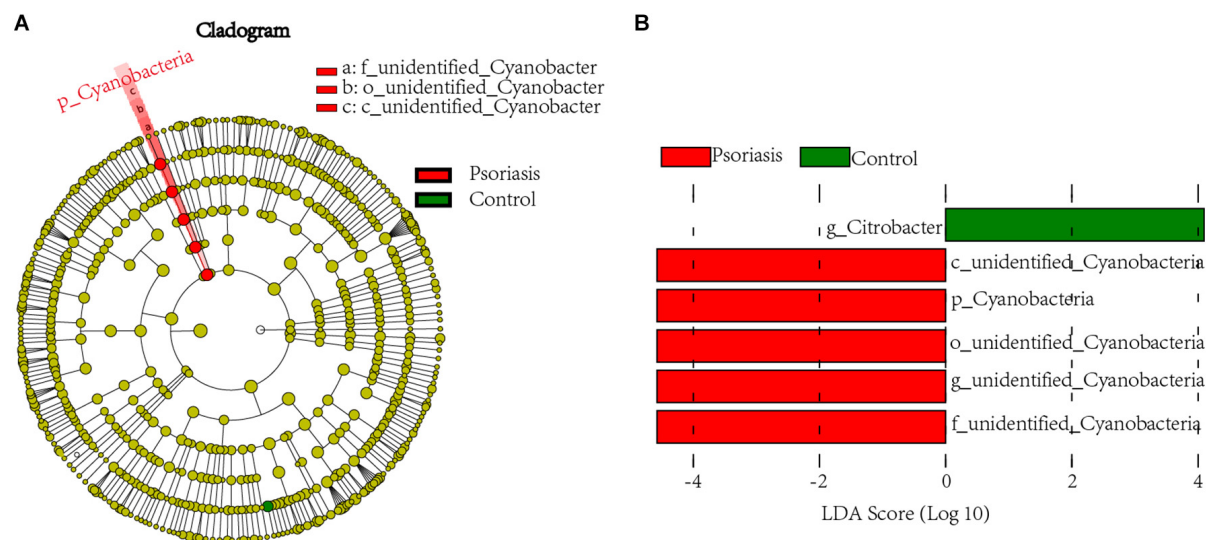
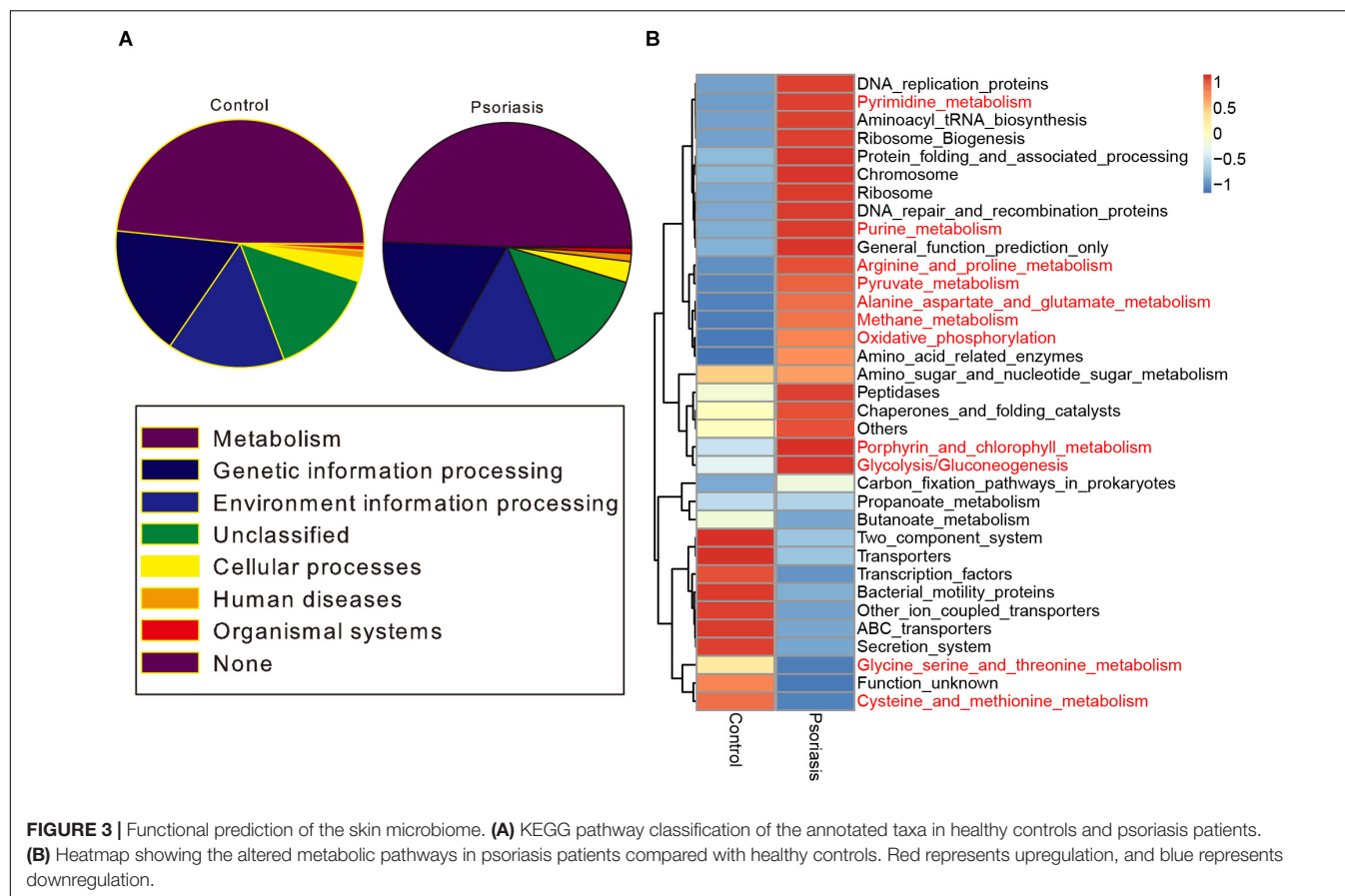


**FIGURE 2 |** Linear discriminant analysis (LDA) effect size. **(A)** Cladogram of LefSe of the skin microbiome from 16S sequencing results. Red and green circles represent the differences of the most abundant microbiome class. The diameter of each circle is proportional to the relative abundance of the taxon. **(B)** Histogram of the LDA scores for differentially abundant microbes in psoriasis patients and healthy controls. Red, enriched in psoriasis patients; green, enriched in healthy controls.



microbiome-generated metabolites that were also significantly changed. These included taurochenodeoxycholic acid (TCDCA), deoxycholic acid glycine conjugate (GDCA), chenodeoxycholic acid glycine conjugate, and L-kynurenine (Chávez-Talavera et al., 2017; Agus et al., 2018; He et al., 2020). To uncover the metabolic pathway alterations, we conducted KEGG pathway analysis of the differentially expressed metabolites by using Metaboanalyst<sup>6</sup> (Figure 4C). Branched-chain amino acid metabolism (valine, leucine, and isoleucine biosynthesis), which was reported to be closely related to microbiota metabolic activity (Liu et al., 2017), was significantly altered. In addition, the metabolism of  $\alpha$ -linolenic acid and linoleic acid, which reflect the inflammation status of tissues (Sergeant et al., 2016), was also significantly altered.

## Novel Interplay Between the Skin Microbiota and Plasma Metabolism

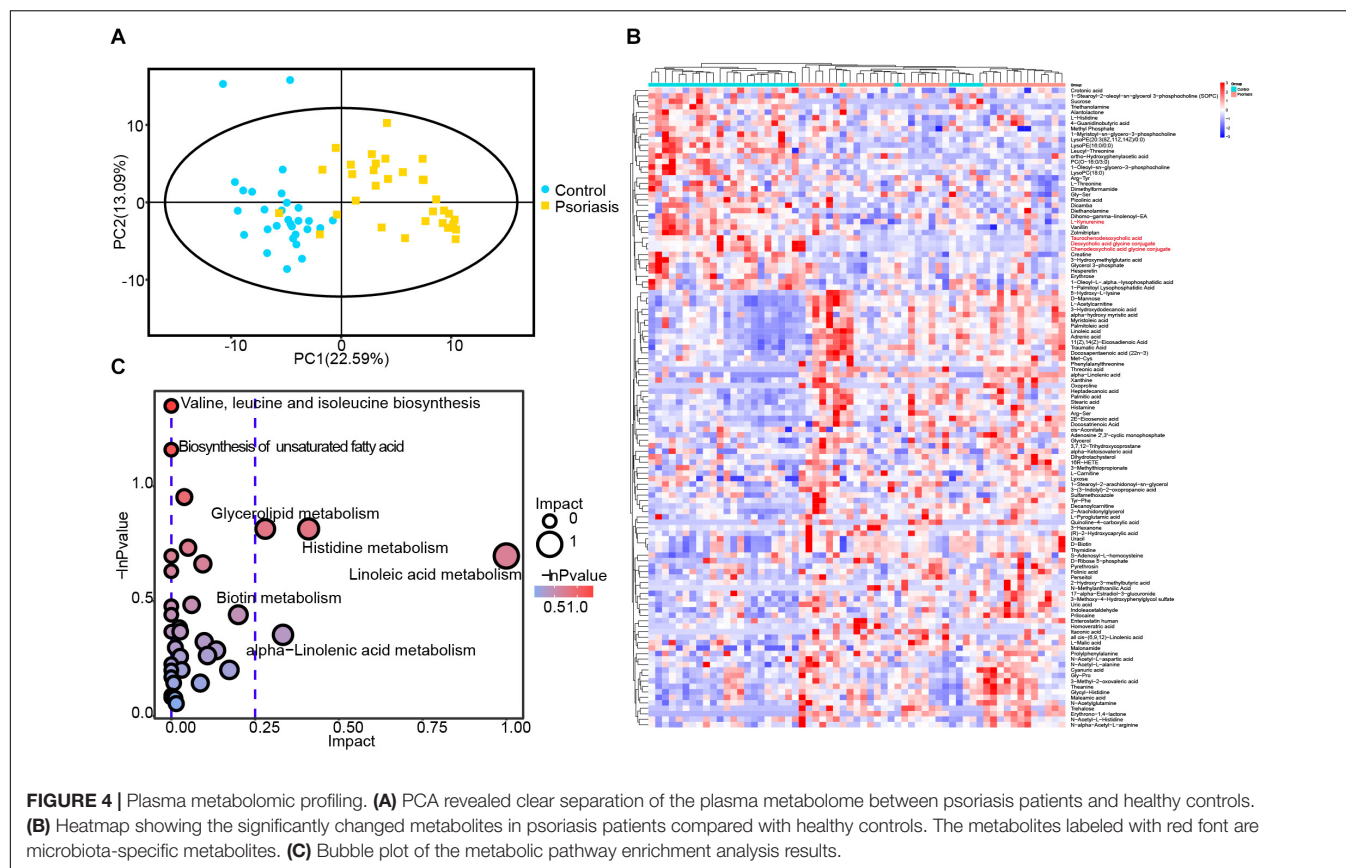
Many articles have reported the correlation of the gut microbiota and blood metabolism (Liu et al., 2017; He et al., 2020), whereas little is known about the relationship of the skin microbiota and blood metabolism. In this study, we carried out Spearman correlation analysis of the annotated skin microbiota at the genus level and the identified plasma metabolites. The association of the skin microbiota and plasma metabolites was different between

healthy controls and psoriasis patients (Figures 5A,B), suggesting that the alteration of plasma metabolites was closely related to the skin microbiome. Interestingly, most of the associations between *Lactobacillus* and plasma metabolites and the associations between *Enterococcus* and plasma metabolites in healthy controls (Figure 5A) disappeared in psoriasis patients (Figure 5B). In addition, new correlations between *Vibrio*, *Ferruginibacter*, *Romboutsia*, and plasma metabolites were established in psoriasis patients (Figure 5B). The metabolites that showed a significant positive association with specific skin bacteria in both healthy controls and psoriasis patients were itaconic acid, crotonic acid, and heptadecanoic acid, which are involved in lipid metabolism (Figures 5A,B). Notably, some plasma metabolites were negatively associated with the skin microbiota in psoriasis patients. In addition to several lipids, xanthine, D-ribose 5-phosphate, and uric acid participate in nucleotide metabolism (Figure 5B). These results suggest a role of the skin microbiota in influencing lipid and nucleotide metabolism in psoriasis patients.

To determine a global relationship between the skin microbiota and plasma metabolism, we then conducted Spearman correlation analysis by using all the samples from healthy controls and systemic lupus erythematosus (SLE) patients. The correlations were shown in a Cytoscape network (Figure 5C), further suggesting a fundamental relationship of the skin microbiota and plasma metabolism. Interestingly, receiver operating characteristic (ROC) curve analysis revealed that many

<sup>6</sup> www.metaboanalyst.ca





skin microbiota-associated plasma metabolites are potential biomarkers for SLE classification (**Supplementary Figure 3**).

## DISCUSSION

Previous studies investigated the changes in the blood metabolome and gut microbiome that occur in psoriasis. However, it is not sufficient to understand the pathogenesis of psoriasis, as the disease primarily occurs on the skin. Here, we analyzed skin microbiota alterations in psoriasis patients by using 16S sequencing and plasma metabolomic changes by applying an LC-MS metabolomics approach. According to our results, the plasma metabolic homeostasis of psoriasis patients was disrupted and was correlated with alterations in the skin microbiome. We further identified some skin microbes at the genus level, such as *Enterococcus* and *Vibrio*, which are critical for plasma metabolism in psoriasis patients. In addition, we also identified some skin microbiota-associated plasma metabolites that are potential biomarkers for strongly discriminating healthy controls from psoriasis patients.

In our untargeted metabolomic study, many plasma metabolites were significantly changed in psoriasis patients. Pathway analysis revealed enrichment in both amino acid metabolism and lipid metabolism pathways (**Figure 4**). The valine, leucine, and isoleucine biosynthesis pathway, which is

a branched-chain amino acid metabolism pathway mediated by the microbiota, has been reported to be related to many diseases (Liu et al., 2017, 2020). In addition, several lipid metabolism pathways were also enriched, including biosynthesis of unsaturated fatty acids, glycerolipid metabolism, linoleic acid metabolism, and  $\alpha$ -linolenic acid metabolism. Glycerolipids that play a very important role in membrane mobility and provide building blocks for membrane biogenesis have also been reported previously as potential diagnostic biomarkers in psoriasis patients (Zeng et al., 2017). Furthermore, the alteration in linoleic acid and  $\alpha$ -linolenic acid metabolism reflects the inflammation status of psoriasis (Boehncke, 2018). In addition, the microbiota-mediated metabolism of bile acids (TCDA, TCDCA, and GDCA) is well known for its role in lipid metabolism, and L-kynurenine is well known for its role in inflammation regulation (Vitek and Haluzik, 2016; Cervenka et al., 2017). Altogether, the metabolomic results indicate the role of the microbiota in the regulation of lipid metabolism and the inflammatory response in psoriasis patients.

Psoriasis is a chronic inflammatory skin disorder. Increasing evidence has suggested the role of the skin microbiome in the pathogenesis of diseases (Grice, 2014; Picardo and Ottaviani, 2014; Li et al., 2019). In our study, some skin microbes were significantly altered in psoriasis patients compared with healthy people, which is consistent with previous research (Chang et al., 2018). Among them, the

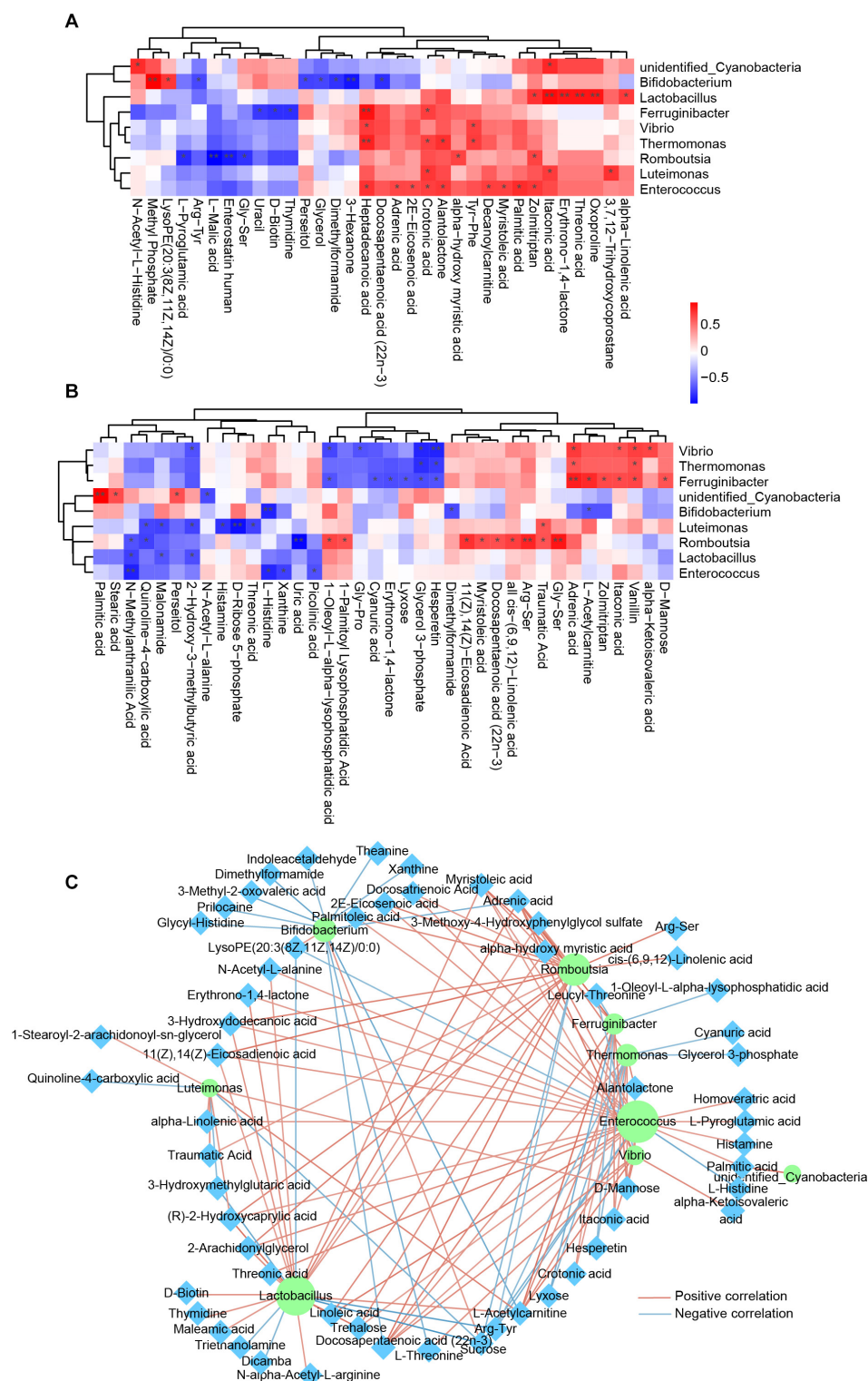


**FIGURE 5 |** Integrated analysis of skin microbes and plasma metabolites. **(A)** Spearman correlation analysis between significantly altered skin microbes and significantly changed plasma metabolites in the healthy control group. Red, positive correlation; blue, negative correlation.  $*p < 0.05$ . **(B)** Spearman correlation analysis between significantly altered skin microbes and significantly changed plasma metabolites in the psoriasis group. Red, positive correlation; blue, negative correlation.  $*p < 0.05$ . **(C)** Spearman correlation network between significantly altered skin microbes and significantly changed plasma metabolites in all samples from both groups. The purple circle represents the skin microbiota, and the cyan diamond represents plasma metabolites. Red line, positive correlation; blue line, negative correlation. Only the correlations with  $p < 0.05$  are shown.  $**p < 0.01$ .

bacteria *Thermomonas* and *Luteimonas* from the pathogenic Proteobacteria (phylum) and Gammaproteobacteria (class) were significantly increased, suggesting the pathological role of these bacteria in psoriasis. *Vibrio*, the most strongly and significantly increased bacterial taxon (**Figure 1B**), is well known for its role as the cholera pathogen (Conner et al., 2016). Because the species of *Vibrio* mainly live in seawater or brackish water (Vasagar et al., 2018), people should be very careful when consuming seafoods or when exposed to seawater. These results indicate that the accumulation of the pathogenic microbiota is a possible reason for the pathogenesis of psoriasis. This conclusion was also confirmed by functional analysis of the skin microbiota. Skin microbiome-mediated nucleotide metabolism and amino acid metabolism activities were elevated in psoriasis patients compared with healthy controls (**Figure 3B**), as small-molecule metabolism pathways are critical for providing building blocks for skin cell proliferation.

The interaction between skin microorganisms and blood metabolism has rarely been investigated. In this article, we analyzed the Spearman correlation of significantly altered skin microbes and significantly changed plasma metabolites (**Figure 5**). The results highlighted the role of the skin microbiota in the regulation of plasma metabolism, especially the role of the pathogens *Enterococcus* and *Vibrio*. These data also suggest the role of the skin microbiome in skin homeostasis, which is critical for the maintenance of the immunological barrier of skin (Belkaid and Tamoutounour, 2016).

In summary, our study integrating skin microbiome 16S sequencing and plasma metabolomic data reveals alterations in global metabolic homeostasis status and the association of the skin microbiota with psoriasis. Considering the impact of many factors, including race, ethnicity, lifestyle, and environmental factors, on the skin microbiome and global metabolome, more studies are needed to address the role of the skin microbiome in the pathogenesis of psoriasis. In addition, additional studies are needed to understand the key skin microbes involved in the pathogenesis of psoriasis, especially through an effect on global metabolism. Our data provide the underlying mechanism of skin microbiome-mediated regulation of blood metabolism in patients with psoriasis. The results will be helpful for understanding the pathological mechanism of psoriasis.

## DATA AVAILABILITY STATEMENT

The datasets presented in this study can be found in online repositories. The names of the repository/repositories and accession number(s) can be found below: EBI metagenomics, accession no: PRJEB42803 (ERP126714).

## ETHICS STATEMENT

The studies involving human participants were reviewed and approved by the Institutional Review Board of the General Hospital of Ningxia Medical University. Written informed

consent to participate in this study was provided by the participants' legal guardian/next of kin.

## AUTHOR CONTRIBUTIONS

HS designed and supervised the study and edited the manuscript. HS, JL, QZ, JS, YG, JY, CL, and FW collected the clinical samples and determined the clinical measurement indexes. HS and QZ analyzed the clinical indicators. DC, JH, TC, and HS performed the metabolomic, 16S sequencing and bioinformatic analyses. HS, JH, and DC interpreted the data and wrote the manuscript. All authors contributed to the article and approved the submitted version.

## FUNDING

This work was supported by grants from the Ningxia Autonomous Region Key R&D Program (Special Project for Foreign Scientific and Technological Cooperation) (No. 2019BFG02008 to HS) and the Construction of Talent Platform Project of Ningxia (Innovation Team for Skin Disease Diagnosis and Treatment Technology & Drug Discovery and Development) (No. NXXJT2019012 to HS).

## ACKNOWLEDGMENTS

We thank all the volunteers who participated in this study. We also thank Shanghai Biotree Biomedical Biotechnology Co., Ltd., for metabolomic and 16S sequencing data acquisition and data analysis.

## SUPPLEMENTARY MATERIAL

The Supplementary Material for this article can be found online at: <https://www.frontiersin.org/articles/10.3389/fmicb.2021.643449/full#supplementary-material>

**Supplementary Figure 1** | Alpha diversity indexes of the skin microbiome in psoriasis patients and healthy controls. **(A)** Curve of accumulated species number in psoriasis patients and healthy controls. **(B–F)** Alpha diversity indexes, including observed species **(B)**, ACE index **(C)**, Shannon index **(D)**, Simpson index **(E)**, and Chao1 index **(F)**, in psoriasis patients and healthy controls.

**Supplementary Figure 2** | Predicted function of the skin microbiome in level 2. The function of the skin microbiome from healthy controls and psoriasis patients was predicted and plotted. Red represents increased pathway annotation. Blue indicates reduced pathway annotation. Metabolic pathways are labeled with red font.

**Supplementary Figure 3** | ROC curve of the metabolites significantly associated with the skin microbiota. Biomarker analysis of the metabolites significantly correlated with the skin microbiota in **Figure 5** shows the high AUCs. Only the metabolites with AUC value >0.8 are shown.

**Supplementary Table 1** | The relative abundance of the annotated skin microbiota measured by 16S sequencing.

**Supplementary Table 2** | The relative abundance of the identified plasma metabolites measured by the LC-MS metabolomic approach.

## REFERENCES

- Agus, A., Planchais, J., and Sokol, H. (2018). Gut microbiota regulation of tryptophan metabolism in health and disease. *Cell Host Microbe* 23, 716–724. doi: 10.1016/j.chom.2018.05.003
- Belkaid, Y., and Tamoutounour, S. (2016). The influence of skin microorganisms on cutaneous immunity. *Nat. Rev. Immunol.* 16, 353–366. doi: 10.1038/nri.2016.48
- Boehncke, W. H. (2018). Systemic inflammation and cardiovascular comorbidity in psoriasis patients: causes and consequences. *Front. Immunol.* 9:579. doi: 10.3389/fimmu.2018.00579
- Boehncke, W. H., and Schön, M. P. (2015). Psoriasis. *Lancet* 386, 983–994. doi: 10.1016/S0140-6736(14)61909-7
- Byrd, A. L., Belkaid, Y., and Segre, J. A. (2018). The human skin microbiome. *Nat. Rev. Microbiol.* 16, 143–155. doi: 10.1038/nrmicro.2017.157
- Cervenka, I., Agudelo, L. Z., and Ruas, J. L. (2017). Kynurenines: tryptophan's metabolites in exercise, inflammation, and mental health. *Science* 357:eaaf9794. doi: 10.1126/science.aaf9794
- Chang, H. W., Yan, D., Singh, R., Liu, J., Lu, X., Ucmak, D., et al. (2018). Alteration of the cutaneous microbiome in psoriasis and potential role in Th17 polarization. *Microbiome* 6:154. doi: 10.1186/s40168-018-0533-1
- Chávez-Talavera, O., Tailleux, A., Lefebvre, P., and Staels, B. (2017). Bile acid control of metabolism and inflammation in obesity, type 2 diabetes, dyslipidemia, and nonalcoholic fatty liver disease. *Gastroenterology* 152, 1679.e3–1694.e3. doi: 10.1053/j.gastro.2017.01.055
- Conner, J. G., Teschler, J. K., Jones, C. J., and Yildiz, F. H. (2016). Staying alive: *Vibrio cholerae*'s cycle of environmental survival, transmission, and dissemination. *Microbiol. Spectr.* 4:10.1128/microbiolspec.VMBF-0015-2015. doi: 10.1128/microbiolspec.VMBF-0015-2015
- Dréno, B., Araviiskaia, E., Berardesca, E., Gontijo, G., Sanchez Viera, M., Xiang, L. F., et al. (2016). Microbiome in healthy skin, update for dermatologists. *J. Eur. Acad. Dermatol. Venereol.* 30, 2038–2047. doi: 10.1111/jdv.13965
- Dubertret, L., Mrowietz, U., Ranki, A., van de Kerkhof, P. C., Chimenti, S., Lotti, T., et al. (2006). European patient perspectives on the impact of psoriasis: the EUPOS patient membership survey. *Br. J. Dermatol.* 155, 729–736. doi: 10.1111/j.1365-2133.2006.07405.x
- Gisondi, P., Fostini, A. C., Fossà, I., Girolomoni, G., and Targher, G. (2018). Psoriasis and the metabolic syndrome. *Clin. Dermatol.* 36, 21–28. doi: 10.1016/j.clindermatol.2017.09.005
- Grice, E. A. (2014). The skin microbiome: potential for novel diagnostic and therapeutic approaches to cutaneous disease. *Semin. Cutan. Med. Surg.* 33, 98–103. doi: 10.12788/j.sder.0087
- He, J., Chan, T., Hong, X., Zheng, F., Zhu, C., Yin, L., et al. (2020). Microbiome and metabolome analyses reveal the disruption of lipid metabolism in systemic lupus erythematosus. *Front. Immunol.* 11:1703. doi: 10.3389/fimmu.2020.01703
- Im, A. R., Lee, B., Kang, D. J., and Chae, S. (2018). Skin moisturizing and antiphotodamage effects of tyndallized *Lactobacillus acidophilus* IDCC 3302. *J. Med. Food* 21, 1016–1023. doi: 10.1089/jmf.2017.4100
- Langille, M. G., Zaneveld, J., Caporaso, J. G., McDonald, D., Knights, D., Reyes, J. A., et al. (2013). Predictive functional profiling of microbial communities using 16S rRNA marker gene sequences. *Nat. Biotechnol.* 31, 814–821. doi: 10.1038/nbt.2676
- Li, C. X., You, Z. X., Lin, Y. X., Liu, H. Y., and Su, J. (2019). Skin microbiome differences relate to the grade of acne vulgaris. *J. Dermatol.* 46, 787–790. doi: 10.1111/1346-8138.14952
- Liu, R., Hong, J., Xu, X., Feng, Q., Zhang, D., Gu, Y., et al. (2017). Gut microbiome and serum metabolome alterations in obesity and after weight-loss intervention. *Nat. Med.* 23, 859–868. doi: 10.1038/nm.4358
- Liu, Y., Wang, Y., Ni, Y., Cheung, C. K. Y., Lam, K. S. L., Wang, Y., et al. (2020). Gut microbiome fermentation determines the efficacy of exercise for diabetes prevention. *Cell Metab.* 31, 77.e5–91.e5. doi: 10.1016/j.cmet.2019.11.001
- Luo, Y., Hara, T., Kawashima, A., Ishido, Y., Suzuki, S., Ishii, N., et al. (2020). Pathological role of excessive DNA as a trigger of keratinocyte proliferation in psoriasis. *Clin. Exp. Immunol.* 202, 1–10. doi: 10.1111/cei.13455
- Mrowietz, U., Kragballe, K., Reich, K., Spuls, P., Griffiths, C. E., Nast, A., et al. (2011). Definition of treatment goals for moderate to severe psoriasis: a European consensus. *Arch. Dermatol. Res.* 303, 1–10. doi: 10.1007/s00403-010-1080-1
- Myers, B., Brownstone, N., Reddy, V., Chan, S., Thibodeaux, Q., Truong, A., et al. (2019). The gut microbiome in psoriasis and psoriatic arthritis. *Best Pract. Res. Clin. Rheumatol.* 33:101494. doi: 10.1016/j.berh.2020.101494
- Nestle, F. O., Kaplan, D. H., and Barker, J. (2009). Psoriasis. *N. Engl. J. Med.* 361, 496–509. doi: 10.1056/NEJMra0804595
- Oh, J., Byrd, A. L., Deming, C., Conlan, S., Kong, H. H., and Segre, J. A. (2014). Biogeography and individuality shape function in the human skin metagenome. *Nature* 514, 59–64. doi: 10.1038/nature13786
- Olson, C. A., Vuong, H. E., Yano, J. M., Liang, Q. Y., Nusbaum, D. J., and Hsiao, E. Y. (2018). The gut microbiota mediates the anti-seizure effects of the ketogenic diet. *Cell* 173, 1728.e13–1741.e13. doi: 10.1016/j.cell.2018.04.027
- Picardo, M., and Ottaviani, M. (2014). Skin microbiome and skin disease: the example of rosacea. *J. Clin. Gastroenterol.* 48(Suppl. 1), S85–S86. doi: 10.1097/MCG.0000000000000241
- Pohla, L., Ottas, A., Kaldvee, B., Abram, K., Soomets, U., Zilmer, M., et al. (2020). Hyperproliferation is the main driver of metabolomic changes in psoriasis lesional skin. *Sci. Rep.* 10:3081. doi: 10.1038/s41598-020-59996-z
- Sergeant, S., Rahbar, E., and Chilton, F. H. (2016). Gamma-linolenic acid, Dihomo-gamma linolenic, Eicosanoids and Inflammatory Processes. *Eur. J. Pharmacol.* 785, 77–86. doi: 10.1016/j.ejphar.2016.04.020
- Thio, H. B. (2018). The microbiome in psoriasis and psoriatic arthritis: the skin perspective. *J. Rheumatol. Suppl.* 94, 30–31.
- Vasagar, B., Jain, V., Germinario, A., Watson, H. J., Ouzts, M., Presutti, R. J., et al. (2018). Approach to aquatic skin infections. *Prim Care* 45, 555–566. doi: 10.1016/j.pop.2018.05.010
- Vitek, L., and Haluzik, M. (2016). The role of bile acids in metabolic regulation. *J. Endocrinol.* 228, R85–R96. doi: 10.1530/JOE-15-0469
- Wolters, M. (2005). Diet and psoriasis: experimental data and clinical evidence. *Br. J. Dermatol.* 153, 706–714. doi: 10.1111/j.1365-2133.2005.06781.x
- Zeeuwen, P. L., Kleerebezem, M., Timmerman, H. M., and Schalkwijk, J. (2013). Microbiome and skin diseases. *Curr. Opin. Allergy Clin. Immunol.* 13, 514–520. doi: 10.1097/ACI.0b013e328364ebeb
- Zeng, C., Wen, B., Hou, G., Lei, L., Mei, Z., Jia, X., et al. (2017). Lipidomics profiling reveals the role of glycerophospholipid metabolism in psoriasis. *Gigascience* 6, 1–11. doi: 10.1093/gigascience/gix087
- Zhu, J., and Thompson, C. B. (2019). Metabolic regulation of cell growth and proliferation. *Nat. Rev. Mol. Cell Biol.* 20, 436–450. doi: 10.1038/s41580-019-0123-5

**Conflict of Interest:** JH and TC are employed by the company Shanghai Biotree Biomedical Biotechnology co., LTD.

The remaining authors declare that this study was conducted in the absence of any commercial or financial relationships.

Copyright © 2021 Chen, He, Li, Zou, Si, Guo, Yu, Li, Wang, Chan and Shi. This is an open-access article distributed under the terms of the Creative Commons Attribution License (CC BY). The use, distribution or reproduction in other forums is permitted, provided the original author(s) and the copyright owner(s) are credited and that the original publication in this journal is cited, in accordance with accepted academic practice. No use, distribution or reproduction is permitted which does not comply with these terms.





# Surface Topography, Bacterial Carrying Capacity, and the Prospect of Microbiome Manipulation in the Sea Anemone Coral Model *Aiptasia*

Rúben M. Costa<sup>1</sup>, Anny Cárdenas<sup>2</sup>, Céline Loussert-Fonta<sup>3</sup>, Gaëlle Toullec<sup>3</sup>, Anders Meibom<sup>3,4</sup> and Christian R. Voolstra<sup>1,2\*</sup>

<sup>1</sup> Division of Biological and Environmental Science and Engineering, Red Sea Research Center, King Abdullah University of Science and Technology, Thuwal, Saudi Arabia, <sup>2</sup> Department of Biology, University of Konstanz, Konstanz, Germany, <sup>3</sup> Laboratory for Biological Geochemistry, School of Architecture, Civil and Environmental Engineering, École Polytechnique Fédérale de Lausanne, Lausanne, Switzerland, <sup>4</sup> Center for Advanced Surface Analysis, Institute of Earth Sciences, University of Lausanne, Lausanne, Switzerland

## OPEN ACCESS

### Edited by:

Aram Mikaelyan,  
North Carolina State University,  
United States

### Reviewed by:

Brittany Leigh,  
Vanderbilt University, United States  
Elizabeth Hambleton,  
University of Vienna, Austria

### \*Correspondence:

Christian R. Voolstra  
chris.voolstra@gmail.com

### Specialty section:

This article was submitted to  
Microbial Symbioses,  
a section of the journal  
Frontiers in Microbiology

**Received:** 04 December 2020

**Accepted:** 19 February 2021

**Published:** 08 April 2021

### Citation:

Costa RM, Cárdenas A, Loussert-Fonta C, Toullec G, Meibom A and Voolstra CR (2021) Surface Topography, Bacterial Carrying Capacity, and the Prospect of Microbiome Manipulation in the Sea Anemone Coral Model *Aiptasia*. *Front. Microbiol.* 12:637834. doi: 10.3389/fmicb.2021.637834

*Aiptasia* is an emerging model organism to study cnidarian symbioses due to its taxonomic relatedness to other anthozoans such as stony corals and similarities of its microalgal and bacterial partners, complementing the existing *Hydra* (Hydrozoa) and *Nematostella* (Anthozoa) model systems. Despite the availability of studies characterizing the microbiomes of several natural *Aiptasia* populations and laboratory strains, knowledge on basic information, such as surface topography, bacterial carrying capacity, or the prospect of microbiome manipulation is lacking. Here we address these knowledge gaps. Our results show that the surface topographies of the model hydrozoan *Hydra* and anthozoans differ substantially, whereas the ultrastructural surface architecture of *Aiptasia* and stony corals is highly similar. Further, we determined a bacterial carrying capacity of  $\sim 10^4$  and  $\sim 10^5$  bacteria (i.e., colony forming units, CFUs) per polyp for aposymbiotic and symbiotic *Aiptasia* anemones, respectively, suggesting that the symbiotic status changes bacterial association/density. Microbiome transplants from *Acropora humilis* and *Porites* sp. to gnotobiotic *Aiptasia* showed that only a few foreign bacterial taxa were effective colonizers. Our results shed light on the putative difficulties of transplanting microbiomes between cnidarians in a manner that consistently changes microbial host association at large. At the same time, our study provides an avenue to identify bacterial taxa that exhibit broad ability to colonize different hosts as a starting point for cross-species microbiome manipulation. Our work is relevant in the context of microbial therapy (probiotics) and microbiome manipulation in corals and answers to the need of having cnidarian model systems to test the function of bacteria and their effect on holobiont biology. Taken together, we provide important foundation data to extend *Aiptasia* as a coral model for bacterial functional studies.

**Keywords:** coral model system, *Exaiptasia diaphana*, metaorganism, holobiont, microbiome, symbiosis, gnotobiotic, axenic

## INTRODUCTION

Corals constitute the foundation species of reef ecosystems that provide a habitat for about a third of all marine life (Fisher et al., 2015), but anthropogenic-driven climate change is now one of the main drivers of coral reef loss (Hughes et al., 2017b, 2018a,b): about half of the Great Barrier Reef corals were lost over the last 30 years (Dietzel et al., 2020) and a 70–99% coral reef decline is projected even under a 1.5–2°C warming, one of the more benign climate change scenarios (Allen et al., 2018). Therefore, it is important to find solutions that can improve coral resilience and mitigate the negative effects of ongoing ocean warming, ocean acidification, and ocean deoxygenation (Allemand and Osborn, 2019; Hughes et al., 2020). Importantly, corals are cnidarian holobionts that consist of the coral animal host, intracellular microalgal symbionts (Symbiodiniaceae), and associated bacteria among many other organisms that all contribute to the stress tolerance and resilience of this metaorganism (Rohwer et al., 2002; Rosenberg et al., 2007; Bang et al., 2018; LaJeunesse et al., 2018; Pogoreutz et al., 2020; Voolstra and Ziegler, 2020). Besides the broad importance of Symbiodiniaceae, which reside within the coral cells and cover almost the entire energy needs of the coral host through provision of photosynthates (Muscatine, 1990; Trench, 1993), bacteria presumably play important roles in metabolism, immunity, and environmental adaptation of the coral host (Ziegler et al., 2017; Ziegler et al., 2019; Robbins et al., 2019; Voolstra and Ziegler, 2020). However, functional studies that detail the specific contributions of specific microbial taxa are still rare, partially due to methodological limitations (Cooke et al., 2019; Robbins et al., 2019). One suggested avenue to elucidate host-bacteria interactions in cnidarians is the use of model organisms, in particular using gnotobiotic (i.e., bearing few remaining known bacteria) or axenic (i.e., bacteria-/germ-free) host systems that allow controlled exposure or provision of cultured bacterial isolates (Jaspers et al., 2019).

Among Cnidarians, the hydrozoan *Hydra* is one of the few models where a germ-free (axenic) closed life cycle is available, which allows the detailed study of associated bacteria and the functions they contribute to the metaorganism, demonstrating the power of such systems to elucidate host-bacterial interactions (Fraune and Bosch, 2007; Fraune et al., 2009; Fraune et al., 2014; Franzenburg et al., 2013b; Augustin et al., 2017; Wein et al., 2018). Similarly, the anthozoan *Nematostella vectensis* is becoming established as a cnidarian model to study host-bacterial interactions (Har et al., 2015; Domin et al., 2018). However, both systems lack the ability to engage in symbioses with microalgal symbionts of the family Symbiodiniaceae (LaJeunesse et al., 2018). Therefore, they may not comprise an ideal model for corals, since association with Symbiodiniaceae affects bacterial assemblage (Ainsworth et al., 2015; Röthig et al., 2016a; Lawson et al., 2018; Maire et al., 2021). To this end, the sea anemone *Aiptasia* is gaining increasing traction as a coral model due to harboring the same or similar Symbiodiniaceae as scleractinian corals, its simplicity of culturing and clonal propagation, and the fact that *Aiptasia* anemones can be kept indefinitely in symbiotic and aposymbiotic states (i.e., with and without their microalgal partners) (Weis et al., 2008; Voolstra, 2013), allowing to study

the mechanistic underpinnings of the cnidarian-dinoflagellate symbiosis in detail (Baumgarten et al., 2015; Biquand et al., 2017; Czieleski et al., 2018; Räder et al., 2018; Gegner et al., 2019; Simona et al., 2019). Of note, the name *Aiptasia* refers to the colloquial model system name, given that different researchers across the world use different strains, and likely species (Weis et al., 2008; Baumgarten et al., 2015; Oakley et al., 2015; Biquand et al., 2017; Dungan et al., 2020). The current proposed species name is *Exaiptasia diaphana* (Dungan et al., 2020), previously *Exaiptasia pallida* (Grajales and Rodríguez, 2014). Following the notion of *Aiptasia* as a model to study the coral-algal symbiosis (Baumgarten et al., 2015), its suitability as a model to study coral-bacterial interactions was suggested (Röthig et al., 2016a). Studies that describe bacterial association of several wild-type and lab-cultured strains could show that (i) microbial assemblages of lab-cultured *Aiptasia* are comparable, (ii) bacterial associations are somewhat “plastic” pending environmental differences and association with or without algal symbionts, and (iii) an overall similarity in the taxonomic composition of microbiomes of corals and *Aiptasia* (Röthig et al., 2016a; Brown et al., 2017; Herrera et al., 2017; Dungan et al., 2020). However, a detailed examination of the surface ectoderm topography, bacterial carrying capacity, and the prospect of microbiome manipulation (e.g., in the form of microbiome transplants) to highlight similarities to corals and demonstrate the efficacy of the *Aiptasia* system as a tool to study bacterial interactions was missing.

In the current work, our aim was to address these knowledge gaps and provide a foundation for *Aiptasia* to be used as a model for the study of coral-bacterial interactions. To do this, we characterized tissue surface topographies of *Aiptasia* and the *Hydra* and *Nematostella* cnidarian model systems and subsequently compared them to three scleractinian corals, in the context of the surface ectoderm as a bacterial habitat. In addition, we determined the bacterial carrying capacity in symbiotic and aposymbiotic *Aiptasia* anemones as a frame of comparison to reef-building corals and to provide a scale of reference for sequencing-based bacterial community studies. Last, using bacteria-depleted sea anemones, we conducted microbiome transplant experiments using coral microbiomes to assess the suitability of this method as a tool to study function of coral-associated bacteria and as a means to assess the ability of changing microbial host association to aid environmental adaptation of coral holobionts.

## MATERIALS AND METHODS

### Animal Rearing

Aposymbiotic and symbiotic *Aiptasia* of the clonal strain CC7 were generated and reared as described previously (Baumgarten et al., 2015) with some modifications. Aposymbiotic animals were generated through repeated 4 h cold-shocks at 4°C and treatment with 50 µM of the photosynthetic inhibitor diuron (Sigma—Aldrich, United States). Aposymbiotic animals were maintained in the dark for >3 years and are routinely inspected by fluorescence microscopy (Leica DMI3000 B) to confirm the absence of Symbiodiniaceae. Symbiotic anemones were generated

by infecting aposymbiotic animals with strain SSB01 (*Breviolum minutum*, former Clade B) (Xiang et al., 2013). Of note, the algal symbiont strain SSB01 is not the native symbiont of Aiptasia CC7 but has been previously used as a stable and characterized Aiptasia host-algal symbiont combination (Röthig et al., 2016a; Wolfowicz et al., 2016; Simona et al., 2019). To obtain symbiotic CC7-SSB01 Aiptasia, individual anemones were exposed to  $10^5$  Symbiodiniaceae cells/ml for 24 h, fed with *Artemia* nauplii after 48 h, and seawater was exchanged thereafter. All Aiptasia anemones were kept in autoclaved natural seawater and reared in 1 L tanks at a 12 h:12 h light:dark cycle at 20–40  $\mu\text{mol photons m}^{-2} \text{ s}^{-1}$  of photosynthetically active radiation at 25°C in an I-36LLVL incubator (Percival Scientific Inc., United States). *Nematostella vectensis* polyps were reared in half liter tanks in half strength artificial seawater at room temperature. Polyps of *Hydra magnipapillata* strain 105 were reared in half liter tanks in commercial spring water at room temperature. *Nematostella* and *Hydra* animals were fed *Artemia* nauplii twice a week.

## Ectoderm Surface Analysis Using Electron Microscopy

We compared ectoderm surface topography of different cnidarian classes, namely Anthozoa (corals, Aiptasia, *Nematostella vectensis*) with Hydrozoa (*Hydra magnipapillata*), using Scanning Electron Microscopy (SEM). Coral colony fragments of *Stylophora pistillata*, *Acropora humilis*, and *Porites* sp. were collected from the central Red Sea at 6 m depth at the Al Fahal forereef (22°15.100'N, 38°57.386'E) by SCUBA and maintained in an open water aquaria system until use (CMOR, KAUST), whereas Aiptasia, *N. vectensis*, and *H. magnipapillata* animals were available from cultured lab strains. Three fragments (in the case of corals) or three polyps (in the case of Aiptasia, *Nematostella*, *Hydra*) were transferred to 24-well plates for processing. Coral fragments and model system cnidarians were left to expand in ~2% magnesium chloride in artificial seawater (ASW) or fresh water for *Hydra*, or half strength ASW for *Nematostella* for 15 min, respectively. After that, specimens were fixed in ~2.5% glutaraldehyde in 0.1 M cacodylate buffer at 4°C overnight. Samples were then washed in 0.1 M cacodylate buffer (pH 7.2–7.4) thrice for 15 min each and post fixed in 1% osmium tetroxide solution in 0.1 M cacodylate buffer for 1 h in the dark. Samples were further washed thrice in ddH<sub>2</sub>O for 15 min each and proceeded for dehydration in an EtOH gradient: 30, 50, 70, 90, and 100%, 15 min each step, with two final incubations in 100% EtOH, also for 15 min. The drying process was initiated by transferring the samples to a 1:2 solution of hexamethyldisilazane (HMDS):100% EtOH (v/v) for 20 min, then to a fresh solution of 2:1 HMDS:100% EtOH for 20 min, 100% HMDS for 20 min, and a final incubation in 100% HMDS. Samples were left to dry loosely covered in the chemical hood for the HMDS to slowly evaporate overnight. Each fragment was then mounted on an SEM specimen mount head pin and sputter coated with 4 nm of platinum/palladium or Iridium. All samples were imaged using a Teneo Volume Scope electron microscope (FEI, United States) operating at 1–3 kV.

Complementary to the SEM analyses, we imaged Aiptasia specimens by Transmission Electron Microscopy (TEM). Briefly, Aiptasia polyps were fixed in 2.5% glutaraldehyde in 0.1 M cacodylate buffer (pH 7.4) for 12 h at 4°C and post fixed with 1% osmium tetroxide in 0.1 M cacodylate buffer for 1 h in the dark at 4°C. After three washes in ddH<sub>2</sub>O, the sample blocks were dehydrated through EtOH and acetone, infiltrated with a mixture of epoxy resin (Electron Microscopy Sciences, United States) and acetone, followed by a final embedding in pure resin. A Leica EM UC6 Ultramicrotome (Leica Microsystems, Germany) was used to cut 150 nm thin sections from the resin block. Finally, thin sections were collected on a 200 mesh copper grid, stained with 1% uranyl acetate (Electron Microscopy Sciences, United States) and Reynold's lead citrate (Electron Microscopy Sciences, United States). Images were acquired using a Titan CT transmission electron microscope (Thermo Fisher Scientific, United States) operating at 300 kV.

To investigate the presence of bacteria inside the mucus layer using TEM, we modified the standard resin embedding protocol by introducing an agarose embedding step with subsequent cryosectioning of the specimens. Aiptasia anemones were prepared as follows: Individual polyps were chemically fixed in phosphate buffer (0.1 M pH 7.4) with 9% sucrose, containing 4% formaldehyde and 2.5% glutaraldehyde. Fixation was done at room temperature for 2 h after which samples were embedded in 4% aqueous agarose to ease the manipulation. Then, polyps were cut into ~4 mm<sup>3</sup> pieces and post stained in 2% osmium aqueous solution for 1 h in the dark. After rinsing in water, samples were dehydrated in a series of ethanol concentrations, ranging from 10 to 100%, then infiltrated with EPON resin (Electron Microscopy Sciences, United States), before polymerization at 60°C for 48 h. Thin sections of 80 nm were cut and mounted onto a Formvar film-coated, carbon-stabilized 100 mesh copper finder grid (Electron Microscopy Sciences, United States). Sections were post stained with UranylLess (Electron Microscopy Sciences, United States) and lead citrate (Electron Microscopy Sciences, United States) before being imaged with a Tecnai-12 transmission electron microscope (Thermo Fisher Scientific, United States) operating at 100 kV with a FEI eagle camera (Thermo Fisher Scientific, United States) using TIA software (Thermo Fisher Scientific, United States). Contrast, brightness, and sharpness of acquired images were adjusted using Adobe Photoshop.

## Generation of Gnotobiotic Aiptasia

Bacteria-depleted Aiptasia polyps were generated using a previously developed protocol consisting of a depletion priming step, followed by an antibiotic treatment, and subsequent recovery from the antibiotic cocktail (Costa et al., 2019). For the depletion priming step, polyps were transferred to 500 ml plastic tanks, reared in 0.22  $\mu\text{m}$  filtered ASW (same light and temperature regime as described above) and fed with sterile decapsulated *Artemia* nauplii for 4 weeks. For the antibiotic treatment, anemones were transferred to petri dishes and washed repeatedly with ASW individually and incubated in antibiotic solution (50  $\mu\text{g/ml}$  of Carbenicillin, Chloramphenicol, Rifampicin, and Nalidixic acid in ASW) for 15 min. Polyps were

then transferred to 24-well tissue culture plates (Corning Costar, United States), one polyp per well, under sterile conditions, and incubated with antibiotic solution for 7 days, with daily media exchange, at a 12 h:12 h light/dark cycle in an incubator (20–40  $\mu\text{mol photons m}^{-2} \text{ s}^{-1}$  of photosynthetically active radiation) at 25°C. After 7 days, anemones were given 24 h for recovery in ASW before microbiome inoculation (see below). Effective bacterial depletion using this protocol was validated using culture-dependent and -independent techniques (Costa et al., 2019): bacterial depletion of treated Aiptasia polyps was confirmed by absence of colony forming units (CFUs) after plating anemone lysates on Marine Agar and subsequent incubation for at least 5 days. In addition, DNA extracted using the DNeasy Blood & Tissue Kit (Qiagen, Germany) from treated Aiptasia anemone lysates were used for PCR amplification of the 16S rRNA gene (95°C for 15 min, followed by 30 cycles of 30 s at 95°C, 90 s at 55°C, and 90 s at 72°C, followed by a final extension for 10 min at 72°C using the 16S universal primer pair 27F-1492R) and subsequent confirmation of absence of a PCR product by means of electrophoresis on an agarose gel.

## Microbial Carrying Capacity

We determined microbial carrying capacity of apo- and symbiotic control Aiptasia polyps (i.e., untreated) as well as of anemones after antibiotic treatment and microbiome transplants. To do this, single polyps from all experimental conditions were placed in 1.5 ml tubes under sterile conditions and 300  $\mu\text{l}$  of ASW were added before the polyps were lysed using a motorized pestle and mortar. Animal lysates and ASW (negative control) were diluted 10-, 100-, and 1000-fold, and 50  $\mu\text{l}$  were plated on Marine Agar (Difco Marine Agar 2216, BD Biosciences, United States) and incubated at 25°C for 24–48 h or 5 days in the case of antibiotic treated anemones, with subsequent counting of bacterial colonies. For statistical analysis, colony counts were log-transformed, normality was tested using the Shapiro–Wilk test, and a one-way ANOVA was conducted. In case of statistical significance, a Dunnett *post hoc* test was conducted. An unpaired *t*-test was used to assess for significant differences between aposymbiotic and symbiotic control conditions. In order to account for putative polyp size differences, CFU counts per polyp were normalized to the host total protein for each polyp, determined using a Micro BCA protein assay kit (Pierce, United States), and the same statistical analysis as above was conducted.

## Microbiome Inocula

Fragments of *Acropora humilis* and *Porites sp.* were collected from the nearshore reef Tahala (22°15.7812'N, 39°3.099'E) (central Red Sea, Saudi Arabia) and processed on the same day. Fragments from three colonies per coral species were collected and combined prior to inoculation (see below). Each coral fragment was placed in a sterile Ziploc bag with 10 ml of ASW, and coral tissue was air blasted off the skeleton using a sterile 1 ml barrier tip inserted to a rubber hose connected to a bench air-pressure outlet. The slurry obtained from fragments from a given coral species were combined and transferred to a 50 ml polypropylene tube and the volume was adjusted to 50 ml

with ASW to reduce viscosity. The slurry was homogenized for 30 s using an Ultra Turrax T18 homogenizer (IKA, Germany) and split in 25 ml preparations per tube. Control inocula were prepared using between 10 and 15 apo- and symbiotic Aiptasia polyps, respectively, in 30 ml of ASW, homogenized as described above, and homogenized a second time with a MicroDisTec homogenizer 125 (Thermo Fisher Scientific, United States) to ensure complete maceration. The final volume of the lysate was adjusted to 50 ml with ASW and split in 25 ml preparations.

Microbiome inocula were further processed in a biosafety cabinet, using sterile work practices. Lysates were centrifuged using a swing-bucket rotor at 500 *g* for 5 min to pellet zooxanthellae. The supernatant was collected and an aliquot was taken for visual inspection on an inverted epifluorescence microscope. All lysates were centrifuged once, except for the *Porites sp.* inoculum, which had one extra centrifugation step to completely remove visible traces of the zooxanthellae. The supernatants were pooled for each inoculum type and centrifuged at 3220 *g* for 30 min to pellet bacteria. The resulting pellet was resuspended in 25 ml of ASW and centrifuged twice. Pellets were resuspended in 15 ml of ASW and a 1 ml aliquot was set aside for quantification of bacteria.

Bacteria were quantified using BacLight Red Bacterial stain (Thermo Fisher Scientific, United States). Aliquots from each inoculum were stained using 1  $\mu\text{M}$  of dye for 10 min and counted using a BD FACSCanto II flow cytometer (BD Biosciences, United States). Gates for bacterial counts were first defined using 1  $\mu\text{m}$  and 2  $\mu\text{m}$  reference beads (Thermo Fisher Scientific, United States) in forward scatter (FSC) vs. side scatter (SSC) and then by using Aiptasia bacterial cultures stained with BacLight Red and acquired in the PerCP-PI channel. Bacterial numbers were calculated after gravimetric calibration of the flow rates and using the positive events acquired using the defined gating strategy. Based on determined counts, inocula were diluted to  $5 \times 10^5$  bacterial cells/ml and 1 ml was used per polyp. In parallel to the flow cytometry-based bacterial counts, an aliquot of all final inocula was plated on Marine Agar (Difco Marine Agar 2216, BD Biosciences, United States) for CFU counts. Bacterial densities of inocula are provided in **Supplementary Table 1**.

## Microbiome Transplants

For the microbiome transplants, we assessed 30 apo- and symbiotic anemones each across five experimental conditions using six biological replicates (60 anemones in total). Experimental conditions were as follows: (1) untreated control anemones from rearing tanks (APO and SYM), (2) gnotobiotic anemones after 1 day of recovery from antibiotic treatment (APO\_AB and SYM\_AB), (3) *Acropora* microbiome inoculum (APO+ACRinoc and SYM+ACRinoc), (4) *Porites* microbiome inoculum (APO+PORinoc and SYM+PORinoc), (5) Aiptasia microbiome inoculum (APO+APIOinoc and SYM+SYMInoc). Anemones were kept in 24-well plates, 1 polyp per well, and gnotobiotic anemones were inoculated by adding 1 ml of the respective microbiome inoculum to the well (final volume of 1 ml,  $5 \times 10^5$  bacterial cells/ml) and subsequent incubation for 3 days. After that, anemones were washed twice with ASW and



kept in ASW for 4 additional days before being collected (7 days after microbiome transplantation).

## RNA Isolation, cDNA Synthesis, and 16S rRNA Amplicon Sequencing

RNA-based 16S rRNA amplicon sequencing was conducted on five biological replicates from each experimental condition and symbiotic state of the microbiome transplant experiment (see above), in addition to no template DNA extraction and no template PCR negative controls. For RNA isolation, the Qiagen AllPrep DNA/RNA kit (Qiagen, Germany) was used. Briefly, 600  $\mu$ l of RLT Plus buffer were added to 150  $\mu$ l of fresh lysate (or artificial seawater for the negative control) followed by snap freezing of the tubes in liquid nitrogen and storage at  $-80^{\circ}\text{C}$  until extraction, following the manufacturer's instructions. RNA quantity and integrity were determined using Qubit (Thermo Fisher Scientific, United States) and BioAnalyzer (Agilent Technologies, United States), respectively. Total RNA was DNase-treated prior to reverse-transcription using the SuperScript First-Strand Synthesis System (Invitrogen, United States), according to the manufacturer's instructions. For amplification of 16S rRNA amplicons from cDNA, the primers 784F and 1061R (Andersson et al., 2008; Bayer et al., 2013) with MiSeq 16S adapter sequences were used (forward: 5'-TCGTCGGCAGCGTCAGATGTGTATAAGAGACAGAGGATTAGATACCCTGGTA-3'; reverse: 5'-GTCTCGTGGGCTCGGAGATGTGTATAAGAGACAGCRRACGAGCTGACGAC-3'; Illumina overhang adaptor sequences are underlined). PCR reactions were performed in triplicate using the Qiagen Multiplex PCR kit (Qiagen, Germany) with 2  $\mu$ l of cDNA and a primer concentration of 0.5  $\mu$ M in a reaction volume of 20  $\mu$ L. PCRs were performed as follows: 1 cycle at  $95^{\circ}\text{C}$  for 15 min, 27 cycles each at  $95^{\circ}\text{C}$  for 30 s,  $55^{\circ}\text{C}$  for 90 s, and  $72^{\circ}\text{C}$  for 30 s, followed by a final extension step at  $72^{\circ}\text{C}$  for 10 min. Triplicate PCRs for each sample were pooled and cleaned with Illustra ExoProStar (GE Healthcare, United States). Samples were subsequently indexed (eight PCR cycles) using Nextera XT barcode sequencing adapters (Illumina, United States). Indexed PCR products were normalized using Invitrogen SequalPrep normalization plates (Thermo Fisher Scientific, United States) and pooled in equimolar ratios. Pooled samples were checked for the presence of primer dimers on a BioAnalyzer (Agilent Technologies, United States) before sequencing. The library was sequenced at the KAUST Bioscience Core Lab using  $2 \times 300$  bp at 6 pM with 20% phiX on the Illumina MiSeq (version 3 chemistry) according to the manufacturer's specifications.

## 16S rRNA Amplicon Analysis

Sequence reads were demultiplexed and adapters and barcodes were removed. Resulting sequences were then processed using mothur v.1.39.5 (Schloss et al., 2009). Briefly, paired-end sequences were assembled using the "make.contigs" command, subsequently trimmed to exclude sequences  $<200$  bp, and rare sequences (appearing once across the entire sequencing dataset) were removed. The remaining sequences were then aligned to the SILVA database (version 132) using "align.seqs,"

then pre-clustered allowing a 2 nt difference, and finally chimeric sequences were removed using VSEARCH (Rognes et al., 2016). Taxonomical classification was done using the Greengenes (release gg\_13\_5\_99, May 2013) and SILVA (release 138, December 2016) databases. Eukaryotic, archaeal, mitochondrial, and chloroplast sequences were removed prior to OTU clustering using a 97% similarity cutoff. Putative contaminants were determined based on their abundance in negative controls and removed from all samples. An OTU was considered a contaminant if:  $[\sum \text{relative abundance OTU}_i \text{ in negative controls}] / [\sum \text{relative abundance OTU}_i \text{ in all samples}] > 0.1$ . Beta diversity was examined via principal coordinate analysis (PCoA) of Bray-Curtis dissimilarity distances of  $\log_{10}(x + 1)$  OTU abundances (**Supplementary Data 1**) using the *phyloseq* package (McMurdie and Holmes, 2013). A permutational multivariate analysis of variance (PERMANOVA) was carried out using the "adonis" function on dissimilarity Bray-Curtis distances of relative OTU abundances to test for differences between conditions and across symbiotic states. Pairwise PERMANOVA tests were conducted using an R wrapper function for multilevel pairwise comparisons (Martinez Arbizu, 2019). To determine overlap of bacterial taxa across microbiome transplants, we determined OTUs that were present across all samples for a given experimental treatment (i.e., APO, APO+APOinoc, ACR+ACRinoc, APO+PORinoc, SYM, SYM+SYMinoc, SYM+ACRinoc, and SYM+PORinoc) and overlapping taxa were represented using the package *VennDiagram* (Chen and Boutros, 2011).

## RESULTS

### Distinct Ectoderm Surface Topographies Across Cnidarians

We compared surface topographies using scanning electron microscopy (SEM) of three model system cnidarians (*Hydra*, *Nematostella*, and *Aiptasia*) and three coral species (*Stylophora pistillata*, *Acropora humilis*, *Porites* sp.) as a first proxy to determine microbial association (**Figure 1**). The ectodermal epithelium of the hydrozoan *Hydra* was composed of a smooth surface with few cilia (i.e., 5–10  $\mu$ m long hair-like plasma membrane projections, made of microtubules in a  $9 + 2$  ultrastructure arrangement) (**Figure 1A**). By comparison, *Hydra* tentacles showed increased ciliation (and a higher density of villi), coinciding with increased mucus and detritus retention, but also exhibited smooth(er) tissue patches scattered across the tentacles, where some bacteria were found to be attached (**Figure 1B**). The ectodermal epithelium surfaces of column and tentacle of *N. vectensis* and *Aiptasia* were highly similar (**Figures 1C–F**). We observed extensive villi (i.e., smaller, numerous plasma membrane projections, lacking microtubules) coverage in the body column of both polyps, with villi protruding from ectodermal cells ranging between 1 and 2  $\mu$ m in length (**Figures 1C,E**) and bigger cilia ranging from 4 to 6  $\mu$ m in the tentacle region (**Figures 1D,F**). In contrast to *Hydra*, we did not detect any bacteria on the column surface or tentacle regions. This suggests two things: (1) bacteria are rather rare

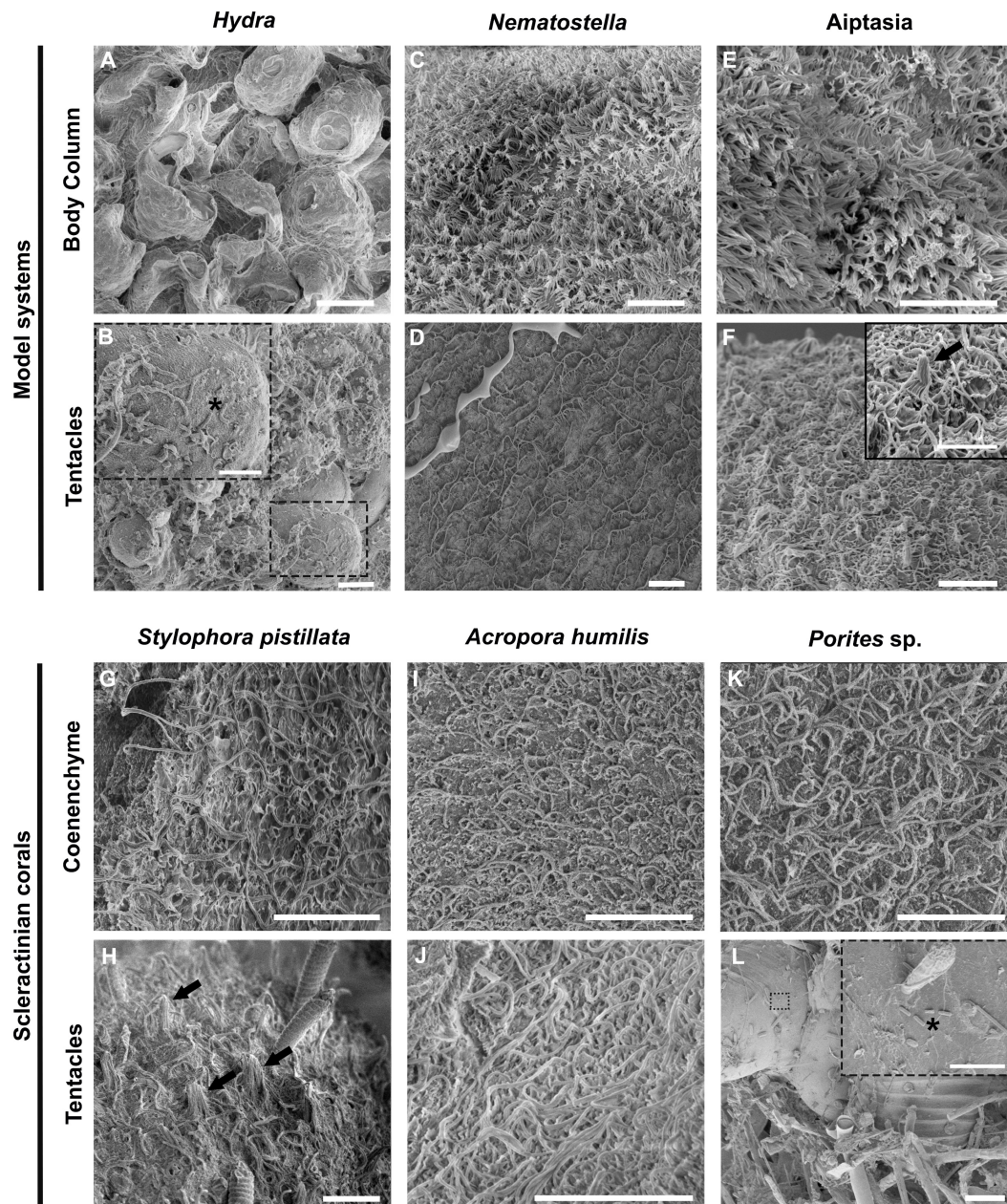


**FIGURE 1 |** Ultrastructural comparison of the surface topography of *Hydra* and Anthozoans. Representative scanning electron microscopy (SEM) images of three model cnidarians (**A–F**) and three reef building corals (**G–L**) show differences between the hydrozoan *Hydra* and anthozoans, but an overall similar topography across anthozoans. (**A,B**) *Hydra* column and tentacle surface topography. (**C,D**) *Nematostella* column and tentacle surface topography. (**E,F**) Aposymbiotic Aiptasia column and tentacle surface topography. (**G,H**) *Stylophora pistillata* coenenchyme and tentacle. (**I,J**) *Acropora humilis* coenenchyme and tentacle. Noticeable are the discharged cnidocytes in the tentacle. (**K,L**) *Porites* sp. coenenchyme and fouled surface topography. Note the presence of microeukaryotes trapped in the fouled region, to which bacteria seem attached. Dashed line boxes denote regions where bacteria can be seen (black asterisks). Black arrows denote mechanoreceptor bundles. Scale bars: (**A–K**): 10  $\mu\text{m}$ ; (**L**): 100  $\mu\text{m}$ ; boxes in (**B,F,L**): 5  $\mu\text{m}$ .

on the surface ectoderm and may be largely constrained to the surface mucus layer in anthozoans, and (2) bacteria may be more abundant on the surface ectoderm in the hydrozoan *Hydra* than in anthozoans. This is corroborated by a complementary TEM analysis of the Aiptasia ectoderm, showing bacteria above the ciliary/villi band, inside the electron dense mucus layer (**Figure 2**

and **Supplementary Figure 1**). The preserved surface mucus layer was estimated around 5–15  $\mu\text{m}$ , extending beyond the villi. Of further note, the surface ectoderms of apo- and symbiotic Aiptasia were indiscriminate (**Supplementary Figure 2**).

We also analyzed the ectodermal epithelium topography of the tentacles and coenenchyme (i.e., coral tissue between the



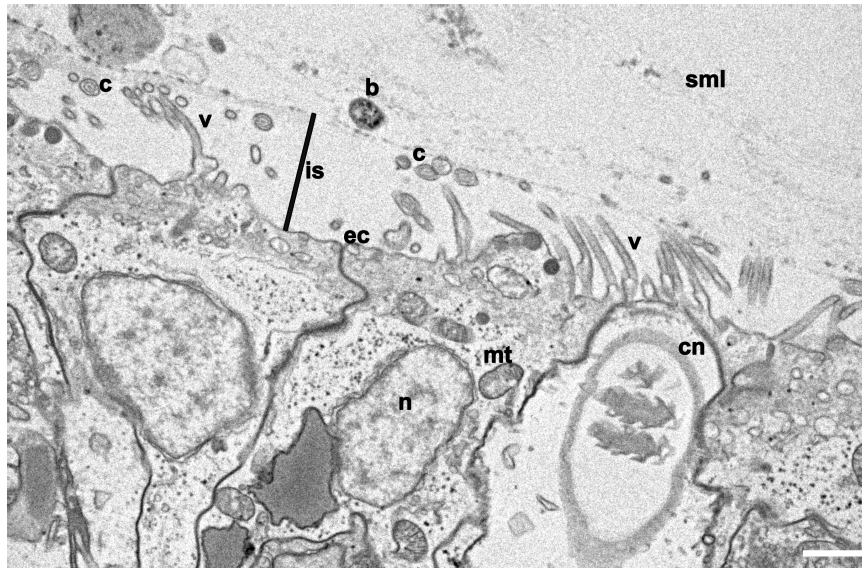


**FIGURE 2 |** Cross section of the surface ectoderm of Aiptasia. Representative transmission electron microscopy (TEM) micrograph of Aiptasia shows the villi coverage on the epidermis and the interspace between villi and the surface mucus layer (SML), where a bacterium can be identified. b, bacterium; c, cilia; cn, cnidocyte; ec, ectoderm; is, Ectoderm-mucus interspace; mt, mitochondria; n, nucleus; sml, surface mucus layer; v, villus. Scale bar- 1  $\mu$ m.

polyps) of the three scleractinian corals *Stylophora pistillata*, *Acropora humilis*, and *Porites* sp. (**Figures 1G–I**). We observed extensive villi coverage with longer cilia ranging from 4 to 6  $\mu$ m extending from the epidermis in all corals. Surface topographies were similar to *N. vectensis* and Aiptasia, but distinct from *Hydra*. In the case of *Porites* sp., a thick mucus sheet was visible on top of the coenenchyme, intercalated with fouled areas (**Supplementary Figure 3**). Further, the surface mucus layer of *Porites* sp. seemed distinct from *S. pistillata* and *A. humilis*, creating a more compact mucus sheet that persisted chemical fixation and several washing steps. Such sheet-like mucus appearances are described for *Porites compressa*, as well as the observation of the presence of fouled regions (Johnston and Rohwer, 2007). Contrary to the coral surface ectoderm that seemed devoid of bacteria, many bacteria were found attached to the smooth epithelial surfaces of other eukaryotes that aggregated in fouled regions of *Porites* sp. (**Figure 1L**), corroborating the notion that the ciliated surface of anthozoans plays a role in preventing bacterial adhesion.

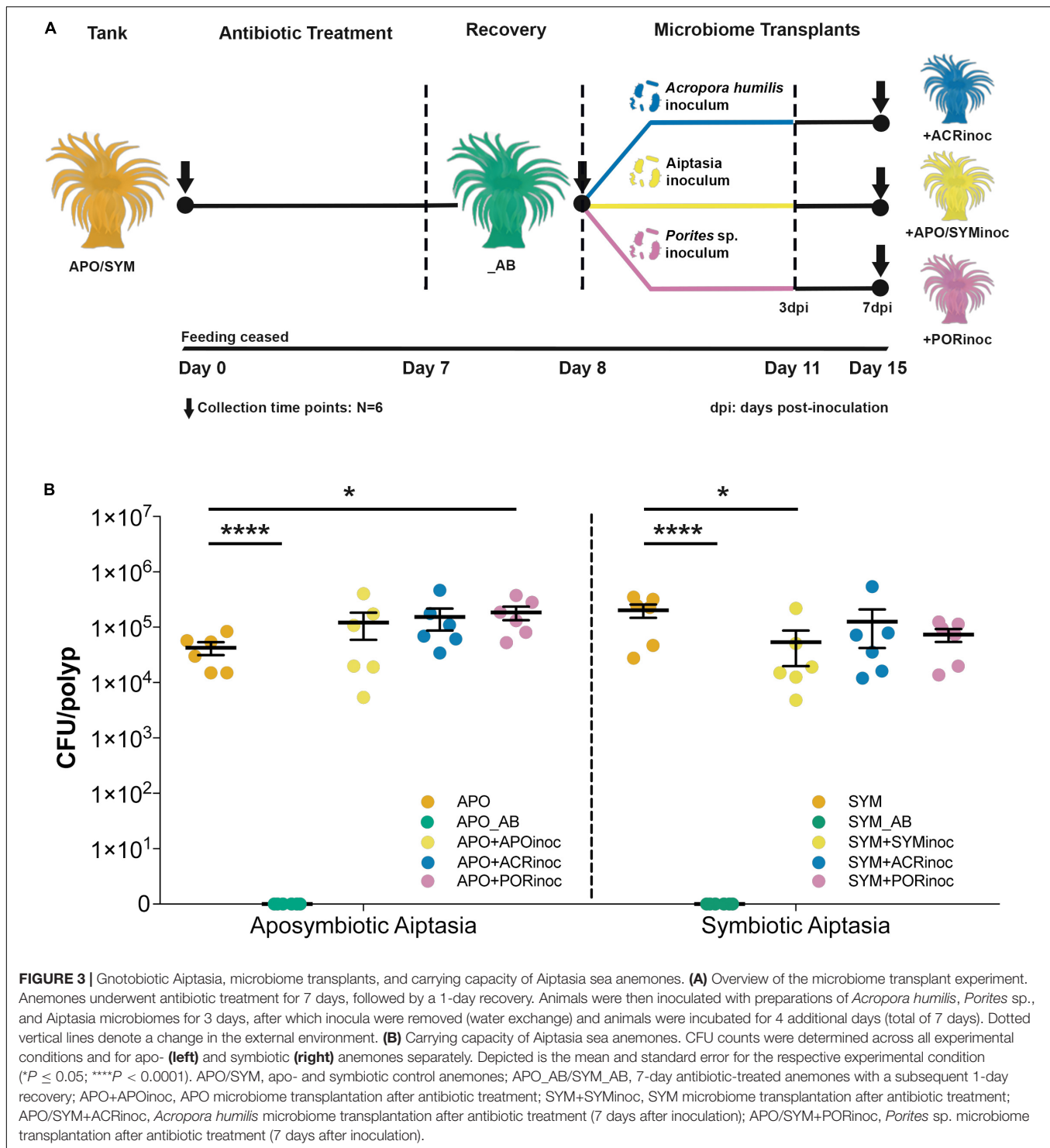
### Distinct Bacterial Carrying Capacity of Apo- and Symbiotic Aiptasia

To determine the putative carrying capacity of Aiptasia anemones, we obtained CFU counts from apo- and symbiotic control anemones that were subsequently compared to the different experimental conditions, i.e., antibiotic treated and microbiome inoculated animals (**Figure 3** and **Supplementary Tables 2, 3**). The average carrying capacity of aposymbiotic Aiptasia anemones was determined as  $4.25 \times 10^4$  CFUs/polyp (control animals). When normalized to protein biomass, we obtained  $1.59 \times 10^5$  CFUs/mg host protein. The carrying capacity of symbiotic anemones was estimated at  $2.02 \times 10^5$  CFUs/polyp and  $1.10 \times 10^6$  CFUs/mg host protein, respectively

(control animals). Thus, the number of CFUs was higher in symbiotic polyps by about an order of magnitude compared to aposymbiotic polyps (unpaired *t*-test,  $P = 0.025$ , **Supplementary Table 4**). We did not obtain CFUs from antibiotic-treated anemones, confirming successful bacterial depletion (**Figure 3B**). Interestingly, in some cases (re-)infection of gnotobiotic Aiptasia with microbiome inocula of either aposymbiotic Aiptasia or corals increased the carrying capacity of aposymbiotic animals. For instance, aposymbiotic anemones exposed to *Porites* sp. inoculum exhibited a significant increase in CFU counts to an average of  $1.85 \times 10^5$  CFUs/polyp (Dunnett's test  $P < 0.05$ , **Figure 3B** and **Supplementary Tables 2, 4**). Conversely, inoculation of symbiotic anemones (SYM+ACRinoc and SYM+PORinoc) did not result in a significant increase in CFU counts (Dunnett's test  $P > 0.3$ , **Figure 3B** and **Supplementary Tables 2, 4**). Overall, the carrying capacity of Aiptasia polyps with  $\sim 5$  mm of oral disk was between  $10^4$  and  $10^5$  CFUs for apo- and symbiotic anemones, respectively. After microbiome inoculation the carrying capacity was at about  $10^5$  CFUs/polyp, irrespective of the symbiotic condition.

### Bacterial Community Composition of Native and Inoculated Aiptasia

We employed RNA-based 16S amplicon sequencing to assess active bacterial community composition and dynamics (in contrast to the resident community based on DNA-based 16S sequencing) associated with Aiptasia under the various experimental treatments (**Figure 4**). Bacterial community composition differed significantly between treatments (PERMANOVA,  $P = 0.001$ ) (**Supplementary Table 5**). As previously reported based on DNA-based 16S marker gene sequencing (Röthig et al., 2016a), bacterial communities of apo-

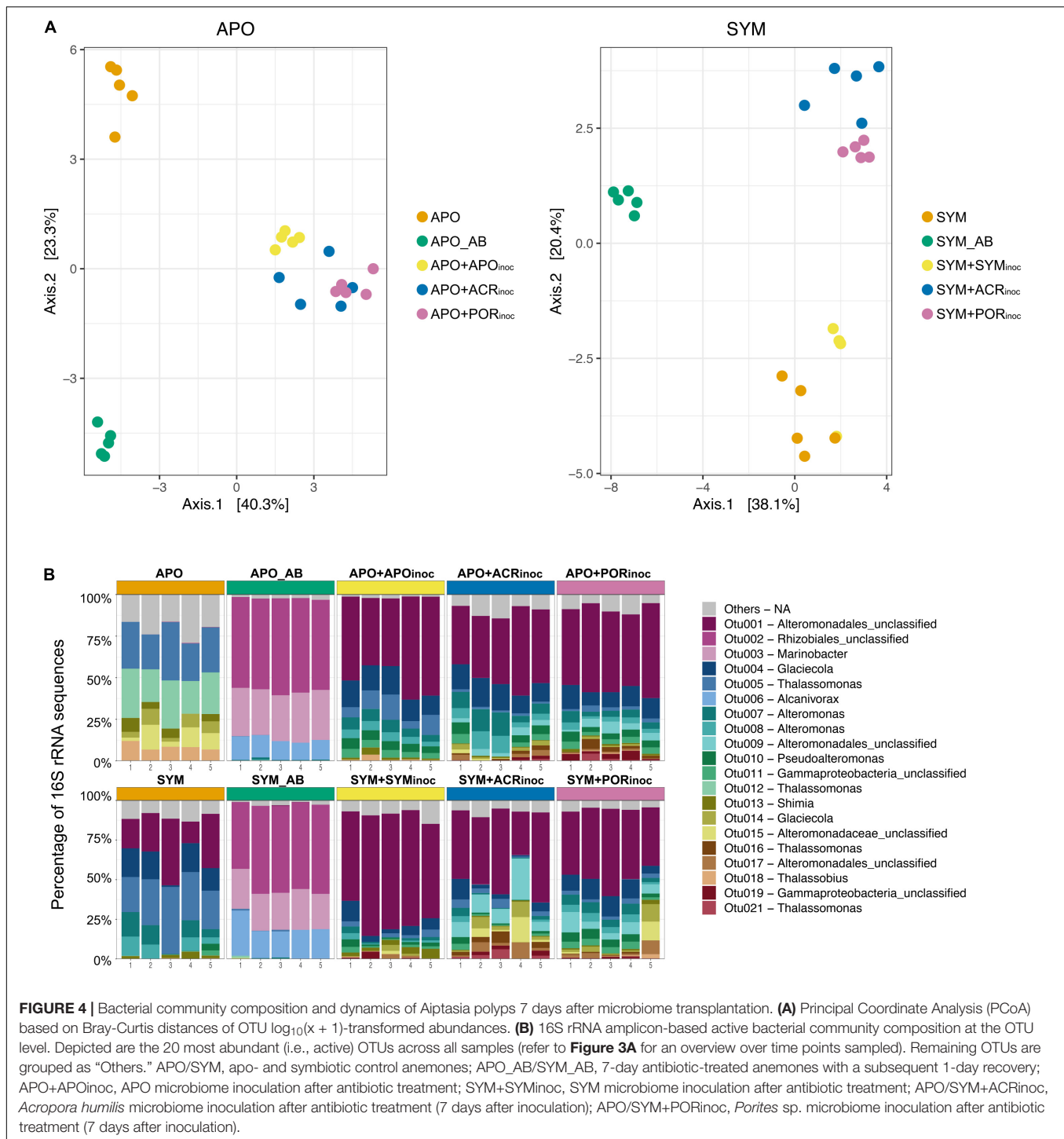


and symbiotic Aiptasia anemones were different (PERMANOVA,  $P = 0.015$ , **Figure 4B**). For this reason, we clustered apo- and symbiotic samples separate to resolve differences within apo- and symbiotic groups as a result of the treatments (**Figure 4A**). For both groups, antibiotic-treated anemones (APO\_AB and SYM\_AB) were clearly separated from control anemones

(APO and SYM) and both were different from gnotobiotic anemones re-inoculated with microbial communities (with the exception of SYM+SYMinoc that closely clustered with SYM anemones) (**Figure 4A**).

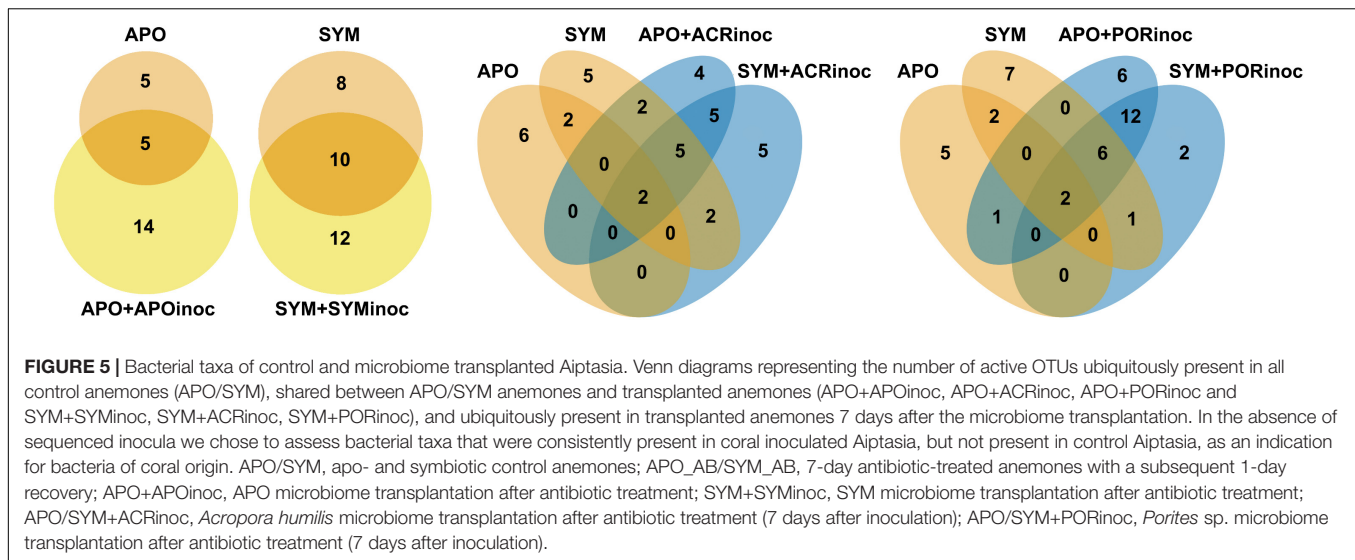
The bacterial assemblage of antibiotic-treated anemones (APO\_AB and SYM\_AB) was markedly different from the





microbiomes of other anemones in that it was considerably less complex. This was highlighted by the notion that >90% of the active community in apo- and symbiotic anemones was comprised of the same three bacterial taxa (OTU0002, OTU0003, and OTU0006) affiliated to the order Rhizobiales and the genera *Marinobacter* and *Alcanivorax* (**Figure 4B**). Conversely, 75% of the active community of aposymbiotic

control anemones was comprised of only six bacterial taxa (OTUs 0005, 0012, 0013, 0014, 0015, 0018, **Figure 4B**), which were largely absent in the antibiotic treated Aiptasia. Notably, >70% of the bacterial communities of all inoculated aposymbiotic anemones were dominated by the same taxa regardless of the inoculum. The dominant bacterial taxa were representatives of the order Alteromonadales (OTU0001, OTU0004, OTU0007,



OTU0008), which were barely detected in aposymbiotic control anemones. For the symbiotic anemones, the active bacterial community of control polyps was dominated by a few bacterial taxa of the order Alteromonadales and the genera *Glaciecola* and *Thalassomonas* (Figure 4B). Similarly, microbiome transplanted symbiotic Aiptasia resembled each other and were dominated by bacteria of the order Alteromonadales (OTU0001, OTU0004, OTU0007, OTU0008, OTU0009), just as the microbiome transplanted aposymbiotic Aiptasia. Thus, despite the differences in microbial community composition of apo- and symbiotic control anemones, microbiome transplanted gnotobiotic apo- and symbiotic anemones look much more alike with regard to their microbiome.

To get better insight into the bacterial taxa that were present in Aiptasia after microbiome transplantation, we compared the active bacterial community of control conditions (APO/SYM) and treatment conditions (Figure 5 and Supplementary Table 6). This comparison shows that all inoculated anemones (+APOinoc, +SYMInoc, +ACRinoc, and +PORinoc) harbored bacterial taxa that were already present (active) in control anemones as well as “novel” (i.e., previously undetected) bacteria. This may point to potential carryover from gnotobiotic anemones (not all bacteria were depleted). In the case of coral microbiome inoculations, we observed association with novel bacteria from the coral microbiomes (as determined by the comparison to APO and SYM anemones, Figure 5 and Supplementary Table 6). In particular, two bacteria taxa, of the genus *Thalassomonas* (OTU0016) and an unclassified Alteromonadales (OTU0021), are worthwhile mentioning because they were both found to be abundant (i.e., active) in coral microbiome transplanted Aiptasia (i.e., APO+ACRinoc, APO+PORinoc, SYM+ACRinoc, and SYM+PORinoc), but absent from Aiptasia transplanted with their own microbiomes (i.e., APO+APOinoc and SYM+SYMInoc) (Supplementary Table 6). Both OTUs are putative coral microbiome bacteria that were able to colonize apo- and symbiotic Aiptasia. On the contrary, a putative coral microbiome taxon from the genus *Glaciecola* (OTU0195) was

only found associated with symbiotic anemones. Further, we found two Gammaproteobacteria (OTU0067 and OTU0099) to be specifically prevalent in anemones inoculated with *Porites* sp. microbiome preparations.

## DISCUSSION

It is becoming increasingly clear that the specific composition and abundance of certain bacterial species affect host health and fitness (McFall-Ngai et al., 2013). At the same time, recent studies highlight that bacterial associations are not stable over time, but rather, assemble flexibly following fluctuations in the prevailing environment(s) (Roder et al., 2015; Ziegler et al., 2017; Ziegler et al., 2019; Voolstra and Ziegler, 2020). On the one hand, such observations support the notion that microbiome community changes can support host ecological adaption to environmental change (Reshef et al., 2006; Voolstra and Ziegler, 2020). On the other hand, the premise of flexibility gives rise to the idea of probiotics, i.e., inoculation with beneficial bacteria to support metaorganism stress resilience (Peixoto et al., 2017, 2019, 2021). The latter is gaining attention with regards to reef-building corals given the alarming loss of coral reef cover over recent decades (Hughes et al., 2017a, 2020). However, besides the acknowledged importance of coral-associated bacteria (Bang et al., 2018; van Oppen and Blackall, 2019) and the promise of coral probiotics to work in principle (Rosado et al., 2019), we are still missing answers to many of the basic questions surrounding cnidarian microbiome building principles and the underlying mechanistic aspects. Aiptasia is an emerging model system to study cnidarian symbioses, and here we set out to build a foundation for bacterial functional studies using the Aiptasia model by characterizing surface topography, carrying capacity, and assessing the prospect of microbiome transplants.

Our results show pronounced differences in the ultrastructure of the surface ectoderm between *Hydra* and anthozoans with implications for microbial association. SEM analyses of *Hydra*,

*N. vectensis*, Aiptasia, and three scleractinian coral species suggest that bacterial epibionts in anthozoans are (more) restricted to the surface mucus layer (SML) in comparison to hydrozoans. Notably, *Hydra* anemones feature a smooth surface ectoderm where the epithelial glycocalyx (i.e., the pericellular matrix made of glycoproteins and glycolipids that cover the plasma membrane of the epithelium) promotes bacterial attachment and lacks extensive ectodermal ciliation that may prevent bacterial adhesion (Kesimer et al., 2013; Fraune et al., 2014; Wein et al., 2018). Other hydrozoans such as *Ectopleura crocea* and *Cladonema* sp. have shown colonizing epibionts attached to the glycocalyx, which ranged from 200 nm to 1  $\mu$ m in thickness from the hydroid ectoderm to the epibiont, and their surface topography was also shown to be smoother, resembling that of *Hydra* (di Camillo et al., 2012; Abouna et al., 2015). Although *Hydra* can be considered a derived hydrozoan due to its life history (e.g., lack of a medusoid stage and freshwater habitat), imaging results from the current and other studies (e.g., di Camillo et al., 2012; Abouna et al., 2015) support the general notion that hydrozoans and anthozoans differ in their surface topographies, with anthozoans featuring a ciliated, rough surface, and a more defined ectoderm-SML separation in contrast to hydrozoans that seem to exhibit a smooth(er) less ciliated surface. It has been shown that the SML of corals is highly dynamic, with SML being cyclically shed (Bythell and Wild, 2011). This is thought to prevent pathogen colonization from the surrounding environment (Shnit-Orland and Kushmaro, 2009; Glasl et al., 2016), but might also explain the flexible microbial association of corals commonly found across different environments (Roder et al., 2015; Röthig et al., 2016b, 2017; Ziegler et al., 2017; Voolstra and Ziegler, 2020) and may contribute to the efficacy of coral probiotics (Peixoto et al., 2017, 2021). At a more basal level, the difference in surface topography between hydrozoans and anthozoans argues for the need of having distinct cnidarian models to reflect the implied microbial association differences. For the two anthozoan models, *N. vectensis* and Aiptasia, there was little difference in terms of ectodermal topography and bacterial colonization between the two organisms, both at the column and tentacle level. However, microalgal symbionts in the family Symbiodiniaceae (Lajeunesse et al., 2018) were shown to putatively contribute to the composition of coral mucus through their exudates (Brown and Bythell, 2005; Nelson et al., 2013), which affect bacterial association (Matthews et al., 2020), and Symbiodiniaceae were also shown to harbor themselves specific bacteria (Maire et al., 2021). As such, Aiptasia is a model system not only for the study of coral-algal symbiosis, but also for the study of bacterial associations and for testing the capacity for microbiome manipulation as further discussed below.

We were surprised by the lack of observed bacterial colonization at the surface ectoderm of Aiptasia (anthozoans more generally) using SEM, which was readily apparent in *Hydra* using the same technique. As alluded to above, this might be a consequence of surface topography differences, which ultimately affect bacterial colonization, but also differences in how the preparation affects sample integrity. In the case of *Hydra*, the accessible glycocalyx was preserved during SEM

preparation, whereas the mucus of the anthozoans species was lost by employing a classical SEM sample protocol. Indeed, a modified TEM protocol developed to preserve the mucus layer also confirmed the presence of bacteria in the surface mucus layer of Aiptasia polyps, but not in the ectodermal layer or glycocalyx (**Supplementary Figure 1**). This highlights the need for continuous development and improvements of protocols to visualize bacterial association (Wada et al., 2016). For instance, TEM analyses may be combined with CARD-FISH staining for improved specificity and visualization of Aiptasia- and coral-associated bacteria besides the exploration of other methods (Kesimer et al., 2013).

Complementary to the visual assessment of bacterial abundance, we determined a bacterial carrying capacity of  $\sim 10^4$  to  $10^5$  bacterial cells per Aiptasia polyp, pending on the symbiotic state. This number is similar to the bacterial density reported for *Hydra* (Wein et al., 2018) and may roughly equate to the  $\sim 10^6$  bacterial cells/cm<sup>2</sup> coral tissue previously reported (Koren and Rosenberg, 2006; Garren and Azam, 2012). It is interesting to note that our bacterial capacity was an order of magnitude higher for symbiotic ( $10^5$  bacterial cells/polyp) in comparison to aposymbiotic ( $10^4$  bacterial cells/polyp) anemones. This difference may arise from the additional niche space provided by the symbiosome, which was previously shown to harbor bacteria (Ainsworth et al., 2015), and through association with Symbiodiniaceae, which harbor their own microbial community (Deines et al., 2020; Maire et al., 2021). Visualization and enumeration of cnidarian-associated bacteria is still relatively rare (Neave et al., 2017; Cooke et al., 2019), in part because of the difficulties associated with fluorescent staining techniques in corals (Wada et al., 2016). As such, we relied on CFU counts, which avoid many of these difficulties but at the cost of media selectivity, as highlighted by the discrepancy between absence of CFUs in marine media and amplicon sequencing-based detection of some bacterial taxa. Literature perusal suggests that the most prevalent bacterial taxa detected in gnotobiotic anemones using sequencing (OTU0002, OTU0003, and OTU0006) cannot grow on our employed media and therefore escape CFU counting (Brooijmans et al., 2009; Yetti et al., 2015; Wang et al., 2016). Nevertheless, the antibiotic-treated anemones were highly bacteria depleted as more than 95% of the sequencing reads represented only three OTUs, which correspond to less than 5% of the active taxa detected in control anemones. As such, we consider animals treated with our gnotobiotic protocol (Costa et al., 2019) highly bacteria depleted. Besides the availability of axenic or gnotobiotic animals, it is desirable to have bacterial isolates with fluorescent reporter plasmids for more accurate estimation, which also allows for tracking location and abundance of said bacteria, as shown in *Hydra* (Wein et al., 2018). On this note, viability-qPCR (Emerson et al., 2017) may comprise a molecular method for enumeration of the density of active bacteria, although we found that it requires significant optimization due to taxon-specific differences with regard to dye permeability. As alluded to above and recently (Röthig et al., 2016a), 75% of the relative microbial abundance is comprised of only a handful of bacterial taxa, making Aiptasia a “non-complex” coral model for microbiome

studies with the promise to obtain bacterial isolates for functional testing and manipulation (Röthig et al., 2016a).

Our RNA-based sequencing analysis revealed that the community of active bacteria was less diverse in comparison to the DNA-based microbial community (Röthig et al., 2016a): we identified an average of 38 and 64 active bacterial taxa associated with apo- and symbiotic anemones, while DNA-based analysis of the standing community retrieved 109 and 118 distinct bacteria, respectively. This may seem like a stark difference; however, it is not straight-forward to compare RNA- and DNA-based bacterial communities. Since abundance estimates are relative, “absence” in the RNA-based community analysis merely indicates that we could identify less bacteria (at the current sequencing depth) and that there is a putative difference between the bacterial community that is “present” (DNA) and the one that is “active” (RNA). Nevertheless, we compared the overlap in OTU-assigned taxonomies at the genus level for CC7 from Röthig et al. (2016a) and this study, which showed that 65% (APO) and 84% (SYM) of the identified bacterial genera in the RNA-based analysis were also found in the DNA-based analysis. Notably, such comparisons have inherent biases due to taxonomic redundancies and differences in the taxonomic classification between different OTU datasets.

To begin to explore the prospect of Aiptasia microbiome manipulation as a tool to interrogate bacterial function and test the effect of probiotics on holobiont biology, we conducted a series of inoculations/transplants on gnotobiotic Aiptasia with microbiomes from control anemones and from two coral species. *Acropora humilis* was chosen because its microbiome is highly uneven and dominated by bacteria of the genus *Endozoicomonas*, which could be used for tracking of the microbial transplant, since Aiptasia CC7 seems devoid of *Endozoicomonas* (Röthig et al., 2016a). However, we did not detect *Endozoicomonas* in the microbiome of inoculated anemones (i.e., SYM+ACRinoc, APO+ACRinoc). This suggests that *Endozoicomonas* exhibit high (coral) host specificity, despite their broad and prevalent distribution across marine invertebrates (Neave et al., 2016, 2017; Rossbach et al., 2019). Moreover, *Endozoicomonas* reside within coral tissues (Neave et al., 2016, 2017), which may explain their absence after microbiome transplantation, because mucus-associated bacteria may be easier to transfer than tissue-associated bacteria. Such differences putatively provide important insight regarding the choice of bacteria targeted for microbiome transplants. In contrast to *A. humilis*, *Porites* sp. was chosen as a donor because it is considered an environmentally resilient species with a more even and diverse microbiome (Hadaidi et al., 2017; Robbins et al., 2019). As such, successful microbiome transplantation would allow for subsequent testing of altered stress susceptibility. First off, our results show that all transplanted animals harbor a significantly different active bacterial community when compared to control anemones with the general notion that inoculated Aiptasia resemble each other more than control animals (Figure 4 and Supplementary Table 5). This is not highly surprising given that formation of an established microbial community may take time and likely goes through processes of inter-bacterial communication, host-bacterial communication,

and winnowing, all of which presumably affect microbiome composition (Franzenburg et al., 2013a; Bernasconi et al., 2019; Shibl et al., 2020). As such, microbial consortia associated with Aiptasia after microbiome transplantation might represent a mix of specific bacteria administered with the inocula and opportunistic, environmentally present bacteria (e.g., resistant bacteria that survived the antibiotic treatment and were attached to the wells of the rearing plate), in particular copiotrophs. Copiotrophs are known to rapidly (re)populate carbon-rich environments such as the surface mucus layer (Nelson et al., 2013; McDewitt-Irwin et al., 2017; Cárdenas et al., 2018; Hadaidi et al., 2019) and as such may “drive” initial microbial repopulation dynamics. This makes the long(er)-term tracking of microbiome assemblage dynamics after transplantation important. It also suggests that antibiotic treated Aiptasia without any subsequent inoculation should be included in future experimental designs as controls for determining load and type of “residual” bacteria. In addition, future experiments should also include microbiome transplantations of untreated Aiptasia, resembling current coral probiotics procedures (Peixoto et al., 2021). This would provide further insight regarding repopulation dynamics and constraints.

Many of the taxa found in control Aiptasia established themselves again after microbiome inoculation, such as bacteria in the genus *Thalassomonas* (OTU0005, OTU0012), *Glaciecola* (OU0014), *Thalassobius* (OTU0018), or *Alteromonas* (OTU0007) (Supplementary Table 6). Microbiome transplantations with inocula from *A. humilis* and *Porites* sp. were successful to the extent that (at least) some foreign bacterial taxa (some of which were specific to the coral species from which the inoculum was obtained) were present (active) in Aiptasia polyps, as evidenced by their detection 7 days after microbiome transplantation. Notably, unavailability of sequenced inocula and coral native microbiomes within the current study limited the extent to which we could identify bacterial taxa with broad host compatibility, suitable for cross-species microbiome manipulation. Due to this, we considered bacterial taxa that were consistently present in coral-inoculated but not present in control Aiptasia as of putative coral origin. Besides treatment-specific differences, we commonly found bacterial taxa belonging to the Alteromonadaceae, Rhodobacteraceae, and Gammaproteobacteria to be transferred. This is encouraging given that bacteria from these taxonomic affiliations are commonly found in coral microbiomes (Roder et al., 2014; Neave et al., 2017; Ziegler et al., 2017, 2019).

At large, our results suggest that cross-species microbiome manipulation via transplantation is possible (to a certain extent). That is to say, Aiptasia is a suitable system to test the function of (at least some) coral bacteria and their effect on holobiont biology. The obvious next step is to test for altered holobiont phenotypes, e.g., increased or decreased stress resilience, using a standardized framework (Voolstra et al., 2020) after microbial transplantation with subsequent elucidation of the underlying mechanism(s). In addition, to achieve consistent and stable changes of microbial host consortia, an improved understanding of inocula persistence, dispersion, location, bacterial load, and any putative long-term effects is wanted. Aiptasia seems like the model system of choice, given its taxonomic relatedness and physiological similarities with regard



to Symbiodiniaceae association, microbiome composition, and surface and tissue complexity.

## CONCLUSION

Bacteria affect the health and fitness of their hosts. Given the worldwide decline of corals and the reefs they build, a better understanding of the function of bacteria and their potential manipulation is important. To achieve this, the development of coral model systems is imperative. Here we set the foundation for Aiptasia as a model for the study of coral-bacterial interactions. We show that the surface ectoderm topography is highly similar between Aiptasia and corals, in line with overall similarities in the microbiome composition established previously. Building on these prospects, we have developed a protocol for the generation of gnotobiotic Aiptasia and determined the bacterial carrying capacity to perform microbiome manipulation experiments. Our results support the principal suitability of Aiptasia to microbiome manipulation and its putative ability to incorporate foreign bacterial species. Although more work is needed, our study is a first step and provides an avenue to study the function of self and foreign bacteria as well as to explore the mechanisms underlying microbial acquisition, association, and host specificity. Future work should incorporate standardized testing to elucidate the effect of altered microbiomes on holobiont phenotypes as well as the generation of fluorescently labeled bacterial isolates, which will allow for spatial/temporal tracking and enumeration of bacterial associates. The work presented here provides a foundation and we will continue to develop Aiptasia as a coral model for bacterial functional studies.

## DATA AVAILABILITY STATEMENT

Data determined in this study are available under NCBI BioProject PRJNA665377 (<https://www.ncbi.nlm.nih.gov/bioproject/665377>). Scripts used for data analysis, curation, and plotting are available at [https://github.com/ajcardenasb/Aiptasia\\_microbiome\\_manipulation](https://github.com/ajcardenasb/Aiptasia_microbiome_manipulation). Abundant bacterial OTU

reference sequences are available under GenBank Accession numbers MW577132 – MW577168 ([https://www.ncbi.nlm.nih.gov/nucleotide/?term=MW577132:MW577168\[accn\]](https://www.ncbi.nlm.nih.gov/nucleotide/?term=MW577132:MW577168[accn])).

## AUTHOR CONTRIBUTIONS

CV, RC, and AC conceived and designed the experiments, analyzed the data, and wrote the manuscript. RC and AC collected and processed the samples. RC, AC, and CL-F generated the data. RC, AC, CL-F, GT, and CV generated the figures. RC, AC, CL-F, GT, AM, and CV interpreted the data. CL-F, AM, and CV provided tools, reagents, and methods. All authors contributed to the article and approved the submitted version.

## FUNDING

Research reported in this publication was supported by KAUST baseline funds to CV.

## ACKNOWLEDGMENTS

We acknowledge the KAUST Imaging and Characterization Core Lab for their support in TEM and SEM analysis and the KAUST Bioscience Core Lab (BCL) for their support with the NGS data generation. We would like to thank all collaborators who tested the bacteria depletion protocol and provided feedback. We would also like to thank Carol Buitrago-Lopez and Hagen Gegner for their help with the coral collection and maintenance. *Hydra magnipapillata* and *Nematostella vectensis* were kindly provided by Prof. Takashi Gojobori's group.

## SUPPLEMENTARY MATERIAL

The Supplementary Material for this article can be found online at: <https://www.frontiersin.org/articles/10.3389/fmicb.2021.637834/full#supplementary-material>

## REFERENCES

- Abouna, S., Gonzalez-Rizzo, S., Grimonprez, A., and Gros, O. (2015). First description of sulphur-oxidizing bacterial symbiosis in a cnidarian (*Medusozoa*) living in sulphidic shallow-water environments. *PLoS One* 10:e0127625. doi: 10.1371/journal.pone.0127625
- Ainsworth, T. D., Krause, L., Bridge, T., Torda, G., Raina, J.-B., Zakrzewski, M., et al. (2015). The coral core microbiome identifies rare bacterial taxa as ubiquitous endosymbionts. *ISME J.* 9, 2261–2274. doi: 10.1038/ismej.2015.39
- Allemand, D., and Osborn, D. (2019). Ocean acidification impacts on coral reefs: from sciences to solutions. *Reg. Stud. Mar. Sci.* 28:100558. doi: 10.1016/j.rsma.2019.100558
- Allen, M. R., Dube, O. P., Solecki, W., Aragón-Durand, F., Cramer, W., Humphreys, S., et al. (2018). "Framing and context," in *Global Warming of 1.5°C. An IPCC Special Report on the Impacts of Global Warming of 1.5°C Above Pre-Industrial Levels and Related Global Greenhouse Gas Emission Pathways, in the Context of Strengthening the Global Response to the Threat of Climate Change, Sustainable Development, and Efforts to Eradicate Poverty*, eds V. Masson-Delmotte et al. (Geneva: IPCC).
- Andersson, A. F., Lindberg, M., Jakobsson, H., Bäckhed, F., Nyrén, P., and Engstrand, L. (2008). Comparative analysis of human gut microbiota by barcoded pyrosequencing. *PLoS One* 3:e2836. doi: 10.1371/journal.pone.0002836
- Augustin, R., Schröder, K., Murillo Rincón, A. P., Fraune, S., Anton-Erxleben, F., Herbst, E.-M., et al. (2017). A secreted antibacterial neuropeptide shapes the microbiome of *Hydra*. *Nat. Commun.* 8:698. doi: 10.1038/s41467-017-00625-1
- Bang, C., Dagan, T., Deines, P., Dubilier, N., Duschl, W. J., Fraune, S., et al. (2018). Metaorganisms in extreme environments: do microbes play a role in organismal adaptation? *Zoology* 127, 1–19. doi: 10.1016/j.zool.2018.02.004
- Baumgarten, S., Simakov, O., Esherrick, L. Y., Liew, Y. J., Lehnert, E. M., Michell, C. T., et al. (2015). The genome of *Aiptasia*, a sea anemone model for coral symbiosis. *Proc. Natl. Acad. Sci. U.S.A.* 112:201513318. doi: 10.1073/pnas.1513318112
- Bayer, T., Neave, M. J., Alsheikh-Hussain, A., Aranda, M., Yum, L. K., Mincer, T., et al. (2013). The microbiome of the red sea coral stylophora pistillata is dominated by tissue-associated endozoicomonas bacteria. *Appl. Environ. Microbiol.* 79, 4759–4762. doi: 10.1128/AEM.00695-13

- Bernasconi, R., Stat, M., Koenders, A., Paparini, A., Bunce, M., and Huggett, M. J. (2019). Establishment of coral-bacteria symbioses reveal changes in the core bacterial community with host ontogeny. *Front. Microbiol.* 10:1529. doi: 10.3389/fmicb.2019.01529
- Biquand, E., Okubo, N., Aihara, Y., Rolland, V., Hayward, D. C., Hatta, M., et al. (2017). Acceptable symbiont cell size differs among cnidarian species and may limit symbiont diversity. *ISME J.* 11, 1702–1712. doi: 10.1038/ismej.2017.17
- Brooijmans, R. J. W., Pastink, M. I., and Siezen, R. J. (2009). Hydrocarbon-degrading bacteria: the oil-spill clean-up crew. *Microb. Biotechnol.* 2, 587–594. doi: 10.1111/j.1751-7915.2009.00151.x
- Brown, B. E., and Bythell, J. C. (2005). Perspectives on mucus secretion in reef corals. *Mar. Ecol. Prog. Ser.* 296, 291–309. doi: 10.3354/meps296291
- Brown, T., Otero, C., Grajales, A., Rodriguez, E., and Rodriguez-Lanetty, M. (2017). Worldwide exploration of the microbiome harbored by the cnidarian model, *Exaiptasia pallida* (Agassiz in Verrill, 1864) indicates a lack of bacterial association specificity at a lower taxonomic rank. *PeerJ* 5:e3235. doi: 10.7717/peerj.3235
- Bythell, J. C., and Wild, C. (2011). Biology and ecology of coral mucus release. *J. Exp. Mar. Biol. Ecol.* 408, 88–93. doi: 10.1016/j.jembe.2011.07.028
- Cárdenas, A., Neave, M. J., Haroon, M. F., Pogoreutz, C., Rädcker, N., Wild, C., et al. (2018). Excess labile carbon promotes the expression of virulence factors in coral reef bacterioplankton. *ISME J.* 12, 59–76. doi: 10.1038/ismej.2017.142
- Chen, H., and Boutros, P. C. (2011). VennDiagram: a package for the generation of highly-customizable venn and euler diagrams in R. *BMC Bioinformatics* 12:35. doi: 10.1186/1471-2105-12-35
- Cooke, I., Mead, O., Whalen, C., Boote, C., Moya, A., Ying, H., et al. (2019). Molecular techniques and their limitations shape our view of the holobiont. *Zoology* 137:125695. doi: 10.1016/j.zool.2019.125695
- Costa, R. M., Cárdenas, A., and Voolstra, C. R. (2019). *Protocol for Bacterial Depletion of Aiptasia Anemones - Towards the Generation of Gnotobiotic/germ-free Cnidarian Host Animals V.2. Protocols IO*. Available online at: [dx.doi.org/10.17504/protocols.io.7mrhk56](https://doi.org/10.17504/protocols.io.7mrhk56).
- Cziesielski, M. J., Liew, J., Cui, G., Schmidt-Roach, S., Campana, S., Marondedze, C., et al. (2018). Multi-omics analysis of thermal stress response in a zooxanthellate cnidarian reveals the importance of associating with thermotolerant symbionts. *Proc. R. Soc. B Biol. Sci.* 285:20172654. doi: 10.1098/rspb.2017.2654
- Deines, P., Hammerschmidt, K., and Bosch, T. C. G. (2020). Microbial species coexistence depends on the host environment. *mBio* 11:e807-20. doi: 10.1128/mBio.00807-20
- di Camillo, C. G., Luna, G. M., Bo, M., Giordano, G., Corinaldesi, C., and Bavestrello, G. (2012). Biodiversity of prokaryotic communities associated with the ectoderm of *Ectopleura crocea* (Cnidaria, Hydrozoa). *PLoS One* 7:e39926. doi: 10.1371/journal.pone.0039926
- Dietzel, A., Bode, M., Connolly, S. R., and Hughes, T. P. (2020). Long-term shifts in the colony size structure of coral populations along the great barrier reef. *Proc. Biol. Sci.* 287:20201432. doi: 10.1098/rspb.2020.1432
- Domin, H., Zurita-Gutiérrez, Y. H., Scotti, M., Buttlar, J., Humeida, U. H., and Fraune, S. (2018). Predicted bacterial interactions affect in vivo microbial colonization dynamics in *Nematostella*. *Front. Microbiol.* 9:728. doi: 10.3389/fmicb.2018.00728
- Dungan, A. M., Hartman, L. M., Tortorelli, G., Belderok, R., Lamb, A. M., Pisan, L., et al. (2020). *Exaiptasia diaphana* from the great barrier reef: a valuable resource for coral symbiosis research. *Symbiosis* 80, 195–206. doi: 10.1007/s13199-020-00665-0
- Emerson, J. B., Adams, R. I., Román, C. M. B., Brooks, B., Coil, D. A., Dahlhausen, K., et al. (2017). Schrödinger's microbes: tools for distinguishing the living from the dead in microbial ecosystems. *Microbiome* 5:86. doi: 10.1186/s40168-017-0285-3
- Fisher, R., O'Leary, R. A., Low-Choy, S., Mengersen, K., Knowlton, N., Brainard, R. E., et al. (2015). Species richness on coral reefs and the pursuit of convergent global estimates. *Curr. Biol.* 25, 500–505. doi: 10.1016/j.cub.2014.12.022
- Franzenburg, S., Fraune, S., Altrock, P. M., Künzel, S., Baines, J. F., Traulsen, A., et al. (2013a). Bacterial colonization of *Hydra* hatchlings follows a robust temporal pattern. *ISME J.* 7, 781–790. doi: 10.1038/ismej.2012.156
- Franzenburg, S., Walter, J., Künzel, S., Wang, J., Baines, J. F., Bosch, T. C. G., et al. (2013b). Distinct antimicrobial peptide expression determines host species-specific bacterial associations. *Proc. Natl. Acad. Sci. U.S.A.* 110, E3730–E3738.
- Fraune, S., Anton-Erxleben, F., Augustin, R., Franzenburg, S., Knop, M., Schröder, K., et al. (2014). Bacteria-bacteria interactions within the microbiota of the ancestral metazoan *Hydra* contribute to fungal resistance. *ISME J.* 9, 1543–1556. doi: 10.1038/ismej.2014.239
- Fraune, S., and Bosch, T. C. G. (2007). Long-term maintenance of species-specific bacterial microbiota in the basal metazoan *Hydra*. *Proc. Natl. Acad. Sci. U.S.A.* 104, 13146–13151. doi: 10.1073/pnas.0703375104
- Fraune, S., Bosch, T. C. G., and Augustin, R. (2009). Exploring host-microbe interactions in *Hydra*. *Microbe Magazine* 4, 457–462. doi: 10.1128/microbe.4.457.1
- Garren, M., and Azam, F. (2012). Corals shed bacteria as a potential mechanism of resilience to organic matter enrichment. *ISME J.* 6, 1159–1165. doi: 10.1038/ismej.2011.180
- Gegner, H. M., Rädcker, N., Ochsenkühn, M., Barreto, M. M., Ziegler, M., Reichert, J., et al. (2019). High levels of floridoside at high salinity link osmoadaptation with bleaching susceptibility in the cnidarian-algal endosymbiosis. *Biol. Open* 8:bio045591. doi: 10.1242/bio.045591
- Glasl, B., Herndl, G. J., and Frade, P. R. (2016). The microbiome of coral surface mucus has a key role in mediating holobiont health and survival upon disturbance. *ISME J.* 10, 2280–2292. doi: 10.1038/ismej.2016.9
- Grajales, A., and Rodríguez, E. (2014). Morphological revision of the genus *Aiptasia* and the family *Aiptasiidae* (Cnidaria, Actiniaria, Etrididae). *Zootaxa* 3826, 55–100. doi: 10.11646/zootaxa.3826.1.2
- Hadaidi, G., Gegner, H. M., Ziegler, M., and Voolstra, C. R. (2019). Carbohydrate composition of mucus from scleractinian corals from the central Red Sea. *Coral Reefs* 38, 21–27. doi: 10.1007/s00338-018-01758-5
- Hadaidi, G., Röthig, T., Yum, L. K., Ziegler, M., Arif, C., Roder, C., et al. (2017). Stable mucus-associated bacterial communities in bleached and healthy corals of *Porites lobata* from the Arabian Seas. *Sci. Rep.* 7:45362. doi: 10.1038/srep45362
- Har, J. Y., Helbig, T., Lim, J. H., Fernando, S. C., Reitzel, A. M., Penn, K., et al. (2015). Microbial diversity and activity in the *Nematostella vectensis* holobiont: insights from 16S rRNA gene sequencing, isolate genomes, and a pilot-scale survey of gene expression. *Front. Microbiol.* 6:818. doi: 10.3389/fmicb.2015.00818
- Herrera, M., Ziegler, M., Voolstra, C. R., and Aranda, M. (2017). Laboratory-cultured strains of the sea anemone *Exaiptasia* reveal distinct bacterial communities. *Front. Mar. Sci.* 4:115. doi: 10.3389/fmars.2017.00115
- Hughes, D. J., Alderdice, R., Cooney, C., Kühl, M., Pernice, M., Voolstra, C. R., et al. (2020). Coral reef survival under accelerating ocean deoxygenation. *Nat. Clim. Chang.* 10, 296–307. doi: 10.1038/s41558-020-0737-9
- Hughes, T. P., Anderson, K. D., Connolly, S. R., Heron, S. F., Kerry, J. T., Lough, J. M., et al. (2018a). Spatial and temporal patterns of mass bleaching of corals in the Anthropocene. *Science* 359, 80–83. doi: 10.1126/science.aan8048
- Hughes, T. P., Kerry, J. T., Baird, A. H., Connolly, S. R., Dietzel, A., Eakin, C. M., et al. (2018b). Global warming transforms coral reef assemblages. *Nature* 556, 492–496. doi: 10.1038/s41586-018-0041-2
- Hughes, T. P., Barnes, M. L., Bellwood, D. R., Cinner, J. E., Cumming, G. S., Jackson, J. B. C., et al. (2017a). Coral reefs in the Anthropocene. *Nature* 546, 82–90. doi: 10.1038/nature22901
- Hughes, T. P., Kerry, J. T., Álvarez-Noriega, M., Álvarez-Romero, J. G., Anderson, K. D., Baird, A. H., et al. (2017b). Global warming and recurrent mass bleaching of corals. *Nature* 543, 373–377. doi: 10.1038/nature21707
- Jaspers, C., Fraune, S., Arnold, A. E., Miller, D. J., Bosch, T. C. G., and Voolstra, C. R. (2019). Resolving structure and function of metaorganisms through a holistic framework combining reductionist and integrative approaches. *Zoology* 133, 81–87. doi: 10.1016/j.zool.2019.02.007
- Johnston, I. S., and Rohwer, F. (2007). Microbial landscapes on the outer tissue surfaces of the reef-building coral *Porites compressa*. *Coral Reefs* 26, 375–383. doi: 10.1007/s00338-007-0208-z
- Kesimer, M., Ehre, C., Burns, K. A., Davis, C. W., Sheehan, J. K., and Pickles, R. J. (2013). Molecular organization of the mucins and glycocalyx underlying mucus transport over mucosal surfaces of the airways. *Mucosal Immunol.* 6, 379–392. doi: 10.1038/mi.2012.81
- Koren, O., and Rosenberg, E. (2006). Bacteria associated with mucus and tissues of the coral *Oculina patagonica* in summer and winter. *Appl. Environ. Microbiol.* 72, 5254–5259. doi: 10.1128/AEM.00554-06
- LaJeunesse, T. C., Parkinson, J. E., Gabrielson, P. W., Jeong, H. J., Reimer, J. D., Voolstra, C. R., et al. (2018). Systematic revision of symbiodiniaceae highlights the antiquity and diversity of coral endosymbionts. *Curr. Biol.* 28, 2570.e6–2580.e6. doi: 10.1016/j.cub.2018.07.008

- Lawson, C. A., Raina, J., Kahlke, T., Seymour, J. R., and Suggett, D. J. (2018). Defining the core microbiome of the symbiotic. *Environ. Microbiol. Rep.* 10, 7–11. doi: 10.1111/1758-2229.12599
- Maire, J., Girvan, S. K., Barkla, S. E., Perez-Gonzalez, A., Suggett, D. J., Blackall, L. L., et al. (2021). Intracellular bacteria are common and taxonomically diverse in cultured and in hospite algal endosymbionts of coral reefs. *ISME J.* doi: 10.1038/s41396-021-00902-4 Online ahead of print
- Martinez Arbizu, P. (2019). *pairwiseAdonis: Pairwise Multilevel Comparison using Adonis. R Package Version 0.3.1*.
- Matthews, J. L., Raina, J. B., Kahlke, T., Seymour, J. R., van Oppen, M. J. H., and Suggett, D. J. (2020). Symbiodiniaceae-bacteria interactions: rethinking metabolite exchange in reef-building corals as multi-partner metabolic networks. *Environ. Microbiol.* 22, 1675–1687. doi: 10.1111/1462-2920.14918
- McDevitt-Irwin, J. M., Baum, J. K., Garren, M., and Vega Thurber, R. L. (2017). Responses of coral-associated bacterial communities to local and global stressors. *Front. Mar. Sci.* 4:262. doi: 10.3389/fmars.2017.00262
- McFall-Ngai, M., Hadfield, M. G., Bosch, T. C. G., Carey, H. V., Domazet-Lošo, T., Douglas, A. E., et al. (2013). Animals in a bacterial world, a new imperative for the life sciences. *Proc. Natl. Acad. Sci. U.S.A.* 110, 3229–3236.
- McMurdie, P. J., and Holmes, S. (2013). Phyloseq: an R package for reproducible interactive analysis and graphics of microbiome census data. *PLoS One* 8:e61217. doi: 10.1371/journal.pone.0061217
- Muscantine, L. (1990). “The role of symbiotic algae in carbon and energy flux in reef corals,” in *Ecosystems of the World*, ed. Z. Dubinsky (Amsterdam: Elsevier).
- Neave, M. J., Apprill, A., Ferrier-Pagès, C., and Voolstra, C. R. (2016). Diversity and function of prevalent symbiotic marine bacteria in the genus *Endozoicomonas*. *Appl. Microbiol. Biotechnol.* 100, 8315–8324. doi: 10.1007/s00253-016-7777-0
- Neave, M. J., Rachmawati, R., Xun, L., Michell, C. T., Bourne, D. G., Apprill, A., et al. (2017). Differential specificity between closely related corals and abundant *Endozoicomonas* endosymbionts across global scales. *ISME J.* 11, 186–200. doi: 10.1038/ismej.2016.95
- Nelson, C. E., Goldberg, S. J., Wegley Kelly, L., Haas, A. F., Smith, J. E., Rohwer, F., et al. (2013). Coral and macroalgal exudates vary in neutral sugar composition and differentially enrich reef bacterioplankton lineages. *ISME J.* 7, 962–979. doi: 10.1038/ismej.2012.161
- Oakley, C. A., Ameisemeier, M. F., Peng, L., Weis, V. M., Grossman, A. R., and Davy, S. K. (2015). Symbiosis induces widespread changes in the proteome of the model cnidarian *Aiptasia*. *Cell Microbiol.* 18, 1009–1023. doi: 10.1111/cmi.12564
- Peixoto, R. S., Rosado, P. M., Leite, D. C., de, A., Rosado, A. S., and Bourne, D. G. (2017). Beneficial microorganisms for corals (BMC): proposed mechanisms for coral health and resilience. *Front. Microbiol.* 8:341. doi: 10.3389/fmicb.2017.00341
- Peixoto, R. S., Sweet, M., and Bourne, D. G. (2019). Customized medicine for corals. *Front. Mar. Sci.* 6:1–5. doi: 10.3389/fmars.2019.00686
- Peixoto, R. S., Sweet, M., Villela, H. D. M., Cardoso, P., Thomas, T., Voolstra, C. R., et al. (2021). Coral probiotics: premise, promise, prospects. *Annu. Rev. Anim. Biosci.* 9, 265–288. doi: 10.1146/annurev-animal-090120-115444
- Pogoreutz, C., Voolstra, C. R., Rädcker, N., Weis, V., Cardenas, A., and Raina, J.-B. (2020). “The coral holobiont highlights the dependence of cnidarian animal hosts on their associated microbes,” in *Cellular Dialogues in the Holobiont*, eds T. C. Bosch and M. G. Hadfield (Boca Raton, FL: CRC Press), 91–118. doi: 10.1201/9780429277375
- Rädcker, N., Raina, J. B., Pernice, M., Perna, G., Guagliardo, P., Kilburn, M. R., et al. (2018). Using *Aiptasia* as a model to study metabolic interactions in cnidarian-symbiodinium symbioses. *Front. Physiol.* 9:214. doi: 10.3389/fphys.2018.00214
- Reshef, L., Koren, O., Loya, Y., Zilber-Rosenberg, I., and Rosenberg, E. (2006). The coral probiotic hypothesis. *Environ. Microbiol.* 8, 2068–2073. doi: 10.1111/j.1462-2920.2006.01148.x
- Robbins, S. J., Singleton, C. M., Chan, C. X., Messer, L. F., Geers, A. U., Ying, H., et al. (2019). A genomic view of the reef-building coral *Porites lutea* and its microbial symbionts. *Nat. Microbiol.* 4, 2090–2100. doi: 10.1038/s41564-019-0532-4
- Roder, C., Arif, C., Daniels, C., Weil, E., and Voolstra, C. R. (2014). Bacterial profiling of white plague disease across corals and oceans indicates a conserved and distinct disease microbiome. *Mol. Ecol.* 23, 965–974. doi: 10.1111/mec.12638
- Roder, C., Bayer, T., Aranda, M., Kruse, M., and Voolstra, C. R. (2015). Microbiome structure of the fungid coral *Ctenactis echinata* aligns with environmental differences. *Mol. Ecol.* 24, 3501–3511. doi: 10.1111/mec.13251
- Rognes, T., Flouri, T., Nichols, B., Quince, C., and Mahé, F. (2016). VSEARCH: a versatile open source tool for metagenomics. *PeerJ* 2016, 1–22. doi: 10.7717/peerj.2584
- Rohwer, F., Seguritan, V., Azam, F., and Knowlton, N. (2002). Diversity and distribution of coral-associated bacteria. *Mar. Ecol. Prog. Ser.* 243, 1–10. doi: 10.3354/meps243001
- Rosado, P. M., Leite, D. C. A., Duarte, G. A. S., Chaloub, R. M., Jospin, G., Nunes da Rocha, U., et al. (2019). Marine probiotics: increasing coral resistance to bleaching through microbiome manipulation. *ISME J.* 13, 921–936. doi: 10.1038/s41396-018-0323-6
- Rosenberg, E., Koren, O., Reshef, L., Efrony, R., and Zilber-Rosenberg, I. (2007). The role of microorganisms in coral health, disease and evolution. *Nat. Rev. Microbiol.* 5, 355–362. doi: 10.1038/nrmicro1635
- Rosbach, S., Cardenas, A., Perna, G., Duarte, C. M., and Voolstra, C. R. (2019). Tissue-specific microbiomes of the red sea giant clam *Tridacna maxima* highlight differential abundance of endozoicomonadaceae. *Front. Microbiol.* 10:2661. doi: 10.3389/fmicb.2019.02661
- Röthig, T., Costa, R. M., Simona, F., Baumgarten, S., Torres, A. F., Radhakrishnan, A., et al. (2016a). Distinct bacterial communities associated with the coral model *Aiptasia* in aposymbiotic and symbiotic states with symbiodinium. *Front. Mar. Sci.* 3:234. doi: 10.3389/fmars.2016.00234
- Röthig, T., Ochsenkühn, M. A., Roik, A., van der Merwe, R., and Voolstra, C. R. (2016b). Long-term salinity tolerance is accompanied by major restructuring of the coral bacterial microbiome. *Mol. Ecol.* 25, 1308–1323. doi: 10.1111/mec.13567
- Röthig, T., Roik, A., Yum, L. K., and Voolstra, C. R. (2017). Distinct bacterial microbiomes associate with the deep-sea coral *Eguchipsammia fistula* from the red sea and from aquaria settings. *Front. Mar. Sci.* 4:259. doi: 10.3389/fmars.2017.00259
- Schloss, P. D., Westcott, S. L., Ryabin, T., Hall, J. R., Hartmann, M., Hollister, E. B., et al. (2009). Introducing mothur: open-source, platform-independent, community-supported software for describing and comparing microbial communities. *Appl. Environ. Microbiol.* 75, 7537–7541. doi: 10.1128/AEM.01541-09
- Shibl, A. A., Isaac, A., Ochsenkühn, M. A., Cárdenas, A., Fei, C., Behringer, G., et al. (2020). Diatom modulation of select bacteria through use of two unique secondary metabolites. *Proc. Natl. Acad. Sci. U.S.A.* 117, 27445–27455. doi: 10.1073/pnas.2012088117
- Shnit-Orland, M., and Kushmaro, A. (2009). Coral mucus-associated bacteria: a possible first line of defense. *FEMS Microbiol. Ecol.* 67, 371–380. doi: 10.1111/j.1574-6941.2008.00644.x
- Simona, F., Zhang, H., and Voolstra, C. R. (2019). Evidence for a role of protein phosphorylation in the maintenance of the cnidarian–algal symbiosis. *Mol. Ecol.* 28, 5373–5386. doi: 10.1111/mec.15298
- Trench, R. K. (1993). Microalgal-invertebrate symbioses - a review. *Endocytobiosis Cell Res.* 9, 135–175.
- van Oppen, M. J. H., and Blackall, L. L. (2019). Coral microbiome dynamics, functions and design in a changing world. *Nat. Rev. Microbiol.* 17, 557–567. doi: 10.1038/s41579-019-0223-4
- Voolstra, C. R. (2013). A journey into the wild of the cnidarian model system *Aiptasia* and its symbionts. *Mol. Ecol.* 22, 4366–4368. doi: 10.1111/mec.12464
- Voolstra, C. R., Buitrago-López, C., Perna, G., Cárdenas, A., Hume, B. C. C., Rädcker, N., et al. (2020). Standardized short-term acute heat stress assays resolve historical differences in coral thermotolerance across microhabitat reef sites. *Glob. Chang. Biol.* 26, 4328–4343. doi: 10.1111/gcb.15148
- Voolstra, C. R., and Ziegler, M. (2020). Adapting with microbial help: microbiome flexibility facilitates rapid responses to environmental change. *BioEssays* 42:e2000004. doi: 10.1002/bies.202000004
- Wada, N., Pollock, F. J., Willis, B. L., Ainsworth, T., Mano, N., and Bourne, D. G. (2016). In situ visualization of bacterial populations in coral tissues: pitfalls and solutions. *PeerJ* 2016:e2424. doi: 10.7717/peerj.2424
- Wang, G., Tang, M., Wu, H., Dai, S., Li, T., Chen, C., et al. (2016). *Pyruvibacter mobilis* gen. nov., sp. nov., a marine bacterium from the culture broth of *Picocylindrum* sp. 122. *Int. J. Syst. Evol. Microbiol.* 66, 184–188. doi: 10.1099/ijsem.0.000692

- Wein, T., Dagan, T., Fraune, S., Bosch, T. C. G., Reusch, T. B. H., and Hülter, N. F. (2018). Carrying capacity and colonization dynamics of *Curvibacter* in the hydra host habitat. *Front. Microbiol.* 9:443. doi: 10.3389/fmicb.2018.00443
- Weis, V. M., Davy, S. K., Hoegh-Guldberg, O., Rodriguez-Lanetty, M., and Pringle, J. R. (2008). Cell biology in model systems as the key to understanding corals. *Trends Ecol. Evol.* 23, 369–376. doi: 10.1016/j.tree.2008.03.004
- Wolfowicz, I., Baumgarten, S., Voss, P. A., Hambleton, E. A., Voolstra, C. R., Hatta, M., et al. (2016). *Aiptasia* sp. larvae as a model to reveal mechanisms of symbiont selection in cnidarians. *Sci. Rep.* 6:32366. doi: 10.1038/srep32366
- Xiang, T., Hambleton, E. A., Denofrio, J. C., Pringle, J. R., and Grossman, A. R. (2013). Isolation of clonal axenic strains of the symbiotic dinoflagellate *Symbiodinium* and their growth and host specificity. *J. Phycol.* 49, 447–458. doi: 10.1111/jpy.12055
- Yetti, E., Thontowi, A., Yopi, Y., and Lisdiyanti, P. (2015). Screening of marine bacteria capable of degrading various polyaromatic hydrocarbons. *Squalen Bull. Mar. Fish. Postharvest Biotechnol.* 10, 121–127. doi: 10.15578/squalen.v10i3.123
- Ziegler, M., Grupstra, C. G. B., Barreto, M. M., Eaton, M., BaOmar, J., Zubier, K., et al. (2019). Coral bacterial community structure responds to environmental change in a host-specific manner. *Nat. Commun.* 10:3092. doi: 10.1038/s41467-019-10969-5
- Ziegler, M., Seneca, F. O., Yum, L. K., Palumbi, S. R., and Voolstra, C. R. (2017). Bacterial community dynamics are linked to patterns of coral heat tolerance. *Nat. Commun.* 8:14213. doi: 10.1038/ncomms14213

**Conflict of Interest:** The authors declare that the research was conducted in the absence of any commercial or financial relationships that could be construed as a potential conflict of interest.

Copyright © 2021 Costa, Cárdenas, Loussert-Fonta, Toullec, Meibom and Voolstra. This is an open-access article distributed under the terms of the Creative Commons Attribution License (CC BY). The use, distribution or reproduction in other forums is permitted, provided the original author(s) and the copyright owner(s) are credited and that the original publication in this journal is cited, in accordance with accepted academic practice. No use, distribution or reproduction is permitted which does not comply with these terms.





# Sex-Dependent Effects of the Microbiome on Foraging and Locomotion in *Drosophila suzukii*

Runhang Shu<sup>1</sup>, Daniel A. Hahn<sup>1,2</sup>, Edouard Jurkevitch<sup>3</sup>, Oscar E. Liburd<sup>1</sup>, Boaz Yuval<sup>4</sup> and Adam Chun-Nin Wong<sup>1,2\*</sup>

<sup>1</sup> Entomology and Nematology Department, University of Florida, Gainesville, FL, United States, <sup>2</sup> UF Genetics Institute, University of Florida, Gainesville, FL, United States, <sup>3</sup> Department of Plant Pathology and Microbiology, Faculty of Agriculture, Food and Environment, The Hebrew University of Jerusalem, Rehovot, Israel, <sup>4</sup> Department of Entomology, Faculty of Agriculture, Food and Environment, The Hebrew University of Jerusalem, Rehovot, Israel

## OPEN ACCESS

### Edited by:

Aram Mikaelyan,  
North Carolina State University,  
United States

### Reviewed by:

Yu Matsuura,  
University of the Ryukyus, Japan  
Brittany Leigh,  
Vanderbilt University, United States

### \*Correspondence:

Adam Chun-Nin Wong  
adamcnwong@ufl.edu

### Specialty section:

This article was submitted to  
Microbial Symbioses,  
a section of the journal  
Frontiers in Microbiology

Received: 20 January 2021

Accepted: 13 April 2021

Published: 10 May 2021

### Citation:

Shu R, Hahn DA, Jurkevitch E,  
Liburd OE, Yuval B and Wong AC-N  
(2021) Sex-Dependent Effects of the  
Microbiome on Foraging  
and Locomotion in *Drosophila suzukii*.  
Front. Microbiol. 12:656406.  
doi: 10.3389/fmicb.2021.656406

There is growing evidence that symbiotic microbes can influence multiple nutrition-related behaviors of their hosts, including locomotion, feeding, and foraging. However, how the microbiome affects nutrition-related behavior is largely unknown. Here, we demonstrate clear sexual dimorphism in how the microbiome affects foraging behavior of a frugivorous fruit fly, *Drosophila suzukii*. Female flies deprived of their microbiome (axenic) were consistently less active in foraging on fruits than their conventional counterparts, even though they were more susceptible to starvation and starvation-induced locomotion was notably more elevated in axenic than conventional females. Such behavioral change was not observed in male flies. The lag of axenic female flies but not male flies to forage on fruits is associated with lower oviposition by axenic flies, and mirrored by reduced food seeking observed in virgin females when compared to mated, gravid females. In contrast to foraging intensity being highly dependent on the microbiome, conventional and axenic flies of both sexes showed relatively consistent and similar fruit preferences in foraging and oviposition, with raspberries being preferred among the fruits tested. Collectively, this work highlights a clear sex-specific effect of the microbiome on foraging and locomotion behaviors in flies, an important first step toward identifying specific mechanisms that may drive the modulation of insect behavior by interactions between the host, the microbiome, and food.

**Keywords: microbiome, *Drosophila*, foraging, sex differences, locomotion, oviposition**

## INTRODUCTION

Food seeking and selection are crucial for the survival, growth, and reproduction of animals. The motivation to seek food and foraging preferences toward particular food sources involve complex integration of intrinsic (e.g., host physiological status and chemosensory perception) and extrinsic (e.g., food nutrient content and chemistry) signals. In most animals, both males and females can adjust their foraging behavior to achieve their nutritional goals and to avoid harmful components, often through the same behavioral and neurophysiological adaptations. Examples include increasing locomotion when starved to promote food searching and acquisition (Zhao et al., 2011; Yu et al., 2016), and the ability to sense or differentiate potential food sources based

on volatile cues released by the food as well as cues released by associated microbes (Becher et al., 2012; Stensmyr et al., 2012; Martini et al., 2014; Karageorgi et al., 2017; Goldberg et al., 2019; Kim et al., 2019). However, males and females are distinct in their foraging motivation and reproductive investments. For example, in many oviparous insects, females make foraging decisions to fulfill both their own nutritional needs (feeding) as well as those of their offspring (oviposition). Females also allocate a large amount of energy and resources to oogenesis, requiring significant nutrient intake from the diet (Simmons and Bradley, 1997; Terashima et al., 2005; Schultzhuis and Carney, 2017). These male and female specific differences in nutritional needs are likely to drive sex-specific patterns of foraging and diet selection behaviors (Lihoreau et al., 2016; Ehl et al., 2018; Roswell et al., 2019).

Symbiosis with microbes is an important intrinsic component of animal nutrition and physiology. Contributions of the gut microbiome to a host can vary from the digestion of dietary substrates to provisioning of essential micronutrients (Larsbrink et al., 2014; Wong et al., 2014; Kovatcheva-Datchary et al., 2015; Hu et al., 2018) among other functions, which can ultimately affect host feeding and diet selection behavior (Alcock et al., 2014; Akami et al., 2019). Specifically, in the model fly *Drosophila melanogaster*, symbiotic gut bacteria can influence host foraging by priming host olfactory-guided preferences toward specific bacteria on food (Wong et al., 2017; Qiao et al., 2019), and feeding by regulating host appetite toward specific food macronutrients (Leitão-Gonçalves et al., 2017; Wong et al., 2017). Other behaviors directly linked to foraging, especially locomotor activity, have also been shown to be modulated by the gut microbiome (Schretter et al., 2018). This emerging evidence supports the notion that symbiotic microbes are an integral part of the behavioral aspects of food-seeking and acquisition. However, how the microbiome interacts with host sex-specific differences in physiology and metabolic needs for reproduction to bring about changes in behavior is unclear. Additionally, the majority of studies on foraging preference and food selection have been conducted using semi- or fully defined artificial diets. The influence of the gut microbiome on host foraging toward more natural food sources remains underexplored.

*Drosophila suzukii* (Matsumura), a close relative of *D. melanogaster*, is a significant agricultural pest with a broad host range that can infest a large variety of small, soft-skinned fruits (Hauser, 2011; Walsh et al., 2011; Asplen et al., 2015). These flies have evolved a serrated ovipositor, unique among related *Drosophila*, to lay eggs inside ripening fruits where larvae feed and develop (Hickner et al., 2016; Cloonan et al., 2018). Like *D. melanogaster*, the *D. suzukii* microbiome is dominated by a few bacterial genera, and the composition can vary significantly by geographical location and across diets (Chandler et al., 2014; Vacchini et al., 2017; Bing et al., 2018; Fountain et al., 2018; Jiménez-Padilla et al., 2020). Research using axenic *D. suzukii* generated in the laboratory has demonstrated the microbiome is essential for *D. suzukii* development on fruit (strawberry and blueberry)-based diets (Bing et al., 2018). Given the known fruit hosts and the importance of the gut microbiome in host nutrition and developmental success, *D. suzukii* can serve as a tractable

model to study the relationship between the gut microbiome and foraging behavior.

In this study, we characterize the role of the gut microbiome in host foraging and locomotion using *D. suzukii* as a model. By quantifying the effects of the microbiome on flies' overall food-seeking and host preference in both sexes (using five different fruits that are considered their natural food sources), we have made several significant discoveries. First, we reveal a strong sex difference in microbiome-mediated effects on fly foraging. Axenic females had lower food-seeking activity than conventional females, even though they were more susceptible to mortality by starvation, and starvation-induced locomotor hyperactivity was exacerbated in axenic females. Yet, we did not observe the same microbiome effects in male flies. Further, we demonstrate that female flies' food seeking is strongly associated with egg production, by showing that axenic females laid significantly fewer eggs than conventional females, similar to virgins who also exhibited lower foraging activity than gravid females. Finally, we show that conventional and axenic flies of both sexes share similar fruit preferences; in females, their foraging and oviposition preferences toward the different fruits are tightly coupled. Altogether, our study provides novel evidence for sex-dependent effects of the microbiome on foraging and locomotion in *D. suzukii*. Sex-specific effects of the microbiome on behavior are likely prevalent across *Drosophila* species and other insects, given the evidence suggesting a significant role of microbial symbionts in insect oogenesis.

## MATERIALS AND METHODS

### Fly Husbandry

Wild *D. suzukii* were collected from blackberries grown in Hawthorne Florida (29°35'17" N 82° 5' 2" W) in August 2017. The population was subsequently raised on Formula 4-24® Instant *Drosophila* Medium (Carolina Biological Supply Company) supplemented with 2.5% brewer's yeast (MP Biomedical) in the laboratory at 24°C, 64% RH, 16:8 L:D cycle. Fruit-based diets were prepared using raspberries (Driscoll's Inc.), nectarines (PLU code: 4378, GEOFRUT Inc.), strawberries (Driscoll's Inc.), grapes (PLU code: 4023, Ahold Inc.), and blueberries (Driscoll's Inc.) purchased from grocery stores. Intact fruits and pitted nectarines were washed with deionized water and then macerated separately in a blender, followed by adding a solution of deionized water (13.7%), agar (0.6%), and Tegosept (0.15%), then dispensed in 50 ml bottles (VWR, United States).

### Generation of Axenic Flies

*Drosophila suzukii* mated females were allowed to lay eggs on the Instant *Drosophila* Medium overnight. Eggs were then collected in a mesh basket (2.54 cm diameter, Genesee Scientific, United States) using paintbrushes. Eggs were soaked in 0.01M sterile phosphate-buffered saline (PBS) to avoid dehydration. Axenic flies were generated using an established procedure (Ridley et al., 2013). Briefly, mesh baskets containing the eggs were soaked in 0.6% hypochlorite for 2.5 min two times. After dechoriation, embryos were rinsed three times with

sterile deionized water and then placed onto fruit-based diets or autoclaved Instant *Drosophila* Medium. These steps were performed in a biosafety level II cabinet (NuAire, United States) with aseptic techniques. Successful elimination of the fly microbiota was confirmed by plating homogenates of fly adults onto MRS medium (VWR, United States).

## Collection of Virgin Flies

*Drosophila suzukii* flies emerged within 18 h were anesthetized on a *Drosophila* Flypad (Genesee Scientific, United States) using CO<sub>2</sub> under a stereomicroscope and the virgin females were identified based on the presence of meconium on the ventral abdomen as well as their distinct ovipositors. Virgin females were then transferred onto autoclaved Instant *Drosophila* Medium for 7 days before conducting the foraging assay.

## Foraging and Oviposition Assays

*Drosophila suzukii* adult foraging assays were performed in transparent plastic arenas (350 × 260 × 150 mm) containing food patches made of 5 g mashed fruits loaded into open lids (25 mm diameter and 10 mm depth) and arranged in a randomized, circular array (Supplementary Figure 1). Groups of ten 5–10-day-old female or male flies were food-deprived for 15 h (provided with water), chilled on ice in microfuge tubes, before being placed at the center of the arena with the tube cap opened. Each arena was used as a biological replicate. A total number of 72 arenas were set up in the entire experiment (Conventional females, *N* = 26; Axenic females, *N* = 14; Conventional males, *N* = 17; Axenic males, *N* = 22). The number of flies on each fruit was scored at each of three-time points 7, 12, and 24 h after introduction to the arena. The number of eggs on each fruit was counted under a stereomicroscope after the 24 h-foraging assay. All fruits were purchased from grocery stores on the same day or a day before the assay. Because the fruits may vary across different batches, all four treatments (age-matched conventional female, axenic female, conventional male, and axenic male) with at least four replicates were set up on the same day. Data were aggregated from assays performed over three separate days, and day was modeled as a random factor.

## Locomotion Assays

*Drosophila suzukii* adult locomotion assays were performed in 9 cm diameter and 0.5 cm depth sterile Petri dishes that allowed free walking movement but restricted flight. Groups of eight 5–10-day-old conventional or axenic flies that had either been given open access to food or had been food-deprived for 15 h (provided with water) were placed into Petri dishes. Locomotion behaviors of flies were filmed in real-time using GigE cameras acA1300-60gc (Basler AG, Germany) for seven consecutive trials of 1 h duration from 12PM to 7PM on a laboratory bench under constant light condition and 23°C ambient temperature throughout the experiments. Each Petri dish contained eight flies that were tracked individually. Each fly in the assay was considered a replicate. For each experiment, four cameras were set up for four different groups of flies (female/male; conventional/axenic; and fed/starved), and each group was repeated once. Video footage was processed and

analyzed in EthoVision XT 15 software (Noldus, Netherlands). Slightly modified from a previous study (Schretter et al., 2018), we set 0.3 mm/s and 0.1 mm/s as the threshold walking speeds for characterizing the start and stop of movement of the flies, respectively. The LOWESS (Locally Weighted Scatterplot Smoothing) method was applied to reduce the tracking noise and the small movements of the fly (“body wobble”).

## Starvation Resistance Assay

Five-ten-day-old conventional or axenic flies were sorted into same-sex groups of 15–20 individuals on ice and placed onto vials provided with 10 ml 2% agar. The number of survivors was monitored twice daily until all flies were dead. Each group of flies was replicated three times in one experiment.

## Statistical Analysis

All analyses were performed using the statistical computing environment R (version 3.5.1). Foraging assay data were analyzed by fitting either a generalized linear mixed model (GLMM) or a linear mixed model with random effects accounting for the experimental arenas and experiment days. The total numbers of foraging flies in each arena at each time point were modeled as a function of foraging time, microbiome status, sex, and their interactions using the “lmer” function. The numbers of flies counted on each fruit at each time point were modeled as a function of fruit types, foraging time, microbiome status, sex, and their interactions using the “glmer” function with Poisson distribution in R package lme4 (Bates et al., 2015). Analysis of variance for the model objects was conducted using Wald chi-square test implemented in R package car (Fox et al., 2020). Inferential statistics for all pairwise comparisons were based on 95% confidence interval of estimated marginal means (EMMs) with Kenward-Roger adjusted degrees of freedom followed by Bonferroni correction. The numbers of eggs (log-transformed) laid on each fruit were modeled as a function of fruit type and microbiome status, and their interactions. Mann-Whitney *U* tests were applied to compare the total number of eggs in each arena laid by the conventional fly population and the axenic fly population. For locomotion data, pairwise comparisons between conventional and axenic flies or between fed and starved flies were analyzed with two-sample *t*-tests after meeting the normality assumption with the Shapiro-Wilk test. Cox proportional hazards regression models and pairwise log-rank tests implemented in the R package “survival” and “survminer” were used to analyze fly mortality under starvation (Kassambara et al., 2020). All plots were generated using the R package ggplot2 (Wickham et al., 2020).

## RESULTS

### Food-Seeking Is Reduced in Axenic Female, but Not Male *Drosophila suzukii*

To examine the microbiome’s impact on *D. suzukii* foraging, we adopted an adult foraging assay as previously described

(Wong et al., 2017). Groups of ten flies of only one sex were placed in arenas provided with five different open choices of fruits that are considered their natural hosts (**Supplementary Figure 1**). Both conventional (flies bearing a full microbiome) and axenic (microbiome-free) flies were tested. The total numbers of flies foraging across all five fruits increased from hour 7 to hour 24 after introduction to the arena for both axenic and conventional females, but not for either treatment in males (time:sex,  $P = 0.009$ , Wald, **Table 1**). Notably, the influence of the microbiome on flies' food-seeking varied by sex (microbiome:sex,  $P = 0.02$ , Wald, **Table 1**). A greater number of female flies with an intact microbiome were observed foraging than axenic flies at all three time points of observation (7 h,  $P < 0.001$ ; 12 h,  $P = 0.01$ ; 24 h,  $P = 0.004$ , Bonferroni adjusted) (**Figure 1**), but the microbiome had a limited effect on male food seeking (7 h,  $P = 0.07$ ; 12 h,  $P = 0.33$ ; 24 h,  $P = 0.99$ , Bonferroni adjusted) (**Figure 1**). We discuss time spent foraging across different fruits in section "The microbiome has subtle

effects on foraging and oviposition preferences toward different fruits" below.

## Axenic Female *D. suzukii* Are More Sensitive to Starvation

Foraging behavior is modulated by nutritional status (Toth et al., 2005; Pradhan et al., 2019). Accordingly, the lower numbers of axenic females observed on food compared to conventional females led us to hypothesize that axenic female *D. suzukii* have reduced hunger or appetite and would thus potentially be less sensitive to starvation. Contrary to our expectation, axenic female *D. suzukii* were more susceptible to death by starvation than conventional females ( $P = 7.4 \times 10^{-5}$ , log-rank) (**Supplementary Figure 2**). Male flies were generally less starvation-resistant than female flies (sex,  $P = 4.4 \times 10^{-10}$ , Cox regression), but no difference was observed between conventional and axenic males ( $P = 1$ , log-rank) (**Supplementary Figure 2**).

**TABLE 1** | Summary of the GLMM/LMM Wald chi-square tests outputs.

Food-seeking: Numbers of foraging flies in response to time, sex, and microbiome status (**Figure 1**).

Fixed effects	Chisq	Df	Pr(>Chisq)
Time	76.37586	2	2.60E-17
Microbiome	11.45179	1	0.000714
Sex	3.554124	1	0.059398
Time:microbiome	2.400064	2	0.301185
Time:sex	9.377775	2	0.009197
Microbiome:sex	5.724997	1	0.016725
Time:microbiome:sex	0.771933	2	0.679793

Oviposition preference: The number of eggs (log-transformed) in response to fruits and microbiome status (**Figure 4**).

Fixed effects	Chisq	Df	Pr(>Chisq)
Fruit	56.42379	4	1.63E-11
Microbiome	17.29838	1	3.19E-05
Fruit:microbiome	6.531558	4	0.162813

Fruit preference: Fruit choice in response to time, fruits, sex, and microbiome status (**Figure 4**).

Fixed effects	Chisq	Df	Pr(>Chisq)
Time	28.43574	2	6.69E-07
Fruits	210.3089	4	2.28E-44
Microbiome	8.975631	1	0.002736
Sex	3.605242	1	0.057598
Time:fruits	9.749983	8	0.283014
Time:microbiome	2.03618	2	0.361284
Fruits:microbiome	2.610014	4	0.62505
Time:sex	2.87031	2	0.238078
Fruits:sex	5.548641	4	0.235487
Microbiome:sex	4.322436	1	0.037613
Time:fruits:microbiome	24.03812	8	0.002258
Time:fruits:sex	9.106219	8	0.333415
Time:microbiome:sex	0.268544	2	0.874352
Fruits:microbiome:sex	2.778305	4	0.595583
Time:fruits:microbiome:sex	7.6383	8	0.469575



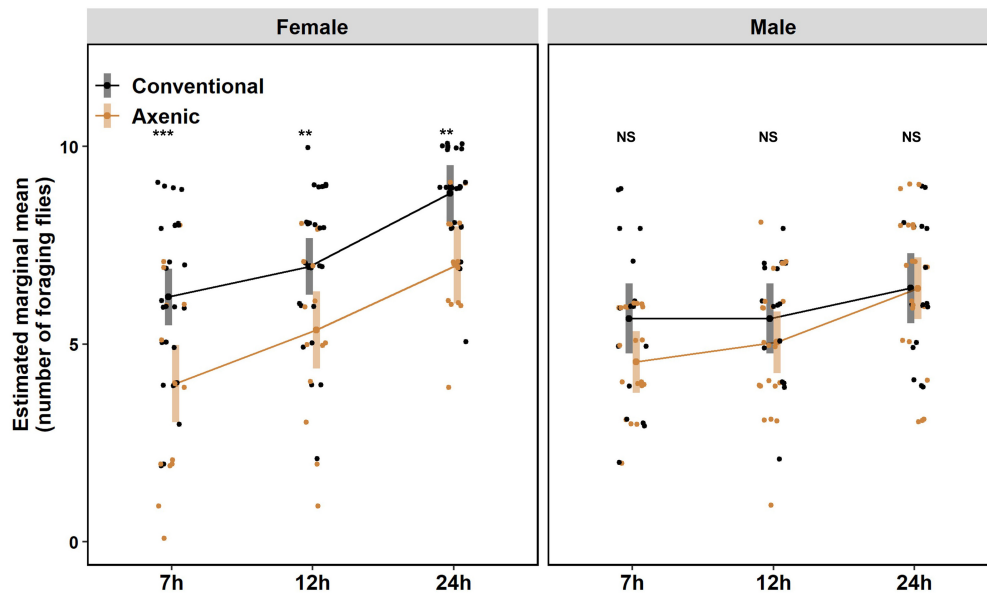


**FIGURE 1 |** Foraging of adult *Drosophila suzukii* on fruit-based foods. Conventional females,  $N = 26$ ; Axenic females,  $N = 14$ ; Conventional males,  $N = 17$ ; Axenic males,  $N = 22$  ( $N$  indicates the number of arenas). The numbers of flies foraging on food (foraging flies) at 7, 12, and 24 h were scored. The data were analyzed by fitting a linear mixed effects model (LMM) with time, microbiome status, and sex as fixed effects (and their interactions tested), while arenas and days were accounted for as random effects. Error bars represent estimated marginal means (EMMs) with 95% confidence interval. The observed number of foraging flies in each arena was represented in dots. Statistical significance between conventional and axenic flies is indicated with \* $P < 0.05$ , \*\* $P < 0.01$ , \*\*\* $P < 0.001$ . NS represents no statistical significance ( $P \geq 0.05$ ).  $P$ -values were adjusted by Bonferroni correction.

Starvation has been shown to increase animal locomotor activity (Lee and Park, 2004; Isabel et al., 2005; Dietrich et al., 2015; Yang et al., 2015; Yu et al., 2016), presumably to facilitate exploration of the environment and promote the chance of locating food. Interestingly, a recent study on *D. melanogaster* showed axenic females were hyperactive compared to conventional females, but male flies were not tested, and the effect of starvation was unknown (Schretter et al., 2018). Therefore, we compared locomotion between axenic and conventional *D. suzukii* of both sexes under fed and starved conditions. Consistent with the observation in *D. melanogaster*, axenic *D. suzukii* females were hyperactive compared to conventional females (Figure 2A). Fed axenic females traveled  $\sim 2.6$  times further ( $P = 3.5 \times 10^{-7}$ , Bonferroni adjusted) and walked for  $\sim 2.4$  times longer ( $P = 1.4 \times 10^{-8}$ , Bonferroni adjusted) than fed conventional females (Figures 2B,C).

Starvation-induced locomotor hyperactivity was more pronounced in axenic females than conventional females. Both distance moved and duration of movement were further increased in axenic females under starvation in the 7-h window, by 129% and 121%, respectively. In conventional females, starvation increased the duration of movement ( $P = 2.5 \times 10^{-10}$ , Bonferroni adjusted) but not the distance moved ( $P = 0.4$ , Bonferroni adjusted), owing to decreased walking speed in starved flies (Figures 2A–D and see Supplementary Table 2 for statistical details).

Male flies exhibited different locomotion patterns from female flies in response to microbiome elimination and starvation. At the beginning of the assay, starved males displayed significantly

greater moving distance and moving duration than fed males, regardless of the microbiome status (Supplementary Figure 3A). Interestingly, toward the later time points (from 4 to 7 h), the locomotion of conventional fed males was significantly elevated, with up to a 7.6 times increase in moving distance and five times increase in moving duration (see Supplementary Figures 3B,C and Supplementary Table 2 for statistical details).

## Egg-Laying on Fruits Is Dramatically Reduced in Axenic *D. suzukii*

The reduced food seeking in axenic *D. suzukii* occurs only in females, seemingly contradicting the higher sensitivity of females to starvation, both in starvation resistance and starvation-induced locomotor response. Based on these observations, we hypothesized that the female-specific microbiome effect on foraging might be associated with oviposition, because females forage for fruits to lay eggs in addition to their own consumption. In fact, we observed that conventional female populations laid over five times more eggs than the axenic female populations 24 h after being placed in the arenas. The average numbers of eggs laid by the conventional females were  $76 \pm 7.3$  (SEM), compared to  $14 \pm 2.8$  (SEM) laid by axenic females in each arena ( $W = 297$ ,  $P = 2.2 \times 10^{-6}$ , Mann-Whitney  $U$  test) (Figure 3). To further elucidate the relationship between food seeking and egg laying, we also compared foraging between virgin (no egg laying) and gravid flies. As expected, conventional virgin flies were less active in seeking food than conventional gravid flies, but the difference was only significant at the early time point

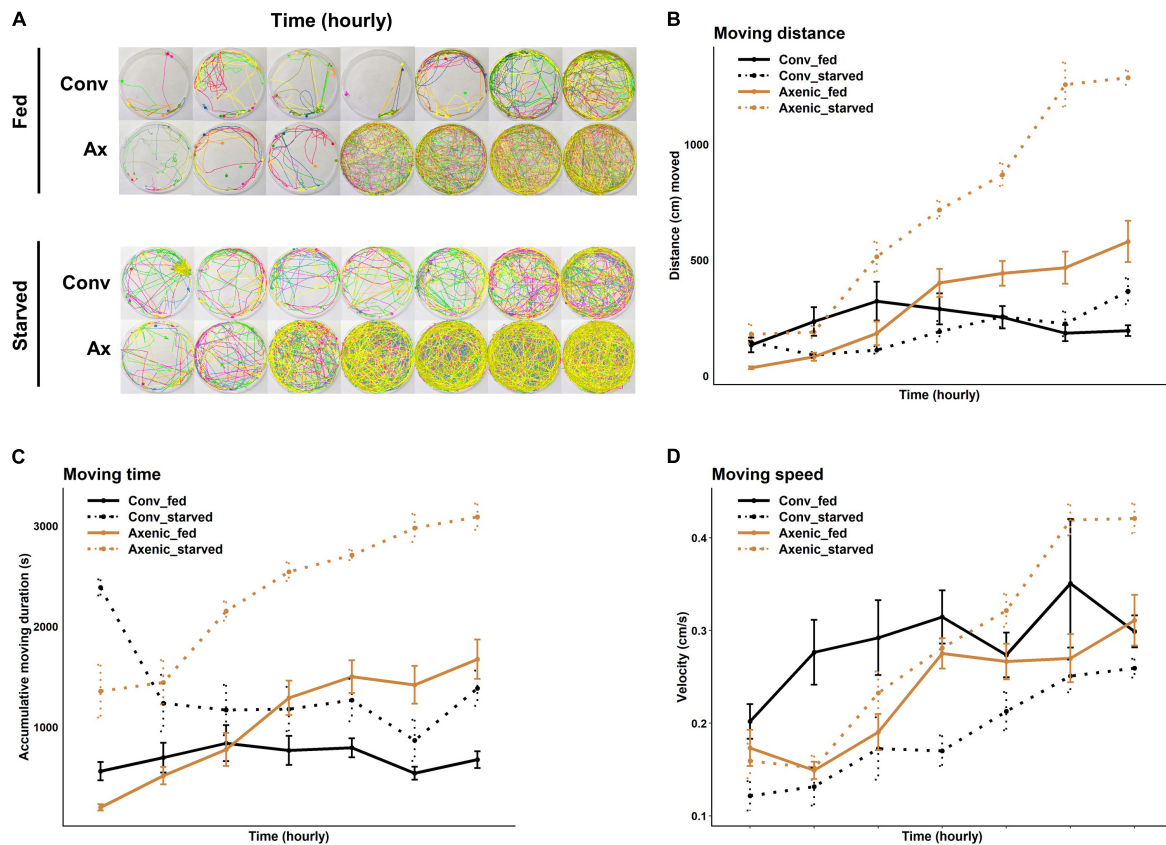


**FIGURE 2 |** Effects of the microbiome on locomotor activities of fed or starved female *Drosophila suzukii*. **(A)** Movement profiles of groups of eight conventional (Conv) and axenic (Ax) flies in the locomotion assay at 1 h intervals. **(B)** Hourly moving distance, **(C)** moving time, and **(D)** moving speed of fed or starved conventional flies (black lines) and axenic flies (golden lines) during the 7 h. **(B–D)** Fed conventional flies,  $n = 16$ ; starved conventional flies,  $n = 16$ ; fed axenic flies,  $n = 16$ ; starved axenic flies,  $n = 16$ .  $n$  indicates the number of flies tracked. The error bars represent the means  $\pm$  SEM (standard error of the means). All pairwise comparisons were analyzed with two-sample  $t$ -tests after meeting the normality assumption with Shapiro-Wilk test. Full statistical details are in **Supplementary Table 2**.

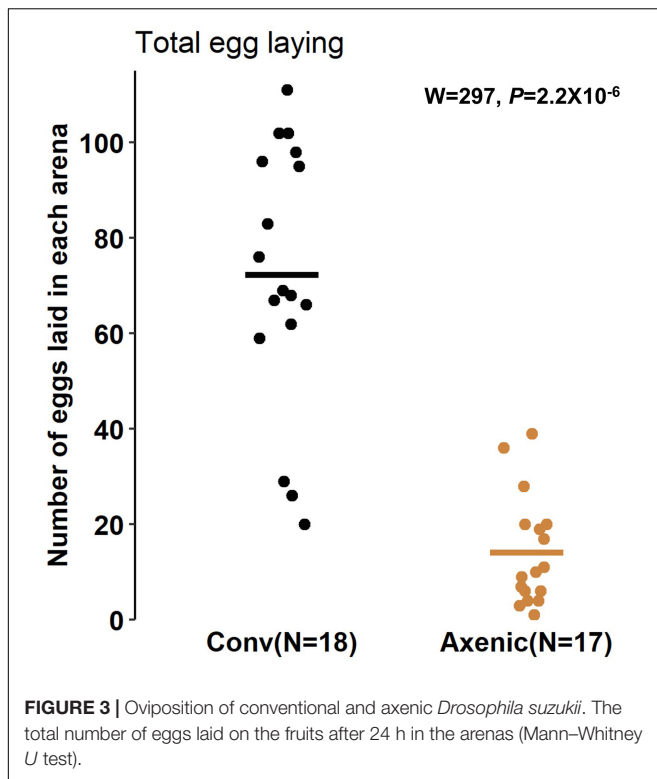
(7 h,  $P = 0.027$ , Bonferroni adjusted) (**Supplementary Figure 4**). Also, no difference in food seeking between virgin and gravid flies was observed when they were axenic (7 h,  $P = 0.24$ ; 12 h,  $P = 0.17$ ; 24 h,  $P = 0.60$ , Bonferroni adjusted) (see **Supplementary Figure 4** and **Supplementary Table 1** for statistical details). Together, our data point to reduce egg production and laying as a possible mechanism for reduced foraging behavior in axenic flies, but additional factors are likely involved in the microbiome-dependent effect on female food seeking.

## The Microbiome Has Subtle Effects on *D. suzukii* Foraging and Oviposition Preferences Toward Different Fruits

In addition to overall food seeking and total egg production, we examined the microbiome's impact on *D. suzukii* fruit preferences. Conventional and axenic flies of both sexes displayed similar relative fruit preferences in foraging (fruit:sex,  $P = 0.24$ ; fruit:microbiome,  $P = 0.63$ ; fruit:microbiome:sex,  $P = 0.60$ , Wald; **Table 1**). In the conventional populations, female flies preferred foraging on raspberries over strawberries ( $P = 0.0002$ , Bonferroni

adjusted), blueberries ( $P < 0.0001$ , Bonferroni adjusted), nectarines ( $P < 0.0001$ , Bonferroni adjusted), and grapes (*Vitis vinifera*) ( $P < 0.0001$ , Bonferroni adjusted) (**Figure 4A**). Male flies were most attracted to raspberries and blueberries, followed by nectarines ( $P = 0.0053$ , Bonferroni adjusted), strawberries ( $P = 0.007$ , Bonferroni adjusted), and grapes ( $P = 0.0001$ , Bonferroni adjusted) (**Figure 4A** and see **Supplementary Table 1** for statistical details). Subtle differences in fruit preferences were observed in axenic flies. Specifically, a reduced preference for blueberries was detected in axenic males, and the preference for raspberries was less pronounced in axenic females than in conventional females.

Aligning with the foraging preference, conventional females preferred laying eggs on raspberries, distributing 41.9% of the eggs on raspberries, followed by 25.7% on nectarines, 15.3% on blueberries ( $P = 0.02$ , Bonferroni adjusted), 9.9% on strawberries ( $P < 0.0001$ , Bonferroni adjusted), and 7.3% on grapes ( $P < 0.0001$ , Bonferroni adjusted) (**Figure 4B**). Although axenic flies laid significantly fewer eggs than conventional flies, microbiome's effect on oviposition preference was not significant (fruit:microbiome,  $P = 0.16$ , Wald, **Table 1**). The



relative proportion of eggs laid on raspberries by axenic females was 43.8%, followed by 21.7% on blueberries, 16.7% on nectarines, 10.8% on grapes ( $P = 0.01$ , Bonferroni adjusted), and 7.1% on strawberries ( $P = 0.001$ , Bonferroni adjusted) (Figure 4C). Together, our results suggest that *D. suzukii* female foraging preference generally aligns with oviposition preferences, regardless of the flies' microbiome status.

Given that female *D. suzukii* distributed their eggs across the different fruits, it raises the question of whether flies developing on different fruits in early life may differ in their later-life foraging preferences. To test this, we raised the flies on three different fruits (raspberry, strawberry, and nectarine) for one (F1) or five generations (F5), then subjected the flies to the foraging assays offered with the different fruits. Our results suggest that the foraging fruit preferences of *D. suzukii* are not dependent on their diet history. Regardless of the fruit they were raised on, the flies maintained the strongest preference toward raspberries and a similar order of preference on the other fruits. The results are consistent regardless of whether the flies were raised on those fruits for one or five generations (Supplementary Figure 5 and Supplementary Table 3).

## DISCUSSION

Using a non-model *Drosophila* system, our experiments show significant effects of the microbiome on three discrete but connected host behaviors: foraging, oviposition, and locomotion. These findings join a growing body of literature demonstrating that the gut microbiome contributes to individual patterns of

animal behavior, by way of modulating internal physiological processes and the nervous system (Ben-Ami et al., 2010; Alcock et al., 2014; Mayer et al., 2015; Wong et al., 2017; Akami et al., 2019; Morimoto et al., 2019; Hosokawa and Fukatsu, 2020). Our results show that food seeking in female, but not male *D. suzukii*, is influenced by the fly's microbiome. Lower food seeking in axenic females is associated with reduced egg production but conflicted with the flies' higher locomotor response and susceptibility to starvation, suggesting that the flies might prioritize foraging for oviposition sites for their progeny over their own feeding. This is also supported by the close alignment between fly foraging and oviposition preferences, with raspberries being the most preferred fruit among the five fruits tested.

Our finding of decreased egg laying in axenic *D. suzukii* is in line with previous studies on other insects showing that symbionts can promote host reproduction, including mosquitoes (Gaio et al., 2011; Coon et al., 2016), olive fruit fly (Jose et al., 2019), Queensland fruit fly (Nguyen et al., 2020), the bean bug *Riptortus pedestris* (Lee et al., 2017), and *Drosophila melanogaster* (Leitão-Gonçalves et al., 2017). Specifically, there is emerging evidence for the role of microbial symbionts in insect oogenesis. In *D. melanogaster*, the gut microbiome has been shown to contribute to oogenesis in two independent studies. Elgart et al. (2016) found that reduction in oogenesis of axenic female flies is associated with reduced transcription and enzymatic activities of *Aldh* (Aldehyde dehydrogenase) in the ovary. *Aldh* expression and the normal oogenesis phenotype could be restored by re-introduction of a specific *Acetobacter* gut bacterium to the flies. Gnainsky et al. (2021) suggested that specific gut bacteria provision an essential B vitamin (riboflavin) and mitochondrial co-enzymes to the host to support oogenesis. While further research is needed to elucidate the involvement of these molecular pathways in microbiome-dependent egg production in *D. suzukii*, our study is the first to discover that the microbiome-dependent effects on egg production could have an effect on the foraging behavior of the host insects.

Egg production requires nutrient acquisition and allocation (i.e., vitellogenin) to the oocytes. A recent study on *D. melanogaster* showed egg production depends on the upregulation of the pentose phosphate pathway in the germline, which in turn affects sugar feeding (Carvalho-Santos et al., 2020). Therefore, foraging signals are likely elicited or suppressed during the pre-oviposition state, corresponding to nutritional needs for egg production. In *Aedes* mosquitoes, vitellogenin synthesis in the fat body is upregulated after a blood or sugar meal, and the elevated expression of a specific vitellogenin gene (*Vg-2*) has been shown to suppress host-seeking behavior (Hansen et al., 2014; Dittmer et al., 2019). Conserved mechanisms governing the equilibrium between foraging, egg production, and egg-laying behavior may also exist in other insects. More recently, a study on Queensland fruit fly highlights transgenerational effects of the parental microbiome on offspring fecundity (Nguyen et al., 2020). Therefore, it is also plausible that the microbiome could exert long-term effects on the host fly germline that ultimately shapes their hosts' foraging and oviposition strategies. Besides effects on

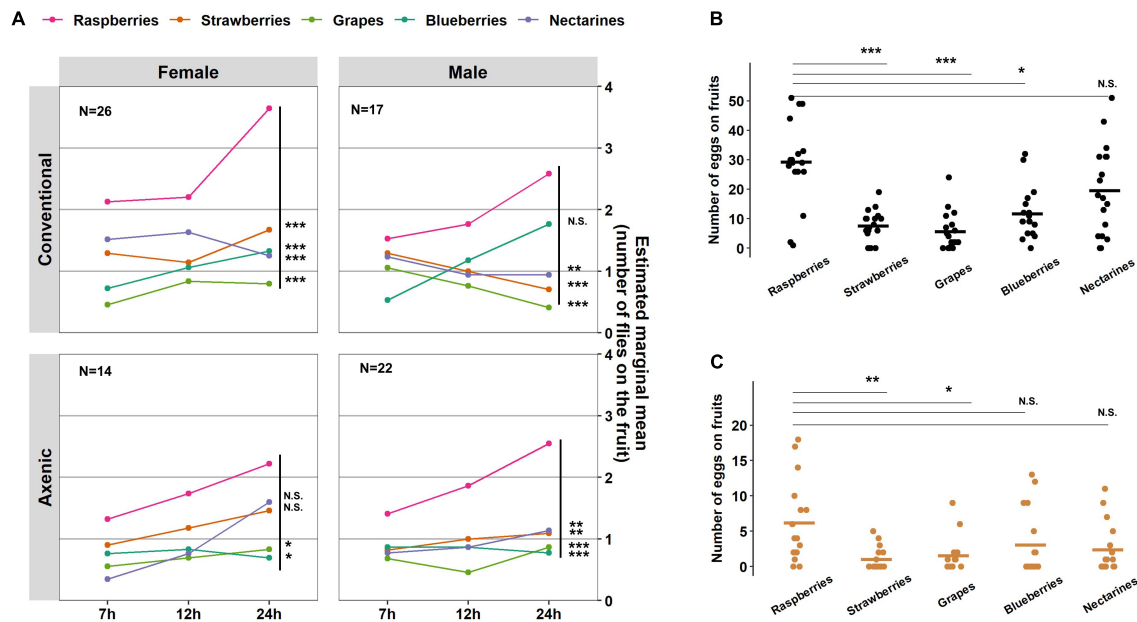


**FIGURE 4 |** Effects of the microbiome on *Drosophila suzukii* fruit preferences and oviposition preference. **(A)** A generalized linear mixed model (GLMM; Poisson) was applied to analyze the number of flies on each fruit in response to time, microbiome status, and sex as fixed effects (and their interactions tested), while arenas and days were accounted for as random effects. The number of eggs laid on each fruit by **(B)** the conventional fly populations or **(C)** the axenic fly populations. Statistical significance between raspberries and the other four fruits is indicated with \* $P < 0.05$ , \*\* $P < 0.01$ , \*\*\* $P < 0.001$ . NS represents no statistical significance ( $P \geq 0.05$ ). The crossbars represent mean values.  $N$  indicates the number of arenas with each containing ten *D. suzukii* adults.  $P$ -values were adjusted by Bonferroni correction.

food seeking and oviposition, our results demonstrate sexual dimorphism in locomotion in axenic flies. Our locomotion data corroborate recent findings in *D. melanogaster*, showing axenic females were inherently hyperactive compared to conventional females (Schretter et al., 2018). We show that starvation-induced hyperactive locomotion was exacerbated in axenic females. In contrast, the locomotion in male *D. suzukii* was less affected by the microbiome. In *D. melanogaster*, it is believed that an enzyme (xylose isomerase) encoded by a specific fly gut commensal bacterium (*Lactobacillus brevis*) can rescue fly locomotion in axenic flies to levels similar to conventional flies by modulating host sugar metabolism and possibly octopamine signaling (Schretter et al., 2018). Interestingly, *Lactobacillus brevis* was not found in our *D. suzukii* flies (data not shown), but other gut bacteria we have detected in *D. suzukii* (including *Bacillus* sp. and *Enterobacter* sp.) might encode this enzyme (Amore et al., 1989; Brat et al., 2009; Taghavi et al., 2010). Assuming the same bacteria-mediated mechanism is at play in controlling *D. suzukii* locomotion as in *D. melanogaster*, a plausible explanation is that there is a sex difference in fly behavioral output in response to the same microbiome-dependent effector(s) (or the lack of such effectors). For instance, octopamine signaling has been shown to drive aggression (Hoyer et al., 2008) and plasticity responses to endurance exercise (Sujkowski et al., 2017) specifically in male *D. melanogaster*, while for females, it can stimulate post-mating behaviors, including oviposition (Rezával et al., 2014).

Taken together, our work, using a non-model fruit fly, provides the first demonstration of a role for the microbiome in host foraging behavior associated with changes in host physiological

state. The interrelationship between host-microbe symbiosis, oviposition, and foraging might be ubiquitous across insect taxa, given that the role of symbiotic microbes in insect oogenesis has been established in different insects. The knowledge of how commonly the microbiome affects foraging and oviposition behaviors opens new research avenues regarding microbiomes as key regulators of animal behavior. It could also serve as a basis for innovative strategies to control pest insects by diminishing their tendency to forage and oviposit on crops, via disruption of their microbiomes to achieve long-term physiological and behavioral changes.

## DATA AVAILABILITY STATEMENT

The original contributions presented in the study are included in the article/**Supplementary Material**, further inquiries can be directed to the corresponding author/s.

## AUTHOR CONTRIBUTIONS

AW and RS conceived the ideas, designed the methodology, and wrote the initial manuscript draft. RS conducted the experiments, collected the data, and led the statistical analyses. DH, EJ, OL, and BY critically reviewed the methodology and results. All authors contributed critically to the manuscript writing and gave approval for the final submission.



## FUNDING

This work was supported by the BARD US-Israel Agricultural Research and Development Fund (US-5179-19).

## ACKNOWLEDGMENTS

We thank Michael Costa, Tiffany Royle, Lewis Culver, and other members of the Wong lab for thoughtful

discussion throughout this study. We also thank Lindsay Campbell and Leo Ohyama for technical advice on statistics.

## SUPPLEMENTARY MATERIAL

The Supplementary Material for this article can be found online at: <https://www.frontiersin.org/articles/10.3389/fmicb.2021.656406/full#supplementary-material>

## REFERENCES

- Akami, M., Andongma, A. A., Zhengzhong, C., Nan, J., Khaeso, K., Jurkevitch, E., et al. (2019). Intestinal bacteria modulate the foraging behavior of the oriental fruit fly *Bactrocera dorsalis* (Diptera: Tephritidae). *PLoS One* 14:e0210109. doi: 10.1371/journal.pone.0210109
- Alcock, J., Maley, C. C., and Aktipis, C. A. (2014). Is eating behavior manipulated by the gastrointestinal microbiota? Evolutionary pressures and potential mechanisms. *Bioessays* 36, 940–949. doi: 10.1002/bies.201400071
- Amore, R., Wilhelm, M., and Hollenberg, C. P. (1989). The fermentation of xylose—an analysis of the expression of *Bacillus* and *Actinoplanes* xylose isomerase genes in yeast. *Appl. Microbiol. Biotechnol.* 30, 351–357. doi: 10.1007/BF00296623
- Asplen, M. K., Anfora, G., Biondi, A., Choi, D.-S., Chu, D., Daane, K. M., et al. (2015). Invasion biology of spotted wing *Drosophila* (*Drosophila suzukii*): a global perspective and future priorities. *J. Pest Sci.* 88, 469–494. doi: 10.1007/s10340-015-0681-z
- Bates, D., Mächler, M., Bolker, B., and Walker, S. (2015). Fitting linear mixed-effects models using lme4. *J. Stat. Softw.* 67, 1–48. doi: 10.18637/jss.v067.i01
- Becher, P. G., Flick, G., Rozpędowska, E., Schmidt, A., Hagman, A., Lebreton, S., et al. (2012). Yeast, not fruit volatiles mediate *Drosophila melanogaster* attraction, oviposition and development. *Funct. Ecol.* 26, 822–828. doi: 10.1111/j.1365-2435.2012.02006.x
- Ben-Ami, E., Yuval, B., and Jurkevitch, E. (2010). Manipulation of the microbiota of mass-reared Mediterranean fruit flies *Ceratitis capitata* (Diptera: Tephritidae) improves sterile male sexual performance. *ISME J.* 4, 28–37. doi: 10.1038/ismej.2009.82
- Bing, X., Gerlach, J., Loeb, G., and Buchon, N. (2018). Nutrient-dependent impact of microbes on *Drosophila suzukii* Development. *mBio* 9:e02199-17. doi: 10.1128/mBio.02199-17
- Brat, D., Boles, E., and Wiedemann, B. (2009). Functional expression of a bacterial xylose isomerase in *Saccharomyces cerevisiae*. *Appl. Environ. Microbiol.* 75, 2304–2311. doi: 10.1128/AEM.02522-08
- Carvalho-Santos, Z., Cardoso-Figueiredo, R., Elias, A. P., Tastekin, I., Baltazar, C., and Ribeiro, C. (2020). Cellular metabolic reprogramming controls sugar appetite in *Drosophila*. *Nat. Metab.* 2, 958–973. doi: 10.1038/s42255-020-0266-x
- Chandler, J. A., James, P. M., Jospin, G., and Lang, J. M. (2014). The bacterial communities of *Drosophila suzukii* collected from undamaged cherries. *PeerJ* 2:e474. doi: 10.7717/peerj.474
- Cloonan, K. R., Abraham, J., Angeli, S., Syed, Z., and Rodriguez-Saona, C. (2018). Advances in the chemical ecology of the spotted wing *Drosophila* (*Drosophila suzukii*) and its applications. *J. Chem. Ecol.* 44, 922–939. doi: 10.1007/s10886-018-1000-y
- Coon, K. L., Brown, M. R., and Strand, M. R. (2016). Gut bacteria differentially affect egg production in the anautogenous mosquito *Aedes aegypti* and facultatively autogenous mosquito *Aedes atropalpus* (Diptera: Culicidae). *Parasit. Vectors* 9:375. doi: 10.1186/s13071-016-1660-9
- Dietrich, M. O., Zimmer, M. R., Bober, J., and Horvath, T. L. (2015). Hypothalamic AgRP neurons drive stereotypic behaviors beyond feeding. *Cell* 160, 1222–1232. doi: 10.1016/j.cell.2015.02.024
- Dittmer, J., Alafndi, A., and Gabrieli, P. (2019). Fat body-specific vitellogenin expression regulates host-seeking behaviour in the mosquito *Aedes albopictus*. *PLoS Biol.* 17:e3000238. doi: 10.1371/journal.pbio.3000238
- Ehl, S., Hostert, K., Korsch, J., Gros, P., and Schmitt, T. (2018). Sexual dimorphism in the alpine butterflies *Boloria pales* and *Boloria napaea*: differences in movement and foraging behavior (Lepidoptera: Nymphalidae). *Insect Sci.* 25, 1089–1101. doi: 10.1111/1744-7917.12494
- Elgart, M., Stern, S., Salton, O., Gnainsky, Y., Heifetz, Y., and Soen, Y. (2016). Impact of gut microbiota on the fly's germ line. *Nat. Commun.* 7, 1–11. doi: 10.1038/ncomms11280
- Fountain, M. T., Bennett, J., Cobo-Medina, M., Ruiz, R. C., Deakin, G., Delgado, A., et al. (2018). Alimentary microbes of winter-form *Drosophila suzukii*. *Insect Mol. Biol.* 27, 383–392. doi: 10.1111/imb.12377
- Fox, J., Weisberg, S., Price, B., Adler, D., Bates, D., Baud-Bovy, G., et al. (2020). *car: Companion to Applied Regression*. Available online at: <https://CRAN.R-project.org/package=car> (accessed December 21, 2020).
- Gaio, A., de, O., Gusmão, D. S., Santos, A. V., Berbert-Molina, M. A., Pimenta, P. F., et al. (2011). Contribution of midgut bacteria to blood digestion and egg production in *Aedes aegypti* (diptera: culicidae) (L.). *Parasit. Vectors* 4:105. doi: 10.1186/1756-3305-4-105
- Gnainsky, Y., Zfanya, N., Elgart, M., Omri, E., Brandis, A., Mehlman, T., et al. (2021). Systemic regulation of host energy and oogenesis by microbiome-derived mitochondrial coenzymes. *Cell Rep.* 34:108583. doi: 10.1016/j.celrep.2020.108583
- Goldberg, J. K., Pintel, G., Weiss, S. L., and Martins, E. P. (2019). Predatory lizards perceive plant-derived volatile odorants. *Ecol. Evol.* 9, 4733–4738. doi: 10.1002/ece3.5076
- Hansen, I. A., Attardo, G. M., Rodriguez, S. D., and Drake, L. L. (2014). Four-way regulation of mosquito yolk protein precursor genes by juvenile hormone-, ecdysone-, nutrient-, and insulin-like peptide signaling pathways. *Front. Physiol.* 5:103. doi: 10.3389/fphys.2014.00103
- Hauser, M. (2011). A historic account of the invasion of *Drosophila suzukii* (Matsumura) (Diptera: Drosophilidae) in the continental United States, with remarks on their identification. *Pest Manag. Sci.* 67, 1352–1357. doi: 10.1002/ps.2265
- Hickner, P. V., Rivaldi, C. L., Johnson, C. M., Siddappaji, M., Raster, G. J., and Syed, Z. (2016). The making of a pest: insights from the evolution of chemosensory receptor families in a pestiferous and invasive fly, *Drosophila suzukii*. *BMC Genomics* 17:648. doi: 10.1186/s12864-016-2983-9
- Hosokawa, T., and Fukatsu, T. (2020). Relevance of microbial symbiosis to insect behavior. *Curr. Opin. Insect Sci.* 39, 91–100. doi: 10.1016/j.cois.2020.03.004
- Hoyer, S. C., Eckart, A., Herrel, A., Zars, T., Fischer, S. A., Hardie, S. L., et al. (2008). Octopamine in male aggression of *Drosophila*. *Curr. Biol.* 18, 159–167. doi: 10.1016/j.cub.2007.12.052
- Hu, Y., Sanders, J. G., Łukasik, P., D'Amelio, C. L., Millar, J. S., Vann, D. R., et al. (2018). Herbivorous turtle ants obtain essential nutrients from a conserved nitrogen-recycling gut microbiome. *Nat. Commun.* 9:964. doi: 10.1038/s41467-018-03357-y
- Isabel, G., Martin, J.-R., Chidami, S., Veenstra, J. A., and Rosay, P. (2005). AKH-producing neuroendocrine cell ablation decreases trehalose and induces behavioral changes in *Drosophila*. *Am. J. Physiol. Regul. Integr. Comp. Physiol.* 288, R531–R538. doi: 10.1152/ajpregu.00158.2004

- Jiménez-Padilla, Y., Esan, E. O., Floate, K. D., and Sinclair, B. J. (2020). Persistence of diet effects on the microbiota of *Drosophila suzukii* (Diptera: Drosophilidae). *Can. Entomol.* 152, 516–531. doi: 10.4039/tce.2020.37
- Jose, P. A., Ben-Yosef, M., Jurkevitch, E., and Yuval, B. (2019). Symbiotic bacteria affect oviposition behavior in the olive fruit fly *Bactrocera oleae*. *J. Insect Physiol.* 117:103917. doi: 10.1016/j.jinsphys.2019.103917
- Karageorgi, M., Bräcker, L. B., Lebreton, S., Minervino, C., Cavey, M., Siju, K. P., et al. (2017). Evolution of multiple sensory systems drives novel egg-laying behavior in the fruit pest *Drosophila suzukii*. *Curr. Biol.* 27, 847–853. doi: 10.1016/j.cub.2017.01.055
- Kassambara, A., Kosinski, M., Biecek, P., and Fabian, S. (2020). *survminer: Drawing Survival Curves using "ggplot2"*. Available online at: <https://CRAN.R-project.org/package=survminer> (accessed December 21, 2020).
- Kim, D.-R., Cho, G., Jeon, C.-W., Weller, D. M., Thomashow, L. S., Paulitz, T. C., et al. (2019). A mutualistic interaction between *Streptomyces* bacteria, strawberry plants and pollinating bees. *Nat. Commun.* 10:4802. doi: 10.1038/s41467-019-12785-3
- Kovatcheva-Datchary, P., Nilsson, A., Akrami, R., Lee, Y. S., De Vadder, F., Arora, T., et al. (2015). Dietary fiber-induced improvement in glucose metabolism is associated with increased abundance of *Prevotella*. *Cell Metab.* 22, 971–982. doi: 10.1016/j.cmet.2015.10.001
- Larsbrink, J., Rogers, T. E., Hemsworth, G. R., McKee, L. S., Tauzin, A. S., Spadiut, O., et al. (2014). A discrete genetic locus confers xyloglucan metabolism in select human gut Bacteroidetes. *Nature* 506, 498–502. doi: 10.1038/nature12907
- Lee, G., and Park, J. H. (2004). Hemolymph sugar homeostasis and starvation-induced hyperactivity affected by genetic manipulations of the adipokinetic hormone-encoding gene in *Drosophila melanogaster*. *Genetics* 167, 311–323. doi: 10.1534/genetics.167.1.311
- Lee, J. B., Park, K.-E., Lee, S. A., Jang, S. H., Eo, H. J., Jang, H. A., et al. (2017). Gut symbiotic bacteria stimulate insect growth and egg production by modulating hexamerin and vitellogenin gene expression. *Dev. Comp. Immunol.* 69, 12–22. doi: 10.1016/j.dci.2016.11.019
- Leitão-Gonçalves, R., Carvalho-Santos, Z., Francisco, A. P., Fioreze, G. T., Anjos, M., Baltazar, C., et al. (2017). Commensal bacteria and essential amino acids control food choice behavior and reproduction. *PLoS Biol.* 15:e2000862. doi: 10.1371/journal.pbio.2000862
- Lihoreau, M., Poissonnier, L.-A., Isabel, G., and Dussutour, A. (2016). *Drosophila* females trade off good nutrition with high-quality oviposition sites when choosing foods. *J. Exp. Biol.* 219, 2514–2524. doi: 10.1242/jeb.142257
- Martini, X., Pelz-Stelinski, K. S., and Stelinski, L. L. (2014). Plant pathogen-induced volatiles attract parasitoids to increase parasitism of an insect vector. *Front. Ecol. Evol.* 2:8. doi: 10.3389/fevo.2014.00008
- Mayer, E. A., Tillisch, K., and Gupta, A. (2015). Gut/brain axis and the microbiota. *J. Clin. Invest.* 125, 926–938. doi: 10.1172/JCI76304
- Morimoto, J., Nguyen, B., Tabrizi, S. T., Lundbäck, I., Taylor, P. W., Ponton, F., et al. (2019). Commensal microbiota modulates larval foraging behaviour, development rate and pupal production in *Bactrocera tryoni*. *BMC Microbiol.* 19:286. doi: 10.1186/s12866-019-1648-7
- Nguyen, B., Than, A., Dinh, H., Morimoto, J., and Ponton, F. (2020). Parental microbiota modulates offspring development, body mass and fecundity in a polyphagous fruit fly. *Microorganisms* 8:1289. doi: 10.3390/microorganisms8091289
- Pradhan, S., Quilez, S., Homer, K., and Hendricks, M. (2019). Environmental programming of adult foraging behavior in *C. elegans*. *Curr. Biol.* 29, 2867–2879.e4. doi: 10.1016/j.cub.2019.07.045
- Qiao, H., Keesey, I. W., Hansson, B. S., and Knaden, M. (2019). Gut microbiota affects development and olfactory behavior in *Drosophila melanogaster*. *J. Exp. Biol.* 222(Pt 5):jeb192500. doi: 10.1242/jeb.192500
- Rezával, C., Nojima, T., Neville, M. C., Lin, A. C., and Goodwin, S. F. (2014). Sexually dimorphic octopaminergic neurons modulate female postmating behaviors in *Drosophila*. *Curr. Biol.* 24, 725–730. doi: 10.1016/j.cub.2013.12.051
- Ridley, E. V., Wong, A. C. N., and Douglas, A. E. (2013). Microbe-dependent and nonspecific effects of procedures to eliminate the resident microbiota from *Drosophila melanogaster*. *Appl. Environ. Microbiol.* 79, 3209–3214. doi: 10.1128/AEM.00206-13
- Roswell, M., Dushoff, J., and Winfree, R. (2019). Male and female bees show large differences in floral preference. *PLoS One* 14:e0214909. doi: 10.1371/journal.pone.0214909
- Schretter, C. E., Vielmetter, J., Bartos, I., Marka, Z., Marka, S., Argade, S., et al. (2018). A gut microbial factor modulates locomotor behaviour in *Drosophila*. *Nature* 563, 402–406. doi: 10.1038/s41586-018-0634-9
- Schultzhaus, J. N., and Carney, G. E. (2017). Dietary protein content alters both male and female contributions to *Drosophila melanogaster* female post-mating response traits. *J. Insect Physiol.* 99, 101–106. doi: 10.1016/j.jinsphys.2017.04.004
- Simmons, F. H., and Bradley, T. J. (1997). An analysis of resource allocation in response to dietary yeast in *Drosophila melanogaster*. *J. Insect Physiol.* 43, 779–788. doi: 10.1016/S0022-1910(97)00037-1
- Stensmyr, M. C., Dweck, H. K. M., Farhan, A., Ibba, I., Strutz, A., Mukunda, L., et al. (2012). A conserved dedicated olfactory circuit for detecting harmful microbes in *Drosophila*. *Cell* 151, 1345–1357. doi: 10.1016/j.cell.2012.09.046
- Sujkowski, A., Ramesh, D., Brockmann, A., and Wessells, R. (2017). Octopamine drives endurance exercise adaptations in *Drosophila*. *Cell Rep.* 21, 1809–1823. doi: 10.1016/j.celrep.2017.10.065
- Taghavi, S., van der Lelie, D., Hoffman, A., Zhang, Y.-B., Walla, M. D., Vangronsveld, J., et al. (2010). Genome sequence of the plant growth promoting endophytic bacterium *Enterobacter* sp. 638. *PLoS Genet.* 6:e1000943. doi: 10.1371/journal.pgen.1000943
- Terashima, J., Takaki, K., Sakurai, S., and Bownes, M. (2005). Nutritional status affects 20-hydroxyecdysone concentration and progression of oogenesis in *Drosophila melanogaster*. *J. Endocrinol.* 187, 69–79. doi: 10.1677/joe.1.06220
- Toth, A. L., Kantarovich, S., Meisel, A. F., and Robinson, G. E. (2005). Nutritional status influences socially regulated foraging ontogeny in honey bees. *J. Exp. Biol.* 208, 4641–4649. doi: 10.1242/jeb.01956
- Vacchini, V., Gonella, E., Crotti, E., Prosdocimi, E. M., Mazzetto, F., Chouaia, B., et al. (2017). Bacterial diversity shift determined by different diets in the gut of the spotted wing fly *Drosophila suzukii* is primarily reflected on acetic acid bacteria. *Environ. Microbiol. Rep.* 9, 91–103. doi: 10.1111/1758-2229.12505
- Walsh, D. B., Bolda, M. P., Goodhue, R. E., Dreves, A. J., Lee, J., Bruck, D. J., et al. (2011). *Drosophila suzukii* (Diptera: Drosophilidae): invasive pest of ripening soft fruit expanding its geographic range and damage potential. *J. Integr. Pest Manag.* 2, G1–G7. doi: 10.1603/IPM10010
- Wickham, H., Chang, W., Henry, L., Pedersen, T. L., Takahashi, K., Wilke, C., et al. (2020). *ggplot2: Create Elegant Data Visualisations Using the Grammar of Graphics*. Available online at: <https://CRAN.R-project.org/package=ggplot2> (accessed December 21, 2020).
- Wong, A. C.-N., Dobson, A. J., and Douglas, A. E. (2014). Gut microbiota dictates the metabolic response of *Drosophila* to diet. *J. Exp. Biol.* 217, 1894–1901. doi: 10.1242/jeb.101725
- Wong, A. C.-N., Wang, Q.-P., Morimoto, J., Senior, A. M., Lihoreau, M., Neely, G. G., et al. (2017). Gut microbiota modifies olfactory-guided microbial preferences and foraging decisions in *Drosophila*. *Curr. Biol.* 27, 2397–2404.e4. doi: 10.1016/j.cub.2017.07.022
- Yang, Z., Yu, Y., Zhang, V., Tian, Y., Qi, W., and Wang, L. (2015). Octopamine mediates starvation-induced hyperactivity in adult *Drosophila*. *Proc. Natl. Acad. Sci. U.S.A.* 112, 5219–5224. doi: 10.1073/pnas.1417838112
- Yu, Y., Huang, R., Ye, J., Zhang, V., Wu, C., Cheng, G., et al. (2016). Regulation of starvation-induced hyperactivity by insulin and glucagon signaling in adult *Drosophila*. *Elife* 5:e15693. doi: 10.7554/eLife.15693
- Zhao, Q., Cheung, S. G., Shin, P. K. S., and Chiu, J. M. Y. (2011). Effects of starvation on the physiology and foraging behaviour of two subtidal nassariid scavengers. *J. Exp. Mar. Biol. Ecol.* 409, 53–61. doi: 10.1016/j.jembe.2011.08.003

**Conflict of Interest:** The authors declare that the research was conducted in the absence of any commercial or financial relationships that could be construed as a potential conflict of interest.

Copyright © 2021 Shu, Hahn, Jurkevitch, Liburd, Yuval and Wong. This is an open-access article distributed under the terms of the Creative Commons Attribution License (CC BY). The use, distribution or reproduction in other forums is permitted, provided the original author(s) and the copyright owner(s) are credited and that the original publication in this journal is cited, in accordance with accepted academic practice. No use, distribution or reproduction is permitted which does not comply with these terms.



OPEN ACCESS

**Edited by:**

David Kamanda Ngugi,  
German Collection of Microorganisms  
and Cell Cultures GmbH (DSMZ),  
Germany

**Reviewed by:**

Christine Ferrier-Pagès,  
Centre Scientifique de Monaco,  
Monaco  
Basak Öztürk,  
German Collection of Microorganisms  
and Cell Cultures GmbH (DSMZ),  
Germany  
Tomihiko Higuchi,  
The University of Tokyo, Japan  
Biao Chen,  
Guangxi University, China

**\*Correspondence:**

Chengyong Li  
cyl@gdou.edu.cn

<sup>†</sup> These authors have contributed  
equally to this work

**Specialty section:**

This article was submitted to  
Microbial Symbioses,  
a section of the journal  
Frontiers in Microbiology

**Received:** 09 February 2021

**Accepted:** 15 April 2021

**Published:** 04 June 2021

**Citation:**

Xiao B, Li D, Liao B, Zheng H,  
Yang X, Xie Y, Xie Z and Li C (2021)  
Effects of Microplastics Exposure on  
the *Acropora* sp. Antioxidant,  
Immunization and Energy Metabolism  
Enzyme Activities.  
Front. Microbiol. 12:666100.  
doi: 10.3389/fmicb.2021.666100

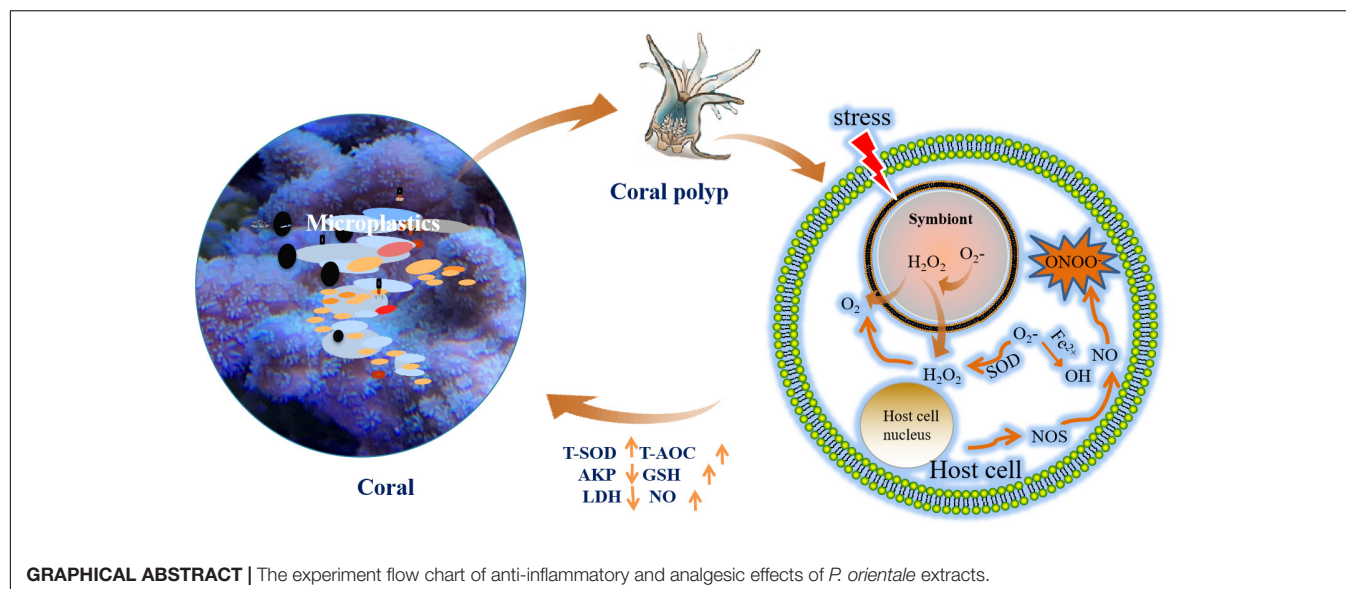
# Effects of Microplastics Exposure on the *Acropora* sp. Antioxidant, Immunization and Energy Metabolism Enzyme Activities

Baohua Xiao<sup>1†</sup>, Dongdong Li<sup>1†</sup>, Baolin Liao<sup>1</sup>, Huina Zheng<sup>1</sup>, Xiaodong Yang<sup>1</sup>, Yongqi Xie<sup>1</sup>, Ziqiang Xie<sup>1</sup> and Chengyong Li<sup>1,2\*</sup>

<sup>1</sup> Shenzhen Institute of Guangdong Ocean University, Shenzhen, China, <sup>2</sup> Southern Marine Science and Engineering Guangdong Laboratory, School of Chemistry and Environment, Guangdong Ocean University, Zhanjiang, China

Microplastic pollution in marine environments has increased rapidly in recent years, with negative influences on the health of marine organisms. Scleractinian coral, one of the most important species in the coral ecosystems, is highly sensitive to microplastic. However, whether microplastic causes physiological disruption of the coral, via oxidative stress, immunity, and energy metabolism, is unclear. In the present study, the physiological responses of the coral *Acropora* sp. were determined after exposure to polyethylene terephthalate (PET), polyamide 66 (PA66), and polyethylene (PE) microplastic for 96 h. The results showed that there were approximately 4–22 items/nubbin on the surface of the coral skeleton and 2–10 items/nubbin on the inside of the skeleton in the MPs exposure groups. The density of endosymbiont decreased ( $1.12 \times 10^5$ – $1.24 \times 10^5$  cell/cm<sup>2</sup>) in MPs exposure groups compared with the control group. Meanwhile, the chlorophyll content was reduced (0.11–0.76  $\mu$ g/cm<sup>2</sup>) after MPs exposure. Further analysis revealed that the antioxidant enzymes in coral tissues were up-regulated (Total antioxidant capacity T-AOC  $2.35 \times 10^{-3}$ – $1.05 \times 10^{-2}$  mmol/mg prot, Total superoxide dismutase T-SOD 3.71–28.67 U/mg prot, glutathione GSH 10.21–10.51 U/mg prot). The alkaline phosphatase (AKP) was inhibited (1.44–4.29 U/mg prot), while nitric oxide (NO) increased (0.69–2.26  $\mu$ mol/g prot) for cell signal. Moreover, lactate dehydrogenase (LDH) was down-regulated in the whole experiment period (0.19–0.22 U/mg prot), and Glucose-6-phosphate dehydrogenase (G6PDH) for cell the phosphate pentoses pathway was also reduced (0.01–0.04 U/mg prot). Results showed that the endosymbiont was released and chlorophyll was decreased. In addition, a disruption could occur under MPs exposure, which was related to anti-oxidant, immune, and energy metabolism.

**Keywords:** microplastics, *Acropora* sp., endosymbiont, enzyme, biochemical evaluation



## INTRODUCTION

*Acropora* sp., a species of scleractinian coral, is a complex symbiosis constituting with scleractinian host, photosynthetic symbionts, and various microbial communities (Besseling et al., 2014; Tian and Niu, 2017; Yu et al., 2020a,b). Corals supply protection and inorganic salt for the endosymbiont, and in return, the endosymbiont provides its host with organic nutrients (Cook and D'Elia, 1987). Although corals can obtain energy from symbiotic endosymbiont, they need to ingest extra exogenous food to satisfy their nutrition (Allen et al., 2017; Tian and Niu, 2017). However, the intricate relationship between coral and endosymbiont symbiosis is threatened by environmental changes such as global climate change and aquatic environment pollution (Hughes et al., 2017; Saliu et al., 2019; Yu et al., 2020a,b). Global coral reefs are suffering from continual and serious degradation in recent years (Veron, 1992; Zhao et al., 2013, 2016; Higuchi et al., 2015a,b; Hughes et al., 2017).

An estimated approximately 8–12 million tons of various plastic waste are transferred into the ocean in multiple ways each year (Carpenter et al., 1972; Hidalgo-Ruz et al., 2012). Previous reports show that plastic waste accounted for 70–90% of marine waste (Lusher, 2015; Walker, 2018). Lamb assessed the influence of plastic waste on reef-building corals in the Asia-Pacific region, and they found that plastic waste increased the risk of diseases in corals from 4 to 89% (Lamb et al., 2018). Furthermore, in the marine environment plastic waste can develop into small fragments through biodegradation, thermal degradation, hydrolysis, and photodegradation (Hidalgo-Ruz et al., 2012; Walker, 2018). Microplastics (MPs) are described as plastic pieces smaller than five millimeters, and they are more difficult to manage than other pollutants due to this small size and global distribution (Antao Barboza and Garcia Gimenez, 2015; Ali Chamas et al., 2020). MPs can be ingested by a wide range of marine organisms, and they bring negative effects, including gastrointestinal obstruction, inflammation, tissue damage, and

growth restriction (Sun et al., 2017; Wang et al., 2020). Due to the stable chemical composition, MPs are difficult for marine organisms to digest. Hence, MPs accumulate continuously in marine organisms (Deudero and Alomar, 2015; Sun et al., 2017).

MPs are mainly discharged from terrestrial environments into the sea, meaning coastal ecosystems such as coral reefs are especially at risk (Hermabessiere et al., 2017; Huang et al., 2019). The threat of numerous MPs to coral reefs has attracted extensive attention (Kirstein et al., 2016; Reichert et al., 2018). Reichert found that MPs could attach to the tentacles or skeleton surface of *Pocillopora damicornis*, and the coral was subject to germ infection, bleaching, and even tissue necrosis (Reichert et al., 2018). Additionally, Hankins evaluated the effects of MPs on *Montastraea cavernosa* and *Orbicella faveolat*. They found that the corals captured MPs actively although they could recognize and repel indigestible substances (Hankins et al., 2018). Interestingly, coral tends to ingest MPs because it is driven by chemoreception (Allen et al., 2017). Furthermore, a previous report suggested that excessive ingestion of MPs could induce the scleractinian coral *P. damicornis* to produce oxidative stress, which can lead to a decrease in the expression of stress-related protein and activate the MAPK/Nrf2 pathway (Jeong et al., 2016). MPs not only cause irreversible damage to coral hosts but also seriously threaten the survival of symbiotic algae. Su found that MPs can inhibit the growth of endosymbiotic algae by affecting its apoptosis and metabolism (Su et al., 2020). MPs negatively affect the photosynthesis activity of coral endosymbiotic microorganisms through reducing chlorophyll content and photochemical efficiency (Mao et al., 2018; Wu et al., 2019). Many studies to date have found that MPs could accumulate in an organism and cause endocrine disruption (Chapron et al., 2018; Syakti et al., 2019). It has been revealed that the reactive oxygen species (ROS) and antioxidant enzymes (SOD, CAT, and GSH) of coral are up-regulated after exposure to MPs (Chen et al., 2017; Tang et al., 2018; Dias et al., 2019). Oxidative damage could be caused by excessive ROS after



exposure to MPs (Paul-Pont et al., 2016; Chen et al., 2017). Although exposure and ingestion of MPs have been reported in many coral reefs, there is still a shortage of research on the adverse effects of MPs on coral *Acropora* sp.

The present study aimed to provide detailed information about the physical and toxicity effects of MPs on corals. The scleractinian coral *Acropora* sp. was chosen to evaluate the effect of MPs. The biochemical level stress response of *Acropora* sp. was determined by the antioxidant enzyme (T-SOD, T-AOC, and GSH), immunocompetence [alkaline phosphatase (AKP), nitric oxide (NO)], phosphate pentoses pathway [lactate dehydrogenase (LDH), Glucose-6-phosphate dehydrogenase (G6PDH)]. This is the first study to assess the physiological responses of scleractinian coral exposed to MPs. It examines the activity of enzymes involving antioxidant capacity, immune response, and energy metabolism in different stages. The results provide new insights into the response of corals and stress reactions caused by different kinds of MPs.

## MATERIALS AND METHODS

### Materials

Polyethylene terephthalate microplastics (PET), Polyethylene microplastics (PE), Nylon 66 microplastics (PA66) were purchased from Saierqun, Shanghai, China. The microscope images and size distributions of MPs are shown in **Supplementary Figure 1**. The BCA protein assay kit was offered by the Beyotime Institute of Biotechnology (Shanghai, China). We 4% paraformaldehyde, acetic acid, 0.9% saline were purchased from Sigma-Aldrich (St Louis, MO, United States). Assay kits for measuring the levels of LDH, G6DPH, GSH, AKP, NO, T-SOD, and T-AOC were purchased from Nanjing Jiancheng Bioengineering Institute (A020, A027, A006, A059, A012, A001, and A015, Nanjing, China).

### Experimental Design

#### Collection and Treatment of Corals

Corals of the genus *Acropora* were used in this investigation. *Acropora* sp. is very sensitive to changes in the anthropogenic ecosystem (Mendrik et al., 2020). *Acropora* sp. was collected from the surrounding waters of Shenzhen Nanao Island (22°33'50.78"—22°40'38.18"N, 114°30'35.62"—114°33'26.90"E, 18–25°C, depth 5–8 m) (**Supplementary Figure 2**), according to the statistical data of Meteorological Bureau of Shenzhen Municipality (1980.01–2018.12). The annual average temperature is 21.5°C, the annual average sunshine is 2,325.3 h, and the annual average rainfall is 1,348.4 mm. There are 6 months in a year when the total solar radiation is above 400 MJ/m<sup>2</sup>. Five corals were collected from this location and quickly put into the holding tank. The oxygen pump was used to supply oxygen to corals.

In the laboratory, the whole origin coral polyps were transferred to open flow system glass tanks (160 cm × 50 cm × 75 cm) at ambient conditions, glued on ceramic plates by cyanoacrylate. The coral's acclimation modular system was conducted according to the previous description (Rocha et al., 2015). They were acclimated to the

experimental conditions for 30 days. Subsequently, 2–5 cm long fragments were cut from the origin colonies and they were attached to the ceramic matrix bases with two-component glue. The branches in the colonies were split as nubbins, and 108 nubbins were thus generated in total. In addition, there were regular shape and single branch experimental corals with intact polyps on each nubbin. All nubbins were distributed equally in 15 L acrylic laboratory tanks filled with seawater. Corals were housed in a controlled tank with a temperature of 24 ± 1°C and a salinity of 35.0 ± 0.2 ppt. The whole coral nubbins were illuminated with blue-white fluorescent bulbs (Chihiros LED lighting system 21 W, A351M, <sup>1</sup>) at a light 70 ± 10 μmol quanta m<sup>-2</sup> s<sup>-1</sup> in a 10 h/14 h light-dark cycle for 30 days to adapt to the experimental environment.

### Exposure of Microplastics

In the experiments, MPs (PET, PE, and PA66) were treated for *Acropora* sp. to optionally ingest. Prior to the experiment, all MPs were confirmed by Raman Spectrometer (RS, SR-510 Pro, Ocean optics Asia, 785 nm laser, Raman shift 50–3,500 cm<sup>-1</sup>).

In detail, seawater containing MPs was prepared by adding 250 mg MPs to a 100 mL beaker. Then 50 mL seawater was added into the beaker, and it was shaken well. The solution in the beaker was ultrasonic for 5 min (200 W). Finally, the solution in the beaker was mixed with 5 L of seawater, and constant stirring prevented MPs from depositing. The final concentration of MPs was 50 mg/L (9.0 × 10<sup>10</sup> particles/L), which is similar to previous reports (Tang et al., 2018; Chantal et al., 2020). The control groups of corals nubbins were maintained in fresh seawater (three tanks). While the experiment groups were carried out in the PET group (three tanks), PA66 group (three tanks), and PE group (three tanks), which were each placed in seawater-containing MPs. Continuous gentle aeration was used to prevent the accumulation of MPs. There were 12 tanks with a capacity of 15 L in the present study. The temperature was controlled at 24–25°C by air conditioning. The seawater in all tanks was replaced once every 24 h with freshly filtered seawater from the coral culture system to ensure a suitable aquaculture water environment, and new MPs were also added at the same time.

### Separation of Microplastics

To obtain the concentration of MPs attached to the coral surface, a test was conducted based on Allen's work (Allen et al., 2017). Briefly, the nubbins were placed in a glass beaker and then immersed in filtered seawater. The nubbins were sonicated (200 W) for 10 min to strip off MPs attached to the surface. The glass beaker was then placed at ambient temperature to settle for 1 day. After 24 h, all the solution was prudently decanted and filtered with 0.8 μm pore size glass fiber membranes (Beyotime Biotechnology, FF338).

To obtain the ingested MPs in corals, the coral tissues after sonic processing were immersed in 30% formic acid solution for 6 h, and then they were placed in excess KOH solution (ω = 10%). All the solution was collected. Filtered seawater was used to rinse undissolved corals to get remnant MPs and the solution was

<sup>1</sup><https://www.aliexpress.com/i/4000118987595.html>

collected. The collected solution was blended and filtered through a glass fiber membrane to obtain MPs. To collect all MPs, the membrane was treated the same way, and then MPs were dried completely at room temperature. Finally, MPs were observed *via* a microscope. The number of MPs represented per coral nubbin (unit: items/nubbin). Because coral is a colony animal, the unit of items/nubbin was used to reflect the number of MPs in the coral during the analysis procedure.

### Measurement of Endosymbiont Density

The density of endosymbiont from corals was measured based on previous studies by Hedouin et al. (2016) and Higuchi et al. (2015a,b). The coral tissues were homogenized (60 Hz, 3 min, 4°C) in 5 ml of filtered seawater. Subsequently, the collected homogenates were mixed with 2 mL 4% paraformaldehyde and stored at 4°C for 30 min. 2 mL homogenate was resuspended with filtered seawater to count the number of endosymbiont per unit area by a hemocytometer (QIUJING, China). The coral nubbins surface area was measured according to the aluminum foil method (Johannes et al., 1970). Finally, the density of endosymbiont was expressed as the number of symbiont per unit area of the coral nubbins.

### Measurement of Chlorophyll

Chlorophyll from symbiotic algae after MPs exposure was analyzed as outlined in previous research by Stimson and Kinzie (1991). 2 mL homogenate was centrifuged at 2,500 rpm for 15 min under 4°C, and then the gathered symbiotic algae was centrifuged at 15,000 rpm for 30 s under 4°C. Subsequently, the centrifuged homogenate was extracted with 2 mL of 100% acetone for 24 h at 4°C. The absorbance of the extract was measured at wavelengths of 634, 647, 664, and 750 nm (Thermo NanoDrop 2000), respectively. The chlorophyll content was obtained according to the equations of Porra and Jeffrey (Jeffrey and Humphrey, 1975; Porra et al., 1989). The weight of chlorophyll was described as the chlorophyll content per unit area of coral nubbins ( $\mu\text{g}/\text{cm}^2$ ).

### Biochemical Evaluation of Coral Tissue

To get tissue homogenates, the coral tissue was moved into a 5 mL tube after weighing accurately, and it was added to nine times the volume of filtered seawater according to the ratio of  $m(\text{g})/V(\text{mL})$ . The tissue was mechanically homogenized under ice bath conditions for making 10% homogenate that used an Automatic Sample Rapid Grinding Instrument (JingXin, Shanghai, China). The homogenate was centrifuged for 15 min at 5,500 rpm. Finally, the supernatant was transferred to a new tube, and then it was diluted with filtered seawater. After the total enzyme activities were obtained, the concentration of total protein in the supernatant was quantified using the BCA method (Zhou et al., 2018). Biochemical parameters were analyzed after the diluted supernatant was transferred to a new tube. The commercial kits were used to detect the activities of T-SOD, T-AOC, AKP, GSH, G6PDH, LDH, and the content of NO.

### Histology Observation

After exposure, the coral nubbins were fixed in 4% formalin-seawater for more than 24 h, then rinsed with filtered seawater and preserved in 70% ethanol and 30% seawater (V/V). The coral samples were immersed in ethylene diamine tetraacetic acid (EDTA) decalcifying solution (pH 7.2) for 2 weeks, and the solution was replaced at 48 h. The tissue was paraffin-embedded and sectioned (6  $\mu\text{m}$ ) in a Jinhua automatic tissue processor (Zhejiang, KEDD-BM-6L). At least five slices were made from each sample (each slide was from a different area and depth in the tissue). Comparisons were made among slides from the same area (tissue depth or polyp area). Chlorophyll distribution was observed and photographed *via* a fluorescence microscope (Japan, Nikon Type 108, blue light excitation).

The green fluorescence was obtained by the camera system (NIS-Elements).

### Statistical Analyses

The values were evaluated by one-way ANOVA and multiple analyses of variation using Statistical Analysis Software (SPSS 17.0 IBM, Armonk, NY, United States). Data were expressed as mean  $\pm$  standard deviation (SD). In all cases,  $p < 0.05$  was considered as a statistically significant difference. The asterisk (\*) expressed as the significant difference between the control and MPs treatment groups. Letter of a, b and c represented the differences of PET vs. PA66, PET vs. PE, and PA66 vs. PE, respectively.

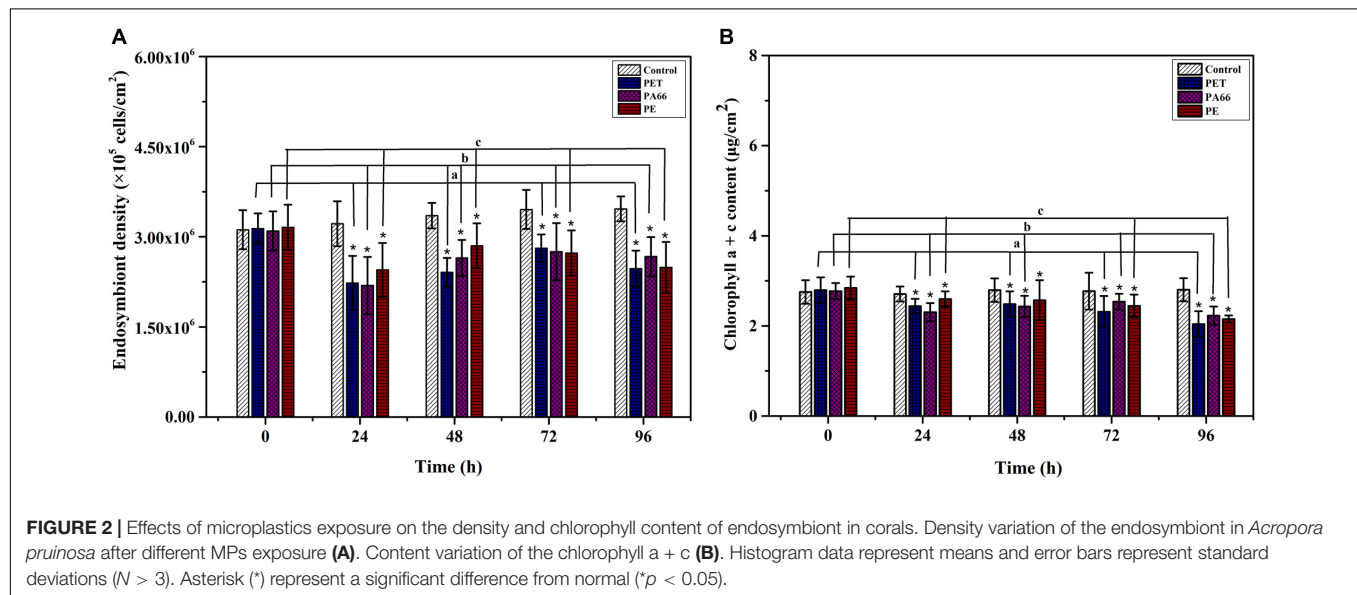
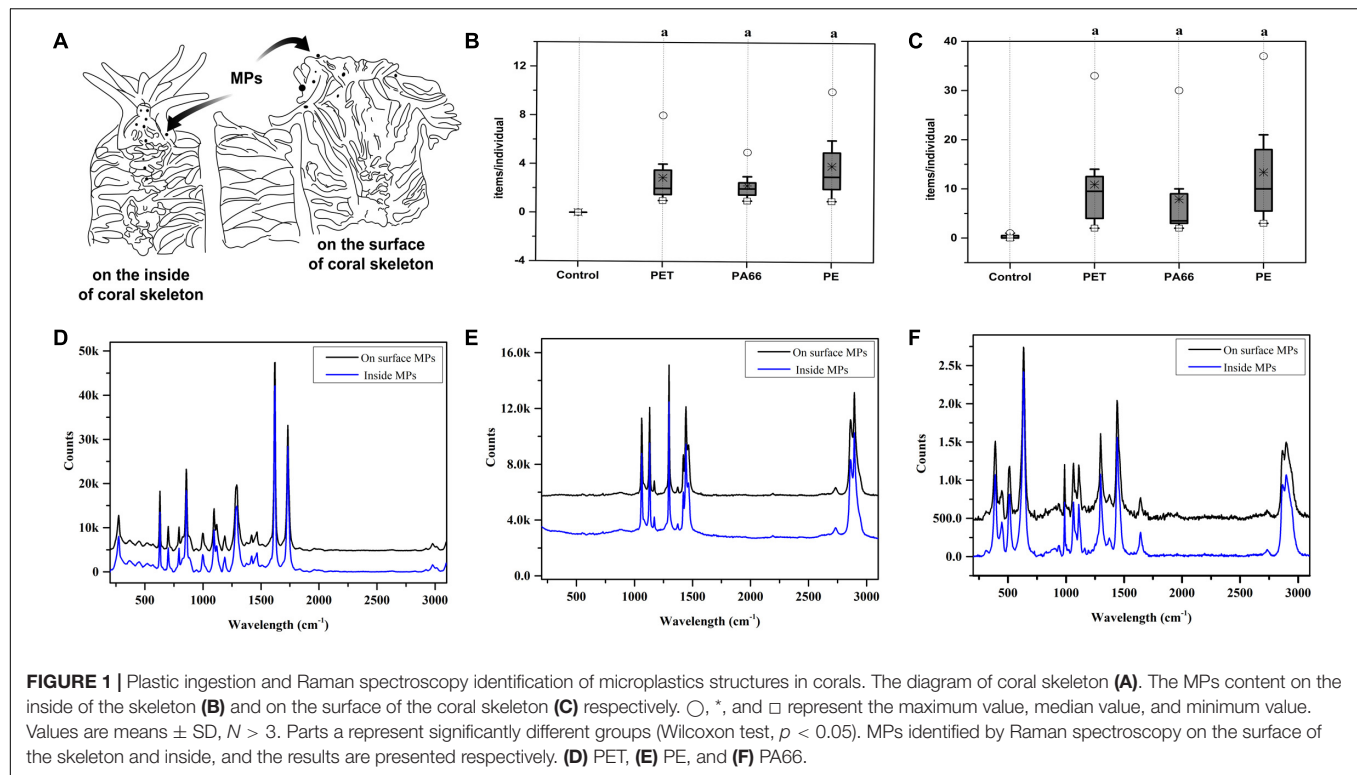
## RESULTS

### Microplastics in Corals

**Figure 1A** is a sketch that displays the distribution of MPs on the inside and outside of corals. Granular aggregation MPs could be found inside of corals (2–10 items/nubbins, **Figure 1B**) and on the surface (4–22 items/nubbins, **Figure 1C**). The contents of the three kinds of MPs (PET, PA66, and PE) on the surface were higher than the ones inside (**Figures 1B,C**). Raman spectroscopy was used to distinguish the constituent (**Figures 1D–F**) of MPs. The results showed that the granular aggregations were PET (D), PE (E), and PA66 (F).

### The Impact of Microplastics Exposure on Endosymbiont and Chlorophyll

The density of endosymbiont in corals is stable in the control group ( $p > 0.05$ ) (**Figure 2A**). However, after exposing for 96 h, their densities were lower ( $p < 0.05$ ) in all MPs exposure groups (PET  $2.47 \times 10^5$  cell/ $\text{cm}^2$ , PA66  $2.67 \times 10^5$  cell/ $\text{cm}^2$ , and PE  $2.49 \times 10^5$  cell/ $\text{cm}^2$ ) compared with the control group ( $3.46 \times 10^5$  cell/ $\text{cm}^2$ ). The density of endosymbiont was the lowest after 24 h of MPs treatment, indicating that endosymbiont was sensitive to MPs toxicological reaction. The chlorophyll content of corals is shown in **Figure 2B**. The chlorophyll a + c content was stable in the control group ( $p > 0.05$ ). Compared with the control group, it reduced to the lowest value ( $p < 0.05$ ) at 96 h in the presence of PET, PA66, and



PE. In general, the chlorophyll content was reduced in all MPs treatment groups at 96 h.

## Fluorescence Analysis of the Chlorophyll in Corals

The chlorophyll green fluorescence of the control group was more than those corals with MPs treatment groups (see in Figure 3). Short-term high concentration of MPs exposure caused damage and disturbed the symbiosis with endosymbiont.

## Effect of Microplastics Exposure on Biochemical Indices of Coral

### The Effect of MPs on Anti-Oxidative Capacity

Figures 4A–C show the anti-oxidative ability of coral tissue. As depicted in Figure 4A, the content of T-AOC ( $p < 0.05$ ) was  $4.26 \times 10^{-2}$ ,  $4.17 \times 10^{-2}$ ,  $4.23 \times 10^{-2}$  mmol/mg prot after 24 h exposure in PET, PA66, and PE. Though it was gradually reduced after 48 h and 96 h, it was still higher than the control group. There was a significant increase in T-SOD activity after exposure

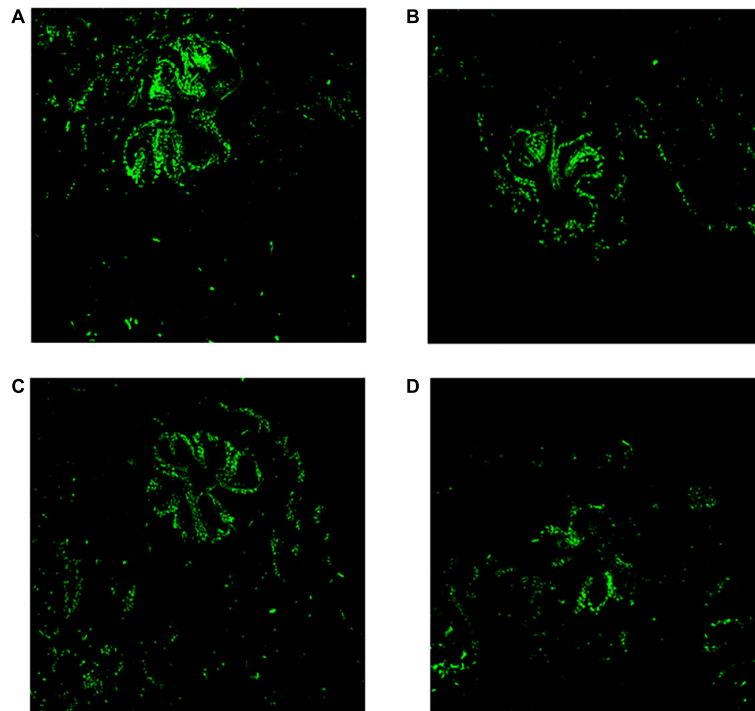


**FIGURE 3 |** Microcosmic analysis of corals after MPs exposure for 96 h. Fluorescence analysis of chlorophyll in coral tissue (20 $\times$ ). **(A)** Control, **(B)** PET, **(C)** PA66, and **(D)** PE.

24 h (137.44 U/mg prot, 137.07 U/mg prot, 142.10 U/mg prot,  $p < 0.05$ ) in PET, PA66, and PE groups. While it was decreasing after 96 h treatment (**Figure 4B**). Comparing with the control group, the GSH activities ( $p < 0.05$ ) were higher in MPs groups after 24 h exposure. After 96 h, the GSH activities decreased (32.23 U/mg prot, 32.43 U/mg prot, 32.92 U/mg prot,  $p < 0.05$ ) in MPs exposure groups (**Figure 4C**). In summary, the levels of T-SOD, T-AOC, and GSH increased after MPs exposure, indicating that MPs could induce coral defense against oxidative stress, which depended on the type of MPs.

### The Effect of MPs on Alkaline Phosphate and Nitric Oxide

As shown in **Figure 5A**, the AKP level showed an inhibiting trend throughout the experimental period (1.44–4.29 U/mg prot,  $p < 0.05$ ) in all MPs exposure groups. At 96 h, the AKP activities ( $p < 0.05$ ) were significantly decreased in MPs exposure corals when compared with the corals in the control group. On the contrary, the NO content in the MPs group sharply increased at 96 h (0.69–2.26  $\mu\text{mol/g prot}$ , **Figure 5B**), and was higher ( $p < 0.05$ ) than the control groups. It was ascending for NO content in all MPs exposure groups, indicating that the coral immune system may be sensitive to MPs.

### The Effect of MPs on Glycolysis Enzymes (LDH) and Phosphate Pentoses Pathway (G6PDH)

An inhibiting effect was observed on LDH activity ( $p < 0.05$ ) after exposure to MPs (**Figure 6A**) and decreased compared with the

one in control coral at 24 h (0.19–0.22 U/mg prot,  $p < 0.05$ ). The activity of LDH presented significantly lower values ( $p < 0.05$ ) in MPs exposure groups at 96 h compared with the control group. As shown in **Figure 6B**, the G6DPH content ( $p < 0.05$ ) decreased in MPs exposure corals compared with the corals in the control group at 24 h. The G6DPH content was sharply reduced ( $p < 0.05$ ) in PET, PA66 and the PE group (0.01–0.04 U/mg port) at 96 h. This indicated that coral glycometabolism was influenced by the type of MPs.

## DISCUSSION

The presence of MPs significantly affected the physiology of corals depending on the types of MPs (Hidalgo-Ruz et al., 2012; Hankins et al., 2018). In this study, we observed that the contents of MPs on the surface of the coral skeleton were significantly different from those of the control groups. Our study also discovered MPs in coral tissues, which aligns with other studies indicating that corals may ingest MPs (Allen et al., 2017; Tang et al., 2018; Reichert et al., 2019). Even though coral calcification depends largely on photosynthesis from the endosymbiont (Porter et al., 1989), the corals still supply carbon sources through predation (Grottoli et al., 2006; Anthony et al., 2009). MPs are ingested as food because they are not easily recognized by zooplankton or corals (Hankins et al., 2018). The large specific surface area and high hydrophobicity of MPs may increase the surface free energy of polar plastics and improve



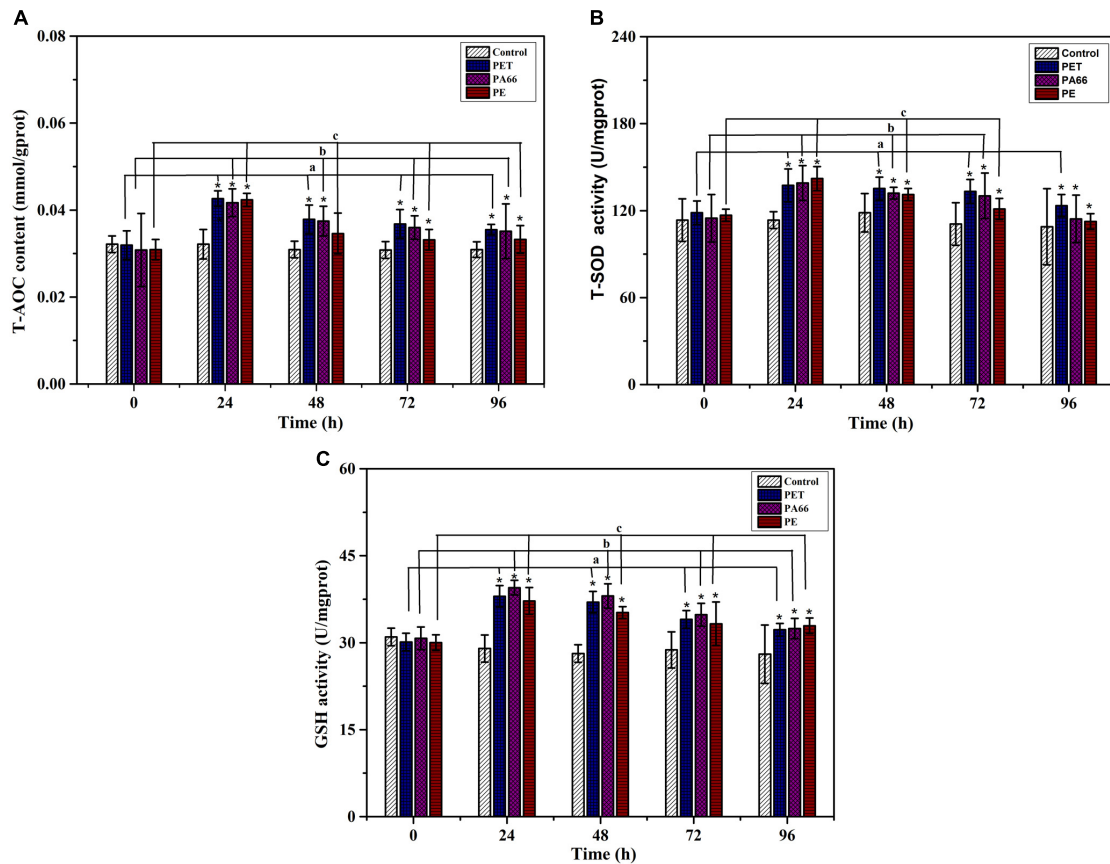


**FIGURE 4 |** Changes in the anti-oxidative enzymes of corals after 96 h exposure to three kinds of microplastics. **(A)** Total antioxidant capacity (T-AOC), **(B)** Total Superoxide Dismutase (T-SOD), and **(C)** Glutathione (GSH) in the coral *Acropora pruinosa* after exposure to different MPs (PET, PA66, and PE 50 mg/L, respectively) in the experiment. Histogram data represent mean and error bars represent standard deviations ( $N > 3$ ). Asterisk (\*) represents a significant difference from normal (\* $p < 0.05$ ).

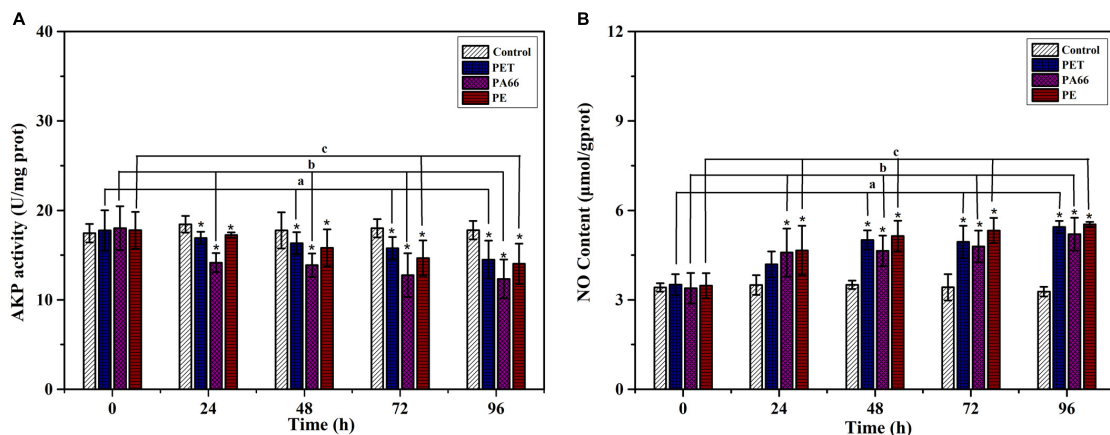
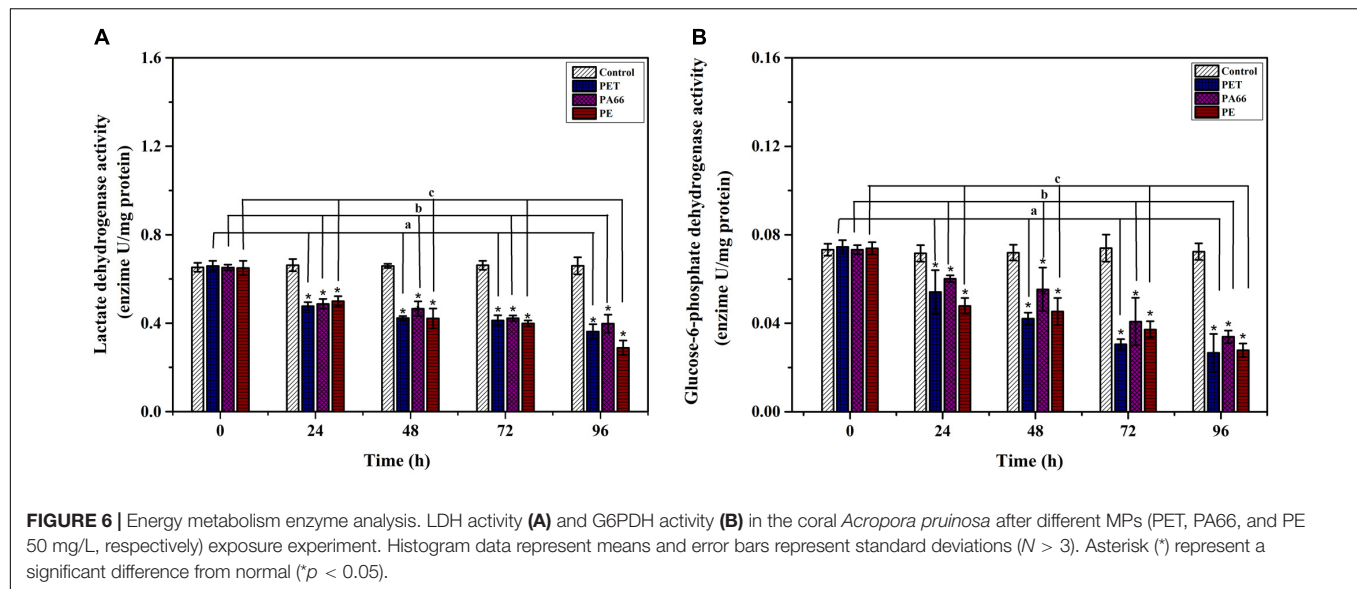


**FIGURE 5 |** Immune ability analysis. AKP activity **(A)** and NO content **(B)** in the coral exposed to different MPs (PET, PA66, and PE 50 mg/L, respectively) for 0, 24, 48, 72, and 96 h. All data are presented as mean  $\pm$  standard error ( $N > 3$ ). Asterisk (\*) represent a significant difference from normal (\* $p < 0.05$ ).

lipophilicity. Therefore, MPs can be adsorbed on the surface of corals (Ainsworth et al., 2007; Hidalgo-Ruz et al., 2012). MPs tend to accumulate on the surface of the coral skeleton,

causing frictional damage and pathogen invasion (Chen et al., 2017; Reichert et al., 2018). They can also be ingested by the coral, leading to coral oxidative stress response or toxic effects



(Chen et al., 2017; Tang et al., 2018). The toxic effect of MPs was determined by measuring the biochemical indicators of coral and further exploration of the relationship between the contents of MPs and physiological activities.

Exposure to MPs caused a stress response in the coral that further impaired its function. Firstly, the heterotrophic feeding may be inhibited due to excessive ingestion of MPs. Several studies have reported that the normal food supply of corals was hindered by MPs. The coral is unable to obtain nutrients owing to the continuous ingestion and excretion of MPs (Chapron et al., 2018; Reichert et al., 2019). When food sources are limited, the endosymbionts play a key role in the energy supply. The endosymbionts provide hosts with colors and energy because they can absorb light. They can also convert light energy into chemical energy through chlorophyll (Besseling et al., 2014; Pierson et al., 2017), meaning that endosymbionts play an important role in the growth and breeding of corals (McLeod, 1957; Pierson et al., 2017). In the present study, the density of endosymbionts in coral decreased and maintained a stable density, which revealed that the corals could recover symbiotic balance in a short time. This is consistent with previous reports (Denis et al., 2013; Reichert et al., 2018; Corona et al., 2020). As expected, the chlorophyll content was reduced in coral symbiosis. The exchange of light energy was reduced due to the attachment of MPs on the surface of the coral skeleton. MPs can easily absorb the toxic metabolites of microorganisms that inhibit the activity of key photosystem II in coral (Hidalgo-Ruz et al., 2012; Mendrik et al., 2020). On balance, these stressors lead to the stress response of corals and their symbionts (Enriquez et al., 2005; Muller-Parker et al., 2015). The content of chlorophyll was closely related to the MPs on the surface of the coral skeleton. Furthermore, the toxicity of MPs increased and the symbiotic algae were reduced with time (Downs et al., 2002). Under different stressors, the chlorophyll content of scleractinian coral decreased temporarily, results that are confirmed by previous studies (Rocha et al., 2015; Long et al., 2017; Zhang et al., 2017; Lanctot et al.,

2020). Lei believed that the change of chlorophyll content was one of the stress response indicators and that it reflected the density and photosynthetic capacity of the endosymbiont in corals (Lei et al., 2009).

Moreover, a disturbance of the symbiotic alga-host relationship could be caused by ROS from MPs stress (Okubo et al., 2018). In the antioxidant enzyme system of marine organisms, T-AOC, T-SOD, and GSH are important active enzymes that synergistically reduce the production of free radicals under negative stress (Levy et al., 2006; Sorianosantiago et al., 2013). The activities of T-SOD and T-AOC were up-regulated after MPs exposure at 24 h, meaning that MPs can induce ROS production and it enhances the anti-oxidative system of coral. The adverse effects of MPs, causing oxidative stress on scleractinian coral, have also been reported in previous research (Sorianosantiago et al., 2013; Tang et al., 2018; Liao et al., 2021). In the present study, there was the same tendency of oxidative stress caused by the three kinds of MPs. In general, the T-AOC content, T-SOD, and GSH activity showed the variation tendency of rising (Tang et al., 2018; Liao et al., 2021). After 96 h of exposure, the coral acclimation to MPs stress can occur through the production of antioxidant enzymes. The antioxidant system of corals (inactive damaging oxygen radicals) can scavenge denatured cellular proteins to reduce the harm of active free radicals (Hofmann and Todgham, 2010; Weis, 2010). The corals can resist external adverse factors by enhancing antioxidants or self-cleaning (Denis et al., 2013; Rocha et al., 2015). When a mass of MPs are ingested by corals, they cause damage to the coral tissues because they accumulate in the gastrointestinal tract and liposomes of corals (Hall et al., 2015). Previous reports have shown that oxidative damage of coral symbiosis increased in the presence of MPs (Jeong et al., 2016; Tang et al., 2018). Tang outlines that exposure to MPs may regulate the JNK and ERK signaling pathways and that it inhibits the phosphorylation process in corals (Tang et al., 2018). It is worth mentioning that these effects directly weaken coral's ability to detoxify. GSH is

a small molecule peptide composed of three amino acids, and it is a special substance for detoxification (Krueger et al., 2014; Nicosia et al., 2014). GSH activity increased under MPs exposure at 24 h. Finally, it was decreased in MPs exposure groups at 96 h. This indicated that short-term MPs exposure could regulate the detoxification system in *Acropora* sp. Under MPs stress, the detoxification system was disturbed, which accelerated the collapse of the host-symbiotic algae relationship (Tang et al., 2018). In summary, MPs could activate the *Acropora* sp. antidotal system in a short time.

The immune system is the host defense system, and AKP is an essential enzyme in corals. It participates in the identification and clearance of pathogenic organisms or materials (Palmer et al., 2011). In scleractinian corals, the immune function of AKP has been confirmed (Palmer et al., 2011; Godinot et al., 2013). Oxidative stress is expected to aggravate the negative immunity effects of MPs exposure on corals (Godinot et al., 2013; Tang et al., 2018). Our results suggested that there was a significant correlation between MPs and AKP in *Acropora* sp. The AKP activities in all MPs exposure groups showed a decreasing trend in the experiment. AKP activity decreased significantly, which suggested that MPs-induced stress may damage the immune system of *Acropora* sp. by regulating the oxidative stress signal pathway. Studies have revealed that the oxidative stress caused by MPs exposure can lead to the occurrence of immunosuppression in corals (Tang et al., 2018). Moreover, some similar results have been reported in other species (Detree and Gallardo-Escarate, 2018; Liao et al., 2021). An imbalance in immunity capacities was induced by MPs, which could disturb pathways or genes of the immune system in coral. Tang's results showed that MPs impacted the immune system in corals by regulating the MAPK signal pathways (Tang et al., 2018). However, the mechanism of immune system suppression still requires further study and research. Besides, NO is the product of inflammatory molecules in corals, which have a significant effect on coral bleaching (Perez and Weis, 2006). When exposed to MPs, the NO content was increased in coral, meaning that the pressure on the immune system in corals increased. The rapid increase of NO in the host may adversely affect the symbiosis of coral-endosymbiont (Perez and Weis, 2006; da Silva Fonseca et al., 2019). The role of NO not only involves host apoptotic-like cell death but also receiving and transmitting information. It can regulate the activity of the host-endosymbiont cells (Hawkins and Davy, 2012; Hawkins et al., 2014; da Silva Fonseca et al., 2019). These results indicate that an immunosuppressive effect could be caused by MPs in the coral host. In addition, the synthesis NO from the host was related to the health of the coral-endosymbiont.

The LDH and G6PDH in coral *Acropora* sp. were investigated to understand the effects of MPs exposure on the energy metabolism of corals. In the presence of MPs, the content of glycolytic enzyme (LDH) was reduced, indicating that the inhibition of LDH activity can compromise the coral energy metabolism. In turn, it reduced the aerobic metabolism because organisms failed to initiate physiological adjustment that leads to severe anaerobic metabolism. The exposure of MPs had an overall inhibitory effect on the enzyme activities related to energy metabolism in corals (Teuten et al., 2009; Andradý, 2011). Therefore, the change of LDH activity directly affected the corals'

energy metabolism (Hosseini et al., 2014; da Silva Fonseca et al., 2019). In addition, G6PDH is responsible for the production of ribose units necessary for nucleotide synthesis that contributes to antioxidant system, lipid synthesis and, bioconversion (Carvalho and Fernandes, 2008; Nelson et al., 2008). After 24 h exposure to MPs, the activity of G6PDH was suppressed, resulting in metabolic and oxidative damages of coral. Besides, a consistent decrease of enzymatic activity was observed after 96 h exposure to MPs. The results from enzymatic activities showed that exposure to stressors induce a state of energy limitation in the scleractinian coral *Acropora* sp. An insufficient energy supply can accelerate the collapse of the symbiotic system of corals.

The results of this study indicate that short-term exposure to high concentrations of MPs could induce the stress response of scleractinian coral *Acropora* sp. as well as inhibit the activity system of major enzymes in energy metabolism. Based on our results, it is clear that short-term exposure to concentrations of MPs is the potential to cause metabolic dysfunction between *Acropora* sp. and its algal symbionts. However, long-term exposure to lower concentrations *in situ* still needs to be studied.

## CONCLUSION

In conclusion, the present study revealed that there were correlations between MPs exposure and physiological parameters in corals *Acropora* sp. The number of MPs ingested by corals was significantly different among PET, PA66, and PE. MPs exposure disrupted the balance between symbiosis and corals by influencing the density of endosymbiont and chlorophyll. The antioxidant enzyme T-AOC content, T-SOD activity, and GSH activity were maintained at higher levels, which suggested that MPs caused the breakdown of the oxidation-reduction enzyme balance in the coral and endosymbiont symbiosis. The AKP enzyme was inhibited to various degrees by MPs. The content of NO in whole MPs exposure groups increased in the whole exposure experiment, which revealed that the immune functions suffered disruption to some extent. LDH activity was significantly down-regulated, which indicated that the energy metabolism and homeostasis of corals were disturbed. The variation of G6PDH activity showed that the coral *Acropora* sp. phosphate pentoses pathway was destroyed. The results showed the MPs ingested by corals would lead to the destruction of oxidative stress, immune suppression, and energy metabolism pathways.

## DATA AVAILABILITY STATEMENT

The original contributions presented in the study are included in the article/**Supplementary Material**, further inquiries can be directed to the corresponding author/s.

## AUTHOR CONTRIBUTIONS

BX: conceptualization and funding acquisition. DL: conceptualization, writing the original draft, and writing, review, and editing the manuscript. CL: supervision, project administration, and funding acquisition. BL: investigation

and formal analysis. HZ: data curation. XY: methodology. YX: software, supervision, and validation. ZX: investigation and formal analysis. All authors contributed to the article and approved the submitted version.

## FUNDING

The study was funded by the Guangdong Oceanic and Fishery Administration (project number: A201708D06), China Guangdong MEPP Fund [project number: GDOE (2019)A01], Shenzhen Science and Technology R&D Fund (project number: KJYY20180213182720347), Shenzhen Science and Technology R&D Fund (project number: JCYJ20200109144803833), Shenzhen Science and Technology R&D Fund (project

number: KCXFZ202002011011057), Guangdong Key Area R&D Program Project (Project number:2020B111030002), and China Guangdong OEDP Fund [project number: GDNRC (2020)040].

## SUPPLEMENTARY MATERIAL

The Supplementary Material for this article can be found online at: <https://www.frontiersin.org/articles/10.3389/fmicb.2021.666100/full#supplementary-material>

**Supplementary Figure 1** | The microscope images and size distribution of three types of MPs (PET, PA66, PE).

**Supplementary Figure 2** | The coral reef field locations (22°33'50.78"–22°40'38.18"N, 114°30'35.62"–114°33'26.90"E) and sample (*Acropora* sp.).

## REFERENCES

- Ainsworth, T. D., Kvennefors, E. C., Blackall, L. L., Fine, M., and Hoegh-Guldberg, O. (2007). Disease and cell death in white syndrome of acroporid corals on the great barrier reef. *Mar. Biol.* 151, 19–29. doi: 10.1007/s00227-006-0449-3
- Ali Chamas, H. M., Zheng, J. J., Yang, Q., Tabassum, T., Jang, J. H., Abu-Omar, M., et al. (2020). Degradation rates of plastics in the environment. *ACS Sustain. Chem. Eng.* 8, 3494–3511.
- Allen, A. S., Seymour, A. C., and Rittschof, D. (2017). Chemoreception drives plastic consumption in a hard coral. *Mar. Pollut. Bull.* 124, 198–205. doi: 10.1016/j.marpolbul.2017.07.030
- Andrady, A. L. (2011). Microplastics in the marine environment. *Mar. Pollut. Bull.* 62, 1596–1605. doi: 10.1016/j.marpolbul.2011.05.030
- Antao Barboza, L. G., and Garcia Gimenez, B. C. (2015). Microplastics in the marine environment: current trends and future perspectives. *Mar. Pollut. Bull.* 97, 5–12. doi: 10.1016/j.marpolbul.2015.06.008
- Anthony, K. R. N., Hoogenboom, M. O., Maynard, J. A., Grottoli, A. G., and Middlebrook, R. (2009). Energetics approach to predicting mortality risk from environmental stress: a case study of coral bleaching. *Funct. Ecol.* 23, 539–550. doi: 10.1111/j.1365-2435.2008.01531.x
- Besseling, E., Wang, B., Lüring, M., and Koelmans, A. A. (2014). Nanoplastic affects growth of *S. obliquus* and reproduction of *D. magna*. *Environ. Sci. Technol.* 48, 12336–12343. doi: 10.1021/es503001d
- Carpenter, E. J., Anderson, S. J., Harvey, G. R., Miklas, H. P., and Peck, B. B. (1972). Polystyrene spherules in coastal waters. *Science* 178, 749–750.
- Carvalho, C. S., and Fernandes, M. N. (2008). Effect of copper on liver key enzymes of anaerobic glucose metabolism from freshwater tropical fish *Prochilodus lineatus*. *Comp. Biochem. Phys. A* 151, 437–442. doi: 10.1016/j.cbpa.2007.04.016
- Chantal, M., Bednarz, V. N., Melvin, S. D., Jacob, H., Oberhaensli, F., Swarzensk, P. W., et al. (2020). Physiological stress response of the scleractinian coral *Stylophora pistillata* exposed to polyethylene microplastics. *Environ. Pollut.* 263:114559. doi: 10.1016/j.envpol.2020.114559
- Chapron, L., Peru, E., Engler, A., Ghiglione, J. F., Meistertzheim, A. L., Pruski, A. M., et al. (2018). Macro- and microplastics affect cold-water corals growth, feeding and behaviour. *Sci. Rep.* 8:15299.
- Chen, Q., Gundlach, M., Yang, S., Jiang, J., Velki, M., Yin, D., et al. (2017). Quantitative investigation of the mechanisms of microplastics and nanoplastics toward zebrafish larvae locomotor activity. *Sci. Total Environ.* 584, 1022–1031. doi: 10.1016/j.scitotenv.2017.01.156
- Cook, C. B., and D'Elia, C. F. (1987). Are natural populations of endosymbiont ever nutrient-limited. *Symbiosis* 4, 199–211.
- Corona, E., Martin, C., Marasco, R., and Duarte, C. M. (2020). Passive and active removal of marine microplastics by a mushroom coral (*Danafungia scruposa*). *Front. Mar. Sci.* 7:128. doi: 10.3389/fmars.2020.00128
- da Silva Fonseca, J., de Barros Marangoni, L. F., Marques, J. A., and Bianchini, A. (2019). Energy metabolism enzymes inhibition by the combined effects of increasing temperature and copper exposure in the coral *Mussismilia harttii*. *Chemosphere* 236, 124–128.
- Denis, V., Guillaume, M. M. M., Goutx, M., Palmas, S., Debreuil, J., Baker, A. C., et al. (2013). Fast growth may impair regeneration capacity in the branching coral *Acropora muricata*. *PLoS One* 8:e72618. doi: 10.1371/journal.pone.0072618
- Detree, C., and Gallardo-Escarate, C. (2018). Single and repetitive microplastics exposures induce immune system modulation and homeostasis alteration in the edible mussel *Mytilus galloprovincialis*. *Fish Shellfish Immun.* 83, 52–60. doi: 10.1016/j.fsi.2018.09.018
- Deudero, S., and Alomar, C. (2015). Mediterranean marine biodiversity under threat: reviewing influence of marine litter on species. *Mar. Pollut. Bull.* 98, 58–68. doi: 10.1016/j.marpolbul.2015.07.012
- Dias, M., Madeira, C., Jogee, N., Ferreira, A., Gouveia, R., Cabral, H., et al. (2019). Oxidative stress on scleractinian coral fragments following exposure to high temperature and low salinity. *Ecol. Indic.* 107:105586. doi: 10.1016/j.ecolind.2019.105586
- Downs, C. A., Fauth, J. E., Halas, J. C., Dustan, P., Bemiss, J., and Woodley, C. M. (2002). Oxidative stress and seasonal coral bleaching. *Free Radic. Biol. Med.* 33, 533–543. doi: 10.1016/s0891-5849(02)00907-3
- Enriquez, S., Mendez, E. R., and Prieto, R. I. (2005). Multiple scattering on coral skeletons enhances light absorption by symbiotic algae. *Limnol. Oceanogr.* 50, 1025–1032. doi: 10.4319/lo.2005.50.4.1025
- Godinot, C., Ferrierpages, C., Sikorski, S., and Grover, R. (2013). Alkaline phosphatase activity of reef-building corals. *Limnol. Oceanogr.* 58, 227–234. doi: 10.4319/lo.2013.58.1.0227
- Grottoli, A. G., Rogridues, L. J., and Palardy, J. E. (2006). Heterotrophic plasticity and resilience in bleached corals. *Nature* 440, 1186–1189. doi: 10.1038/nature04565
- Hall, N. M., Berry, K. L. E., Rintoul, L., and Hoogenboom, M. O. (2015). Microplastic ingestion by scleractinian corals. *Mar. Biol.* 162, 725–732. doi: 10.1007/s00227-015-2619-7
- Hankins, C., Duffy, A., and Drisco, K. (2018). Scleractinian coral microplastic ingestion: potential calcification effects, size limits, and retention. *Mar. Pollut. Bull.* 135, 587–593. doi: 10.1016/j.marpolbul.2018.07.067
- Hawkins, T. D., and Davy, S. K. (2012). Nitric oxide production and tolerance differ among symbiodinium types exposed to heat stress. *Plant Cell Physiol.* 53, 1889–1898. doi: 10.1093/pcp/pcs127
- Hawkins, T. D., Krueger, T., Becker, S., Fisher, P. L., and Davy, S. K. (2014). Differential nitric oxide synthesis and host apoptotic events correlate with bleaching susceptibility in reef corals. *Coral Reefs* 33, 141–153. doi: 10.1007/s00338-013-1103-4
- Hedouin, L. S., Wolf, R. E., Phillips, J., and Gates, R. D. (2016). Improving the ecological relevance of toxicity tests on scleractinian corals: influence of season, life stage, and seawater temperature. *Environ. Pollut.* 213, 240–253. doi: 10.1016/j.envpol.2016.01.086



- Hidalgo-Ruz, V., Gutow, L., Thompson, R. C., and Thiel, M. (2012). Microplastics in the marine environment: a review of the methods used for identification and quantification. *Environ. Sci. Technol.* 46, 3060–3075. doi: 10.1021/es2031505
- Higuchi, T., Agostini, S., Casareto, B. E., Suzuki, Y., and Yuyama, I. (2015a). The northern limit of corals of the genus *Acropora* in temperate zones is determined by their resilience to cold bleaching. *Sci. Rep.* 5:18467.
- Higuchi, T., Yuyama, I., and Nakamura, T. (2015b). The combined effects of nitrate with high temperature and high light intensity on coral bleaching and antioxidant enzyme activities. *Reg. Stud. Mar. Sci.* 2, 27–31. doi: 10.1016/j.rsma.2015.08.012
- Hofmann, G. E., and Todgham, A. E. (2010). Living in the now: physiological mechanisms to tolerate a rapidly changing environment. *Annu. Rev. Physiol.* 72, 127–145. doi: 10.1146/annurev-physiol-021909-135900
- Hermabessiere, L., Dehaut, A., Paul-Pont, I., and Lacroix, C. (2017). Occurrence and effects of plastic additives on marine environments and organisms: a review. *Chemosphere* 182, 781–793. doi: 10.1016/j.chemosphere.2017.08.012
- Hosseini, M. J., Shaki, F., Khansari, M. G., and Pourahmad, J. (2014). Toxicity of copper on isolated liver mitochondria: impairment at complexes I, II, and IV leads to increased ROS production. *Cell Biochem. Biophys.* 70, 367–381. doi: 10.1007/s12013-014-9922-7
- Huang, Y., Yan, M., Xu, K., Nie, H., Gong, H., and Wang, J. (2019). Distribution characteristics of microplastics in Zhubi Reef from South China Sea. *Environ. Pollut.* 255, 123–133.
- Hughes, T. P., Barnes, M. L., Bellwood, D. R., Cinner, J. E., Cumming, G. S., and Jackson, J. B. C. (2017). Coral reefs in the anthropocene. *Nature* 546, 82–90.
- Jeffrey, S. W., and Humphrey, G. F. (1975). New spectrophotometric equations for determining chlorophylls a, b, c1 and c2 in higher plants, algae and natural phytoplankton. *Biochem. Physiol. Der Pflanz.* 167, 191–194. doi: 10.1016/s0015-3796(17)30778-3
- Jeong, C. B., Won, E. J., Kang, H. M., Lee, M. C., Hwang, D. S., and Hwang, U. K. (2016). Microplastic size-dependent toxicity, oxidative stress induction, and p-jnk and p-p38 activation in the monogonot rotifer (*brachionus koreanus*). *Environ. Sci. Technol.* 50, 8849–8857. doi: 10.1021/acs.est.6b01441
- Johannes, R., Coles, S. L., and Kuenzel, N. T. (1970). The role of zooplankton in the nutrition of some scleractinian corals. *Limnol. Oceanogr.* 15, 579–586. doi: 10.4319/lo.1970.15.4.0579
- Kirstein, I. V., Kirmizi, S., Wichels, A., Garin-Fernandez, A., Erler, R., Löder, M., et al. (2016). Dangerous hitchhikers? Evidence for potentially pathogenic *Vibrio* spp. on microplastic particles. *Mar. Environ. Res.* 120, 1–8. doi: 10.1016/j.marenvres.2016.07.004
- Krueger, T., Becker, S., and Pontasch, S. (2014). Antioxidant plasticity and thermal sensitivity in four types of *Symbiodinium* sp. *J. Phycol.* 50, 1035–1047. doi: 10.1111/jpy.12232
- Lamb, J. B., Willis, B. L., Fiorenza, E. A., Couch, C. S., Howard, R., and Rader, D. N. (2018). Plastic waste associated with disease on coral reefs. *Science* 359, 460–462.
- Lancot, C. M., Bednarz, V. N., Melvin, S., Jacob, H., Oberhaensli, F., Swarzenski, P. W., et al. (2020). Physiological stress response of the scleractinian coral *Stylophora pistillata* exposed to polyethylene microplastics. *Environ. Pollut.* 263, 114–129.
- Lei, X. M., Huang, H., Wang, H. J., and Lian, J. S. (2009). Study on the responses of the symbiotic endosymbiont of hermatypic coral to eutrophication. *Mar. Sci. Bull.* 28, 43–49.
- Levy, O., Achituv, Y., Yacobi, Y. Z., Stambler, N., and Dubinsky, Z. (2006). The impact of spectral composition and light periodicity on the activity of two antioxidant enzymes (SOD and CAT) in the coral *Favia fava*. *J. Exp. Mar. Biol. Ecol.* 328, 35–46. doi: 10.1016/j.jembe.2005.06.018
- Liao, B., Wang, J., Xiao, B., Yang, X., and Li, C. (2021). Effects of acute microplastic exposure on physiological parameters in *tubastrea aurea* corals. *Mar. Pollut. Bull.* 165:112173. doi: 10.1016/j.marpolbul.2021.112173
- Long, M., Paul-Pont, I., Hégaret, H., Moriceau, B., Lambert, C., Huvet, A., et al. (2017). Interactions between polystyrene microplastics and marine phytoplankton lead to species-specific hetero-aggregation. *Environ. Pollut.* 228, 454–463. doi: 10.1016/j.envpol.2017.05.047
- Lusher, A. (2015). “Microplastics in the marine environment: distribution, interactions and effects,” in *Marine Anthropogenic Litter*, Vol. 10, eds M. Bergmann, L. Gutow, and M. Klages (Cham: Springer), 245–307. doi: 10.1007/978-3-319-16510-3\_10
- Mao, Y., Ai, H., Chen, Y., Zhang, Z., Zeng, P., Kang, L., et al. (2018). Phytoplankton response to polystyrene microplastics: perspective from an entire growth period. *Chemosphere* 208, 59–68. doi: 10.1016/j.chemosphere.2018.05.170
- McLeod, G. C. (1957). The effect of circularly polarized light on the photosynthesis and chlorophyll a synthesis of certain marine algae. *Limnol. Oceanogr.* 2, 360–362. doi: 10.1002/lno.1957.2.4.0360
- Mendrik, F. M., Henry, T. B., Burdett, H., Hackney, C. R., Waller, C., and Parsons, D. R. (2020). Species-specific impact of microplastics on coral physiology. *Environ. Pollut.* 269:116238. doi: 10.1016/j.envpol.2020.116238
- Muller-Parker, G., D’Elia, C. F., and Cook, C. B. (2015). “Interactions between corals and their symbiotic algae,” in *Coral Reefs in the Anthropocene*, Vol. 5, ed. C. Birkeland (Dordrecht: Springer), 99–116. doi: 10.1007/978-94-017-7249-5\_5
- Nelson, D. L., Albert, L. L., and Cox, M. M. (2008). *Lehninger Principles of Biochemistry*, 5th Edn. New York, NY: W.H. Freeman.
- Nicosia, A., Celi, M., Vazzana, M., Damiano, M. A., Parrinello, N., and D’Agostino, F. (2014). Profiling the physiological and molecular response to sulfonamidic drug in *procamburus clarkii*. *Comp. Biochem. Phys. C* 166, 14–23. doi: 10.1016/j.cbpc.2014.06.006
- Okubo, N., Takahashi, S., and Nakano, Y. (2018). Microplastics disturb the anthozoanalgae symbiotic relationship. *Mar. Pollut. Bull.* 135, 83–89. doi: 10.1016/j.marpolbul.2018.07.016
- Palmer, C. V., Bythell, J. C., and Willis, B. L. (2011). A comparative study of phenoloxidase activity in diseased and bleached colonies of the coral *Acropora millepora*. *Dev. Comp. Immunol.* 35, 1098–1101. doi: 10.1016/j.dci.2011.04.001
- Paul-Pont, I., Lacroix, C., Gonzalez Fernandez, C., and Hegaret, H. (2016). Exposure of marine mussels *Mytilus* spp. to polystyrene microplastics: toxicity and influence on fluoranthene bioaccumulation. *Environ. Pollut.* 216, 724–737. doi: 10.1016/j.envpol.2016.06.039
- Perez, S., and Weis, V. (2006). Nitric oxide and cnidarian bleaching: an eviction notice mediates breakdown of a symbiosis. *J. Exp. Biol.* 209, 2804–2810. doi: 10.1242/jeb.02309
- Pierson, D. C., Colom, W., and Rodrigo, M. A. (2017). The influence of photoinhibition and algal size on vertical variations in chlorophyll-a specific photosynthesis. *SIL Proc.* 25, 516–519.
- Porra, R. J., Thompson, W. A., and Kriedemann, P. E. (1989). Determination of accurate extinction coefficients and simultaneous equations for assaying chlorophylls a and b extracted with four different solvents: verification of the concentration of chlorophyll standards by atomic absorption spectroscopy. *Biochim. Biophys. Acta Biomembr.* 975, 389–394.
- Porter, J. W., Fitt, W., Spero, H., Rogers, C. S., and White, M. W. (1989). Bleaching in reef corals: physiological and stable isotopic responses. *Proc. Natl. Acad. Sci. U.S.A.* 86, 9342–9346. doi: 10.1073/pnas.86.23.9342
- Reichert, J., Arnold, A. L., Hoogenboom, M. O., Schubert, P., and Wilke, T. (2019). Impacts of microplastics on growth and health of hermatypic corals are species-specific. *Environ. Pollut.* 254:113074. doi: 10.1016/j.envpol.2019.113074
- Reichert, J., Schellenberg, J., Schubert, P., and Wilke, T. (2018). Responses of reef building corals to microplastic exposure. *Environ. Pollut.* 237, 955–960. doi: 10.1016/j.envpol.2017.11.006
- Rocha, R. J., Bontas, B., Cartaxana, P., Leal, M. C., Ferreira, J. M., Rosa, R., et al. (2015). Development of a standardized modular system for experimental coral culture. *J. World Aquacult. Soc.* 46, 235–251. doi: 10.1111/jwas.12186
- Saliu, F., Montano, S., Leoni, B., Lasagni, M., and Galli, P. (2019). Microplastics as a threat to coral reef environments: detection of phthalate esters in neuston and scleractinian corals from the Faafu Atoll, Maldives. *Mar. Pollut. Bull.* 142, 234–241. doi: 10.1016/j.marpolbul.2019.03.043
- Soriano-santiago, O., Linancabello, M. A., Delgadillonuno, M. A., Ortegaortiz, C. D., and Cuevasvenegas, S. (2013). Physiological responses to oxidative stress associated with pH variations in host tissue and endosymbiont of hermatypic coral *Pocillopora capitata*. *Mar. Freshw. Behav. Phys.* 46, 275–286. doi: 10.1080/10236244.2013.827877
- Stimson, J., and Kinzie, R. A. (1991). The temporal pattern and rate of release of endosymbiont from the reef coral *Pocillopora damicornis* (Linnaeus) under

- nitrogen-enrichment and control conditions. *J. Exp. Mar. Biol. Ecol.* 153, 63–74. doi: 10.1016/s0022-0981(05)80006-1
- Su, Y., Zhang, K., Zhou, Z., Wang, J., and Lin, S. (2020). Microplastic exposure represses the growth of endosymbiotic dinoflagellate *Cladocinium goreau* in culture through affecting its apoptosis and metabolism. *Chemosphere* 244, 125485. doi: 10.1016/j.chemosphere.2019.125485
- Sun, X., Li, Q., Zhu, M., Liang, J., Zheng, S., and Zhao, Y. (2017). Ingestion of microplastics by natural zooplankton groups in the northern south china sea. *Mar. Pollut. Bull.* 115, 217–224. doi: 10.1016/j.marpolbul.2016.12.004
- Syakti, A. D., Jaya, J. V., Rahman, A., Hidayati, N. V., Raza'i, T. S., Idris, F., et al. (2019). Bleaching and necrosis of staghorn coral (*Acropora formosa*) in laboratory assays: immediate impact of LDPE microplastics. *Chemosphere* 228, 528–535. doi: 10.1016/j.chemosphere.2019.04.156
- Tang, J., Ni, X., Zhou, Z., Wang, L., and Lin, S. (2018). Acute microplastic exposure raises stress response and suppresses detoxification and immune capacities in the scleractinian coral *Pocillopora damicornis*. *Environ. Pollut.* 243, 66–74. doi: 10.1016/j.envpol.2018.08.045
- Teuten, E. L., Saquing, J. M., Knappe, D. R. U., Barlaz, M. A., Jonsson, S., Bjorn, A., et al. (2009). Transport and release of chemicals from plastics to the environment and to wildlife. *Philos. Trans. R. Soc. Lond. B* 364, 2027–2045.
- Tian, P., and Niu, W. (2017). The complete mitochondrial genome of the *Acropora* sp. *Mitochondrial DNA B Resour.* 2, 652–653. doi: 10.1080/23802359.2017.1375882
- Veron, J. E. N. (1992). Conservation of biodiversity: a critical time for the hermatypic corals of Japan. *Coral Reefs* 11, 13–21. doi: 10.1007/bf00291930
- Walker, T. R. (2018). Drowning in debris: solutions for a global pervasive marine pollution problem. *Mar. Pollut. Bull.* 126:338. doi: 10.1016/j.marpolbul.2017.11.039
- Wang, W., Ge, J., and Yu, X. (2020). Bioavailability and toxicity of microplastics to fish species: a review. *Ecotox. Environ. Safe.* 189:109913. doi: 10.1016/j.ecoenv.2019.109913
- Weis, V. M. (2010). The susceptibility and resilience of corals to thermal stress: adaptation, acclimatization or both?: NEWS and VIEWS. *Mol. Ecol.* 19, 1515–1517. doi: 10.1111/j.1365-294x.2010.04575.x
- Wu, Y., Guo, P., Zhang, X., Zhang, Y., Xie, S., and Deng, J. (2019). Effect of microplastics exposure on the photosynthesis system of freshwater algae. *J. Hazard. Mater.* 374, 219–227. doi: 10.1016/j.jhazmat.2019.04.039
- Yu, X., Yu, K., Liao, Z., Liang, J., Deng, C., Huang, W., et al. (2020a). Potential molecular traits underlying environmental tolerance of *Pavona decussata* and *Acropora pruinosa* in Weizhou Island, northern South China Sea. *Mar. Pollut. Bull.* 156:111199. doi: 10.1016/j.marpolbul.2020.111199
- Yu, X., Yu, K. F., Huang, W., Liang, J., and Liao, Z. (2020b). Thermal acclimation increases heat tolerance of the scleractinian coral *Acropora pruinosa*. *Sci. Total Environ.* 733:139319. doi: 10.1016/j.scitotenv.2020.139319
- Zhang, C., Chen, X., Wang, J., and Tan, L. (2017). Toxic effects of microplastic on marine microalgae *Skeletonema costatum*: interactions between microplastic and algae. *Environ. Pollut.* 220, 1282–1288. doi: 10.1016/j.envpol.2016.11.005
- Zhao, M., Yu, K., Shi, Q., Yang, H., Riegl, B., Zhang, Q., et al. (2016). The coral communities of Yongle atoll: status, threats and conservation significance for coral reefs in South China Sea. *Mar. Freshw. Res.* 67:1888. doi: 10.1071/mf15110
- Zhao, M. X., Yu, K. F., Shi, Q., Chen, T. R., Zhang, H. L., and Chen, T. G. (2013). Coral communities of the remote atoll reefs in the Nansha Islands, southern South China Sea. *Environ. Monit. Assess.* 185, 7381–7392. doi: 10.1007/s10661-013-3107-5
- Zhou, Z., Zhao, S., Ni, J., Su, Y., Wang, L., and Xu, Y. (2018). Effects of environmental factors on C-type lectin recognition to zooxanthellae in the stony coral *Pocillopora damicornis*. *Fish Shellfish Immun.* 79, 228–233. doi: 10.1016/j.fsi.2018.05.026

**Conflict of Interest:** The authors declare that the research was conducted in the absence of any commercial or financial relationships that could be construed as a potential conflict of interest.

Copyright © 2021 Xiao, Li, Liao, Zheng, Yang, Xie, Xie and Li. This is an open-access article distributed under the terms of the Creative Commons Attribution License (CC BY). The use, distribution or reproduction in other forums is permitted, provided the original author(s) and the copyright owner(s) are credited and that the original publication in this journal is cited, in accordance with accepted academic practice. No use, distribution or reproduction is permitted which does not comply with these terms.



# Disentangling the Complexity of the Rumen Microbial Diversity Through Fractionation Using a Sucrose Density Gradient

Ruth Hernández<sup>1,2</sup>, Hugo Jimenez<sup>2</sup>, Cesar Vargas-Garcia<sup>3</sup>, Alejandro Caro-Quintero<sup>2,4\*</sup> and Alejandro Reyes<sup>1,5\*</sup>

<sup>1</sup> Computational Biology and Microbial Ecology Group, Max Planck Tandem Group in Computational Biology, Department of Biological Sciences, Universidad de los Andes, Bogotá, Colombia, <sup>2</sup> Animal Microbiology Laboratory, Agrodiversity Department, Corporación Colombiana de Investigación Agropecuaria – AGROSAVIA, Bogotá, Colombia, <sup>3</sup> Grupo de Investigación en Sistemas Agropecuarios Sostenibles, Corporación Colombiana de Investigación Agropecuaria – AGROSAVIA, Bogotá, Colombia, <sup>4</sup> Departamento de Biología, Facultad de Ciencias, Universidad Nacional de Colombia, Bogotá, Colombia, <sup>5</sup> The Edison Family Center for Genome Sciences and Systems Biology, Washington University School of Medicine, St. Louis, MO, United States

## OPEN ACCESS

### Edited by:

David Kamanda Ngugi,  
German Collection of Microorganisms  
and Cell Cultures GmbH (DSMZ),  
Germany

### Reviewed by:

Shengguo Zhao,  
Chinese Academy of Agricultural  
Sciences, China  
Derek M. Bickhart,  
United States Department  
of Agriculture (USDA), United States

### \*Correspondence:

Alejandro Reyes  
a.reyes@uniandes.edu.co  
Alejandro Caro-Quintero  
acarq@unal.edu.co

### Specialty section:

This article was submitted to  
Microbial Symbioses,  
a section of the journal  
Frontiers in Microbiology

**Received:** 05 February 2021

**Accepted:** 15 June 2021

**Published:** 08 July 2021

### Citation:

Hernández R, Jimenez H,  
Vargas-García C, Caro-Quintero A  
and Reyes A (2021) Disentangling  
the Complexity of the Rumen  
Microbial Diversity Through  
Fractionation Using a Sucrose Density  
Gradient.  
Front. Microbiol. 12:664754.  
doi: 10.3389/fmicb.2021.664754

The ruminal microbial community is an important element in health, nutrition, livestock productivity, and climate impact. Despite the historic and current efforts to characterize this microbial diversity, many of its members remain unidentified, making it challenging to associate microbial groups with functions. Here we present a low-cost methodology for rumen sample treatment that separates the microbial community based on cell size, allowing for the identification of subtle compositional changes. In brief, the sample is centrifuged through a series of sucrose density gradients, and cells migrate to their corresponding density fraction. From each fraction, DNA is extracted and 16S rRNA gene amplicons are sequenced. We tested our methodology on four animals under two different conditions, fasting, and post-feeding. Each fraction was examined by confocal microscopy showing that the same sucrose fraction consistently separated similar cell-sized microorganisms independent of the animal or treatment. Microbial composition analysis using metabarcoding showed that our methodology detected low abundance bacterial families and population changes between fasting and post-feeding treatments that could not be observed by bulk DNA analysis. In conclusion, the sucrose-based method is a powerful low-cost approximation to untwine, enrich, and potentially isolate uncharacterized members of the ruminal microbiome.

**Keywords:** ruminal microbiota, microbial diversity, sucrose density gradient, fractionation, low abundant microorganisms

## INTRODUCTION

Ruminants contribute to food security by providing adequate protein and energy to the human population (Matthews et al., 2018). These animals have developed a unique ability to convert plant cell wall carbohydrates into meat and milk, mostly due to the complex and not completely characterized symbiotic microbiota in their rumen (Morgavi et al., 2013; Ribeiro et al., 2016).

The ruminal microbiota is composed of diverse populations of obligate anaerobic microorganisms belonging to all life domains such as Bacteria, Eukarya, and Archaea (Nagaraja, 2016), which interact with each other to degrade the plant material and convert it into metabolic by-products and microbial protein (Ribeiro et al., 2016).

For decades, many studies conducted in the rumen have tried to understand the numbers, composition, and function of the ruminal microbial community, mostly using conventional culture-based methods (Morgavi et al., 2013; Ribeiro et al., 2016). These types of methods have only allowed for the isolation and cultivation of about 15% of the estimated bacterial species potentially present in the rumen (Ribeiro et al., 2016). However, for most of the ruminal microorganisms, little is known about their functional role, and many of them have not been taxonomically classified at the genus or species level (Henderson et al., 2015; Puniya et al., 2015).

The modulation of the microbial community structure and function of the rumen has been an area of intense research, particularly in the development of food additives, probiotics, chemical compounds, and diets, which may lead to improved productivity and animal health, as well as the reduction of environmental impacts (Fernando et al., 2010; Poulsen et al., 2013; van Lingen et al., 2017; Teoh et al., 2019; Petri et al., 2020; Stanton et al., 2020). Several recent studies have used the high-throughput sequencing of universal phylogenetic markers such as 16S rRNA gene to evaluate bacterial community shifts under different treatments (Wang et al., 2017; Yang B. et al., 2018). In many cases, even though these interventions seem to affect animals' productivity or health, the direct relationship between such treatments and the identification of microbial community members responding to them remains unclear. Various factors might hinder the identification of such differences. For instance, one factor is the population-level diversity not observable with the current methodologies, which obscures the response of specific populations (Caro-Quintero and Ochman, 2015). Another factor is the effect of bulk DNA extraction that destroys the distinct levels of microbial organization and favors the amplification of the most abundant members of the communities, missing important functional organisms that might have lower abundances (Puniya et al., 2015; Eisenstein, 2018). For these reasons, it is necessary to develop new methodological approaches to disentangle the complexity of the ruminal microbiota that favor the recovery of a greater variety of taxonomic groups, allowing a higher resolution for the microbes' identification affected by treatments and conditions.

The fractionation of the microbial community by cell size and density prior to DNA extraction is an alternative methodological approach that can unravel the enormous microbial diversity present in complex samples. Density gradients are used in different disciplines to separate particles based on size and density (York and Tang, 2015; Lianidou and Hoon, 2018). The principle of the method is simple; first, the sample is deposited on top of either a continuous or step gradient. Then, using centrifugal forces, the different particles in the sample migrate to their corresponding density equilibrium (Brakke, 1951). Different types of media have been used to build density gradients for

biological applications; however, one of the most common is a sucrose medium, which has been used for the separation of molecules such as DNA, RNA, and proteins (Raschke et al., 2009; Kleene et al., 2010). In microbiology, the sucrose density gradient has been used for the purification and concentration of viruses (Huhti et al., 2010; Urbas et al., 2011), the separation of *Burkholderia* sp. from a consortium of microorganisms (Chee et al., 2010), and the separation of prokaryotes from eukaryotes (protozoa) in aquatic environments (Garrison and Bochdansky, 2015). Sieving the microbial community through these gradients has the potential for the identification of more subtle differences among less abundant organisms, providing a greater resolution when compared to currently used methods.

In this study, we present a methodology that incorporates a sucrose density gradient as a simple approach for separating ruminal microbial communities by size and density. This approach allows for a more thorough recovery of the diversity of taxonomic groups from the ruminal microbiota compared to commonly used methods for microbial community characterization. To demonstrate the utility of the fractionation methodology, we evaluated the taxonomic diversity shifts of the ruminal microbial community in two different treatments: fasting and post-feeding. We used fractionated and non-fractionated (total) samples and compared the microbial composition using 16S rRNA gene amplicon sequencing. We hypothesized that density fractionation provides a higher resolution by disentangling the microbial community's complexity, allowing for a more sensitive identification of taxonomic bacterial groups.

## MATERIALS AND METHODS

### Experimental Design and Sampling

Three female adults of the creole Colombian cattle breed Blanco Oreginegro (BON) and one male of the Holstein breed were used in the study. These animals were kept at the same location and fed *ad libitum* with fresh grass (*Cenchrus clandestinus*) at the Colombian Agricultural Research Corporation Agrosavia, Tibaitatá (Mosquera, Cundinamarca, Colombia).

Two ruminal samples were collected for each animal after fasting and post-feeding. The animals were initially fed *ad libitum* in a closed grass field, then they were moved to a different enclosure without the availability of food for 16 h. After that time, the fasting sample was taken, registering the order of sampling for the different animals. Once these samples were taken, the animals were moved back to the grass field where they were fed *ad libitum* again. Although no quantification was performed on the amount of grass consumed, all the animals registered similar grassing activities and after 1 h they were all removed from the grass field back to the enclosure where they were sampled for post-feeding in the same order as in the first sampling. One animal, BON-C, bled during the post-feeding sampling, which contaminated the sample. Consequently, this sample was discarded.

The ruminal fluid samples of the BON animals were collected using a nasogastric probe, and the ruminal fluid of the Holstein animal was obtained directly from the rumen through a fistula according to the standard procedure published



in Minor et al. (1977). The ruminal fluid samples were initially filtered through a sterile cheesecloth to remove plant material, then 200 mL of ruminal fluid was stored in 50 mL tubes with 10% (v/v) formal saline solution. The samples were refrigerated at 4°C until further use.

All animal procedures were conducted by a veterinary doctor after the previous approval of Agrosavia's bioethics committee and followed all the guidelines and standards for animal care. In addition, the Institutional Committee for the Care and Use of Laboratory Animals (CICUAL) at the Universidad de los Andes also approved these procedures. The number of individuals used in this study was maintained to a minimum to avoid any negative impact of the research on animal health and wellness.

## Sucrose Density Gradient Construction

Eight solutions were prepared in a PBS buffer at different sucrose concentrations of 5, 10, 20, 30, 40, 50, 60, and 70% (w/v% or g/L). Each solution was prepared to a final volume of 100 mL. The sucrose gradient was assembled as follows. First, a 5 mL of a sucrose solution at 70% was added to a 50 mL tube, which was immediately immersed into liquid nitrogen for approximately 60–80 s, until the solution was completely frozen. Next, 5 mL of the 60% solution was added and fast-frozen as mentioned before. The process was repeated with the other sucrose solutions from the highest (50%) to the lowest (5%) sucrose concentration. The 50 mL tube was kept frozen at –20°C until further use.

From each of the three 50 mL samples collected for each animal for each treatment, a sucrose gradient was prepared. To prepare the sucrose density gradient for analysis, it was thawed for 2 h at room temperature, keeping it still to prevent the different sucrose solutions from mixing. A total volume of 5 mL of ruminal fluid was carefully added on top of the sucrose density gradient. The tube was centrifuged at  $5,000 \times g$  for 35 min at 4°C to prevent damage to the protozoan cells. After centrifugation, the fractions of each gradient were retrieved separately using a sterile 16 G needle, which was inserted through the wall of the falcon tube at the bottom end of each fraction. This process was performed sequentially starting from the top of the tube with the lowest concentration fraction (5%). The individual gradient fractions obtained from the previous procedure were stored in 15 mL tubes at 4°C until further use. The experimental replicates from each animal and treatment were pooled together in order to obtain DNA concentrations suitable for sequencing at specific sucrose gradient levels, this will hinder estimates of reproducibility as technical replicates were not assessed. In total, 69 samples were processed in this study.

## Microscopy Analysis of Sucrose Gradient Fractions

To evaluate the size distribution of the microorganisms in the different gradient fractions, an aliquot of 10 µL of each sample was examined under a light microscope. Some selected samples were used to visualize the microorganisms under the scanning electron microscope and confocal microscope. To reduce focal problems due to microbial cells accumulating at different depths, we used Colorfrost Plus Slide Glass, which electrostatically adhered the microbial cells to the

slides (ThermoFisher, United States). All observations were performed at the Microscopy Center of the Universidad de los Andes. High-resolution pictures were taken with the scanning electron microscope to confirm the cell size observations. The size of the microorganisms in each fraction was measured using the confocal microscope and five independent photographs were analyzed using a custom ImageJ (Abramoff et al., 2003) script on each fraction from each sample (available upon request). The ImageJ script includes image preprocessing steps (background subtraction algorithms, noise filtering), segmentation (Phansalkar Local threshold method), and post-processing routines (watershed, hole filling, erode-dilate morphological filtering). We gaged the convex hull of each cell and computed its area value in square microns. We assessed image quality by using the deep neural network model proposed in Yang S. J. et al. (2018).

## DNA Extraction in Different Sucrose Gradient Fractions

DNA extraction of each gradient fraction was done as follows. First, 5 mL of each gradient fraction were centrifuged at 19,064 RCF at 1°C for 1 h. The supernatant was discarded and the pellet was washed with a PBS buffer to remove sucrose residues. The suspension was centrifuged again at 11,769 RCF at 4°C. The supernatant was discarded, and the pellet was resuspended in 200 µL of PBS buffer for a second time. The three experimental replicates for each gradient were pooled in a 2 mL centrifuge tube to make a single DNA extraction. In addition, 500 µL of a homogenized, composite ruminal fluid sample that did not undergo a separation by sucrose density gradient was also extracted and used as a total community for reference comparisons (bulk DNA extraction). The samples were frozen in liquid nitrogen for 5 min and were then placed in a water bath at 65°C for 5 min. This procedure was repeated three times in order to promote the lysis of the cells. DNA extraction was performed using the kit ZR Fungal/Bacterial DNA MiniPrep™ from Zymo research following manufacturer's instructions. Samples were initially homogenized using bead beating for 5 min. The DNA concentration was measured using the Nanodrop (ThermoFisher, United States) and the quality of the DNA was verified by electrophoresis in a 2% (w/v) agarose gel. The DNA extractions from the different fractions were quantified, obtaining concentrations ranging from 8 to 100 ng/µL (see **Supplementary Table 1**). All samples with concentration greater than 30 ng/µL were diluted to 30 ng/µL. For PCR (see below) 30 ng of DNA was used as template, implying 1 µL for all dilutions and the corresponding volume from the stock sample in order to reach 30 ng for samples with less than 30 ng/µL.

## Construction of Amplicon Libraries of the 16S rRNA Gene and Sequencing

The construction of metabarcoding libraries for 16S rRNA gene was performed in two steps, following the protocol described by Caro-Quintero and Ochman (2015) which targeted the hypervariable region V4. In the first step, a triplicate PCR reaction was prepared for each of the samples. Amplification was performed using 30 ng of DNA template, 12 µL of the Promega

GoTag® Green Master Mix (United States), 10 µL of ddH<sub>2</sub>O, and 1 µL of each of the primers 515F and 806R at a concentration of 10 µM (Caporaso et al., 2012) with customized modifications to include a partial sequence of the Illumina amplification primers as shown in Faith et al. (2013); see **Supplementary Table 2**). The PCR amplification reactions were carried out under the following conditions: initial denaturation of 3 min at 94°C; three cycles of 45 s at 94°C, 30 s at 62°C, and 30 s at 72°C; three cycles of 45 s at 94°C, 30 s at 60°C, and 30 s at 72°C; three cycles of 45 s at 94°C, 30 s at 58°C, and 30 s at 72°C; 25 cycles of 45 s at 94°C, 30 s at 56°C, and 30 s at 72°C; and a final extension of 10 min at 72°C. PCR products were purified using AMPure XP beads (Beckman Coulter) following the manufacturer's instructions.

In the second step, the triplicate amplification products were pooled together. Five microliters of this pool were used as a template for a second PCR reaction where the indexes and the Illumina adaptors were added to the sequences (**Supplementary Table 2**). The second PCR reaction was performed with the same conditions as described in the first PCR reaction. The PCR conditions included an initial denaturation of 3 min at 94°C, 12 cycles of denaturation for 45 s at 94°C, annealing for 1 min at 56°C, an extension for 1.5 min at 72°C, and a final extension of 10 min at 72°C. PCR products were cleaned using AMPure XP beads (Beckman Coulter). The quality of the DNA was verified by electrophoresis in a 2% (w/v) agarose gel. The DNA concentration was measured using Qubit 2 fluorometer (ThermoFisher, United States). An equimolar pool of all the PCR products was made with a final concentration of 10 nM. Pair-end libraries were sequenced in an Illumina MiSeq machine at the Universidad del Bosque in Bogotá, Colombia.

## Bioinformatic Analysis

Samples were demultiplexed with an in-house script (available upon request). The quality of the sequences was verified using FastQC v0.11.7 (Andrews, 2010). The adapters and linker sequences were removed from the 16S rRNA gene partial sequences, using cutadapt v1.12 (Martin, 2011). Low-quality sequences, with an average Phred score <20 and having a read length <200 nts, were detected and removed from the datasets using trimmomatic v0.38 (Bolger et al., 2014). Qiime2 pipeline v\_2018 (Bolyen et al., 2019) was used to analyze the 16S rRNA gene amplicon libraries. Dada2 (Callahan et al., 2016) was the algorithm used to denoise and generate Amplicon Sequence Variants (ASVs). Pair-end sequences were used as input for Dada2 with a truncation length of 200 bp. The ASVs present in less than two samples or had less than 4 sequences in all the samples in the feature table were eliminated from further analyses. The taxonomic assignment of the ASVs was performed using the Silva Database version 132 (Glöckner et al., 2017).

## Microbial Community Structure and Diversity Estimates

All samples were rarefied to a depth of 7,200 sequences, which was the minimum number obtained for any given sample. We used Observed OTUs, Shannon and Faith's PD indices as alpha diversity metrics to explore within-sample microbial heterogeneity. Beta diversity (between-sample diversity) was

calculated using the weighted UniFrac metric (Lozupone et al., 2011). A principal coordinate analysis (PCoA) was used to visualize the results and the effect of the different variables under study such as the sucrose concentration, breed, individual, and sampling time. Rarefaction curves and beta diversity metrics were estimated using the "core-metrics-phylogenetic" plug-in implemented in the Qiime2 pipeline.

## Statistical Analysis

A permutational multivariate analysis of variance, PERMANOVA (Anderson, 2017), was performed using weighted UniFrac distance matrix on the ASVs table to establish if there were significant differences among groups of samples according to variables such as fractions of the gradient, the breed, and the individual animals. Distances were calculated among the different fractions of the sucrose gradient as well as the total sample of ruminal fluid. Pairwise comparisons (PERMANOVA between two groups) were made between gradient's fractions and between animals to establish significant differences.

Welch's test (White et al., 2009) was used to establish if there were significant differences in taxonomic families' abundance or ASVs between fractions, and total, and between fasting and post-feeding treatments. In addition, the Fisher exact test (Ironyt and Pereirat, 1986) was used to quantify the enrichment of a given taxonomic group in the different fractions of the gradient. The taxonomic groups were filtered in both tests using a difference between proportions >1% together with an FDR adjusted *p*-value < 0.01. These two tests were implemented in the software STAMP-v2 (Statistical Analysis of taxonomic and functional Profiles) (Parks et al., 2014). To visualize if a taxonomic group (family or an ASV) was significantly enriched, an extended error bar plot was performed in the STAMP-v2 program.

An abundance matrix was generated with the taxonomic groups that had a statistically significant difference in at least two fractions of the gradient for the same animal. This matrix allowed us to identify in which fractions of the gradient a specific taxonomic group was enriched. The enrichment of the taxonomic groups across the gradient fractions was analyzed for each animal.

## RESULTS

### The Sucrose Density Gradient Allows for the Separation of the Microbial Community by Size

We developed a methodology to disentangle the complex composition of the ruminal microbial community using sucrose-based fractionation of microbial cells. Our approach incorporated a sucrose step gradient using a range of eight sucrose (w/v) concentrations: 5, 10, 20, 30, 40, 50, 60, and 70%. We also included the densest fraction of the community that moved through all gradients and formed a large pellet at the bottom of the tube (labeled 70%\_F) which was enriched with protozoa that were not observed in any of the other fractions. Ruminal samples were collected from four animals at *fasting* and *post-feeding* treatments, with the exception of one animal (BON-C) who was not possible to sample at 1 h post-feeding, for a total of

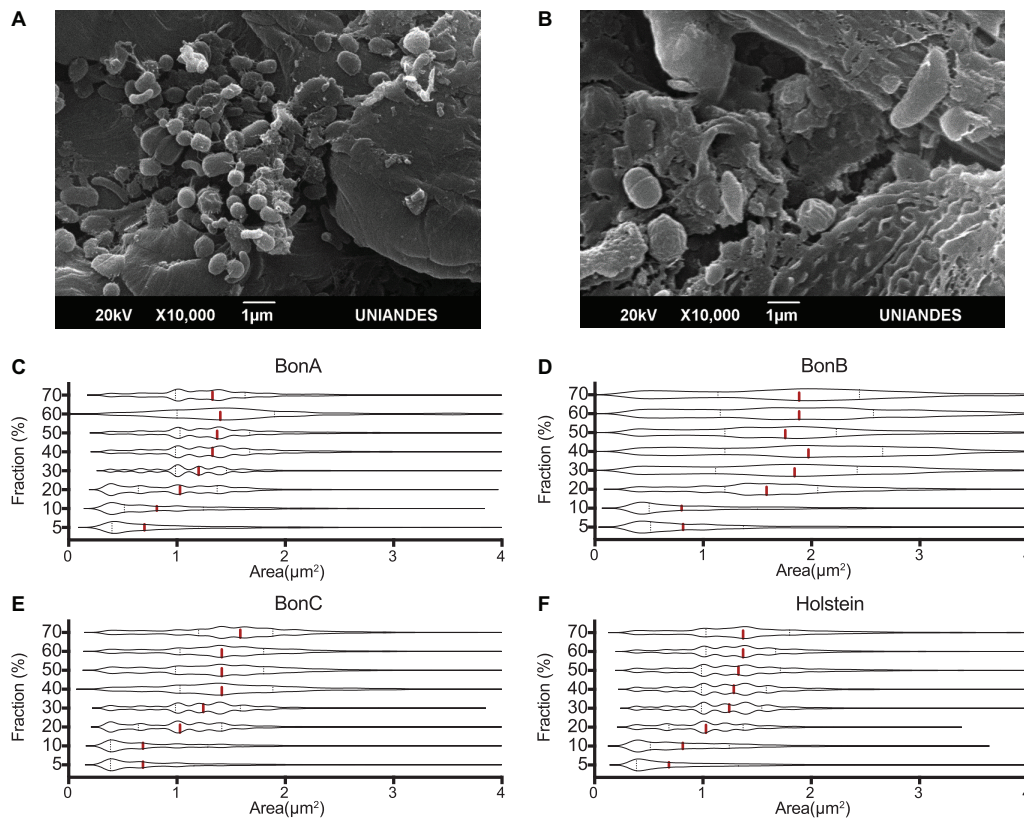


**FIGURE 1 |** Cell size distribution of rumen microorganisms retained by the different sucrose fractions. The transmission electron microscope images show the differences in the size of microorganisms present in the (A) 20% and (B) 70% sucrose fractions. Violin plots represent the distribution of cells' area quantified by confocal microscopy, five confocal microscopy microphotographs were analyzed for each gradient and animal. The panels show the distributions of the 70, 60, 50, 40, 30, 20, 10, and 5% fractions, for the animals (C) BON-A, (D) BON-B, (E) BON-C and (F) Holstein.

seven ruminal samples. For each of those samples, the nine step gradient fractions were obtained as well as a total non-fragmented sample, resulting in 69 samples.

Using electron microscopy, it was observed that the lowest density fraction (5%) enriched the smallest bacteria, with an average size ranging from 0.2 to 0.8  $\mu\text{m}^2$ , while the larger microorganisms of about 1–4  $\mu\text{m}^2$  in area were enriched in the larger fractions (30–60%) (Figure 1A). Other large microorganisms such as protozoa and bacterial clusters (i.e., chains and aggregates) were found in the highest density fractions (i.e., 70 and 70%\_F) (Figure 1B).

To assess the consistent separation of similar size microorganisms, five confocal microscopy microphotographs were analyzed for each gradient and animal. The cell size (area) was determined for each microphotograph, and the area distribution was represented as violin plots. Although an overlapping distribution in cell sizes along the gradient was observed, different cell sizes were clearly enriched at different concentrations of the gradient. The cell size distribution for samples corresponding to the BON-A (Figure 1C), BON-B (Figure 1D), BON-C (Figure 1E), and Holstein (Figure 1F) showed that the step gradients demonstrated similar size selection across animals. For instance, the distributions of the 5 and 10% fractions showed an enrichment of small cell-sizes,

with the first quartile and median of the cell size around 0.3 and 0.7  $\mu\text{m}^2$ , respectively. In the case of the 20% gradient, the first quartile was around 0.75  $\mu\text{m}^2$  with a median around 1  $\mu\text{m}^2$ . For the 30% gradient, the first quartile was around 1  $\mu\text{m}^2$  with a median around 1.3  $\mu\text{m}^2$ . Finally, for the concentrations between 40 and 70%, the first quartile was around 1  $\mu\text{m}^2$  and the median was around 1.5  $\mu\text{m}^2$ . For BON-B, cell size distribution for all gradients seems to have a larger variability and wider distribution due to suboptimal focus quality. We obtained absolute measure predictions of image focus with no user-specified parameters, using the deep learning trained model (Yang S. J. et al., 2018), combining all images for BON-B and comparing the focus accuracy with that of the images from BON-A. A clear decrease in accuracy could be observed (Supplementary Figure 1).

## Diversity Is Mainly Driven by Sucrose-Based Fractionation

To analyze the microbial community structure in bovine ruminal fluid and the effect of the sucrose-based fractionation, we sequenced the V4 region of the 16S *rRNA* gene. An average sequence depth of  $33.661 \pm 60.044$  (mean  $\pm$  SD) reads were obtained per sample. ASVs were identified using Dada2 and rarefaction curves for each sample were calculated for all samples



(**Supplementary Figure 2**). Given the diversity saturation observed for most samples at  $\sim 7,000$  reads, a rarefaction was performed at 7,200 sequences to prevent sample loss and used for downstream analyses.

The PCoA with weighted UniFrac distance metric on the ASVs abundances was used to visualize similarities between the bacterial communities and evaluate the effect of variables such as sucrose concentration, breed/sampling method, individual, and treatments. Interestingly, the sucrose concentration was the variable with the highest contribution at inter-sample diversity, as it corresponded to the variable that principally explained the variation in the first two axis of the PCoA with 32 and 28% of the variability explained, respectively (**Figure 2A** and **Supplementary Figure 3**). In general, a distinction was observed for the 5, 10, and 20% fractions compared to the rest of the fractions, suggesting that they share a similar bacterial composition, confirming what was also observed on the cell size distribution by the confocal microscopy (**Figure 1**). The total (non-fragmented) samples of ruminal fluid were grouped closely together with the largest gradient fractions (50, 60, 70, and 70%<sub>F</sub>), suggesting that the total ruminal fragment is enriched with bacterial taxons more commonly identified in the medium-high density gradients.

Given that most of the variation was explained by the fractionation of density gradients, a PERMANOVA analysis was performed to test whether the weighted UniFrac distances among the different gradients were significantly different (pseudo- $F = 5.39$ ,  $p$ -value 0.001, 999 permutations; see **Supplementary Table 3A** for pairwise comparisons). This analysis showed that the smallest fractions of the gradient (5 and 10%) and the larger fractions (50, 60, 70, 70%<sub>F</sub>, and Total) are more similar. This can also be observed when comparing weighted UniFrac distances within and between gradient fractions (**Figure 3**). For example, when comparing the distances within the different samples of the 5% fraction (**Figure 3A**, it is possible to observe black box) that they had lower variation. This low beta diversity or distance was also observed when comparing the samples of the 5% fraction with the 10 or 20% fractions. In contrast, significantly higher distances were observed when comparing the 5% fraction with the larger fractions (50, 60, and 70%). The behavior observed with the distances based on the composition of the microbial communities was similar to what was observed in the microscopy pictures. Importantly, some of the lowest inter-sample distances observed were between the total sample and each gradient, showing that the total is a composite of all the other samples.

Beyond the sucrose density gradient effect, a separation between breeds was observed in the PCoA plot on axis 3 (8.6% of total variation), where the samples belonging to animal of the Holstein breed were separated from those from the BON breed (**Supplementary Figure 3B**). It is important to mention that the Holstein animal was the only one sampled by cannula and not by nasogastric tube as the other BON animals. Several studies have suggested that there are no, or very minor, variations in the microbial communities obtained depending on the sampling method of rumen microorganisms (Kittelman et al., 2015; Tapio et al., 2016; de Assis Lage et al., 2020). However, due to this complete co-variation between the

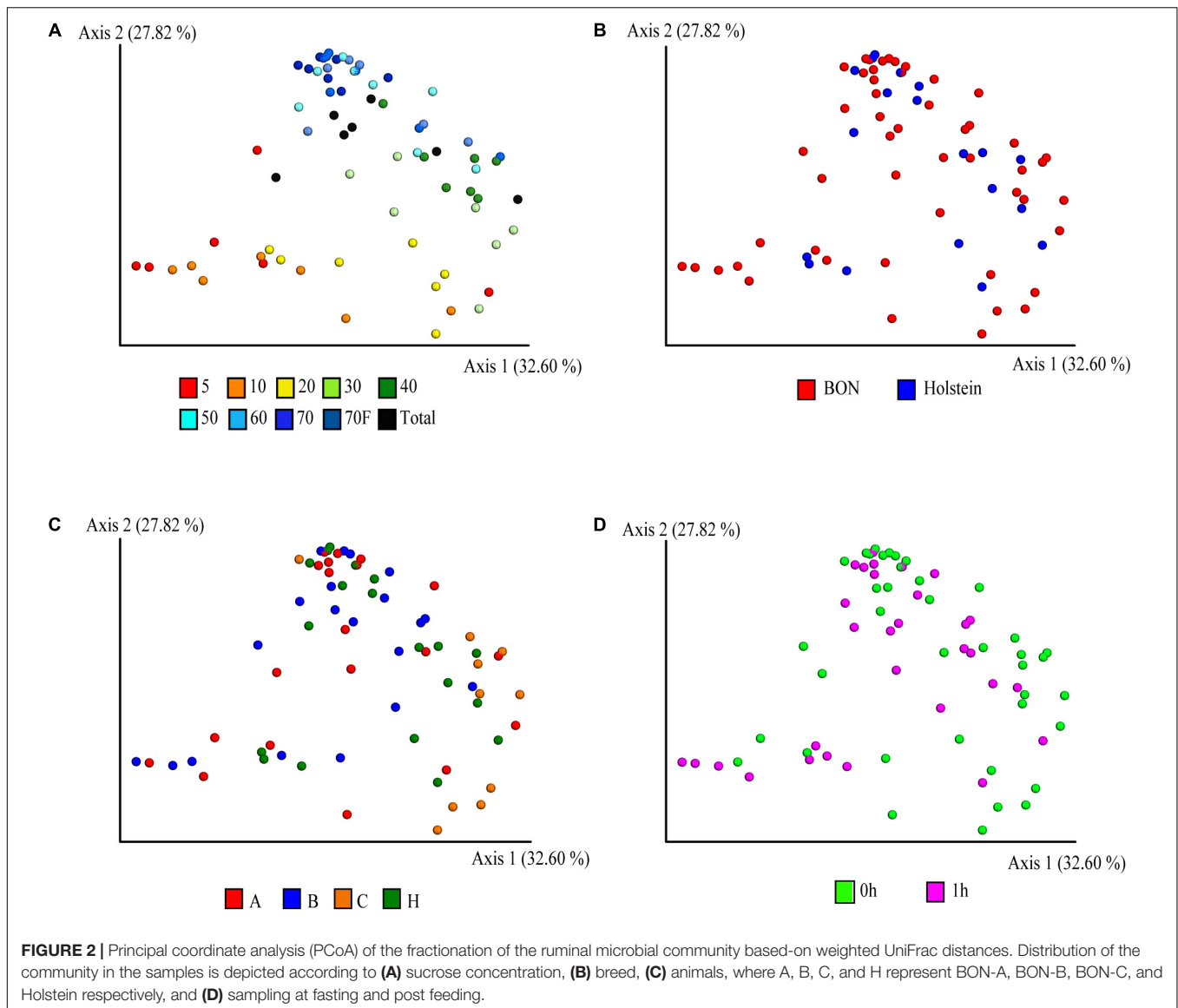
sample treatment and the breed of the animals, it is impossible for us to determine if the breed was the main factor affecting the observed variation and not the sampling method. The samples belonging to the three BON animals were similar among them and no clear separation was observed (**Figure 2C** and **Supplementary Figure 3C**). Those results were further confirmed with the ANOVA analysis, where we found significant differences driven by breed/sampling method (pseudo- $F = 3$ , 11,131,  $p$ -value = 0.003, 999 permutations) and individuals (pseudo- $F = 4.154$ ,  $p$ -value = 0.001, permutations = 999), although no significant differences were found between the individuals of BON-A and BON-B (**Supplementary Table 3B**). Finally, no apparent effect of the feeding was observed on the first 3 PCoA axes (**Figure 2D** and **Supplementary Figure 3D**).

## Enrichment of Bacterial Families and ASVs Throughout the Sucrose Density Gradient

Bacterial taxonomic groups were enriched in specific sucrose fractions compared to the total ruminal fluid. **Figure 4** shows bacterial abundance at the family level for all the individual animals during fasting and post-feeding, for the families comprising up to 70% of the relative abundance. Several interesting observations can be derived from **Figure 4**. First, the families present in any gradient were also found in the total samples; additionally, all 27 bacterial families were present in all four animals. Second, as noted above, the 5 and 10% fractions have very similar composition, and for most of the animals this similarity extended to the 20% or even 30% fraction. However, the abundance of the families that were enriched in the 5 and 10% fractions began to decrease as the sucrose concentration increased. Examples of the families enriched in the 5 and 10% fractions included members from the Bacteroidales order, such as Bacteroidaceae and RF16, the Clostridiaceae and Erysipelotrichaceae from the Firmicutes, and the Anaeroplasmataceae from the Tenericutes. There were few families enriched in the 40 and 50% fractions, with the Enterobacteriaceae among those, suggesting that these fractions are a transition between smaller and larger bacteria. Additionally, other families were enriched only in 60, 70, and 70%<sub>F</sub>, such as the families Mogibacteriaceae, Veillonellaceae, Methanobacteriaceae, Anaerolinaceae and S24-7 from Bacteroidales. Lastly, the 70%<sub>F</sub> fraction shows different abundance patterns with respect to other fractions immediately preceding it, likely due to the presence of sessile bacteria that were attached to large particles and the absence of planktonic cells, prevalent in the other fractions. Families such as Prevotellaceae, Ruminococcaceae, Lachnospiraceae, and Spirochaetaceae were present in all the gradient fractions and were the most abundant bacterial families for all the animals.

Looking deeper in the taxonomic level, the distribution of genera per gradient shows three different patterns based on their relative abundance (**Supplementary Figure 4**), confirming the results observed at the family level. First, some genera were enriched at the lower sucrose concentrations (5, 10, and 20%), such as *Anaeroplasma* (*Anaeroplasmataceae* family), RFN20 (*Erysipelotrichaceae*), *Clostridium* (*Clostridiaceae* family), BF311





(*Bacteroidaceae* family); all those genera belong to families identified as enriched in the smaller gradients. Furthermore, the genus *Anaerostipes* from the Lachnospiraceae family also was identified in these fractions. Second, we observed microorganisms with a higher relative abundance at more dense gradient concentrations (50, 60, and 70%); among these we found genera with species that have very large cell sizes such as *Selenomonas* (Veillonellaceae), *Oscillospira* and *Ruminococcus* (Ruminococcaceae), and *Butyrivibrio* (Lachnospiraceae). Finally, some genera have a higher relative abundance at the intermediate gradients (30, 40, and 50%); among these we found *Prevotella*, *Fibrobacter*, *Pseudobutyrivibrio*, *Treponema*, and *Coprococcus*. Interestingly, when analyzed at the genus level, families such as Lachnospiraceae and Ruminococcaceae that were reported at high abundance in all fractions of the gradient were composed by different genera, each one with specific distribution of cell sizes highlighting the large diversity within these taxonomic groups.

## Bacterial Community Changes Are Better Detected Using the Sucrose-Based Fractionation

In order to evaluate the usefulness of the fractionation on the identification of subtle changes in the composition of the microbial community, we identified the taxonomic groups that show significant differences when comparing the fasting and post-feeding treatment for the same animal. It is important to highlight that the BON-C is excluded from these analyses due to the lack of post-feeding samples. We found significant differences in the abundance of bacterial families before and after feeding; many of those differences were not detected in the total samples (Supplementary Table 4). Using the program STAMP, we evaluated the differential abundance between fasting and post-feeding conditions at the family level (Fisher's exact test, FDR corrected  $q$ -value <  $1e-2$ ) for each of the animals.

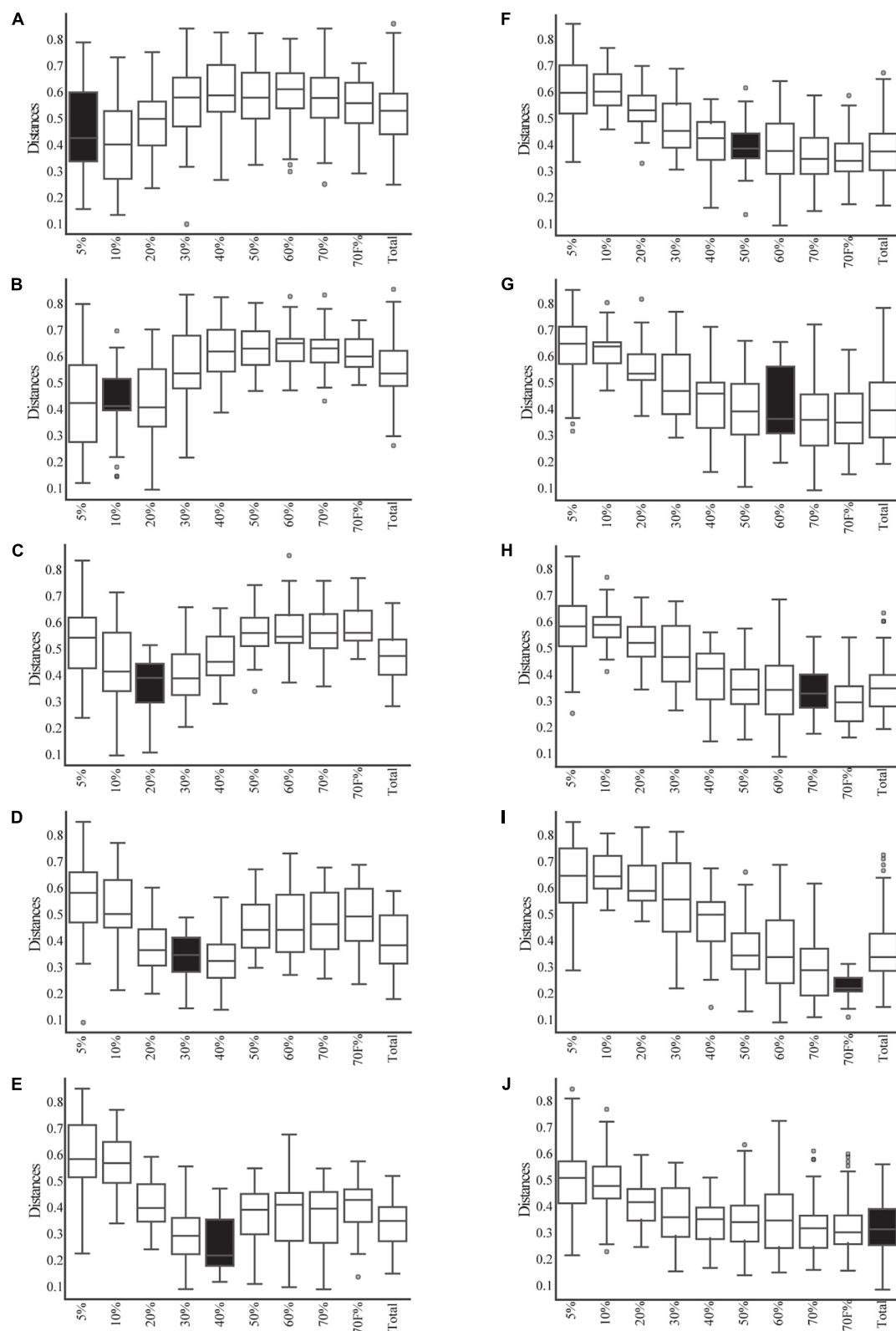
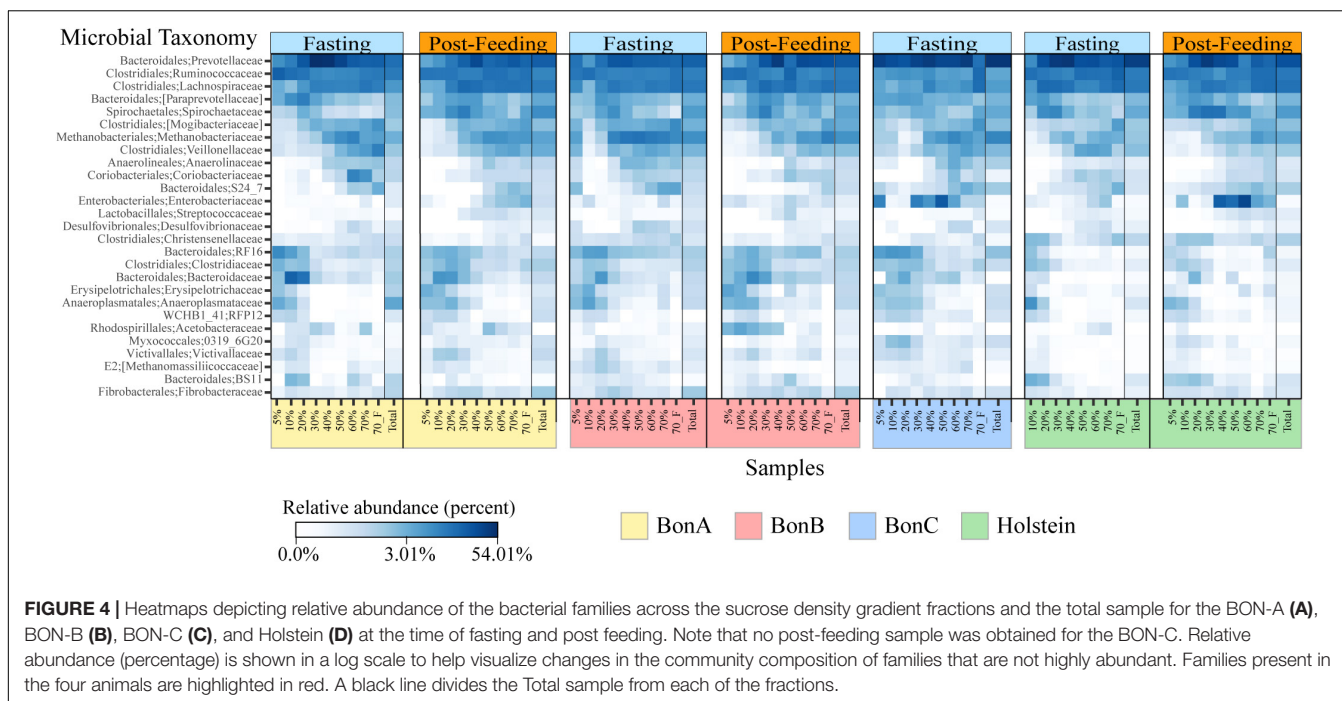


**FIGURE 3 |** Beta-diversity analysis based on weighted UniFrac between and within the fractions of the gradient and total samples. The distribution of the distances between each sample from each fraction of the gradient (and the total) and the samples from each other fraction of the gradient are shown in open box plots. The distances of samples within a given fraction of the gradient are shown in black box plots. **(A–I)** Correspond to each fraction of the gradient. **(J)** Corresponds to the distance of the total samples compared to all gradients and itself.



We chose families that had an effect size (differences between proportions) greater than 1 (significantly enriched in fasting) or less than  $-1$  (significantly enriched in post-feeding), comparing equivalent fractions (**Supplementary Table 4**). In general, it was observed that all the enriched families were identified either uniquely in the fractions or shared by the fractions and the total. Furthermore, the magnitude of the effect size and the percent of families enriched were greater in the fractions compared to the total sample. Specifically in terms of percentage of enriched families in fragments vs. totals, we have in BON-A: 81.5 vs. 37.0%; BON-B: 77.8 vs. 7.4%; Holstein: 66.7 vs. 22.2%. These results indicate that the gradients allowed the detection of a stronger family enrichment signal.

The families enriched exclusively in the fractions of the gradient included Coriobacteriaceae, Bacteroidales RF16 and Methanomassiliicoccaceae. On the other hand, the families that were present in all fractions showing consistent enrichment patterns included Ruminococcaceae, Lachnospiraceae, Spirochaetaceae, and Prevotellaceae. Interestingly, the enrichment direction was not the same on all animals or between the fractions and the total. An example of this is Prevotellaceae, which shows opposite treatment enrichment. In BON-B, this family is enriched in post-feeding in most of the gradients, while in BON-A it is highly enriched in the 20–50% gradients during fasting and in the total during post-feeding. Given that within a bacterial family a large functional and phenotypic diversity of microorganisms is expected, we examined the enrichment of microorganisms using ASV as a proxy for species level. We wanted to determine if at a finer level of taxonomic classification implying closer evolutionary relationships, a defined group may have a more restricted associated cell size, and therefore it would be possible to see stronger effects of separation on the enrichment at this level.

Using the total number of ASVs, we calculated the difference in proportions between fasting and post-feeding, analogous to what was performed at the family level, selecting those with enrichment in fasting (as a difference greater than 1) or post-feeding (with values less than  $-1$ ). We selected only those ASVs that were significantly enriched in at least two fractions of the gradient (**Supplementary Table 5**). Analogously to what was observed at the family level, there was a higher number of ASVs enriched in the gradients compared to the number enriched in total samples. In summary, the proportion of enriched ASVs in fractions vs. the total samples is 29 vs. 7 for BON-A, 18 vs. 2 for BON-B; and 21 vs. 3 for Holstein. The ASVs that belong to the taxonomic groups Bacteroidaceae BF311, Bacteroidales RF16, Ruminococcaceae, Clostridiales, and Tenericutes ML615J-28 were enriched in the smallest fractions (5, 10, and 20%) for the BON-A and BON-B. Meanwhile, ASVs belonging to *Prevotella* were mostly enriched in the middle fractions (30, 40, and 50%) for all the animals, as well as ASVs from Enterobacteriaceae in the Holstein. The ASVs that belong to *Methanobrevibacter* genus were enriched in the largest fractions (60, 70, and 70%\_F) of the gradient for the BON-B and Holstein, and the ASVs belonging to the bacterial group WPS-2 were enriched in the biggest fractions of the gradient in the Holstein. **Supplementary Figure 5** shows the unique and shared ASVs enriched in the three animals. Only four ASVs were shared by all three animals, two of them belonging to the *Prevotella* genus, and the other ones to the taxonomic groups Clostridiales and Achaeobacteriaceae. The larger number of enriched ASVs was found uniquely in Holstein and BON-A, with 13 and 12 ASVs, respectively. Another group of enriched ASVs is those present in BON-A and BON-B, 12 ASVs, while no ASVs were found shared between Holstein and BON-B. This shows that each animal has their unique ASV profile, with animals from the same breed sharing higher numbers of bacteria.

As observed at the family level, there were also some ASVs that were present in all the fractions of the gradients studied and in the total samples. It was possible to identify those ASVs enriched using a Welch test due to the treatment in most of the fractions (Figure 5), and for some selected representatives we plotted their abundance as a function of the sucrose fraction (Figure 6). The enriched ASVs are members of the genera *Prevotella*, *Butyrivibrio*, *Ruminococcus*, *Succinivibrillum*, *Paraprevotella*, and *Treponema*. Interestingly, some ASVs were enriched in between treatments but only in a few specific fractions of the gradient (Figure 7). Some ASVs were enriched in the smallest fractions of the gradient such as *Acetobacter* variants in the animal BON-B, other ASVs were enriched in the middle gradient fractions such as *Prevotella* variants in the animal BON-A, and other ASVs were enriched in the largest gradient fractions such as Enterobacteriaceae variants in the animal BON-A. The identification of those ASVs shows that the fractionation of the microbial community can detect changes in the abundance that total DNA extraction without fractionation cannot.

## DISCUSSION

### The Sucrose Density Gradient and the Separation of the Ruminal Microorganisms

The ruminal microbial diversity is a key factor in improving productivity, health, and reducing methane emission in cattle (Matthews et al., 2018). Despite its importance, there are still gaps in the knowledge of the diversity of ruminal microbiota and we are still exploring how treatments and conditions affect the abundance and composition of ruminal microbes (Malmuthuge and Guan, 2017). In this study, we developed an alternative approach to study the composition and diversity of the ruminal microbiota by fractionating the microbial community based on cell size and density.

We were able to show that the sucrose gradient is a simple method for microbial community analysis, which showed consistent fractionation in four different animals tested. These results were confirmed both qualitatively and quantitatively by the cell size distribution of samples measured by confocal microscopy. Furthermore, it was shown that most cells are maintained intact in the different fractions, allowing the recovery of enriched cells viable for culture and other downstream analysis. A similar use has been reported in the human gut, where bacteria has been separated from the rest of the fecal material using a NICODENZ density gradient and could be recovered alive and preserved for a fecal microbiota transplantation (Hevia et al., 2015). We observed that the cell morphology and size distribution corresponded to that of bacteria, archaea, and protozoa; however, we did not observe fungi zoospores, an important part of this microbial community. A potential explanation is that zoospores attach to the plant material in a sessile state (Orpin and Bountiff, 1978). This matches with the observation that a very low number of motile zoospores have been observed in the ruminal fluid (Lee et al., 2000) and with our

observation from the images obtained with the scanning electron microscope for the 40% fraction.

The analysis of cell size distribution clearly shows that even though breed/sampling method has an important effect on the ruminal microbial composition, same sucrose percentage fractions between different animals recover similar microbial taxonomic composition. In this sense, the cell size distribution obtained by microscopy and the taxonomic composition analysis showed a similarity between the 5, 10, and 20% fractions, significantly different from the 40, 50, 60, and 70% fractions. One possible explanation is that in the environment, cell sizes and their densities may differ to what has been characterized in laboratory conditions. They may depend on factors such as age, growth phase, or cell arrangement morphology (e.g., aggregates or chains); in consequence, the cell density might vary, as well as their distribution in the different gradient fractions. Because of this, it is expected to find ASVs in different fractions of the gradient. The lack of a finer resolution or separation among the fractions could be due to technical difficulties in recovering the purified fraction and/or incomplete fractionation during the centrifugation. A strong separation of the fractions by centrifugation was avoided to maintain the viability and integrity of the cells. Other plausible explanations of that seemingly bimodal distribution of bacterial sizes could be due to factors like protozoa predation and the anoxic environment. This variation in bacterial size has been reported as a consequence of predation of bacteria by the protozoa (Chrzanowski and Šimek, 1990; Gonzalez et al., 1990). Studies in aquatic environments have demonstrated that when bacteria are under grazing pressure, the bacterial size tends to become smaller or very large (Hahn and Höfle, 2001) as a size-defensive mechanism because protozoans prefer to feed on intermediate-sized bacteria (1  $\mu\text{m}$ ). Bacteria with a size smaller than 1  $\mu\text{m}$  or greater than 2  $\mu\text{m}$  have a predation rate 10–200 times lower than in an intermediate size bacterium. Another factor that could influence the similarity in the microbial composition in the fractions of 40–70% is the possibility of the protozoa disrupting the gradient as they pass through, generating a homogenization of the fractions.

### The Enrichment of Families and ASVs in the Sucrose Density Gradient

During the development of this research, it was possible to observe that the most important factor affecting the taxonomic composition of the samples was the sucrose gradient. This observation shows the possibility to use such methods for enrichment of certain bacterial species, genera, or families based on their size or density. At higher taxonomic ranks (i.e., family), it was possible to observe a consistency in the enrichment among the different gradients between animals, even from different breeds. For example, the taxonomic groups Anaeroplasmataceae, Bacteroidaceae, and Clostridiaceae were enriched in the smallest fractions of the gradient, which was consistent with what was observed at the genus level, with genera such as *Clostridium* (Ruminococcaceae); *Anaerostipes* (Lachnospiraceae); *Clostridium* (Clostridiaceae); BF311 (Bacteroidaceae); *Anaeroplasma* (Anaeroplasmataceae);



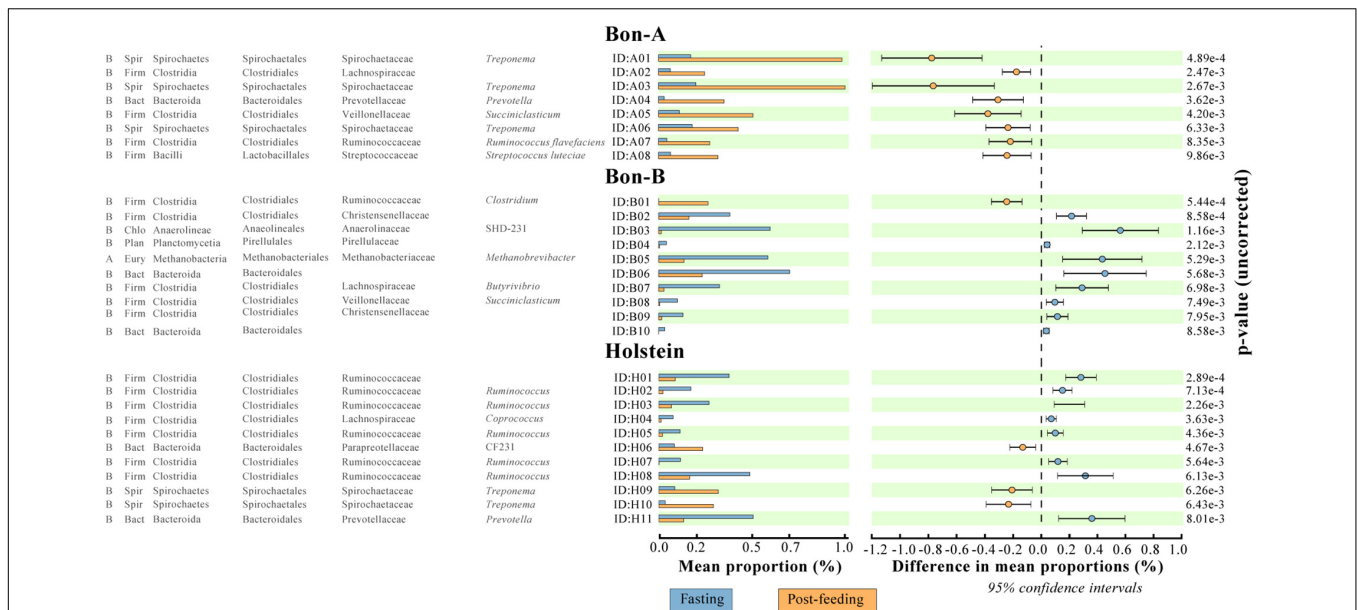


**FIGURE 5 |** ASVs that were significantly enriched in all the fractions of the gradient before or after feeding. **(A)** BON-A, **(B)** BON-B, and **(C)** Holstein. The graphics were made using the program STAMP program using Welch's test with a  $p$ -value  $< 0.01$ . No FDR correction was made.

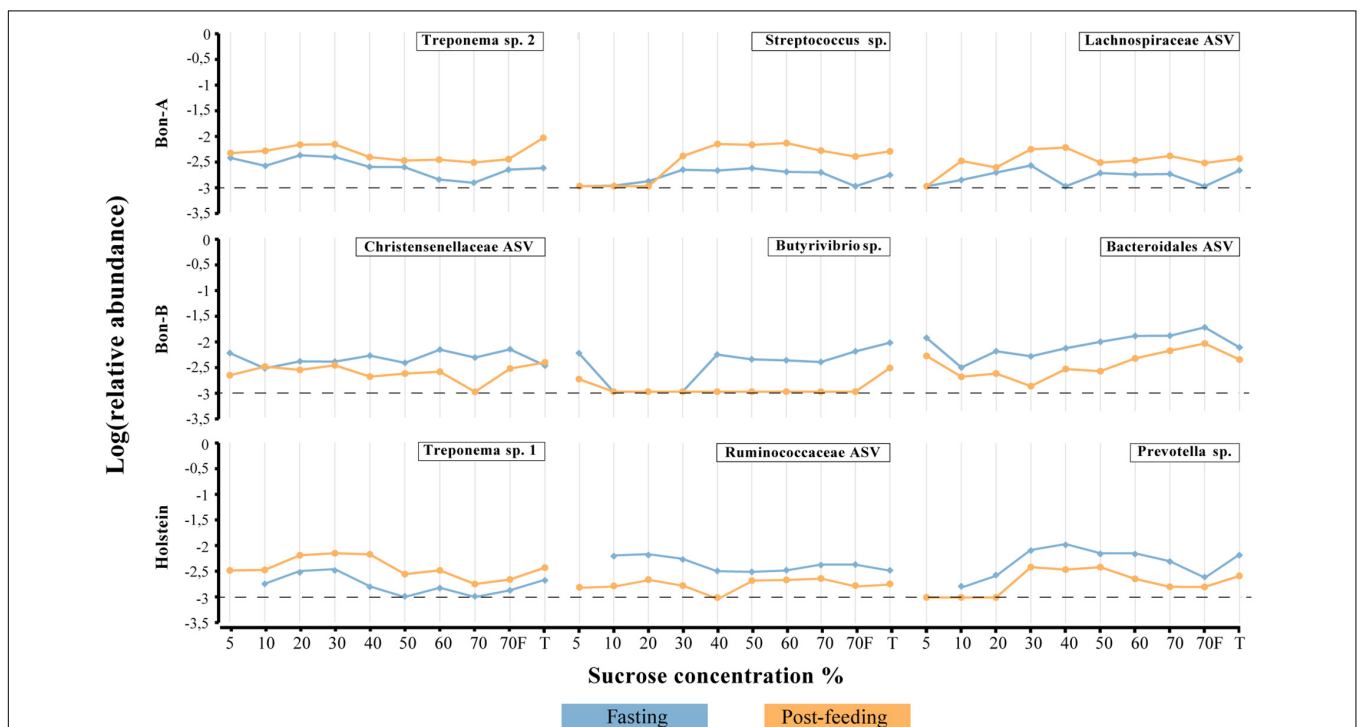
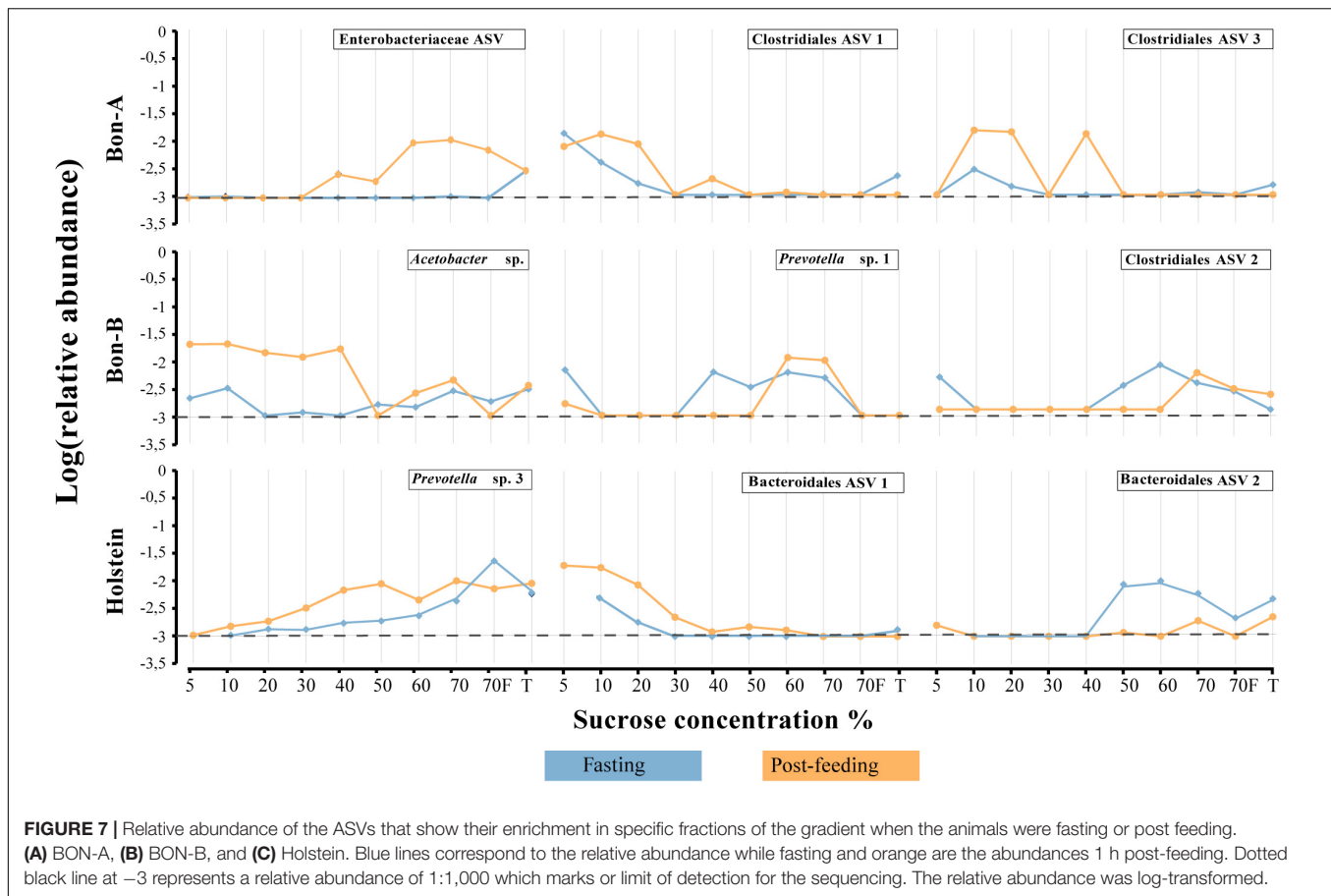


**FIGURE 6 |** Relative abundance of the ASVs that show their enrichment throughout all, or almost all, the fractions of the gradient. **(A)** BON-A, **(B)** BON-B, and **(C)** Holstein. Blue lines correspond to the relative abundance while fasting and orange are the abundances 1 h post-feeding. Dotted black line at  $-3$  represents a relative abundance of 1:1,000 which marks or limit of detection for the sequencing. The relative abundance was log-transformed.

RFN20 (Erysipelotrichaceae). Most of these genera have a reported small cell size, for instance *Anaeroplasma* and anaerobic mycoplasmas have an average cell size of  $0.5 \mu\text{m}$  and *Anaerostipes* has a described cell size of  $0.5\text{--}0.6 \mu\text{m}$  wide  $\times$   $2.0\text{--}4.3 \mu\text{m}$  long.

Families enriched in the larger fractions of the gradients included Mogibacteriaceae, Veillonellaceae, Anaerolinaceae, Coriobacteriaceae, and S24-7. These families were further confirmed at the genus level, with members of the



*Selenomonas*, *Anaerovibrio* (Veillonellaceae); *Ruminococcus*, *Oscillospira* (Ruminococcaceae); *Butyrivibrio* (Lachnospiraceae); *Methanobrevibacter* (Methanobrevibacteriaceae); SHD-231 (Anaerolinales); and *Desulfovibrio* (Desulfovibrionales). This includes organisms known for a large cell size such as the genus *Selenomonas* with an average cell size of  $2.0\text{--}3.0 \times 5.0\text{--}10.0 \mu\text{m}$  (Falkow et al., 2006) and *Oscillospira* has an average size of  $3\text{--}6 \times 10\text{--}40 \mu\text{m}$  (Gophna et al., 2017). Other genera, even though they have smaller reported cell size, are known to grow in filamentous and chain structures, such as *Butyrivibrio* ( $0.21\text{--}0.32 \times 2\text{--}4 \mu\text{m}$ ) (Sewell et al., 1988) and *Ruminococcus* ( $0.9 \times 1.3 \mu\text{m}$ ) (Latham et al., 1978). Another example of how the cell size influences the distribution across the fractions of the gradient of the bacterial group at the genus level is the *Ruminococcus* genus. The *Ruminococcus* are prevalent in most of the ruminant species, and they are major cellulose and cellobiose degraders (Krause et al., 1999). The bacterial morphology of *R. albus* is mainly coccus and diplococcus with diameters varying from 0.8 to 2.0  $\mu\text{m}$ . The cells of *R. flavefaciens* are spherical with a diameter varying from 0.7 to 1.6  $\mu\text{m}$ ; however, this species grows in chains (Puniya et al., 2015), which is likely the reason why they were enriched in the 60 and 70% fractions. There were also families that appeared throughout the whole range of fractions such as Ruminococcaceae, Lachnospiraceae, Prevotellaceae, and

families belonging to Clostridiales. Interestingly, at the genus level, we observe genera from these families being enriched in different fractions. These families, which are among the most abundant and prevalent in the ruminal microbiota (Henderson et al., 2015), have been described with large morphological diversity living as single cells, filaments, chains, and flocs (Parte et al., 2011).

One important aspect is the enrichment of unclassified or poorly characterized bacteria in different gradients. We observed ASVs from the candidate division SR1 (SR1c) and Tenericutes phylum were only enriched in the small fractions of the gradient. The SR1c group is also found in diverse environments like sea sediments (Corre, 2001), termite gut (Hongoh et al., 2003), and sulfur rich springs (Blank et al., 2002) and do not have any representative isolated strains. The SR1c has been reported in several of the rumen microbiota studies (Davis et al., 2009; Zhong et al., 2018). However, the diversity of this group in the rumen is low, and only two OTUs from this group have been reported in the rumen and belonging to the BD2-14 sub-group III (Davis et al., 2009; Ghotra, 2014; AlZahal et al., 2017). The SR1c was also present in all the fractions of the gradient indicating that there are other bacterial sizes of this group in the ruminal fluid.

## The Sucrose Density Gradient as a Tool to Disentangle Subtle Changes in Microbial Composition in Response to Treatments

In our experimental design, we aimed at using the fractionation of cells according to their density to allow for a higher resolution of changes and enrichments upon treatments such as feeding. Although the treatment used (fasting vs. feeding) does not necessarily imply a drastic change in the microbial community, most of the variations and enrichments observed were found precisely in the fractions and not in the total samples. In this experiment, the post-feeding time could actually represent an active phase of transitions with a reported peak of increased abundance of fibrolytic bacteria at 1–2 h post feeding (Huws et al., 2018). Examples of these increases in abundance were the families Bacteroidales BS11 and Bacteroidales S24-7. These families are commonly present in the rumen but are found in low abundance and do not have cultured representatives yet. In our study, the family BS11 was enriched in the 10 and 20% fractions, for the BON-A when fasting, in the 5 and 10% for the Holstein, and in the 50% fraction in the BON-B post-feeding (**Figure 4**), suggesting a niche partitioning of this family in the rumen (Solden et al., 2017). The presence of this family in different fractions could indicate different genera with different size and functional profiles in the rumen. The family Bacteroidetes S24-7 was enriched in 60, 70, and 70%\_F for most of the animals when they were fasting (**Figure 4**), which could be explained by the bacterial cells floating in the ruminal fluid waiting to adhere to the plant material that enters the rumen when the animal feeds on grass. To obtain more precise results about the enrichment of the different taxonomic groups when fasting or post feeding, it would be desirable to sample a larger number of animals to observe more robust and homogeneous trends. On the other hand, the functional response of the low abundant microorganism, such as the families Bacteroidales BS11 and S24-7, is not well understood in ruminal animals. The enrichment of these families in the gradient will provide an opportunity to explore the genome of these low abundant groups. In this sense, recent studies performed in the human gut microbiome demonstrated the importance of the low abundant microorganisms as a source of new functional genes with antimicrobial and biotechnological applications (Almeida et al., 2019).

We believe that the current method is widely applicable and of potential interest in different relevant situations, particularly when studying the effect of treatments such as prebiotics and probiotics in the animal microbial community since some of those effects are more subtle and may not affect the most abundant bacteria. However, even small changes may bring significant biological variation. The method presented here can be further optimized, for instance, the addition of a cell dissociating step prior to the fractionation in order to separate those microorganisms that can flock together, or those that are attached to large plant material. The dissociation can be performed using treatment such as Tween or physical methods such as sonication. Based on our results is not clear whether the complete set of different gradients is needed in order to obtain

the observed separation, as each gradient sieves the bacteria that pass to the next gradient, or if a selected subset of gradients could have the same effect. However, from the obtained results it is clear that is not needed to sequence all fractions. We suggest that in future studies a focus could be made on the 5, 30, 60, and 70\_F fractions. We think this will reduce the sequencing cost, while still representing all of the taxonomic groups that inhabit in the rumen. As with any enrichment method, it is important to consider that any bias or noise that could be present in the samples could be artificially enriched when separated throughout the sucrose gradient.

For other microorganisms, an optimization of the gradient or even the solution will still be necessary. In the current setup, the viral component of the rumen community will be present only in the 5% gradient fraction. If what is desired is to fractionate the different members of the viral community, a Cesium Chloride gradient with ultracentrifugation should be used instead. On the other hand, when considering large organisms such as protozoa, the sucrose density gradient facilitates the isolation and concentration of these microorganisms in a unique fraction making it easy to determine the effect of a treatment on their abundance.

Finally, caution is important when analyzing the enrichment based on specific fractions of the gradient. If the total DNA yield of a given fraction is too low or the alpha diversity is significantly affected compared to the total sample, it is possible that sampling bias could affect the relative abundance of the taxons and thus the enrichment observed. Furthermore, if biological inferences will be made based on enrichments identified in particular fractions, verification through qPCR or other methods such as CFU counts on selective media should be done, starting from the total sample, to confirm the results obtained from the fractions.

In conclusion, in this study we describe a low-cost methodology to expand the knowledge of the ruminal microbial diversity in the ruminal fluid compared to a standard procedure. Using the sucrose density gradient methodology, we separated the ruminal microbiota based on their size and density in different fractions of a gradient. We demonstrated that fractions of the gradient of ruminal sample fluid have different compositions and abundance, which allowed us to enhance the resolution of the study of bacterial diversity in the rumen. We found an enrichment of the less abundant bacterial families and ASVs in different fractions of the gradient compared with a total sample without separation. Lastly, the sucrose density gradient was able to detect subtle changes in the differential abundance, not only for the most abundant and prevalent groups of bacteria in the rumen before and after feeding, but also for the less abundant groups. These less abundant groups are likely equally important groups in the rumen. Hence, this method will allow an improved diversity analysis of the effect of a treatment on the ruminal microbiota. The enrichment of specific or less abundant taxonomic groups in specific fractions of the gradient maintaining their viability in a less complex mixture open the possibilities for culturing strategies or even whole-genome shotgun sequencing for genomic reconstruction, paving the way for a more exhaustive functional characterization of those elusive members of the ruminal microbiome.

## DATA AVAILABILITY STATEMENT

The datasets presented in this study can be found in online repositories. The names of the repository/repositories and accession number(s) can be found below: <https://www.ebi.ac.uk/ena>, PRJEB42578.

## ETHICS STATEMENT

The animal study was reviewed and approved by Committee for the Care and Use of Laboratory Animals (CICUAL), Universidad de los Andes.

## AUTHOR CONTRIBUTIONS

HJ, AC-Q, RH, and AR contributed to the conception, design, and supervision of this study. HJ and AC-Q provided resources for the field sampling and the processing of the samples in the laboratory. AR supplied the computational resources for the bioinformatic analysis. Data collections were made by RH and HJ and the processing and analysis of the data was made principally by RH with collaboration from AR and AC-Q. CV-G processed and analyzed the data of the images obtained with confocal microscopy. The statistical analysis was made by RH and AR. RH wrote the first draft of the manuscript. HJ, AC-Q, CV-G, and AR participated in the writing of different sections of the manuscript. All authors read, contributed to manuscript revision, and approved the submitted version.

## REFERENCES

- Abramoff, M., Magalhães, P., and Ram, S. J. (2003). Image Processing with ImageJ. *Biophotonics Int.* 11, 36–42.
- Almeida, A., Mitchell, A. L., Boland, M., Forster, S. C., Gloor, G. B., Tarkowska, A., et al. (2019). A new genomic blueprint of the human gut microbiota. *Nature* 568, 499–504. doi: 10.1038/s41586-019-0965-1
- AlZahal, O., Li, F., Guan, L. L., Walker, N. D., and McBride, B. W. (2017). Factors influencing ruminal bacterial community diversity and composition and microbial fibrolytic enzyme abundance in lactating dairy cows with a focus on the role of active dry yeast. *J. Dairy Sci.* 100, 4377–4393. doi: 10.3168/jds.2016-11473
- Anderson, M. J. (2017). *Permutational Multivariate Analysis of Variance (PERMANOVA)*. New York, NY: Wiley, 1–15.
- Andrews, S. (2010). *FastQC: A Quality Control Tool for High Throughput Sequence Data*. Available online at: <http://www.bioinformatics.babraham.ac.uk/projects/fastqc>
- Blank, C. E., Cady, S. L., and Pace, N. R. (2002). Microbial composition of near-boiling silica-depositing thermal springs throughout Yellowstone National Park. *Appl. Environ. Microbiol.* 68, 5123–5135. doi: 10.1128/AEM.68.10.5123-5135.2002
- Bolger, A. M., Lohse, M., and Usadel, B. (2014). Trimmomatic: a flexible trimmer for Illumina sequence data. *Bioinformatics* 30, 2114–2120. doi: 10.1093/bioinformatics/btu170
- Bolyen, E., Rideout, J. R., Dillon, M. R., Bokulich, N. A., Abnet, C. C., Al-Ghalith, G. A., et al. (2019). Reproducible, interactive, scalable and extensible microbiome data science using QIIME 2. *Nat. Biotechnol.* 37, 852–857. doi: 10.1038/s41587-019-0209-9
- Brakke, M. K. (1951). Density gradient centrifugation: a new separation technique. *J. Am. Chem. Soc.* 73, 1847–1848. doi: 10.1021/ja01148a508

## FUNDING

This study was supported by the agriculture and rural development Ministry of Colombia, and the Max Planck Tandem Group in Computational Biology at the Universidad de los Andes. RH had a graduate student scholarship provided by Colciencias, grant 647.

## ACKNOWLEDGMENTS

We want to give special thank to the professor Martha Vives and our colleagues at the CIMIC Lab for their invaluable support and advice in the experimental work. We would also like to thank the members of the BEM laboratory for their help with the Bioinformatic analysis; Humberto Ibarra and the microscopy center in the University of Los Andes for their help in optimizing the microscopy photographs; the IT Services Department and ExaCore – IT Core-facility of the Vice Presidency for Research and Creation at the Universidad de Los Andes for high-performance computing services; the lab technicians who were always ready to help in the laboratory work; and Kelley Crites for her revision to the language of this manuscript.

## SUPPLEMENTARY MATERIAL

The Supplementary Material for this article can be found online at: <https://www.frontiersin.org/articles/10.3389/fmicb.2021.664754/full#supplementary-material>

- Callahan, B. J., McMurdie, P. J., Rosen, M. J., Han, A. W., Johnson, A. J. A., and Holmes, S. P. (2016). DADA2: high-resolution sample inference from Illumina amplicon data. *Nat. Methods* 13, 581–583. doi: 10.1038/nmeth.3869
- Caporaso, J. G., Lauber, C. L., Walters, W. A., Berg-Lyons, D., Huntley, J., Fierer, N., et al. (2012). Ultra-high-throughput microbial community analysis on the Illumina HiSeq and MiSeq platforms. *ISME J.* 6, 1621–1624. doi: 10.1038/ismej.2012.8
- Caro-Quintero, A., and Ochman, H. (2015). Assessing the unseen bacterial diversity in microbial communities. *Genome Biol. Evol.* 7, 3416–3425. doi: 10.1093/gbe/evv234
- Chee, J.-Y., Tan, Y., Samian, M.-R., and Sudesh, K. (2010). Isolation and characterization of a *Burkholderia* sp. USM (JCM15050) capable of producing polyhydroxyalkanoate (PHA) from triglycerides, fatty acids and glycerols. *J. Polym. Environ.* 18, 584–592. doi: 10.1007/s10924-010-0204-1
- Chrzanowski, T. H., and Šimek, K. (1990). Prey-size selection by freshwater flagellated protozoa. *Limnol. Oceanogr.* 35, 1429–1436. doi: 10.4319/lo.1990.35.7.1429
- Corre, E. (2001). ε-Proteobacterial diversity from a deep-sea hydrothermal vent on the mid-atlantic ridge. *FEMS Microbiol. Lett.* 205, 329–335. doi: 10.1016/S0378-1097(01)00503-1
- Davis, J. P., Youssef, N. H., and Elshahed, M. S. (2009). Assessment of the diversity, abundance, and ecological distribution of members of candidate division sr1 reveals a high level of phylogenetic diversity but limited morphotypic diversity. *Appl. Environ. Microbiol.* 75, 4139–4148. doi: 10.1128/AEM.00137-09
- de Assis Lage, C. F., Räisänen, S. E., Melgar, A., Nedelkov, K., Chen, X., Oh, J., et al. (2020). Comparison of two sampling techniques for evaluating ruminal fermentation and microbiota in the planktonic phase of rumen digesta in dairy cows. *Front. Microbiol.* 11. doi: 10.3389/fmicb.2020.618032
- Eisenstein, M. (2018). Microbiology: making the best of PCR bias. *Nat. Methods* 15, 317–320. doi: 10.1038/nmeth.4683



- Faith, J. J., Guruge, J. L., Charbonneau, M., Subramanian, S., Seedorf, H., Goodman, A. L., et al. (2013). The long-term stability of the human gut microbiota. *Science* 341:1237439. doi: 10.1126/science.1237439
- Falkow, S., Rosenberg, E., Schleifer, K.-H., and Stackebrandt, E. (2006). *The Prokaryotes: Vol. 4: Bacteria: Firmicutes, Cyanobacteria*. Springer Science & Business Media.
- Fernando, S. C., Purvis, H. T., Najar, F. Z., Sukharnikov, L. O., Krehbiel, C. R., Nagaraja, T. G., et al. (2010). Rumen microbial population dynamics during adaptation to a high-grain Diet. *Appl. Environ. Microbiol.* 76, 7482–7490. doi: 10.1128/AEM.00388-10
- Garrison, C. E., and Bochdansky, A. B. (2015). A simple separation method for downstream biochemical analysis of aquatic microbes. *J. Microbiol. Methods* 111, 78–86. doi: 10.1016/j.mimet.2015.01.025
- Ghota, S. K. (2014). *Novel Bacterial Lineages in the Uncultured Candidate Division SRI*. Masters Theses. San Jose, CA: San José State University.
- Glöckner, F. O., Yilmaz, P., Quast, C., Gerken, J., Beccati, A., Ciuprina, A., et al. (2017). 25 years of serving the community with ribosomal RNA gene reference databases and tools. *J. Biotechnol.* 261, 169–176. doi: 10.1016/j.jbiotec.2017.06.1198
- Gonzalez, J. M., Sherr, E. B., and Sherr, B. F. (1990). Size-selective grazing on bacteria by natural assemblages of estuarine flagellates and ciliates. *Appl. Environ. Microbiol.* 56:7.
- Gophna, U., Konikoff, T., and Nielsen, H. B. (2017). Oscillospira and related bacteria - from metagenomic species to metabolic features. *Environ. Microbiol.* 19, 835–841. doi: 10.1111/1462-2920.13658
- Hahn, M. W., and Höfle, M. G. (2001). Grazing of protozoa and its effect on populations of aquatic bacteria. *FEMS Microbiol. Ecol.* 35, 113–121. doi: 10.1111/j.1574-6941.2001.tb00794.x
- Henderson, G., Cox, F., Ganesh, S., Jonker, A., Young, W., and Janssen, P. H. (2015). Rumen microbial community composition varies with diet and host, but a core microbiome is found across a wide geographical range. *Sci. Rep.* 5, 1–15. doi: 10.1038/srep14567
- Hevia, A., Delgado, S., Margolles, A., and Sánchez, B. (2015). Application of density gradient for the isolation of the fecal microbial stool component and the potential use thereof. *Sci. Rep.* 5:16807. doi: 10.1038/srep16807
- Hongoh, Y., Ohkuma, M., and Kudo, T. (2003). Molecular analysis of bacterial microbiota in the gut of the termite *Reticulitermes speratus* (Isoptera; Rhinotermitidae). *FEMS Microbiol. Ecol.* 44, 231–242. doi: 10.1016/S0168-6496(03)00026-6
- Huhtinen, L., Blazevic, V., Nurminen, K., Koho, T., Hytönen, V. P., and Vesikari, T. (2010). A comparison of methods for purification and concentration of norovirus GII-4 capsid virus-like particles. *Arch. Virol.* 155, 1855–1858. doi: 10.1007/s00705-010-0768-z
- Huws, S. A., Creevey, C. J., Oyama, L. B., Mizrahi, I., Denman, S. E., Popova, M., et al. (2018). Addressing global ruminant agricultural challenges through understanding the rumen microbiome: past, present, and future. *Front. Microbiol.* 9:2161. doi: 10.3389/fmicb.2018.02161
- Irony, T. Z., and Pereir, C. A. B. (1986). Exact tests for equality of two proportions: fisher v. bayes. *J. Stat. Comput. Simul.* 25, 93–114. doi: 10.1080/00949658608810926
- Kittmann, S., Kirk, M. R., Jonker, A., McCulloch, A., and Janssen, P. H. (2015). Buccal swabbing as a noninvasive method to determine bacterial, archaeal, and eukaryotic microbial community structures in the rumen. *Appl. Environ. Microbiol.* 81, 7470–7483. doi: 10.1128/AEM.02385-15
- Kleene, K. C., Bagarova, J., Hawthorne, S. K., and Catado, L. M. (2010). Quantitative analysis of mRNA translation in mammalian spermatogenic cells with sucrose and Nycodenz gradients. *Reprod. Biol. Endocrinol.* 8:155. doi: 10.1186/1477-7827-8-155
- Krause, D., Dalrymple, B., Smith, W., Mackie, R., and McSweeney, C. (1999). 16S rDNA sequencing of *Ruminococcus albus* and *Ruminococcus flavefaciens*: design of a signature probe and its application in adult sheep. *Microbiol. Read. Engl.* 145(Pt 7), 1797–1807. doi: 10.1099/13500872-145-7-1797
- Latham, M. J., Brooker, B. E., Pettipher, G. L., and Harris, P. J. (1978). *Ruminococcus flavefaciens* cell coat and adhesion to cotton cellulose and to cell walls in leaves of perennial ryegrass (*Lolium perenne*). *Appl. Environ. Microbiol.* 35, 156–165. Available online at: <https://aem.asm.org/content/35/1/156>
- Lee, S. S., Ha, J. K., and Cheng, K.-J. (2000). Relative contributions of bacteria, protozoa, and fungi to in vitro degradation of orchard grass cell walls and their interactions. *Appl. Environ. Microbiol.* 66, 3807–3813. doi: 10.1128/aem.66.9.3807-3813.2000
- Lianidou, E., and Hoon, D. (2018). “9 - circulating tumor cells and circulating tumor DNA,” in *Principles and Applications of Molecular Diagnostics*, eds N. Rifai, A. R. Horvath, and C. T. Wittwer (Amsterdam: Elsevier), 235–281. doi: 10.1016/b978-0-12-816061-9.00009-6
- Lozupone, C., Lladser, M. E., Knights, D., Stombaugh, J., and Knight, R. (2011). UniFrac: an effective distance metric for microbial community comparison. *ISME J.* 5, 169–172. doi: 10.1038/ismej.2010.133
- Malmuthuge, N., and Guan, L. L. (2017). Understanding host-microbial interactions in rumen: searching the best opportunity for microbiota manipulation. *J. Anim. Sci. Biotechnol.* 8:8. doi: 10.1186/s40104-016-0135-3
- Martin, M. (2011). Cutadapt removes adapter sequences from high-throughput sequencing reads. *EMBnet.journal* 17, 10–12. doi: 10.14806/ej.17.1.200
- Matthews, C., Crispie, F., Lewis, E., Reid, M., O’Toole, P. W., and Cotter, P. D. (2018). The rumen microbiome: a crucial consideration when optimising milk and meat production and nitrogen utilisation efficiency. *Gut Microbes* 10, 115–132. doi: 10.1080/19490976.2018.1505176
- Minor, S., MacLeod, N. A., and Preston, T. R. (1977). Effect of sampling by fistula or at slaughter on estimation of rumen protozoa. *Trop. Anim. Prod.* 2:1. doi: 10.1016/b978-0-12-426013-9.50006-4
- Morgavi, D. P., Kelly, W. J., Janssen, P. H., and Attwood, G. T. (2013). Rumen microbial (meta)genomics and its application to ruminant production. *Anim. Int. J. Anim. Biosci.* 7(Suppl. 1), 184–201. doi: 10.1017/S175173112000419
- Nagaraja, T. G. (2016). “Microbiology of the rumen,” in *Rumenology*, eds D. D. Millen, M. De Beni Arrigoni, and R. D. Lauritano Pacheco (Cham: Springer International Publishing), 39–61.
- Orpin, C. G., and Bountiff, L. (1978). Zoospore chemotaxis in the rumen phycomycete *Neocallimastix frontalis*. *Microbiology* 104, 113–122. doi: 10.1099/00221287-104-1-113
- Parks, D. H., Tyson, G. W., Hugenholtz, P., and Beiko, R. G. (2014). STAMP: statistical analysis of taxonomic and functional profiles. *Bioinformatics* 30, 3123–3124. doi: 10.1093/bioinformatics/btu494
- Parte, A., Krieg, N. R., Ludwig, W., Whitman, W. B., Hedlund, B. P., Paster, B. J., et al. (2011). *Bergey’s Manual of Systematic Bacteriology: Volume 4: The Bacteroidetes, Spirochaetes, Tenericutes (Mollicutes), Acidobacteria, Fibrobacteres, Fusobacteria, Dictyoglomi, Gemmatimonadetes, Lentisphaerae, Verrucomicrobia, Chlamydiae, and Planctomycetes*. Cham: Springer Science & Business Media.
- Petri, R. M., Neubauer, V., Humer, E., Kröger, I., Reisinger, N., and Zebeli, Q. (2020). Feed additives differentially impact the epimural microbiota and host epithelial gene expression of the bovine rumen fed diets rich in concentrates. *Front. Microbiol.* 11:119. doi: 10.3389/fmicb.2020.00119
- Poulsen, M., Schwab, C., Borg Jensen, B., Engberg, R. M., Spang, A., Canibe, N., et al. (2013). Methylophilic methanogenic Thermoplasmata implicated in reduced methane emissions from bovine rumen. *Nat. Commun.* 4, 1–9. doi: 10.1038/ncomms2432
- Puniya, A. K., Singh, R., and Kamra, D. N. (eds) (2015). *Rumen Microbiology: From Evolution to Revolution*. Berlin: Springer.
- Raschke, S., Guan, J., and Iliakis, G. (2009). “Application of alkaline sucrose gradient centrifugation in the analysis of DNA replication after DNA damage,” in *DNA Replication: Methods and Protocols Methods in Molecular Biology*, eds S. Vengrova and J. Z. Dalgard (Totowa, NJ: Humana Press), 329–342. doi: 10.1007/978-1-60327-815-7\_18
- Ribeiro, G. O., Gruninger, R. J., Badhan, A., and McAllister, T. A. (2016). Mining the rumen for fibrolytic feed enzymes. *Anim. Front.* 6, 20–26. doi: 10.2527/af.2016-0019
- Sewell, G. W., Aldrich, H. C., Williams, D., Mannarelli, B., Wilkie, A., Hespell, R. B., et al. (1988). Isolation and characterization of xylan-degrading strains of butyrivibrio fibrisolvens from a napier grass-fed anaerobic digester. *Appl. Environ. Microbiol.* 54, 1085–1090. Available online at: <https://www.ncbi.nlm.nih.gov/pmc/articles/PMC202607/>
- Solden, L. M., Hoyt, D. W., Collins, W. B., Plank, J. E., Daly, R. A., Hildebrand, E., et al. (2017). New roles in hemicellulosic sugar fermentation for the uncultivated bacteroidetes family BS11. *ISME J.* 11, 691–703. doi: 10.1038/ismej.2016.150
- Stanton, C., Leahy, S., Kelly, B., Ross, R. P., and Attwood, G. (2020). Manipulating the rumen microbiome to address challenges facing Australasian dairy farming. *Anim. Prod. Sci.* 60, 36–45. doi: 10.1071/AN18611
- Tapio, I., Shingfield, K. J., McKain, N., Bonin, A., Fischer, D., Bayat, A. R., et al. (2016). Oral samples as non-invasive proxies for assessing the composition

- of the rumen microbial community. *PLOS ONE* 11:e0151220. doi: 10.1371/journal.pone.0151220
- Teoh, R., Caro, E., Holman, D. B., Joseph, S., Meale, S. J., and Chaves, A. V. (2019). Effects of hardwood biochar on methane production, fermentation characteristics, and the rumen microbiota using rumen simulation. *Front. Microbiol.* 10:1534. doi: 10.3389/fmicb.2019.01534
- Urbas, L., Jarc, B. L., Barut, M., Zochowska, M., Chroboczek, J., Pihlar, B., et al. (2011). Purification of recombinant adenovirus type 3 dodecahedral virus-like particles for biomedical applications using short monolithic columns. *J. Chromatogr. A* 1218, 2451–2459. doi: 10.1016/j.chroma.2011.01.032
- van Lingen, H. J., Edwards, J. E., Vaidya, J. D., van Gastelen, S., Saccenti, E., van den Bogert, B., et al. (2017). Diurnal dynamics of gaseous and dissolved metabolites and microbiota composition in the bovine rumen. *Front. Microbiol.* 8:425. doi: 10.3389/fmicb.2017.00425
- Wang, Z., Elekwachi, C., Jiao, J., Wang, M., Tang, S., Zhou, C., et al. (2017). Changes in metabolically active bacterial community during rumen development, and their alteration by rhubarb root powder revealed by 16S rRNA amplicon sequencing. *Front. Microbiol.* 8:159. doi: 10.3389/fmicb.2017.00159
- White, J. R., Nagarajan, N., and Pop, M. (2009). Statistical methods for detecting differentially abundant features in clinical metagenomic samples. *PLoS Comput. Biol.* 5. doi: 10.1371/journal.pcbi.1000352
- Yang, B., Le, J., Wu, P., Liu, J., Guan, L. L., and Wang, J. (2018). Alfalfa intervention alters rumen microbial community development in hu lambs during early life. *Front. Microbiol.* 9:574. doi: 10.3389/fmicb.2018.00574
- Yang, S. J., Berndt, M., Michael Ando, D., Barch, M., Narayanaswamy, A., Christiansen, E., et al. (2018). Assessing microscope image focus quality with deep learning. *BMC Bioinformatics* 19:77. doi: 10.1186/s12859-018-2087-4
- York, T. M., and Tang, H.-B. (2015). “Chapter 8 - hydromagnetics—fluid behavior of plasmas,” in *Introduction to Plasmas and Plasma Dynamics*, eds T. M. York and H.-B. Tang (Oxford: Academic Press), 137–193. doi: 10.1016/b978-0-12-801661-9.00008-8
- Zhong, Y., Xue, M., and Liu, J. (2018). Composition of rumen bacterial community in dairy cows with different levels of somatic cell counts. *Front. Microbiol.* 9:3217. doi: 10.3389/fmicb.2018.03217

**Conflict of Interest:** The authors declare that the research was conducted in the absence of any commercial or financial relationships that could be construed as a potential conflict of interest.

Copyright © 2021 Hernández, Jimenez, Vargas-Garcia, Caro-Quintero and Reyes. This is an open-access article distributed under the terms of the Creative Commons Attribution License (CC BY). The use, distribution or reproduction in other forums is permitted, provided the original author(s) and the copyright owner(s) are credited and that the original publication in this journal is cited, in accordance with accepted academic practice. No use, distribution or reproduction is permitted which does not comply with these terms.



# The Axenic and Gnotobiotic Mosquito: Emerging Models for Microbiome Host Interactions

Blaire Steven<sup>1\*</sup>, Josephine Hyde<sup>1†</sup>, Jacquelyn C. LaReau<sup>1</sup> and Doug E. Brackney<sup>1,2</sup>

<sup>1</sup>Department of Environmental Sciences, Connecticut Agricultural Experiment Station, New Haven, CT, United States,

<sup>2</sup>Center for Vector Biology and Zoonotic Diseases, Connecticut Agricultural Experiment Station, New Haven, CT, United States

## OPEN ACCESS

### Edited by:

Aram Mikaelyan,  
North Carolina State University,  
United States

### Reviewed by:

Emily Derbyshire,  
Duke University, United States  
Ottavia Romoli,  
Institut Pasteur de la Guyane, French  
Guiana

### \*Correspondence:

Blaire Steven  
blaire.steven@ct.gov

### <sup>†</sup>Present address:

Josephine Hyde,  
Western Australia Department of  
Biodiversity Conservation and  
Attractions, Kensington, WA,  
Australia

### Specialty section:

This article was submitted to  
Microbial Symbioses,  
a section of the journal  
Frontiers in Microbiology

**Received:** 24 May 2021

**Accepted:** 15 June 2021

**Published:** 12 July 2021

### Citation:

Steven B, Hyde J, LaReau JC and  
Brackney DE (2021) The Axenic and  
Gnotobiotic Mosquito: Emerging  
Models for Microbiome  
Host Interactions.  
Front. Microbiol. 12:714222.  
doi: 10.3389/fmicb.2021.714222

The increasing availability of modern research tools has enabled a revolution in studies of non-model organisms. Yet, one aspect that remains difficult or impossible to control in many model and most non-model organisms is the presence and composition of the host-associated microbiota or the microbiome. In this review, we explore the development of axenic (microbe-free) mosquito models and what these systems reveal about the role of the microbiome in mosquito biology. Additionally, the axenic host is a blank template on which a microbiome of known composition can be introduced, also known as a gnotobiotic organism. Finally, we identify a “most wanted” list of common mosquito microbiome members that show the greatest potential to influence host phenotypes. We propose that these are high-value targets to be employed in future gnotobiotic studies. The use of axenic and gnotobiotic organisms will transition the microbiome into another experimental variable that can be manipulated and controlled. Through these efforts, the mosquito will be a true model for examining host microbiome interactions.

**Keywords:** axenic, gnotobiotic, mosquito, microbiome, model system

## THE ORIGINS OF AN AXENIC MOSQUITO MODEL

The term axenic refers to the growth of a single strain or species entirely free from contamination of any other organisms. The axenic state has also been referred to as “germ free.” We discourage this practice as it tends to implicate the microbes associated with a host with disease, ignoring the myriad of commensal and beneficial associations between microorganisms and their host. In its original usage, the term axenic was generally applied to cultures of bacteria or single-celled eukaryotes. As early as 1885, Louis Pasteur hypothesized the potential of an axenic animal host, although he was of the belief that the resulting axenic animal would not be viable (Pasteur, 1885). His views seemed to be borne out in 1896 when the production of axenic guinea pigs failed to survive past 13 days (Nuttall and Thierfelder, 1896). An axenic fly (*Calliphora vomitoria*) was first reported by Wollman in 1911, raising the potential for producing axenic insects (Wollman, 1911). With advancements in nutrition, handling facilities, and aseptic techniques, species, such as mice and fruit flies, are now routinely reared for multiple generations under axenic conditions, demonstrating that the axenic state is not a death sentence for the host organism (Sang and King, 1961; Smith et al., 2007; Douglas, 2018).

In 1930s, researchers turned their efforts to rear axenic mosquitoes, reporting the production of aseptic *Aedes aegypti* larvae in sterile media (Trager, 1935a,b, 1937). A series of studies would go on to refine the axenic techniques and were generally focused on determining the nutritional requirements of mosquito larvae (Lea et al., 1956; Singh and Brown, 1957; Akov, 1962; Lang et al., 1972; Rosales-Ronquillo et al., 1973). From the earliest studies, it was recognized that the microbiome was a potential source of essential nutrients. In 1935, Trager reported that sterile larval rearing media needed to be supplemented with particular nutrients, reporting that an essential ingredient in the media formulation was “heat-and-alkali-stable...it seems to belong to the B group of vitamins” (Trager, 1935b). In fact, it was these studies that established a diet of liver and yeast extract for larval rearing, which is employed in many mosquito laboratories to this day. However, these studies occurred before the molecular revolution in microbiology in which we learned that the majority of microorganisms in the environment are often recalcitrant to laboratory cultivation (Hug, 2018; Lewis et al., 2021). Thus, there was some concern as to whether reports of axenic mosquitoes were reliable, as they may have been colonized by some of this biological “dark matter” (Rinke et al., 2013). Then, in 2014, a study called into question whether mosquitoes could be reared axenically at all, and proposed a potentially novel mechanism for the role of microbes in mosquito biology (Coon et al., 2014, 2017).

## MICROBIAL INDUCED HYPOXIA AND LARVAL DEVELOPMENT

It was recently reported that removing the mosquito larval microbiome by surface sterilizing eggs resulted in the production of axenic larvae that would expire in the first instar stage of development. However, larval development could be rescued if the larvae were provided with a live culture of a laboratory strain of *Escherichia coli* (Coon et al., 2014). In a follow-up experiment, the researchers performed a transposon mutant screen to identify the genetic determinants allowing for *E. coli* to rescue larval development. Through this screen, they identified that axenic larvae colonized by mutants in *cydB* and *cydD*, which encode cytochrome *bd* oxidase, failed to develop (Coon et al., 2017). The respiratory oxidase cytochrome *bd* allows *E. coli* to grow in oxygen-replete conditions, with maximal activity at oxygen concentrations of 25–50 nM (D’mello et al., 1996). This suggested an important role for this terminal electron transporter in bacteria-host interactions. Coon et al. observed that the guts of larvae colonized by wild-type *E. coli* showed a cyclical behavior in oxic conditions over development, with declining oxygen levels prior to molting. When colonized by the *cydB/cydD* mutants, gut anoxia did not manifest, and the larvae failed to develop. Furthermore, expression of mosquito-encoded hypoxia-inducible transcription factor was associated with larval development, supporting a connection between anoxia and larval growth (Valzania et al., 2018a). Therefore, the hypoxic model proposes that

*E. coli* cytochrome *bd* mutants do not scavenge O<sub>2</sub> from the gut lumen, thereby not producing anoxic conditions, and thus, the larvae failed to develop (Coon et al., 2017). This would require that microbes are not just a passive source of nutrients to the larvae, but a living respiring microbial population was necessary for larval development. These observations would make mosquitoes unique from other insects, like *Drosophila*, which are routinely reared in an axenic state and would seem to support Pasteur’s original thesis that some hosts may require a living microbiome for survival.

## REEMERGENCE OF AXENIC MOSQUITO MODELS

In 2018, we reported the generation of axenic *Ae. aegypti* larvae that were capable of developing into adults. The sterility of the mosquito host was verified by both culture-dependent and culture-independent methods (Correa et al., 2018). More recently, Romoli et al. described a method to produce axenic *Ae. aegypti* larvae through a process of “transient colonization.” Briefly, axenic larvae are colonized by a genetically modified strain of *E. coli* that can be removed during larval development, referred to as decolonization. The decolonized larvae go on to produce axenic adult mosquitoes (Romoli et al., 2021).

The description of axenic mosquitoes seems to contradict the microbial-driven hypoxia model described above, which would require a living functional microbiome. Yet, several lines of evidence suggest that the hypoxic model may be incorrect. First, there was no difference in oxygen concentration between colonized larvae and decolonized axenic larvae (Romoli et al., 2021). Here, we show that axenic *Ae. aegypti* mosquitoes raised in the complete absence of a microbiome and stained with a fluorescent dye as a hypoxia marker maintain anoxic conditions in the gut (Figure 1). This indicates that mosquitoes themselves are capable of scavenging oxygen from the gut lumen. We thusly propose an alternative explanation to the observation that *E. coli* cytochrome *bd* mutants are unable to rescue larval development. Cytochrome *bd* mutants of *E. coli* demonstrate slower growth and produce lower biomass than their wild-type counterparts (Goojani et al., 2020). This suggests that the reproduction rate of cytochrome *bd* mutants may not be sufficient to support larval growth, not their ability to drawdown oxygen. In this view, the defects in the electron transport chain of *E. coli* lead to slower growth, which is then insufficient to support the high levels of metabolism required for larval development. A similar phenomenon has been observed in *Drosophila*, where it was reported that the quantity of bacteria present determined fly development and longevity rather than a particular microbial species or traits. In fact, the best predictor of how well a microbe would affect *Drosophila* development was how well that microbe grew on fruit fly culture medium (Keebaugh et al., 2018). This may also explain why *E. coli* K12, a laboratory-adapted bacterium, is still able to rescue larval development



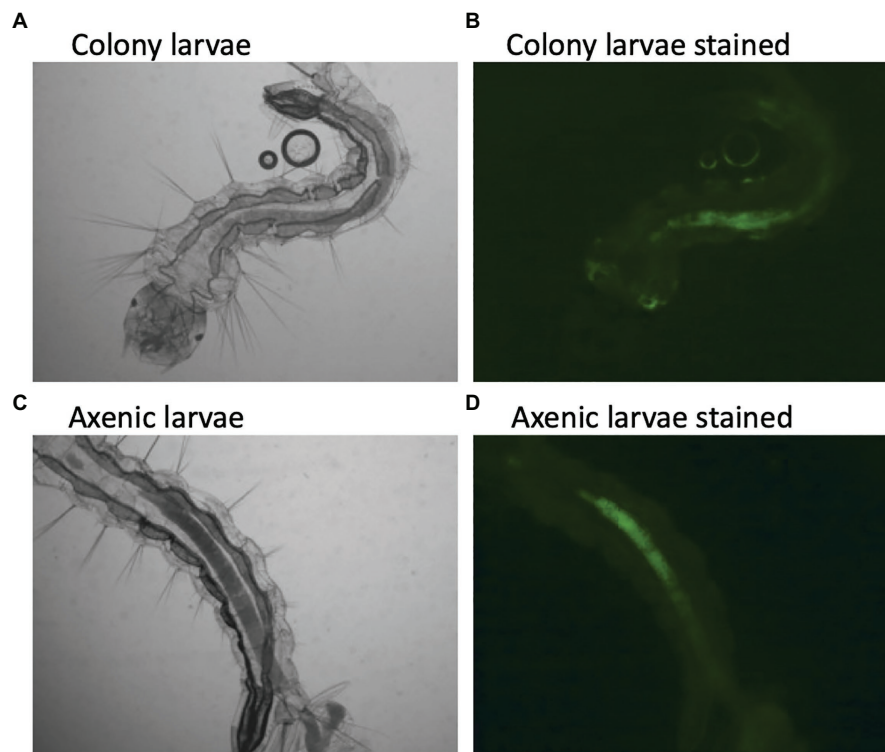


**FIGURE 1** | Hypoxic conditions in the guts of conventionally reared and axenic *Aedes aegypti* larvae. Larvae were reared to the third instar of development and stained with Image-iT Hypoxia Reagent, which fluoresces in anoxic conditions (<5% oxygen). Axenic larvae were reared in the dark to protect light sensitive B-vitamins in the culture medium. A subset of axenic larvae were subsequently verified to be free of microbial contamination by both culture-dependent and culture-independent (16S rRNA and fungal rRNA gene PCR) methods.

(Correa et al., 2018). *E. coli* K12 maintains high growth levels in larval growth media and thus can act as a source of larval nutrition, despite presumably losing many characteristics that would normally facilitate host colonization (Liu and Reeves, 1994; Browning et al., 2013).

Data from the newly developed axenic models also support a nutritional role of the microbiome. For instance, larvae reared on a high-density diet of liver and yeast extract have to be reared in the dark to protect a light-sensitive component in the food, presumably a B vitamin (Hyde et al., 2019a). Transcriptional data from decolonized axenic larvae showed that folate biosynthesis, folate transport, and thiamine metabolism were all upregulated in comparison with their microbially colonized cohorts, additionally pointing to a B vitamin deficiency in axenic larvae (Romoli et al., 2021). Furthermore, supplementing the diet of axenic larvae with folate increased larval survival 4-fold (Romoli et al., 2021). Finally, using data from the axenic and decolonized mosquito models, Wang et al. verified and replicated the observation that supplementing the diet of axenic larvae with B vitamins, in this case riboflavin, can rescue development. They further showed that axenic larvae undergo gut hypoxia when reared under appropriate conditions, verifying that microorganisms are not required to produce anoxic conditions (Wang et al., 2021a). Thus, axenic studies of mosquito larvae have come full circle, highlighting the role of the

microbiome in supplying essential nutrients, B-vitamins, such as folate and riboflavin, as the key function of the microbiome in mosquito larval development.

## ARE MICROBES ESSENTIAL FOR LARVAL DEVELOPMENT?

The development of axenic larvae seems to suggest that living microorganisms are dispensable to larval growth. Yet, the microbes that make up the microbiome are clearly providing high amounts of biomass, food, and essential vitamins. It is unlikely any of these nutrients would be present in the environment in sufficient quantities to support larval growth in the absence of living microbes. In this regard, a living microbiome is likely required to support mosquito development in the wild. The fact that axenic larvae took longer to develop and produced smaller adults indicates that the axenic diet has not yet been optimized (Correa et al., 2018). In addition, several nutrients, such as amino acids and vitamin mixes, were lethal to the larvae when provided in high concentrations in the rearing water, which was only overcome when nutrients were provided in a semi-solid agar plug (Correa et al., 2018). This provides information on how mosquito larvae feed and acquire nutrients in the environment. Larval nutrition has long

been recognized as a potential target for mosquito control and influences the development and fitness of adult mosquitoes (Souza et al., 2019; Dittmer and Gabrieli, 2020). Thus, the axenic model will continue to be important in defining and characterizing the nutritional requirements of mosquito larvae and the potential for identifying diet or microbial-based larval control programs.

## THE ROLE OF THE MICROBIOME IN ADULT MOSQUITOES

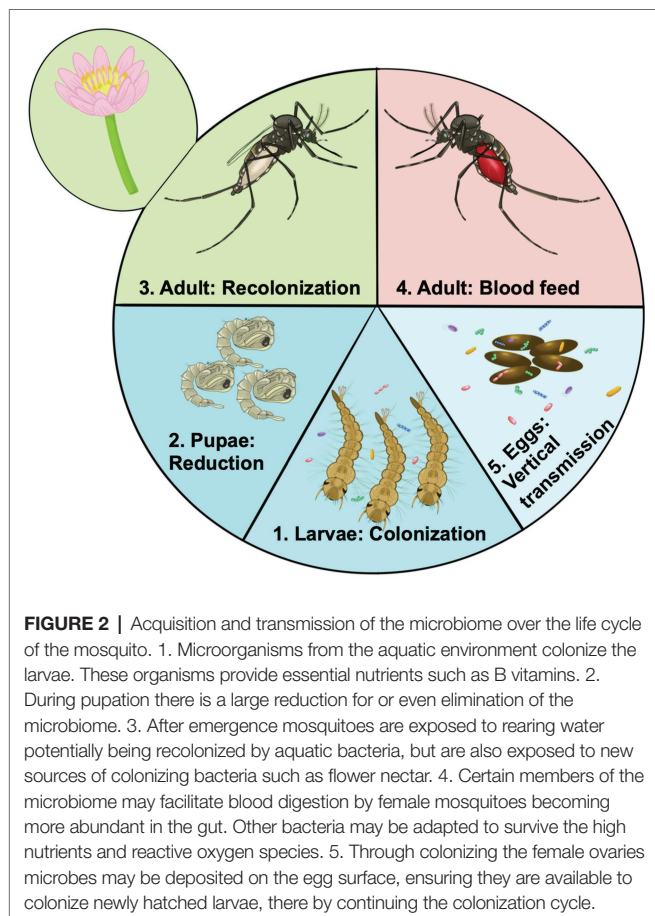
The microbiome of mosquito larvae is thought to be largely acquired from their aquatic environment (Coon et al., 2016b; Saab et al., 2020). As mosquitoes are holometabolous, going through a complete metamorphosis from larvae to adults through a “resting” pupal phase (Figure 2), larval nutrition and health have direct consequences on the fitness of the adult (Moller-Jacobs et al., 2014; Linenberg et al., 2016). Presumably, this means the status of the larval microbiome will also affect traits of the adult mosquito. Evidence suggests that many microbes are lost during metamorphosis when mosquitoes develop from larvae to pupae and emerge as adults (Lindh et al., 2008; Chavshin et al., 2015). The adult mosquito is exposed to new food sources, such as flower

nectar, as well as being more mobile and able to visit other locations, and the anautogenous female mosquito requires a blood meal for reproduction (Figure 2). Thus, the microbiome of adult mosquitoes differs from larvae, in both composition and diversity (Muturi et al., 2017; Wang et al., 2018; Hyde et al., 2019b). Yet, no serious detrimental effects of the axenic state on adult *Ae. aegypti* mosquitoes have been documented. Axenic mosquitoes had similar, if not slightly longer lifespans than their bacterially colonized cohorts, and female mosquitoes took a blood meal, laid a similar number of eggs, and the eggs of the axenic *Ae. aegypti* females gave rise to viable offspring (Correa et al., 2018). Similarly, there were no detrimental effects of the axenic state on longevity of fecundity of decolonized mosquitoes (Romoli et al., 2021). Additionally, transcriptomic analysis of axenic adult mosquitoes showed a muted response in terms of gene expression change between axenic and conventionally reared mosquitoes, indicating similar physiological states for colonized and axenic mosquitoes (Hyde et al., 2020). Thus, it appears that the axenic state is not an obvious burden for the adult mosquito, at least in the case of *Ae. aegypti*.

Mosquitoes pose a significant and continued public health threat worldwide as they are responsible for transmitting numerous pathogenic viruses and parasites, such as dengue virus, West Nile virus, malaria parasites, and filarial nematodes, resulting in millions of infections each year. As such, there has been considerable research interest into the interactions between the mosquito microbiota and the pathogens they carry. Different microbial taxa have shown both positive and negative associations with the vectorial capacity of mosquitoes (Cirimotich et al., 2011; Guégan et al., 2018; Romoli and Gendrin, 2018; Caragata et al., 2019). Additionally, the composition and membership of the microbiome have been associated with a long list of other mosquito phenotypes. These include insecticide resistance, lifespan, and fecundity (Minard et al., 2013a; Dada et al., 2018; Wang et al., 2021b). Yet, all these studies have one thing in common, and they assume an interaction between microbiome members and host phenotypes. In this regard, these associations are not addressable with an axenic model, which can only investigate phenotypes in the presence or absence of a microbiome. What is required to link the status of the microbiome to host phenotypes is a model in which the diversity and composition of the microbiome can be mechanistically controlled and altered.

## A DEFINED MICROBIOME: GNOTOBIOTIC MOSQUITOES

The ability to perform the microbiome presence/absence studies is important, but they are binary in nature and, therefore, somewhat limited. The true power of axenic models is their ability to be manipulated so that defined microbiomes, whether it be an individual or multiple community members, can be introduced, thereby allowing the systematic examination of the effects that specific community members have on host biology. These systems, referred to as gnotobiotics, allow



microbiome research to move beyond correlational studies to hypothesis-driven examinations of causation.

A gnotobiotic host is one in which every living organism in association with the host is defined. Consequently, gnotobiotic systems are limited by the availability of both an axenic host and microbiome community members that can be cultured. Despite these limitations, our ability to decipher the complexity of host-microbiome interactions has accelerated in recent years through advancements in genomics, proteomics, metabolomics, and culturing techniques. Initial studies in axenic flies revealed that developmental delays could be avoided through the introduction of a single community member and that certain community members were more effective at counteracting these delays (Bakula, 1969; Storelli et al., 2011). Functional characterization of these observations through a transposon mutagenesis screen and metagenome-wide association analysis determined that *Drosophila* larval development and adult fly metabolic homeostasis were significantly affected by the bacterial community members' ability to synthesize pyrroloquinoline quinone, which is an important modulator of the flies insulin/insulin-like growth factor signaling (Shin et al., 2011; Chaston et al., 2014).

Monoculture gnotobiotics are a very useful tool for elucidating the contributions that the microbiota has on host development and physiology but are reductionist and cannot measure the influence of intra-community interactions on the system at large. Early on it was demonstrated that the microbiomes influence on host biology can be greater than the sum of its parts (Schaedler et al., 1965). Axenic flies colonized with communities of varying complexity reveal that some phenotypic traits are highly influenced by community interactions (Newell and Douglas, 2014; Gould et al., 2018). For instance, axenic *Drosophila* showed prolonged development times and elevated triglyceride contents in comparison with conventionally reared bacterial colonized flies. When the flies were recolonized with individual members cultivated from the microbiome, there were strain specific responses of the flies in triglyceride levels and longevity, but it was only when strains of both *Acetobacter* and *Lactobacillus* (the dominant members of the *Drosophila* microbiome) were presented to the axenic flies that the flies phenotypes returned to wildtype levels (Newell and Douglas, 2014).

Another approach for examining community scale effects and interactions is through transfer studies. While not truly gnotobiotic, transfer studies in which the microbiome of an individual with a specific disease state is introduced into an axenic host have become a useful tool for examining microbiome correlates of disease (Vrieze et al., 2012; Fei and Zhao, 2013; Schulz et al., 2014). For instance, the now famous study documents that transferring the microbiome from lean and obese mice results in increased capacity for energy harvest and weight gain for the mice receiving the "obese microbiome" (Turnbaugh et al., 2006). These systems have the benefit of more realistically capturing the complexity of interactions associated with the microbiome but suffer from an incomplete understanding of the members within the community and their individual contributions to host phenotypes.

Until recently, mosquito-microbiome studies have been limited due to the lack of an axenic model. Consequently, most studies have relied upon the use of antibiotics to clear the resident bacteria in order to interrogate microbiome-mosquito interactions. Using this approach, several groups have reported that the microbiome plays a role in modulating gut immunity thereby effecting susceptibility to viral and parasitic pathogens (Xi et al., 2008; Dong et al., 2009; Kalappa et al., 2018; Wu et al., 2019). Similarly, antibiotic clearance of the microbiota has demonstrated a role for the microbiome in mosquito metabolism and sensitivity to insecticides (Xiao et al., 2017; Barnard et al., 2019; Chabanol et al., 2020). These studies, like the presence/absence studies used in axenic models, offer generalizable insights into the effects of the microbiota on host phenotypes. While these studies support that the presence of a microbiome is linked to mosquito phenotypes, it is difficult to parse out microbiome impacts from those potentially associated with sustained antibiotic exposure. It has been demonstrated in mammalian systems that antibiotics can induce immunologic and metabolic changes in the host, inhibit eukaryotic translation, and alter mitochondrial function (Kalghatgi et al., 2013; Badal et al., 2015; Moullan et al., 2015; Yang et al., 2017; Gopinath et al., 2018). In addition to potential side effects, it has been shown that antibiotics do not eliminate resident microbiota, but rather cause a dysbiosis, as some members of the mosquito microbiome likely harbor antibiotic resistance (Hughes et al., 2014; Schubert et al., 2015; Hyde et al., 2019b). This may also explain contrasting results between studies that employ antibiotic clearance, as the net result may be an altered microbial composition rather than a comparison between the presence and absence of a microbiome. For instance, Xi et al. (2008) reported a significant reduction in dengue virus infection after antibiotic treatment of *Ae. aegypti* mosquitoes, whereas Audsley et al. reported no effect of antibiotic treatment on the permissiveness of *Ae. aegypti* to infection by dengue virus (Audsley et al., 2017). In addition, several studies have employed antibiotic clearance in attempts to recapitulate monoculture gnotobiotics in mosquitoes, by "clearing" the resident microbiota with antibiotics and then exposing the mosquitoes to a bacterium of interest. These studies demonstrate that specific bacterial community members may affect mosquito susceptibility to pathogens and host physiology (Dong et al., 2009; Apte-Deshpande et al., 2012; Ramirez et al., 2012; Hughes et al., 2014; Xiao et al., 2017; Wu et al., 2019). However, there is no way to separate the possible influence of antibiotics on these traits, or little to no verification that the mosquitoes are true gnotobiotics.

Recent efforts have been made to examine mosquito-microbiome interactions using axenic mosquitoes. Introduction of individual bacterial isolates at the larval stage revealed strain-specific effects on larval survivorship and development time as well as adult mosquito biometrics, such as body size and reproductive fitness as well as susceptibility to dengue virus and Zika virus (Coon et al., 2016a; Dickson et al., 2017; Correa et al., 2018; Carlson et al., 2020; Giraud et al., 2021). It has also been demonstrated that simplified communities can successfully colonize both axenic larvae and adult mosquitoes



(Correa et al., 2018). Correa et al. found that the composition and function of the microbiome may be important determinants of phenotypic plasticity observed between individual mosquitoes. The generation of axenic/gnotobiotic mosquito models now make it possible to systematically interrogate the effects of the microbiome on mosquito biology without the use of antibiotics.

## OPPORTUNITIES AND CHALLENGES FOR AXENIC AND GNOTOBIOTIC MOSQUITOES

The advent of the axenic/gnotobiotic mosquitoes opens up a wide range of questions that can be addressed by the research community. The method for generating and rearing axenic mosquitoes has been published and is achievable by any laboratory with the ability to maintain aseptic conditions, sterilize the required equipment, and perform basic microbiology (see Hyde et al., 2019a for a detailed protocol). To date, axenic rearing from larvae to adults has only been reported for *Ae. aegypti*, but gnotobiotic *Aedes atropalpus*, *Aedes albopictus*, *Anopheles gambiae*, *Culex quinquefasciatus*, and *Toxorhynchites amboinensis* have all been reported (Coon et al., 2016a,b, 2020; Valzania et al., 2018b). In this respect, gnotobiotic models may be achievable for a wider range of host species. Implementing these gnotobiotic studies will require an appropriate mosquito host and bacterial strains capable of supporting larval development.

Perhaps, one of the greatest opportunities for gnotobiotics is the potential for standardizing mosquito studies. It stands to reason that different research laboratories employing varied diets, rearing conditions, and being geographically separated are likely to harbor differing microbiome compositions in the mosquitoes they rear. Thus, at least a portion of variability reported between studies is likely due to heterogeneity in microbiome composition and structure between laboratories. Gnotobiotic models allow for standardization of the microbiome and transitioning the microbiome to a controlled variable. The creation of a defined tractable model microbiome, similar to the altered Schaedler flora employed in gnotobiotic mouse studies (Biggs et al., 2017), would be a resource that could be shared among researchers, and act as a baseline to investigate the consequences of microbiome manipulation on mosquito phenotypes. This will require identifying those bacteria that would serve the greatest utility for a defined microbiome.

## A PATH FORWARD: A MOST WANTED LIST FOR MICROBES IN GNOTOBIOTIC STUDIES

In general, the diversity of the microbiome in an individual mosquito is rather low, being comprised of ~10–50 bacterial species (Minard et al., 2013a). Yet, there are certain microbial members that appear to be commonly associated with mosquitoes or that have been correlated to particular phenotypic outcomes,

which makes them particularly attractive targets to investigate in a gnotobiotic model. Below, we list five microbiome members that are high-value targets for future gnotobiotic studies (Figure 3). This is by no means an extensive list of microbiome members that may play a role in mosquito physiology but is a review of some of the mosquito microbiome members that show the greatest promise for untangling host microbe interactions or potential microbes that could be employed in microbial-based mosquito borne disease control. Notably, not included on the list is the bacterial endosymbiont *Wolbachia*. This maternally inherited organism may be the most well-studied mosquito-associated bacterium, with over 100 years of active study (Kaur et al., 2021). However, the difficulty in growth and maintenance of *Wolbachia* in pure culture, its biology, host range, and inheritance makes it a difficult organism to employ in gnotobiotic studies (Voronin et al., 2010; Hughes et al., 2012). Despite the myriad of effects *Wolbachia* plays in mosquito biology, reproduction, and control of mosquito carried pathogens (Turley et al., 2009; Hancock et al., 2011; Iturbe-Ormaetxe et al., 2011; Jiggins, 2017), it does not make the list.

### Genus *Asaia*

Bacteria in the genera *Asaia* (phylum Proteobacteria) are acetic acid bacteria within the family Acetobacteraceae. Acetic acid bacteria are differentiated from other bacteria as they are

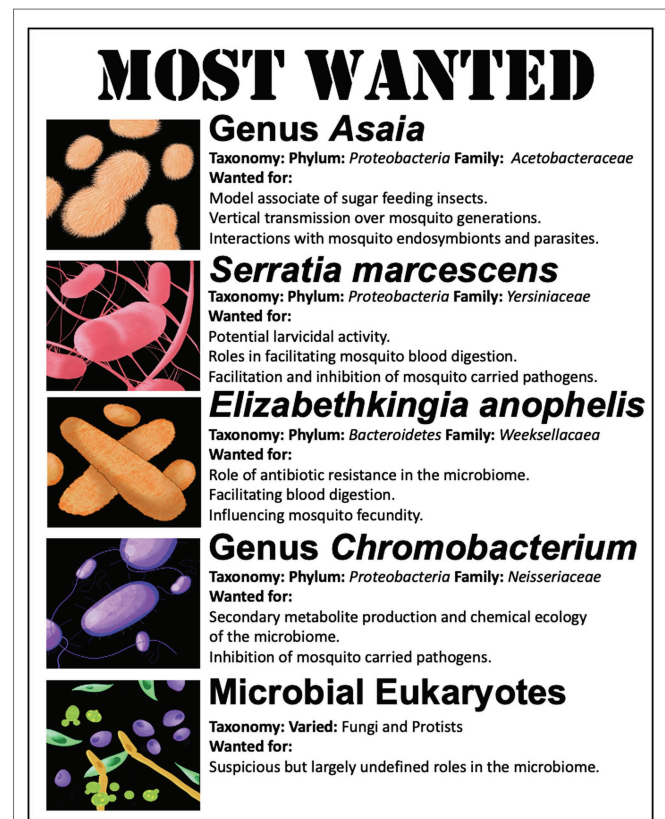


**FIGURE 3 |** List of organisms of significant interest for gnotobiotic studies in mosquitoes.



obligate aerobes that oxidize sugars, sugar alcohols, and ethanol with the production of acetic acid as the major end product (Raspor and Goranovič, 2008). Bacteria of the genus *Asaia* colonize multiple insects, across multiple orders, such as the Diptera, Hymenoptera, Hemiptera, and Homoptera (Crotti et al., 2010). This includes mosquitoes within *Aedes* sp., *Anopheles* sp., and *Culex* sp. (Crotti et al., 2009; Freece et al., 2014; Ramos-Nino et al., 2020). *Asaia* is among the numerically dominant bacterial populations that colonize mosquitoes as assessed by sequencing surveys (Chouaia et al., 2010; Damiani et al., 2010) and can be found in larval and adult mosquitoes and multiple tissues (e.g., the adult gut, testes, ovaries, and salivary glands; Favia 2007, 2008; Mancini, 2018). Geographically dispersed, *Asaia* has been identified in mosquitoes from Brazil (Oliveira et al., 2020), Canada (Novakova et al., 2017), Iran (Rami et al., 2018), Italy (Alfano et al., 2019), Kenya (Osei-Poku et al., 2012), Madagascar (Minard et al., 2013b), and the United States (Muturi et al., 2017), among others. Species of *Asaia* are often found in flower nectar, the food source of newly emerged mosquitoes (Bassene et al., 2020). They can also spread through mosquito populations by paternal transmission during mating (Damiani et al., 2008). *Asaia* may use their colonization of the female reproductive tract to ensure vertical transmission through a process of egg smearing, whereby they colonize the egg surface in order to be ingested by newly hatched larvae (Damiani et al., 2010). The importance of the bacteria to the larvae is demonstrated by the fact that reduction of *Asaia* bacterial load by treatment with antibiotics slows larval growth. Subsequently, supplementing larval diets with *Asaia* bacteria accelerated larval development time (Mitraka et al., 2013). This suggests that these bacteria are able to meet the nutritional needs of developing larvae (Chouaia et al., 2012). Evolutionary analysis of *Asaia* genomes indicates that these organisms have undergone a process of genome reduction as they became associated with insects, yet preserved an insecticide degrading gene, pyrethroid hydrolase (Comandatore et al., 2021). Thus, beyond providing a source of nutrition to developing larvae, *Asaia* may play a role in protecting mosquitoes from insecticides.

*Asaia* bacteria appear to interact with the endosymbiotic bacteria and parasites carried by mosquitoes. When the mosquito microbiome was supplemented with *Asaia* bacteria, there was an observed impediment to the vertical transmission of *Wolbachia*, a mosquito endosymbiont, suggesting inter-species competition (Hughes et al., 2014). Additionally, several studies have documented a negative relationship between *Asaia* bacteria and *Plasmodium*, the causative agent of malaria (Capone et al., 2013; Cappelli et al., 2019a). It is thought that *Asaia* bacteria prime an immune response that prevents the malarial parasite from developing in the mosquito (Cappelli et al., 2019a). In this regard, the *Asaia*-mosquito symbiosis may be a relationship with significant public health implications.

These data and observations show that *Asaia* sp. colonize multiple mosquito hosts as well as other sugar-feeding insects. *Asaia* sp. are present across multiple life stages, in multiple tissues, and are reliably inherited between mosquito generations. *Asaia* bacteria are also amenable to genetic modification and

mosquito recolonization, which makes them an attractive tool for studying the genetic determinants of mosquito colonization (Favia et al., 2007). Additionally, because bacteria in the genus *Asaia* are generally non-pathogenic they are attractive targets for paratransgenic strategies for mosquito vector control. Thus, *Asaia* is on the list of most wanted as they represent an ideal model bacterium to study an apparent beneficial relationship between a bacterium and the mosquito host.

## ***Serratia marcescens***

*Serratia* (phylum Proteobacteria) is a genus of facultatively anaerobic bacteria within the family Yersiniaceae. Bacteria in the genus *Serratia* are common among the bacteria that make up the mosquito microbiome (Sharma et al., 2020). Several different species of *Serratia* have been identified in mosquitoes, including *Serratia odorifera* (Apte-Deshpande et al., 2012), *Serratia nematodiphila* (Patil et al., 2012), and *Serratia fonticola* (Chen and Walker, 2020, 14). Yet, one bacterium in particular has received a considerable research focus as a mosquito associate, *Serratia marcescens*.

*Serratia marcescens* is a cosmopolitan bacterium with multiple environmental reservoirs, including soil and water (Abreo and Altier, 2019). It is often found in hospital settings and is a significant cause of nosocomial infections (Mahlen, 2011; Khanna et al., 2013). Mosquitoes are also an environmental reservoir. Strains of *S. marcescens* have been found to colonize mosquito larvae, the adult midgut, female ovaries, and male accessory glands, and on the surface of newly laid eggs (Tchioffo et al., 2016; Wang et al., 2017). Various isolates of *Serratia* demonstrate larvicidal activity. A strain of *S. nematodiphila* demonstrated high mortality to several mosquitoes species: *C. quinquefasciatus* (100%), *Anopheles stephensi* (95%), and *Ae. aegypti* (91%) after 48 h of exposure (Patil et al., 2012). Similarly, gnotobiotic *Ae. aegypti* mosquito larvae colonized with a strain of *S. marcescens* experienced >85% mortality, and the surviving larvae took approximately twice as long to develop (Correa et al., 2018). The characteristic red coloration of *S. marcescens* may play a role in its antagonism to larval development. Prodigiosin, the red pigment produced by *S. marcescens* shows larvicidal activity when introduced to larvae (Patil et al., 2011; Suryawanshi et al., 2015).

In contrast, *S. marcescens* seems to play a beneficial or at least neutral role in the adult mosquito. Gnotobiotic adult *Ae. aegypti* mosquitoes colonized by *S. marcescens* showed no increase in mortality (Correa et al., 2018). Similarly, no fitness defects were noted for adult *An. gambiae* or *Culex pipiens* mosquitoes colonized by *S. marcescens* (Koosha et al., 2019; Ezemuoka et al., 2020). In fact, *S. marcescens* may participate in mosquito blood digestion. The genome of *S. marcescens* encodes several genes for heme uptake and storage, as well as demonstrating alpha-hemolytic activity, i.e., the complete lysis of blood cells (Chen et al., 2017). Yet, fewer females infected with *S. marcescens* took blood meals in comparison with their uninfected cohorts (Kozlova et al., 2021).

*Serratia marcescens* has also been shown to interact with the capacity of mosquitoes to transmit disease. For instance by inhibiting *Plasmodium* development in the mosquito, thereby

reducing the spread of malaria (Seitz et al., 1987; Bahia et al., 2014; Bai et al., 2019). Yet, there is high intra-specific diversity between *S. marcescens* strains capable of inhibiting *Plasmodium*. This indicates the anti-parasitic ability is likely due to a small number of genetic determinants, such as flagellum biosynthesis, that may not be conserved among all members of the species (Bando et al., 2013). Genome sequencing of mosquito-associated strains of *S. marcescens* showed various virulence factors and antibiotic production which may be involved in controlling pathogen infection of the mosquito (Chen et al., 2017). A recently described class of natural products, the stephensiolides, was isolated from a mosquito-associated *Serratia*. It is posited that these compounds have antimicrobial properties, which may also antagonize *Plasmodium*, as well as facilitate motility and transfer of bacterial cells within and between mosquitoes (Ganley et al., 2018). Additionally, colonization of the mosquito with *S. marcescens* induces gene expression changes in pathways, such as peptidoglycan recognition receptors that may enhance anti-parasitic immune responses that act to inhibit *Plasmodium* (Stathopoulos et al., 2014). In contrast, mosquito colonization by *S. marcescens* has been reported to increase the infection rate of mosquitoes by particular arboviruses. Specifically, *S. marcescens* colonization has been linked to increases in the infection of mosquitoes with dengue-2 and chikungunya virus (Apte-Deshpande et al., 2012). This increased permissiveness to viral infection is thought to occur through bacterial excretion of a protein *SmEnhancin*, which interferes with mucins of the mosquito gut epithelia, allowing dissemination of viral particles (Wu et al., 2019). In this regard, *S. marcescens* appears to inhibit or facilitate the vector competence of mosquitoes depending on the pathogen under consideration.

*Serratia marcescens* is on the target of most wanted mosquito which associates to study in gnotobiotic systems due to its complex interactions with the mosquito host. Colonization outcomes vary widely between larvae and adults. The potential relationships and mechanisms driving interactions between *S. marcescens* and the pathogens vectored by mosquitoes vary from the general, such as a priming of the immune system to the specific production of metabolites that aid or hinder pathogen infection or spread. In this respect, there is a rich list of potential host microbe interactions and phenotypic outcomes to characterize in regard to the association between *S. marcescens* and mosquitoes.

### ***Elizabethkingia anophelis***

*Elizabethkingia* (phylum Bacteroidetes) is a genus within the family Weeksellaceae. This bacterium is unique on this list as its origins are from mosquitoes, being first isolated from the midguts of *An. gambiae* (Kämpfer et al., 2011). However, the genus *Elizabethkingia* is considered to be ubiquitous in the environment. Although genomic-based analyses suggest that the mosquito-associated strains form a distinct evolutionary sublineage within the *Elizabethkingia anophelis* species complex (Breurec et al., 2016).

*Elizabethkingia anophelis* is an opportunistic human pathogen, causing pneumonia, bacteremia, neonatal meningitis, nosocomial bacteremia, and neutropenic fever (Lau et al., 2016). Cases of

bacteremia are often associated with poor clinical outcomes, with mortality rates as high as 23.5% (Lau et al., 2016). Cases of *E. anophelis* infections have been reported from Singapore, Hong Kong, Taiwan, and the United States (Janda and Lopez, 2017). Because of the association between *E. anophelis* and mosquitoes, it was initially posited that mosquitoes may be a vector (Frank et al., 2013). Subsequent studies suggest that *E. anophelis* cases are far more likely to be hospital acquired infections, although sporadic, community-acquired cases have been reported (Hayek et al., 2013; Perrin et al., 2017; Lee et al., 2021). One characteristic that makes *E. anophelis* infections particularly challenging in the clinical environment is that the bacterium is resistant to multiple antibiotics including cephalosporins, aminoglycosides, and carbapenems (González and Vila, 2012; Breurec et al., 2016). A notable 112 predicted proteins identified in the genome of mosquito-associated strains of *E. anophelis* were annotated to features involved in resistance to antibiotics or other toxic compounds (Kukutla et al., 2013). Indeed, in recent surveys of antibiotic-resistant bacteria in the mosquito microbiome, isolates of *Elizabethkingia* were identified to possess multi-drug resistance against ampicillin, carbenicillin, gentamycin, tetracycline, and kanamycin (Hyde et al., 2019b; Ganley, 2020). It is not clear what, if any, role this multi-drug resistance may play in colonizing the mosquito host, other than a potential fitness advantage against other bacteria making up the mosquito microbiome.

*Elizabethkingia anophelis* shows differential preferences for mosquito hosts. The bacterium showed high colonization rates for *An. gambiae* and *A. stephensi* but was rarely detected in *Aedes triseriatus* (Chen et al., 2015). Like other bacteria on this list, *Elizabethkingia* sp. can be found in high numbers in the mosquito ovaries and may be vertically transmitted from mother to offspring (Akhouayri et al., 2013). Yet, colonization by *Elizabethkingia* sp. may induce melanotic lesions in the fat bodies of mosquito larvae and adults, suggesting a potential antagonistic relationship (Akhouayri et al., 2013). *E. anophelis* may be particularly important in mosquito blood digestion. Cell counts of *E. anophelis* increased approximately 3-fold in the guts of post-blood fed mosquitoes, and animal erythrocytes promoted *E. anophelis* growth in cell culture (Chen et al., 2015, 2020). The bacterium also displays hemolytic activity and encodes several hemolysins that may participate in the digestion of erythrocytes in the mosquito gut, along with antioxidant genes, which could provide defense against the oxidative stress that is associated with blood digestion (Kukutla et al., 2014). Mosquitoes colonized with *E. anophelis* produced more eggs than did those treated with erythromycin or with a standard microbiome, suggesting *E. anophelis* may increase mosquito fecundity, potentially by increasing available nutrients from the blood meal (Chen et al., 2020).

*Elizabethkingia anophelis* makes this list as it is a true mosquito associate that may shed light on specific genomic adaptations for colonizing the mosquito host. Furthermore, with the high levels of antibiotic resistance, *E. anophelis* is a model to study competition among microbiome members. Finally, *E. anophelis* appears to play a significant role in blood digestion a key point in the mosquito lifecycle.

## Genus *Chromobacterium*

The genus *Chromobacterium* (phylum Proteobacteria) is facultatively anaerobic bacteria withing the family Neisseriaceae. Like the other bacteria on this list, species of *Chromobacterium* are abundant in the environment and can be readily isolated from soils and water sources (Batista and da Silva Neto, 2017). Much of the research interest in *Chromobacterium* has been driven by the biotechnological and pharmaceutical importance of secondary metabolites produced by the strains, which include antibiotics, quorum sensing molecules, lipopolysaccharides, and the pigment violacein that gives *Chromobacterium violaceum* its characteristic purple coloration (McClean et al., 1997; Durán and Menck, 2008; Kothari et al., 2017).

*Chromobacterium* strains are not particularly abundant in the mosquito microbiome, although they are among bacterial members commonly identified in several species of mosquito (Minard et al., 2013a). Instead, the research focuses on the *Chromobacterium* predominately derives for their role in control of mosquito populations and their interactions with mosquito vector competence. Various strains have shown detrimental effects of mosquito survival, lifespan, blood feeding, and fecundity (Gnambani et al., 2020). Colonization of *Ae. aegypti* or *An. gambiae* with a strain of *Chromobacterium* isolated from mosquito midguts resulted in rapid mortality of both larvae and adults (Ramirez et al., 2014). Larvae exposed to sublethal doses of the bacterium had lengthened developed time, suggesting chronic effects of even small populations of the bacteria (Short et al., 2018a). In the adult mosquito, *C. violaceum* exposure decreased the proportion of females seeking a blood meal, significantly reduced the numbers of eggs laid, and reduced hatches from the resulting eggs (Gnambani et al., 2020). A preparation of a strain of *Chromobacterium* with no living cells maintained strong lethal effects in mosquitoes, indicating this bacterium was producing one or several bioactive compounds (Caragata et al., 2020). Transcriptional analysis of mosquitoes with chromobacterium exposure revealed gene expression changes in pathways related to detoxification, xenobiotic response, and stress response, similar to that of an insecticide exposure (Short et al., 2018b). The same strain was also observed to produce hydrogen cyanide in larval water at sufficient concentrations to induce larval mortality, offering another possible mechanism for larvicidal activity (Short et al., 2018a). The effects of chromobacteria exposure can be transgenerational with the offspring of exposed females showing developmental delays and increased mortality (Short et al., 2018b). The genome of *Chromobacterium vaccinii*, another bacterium with potential roles in mosquito biocontrol, encodes several genes for virulence factors that may explain their toxicity, and these include siderophores, production of hydrogen cyanide, as well as multiple chitinase genes (Vöing et al., 2020).

*Chromobacterium* sp. are among the microbes that show inhibitory activity against the pathogens carried by mosquitoes. Chromobacteria cell extracts and cultures show anti-pathogen activity outside of the mosquito host, indicating the potential production of secreted metabolites inhibiting pathogen growth (Ramirez et al., 2014). For example, violacein, the violet pigment compound produced by many species of *Chromobacteria*, is

potent antimicrobial with antiparasitic activities against *Plasmodium* (Lopes et al., 2009). A specific compound produced by *Chromobacterium* sp. Panama, romidepsin a histone deacetylase inhibitor, also showed high activity against *Plasmodium* (Saraiva et al., 2018b). Additionally, the *Chromobacterium* sp. Panama produces a protease that attacks the envelope protein of dengue virus, thereby blocking its ability to bind to and infect cells (Saraiva et al., 2018a). Thus, these observations point to the wealth of chemical compounds produced by species of *Chromobacterium* and their potential to influence the biology, behavior, and vector competence of their mosquito hosts.

The genus *Chromobacterium* makes the list based on the assortment of potentially bioactive compounds that are produced by these bacteria. In this regard, these bacteria offer a unique insight into the chemical ecology of the mosquito microbiome.

## Microbial Eukaryotes

The microbiome of mosquitoes consists of more than just bacteria. Yet, there is a significant knowledge gap concerning the single-celled eukaryotes that inhabit the mosquito microbiome.

Fungal diseases are common in insects, including mosquitoes. These entomopathogenic fungi have been extensively described elsewhere (e.g., Scholte et al., 2004; Kanzok and Jacobs-Lorena, 2006; Shen et al., 2020). However, it is not so clear that these organisms can be considered part of the normal microflora of the mosquito microbiome. Far less is known of the commensal fungi that are common residents of the microbiome and are the next set of organisms on the most wanted list. A survey of culturable fungal isolates among laboratory reared and field caught mosquitoes found fungal isolates in the class *Microbotryomycetes* to be common among field caught mosquitoes, but absent in the microbiome of laboratory-reared mosquitoes (Hyde et al., 2019b). This suggests fungi may play an important role in the microbiome, but normal colony conditions may not be favorable to commensal fungi (Hyde et al., 2019b). As to the role fungi may play in the environment, certain fungi may exert their effect on the microbiome by attracting gravid females to a breeding site. Particularly, yeasts produce CO<sub>2</sub> and other volatile compounds through fermentation, which can signal to the mosquito, a suitable habitat with sufficient sugar and microbial resources to support larval development (Malassigné et al., 2020). In this manner, these fungi can ensure colonization of the newly hatched larvae (Reeves, 2004). Gnotobiotic larvae colonized by *Saccharomyces cerevisiae* develop normally, indicating yeast can supply all the required nutrients for larval development (Correa et al., 2018). Certain fungi, such as *Cladosporium*, *Aspergillus*, *Ampullimonas*, and *Cyberlindnera*, actively participate in digesting the fructose that mosquitoes ingest from flower nectar (Guégan et al., 2020). Thus, fungi appear to play roles in both larval and adult nutrition. Other yeasts, such as *Wickerhamomyces anomalus*, colonize the reproductive organs of both male and female mosquitoes, indicating the potential for vertical transmission between generations, suggesting a stable multi-generational association (Ricci et al., 2011). Several fungi have also shown potential in inhibiting the pathogens carried by mosquitoes.



For instance, mosquitoes colonized by microsporidian fungi demonstrated a significant decline in *Plasmodium* development in the mosquito, potentially through priming the mosquito immune response to the malarial parasite (Bargielowski and Koella, 2009; Herren et al., 2020). Similarly, protein toxins produced by the yeast *Wickerhamomyces anomalus* inhibit *Plasmodium* and other entomopathogenic fungi (Cappelli et al., 2019b). In contrast, fungi of the species *Talaromyces* may promote mosquito infection by dengue virus through suppression of the digestive enzyme trypsin (Angleró-Rodríguez et al., 2017). In this regard, fungi clearly have the potential to play a multitude of roles in the mosquito microbiome, yet remain an enigma.

Beyond the protist parasite *Plasmodium*, there is very little knowledge concerning whether mosquitoes harbor a stable population of protists in their microbiome (Guégan et al., 2018). Belda et al. employed a method based on peptide-nucleic acid clamps to suppress amplification of host DNA and specifically interrogate the eukaryotic members of the mosquito microbiome (Belda et al., 2017; Taerum et al., 2020). The eukaryotic microbiome of larval samples was dominated by the *Ichthyosporea* group, a lineage of unicellular organisms that includes parasites and commensals of a wide range of animals (Glockling et al., 2013). Similarly, metabarcoding and sequencing of the 18S rRNA genes from mosquitoes in Thailand identified *Ascogregarina* as the dominant microbial eukaryote in the mosquito microbiome (Thongsripong et al., 2018). This protist has been shown to have a range of fitness consequences on host mosquitoes ranging from detrimental to neutral (Erthal et al., 2012). Yet, the organism displays the hallmarks of a parasitic infection as oocysts are ingested from the larval water, enter epithelial cells, and use host cell mitochondria to supply the energy required to mature (Chen and Wu, 1997). *Trypanosoma brucei*, a protist parasite and causative agent of trypanosomiasis, normally carried by tsetse flies, can survive in mosquito midguts for up to 48 h. Co-infection of mosquitoes with *Trypanosoma* and *Plasmodium* increased the malarial parasite load in the mosquito, potentially increasing the risk of malarial spread (Dieme et al., 2020). Thus, there is evidence that the microbiome of the mosquito may host a population of protists, but their roles and interactions with the host are essentially undescribed.

The microbial eukaryotes carried by mosquitoes represent a virtually uncharted territory for discovery in the mosquito microbiome. As such, they are the final members to make the list of high-value targets for gnotobiotic studies.

## COMMUNITY ECOLOGY AND MICROBIOME INTERACTIONS

Bacteria are unlikely to find themselves in the mosquito as a monoculture. Instead, mosquitoes are colonized by a community of interacting individuals and populations.

Microbial interactions may be parasitic, where one organism benefits at the cost of another: mutualistic, such that both organisms benefit, or commensal, when one organism benefits

at no cost or benefit to the other. These interactions are facilitated by mechanisms, such as metabolite exchange, cross-feeding, and antibiotic production (Phelan et al., 2012; Pacheco and Segrè, 2019). Thus, the properties of the community are determined by the separate functional contributions from each species and their interactions. In this respect, the attributes of a community are difficult to predict from the traits of its members when they are reared in a mono-culture (Sanchez-Gorostiaga et al., 2019). It is increasingly apparent that the microbiome of mosquitoes acts as a community, rather than a collection of individuals. Co-occurrence networks based on bacterial census data identified multiple pairwise and higher order interactions, indicating an interwoven and linked microbial community (Hegde et al., 2018). More direct evidence of microbial interactions within the mosquito has also been documented. For example, when a strain of *S. marcescens* was introduced to *Ae. aegypti* larvae as a monoculture, 89% of the larvae died. The same strain inoculated in a simple three-member community reduced mortality to 50%. Yet, *Serratia* was identified among all of the assayed mosquitoes, suggesting that the larvicidal activity of *Serratia* is attenuated by the presence of other microbes (Correa et al., 2018). Microbial interactions also influence the digestion of mosquito food sources. The fructose that mosquitoes obtain through feeding on flower nectar can be digested in a trophic interaction involving both fungi and bacteria (Guégan et al., 2020). In another example, it was shown that when *E. anopheles* was co-cultured with a strain of *Pseudomonas* in the midguts of mosquitoes, *E. anopheles* upregulated gene products for heme degradation. This activity presumably facilitates blood digestion in the mosquito but also produced a metabolite of the class biliverdin, which may inhibit *Pseudomonas* growth. In this manner, *E. anopheles* gains a competitive advantage and may indirectly benefit the mosquito host (Ganley, 2020). These observations all point to the importance of viewing the mosquito microbiome as a community and taking a population ecology viewpoint when linking the status of the mosquito microbiome to host phenotypes. Thus, an important step going forward will be to employ gnotobiotic mosquitoes as a resource to characterize microbiome interaction networks.

## CONCLUSION AND PERSPECTIVES

The development of axenic and gnotobiotic mosquito models offers the potential to transform the study of the mosquito microbiome. These models transition microbiome studies from correlational associations between microbes and their host to controlled experiments that can systematically manipulate the composition, genetics, and biochemistry of the microbiome. In this manner, the mechanistic underpinnings of the relationship between the mosquito and its microflora can begin to be uncovered. The wealth of studies that have already linked the microbiome to mosquito biology and the diseases they carry have already provided an abundance of hypotheses to test and will be an excellent foundation for future studies. We have provided a list of potential microbiome members



that represent particularly high-value targets for future gnotobiotic studies, but they are only the forefront of a broad field of investigation. Recently, researchers proposed the formation of a “Mosquito Microbiome Research Consortium” and laid out recommendations for best practices for collecting, analyzing, and sharing mosquito microbiome data (Dada et al., 2021). We propose that properly designed and controlled axenic and gnotobiotic studies should be central pillars to a unified effort to disentangle the role of the microbiome in mosquito biology and microbe-mosquito control programs.

## REFERENCES

- Abreo, E., and Altier, N. (2019). Pangenome of *Serratia marcescens* strains from nosocomial and environmental origins reveals different populations and the links between them. *Sci. Rep.* 9:46. doi: 10.1038/s41598-018-37118-0
- Akhouayri, I. G., Habtewold, T., and Christophides, G. K. (2013). Melanotic pathology and vertical transmission of the gut commensal *Elizabethkingia meningoseptica* in the major malaria vector *Anopheles gambiae*. *PLoS One* 8:e77619. doi: 10.1371/journal.pone.0077619
- Akov, S. (1962). A qualitative and quantitative study of the nutritional requirements of *Aedes aegypti* L. larvae. *J. Insect Physiol.* 8, 319–335. doi: 10.1016/0022-1910(62)90035-5
- Alfano, N., Tagliapietra, V., Rosso, F., Manica, M., Arnoldi, D., Pindo, M., et al. (2019). Changes in microbiota across developmental stages of *Aedes koreicus*, an invasive mosquito vector in Europe: indications for microbiota-based control strategies. *Front. Microbiol.* 10:2832. doi: 10.3389/fmicb.2019.02832
- Angleró-Rodríguez, Y. I., Talyuli, O. A., Blumberg, B. J., Kang, S., Demby, C., Shields, A., et al. (2017). An *Aedes aegypti*-associated fungus increases susceptibility to dengue virus by modulating gut trypsin activity. *eLife* 6:e28844. doi: 10.7554/eLife.28844
- Apte-Deshpande, A., Paingankar, M., Gokhale, M. D., and Deobagkar, D. N. (2012). *Serratia odorifera* a midgut inhabitant of *Aedes aegypti* mosquito enhances its susceptibility to dengue-2 virus. *PLoS One* 7:e40401. doi: 10.1371/journal.pone.0040401
- Audsley, M. D., Ye, Y. H., and McGraw, E. A. (2017). The microbiome composition of *Aedes aegypti* is not critical for Wolbachia-mediated inhibition of dengue virus. *PLoS Negl. Trop. Dis.* 11:e0005426. doi: 10.1371/journal.pntd.0005426
- Badal, S., Her, Y. F., and Maher, L. J. (2015). Nonantibiotic effects of fluoroquinolones in mammalian cells. *J. Biol. Chem.* 290, 22287–22297. doi: 10.1074/jbc.M115.671222
- Bahia, A. C., Dong, Y., Blumberg, B. J., Mlambo, G., Tripathi, A., BenMarzouk-Hidalgo, O. J., et al. (2014). Exploring *Anopheles* gut bacteria for *Plasmodium* blocking activity. *Environ. Microbiol.* 16, 2980–2994. doi: 10.1111/1462-2920.12381
- Bai, L., Wang, L., Vega-Rodríguez, J., Wang, G., and Wang, S. (2019). A gut symbiotic bacterium *Serratia marcescens* renders mosquito resistance to *Plasmodium* infection through activation of mosquito immune responses. *Front. Microbiol.* 10:1580. doi: 10.3389/fmicb.2019.01580
- Bakula, M. (1969). The persistence of a microbial flora during postembryogenesis of *Drosophila melanogaster*. *J. Invertebr. Pathol.* 14, 365–374. doi: 10.1016/0022-2011(69)90163-3
- Bando, H., Okado, K., Guelbeogo, W. M., Badolo, A., Aonuma, H., Nelson, B., et al. (2013). Intra-specific diversity of *Serratia marcescens* in *Anopheles* mosquito midgut defines *Plasmodium* transmission capacity. *Sci. Rep.* 3:1641. doi: 10.1038/srep01641
- Bargielowski, I., and Koella, J. C. (2009). A possible mechanism for the suppression of *Plasmodium berghei* development in the mosquito *Anopheles gambiae* by the microsporidian *Vavraia culicis*. *PLoS One* 4:e4676. doi: 10.1371/journal.pone.0004676
- Barnard, K., Jeanrenaud, A. C. S. N., Brooke, B. D., and Oliver, S. V. (2019). The contribution of gut bacteria to insecticide resistance and the life histories of the major malaria vector *Anopheles arabiensis* (Diptera: Culicidae). *Sci. Rep.* 9:9117. doi: 10.1038/s41598-019-45499-z
- Bassene, H., Niang, E. H. A., Fenollar, F., Doucoure, S., Faye, O., Raoult, D., et al. (2020). Role of plants in the transmission of *Asaia* sp., which potentially inhibit the *Plasmodium* sporogonic cycle in *Anopheles* mosquitoes. *Sci. Rep.* 10:7144. doi: 10.1038/s41598-020-64163-5
- Batista, J. H., and da Silva Neto, J. F. (2017). *Chromobacterium violaceum* pathogenicity: updates and insights from genome sequencing of novel *Chromobacterium* species. *Front. Microbiol.* 8:2213. doi: 10.3389/fmicb.2017.02213
- Belda, E., Coulibaly, B., Fofana, A., Beavogui, A. H., Traore, S. F., Gohl, D. M., et al. (2017). Preferential suppression of *Anopheles gambiae* host sequences allows detection of the mosquito eukaryotic microbiome. *Sci. Rep.* 7:3241. doi: 10.1038/s41598-017-03487-1
- Biggs, M. B., Medlock, G. L., Moutinho, T. J., Lees, H. J., Swann, J. R., Kolling, G. L., et al. (2017). Systems-level metabolism of the altered Schaedler flora, a complete gut microbiota. *ISME J.* 11, 426–438. doi: 10.1038/ismej.2016.130
- Breurec, S., Criscuolo, A., Diancourt, L., Rendueles, O., Vandenbogaert, M., Passet, V., et al. (2016). Genomic epidemiology and global diversity of the emerging bacterial pathogen *Elizabethkingia anophelis*. *Sci. Rep.* 6:30379. doi: 10.1038/srep30379
- Browning, D. F., Wells, T. J., França, F. L. S., Morris, F. C., Sevastyanovich, Y. R., Bryant, J. A., et al. (2013). Laboratory adapted *Escherichia coli* K-12 becomes a pathogen of *Caenorhabditis elegans* upon restoration of O antigen biosynthesis. *Mol. Microbiol.* 87, 939–950. doi: 10.1111/mmi.12144
- Capone, A., Ricci, I., Damiani, C., Mosca, M., Rossi, P., Scuppa, P., et al. (2013). Interactions between *Asaia*, *Plasmodium* and *Anopheles*: new insights into mosquito symbiosis and implications in malaria symbiotic control. *Parasit. Vectors* 6:182. doi: 10.1186/1756-3305-6-182
- Cappelli, A., Damiani, C., Mancini, M. V., Valzano, M., Rossi, P., Serrao, A., et al. (2019a). *Asaia* activates immune genes in mosquito eliciting an anti-*Plasmodium* response: implications in malaria control. *Front. Genet.* 10:836. doi: 10.3389/fgene.2019.00836
- Cappelli, A., Valzano, M., Cecarini, V., Bozic, J., Rossi, P., Mensah, P., et al. (2019b). Killer yeasts exert anti-plasmodial activities against the malaria parasite *Plasmodium berghei* in the vector mosquito *Anopheles stephensi* and in mice. *Parasit. Vectors* 12:329. doi: 10.1186/s13071-019-3587-4
- Caragata, E. P., Otero, L. M., Carlson, J. S., Dizaji, N. B., and Dimopoulos, G. (2020). A nonlive preparation of *Chromobacterium* sp. *Panama* (Csp\_P) is a highly effective larval mosquito biopesticide. *Appl. Environ. Microbiol.* 86:e00240-2. doi: 10.1128/AEM.00240-20
- Caragata, E. P., Tikhe, C. V., and Dimopoulos, G. (2019). Curious entanglements: interactions between mosquitoes, their microbiota, and arboviruses. *Curr. Opin. Virol.* 37, 26–36. doi: 10.1016/j.coviro.2019.05.005
- Carlson, J. S., Short, S. M., Angleró-Rodríguez, Y. I., and Dimopoulos, G. (2020). Larval exposure to bacteria modulates arbovirus infection and immune gene expression in adult *Aedes aegypti*. *Dev. Comp. Immunol.* 104:103540. doi: 10.1016/j.dci.2019.103540
- Chabanol, E., Behrends, V., Prévot, G., Christophides, G. K., and Gendrin, M. (2020). Antibiotic treatment in *Anopheles coluzzii* affects carbon and nitrogen metabolism. *Pathogens* 9:679. doi: 10.3390/pathogens9090679
- Chaston, J. M., Newell, P. D., and Douglas, A. E. (2014). Metagenome-wide association of microbial determinants of host phenotype in *Drosophila melanogaster*. *MBio* 5:e01631-14. doi: 10.1128/mBio.01631-14
- Chavshin, A., Oshaghi, M., Vatandoost, H., Yakhchali, B., Zarenejad, F., and Terenius, O. (2015). Malpighian tubules are important determinants of

## AUTHOR CONTRIBUTIONS

BS and DB contributed to manuscript conception and writing. JH contributed to data for **Figure 1** and manuscript editing. JL contributed to figure production. All authors contributed to the article and approved the submitted version.

## FUNDING

JH was supported by a Louis A Magnarelli grant to BS and DB.

- Pseudomonas* transstadial transmission and longtime persistence in *Anopheles stephensi*. *Parasit. Vectors* 8:36. doi: 10.1186/s13071-015-0635-6
- Chen, S., Bagdasarian, M., and Walker, E. D. (2015). *Elizabethkingia anophelis*: molecular manipulation and interactions with mosquito hosts. *Appl. Environ. Microbiol.* 81, 2233–2243. doi: 10.1128/AEM.03733-14
- Chen, S., Blom, J., and Walker, E. D. (2017). Genomic, physiologic, and symbiotic characterization of *Serratia marcescens* strains isolated from the mosquito *Anopheles stephensi*. *Front. Microbiol.* 8:1483. doi: 10.3389/fmicb.2017.01483
- Chen, S., Johnson, B. K., Yu, T., Nelson, B. N., and Walker, E. D. (2020). *Elizabethkingia anophelis*: physiologic and transcriptomic responses to iron stress. *Front. Microbiol.* 11:804. doi: 10.3389/fmicb.2020.00804
- Chen, S., and Walker, E. D. (2020). Genome sequence of *Serratia fonticola* strain S14, isolated from the mosquito *Aedes triseriatus*. *Microbiol. Resour. Announc.* 9, e00099–e00020. doi: 10.1128/MRA.00099-20
- Chen, W.-J., and Wu, S.-T. (1997). Ultrastructure of infection, development and gametocyst formation of *Ascogregarina taiwanensis* (Apicomplexa: Lecudinidae) in its mosquito host, *Aedes albopictus* (Diptera: Culicidae). *J. Eukaryot. Microbiol.* 44, 101–108. doi: 10.1111/j.1550-7408.1997.tb05945.x
- Chouaia, B., Rossi, P., Epis, S., Mosca, M., Ricci, I., Damiani, C., et al. (2012). Delayed larval development in *Anopheles* mosquitoes deprived of *Asaia* bacterial symbionts. *BMC Microbiol.* 12:S2. doi: 10.1186/1471-2180-12-S1-S2
- Chouaia, B., Rossi, P., Montagna, M., Ricci, I., Crotti, E., Damiani, C., et al. (2010). Molecular evidence for multiple infections as revealed by typing of *Asaia* bacterial symbionts of four mosquito species. *Appl. Environ. Microbiol.* 76, 7444–7450. doi: 10.1128/AEM.01747-10
- Cirimotich, C. M., Dong, Y., Clayton, A. M., Sandiford, S. L., Souza-Neto, J. A., Mulenga, M., et al. (2011). Natural microbe-mediated refractoriness to *Plasmodium* infection in *Anopheles gambiae*. *Science* 332, 855–858. doi: 10.1126/science.1201618
- Comandatore, F., Damiani, C., Cappelli, A., Ribolla, P. E. M., Gasperi, G., Gradoni, F., et al. (2021). Phylogenomics reveals that *Asaia* symbionts from insects underwent convergent genome reduction, preserving an insecticide-degrading gene. *mBio* 12:e00106-21. doi: 10.1128/mBio.00106-21
- Coon, K. L., Brown, M. R., and Strand, M. R. (2016a). Gut bacteria differentially affect egg production in the anaerobic mosquito *Aedes aegypti* and facultatively autogenous mosquito *Aedes atropalpus* (Diptera: Culicidae). *Parasit. Vectors* 9:375. doi: 10.1186/s13071-016-1660-9
- Coon, K. L., Brown, M. R., and Strand, M. R. (2016b). Mosquitoes host communities of bacteria that are essential for development but vary greatly between local habitats. *Mol. Ecol.* 25, 5806–5826. doi: 10.1111/mec.13877
- Coon, K. L., Valzania, L., Brown, M. R., and Strand, M. R. (2020). Predaceous *Toxorhynchites* mosquitoes require a living gut microbiota to develop. *Proc. R. Soc. B Biol. Sci.* 287:20192705. doi: 10.1098/rspb.2019.2705
- Coon, K. L., Valzania, L., McKinney, D. A., Vogel, K. J., Brown, M. R., and Strand, M. R. (2017). Bacteria-mediated hypoxia functions as a signal for mosquito development. *PNAS* 114, E5362–E5369. doi: 10.1073/pnas.1702983114
- Coon, K. L., Vogel, K. J., Brown, M. R., and Strand, M. R. (2014). Mosquitoes rely on their gut microbiota for development. *Mol. Ecol.* 23, 2727–2739. doi: 10.1111/mec.12771
- Correa, M. A., Matusovsky, B., Brackney, D. E., and Steven, B. (2018). Generation of axenic *Aedes aegypti* demonstrate live bacteria are not required for mosquito development. *Nat. Commun.* 9:4464. doi: 10.1038/s41467-018-07014-2
- Crotti, E., Damiani, C., Pajoro, M., Gonella, E., Rizzi, A., Ricci, I., et al. (2009). *Asaia*, a versatile acetic acid bacterial symbiont, capable of cross-colonizing insects of phylogenetically distant genera and orders. *Environ. Microbiol.* 11, 3252–3264. doi: 10.1111/j.1462-2920.2009.02048.x
- Crotti, E., Rizzi, A., Chouaia, B., Ricci, I., Favia, G., Alma, A., et al. (2010). Acetic acid bacteria, newly emerging symbionts of insects. *Appl. Environ. Microbiol.* 76, 6963–6970. doi: 10.1128/AEM.01336-10
- D'mello, R., Hill, S., and Poole, R. K. (1996). The cytochrome *bd* quinol oxidase in *Escherichia coli* has an extremely high oxygen affinity and two oxygen-binding haems: implications for regulation of activity *in vivo* by oxygen inhibition. *Microbiology* 142, 755–763. doi: 10.1099/00221287-142-4-755
- Dada, N., Jupatanakul, N., Minard, G., Short, S. M., Akorli, J., and Villegas, L. M. (2021). Considerations for mosquito microbiome research from the mosquito microbiome consortium. *Microbiome* 9:36. doi: 10.1186/s40168-020-00987-7
- Dada, N., Sheth, M., Liebman, K., Pinto, J., and Lenhart, A. (2018). Whole metagenome sequencing reveals links between mosquito microbiota and insecticide resistance in malaria vectors. *Sci. Rep.* 8:2084. doi: 10.1038/s41598-018-20367-4
- Damiani, C., Ricci, I., Crotti, E., Rossi, P., Rizzi, A., Scuppa, P., et al. (2008). Paternal transmission of symbiotic bacteria in malaria vectors. *Curr. Biol.* 18, R1087–R1088. doi: 10.1016/j.cub.2008.10.040
- Damiani, C., Ricci, I., Crotti, E., Rossi, P., Rizzi, A., Scuppa, P., et al. (2010). Mosquito-bacteria symbiosis: the case of *Anopheles gambiae* and *Asaia*. *Microb. Ecol.* 60, 644–654. doi: 10.1007/s00248-010-9704-8
- Dickson, L. B., Jirolle, D., Minard, G., Moltini-Conclois, I., Volant, S., Ghazlane, A., et al. (2017). Carryover effects of larval exposure to different environmental bacteria drive adult trait variation in a mosquito vector. *Sci. Adv.* 3:e1700585. doi: 10.1126/sciadv.1700585
- Dieme, C., Zmarlak, N. M., Brito-Fravallo, E., Travaillé, C., Pain, A., Cherrier, F., et al. (2020). Exposure of *Anopheles* mosquitoes to trypanosomes reduces reproductive fitness and enhances susceptibility to *Plasmodium*. *PLoS Negl. Trop. Dis.* 14:e0008059. doi: 10.1371/journal.pntd.0008059
- Dittmer, J., and Gabrieli, P. (2020). Transstadial metabolic priming mediated by larval nutrition in female *Aedes albopictus* mosquitoes. *J. Insect Physiol.* 123:104053. doi: 10.1016/j.jinsphys.2020.104053
- Dong, Y., Manfredini, F., and Dimopoulos, G. (2009). Implication of the mosquito midgut microbiota in the defense against malaria parasites. *PLoS Pathog.* 5:e1000423. doi: 10.1371/journal.ppat.1000423
- Douglas, A. E. (2018). The *Drosophila* model for microbiome research. *Lab Anim.* 47, 157–164. doi: 10.1038/s41684-018-0065-0
- Durán, N., and Menck, C. F. M. (2008). *Chromobacterium violaceum*: a review of pharmacological and industrial perspectives. *Crit. Rev. Microbiol.* 27, 201–222. doi: 10.1080/20014091096747
- Erthal, J. A., Soghigian, J. S., and Livdahl, T. (2012). Life cycle completion of parasite *Ascogregarina taiwanensis* (Apicomplexa: Lecudinidae) in non-native host *Ochlerotatus japonicus* (Diptera: Culicidae). *J. Med. Entomol.* 49, 1109–1117. doi: 10.1603/MEI12018
- Ezemuoka, L. C., Akorli, E. A., Aboagye-Antwi, F., and Akorli, J. (2020). Mosquito midgut *Enterobacter cloacae* and *Serratia marcescens* affect the fitness of adult female *Anopheles gambiae* s.l. *PLoS One* 15:e0238931. doi: 10.1371/journal.pone.0238931
- Favia, G., Ricci, I., Damiani, C., Raddadi, N., Crotti, E., Marzorati, M., et al. (2007). Bacteria of the genus *Asaia* stably associate with *Anopheles stephensi*, an Asian malarial mosquito vector. *Proc. Natl. Acad. Sci.* 104, 9047–9051. doi: 10.1073/pnas.0610451104
- Favia, G., Ricci, I., Marzorati, M., Negri, I., Alma, A., Sacchi, L., et al. (2008). "Bacteria of the genus *Asaia*: a potential paratransgenic weapon against malaria," *Transgenesis and the Management of Vector-Borne Disease*. Vol. 627. ed. S. Aksoy (New York, NY: Springer), 49–59.
- Fei, N., and Zhao, L. (2013). An opportunistic pathogen isolated from the gut of an obese human causes obesity in germfree mice. *ISME J.* 7, 880–884. doi: 10.1038/ismej.2012.153
- Frank, T., Gody, J. C., Nguyen, L. B. L., Berthet, N., Fleche-Mateos, A. L., Bata, P., et al. (2013). First case of *Elizabethkingia anophelis* meningitis in the Central African Republic. *Lancet* 381:1876. doi: 10.1016/S0140-6736(13)60318-9
- Freece, C. D., Damiani, C., Valzano, M., D'amelio, S., Cappelli, A., Ricci, I., et al. (2014). Detection and isolation of the  $\alpha$ -proteobacterium *Asaia* in *Culex* mosquitoes. *Med. Vet. Entomol.* 28, 438–442. doi: 10.1111/mve.12045
- Gainley, J. G. (2020). Coculturing of mosquito-microbiome bacteria promotes heme degradation in *Elizabethkingia anophelis*. *Chembiochem* 21, 1279–1284. doi: 10.1002/cbic.201900675
- Gainley, J. G., Carr, G., Ioerger, T. R., Sacchettini, J. C., Clardy, J., and Derbyshire, E. R. (2018). Discovery of antimicrobial lipodepsipeptides produced by a *Serratia* sp. within mosquito microbiomes. *Chembiochem* 19, 1590–1594. doi: 10.1002/cbic.201800124
- Giraud, E., Varet, H., Legendre, R., Sismeiro, O., Aubry, F., Dabo, S., et al. (2021). Mosquito-bacteria interactions during larval development trigger metabolic changes with carry-over effects on adult fitness. *bioRxiv* [Preprint]. doi: 10.1101/2021.05.20.444942
- Glockling, S. L., Marshall, W. L., and Gleason, F. H. (2013). Phylogenetic interpretations and ecological potentials of the Mesomycetozoa (Ichthyosporidia). *Fungal Ecol.* 6, 237–247. doi: 10.1016/j.funeco.2013.03.005
- Gnambani, E. J., Bilgo, E., Sanou, A., Dabiré, R. K., and Diabaté, A. (2020). Infection of highly insecticide-resistant malaria vector *Anopheles coluzzii* with entomopathogenic bacteria *Chromobacterium violaceum* reduces its

- survival, blood feeding propensity and fecundity. *Malar. J.* 19:352. doi: 10.1186/s12936-020-03420-4
- González, L. J., and Vila, A. J. (2012). Carbapenem resistance in *Elizabethkingia meningoseptica* is mediated by metallo- $\beta$ -lactamase BlaB. *Antimicrob. Agents Chemother.* 56, 1686–1692. doi: 10.1128/AAC.05835-11
- Goojani, H. G., Konings, J., Hakvoort, H., Hong, S., Gennis, R. B., Sakamoto, J., et al. (2020). The carboxy-terminal insert in the Q-loop is needed for functionality of *Escherichia coli* cytochrome bd-I. *Biochim. Biophys. Acta Bioenerg.* 1861:148175. doi: 10.1016/j.bbmbio.2020.148175
- Gopinath, S., Kim, M. V., Rakib, T., Wong, P. W., van Zandt, M., Barry, N. A., et al. (2018). Topical application of aminoglycoside antibiotics enhances host resistance to viral infections in a microbiota-independent manner. *Nat. Microbiol.* 3, 611–621. doi: 10.1038/s41564-018-0138-2
- Gould, A. L., Zhang, V., Lamberti, L., Jones, E. W., Obadia, B., Korasidis, N., et al. (2018). Microbiome interactions shape host fitness. *PNAS* 115, E11951–E11960. doi: 10.1073/pnas.1809349115
- Guégan, M., Minard, G., Tran, F.-H., Fel, B., Hay, A.-E., Simon, L., et al. (2020). Who is eating fructose within the *Aedes albopictus* gut microbiota? *Environ. Microbiol.* 22, 1193–1206. doi: 10.1111/1462-2920.14915
- Guégan, M., Zouache, K., Démichel, C., Minard, G., Tran Van, V., Potier, P., et al. (2018). The mosquito holobiont: fresh insight into mosquito-microbiota interactions. *Microbiome* 6:49. doi: 10.1186/s40168-018-0435-2
- Hancock, P. A., Sinkins, S. P., and Godfray, H. C. J. (2011). Strategies for introducing *Wolbachia* to reduce transmission of mosquito-borne diseases. *PLoS Negl. Trop. Dis.* 5:e1024. doi: 10.1371/journal.pntd.0001024
- Hayek, S. S., Abd, T. T., Cribbs, S. K., Anderson, A. M., Melendez, A., Kobayashi, M., et al. (2013). Rare *Elizabethkingia meningoseptica* meningitis case in an immunocompetent adult. *Emerging Microbes Infect.* 2, 1–4. doi: 10.1038/emi.2013.16
- Hegde, S., Khanipov, K., Albayrak, L., Golovko, G., Pimenova, M., Saldaña, M. A., et al. (2018). Microbiome interaction networks and community structure from laboratory-reared and field-collected *Aedes aegypti*, *Aedes albopictus*, and *Culex quinquefasciatus* mosquito vectors. *Front. Microbiol.* 9:2160. doi: 10.3389/fmicb.2018.02160
- Herren, J. K., Mbaisi, L., Mararo, E., Makhulu, E. E., Mobegi, V. A., Butungi, H., et al. (2020). A microsporidian impairs *Plasmodium falciparum* transmission in *Anopheles arabiensis* mosquitoes. *Nat. Commun.* 11:2187. doi: 10.1038/s41467-020-16121-y
- Hug, L. A. (2018). Sizing up the uncultured microbial majority. *mSystems* 3:e00185-18. doi: 10.1128/mSystems.00185-18
- Hughes, G. L., Dodson, B. L., Johnson, R. M., Murdock, C. C., Tsujimoto, H., Suzuki, Y., et al. (2014). Native microbiome impedes vertical transmission of *Wolbachia* in *Anopheles* mosquitoes. *Proc. Natl. Acad. Sci.* 111, 12498–12503. doi: 10.1073/pnas.1408888111
- Hughes, G. L., Pike, A. D., Xue, P., and Rasgon, J. L. (2012). Invasion of *Wolbachia* into *Anopheles* and other insect germlines in an *ex vivo* organ culture system. *PLoS One* 7:e36277. doi: 10.1371/journal.pone.0036277
- Hyde, J., Correa, M. A., Brackney, D. E., and Steven, B. (2019a). Generation and rearing of axenic *Aedes aegypti* mosquitoes. [Preprint]. doi:10.21203/rs.2.17705/v1
- Hyde, J., Correa, M. A., Hughes, G. L., Steven, B., and Brackney, D. E. (2020). Limited influence of the microbiome on the transcriptional profile of female *Aedes aegypti* mosquitoes. *Sci. Rep.* 10:10880. doi: 10.1038/s41598-020-67811-y
- Hyde, J., Gorham, C., Brackney, D. E., and Steven, B. (2019b). Antibiotic resistant bacteria and commensal fungi are common and conserved in the mosquito microbiome. *PLoS One* 14:e0218907. doi: 10.1371/journal.pone.0218907
- Iturbe-Ormaetxe, I., Walker, T., and O' Neill, S. L. (2011). *Wolbachia* and the biological control of mosquito-borne disease. *EMBO Rep.* 12, 508–518. doi: 10.1038/embor.2011.84
- Janda, J. M., and Lopez, D. L. (2017). Mini review: new pathogen profiles: *Elizabethkingia anophelis*. *Diagn. Microbiol. Infect. Dis.* 88, 201–205. doi: 10.1016/j.diagmicrobio.2017.03.007
- Jiggins, F. M. (2017). The spread of *Wolbachia* through mosquito populations. *PLoS Biol.* 15:e2002780. doi: 10.1371/journal.pbio.2002780
- Kalappa, D. M., Subramani, P. A., Basavanna, S. K., Ghosh, S. K., Sundaramurthy, V., Uragayala, S., et al. (2018). Influence of midgut microbiota in *Anopheles stephensi* on *Plasmodium berghei* infections. *Malar. J.* 17:385. doi: 10.1186/s12936-018-2535-7
- Kalghatgi, S., Spina, C. S., Costello, J. C., Liesa, M., Morones-Ramirez, J. R., Slomovic, S., et al. (2013). Bactericidal antibiotics induce mitochondrial dysfunction and oxidative damage in mammalian cells. *Sci. Transl. Med.* 5:192ra85. doi: 10.1126/scitranslmed.3006055
- Kämpfer, P., Matthews, H., Glaeser, S. P., Martin, K., Lodders, N., and Faye, I. (2011). *Elizabethkingia anophelis* sp. nov., isolated from the midgut of the mosquito *Anopheles gambiae*. *Int. J. Syst. Evol. Microbiol.* 61, 2670–2675. doi: 10.1099/ijs.0.026393-0
- Kanzok, S. M., and Jacobs-Lorena, M. (2006). Entomopathogenic fungi as biological insecticides to control malaria. *Trends Parasitol.* 22, 49–51. doi: 10.1016/j.pt.2005.12.008
- Kaur, R., Shropshire, J. D., Cross, K. L., Leigh, B., Mansueti, A. J., Stewart, V., et al. (2021). Living in the endosymbiotic world of *Wolbachia*: a centennial review. *Cell Host Microbe* 29, 879–893. doi: 10.1016/j.chom.2021.03.006
- Keebaugh, E. S., Yamada, R., Obadia, B., Ludington, W. B., and Ja, W. W. (2018). Microbial quantity impacts *Drosophila* nutrition, development, and lifespan. *iScience* 4, 247–259. doi: 10.1016/j.isci.2018.06.004
- Khanna, A., Khanna, M., and Aggarwal, A. (2013). *Serratia marcescens*-a rare opportunistic nosocomial pathogen and measures to limit its spread in hospitalized patients. *J. Clin. Diagn. Res.* 7, 243–246. doi: 10.7860/JCDR/2013/5010.2737
- Koosha, M., Vatandoost, H., Karimian, F., Choubdar, N., Abai, M. R., and Oshaghi, M. A. (2019). Effect of *Serratia* AS1 (Enterobacteriaceae: Enterobacteriales) on the fitness of *Culex pipiens* (Diptera: Culicidae) for paratransgenic and RNAi approaches. *J. Med. Entomol.* 56, 553–559. doi: 10.1093/jme/tjy183
- Kothari, V., Sharma, S., and Padia, D. (2017). Recent research advances on *Chromobacterium violaceum*. *Asian Pac J Trop Med* 10, 744–752. doi: 10.1016/j.apjtm.2017.07.022
- Kozlova, E. V., Hegde, S., Roundy, C. M., Golovko, G., Saldaña, M. A., Hart, C. E., et al. (2021). Microbial interactions in the mosquito gut determine *Serratia* colonization and blood-feeding propensity. *ISME J.* 15, 93–108. doi: 10.1038/s41396-020-00763-3
- Kukutla, P., Lindberg, B. G., Pei, D., Rayl, M., Yu, W., Steritz, M., et al. (2013). Draft genome sequences of *Elizabethkingia anophelis* strains R26T and Ag1 from the midgut of the malaria mosquito *Anopheles gambiae*. *Genome Announc.* 1:e01030-13. doi: 10.1128/genomeA.01030-13
- Kukutla, P., Lindberg, B. G., Pei, D., Rayl, M., Yu, W., Steritz, M., et al. (2014). Insights from the genome annotation of *Elizabethkingia anophelis* from the malaria vector *Anopheles gambiae*. *PLoS One* 9:e97715. doi: 10.1371/journal.pone.0097715
- Lang, C. A., Basch, K. J., and Storey, R. S. (1972). Growth, composition and longevity of the axenic mosquito. *J. Nutr.* 102, 1057–1066. doi: 10.1093/jn/102.8.1057
- Lau, S. K. P., Chow, W.-N., Foo, C.-H., Curreem, S. O. T., Lo, G. C.-S., Teng, J. L. L., et al. (2016). *Elizabethkingia anophelis* bacteremia is associated with clinically significant infections and high mortality. *Sci. Rep.* 6:26045. doi: 10.1038/srep26045
- Lea, A. O., Dimond, J. B., and Delong, D. M. (1956). A chemically defined medium for rearing *Aedes aegypti* larvae. *J. Econ. Entomol.* 49, 313–315. doi: 10.1093/jee/49.3.313
- Lee, Y.-L., Liu, K.-M., Chang, H.-L., Lin, J.-S., Kung, F.-Y., Ho, C.-M., et al. (2021). A dominant strain of *Elizabethkingia anophelis* emerged from a hospital water system to cause a three-year outbreak in a respiratory care center. *J. Hosp. Infect.* 108, 43–51. doi: 10.1016/j.jhin.2020.10.025
- Lewis, W. H., Tahon, G., Geesink, P., Sousa, D. Z., and Ettema, T. J. G. (2021). Innovations to culturing the uncultured microbial majority. *Nat. Rev. Microbiol.* 19, 225–240. doi: 10.1038/s41579-020-00458-8
- Lindh, J. M., Borg-Karlson, A.-K., and Faye, I. (2008). Transstadial and horizontal transfer of bacteria within a colony of *Anopheles gambiae* (Diptera: Culicidae) and oviposition response to bacteria-containing water. *Acta Trop.* 107, 242–250. doi: 10.1016/j.actatropica.2008.06.008
- Linenberg, I., Christophides, G. K., and Gendrin, M. (2016). Larval diet affects mosquito development and permissiveness to *Plasmodium* infection. *Sci. Rep.* 6:38230. doi: 10.1038/srep38230
- Liu, D., and Reeves, P. R. Y. (1994). *Escherichia coli* K12 regains its O antigen. *Microbiology* 140, 49–57. doi: 10.1099/13500872-140-1-49
- Lopes, S. C. P., Blanco, Y. C., Justo, G. Z., Nogueira, P. A., Rodrigues, F. L. S., Goelnitz, U., et al. (2009). Violacein extracted from *Chromobacterium violaceum*



- inhibits *Plasmodium* growth *in vitro* and *in vivo*. *Antimicrob. Agents Chemother.* 53, 2149–2152. doi: 10.1128/AAC.00693-08
- Mahlen, S. D. (2011). *Serratia* infections: from military experiments to current practice. *Clin. Microbiol. Rev.* 24, 755–791. doi: 10.1128/CMR.00017-11
- Malassigné, S., Valiente Moro, C., and Luis, P. (2020). Mosquito mycobiota: an overview of non-entomopathogenic fungal interactions. *Pathogens* 9:564. doi: 10.3390/pathogens9070564
- Mancini, M. V., Damiani, C., Accoti, A., Tallarita, M., Nunzi, E., Cappelli, A., et al. (2018). Estimating bacteria diversity in different organs of nine species of mosquito by next generation sequencing. *BMC microbiol.* 18:126. doi: 10.1186/s12866-018-1266-9
- McClean, K. H., Winson, M. K., Fish, L., Taylor, A., Chhabra, S. R., Camara, M., et al. (1997). Quorum sensing and *Chromobacterium violaceum*: exploitation of violacein production and inhibition for the detection of N-acylhomoserine lactones. *Microbiology* 143, 3703–3711. doi: 10.1099/00221287-143-12-3703
- Minard, G., Mavingui, P., and Moro, C. V. (2013a). Diversity and function of bacterial microbiota in the mosquito holobiont. *Parasit. Vectors* 6:146. doi: 10.1186/1756-3305-6-146
- Minard, G., Tran, F. H., Raharimalala, F. N., Hellard, E., Ravelonandro, P., Mavingui, P., et al. (2013b). Prevalence, genomic and metabolic profiles of *Acinetobacter* and *Asaia* associated with field-caught *Aedes albopictus* from Madagascar. *FEMS Microbiol. Ecol.* 83, 63–73. doi: 10.1111/j.1574-6941.2012.01455.x
- Mitraka, E., Stathopoulos, S., Siden-Kiamos, I., Christophides, G. K., and Louis, C. (2013). *Asaia* accelerates larval development of *Anopheles gambiae*. *Pathog. Global Health* 107, 305–311. doi: 10.1179/2047773213Y.0000000106
- Moller-Jacobs, L. L., Murdock, C. C., and Thomas, M. B. (2014). Capacity of mosquitoes to transmit malaria depends on larval environment. *Parasit. Vectors* 7:593. doi: 10.1186/s13071-014-0593-4
- Moullan, N., Mouchiroud, L., Wang, X., Ryu, D., Williams, E. G., Mottis, A., et al. (2015). Tetracyclines disturb mitochondrial function across eukaryotic models: a call for caution in biomedical research. *Cell Rep.* 10, 1681–1691. doi: 10.1016/j.celrep.2015.02.034
- Muturi, E. J., Ramirez, J. L., Rooney, A. P., and Kim, C.-H. (2017). Comparative analysis of gut microbiota of mosquito communities in central Illinois. *PLoS Negl. Trop. Dis.* 11:e0005377. doi: 10.1371/journal.pntd.0005377
- Newell, P. D., and Douglas, A. E. (2014). Interspecies interactions determine the impact of the gut microbiota on nutrient allocation in *Drosophila melanogaster*. *Appl. Environ. Microbiol.* 80, 788–796. doi: 10.1128/AEM.02742-13
- Novakova, E., Woodhams, D. C., Rodríguez-Ruano, S. M., Brucker, R. M., Leff, J. W., Maharaj, A., et al. (2017). Mosquito microbiome dynamics, a background for prevalence and seasonality of West Nile virus. *Front. Microbiol.* 8:526. doi: 10.3389/fmicb.2017.00526
- Nuttall, G. H. F., and Thierfelder, H. (1896). *Thierisches Leben ohne Bakterien im Verdauungskanal*. Berlin/New York: Walter de Gruyter.
- Oliveira, T. M. P., Sanabani, S. S., Sallum, M. A. M., Oliveira, T. M. P., Sanabani, S. S., and Sallum, M. A. M. (2020). *Asaia* (Rhodospirillales: Acetobacteraceae) and *Serratia* (Enterobacterales: Yersiniaceae) associated with *Nyssorhynchus brasiliensis* and *Nyssorhynchus darlingi* (Diptera: Culicidae). *Revista Brasileira de Entomologia* 64. doi: 10.1590/1806-9665-rbent-2019-0010
- Osei-Poku, J., Mbogo, C. M., Palmer, W. J., and Jiggins, F. M. (2012). Deep sequencing reveals extensive variation in the gut microbiota of wild mosquitoes from Kenya. *Mol. Ecol.* 21, 5138–5150. doi: 10.1111/j.1365-294X.2012.05759.x
- Pacheco, A. R., and Segrè, D. (2019). A multidimensional perspective on microbial interactions. *FEMS Microbiol. Lett.* 366:fnz125. doi: 10.1093/femsle/fnz125
- Pasteur, L. (1885). Observations relatives à la note précédente de M. Duclaux. *C.R. Acad. Sci* 100:68.
- Patil, C. D., Patil, S. V., Salunke, B. K., and Salunkhe, R. B. (2011). Prodigiosin produced by *Serratia marcescens* NMCC46 as a mosquito larvicidal agent against *Aedes aegypti* and *Anopheles stephensi*. *Parasitol. Res.* 109, 1179–1187. doi: 10.1007/s00436-011-2365-9
- Patil, C. D., Patil, S. V., Salunke, B. K., and Salunkhe, R. B. (2012). Insecticidal potency of bacterial species *Bacillus thuringiensis* SV2 and *Serratia nematodiphila* SV6 against larvae of mosquito species *Aedes aegypti*, *Anopheles stephensi*, and *Culex quinquefasciatus*. *Parasitol. Res.* 110, 1841–1847. doi: 10.1007/s00436-011-2708-6
- Perrin, A., Larssonneur, E., Nicholson, A. C., Edwards, D. J., Gundlach, K. M., Whitney, A. M., et al. (2017). Evolutionary dynamics and genomic features of the *Elizabethkingia anophelis* 2015 to 2016 Wisconsin outbreak strain. *Nat. Commun.* 8:15483. doi: 10.1038/ncomms15483
- Phelan, V. V., Liu, W.-T., Pogliano, K., and Dorrestein, P. C. (2012). Microbial metabolic exchange—the chemotype-to-phenotype link. *Nat. Chem. Biol.* 8, 26–35. doi: 10.1038/nchembio.739
- Rami, A., Raz, A., Zakeri, S., and Dinparast Djadid, N. (2018). Isolation and identification of *Asaia* sp. in *Anopheles* spp. mosquitoes collected from Iranian malaria settings: steps toward applying paratransgenic tools against malaria. *Parasit. Vectors* 11:367. doi: 10.1186/s13071-018-2955-9
- Ramirez, J. L., Short, S. M., Bahia, A. C., Saraiva, R. G., Dong, Y., Kang, S., et al. (2014). *Chromobacterium* Csp\_P reduces malaria and dengue infection in vector mosquitoes and has entomopathogenic and in vitro anti-pathogen activities. *PLoS Pathog.* 10:e1004398. doi: 10.1371/journal.ppat.1004398
- Ramirez, J. L., Souza-Neto, J., Cosme, R. T., Rovira, J., Ortiz, A., Pascale, J. M., et al. (2012). Reciprocal tripartite interactions between the *Aedes aegypti* midgut microbiota, innate immune system and dengue virus influences vector competence. *PLoS Negl. Trop. Dis.* 6:e1561. doi: 10.1371/journal.pntd.0001561
- Ramos-Nino, M. E., Fitzpatrick, D. M., Eckstrom, K. M., Tighe, S., Hattaway, L. M., Hsueh, A. N., et al. (2020). Metagenomic analysis of *Aedes aegypti* and *Culex quinquefasciatus* mosquitoes from Grenada, West Indies. *PLoS One* 15:e0231047. doi: 10.1371/journal.pone.0231047
- Raspor, P., and Goranovič, D. (2008). Biotechnological applications of acetic acid bacteria. *Crit. Rev. Biotechnol.* 28, 101–124. doi: 10.1080/07388550802046749
- Reeves, W. K. (2004). Oviposition by *Aedes aegypti* (Diptera: Culicidae) in relation to conspecific larvae infected with internal symbionts. *J. Vector Ecol.* 29, 159–63.
- Ricci, I., Damiani, C., Scuppa, P., Mosca, M., Crotti, E., Rossi, P., et al. (2011). The yeast *Wickerhamomyces anomalus* (Pichia anomala) inhabits the midgut and reproductive system of the Asian malaria vector *Anopheles stephensi*. *Environ. Microbiol.* 13, 911–921. doi: 10.1111/j.1462-2920.2010.02395.x
- Rinke, C., Schwientek, P., Szczyrba, A., Ivanova, N. N., Anderson, I. J., Cheng, J.-F., et al. (2013). Insights into the phylogeny and coding potential of microbial dark matter. *Nature* 499, 431–437. doi: 10.1038/nature12352
- Romoli, O., and Gendrin, M. (2018). The tripartite interactions between the mosquito, its microbiota and *Plasmodium*. *Parasit. Vectors* 11:200. doi: 10.1186/s13071-018-2784-x
- Romoli, O., Schönbeck, J. C., Hapfelmeier, S., and Gendrin, M. (2021). Production of germ-free mosquitoes via transient colonisation allows stage-specific investigation of host-microbiota interactions. *Nat. Commun.* 12:942. doi: 10.1038/s41467-021-21195-3
- Rosales-Ronquillo, M. C., Simons, R. W., and Silverman, P. H. (1973). Aseptic rearing of *Anopheles stephensi* (Diptera: Culicidae). *Ann. Entomol. Soc. Am.* 66, 949–954. doi: 10.1093/aesa/66.5.949
- Saab, S. A., Dohna, H. z., Nilsson, L. K. J., Onorati, P., Nakhleh, J., Terenius, O., et al. (2020). The environment and species affect gut bacteria composition in laboratory co-cultured *Anopheles gambiae* and *Aedes albopictus* mosquitoes. *Sci. Rep.* 10:3352. doi: 10.1038/s41598-020-60075-6
- Sanchez-Gorostiaga, A., Bajić, D., Osborne, M. L., Poyatos, J. F., and Sanchez, A. (2019). High-order interactions distort the functional landscape of microbial consortia. *PLoS Biol.* 17:e3000550. doi: 10.1371/journal.pbio.3000550
- Sang, J. H., and King, R. C. (1961). Nutritional requirements of axenically cultured *Drosophila melanogaster* adults. *J. Exp. Biol.* 38, 793–809. doi: 10.1242/jeb.38.4.793
- Saraiva, R. G., Fang, J., Kang, S., Angleró-Rodríguez, Y. I., Dong, Y., and Dimopoulos, G. (2018a). Aminopeptidase secreted by *Chromobacterium* sp. Panama inhibits dengue virus infection by degrading the E protein. *PLoS Negl. Trop. Dis.* 12:e0006443. doi: 10.1371/journal.pntd.0006443
- Saraiva, R. G., Huitt-Roehl, C. R., Tripathi, A., Cheng, Y.-Q., Bosch, J., Townsend, C. A., et al. (2018b). *Chromobacterium* spp. mediate their anti-*Plasmodium* activity through secretion of the histone deacetylase inhibitor romidepsin. *Sci. Rep.* 8:6176. doi: 10.1038/s41598-018-24296-0
- Schaedler, R. W., Dubos, R., and Costello, R. (1965). Association of germfree mice with bacteria isolated from normal mice. *J. Exp. Med.* 122, 77–82. doi: 10.1084/jem.122.1.77
- Scholte, E.-J., Knols, B. G. J., Samson, R. A., and Takken, W. (2004). Entomopathogenic fungi for mosquito control: a review. *J. Insect Sci.* 4:19. doi: 10.1093/jis/4.1.19



- Schulz, M. D., Atay, Ç., Heringer, J., Romrig, F. K., Schwitalla, S., Aydin, B., et al. (2014). High-fat-diet-mediated dysbiosis promotes intestinal carcinogenesis independently of obesity. *Nature* 514, 508–512. doi: 10.1038/nature13398
- Seitz, H. M., Maier, W. A., Rottok, M., and Becker-Feldmann, H. (1987). Concomitant infections of *Anopheles stephensi* with *Plasmodium berghei* and *Serratia marcescens*: additive detrimental effects. *Zentralbl. Bakteriol. Mikrobiol. Hyg. Ser. A* 266, 155–166. doi: 10.1016/S0176-6724(87)80029-9
- Sharma, P., Rani, J., Chauhan, C., Kumari, S., Tevatiya, S., Das De, T., et al. (2020). Altered gut microbiota and immunity defines *Plasmodium vivax* survival in *Anopheles stephensi*. *Front. Immunol.* 11:609. doi: 10.3389/fimmu.2020.00609
- Shen, D., Nyawira, K. T., and Xia, A. (2020). New discoveries and applications of mosquito fungal pathogens. *Curr. Opin. Insect Sci.* 40, 111–116. doi: 10.1016/j.cois.2020.05.003
- Shin, S. C., Kim, S.-H., You, H., Kim, B., Kim, A. C., Lee, K.-A., et al. (2011). *Drosophila* microbiome modulates host developmental and metabolic homeostasis via insulin signaling. *Science* 334, 670–674. doi: 10.1126/science.1212782
- Short, S. M., van Tol, S., MacLeod, H. J., and Dimopoulos, G. (2018a). Hydrogen cyanide produced by the soil bacterium *Chromobacterium* sp. Panama contributes to mortality in *Anopheles gambiae* mosquito larvae. *Sci. Rep.* 8:8358. doi: 10.1038/s41598-018-26680-2
- Short, S. M., van Tol, S., Smith, B., Dong, Y., and Dimopoulos, G. (2018b). The mosquito adulticidal *Chromobacterium* sp. Panama causes transgenerational impacts on fitness parameters and elicits xenobiotic gene responses. *Parasit. Vectors* 11:229. doi: 10.1186/s13071-018-2822-8
- Schubert, A. M., Sinani, H., and Schloss, P. D. (2015). Antibiotic-induced alterations of the murine gut microbiota and subsequent effects on colonization resistance against *Clostridium difficile*. *MBio* 6:e00974. doi: 10.1128/mBio.00974-15
- Singh, K. R. P., and Brown, A. W. A. (1957). Nutritional requirements of *Aedes aegypti* L. *J. Insect Physiol.* 1, 199–220. doi: 10.1016/0022-1910(57)90036-7
- Smith, K., McCoy, K. D., and Macpherson, A. J. (2007). Use of axenic animals in studying the adaptation of mammals to their commensal intestinal microbiota. *Semin. Immunol.* 19, 59–69. doi: 10.1016/j.smim.2006.10.002
- Souza, R. S., Virginio, F., Riback, T. I. S., Suesdek, L., Barufi, J. B., and Genta, F. A. (2019). Microorganism-based larval diets affect mosquito development, size and nutritional reserves in the yellow fever mosquito *Aedes aegypti* (Diptera: Culicidae). *Front. Physiol.* 10:152. doi: 10.3389/fphys.2019.00152
- Stathopoulos, S., Neafsey, D. E., Lawniczak, M. K. N., Muskavitch, M. A. T., and Christophides, G. K. (2014). Genetic dissection of *Anopheles gambiae* gut epithelial responses to *Serratia marcescens*. *PLoS Pathog.* 10:e1003897. doi: 10.1371/journal.ppat.1003897
- Storelli, G., Defaye, A., Erkosar, B., Hols, P., Royet, J., and Leulier, F. (2011). Lactobacillus plantarum promotes *Drosophila* systemic growth by modulating hormonal signals through TOR-dependent nutrient sensing. *Cell Metab.* 14, 403–414. doi: 10.1016/j.cmet.2011.07.012
- Suryawanshi, R. K., Patil, C. D., Borase, H. P., Narkhede, C. P., Salunke, B. K., and Patil, S. V. (2015). Mosquito larvicidal and pupacidal potential of prodigiosin from *Serratia marcescens* and understanding its mechanism of action. *Pestic. Biochem. Physiol.* 123, 49–55. doi: 10.1016/j.pestbp.2015.01.018
- Taerum, S. J., Steven, B., Gage, D. J., and Triplett, L. R. (2020). Validation of a PNA clamping method for reducing host DNA amplification and increasing eukaryotic diversity in rhizosphere microbiome studies. *Phytobiomes J.* 4, 291–302. doi: 10.1094/PBIOMES-05-20-0040-TA
- Tchioffo, M. T., Boissière, A., Abate, L., Nsango, S. E., Bayibéki, A. N., Awono-Ambéné, P. H., et al. (2016). Dynamics of bacterial community composition in the malaria mosquito's epithelia. *Front. Microbiol.* 6:1500. doi: 10.3389/fmicb.2015.01500
- Thongsripong, P., Chandler, J. A., Green, A. B., Kittayapong, P., Wilcox, B. A., Kapan, D. D., et al. (2018). Mosquito vector-associated microbiota: metabarcoding bacteria and eukaryotic symbionts across habitat types in Thailand endemic for dengue and other arthropod-borne diseases. *Ecol. Evol.* 8, 1352–1368. doi: 10.1002/ece3.3676
- Trager, W. (1935a). On the nutritional requirements of mosquito larvae (*Aedes aegypti*). *Am. J. Hyg.* 22, 475–493.
- Trager, W. (1935b). The culture of mosquito larvae free from living microorganisms. *Am. J. Epidemiol.* 22, 18–25.
- Trager, W. (1937). A growth factor required by mosquito larvae. *J. Exp. Biol.* 14, 240–251. doi: 10.1242/jeb.14.2.240
- Turley, A. P., Moreira, L. A., O'Neill, S. L., and McGraw, E. A. (2009). *Wolbachia* infection reduces blood-feeding success in the dengue fever mosquito, *Aedes aegypti*. *PLoS Negl. Trop. Dis.* 3:e516. doi: 10.1371/journal.pntd.0000516
- Turnbaugh, P. J., Ley, R. E., Mahowald, M. A., Magrini, V., Mardis, E. R., and Gordon, J. I. (2006). An obesity-associated gut microbiome with increased capacity for energy harvest. *Nature* 444, 1027–1031. doi: 10.1038/nature05414
- Valzania, L., Coon, K. L., Vogel, K. J., Brown, M. R., and Strand, M. R. (2018a). Hypoxia-induced transcription factor signaling is essential for larval growth of the mosquito *Aedes aegypti*. *Proc. Natl. Acad. Sci. U. S. A.* 115, 457–465. doi: 10.1073/pnas.1719063115
- Valzania, L., Martinson, V. G., Harrison, R. E., Boyd, B. M., Coon, K. L., Brown, M. R., et al. (2018b). Both living bacteria and eukaryotes in the mosquito gut promote growth of larvae. *PLoS Negl. Trop. Dis.* 12:e0006638. doi: 10.1371/journal.pntd.0006638
- Vöing, K., Harrison, A., and Soby, S. D. (2020). Draft genome sequence of *Chromobacterium vaccinii*, a potential biocontrol agent against mosquito (*Aedes aegypti*) larvae. *Genome Announc.* 2:e00477-15. doi: 10.1128/genomeA.00477-15
- Voronin, D., Tran-Van, V., Potier, P., and Mavingui, P. (2010). Transinfection and growth discrepancy of *Drosophila Wolbachia* strain wMel in cell lines of the mosquito *Aedes albopictus*. *J. Appl. Microbiol.* 108, 2133–2141. doi: 10.1111/j.1365-2672.2009.04621.x
- Vrieze, A., Van Nood, E., Holleman, F., Salojärvi, J., Koote, R. S., Bartelsman, J. F. W. M., et al. (2012). Transfer of intestinal microbiota from lean donors increases insulin sensitivity in individuals with metabolic syndrome. *Gastroenterology* 143, 913.e7–916.e7. doi: 10.1053/j.gastro.2012.06.031
- Wang, S., Dos-Santos, A. L. A., Huang, W., Liu, K. C., Oshaghi, M. A., Wei, G., et al. (2017). Driving mosquito refractoriness to *Plasmodium falciparum* with engineered symbiotic bacteria. *Science* 357, 1399–1402. doi: 10.1126/science.aan5478
- Wang, Y., Eum, J. H., Harrison, R. E., Valzania, L., Yang, X., Johnson, J. A., et al. (2021a). Riboflavin instability is a key factor underlying the requirement of a gut microbiota for mosquito development. *PNAS* 118:e2101080118. doi: 10.1073/pnas.2101080118
- Wang, X., Liu, T., Wu, Y., Zhong, D., Zhou, G., Su, X., et al. (2018). Bacterial microbiota assemblage in *Aedes albopictus* mosquitoes and its impacts on larval development. *Mol. Ecol.* 27, 2972–2985. doi: 10.1111/mec.14732
- Wang, Y., Shen, R., Xing, D., Zhao, C., Gao, H., Wu, J., et al. (2021b). Metagenome sequencing reveals the midgut microbiota makeup of *Culex pipiens quinquefasciatus* and its possible relationship with insecticide resistance. *Front. Microbiol.* 12:625539. doi: 10.3389/fmicb.2021.625539
- Wollman, E. (1911). Sur l'élevage des mouches stériles. Contribution à la connaissance du rôle des microbes dans les voies digestives. *Ann. Inst. Pasteur* 25, 79–88.
- Wu, P., Sun, P., Nie, K., Zhu, Y., Shi, M., Xiao, C., et al. (2019). A gut commensal bacterium promotes mosquito permissiveness to arboviruses. *Cell Host Microbe* 25, 101.e5–112.e5. doi: 10.1016/j.chom.2018.11.004
- Xi, Z., Ramirez, J. L., and Dimopoulos, G. (2008). The *Aedes aegypti* toll pathway controls dengue virus infection. *PLoS Pathog.* 4:e1000098. doi: 10.1371/journal.ppat.1000098
- Xiao, X., Yang, L., Pang, X., Zhang, R., Zhu, Y., Wang, P., et al. (2017). A Mesh–Duox pathway regulates homeostasis in the insect gut. *Nat. Microbiol.* 2, 17020–17012. doi: 10.1038/nmicrobiol.2017.20
- Yang, J. H., Bhargava, P., McCloskey, D., Mao, N., Palsson, B. O., and Collins, J. J. (2017). Antibiotic-induced changes to the host metabolic environment inhibit drug efficacy and alter immune function. *Cell Host Microbe* 22, 757.e3–765.e3. doi: 10.1016/j.chom.2017.10.020

**Conflict of Interest:** The authors declare that the research was conducted in the absence of any commercial or financial relationships that could be construed as a potential conflict of interest.

Copyright © 2021 Steven, Hyde, LaReau and Brackney. This is an open-access article distributed under the terms of the Creative Commons Attribution License (CC BY). The use, distribution or reproduction in other forums is permitted, provided the original author(s) and the copyright owner(s) are credited and that the original publication in this journal is cited, in accordance with accepted academic practice. No use, distribution or reproduction is permitted which does not comply with these terms.



# Pathogen Challenge and Dietary Shift Alter Microbiota Composition and Activity in a Mucin-Associated *in vitro* Model of the Piglet Colon (MPigut-IVM) Simulating Weaning Transition

Raphaële Gresse<sup>1,2</sup>, Frédérique Chaucheyras-Durand<sup>1,2</sup>, Juan J. Garrido<sup>3</sup>, Sylvain Denis<sup>1</sup>, Angeles Jiménez-Marín<sup>3</sup>, Martin Beaumont<sup>4</sup>, Tom Van de Wiele<sup>5</sup>, Evelyne Forano<sup>1</sup> and Stéphanie Blanquet-Diot<sup>1\*</sup>

<sup>1</sup> INRAE, UMR 454 MEDIS, Université Clermont Auvergne, Clermont-Ferrand, France, <sup>2</sup> Lallemand SAS, Blagnac, France, <sup>3</sup> Grupo de Genómica y Mejora Animal, Departamento de Genética, Facultad de Veterinaria, Universidad de Córdoba, Córdoba, Spain, <sup>4</sup> GenPhySE, INRAE, ENVT, Université de Toulouse, Castanet-Tolosan, France, <sup>5</sup> Center for Microbial Ecology and Technology, Ghent University, Ghent, Belgium

## OPEN ACCESS

### Edited by:

Wakako Ikeda-Ohtsubo,  
Tohoku University, Japan

### Reviewed by:

Katie Lynn Summers,  
United States Department  
of Agriculture (USDA), United States  
Åsa Sjöling,  
Karolinska Institutet (KI), Sweden

### \*Correspondence:

Stéphanie Blanquet-Diot  
Stephanie.blanquet@uca.fr

### Specialty section:

This article was submitted to  
Microbial Symbioses,  
a section of the journal  
Frontiers in Microbiology

Received: 30 April 2021

Accepted: 24 June 2021

Published: 19 July 2021

### Citation:

Gresse R, Chaucheyras-Durand F, Garrido JJ, Denis S, Jiménez-Marín A, Beaumont M, Van de Wiele T, Forano E and Blanquet-Diot S (2021) Pathogen Challenge and Dietary Shift Alter Microbiota Composition and Activity in a Mucin-Associated *in vitro* Model of the Piglet Colon (MPigut-IVM) Simulating Weaning Transition. *Front. Microbiol.* 12:703421. doi: 10.3389/fmicb.2021.703421

Enterotoxigenic *Escherichia coli* (ETEC) is the principal pathogen responsible for post-weaning diarrhea in newly weaned piglets. Expansion of ETEC at weaning is thought to be the consequence of various stress factors such as transient anorexia, dietary change or increase in intestinal inflammation and permeability, but the exact mechanisms remain to be elucidated. As the use of animal experiments raise more and more ethical concerns, we used a recently developed *in vitro* model of piglet colonic microbiome and mucobiome, the MPigut-IVM, to evaluate the effects of a simulated weaning transition and pathogen challenge at weaning. Our data suggested that the tested factors impacted the composition and functionality of the MPigut-IVM microbiota. The simulation of weaning transition led to an increase in relative abundance of the *Prevotellaceae* family which was further promoted by the presence of the ETEC strain. In contrast, several beneficial families such as *Bacteroidiaceae* or *Ruminococcaceae* and gut health related short chain fatty acids like butyrate or acetate were reduced upon simulated weaning. Moreover, the incubation of MPigut-IVM filtrated effluents with porcine intestinal cell cultures showed that ETEC challenge in the *in vitro* model led to an increased expression of pro-inflammatory genes by the porcine cells. This study provides insights about the etiology of a dysbiotic microbiota in post-weaning piglets.

**Keywords:** *in vitro* model of colonic microbiota, piglet, weaning, ETEC, intestinal cells, gene expression

## INTRODUCTION

In early life, the gut microbiota is shaped by its host and by external factors, including diet (Frese et al., 2015). At weaning, piglets are exposed to social, environmental and dietary stresses engendering disruptions of the balance between intestinal microbial communities, also called dysbiosis (Gresse et al., 2017). Gut dysbiosis in post-weaning piglets is associated with a higher

risk of developing infectious post-weaning diarrhea (Gresse et al., 2017), raising a major economic burden in swine industry because of the reduced growth performance and high mortality of infected animals (Amezcu et al., 2002; Fairbrother et al., 2005; Luppi et al., 2016). Additionally, the massive use of antibiotics as preventive and curative treatment increases public health concerns due to the expansion of bacteria resistance against antibiotics (Gresse et al., 2017). The major pathogenic agent responsible for post-weaning diarrhea is Enterotoxigenic *Escherichia coli* (ETEC) (Amezcu et al., 2002; Fairbrother et al., 2005; Dubreuil et al., 2016; Luppi et al., 2016; Rhouma et al., 2017). This pathotype is characterized by both the presence of fimbrial adhesins inducing cell attachment to porcine intestinal epithelial cells and secretion of enterotoxins which impact intestinal homeostasis (Dubreuil et al., 2016; Luppi et al., 2016). The most prevalent ETEC strains found in 45.1% of diarrheic post-weaning piglets harbor the fimbriae F4 (also designated K88) and secrete heat-labile toxin (LT) and heat-stable toxins (St a or b) (Fairbrother et al., 2005; Dubreuil et al., 2016; Luppi et al., 2016). If contributing factors to the progression and severity of ETEC infections such as housing conditions, early weaning, feed management, and genetic predispositions were previously identified (Madec et al., 1998; Main et al., 2004; Laine et al., 2008; Rhouma et al., 2016), the exact etiology of post-weaning diarrhea and ETEC infections remains far from understood. One hypothesis incriminates the reduced feed intake encountered by piglets at weaning which contributes to intestinal inflammation and morphology disruptions and strongly correlates with the risk of developing enteric diseases (McCracken et al., 1999; Le Dividich and Sève, 2000; Main et al., 2004; Rhouma et al., 2017). In particular, the disturbance of the mucosa intestinal environment and its associated microbiota could promote the expansion of opportunistic pathogens such as *Enterobacteriaceae* and increase the susceptibility toward bacteria and their toxins (Gresse et al., 2017). At the end of the weaning-induced feed deprivation period, the ingestion of plant-based derived solid feed further remodels the composition of the gut microbiota that was adapted to maternal milk during the suckling period (Frese et al., 2015). Understanding the origin of post-weaning diarrhea is challenging since the mechanisms involved are very complex and probably caused by nutrition and both host and microbe-derived factors. *In vitro* models of the piglet intestine including gut microbiota are adequate tools to remove host influence and thus exclusively evaluate factors impacting or influenced by commensal microbes. Especially, the use of such *in vitro* techniques offers advantageous conditions when pathogenic strains are involved due to more standardized conditions, good reproducibility and ethical reasons (Payne et al., 2012). Hitherto, the PigutIVM (Piglet Gut *In vitro* Model) and the BABY-SPIME (Baby Simulator of Pig Intestinal Microbial Ecosystem) were the only developed *in vitro* models mimicking the specific physicochemical and microbial conditions encountered in the colon of piglets (Fleury et al., 2017; Dufourny et al., 2019). However, the recently designed MPigut-IVM (Mucin associated Piglet Gut *In vitro* Model) brought the unique feature of reproducing the mucus-associated microbiota of piglet colon using specifically developed mucin beads. In a previous

study using the MPigut-IVM, a 48 h feed deprivation stress remodeled piglet gut microbiota composition and functionality (Gresse et al., 2021).

In this study, we used the MPigut-IVM to evaluate the impact of a dietary change on the gut microbiota of 4-week-old piglets after a 48 h feed deprivation period. The MPigut-IVM was then exposed to an ETEC strain isolated from diarrheic piglets to study the interactions between the pathogen and gut microbiota. Finally, to unravel the consequences of microbiota perturbation on the host epithelium metabolism, filtrated effluents of control and ETEC-inoculated MPigut-IVM bioreactors were incubated with a porcine cell line.

## MATERIALS AND METHODS

### Fecal Sample Collection and Treatments

All animals were housed in a conventional pig farm located in the Haute-Loire area of the Auvergne-Rhône-Alpes region in France. Piglets remained with their mother and siblings during the suckling period. In addition to sow milk, piglets received water and pre-weaning diet *ad libitum*. None of the piglets had signs of enteric or metabolic disturbances. The animals did not receive any antibiotic in the 27 days prior to the day of fecal collection. As freezing process showed to affect bacterial abundances in pig feces (Metzler-Zebeli et al., 2016), fecal samples from six 4-weeks old healthy male unweaned suckling piglets (Landrace × Large White) were collected directly from the pig while holding using sterile bottles and preserved under anaerobic conditions using GENbag anaer gas pack systems (bioMérieux, Marcy-l'Etoile, France) during transport to laboratory where they were immediately processed upon their arrival.

### MPigut-IVM Parameters

Five hundred milliliters MiniBio bioreactors (Applikon Biotechnology, Delft, Netherlands) equipped with stirrers, ports and probes and inoculated with fecal samples from piglets were prepared as previously described (Gresse et al., 2021). Briefly, 150 mL of fecal suspension prepared in an anaerobic chamber were added in each bioreactor containing 150 mL of nutritive medium (see below), previously reduced by flushing with O<sub>2</sub>-free N<sub>2</sub> gas. Ten minutes after inoculation and during the fermentation course, flushing was stopped and anaerobic conditions were maintained exclusively by the activity of the resident microbiota and by ensuring the airtightness of the system. The temperature of the fermentation was set up to 39°C, pH was maintained to a physiological value of 6.0, and redox potential was constantly measured. The fermentation medium was stirred at a constant speed of 300 rpm. After a 24 h-batch fermentation period, nutritive medium was continuously introduced at a flow rate of 0.17 mL/min except during the feed deprivation period (see below). The fermentation medium volume was maintained at 200 mL using a drainage pump controlled by a level sensor. Indeed, the system ensured a retention time of 18 h to mimic the colonic transit time of 4-week old piglets (Wilson and Leibholz, 1981). Anaerobic conditions and gas composition were checked every day by analyzing N<sub>2</sub>,

O<sub>2</sub>, CO<sub>2</sub>, CH<sub>4</sub>, and H<sub>2</sub> present in the atmospheric phase of the bioreactors using a 490 Micro gas chromatograph (Agilent Technologies, Inc., Santa Clara, CA, United States) equipped with two columns, Molecular Sieve 5A and PoraPlot U, coupled with TCD detectors. Argon was used as gas carrier.

## Composition of MPigut-IVM Nutritive Media

Two nutritive media were used during *in vitro* fermentative procedure (see **Figure 1**). A pre-weaning diet was given during the first 7 days of fermentation (Stabilization period, **Figure 1**). Its formula was elaborated as previously described (Gresse et al., 2021) and considered as a digested pre-weaning diet (**Supplementary Table 1**). Following the 48 h feed deprivation period, which was simulated by stopping the nutrient supply to MPigut-IVM bioreactors, corn meal, potato protein and a higher concentration of soy proteins were included in the diet whereas milk derived proteins and products were reduced to simulate a post-weaning diet as commonly fed to piglets (**Supplementary Table 1**).

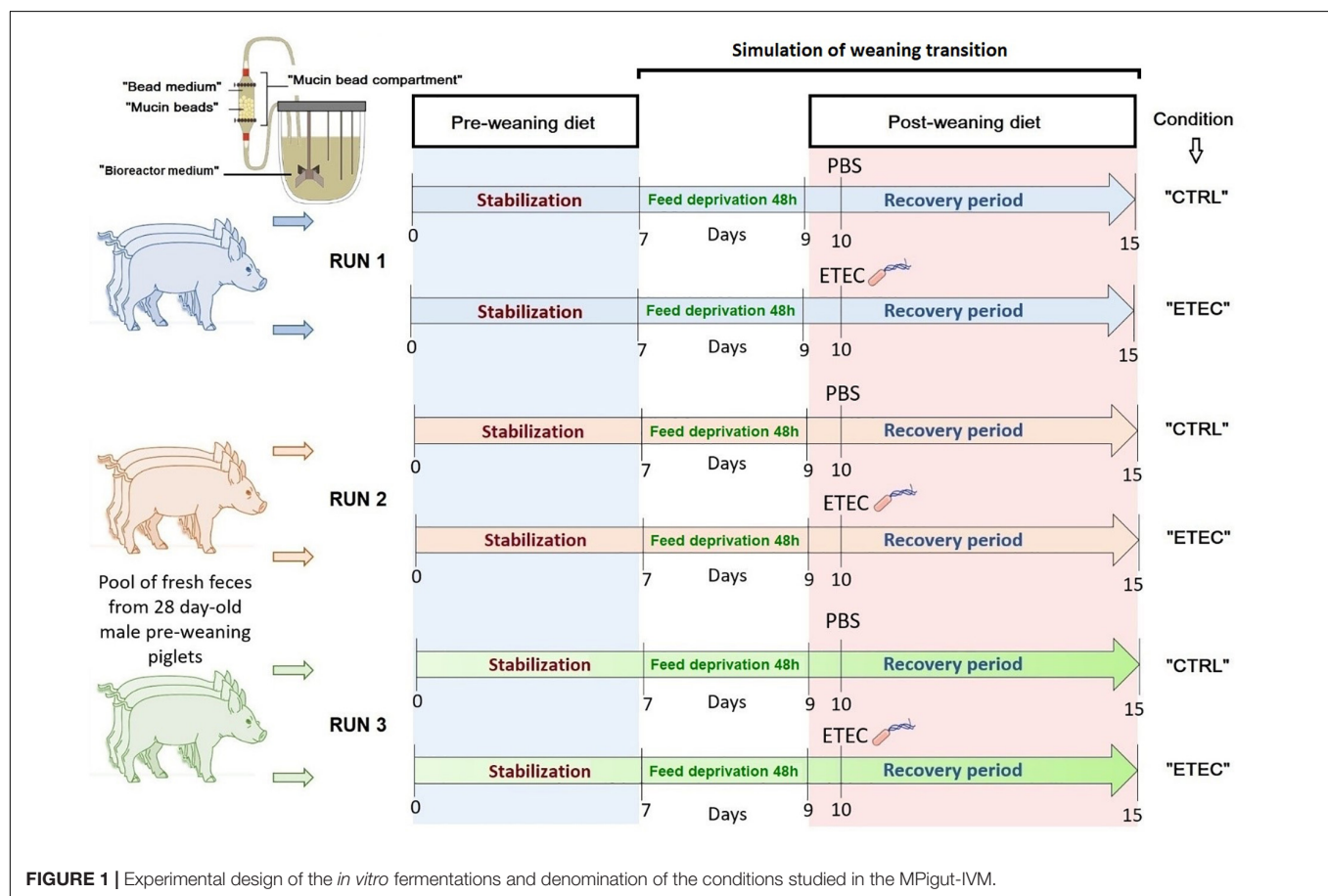
## Mucin Bead Production and Compartment

Mucin beads were prepared as previously described (Gresse et al., 2021). At the beginning of fermentation, 350 ± 20 mucin beads

were introduced into their specific glass compartment. The latter was maintained at 39°C in a water-bath and the fermentative medium continuously flowed through it (re-circulating loop). Mucin beads were completely replaced every 48 h to ensure a continuous availability of mucin adherent surfaces. During the time of bead replacement, the medium of the bead compartment was kept under CO<sub>2</sub> flushing to avoid oxygenation.

## *In vitro* Fermentation Procedures and Sampling

The first 7 days of the fermentation procedures represented the stabilization period and corresponded to the appropriate time to achieve stabilization of microbiota composition, diversity and activity inside the MPigut-IVM (Gresse et al., 2021). At day 7, the flow of nutritive medium was interrupted during 48 h to simulate feed deprivation observed at weaning. At day 9, the flow of nutritive medium restarted with a simulated post-weaning diet. Taken together the feed deprivation stress and the dietary change applied during the recovery period aimed to simulate weaning transition (**Figure 1**). Experiments were designed as presented on **Figure 1**, three independent runs of fermentation were performed with different pools of piglet fecal samples. Samples from the bioreactor medium were collected on day 7 (before the start of the feed deprivation period), day 9 (right at the end of the feed deprivation), and days 10, 10.5, 11, 12,





and 15 (corresponding to the recovery period). Mucin beads and bead medium from the bead compartment were collected on days 7, 9, 11, and 15. Samples from the bioreactor medium and bead medium were centrifuged (4°C, 10,000 g, 45 min). Pellets and supernatants were stored until analysis at −20 and −80°C, respectively. After collection, mucin beads were gently washed three times in sterile 1X PBS and stored at −20°C.

## ETEC Strain, Culture and Challenge Conditions

The ETEC Ec105 strain (F4, Stb+, East1+, LT+) was isolated from a diarrheic piglet (Dr. J. J. Garrido, Department of Animal Genetics, University of Córdoba, Spain). Prior to ETEC challenge in the *in vitro* model, bacteria were grown until OD<sub>600nm</sub> = 0.6 in Luria Bertani (LB) broth (BD Difco, NJ, United States), at 39°C to be consistent with the temperature of the MPigut-IVM (body temperature of piglets). The bacterial culture was then centrifuged (4°C, 10,000 g, 15 min) and the pellet was rinsed using sterile PBS 1X (Phosphate Buffered Saline, Sigma-Aldrich), resuspended in 1 mL of sterile PBS and inoculated to the bioreactor medium of the “ETEC” condition on day 10 (see **Figure 1**) at a final concentration of 10<sup>7</sup> CFU/mL of fermentation medium. The control condition, referred as “CTRL,” received 1 mL of sterile PBS 1X at the same time.

## PMA Treatments for qPCR

Samples from the bioreactor medium and bead medium were collected in duplicate at all time points. They were stained with 50 μM PMAxx (Interchim, Montluçon, France) as described by Roussel et al. (2018) to avoid PCR amplification of DNA from dead cells. The stained samples were incubated for 5 min in the dark at room temperature, under shaking (100 rpm). After incubation, samples were exposed to the blue light PMA-Lite LED Photolysis (Interchim, Montluçon, France) during 15 min to activate the PMAxx dye. Samples were then centrifuged (4,400 g, 4°C, 45 min). Pellets were washed twice with milli-Q water and stored at −20°C until DNA extraction.

## DNA Extraction From MPigut-IVM Samples

Total DNA was extracted from all samples using the Quick-DNA Fecal/Soil Microbe Miniprep Kit (Zymo Research, Irvine, CA, United States) according to the manufacturer's instructions. The quality of the eluted DNA was assessed by agarose gel electrophoresis. Extracts were quantified using the Qubit dsDNA Broad Range Assay Kit (Invitrogen, Carlsbad, CA, United States) with a Qubit 2.0 Fluorometer (Invitrogen, Carlsbad, CA, United States). Samples were stored at −20°C prior to analyses.

## Microbial Quantification by qPCR

The list of primer pairs and their optimal conditions used for quantitative PCR of total bacteria, Methanogenic archaea and *Escherichia/Shigella* group are presented in **Supplementary Table 2** (Huijsdens et al., 2002; Yu et al., 2005; Ohene-Adjei et al., 2008). Standard curves assessment was performed as specified in Gresse et al. (2021). Real-time PCR assays were performed on a

Rotor-Gene Q (Qiagen, Venlo, Netherlands) in 20 μL reactions with QuantiFast SYBR GREEN master mix (Qiagen, Venlo, Netherlands) or TaqMan Fast Advanced Master mix (Applied Biosystems, Foster City, CA, United States) with the addition of each primer at their optimal concentration (**Supplementary Table 2**). The 16S rDNA genes were amplified using the following program: 2 min denaturation at 95°C and 10 min denaturation at 95°C; 40 and 45 cycles of 20 s at 95°C and 60 s elongation and extension at the optimum annealing temperature, and when performing SYBR GREEN based assay, a melting curve step was performed from 60°C to 95°C. Each reaction was run in duplicate. The melting curves of PCR amplicons from SYBR GREEN based assays were checked to ensure primer specificity. The 16S rDNA gene copy number was calculated using the formula: copy number/μl = (C/X)\*0.912.1012 with C: DNA concentration measured (ng/μL) and X: PCR fragment length (bp/copy) and diluted in 10-fold dilution series to be used as qPCR standards. Efficiency of the qPCR for each target varied between 95 and 105% with a slope from −3.0 to −3.4 and a regression coefficient above 0.95, which was in accordance with the MIQE guidelines (Bustin et al., 2009). Ten-fold dilutions series of DNA extracted from the ETEC Ec105 pure culture stained or not with PMA were used to control the reliability of the PMA treatment. A sample from the same bacterial pure culture was subjected to a lethal treatment (95°C, 15 min) and stained or not with PMA and used as a negative control for PMA-qPCR. The survival of the ETEC strain was monitored from day 10, i.e., the time of inoculation, to day 15 in the bioreactor medium, bead medium and on mucin beads *via* the quantification of the labile enterotoxin (LT) gene [**Supplementary Table 3**, references (Ngeleka et al., 2003; Rahman et al., 2006; Madoroba et al., 2009; Nicklasson et al., 2012; Roussel, 2019)]. After log transformation of the data, a mixed-model one-way ANOVA (lmer and ANOVA functions) with time point (days of fermentation) and ETEC treatment as fixed effects and fermentation experiment as a random effect was used to compare the number of 16S gene copy per g of samples between days of fermentation using the R packages lme4 package version 1.1.21 and car package version 3.0-6. The means of each group were compared pairwise with the lsmeans package (version 2.30-0) with the Tukey correction.

## MiSeq 16S rDNA Sequencing and Bioinformatic Analysis

The DNA concentration of all samples was measured using the Qubit dsDNA High Sensitivity Assay Kit (Invitrogen, Carlsbad, CA, United States) with a Qubit 2.0 Fluorometer (Invitrogen, Carlsbad, CA, United States) and diluted to 2 ng/μL prior to PCR amplification. The Bacterial V3–V4 region of 16S rDNA and the Archaeal 16S rDNA were, respectively, amplified with primers 357F 5'-CCTACGGGNGGCWGCAG-3' (Yu et al., 2005) and 805R 5'-GACTACHVGGGTATCTAATCC-3' (Lane et al., 1985) and primers 349F 5'-GYGCASCAGKCGMGAAW-3' and 806R 5'-GGACTACVSGGGTATCTAAT-3' (Ohene-Adjei et al., 2008). Amplicons were generated using a Fluidigm Access Array followed by high-throughput sequencing on an Illumina MiSeq system (Illumina, San Diego, CA, United States)

performed at the Carver Biotechnology Center of the University of Illinois (Urbana, IL, United States). The demultiplexed paired end Illumina sequence reads in the FastQ format were uploaded into the Galaxy instance (v.2.3.0) of the Genotoul bioinformatics platform<sup>1</sup> to be used in the FROGS (Find Rapidly OTU with Galaxy Solution) pipeline (Escudié et al., 2018). During the FROGS pre-process, sequences were depleted of barcode and the sequences with a non-appropriate length or containing ambiguous bases were removed. Next, reads were clustered into *de novo* operational taxonomic units (OTUs) using SWARM algorithm (Mahé et al., 2014) with, at first, a denoising step to build very fine cluster using the minimal distance equal to 1 and, secondly, with an aggregation distance equal to 3. Chimeras were then detected and removed with VSEARCH (Rognes et al., 2016). Additionally, filters were applied to the OTUs in order to remove singletons (Bokulich et al., 2013; Auer et al., 2017). The OTUs selected were taxonomically assigned using the Silva release 132 reference database (Quast et al., 2013).

## Statistical Analysis of Sequencing Data

The Illumina MiSeq run generated a total of 8,107,484 and 1,467,731 high quality sequences, respectively, for the V3–V4 and archaeal sets of primers. Removal of PhiX control reads, removal of chimeras and filtering of singletons lead to a number of  $51,703 \pm 13,520$  sequences for V3–V4 primers and  $5,377 \pm 4,645$  sequences for archaeal primers per sample. To avoid any bias, samples containing less than 500 sequences after abundance filtering were removed from the dataset. Statistical analysis was processed using the RStudio software version 1.0 (with R software version 3.5.1, R Development Core Team)<sup>2</sup>. OTU structure and composition analyses were performed using the phyloseq R package version 1.30.0 (McMurdie and Holmes, 2013). Visualization of data was performed using the ggplot2 R package version 3.2.1. Prior to alpha and beta diversity calculations, rarefaction using the transform count methods was applied to the dataset. The following alpha diversity indices were calculated: number of observed OTU phylogenetic diversity and Shannon index. Statistical differences in Bray Curtis distance between the mucin beads, bead medium and the bioreactor medium and between the pre and post-weaning diet were tested using a multi-analysis of variance (MANOVA) performed with ADONIS using the vegan R package with 9999 permutations and represented by principal coordinate analysis (PCoA) plots. The relative abundances of bacterial groups were log transformed prior to univariate statistical analyses. All univariate statistical analyses were performed using linear mixed-models (lme4 package version 1.1.21) with time point (days of fermentation) and ETEC treatment as fixed effects and fermentation experiment as a random effect. Analysis of variance tables was calculated with the car package (version 3.0.6). The means of each group were compared pairwise with the lsmeans package (version 2.30-0) with the Tukey correction (Supplementary Table 4). Statistical comparisons of samples

from the recovery phase of the fermentation containing or not the ETEC Ec105 strain were also performed using the Wald test of the DESeq2 R package version 1.26.0 at the genus level. In all statistical analyses, only *P*-values below 0.05 were considered as significant.

## RNA Isolation of MPigut-IVM Samples

Total RNAs from bioreactor medium, mucin beads, and bead medium were extracted using Trizol reagent (Invitrogen, Thermo Fisher Scientific, Waltham, MA, United States) as described by Comtet-Marre et al. (2017). DNase treatment with the rDNase Set (Macherey-Nagel, Hérédité, France) was performed to remove any contamination of genomic DNA according to the manufacturer's instructions. The integrity of few samples representative from the whole set was assessed using the Agilent 2100 Bioanalyzer using RNA Nano Chip (Agilent Technologies, Inc., Santa Clara, CA, United States) to ensure sufficient quality for RT-qPCR. Quantity and purity of RNAs were measured using the Nanodrop One (Thermo Fisher Scientific, Waltham, MA, United States) and RNAs were stored at  $-80^{\circ}\text{C}$  until cDNA synthesis.

## RT-qPCR of ETEC Virulence Genes

First, 1  $\mu\text{g}$  of RNA per sample was reverse transcribed into complementary DNA (cDNA) with the SuperScript IV Reverse Transcriptase kit (Invitrogen, Thermo Fisher Scientific, Waltham, MA, United States) in conformity with the manufacturer's instructions. QPCR was performed on the cDNAs as outlined in the section above. Primers and conditions used for qPCR on cDNAs are listed in **Supplementary Table 3**. cDNAs and DNA samples from the ETEC Ec105 pure culture and from the MPigut-IVM challenged with ETEC were used as a positive control. The comparative  $E-\Delta\Delta\text{Ct}$  method was applied to calculate the relative fold changes in the expression of ETEC virulence genes in the samples from the MPigut-IVM. The BestKeeper excel-based tool (Pfaffl et al., 2004) was used to determine the geometric means of the three quantified reference genes, *arcA*, *gapA*, and *rpos* considered for normalization. Primer efficiency was determined using 10-fold dilution series of a set of samples representative from mucin beads, bead medium, and bioreactor medium. The efficiency was calculated from the slope of the standard curves using the following equation  $E = 10^{-1/\text{slope}}$ , where *E* corresponds to high/acceptable amplification efficiency equals to 90–110%.

## Quantification of Short Chain Fatty Acids (SCFAs) by Gas Chromatography

The SCFAs were quantified in the bioreactor medium and bead medium by gas chromatography. Eight hundred microliters of supernatants from bioreactor medium and bead medium were mixed with 500  $\mu\text{L}$  of 0.4% (w:v) crotonic acid and 2% (w:v) metaphosphoric acid solutions. This mixture was centrifuged and the supernatant obtained was injected into a PerkinElmer Clarus 580 gas chromatograph (Waltham, MA,

<sup>1</sup><http://signae-workbench.toulouse.inra.fr>

<sup>2</sup>[www.R-project.org](http://www.R-project.org)

United States) for quantification of SCFAs. A mixed-model one-way ANOVA (lmer and ANOVA functions) with time point and ETEC treatment (days of fermentation) as fixed effects and fermentation experiment as a random effect was used to compare the concentration of the main SCFAs between days of fermentation using the R packages lme4 and car.

## Metabolome Analysis by <sup>1</sup>H Nuclear Magnetic Resonance (NMR)

Supernatants of mucin bead medium collected on days 7 and 11 were used for metabolomic profiling using NMR spectroscopy. After two centrifugation steps (18,000 g, 4°C, 10 min) to remove particles, 50 µL of supernatant were mixed with 600 µL of buffer composed of sodium phosphate 0.2 M, pH 7.4, trimethylsilylpropanoic acid 1 mmol/L, 80% deuterated water, and 20% water. Spectra acquisition, processing, and metabolite identifications were performed as described previously in the MetaboHUB MetaToul-AXIOM metabolomics platform (Beaumont et al., 2020). The list of metabolites identified in the bead medium is presented in **Supplementary Table 5**.

Statistical analysis for NMR metabolomics was performed using the R software (version 3.5.1). Partial-least square discriminant analysis (PLS-DA) was performed with mixOmics package (Rohart et al., 2017). Metabolite relative concentration was used as variable matrix (X). Groups (Day 7, Day 11 CTRL, Day 11 ETEC) were used as predictors (Y) and time-repeated measurement were considered by using a multilevel approach. Univariate statistical analysis was also performed on each metabolite relative concentration with the R packages lme4 and car. A mixed-model one-way ANOVA (lmer and ANOVA functions) with group (Day 7, Day 11 CTRL, Day 11 ETEC) as a fixed effect and fermentation experiment as a random effect was used. A *post hoc* test was used to compare the mean relative concentrations with Tukey correction. *P*-values were corrected for multiple testing (false discovery rate).

## Incubation of MPigut-IVM Effluents on the IPI Porcine Cell Line

### IPI-2I Cell Culture

The IPI-2I cell line is derived from the ileum of an adult male pig and was immortalized by transfection with an SV40 plasmid (pSV3-neo) (Kaeffer et al., 1993). IPI-2I cells were maintained in Dulbecco's Modified Eagle Medium (DMEM)/Ham's F-12 (1:1) medium (Invitrogen Life Technologies, Carlsbad, CA, United States) supplemented with 10% Fetal Calf Serum (FCS, PAA Laboratories GmbH, Austria) and 4 mM L-glutamine (Sigma, St. Louis, MO, United States). Cells were seeded onto 48-well tissue culture plates at 25,000 cell/well in a volume of 200 µL and grown 24 h in an atmosphere of 5% CO<sub>2</sub> at 37°C to allow for confluency for the day of experiment.

### Exposure of IPI-2I Cells to MPigut-IVM Effluents

Supernatants from bioreactor and bead medium at days 7, 9, 11, 13, and 15 were filtered using 0.2 µm sterile Minisart syringe filters (Sartorius, Göttingen, Germany) and 30 times diluted with DMEM (10% Fetal Calf Serum and 4 mM L-glutamine).

A thirty-fold dilution of each sample was established as the best compromise following preliminary tests estimating the survival of IPI-2I cells exposed to dilution series of MPigut-IVM supernatants. After 2 h of incubation with the 30 fold diluted supernatants, the viability of cells was comprised between 70 and 100% with a mean of 86.5% (*n* = 8, data not shown). The diluted samples were added in duplicate to confluent monolayers of IPI-2I cells in 48-well plates, as described above. Plates were incubated for 2 h at 37°C, 5% CO<sub>2</sub>. Then, the supernatants were removed and IPI-2I cells were lysed by addition of 500 µL of NucleoZOL (Macherey-Nagel, Hœrdt, France). Cell lysates were stored at −80°C prior to RNA isolation.

### RNA Isolation From IPI-2I Lysates

Total cellular RNA was extracted from IPI-2I lysed cells following the guidelines provided by the NucleoZOL user manual (Macherey-Nagel, Hœrdt, France). The TURBO DNA-free™ kit (Applied Biosystems, Foster City, CA, United States) was used according to the manufacturer's instructions to prevent DNA contamination. Purity and quality of the RNA extracts were controlled on 1% agarose gels. RNAs were then quantified using a Nanodrop 1000 spectrophotometer (Thermo Fisher Scientific, Waltham, MA, United States) using an optical density of 260 nm.

### RT-qPCR on IPI-2I RNA Extracts

Reverse transcription was performed using the qScript cDNA Synthesis Kit (Quantabio, Beverly, MA, United States). Briefly, 350 ng of RNA per sample were added to 5 µL of sScript Reaction Mix (5x) and 1 µL of qScript Reverse Transcriptase in a final volume of 15 µL. The reverse transcription mix was successively incubated 5 min at 22°C, 30 min at 42°C, and 5 min at 85°C. The synthesized cDNAs were stored at −20°C until used. The targeted genes are listed in **Supplementary Table 5** (Mariani et al., 2009). Quantifications were carried out in triplicate for each cDNA using a QuantStudio™ 12K Flex Real-Time PCR system (Applied Biosystems, Foster City, CA, United States). The cyclophilin A and β-actin genes were used as reference genes. PCR reactions were carried out in 96 well plates using 3 µL of 5x HOT FIREPol® EvaGreen® qPCR Mix Plus (ROX) (Solis BioDyne, Tartu, Estonia), 0.4 µL of forward and reverse primer, 9.2 µL of milli-Q water, and 2 µL of cDNA. Tenfold dilution series of each primer pair were used as standard curves to determine primer efficiencies. Real time PCR efficiencies were calculated according to the equation:  $E = 10 (-1/\text{slope})$ . The appropriate reference gene and the Log2 fold change of each gene, compared with the IPI-2I cells which had not been exposed to bead medium supernatants, were determined by GenEx software<sup>3</sup>. A mixed-model one-way ANOVA (lmer and ANOVA functions) with time point (days of fermentation) and ETEC treatment as fixed effects and fermentation number as a random effect was used to compare the significance between gene expression profile of the IPI-2I cells which were exposed to bead medium supernatants containing or not the ETEC Ec105 strain using the R packages lme4 and car. In all statistical analyses, only *P*-values below 0.05 were considered as significant.

<sup>3</sup><http://genex.gene-quantification.info/>



## RESULTS

Analyses of the microbial profile and SCFA proportions of the three pooled fecal inocula for the runs #1, 2, and 3 are available in **Supplementary Figure 1**. Redox potential was followed throughout the whole fermentation runs and was representative of a feed deprivation stress by displaying an important increase during this period such as detailed in Gresse et al. (2021) (data not shown). Gas composition was also monitored every day during the fermentation runs. At the end of the stabilization period [Day 7, the mean relative proportions of H<sub>2</sub>, O<sub>2</sub>, CO<sub>2</sub>, N<sub>2</sub>, and CH<sub>4</sub> for the six bioreactors were, respectively,  $2.1 \pm 1.2$ ,  $0.3 \pm 0.1$ ,  $73.7 \pm 0.4$ ,  $5.9 \pm 0.8$ , and  $6.8 \pm 1.1\%$  (data not shown)].

### Simulation of Weaning Transition Affects the Metabolic Activity of the MPigut-IVM Microbiota

In the bioreactor medium of the CTRL group, propionate and caproate proportions increased while acetate, isovalerate and butyrate proportions decreased from day 10 to 15 compared to day 7 (**Figure 2A**). In the mucin bead medium of the CTRL group, the proportions of propionate, isovalerate and valerate increased while the proportions of acetate and butyrate decreased from day 11 to 15 compared to day 7 (**Figure 2A**). The total concentration of SCFA significantly ( $P < 0.05$ ) increased between day 9.5 and 15 both in the bioreactor medium and the bead medium (**Figure 2B**).

Nuclear magnetic resonance-based metabolomics revealed a strong modification of the mucin bead medium metabolome between day 7 and day 11 in the CTRL group (**Figure 3**). The relative concentration of isovalerate and 3-phenylpropionate increased significantly after the simulation of weaning transition (day 11 CTRL).

### Simulation of Weaning Transition Impacts MPigut-IVM Microbiota Composition

Q-PCR quantifications of targeted bacterial groups showed that total bacteria concentrations were not affected by the 48 h feed deprivation stress nor the diet change (**Figure 4A**). The abundance of *Escherichia/Shigella* group increased significantly ( $P < 0.05$ ) at day 9 and 15 in the bioreactor medium, when compared to day 7. In the mucin beads, the concentration of *Escherichia/Shigella* increased significantly ( $P < 0.05$ ) at day 15 compared to day 9 and 11 for both (**Figure 4B**). PMA-qPCR confirmed that bacteria from *Escherichia/Shigella* genus were viable across time for all the fermentation runs in both the bioreactor and bead medium of the MPigut-IVM (data not shown).

16S DNA sequencing analysis showed a certain variability of microbiota composition between runs #1, 2, and 3. However, several populations responded in a similar manner and were significantly impacted by the simulated weaning transition. In more details, on the mucin beads, the Spirochaetes phylum significantly decreased from a relative abundance of  $6.8 \pm 5.7\%$  at day 7 to  $0.3 \pm 0.3\%$  of mean relative abundance from day

10 to 15 (**Supplementary Figure 2**). In the bioreactor, the *Proteobacteria* significantly increased from a relative abundance of  $4.0 \pm 2.5\%$  at day 7 to  $17.1 \pm 4.1\%$  at day 9 and to  $7.9 \pm 5.6\%$  from day 10 to 15 (**Supplementary Figure 2**). Looking at lower taxonomy level, some families were also significantly impacted by the simulation of weaning transition (**Figure 5**). In the bioreactor medium, *Coriobacteriaceae* significantly decreased from a mean relative abundance of  $11.9 \pm 6.6\%$  at day 7 to a mean relative abundance of  $2.2 \pm 2\%$  from day 9 to day 15. In contrast, the *Enterobacteriaceae* and *Erysipelotrichaceae* families significantly increased from a mean relative abundance of, respectively,  $0.9 \pm 0.7\%$  and  $1.5 \pm 2\%$  at day 7 to mean relative abundances of  $6.2 \pm 5.4\%$  and  $4.7 \pm 4.1\%$  from day 9 to day 15 (**Figure 5A**). Finally, the *Prevotellaceae* significantly decreased from  $6.5 \pm 6.3\%$  at day 7 to  $4 \pm 2.7\%$  at day 9 prior to significantly increase from day 10 to day 15 with a mean relative abundance of  $27.1 \pm 20\%$ . On the mucin beads, the average relative abundances of *Bacteroidiaceae* and *Coriobacteriaceae* for the day 11–day 15 period ( $10.3 \pm 8.8\%$  and  $1.3 \pm 0.9\%$ , respectively) significantly decreased as compared to those calculated for the day 7–day 9 period ( $24.9 \pm 9\%$  and  $5 \pm 2.7\%$ , respectively) (**Figure 5B**). In contrast, the average relative abundances of *Prevotellaceae* and *Atopobiaceae* were significantly higher for the day 11–day 15 period ( $9.7 \pm 7\%$  and  $6.8 \pm 4\%$ , respectively) than those calculated for the day 7–day 9 period ( $3.1 \pm 2.4\%$  and  $2.4 \pm 1.5\%$ , respectively) (**Figure 5B**). The simulation of weaning transition also led to modifications in relative proportions of several genera, both in bioreactor medium and mucin beads (**Figure 6**). Statistical results of this section are detailed in **Supplementary Table 6**.

In the bioreactor medium and the mucin beads of control fermentations, the *Methanospaera* genus was found in significantly higher mean relative abundance during the recovery period compared to the end of the stabilization period (**Figure 7A**), and feed deprivation stress also affected *Methanobrevibacter* relative abundance which was significantly lower after stress but only on mucin beads (**Figure 7B**). Regarding qPCR data, on the mucin beads, the abundance of archaea increased significantly ( $P < 0.05$ ) at day 15 compared to day 9 and 11 for the CTRL conditions (**Figure 4B**).

### Survival of Ec105 in the MPigut-IVM

The presence of the ETEC strain was monitored in all the MPigut-IVM samples by quantifying the LT gene using qPCR. In the bioreactor medium of the ETEC condition, the LT gene was quantified at a mean of  $8.0 \pm 0.2 \log_{10}$  of gene copy/g of sample at day 10 (ETEC inoculation) prior to slowly decrease over time to reach a mean of  $4.9 \pm 1.1 \log_{10}$  of gene copy/g of sample at day 15 (end of recovery period). On the mucin beads of ETEC condition, the LT gene was quantified at mean values of  $4.5 \pm 1.6$  and  $3.3 \pm 2.9 \log_{10}$  of gene copy/g of sample, respectively, at day 11 and 15. However, the LT gene was quantified in higher concentration in the bead medium at mean values of  $7.6 \pm 1.6$  and  $6.4 \pm 2.1 \log_{10}$  of gene copy/g of sample, respectively, at day 11 and 15. It can be noticed that the LT gene was quantified in much lower quantity from day 11 in all samples from run #1 (**Figure 8**). Finally, a low copy number



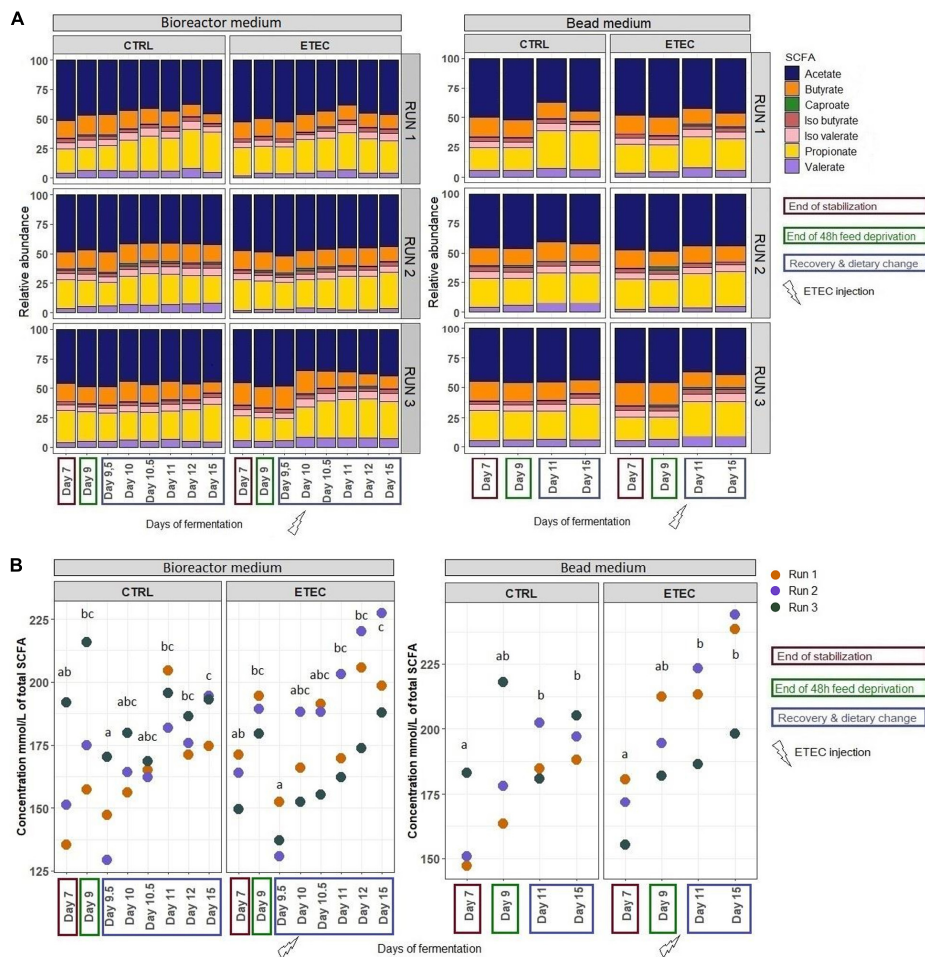


**FIGURE 2 |** Short chain fatty acids (SCFA) relative abundances **(A)** and Evolution of the total concentration of SCFAs **(B)** produced by fermentation activity of the microbiota inhabiting the MPigut-IVM in the CTRL and ETEC conditions for the runs #1, 2, and 3. Groups (days) associated with different letters are significantly different ( $P < 0.05$ ).

of LT gene could also be detected in the CTRL condition at mean values of  $2.9 \pm 1.6$ ,  $3.4 \pm 1.6$ , and  $3.9 \pm 0.2 \log_{10}$  of gene copy/g of sample, respectively, in the bioreactor medium, mucin beads, and bead medium, however, these values are close to the detection limit (**Figure 8**). The activity of the ETEC strain in the MPigut-IVM was evaluated by quantification of virulence gene expression using RT-qPCR. Even though the expression of virulence genes was detected in the bioreactor medium and bead medium in the ETEC condition on the day 10, 11, and 15, none of the targeted virulence genes (EAST1, LT, and K88 genes) was expressed in the CTRL condition (data not shown).

## Effects of the ETEC Ec105 Strain on MPigut-IVM Microbiota Metabolic Activity

Relative abundances of SCFAs were compared between the conditions ETEC and CTRL during the recovery period from day 10 to 15. The proportion of caproate and propionate tended ( $0.05 < P < 0.1$ ) to be higher in the ETEC condition

versus CTRL in the bead medium and bioreactor medium, respectively (**Figure 2A**).

The mucin bead medium metabolome shifted strongly between day 7 and day 11 in the presence of ETEC Ec105 (**Figure 3**). Indeed, the relative concentrations of isovalerate, valerate, 3-phenylpropionate and tyramine increased significantly, while the relative concentration of ethanol decreased. Multivariate PLS-DA analysis also suggested metabolome differences between CTRL and ETEC groups at day 11 (**Figure 3**). However, the relative concentrations of individual metabolites were not significantly different at this time point.

## ETEC Challenge Triggers Microbiota Composition Disruptions in the MPigut-IVM Subjected to a Simulated Weaning Transition

No effect of the presence of the ETEC Ec105 strain on bacterial populations was detected by qPCR (**Figure 4**). However, a

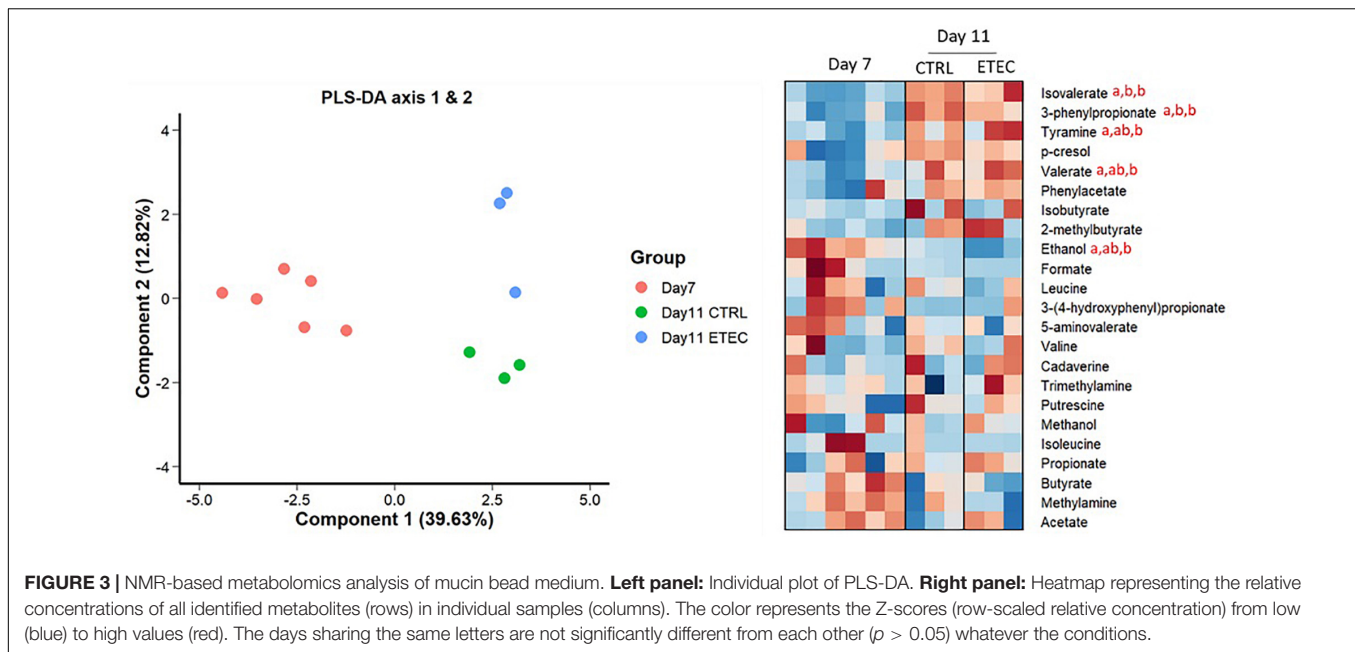


**FIGURE 3 |** NMR-based metabolomics analysis of mucin bead medium. **Left panel:** Individual plot of PLS-DA. **Right panel:** Heatmap representing the relative concentrations of all identified metabolites (rows) in individual samples (columns). The color represents the Z-scores (row-scaled relative concentration) from low (blue) to high values (red). The days sharing the same letters are not significantly different from each other ( $p > 0.05$ ) whatever the conditions.

significant impact of the ETEC challenge on the microbiota was highlighted by the Illumina MiSeq data from day 10 to 15. Indeed, in the bioreactor medium, the presence of Ec105 led to significant higher average relative abundance of the Bacteroidetes phylum ( $35.4 \pm 15.4\%$  for the CTRL condition and  $50.7 \pm 10.5\%$  for the ETEC condition for the day 10 to day 15 period), and lower mean relative abundance of Actinobacteria from  $9.2 \pm 7.4\%$  in the CTRL condition to  $2.7 \pm 2.7\%$  in the ETEC condition during the same period (Supplementary Figure 2A). On the mucin beads, the Firmicutes were significantly increased from  $48.9 \pm 7.7\%$  in the CTRL condition to  $58.1 \pm 6.6\%$  in the ETEC condition from day 11 to 15 (Supplementary Figure 2B). At the family level in the bioreactor medium (Figure 5A), the *Prevotellaceae* average relative abundance was significantly increased ( $23.2 \pm 23\%$  in the CTRL condition,  $30.9 \pm 18.8\%$  in the ETEC condition for the day 10 – day 15 period) (Figure 5A). In contrast, *Acidaminococcaceae*, *Atopobiaceae*, *Veillonellaceae*, and *Erysipelotrichaceae* were significantly reduced with average relative abundances of, respectively,  $24.2 \pm 8.4\%$ ,  $6.3 \pm 7\%$ ,  $4.1 \pm 2.8\%$ , and  $6 \pm 4.8\%$  in the CTRL condition to  $18.2 \pm 7.4\%$ ,  $0.3 \pm 0.4\%$ ,  $2.2 \pm 2.1\%$ , and  $2.7 \pm 2.8\%$  in the ETEC condition during the same recovery period (Figure 5A). On the mucin beads, the *Atopobiaceae* family was significantly decreased from mean relative abundance of  $11.5 \pm 3.2\%$  in the CTRL condition to  $5.8 \pm 2.1\%$  in the ETEC condition while the *Enterococcaceae* was significantly increased from  $0.5 \pm 0.6\%$  in the CTRL condition to  $10.3 \pm 5.7\%$  in the ETEC condition in the day 11 – day 15 period (Figure 5B). At the genus level, the introduction of the ETEC strain significantly affected the abundance of several genera. For example, the genera *Eisenbergiella*, *Peptoniphilus*, *Morganella*, *Tyzzerella*, and *Enterococcus* were particularly enhanced in the ETEC-challenged bioreactors and mucin beads (Figures 6, 9). The MPigut-IVM archaeal microbiota was not significantly impacted by ETEC inoculation (Figure 7).

The MPigut-IVM microbiota alpha diversity indices were not significantly modified by any of the treatment (Supplementary Figure 4). Yet, beta diversity analysis using principal component analysis on Bray-Curtis distance showed that samples of MPigut-IVM clustered by diet (Supplementary Figure 4). No effect of ETEC was detected (data not shown).

## Gene Expression in IPI-2I Cells Is Modulated When Exposed to the Bead Medium of MPigut-IVM Challenged by ETEC

The expression of selected genes involved in innate inflammatory immune response targeting inflammatory cytokines and chemokines, tight junctions or mucus secretion (Supplementary Table 5) of IPI-2I porcine cells incubated with filtrated effluents of the bead medium of MPigut-IVM were quantified using RT-qPCR (Figure 10). The effluents from the ETEC-inoculated bioreactors collected at day 15 led to a significant increase in the expression of *TNF $\alpha$* , *MYD88*, *MUC1*, and *CLDN4* genes compared to effluents from control bioreactors collected at same day. Differences in IPI-2I gene expression caused by effluents from the other days of fermentation (day 11 and 13) remained non-significant.

## DISCUSSION

The MPigut-IVM has been developed to simulate the gut microbiome and mucobiome of weaning piglet (Gresse et al., 2021). In this previous paper, we demonstrated that, due to unique features such as the presence of mucin beads and a self-maintained anaerobiosis, the MPigut-IVM harbored an *in vitro* microbiota very close to that of the proximal colon of piglets

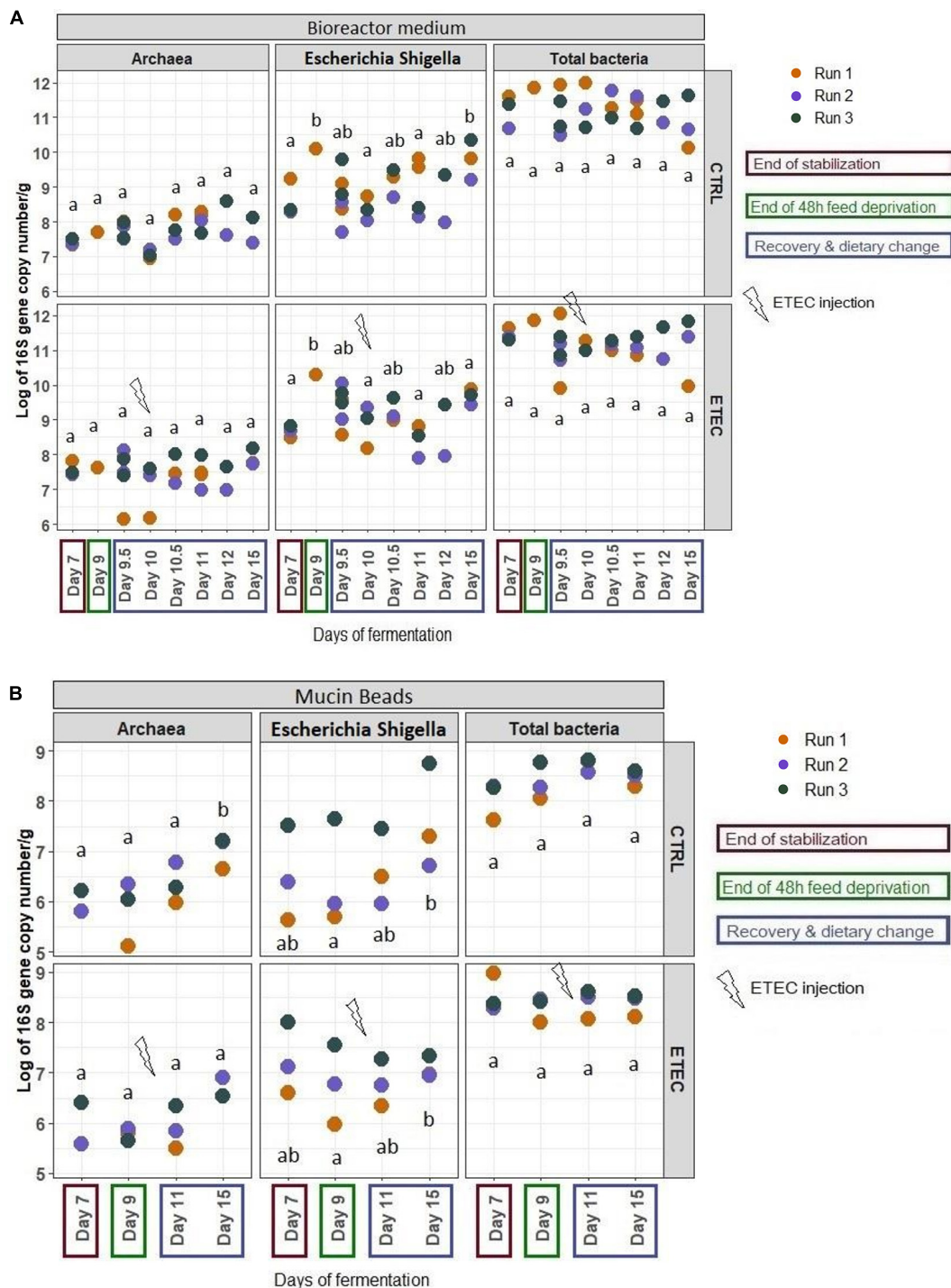


**FIGURE 4 |** Q-PCR quantification of total bacteria, *Escherichia/Shigella* and methanogenic archaea populations in the bioreactor medium **(A)** and the mucin beads **(B)** of the MPigut-IVM for the runs #1, 2, and 3 in the CTRL and ETEC conditions. The days sharing the same letters are not significantly different from each other ( $p > 0.05$ ) whatever the conditions.

originating from the same farm, after a stabilization period of 7 days (Gresse et al., 2021). To further understand the impact of weaning stressors on the colonic microbiota of piglets and their roles in the etiology of post-weaning diarrhea, a diet change

focused on the introduction of more diversified plant protein sources and of higher amounts of these nutrients was introduced into the MPigut-IVM right after the 48 h- feed deprivation period to evaluate the impact of stressful events close to weaning



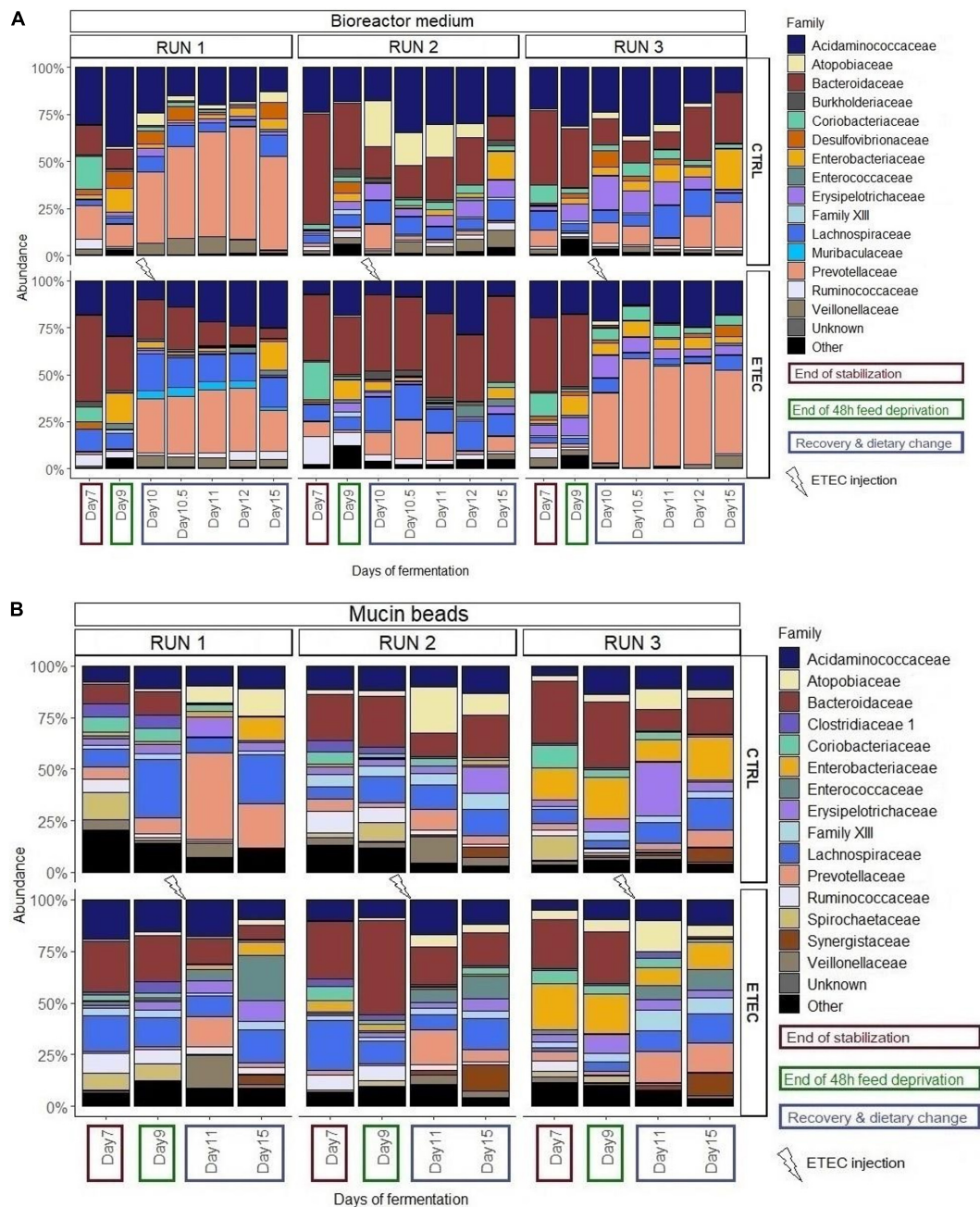


**FIGURE 5 |** Relative abundances of the main bacterial families in the bioreactor medium **(A)** and the mucin beads **(B)** in MPigut-IVM during the runs #1, 2, and 3 which were subjected to a simulated weaning transition and challenged or not with the ETEC Ec105 strain.

as encountered in commercial pig farms. First, in the present work, the simulated weaning transition induced modifications in the archaeal microbiota of the MPigut-IVM, shifting from a *Methanobrevibacter* to a *Methanosphaera* dominant microbiota. Modifications of the archaeal microbiota associated with weaning transitions are not yet well documented in piglets. This shift could, however, impact the metabolites present in the piglet gut, considering the high abundance of archaea populations in piglet lower gut (Gresse et al., 2019). Indeed, *Methanobrevibacter*

and *Methanosphaera* are mainly known as hydrogenotrophic and methylotrophic archaea genera, respectively, although recent genomic studies suggest that they may have other metabolic differences (Poehlein et al., 2018). Second, regarding bacterial microbiota, the simulated weaning transition induced an increase in the relative abundance of several bacterial communities in the MPigut-IVM, including *Prevotellaceae* and *Enterobacteriaceae* family members while the *Bacteroidiaceae* was decreased. Our findings are in agreement with *in vivo* studies reporting a shift



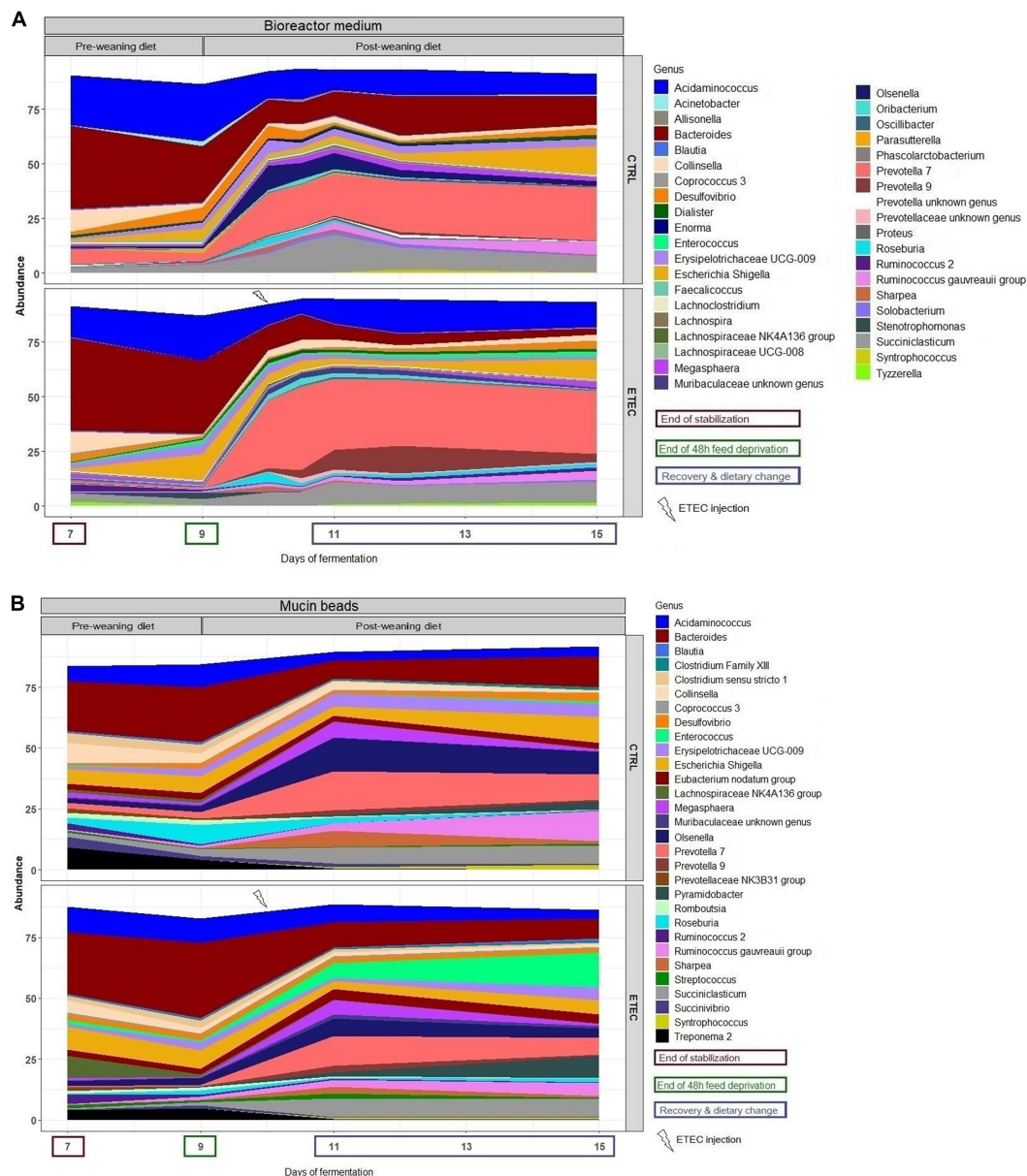


**FIGURE 6 |** Mean relative abundance of the 30 more abundant bacterial genera in the bioreactor medium (A) and mucin beads (B) of MPigut-IVM in the CTRL and ETEC conditions ( $n = 3$ ).

from a high relative abundance of *Bacteroides* in pre-weaning piglet feces toward a high relative abundance of *Prevotella* coupled with a reduced *Bacteroides* proportion in post-weaning piglet fecal samples (Alain B. Pajarillo et al., 2014; Frese et al., 2015; Guevarra et al., 2018; Trckova et al., 2018; Yang et al., 2019) and Adhikari et al. (2019) reported similar results in the piglet colon. *Prevotella* is a common commensal genus which plays important roles in the digestion of nutrients, particularly in the degradation of starch, proteins and other plant polysaccharides (Ivarsson et al., 2014; Sandberg et al., 2019). In the study from Yang et al. (2019), *Prevotella* was the most abundant genus in both healthy and diarrheic weaning piglets. However,

piglets that developed diarrhea after weaning harbored a higher relative abundance of *Prevotella* and less *Escherichia coli* in their pre-weaning period compared to piglets that remained healthy after weaning (Yang et al., 2019). A reduced number of *Bacteroides* in weaned piglet feces was also associated with diarrhea (Yang et al., 2019). Therefore, disturbed ratios between *Prevotella*, *Bacteroides*, and *Escherichia* populations in early life could be associated with the onset of post-weaning diarrhea. Also, the simulated weaning transition in the MPigut-IVM led to a decrease of the *Collinsella* genus from the *Coriobacteriaceae* family. A decreased proportion of *Collinsella* in human gut was previously linked to the development of a dysbiotic microbiota

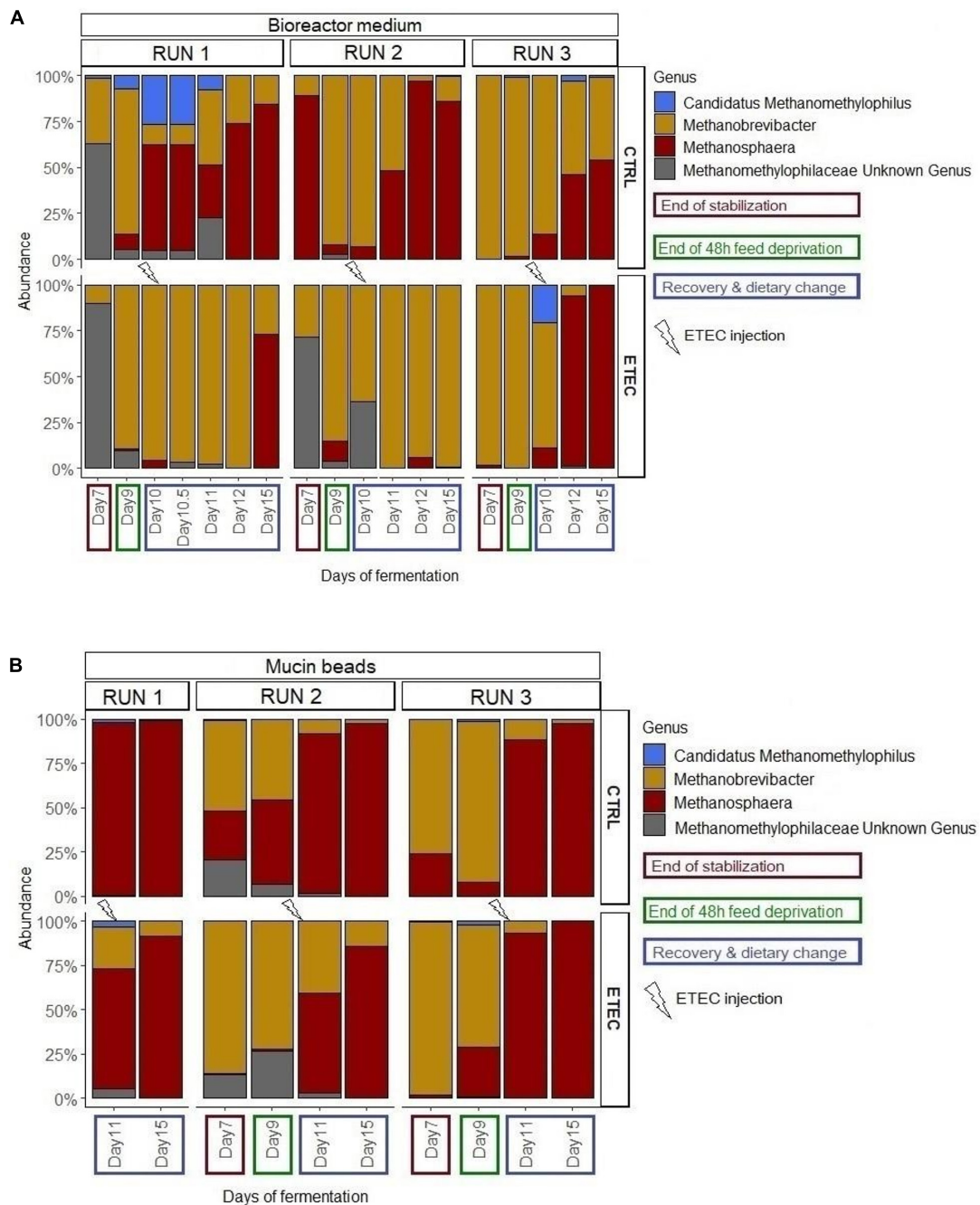


**FIGURE 7 |** Relative abundance of the archaeal genera in the bioreactor medium (A) and mucin beads (B) of the MPigut-IVM for the runs #1, 2, and 3, in the CTRL and ETEC conditions. Day 7 and 9 of run #1 were removed due to their low number of sequences.

in inflammatory bowel disease (Kassinen et al., 2007) while an increase of *Collinsella* was positively correlated with protection against rotavirus diarrhea in gnotobiotic pigs (Twitchell et al., 2016) suggesting of potential role of *Collinsella* in pigs' health. In our study, microbial activity was also significantly modified by the simulated weaning transition probably associated to microbiota composition changes. Redox potential was considerably impacted by the feed deprivation period which is in agreement with

our previous findings (Gresse et al., 2021). In the bioreactor and on the mucin beads, butyrate, acetate and isovalerate relative abundances significantly decreased after the simulated weaning transition. In contrast, propionate, valerate and caproate increased both in the bioreactor and on the mucin beads of the MPigut-IVM. The total SCFA concentration increased during the feed deprivation period. This particular point could be due to the accumulation of these metabolites inside the bioreactors

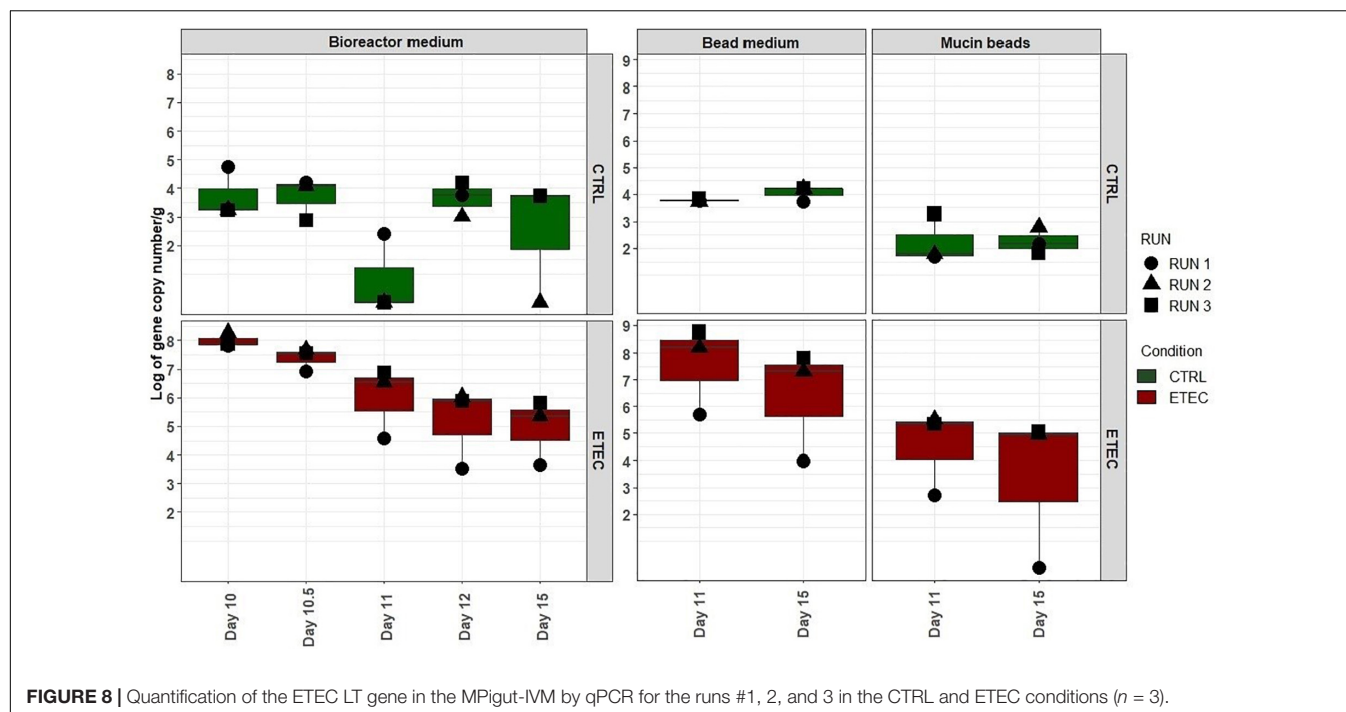


**FIGURE 8** | Quantification of the ETEC LT gene in the MPigut-IVM by qPCR for the runs #1, 2, and 3 in the CTRL and ETEC conditions ( $n = 3$ ).

due the absence of feeding and consequently medium flushing. Besides, the bacterial metabolite 3-phenylpropionate increased after weaning simulation in the mucin bead medium, maybe due to an increased availability of its polyphenol precursors present in the post-weaning diet. Butyrate proved to be very beneficial to piglet health by improving the performance of piglets around weaning due to the stimulation of intestinal epithelium (Lu et al., 2008), improved immune response (Melo et al., 2016), and modulation of intestinal microbiota (Castillo et al., 2006; Xu et al., 2016; López-Colom et al., 2019). Also, supplementation of early weaned piglets with sodium butyrate was shown to attenuate diarrhea symptoms and decrease intestinal permeability (Feng et al., 2018). Thus, fluctuations of both bacterial composition and activity were observed in the MPigut-IVM following the simulated weaning transition which could favor the emergence of opportunistic pathogens such as ETEC.

To further simulate the conditions leading to post-weaning diarrhea at weaning (Gresse et al., 2017), a porcine ETEC strain was inoculated to the MPigut-IVM after the simulated weaning transition. Interestingly, 2 days after the inoculation of ETEC Ec105, the Labile Toxin (LT) gene was detected in high concentration in the bead medium of the MPigut-IVM, showing a preferential localization of ETEC Ec105 close to an area rich in mucins which are indeed known to be a privileged site of adhesion *in vivo* (González-Ortiz et al., 2014). Only one replicate displayed a strong decrease in the pathogenic strain concentration after few days in the MPigut-IVM. This difference could be explained by some variability in the microbial composition of the fecal inocula, probably reflecting the *in vivo* situation. A more robust microbial community could lead to less susceptibility to the introduction of a pathogen. The differences of microbiota composition observed between the three replicates

could also induces different responses toward the ETEC challenge and the simulated weaning transition such as observed *in vivo*. The ETEC challenge did not influence the relative abundance of *Escherichia/Shigella* genus, probably because the concentration of the ETEC strain after inoculation was in the range of that of commensal *Escherichia/Shigella*. In addition, López-Colom et al. (2019) reported previously that an ETEC challenge was not associated with the increase of commensal *E. coli* in the ileum and ileal mucosa of weaned piglets. In this study, piglets which received butyrate and heptanoate preventive treatments to ETEC F4 displayed higher levels of commensal Enterobacteria in the ileum and ileal mucosa few days after the infection (López-Colom et al., 2019). One hypothesis, supported by Leatham et al. (2009), was the phenomenon of colonization resistance described as an increase in coliforms in the gut to fight against colonization of pathogenic strains. In the present work, several families and genera were, however, significantly impacted by the introduction of ETEC after the simulated weaning transition in the MPigut-IVM. The most spectacular change was the increase in *Enterococcus* in the ETEC conditions, especially on the mucin beads. Some *Enterococcus* members are known to bind to mucus *in vivo* (Hendrickx et al., 2015; Tytgat et al., 2016). Consistently with our findings, several *in vivo* studies reported a higher relative abundance or quantity of *Enterococcus* and *E. coli* or ETEC strains in the digestive content or mucosa of neonatal diarrheic piglets (Cheon and Chae, 1996; Jonach et al., 2014; Larsson et al., 2014; Hermann-Bank et al., 2015). A co-occurrence of *Enterococcus* and pathogenic *E. coli* could thus be involved in the pathogenesis of diarrhea episodes in piglets. Considering the several reports of this observation, it has been hypothesized that *Enterococcus* and *E. coli*/ETEC members could be able to naturally cooperate possibly by mechanisms of cross feeding

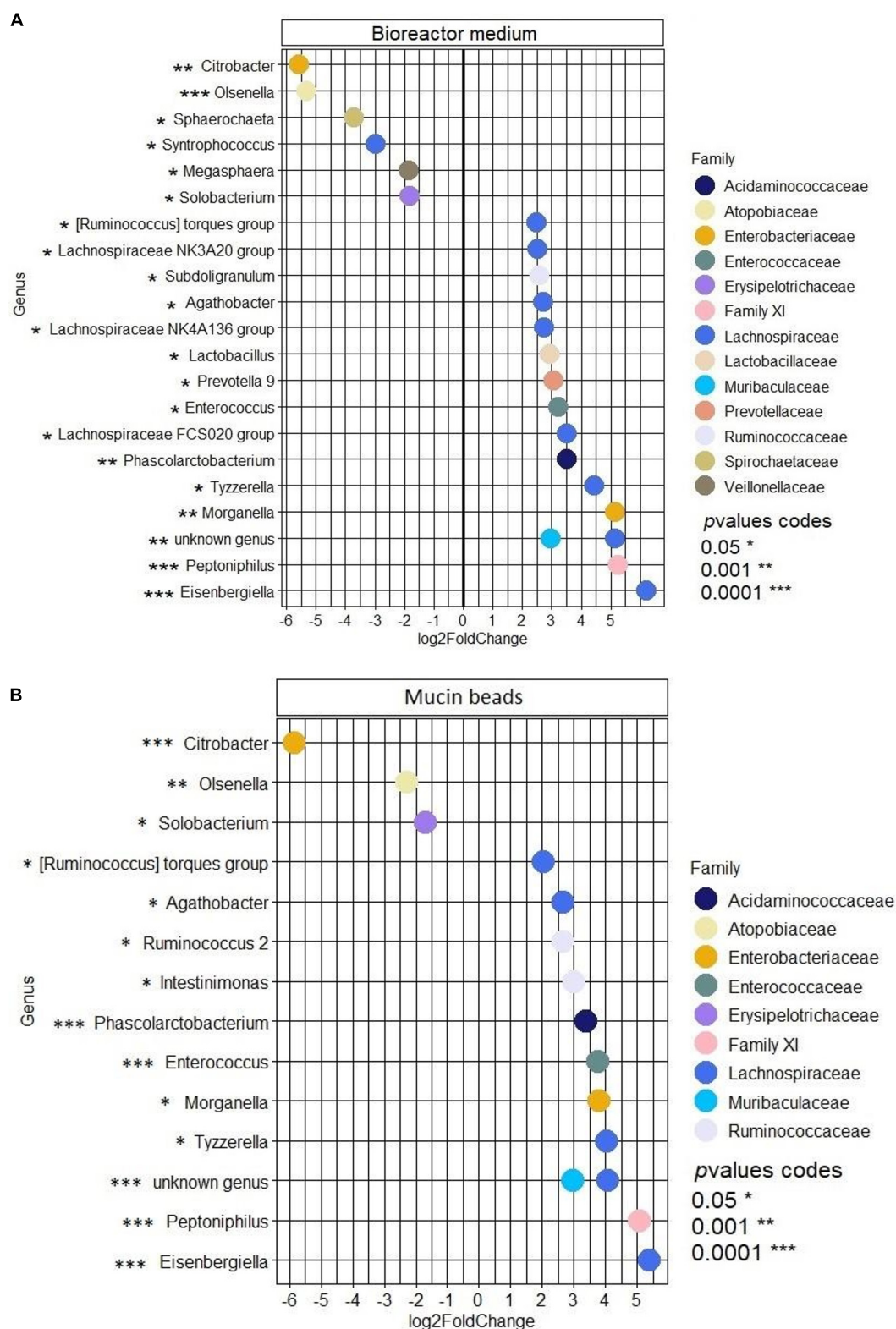


**FIGURE 9 |** Differentially abundant genera between the samples of the recovery period containing the ETEC Ec105 strain or not in the bioreactor medium (**A**) and mucin beads (**B**) of the MPigut-IVM. Only significant Log2 fold changes are represented on the figure. Positive Log2 fold changes indicate genera that were significantly more abundant in the presence of the pathogen. *P* values were corrected for multiple testing.



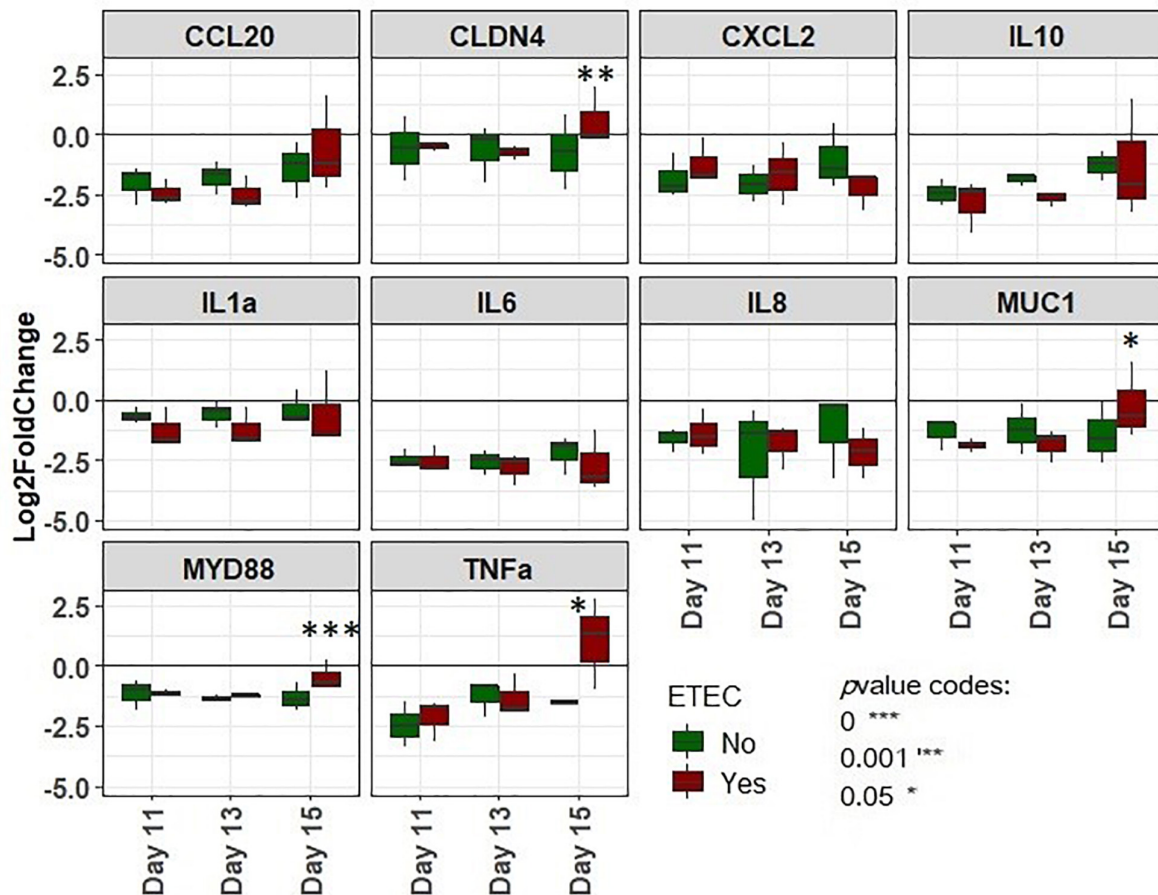


**FIGURE 10 |** Log2 fold changes of gene expression of IPI-2I cells incubated with bead medium supernatants of the MPigut-IVM collected at days 11, 13, and 15 and challenged or not with the ETEC Ec105 strain. Values were normalized with basal gene expression profiles for the targeted genes from IPI-2I cells incubated with their usual glutamine and FCS complemented DMEM medium ( $n = 3$ ).

or mutualism (Germerodt et al., 2016). Finally, the *Morganella* genus, which was found to be four times more abundant in the ETEC condition both in the mucin beads and the bioreactor by the differential analysis, has been previously associated with diarrhea in humans (Müller, 1986; Jertborn and Svennerholm, 1991; Ikeobi et al., 1996) and was even positively correlated with diarrhea indices during an ETEC F4 challenge in mice (Xu et al., 2020). The MPigut-IVM is thus able to reproduce several characteristics of ETEC pathogenesis consistent with *in vivo* data. In consequence, the other populations which correlated with the ETEC conditions but are not currently described in the literature such as *Peptoniphilus* or *Eisenbergiella* should be considered as populations of interest for future investigations.

To increase our understanding of the etiology of post-weaning diarrhea and how microbiota disruptions and pathogen presence affect host cells, we incubated diluted filtrated effluents collected from bead medium from MPigut-IVM with the IPI-2I pig intestinal cell line. *In vitro* models of the human colon were previously successfully coupled with eukaryotic cell cultures (Marzorati et al., 2014; Defois et al., 2018) but, to our knowledge,

this is the first time that this was performed with an *in vitro* model of the piglet colon. In this study, supernatants from the bead medium of the ETEC condition induced significant increases in expression of genes coding for the myeloid differentiation primary response 88 (MyD88), tumor necrosis factor  $\alpha$  (TNF $\alpha$ ), claudin 4 (CLDN4), and mucin 1 (MUC1) in IPI-2I cells. The relation between mucins, commensals and pathogens have been widely studied (Etienne-Mesmin et al., 2019). MUC1 is a high molecular mass glycoprotein expressed at the apical surface of mucosal epithelial cells. MUC1 secretion can be stimulated by lipopolysaccharides produced by Gram negative bacteria and mucin is thought to play an important role against infections of epithelial cells (Kato et al., 2017). Expression of the MUC1 gene notably limited the access of *Helicobacter pylori* in infected mice (McGuckin et al., 2007). In our study, claudin 4 gene was over-expressed in cells exposed to supernatants collected at day 15 of ETEC conditions. This gene belongs to claudins' family which are, with occludin proteins, tight junction proteins located at the apical side of piglet enterocytes (Pasternak et al., 2015) and thus play a role in intestinal permeability and infection. Consistently

with our findings, claudin protein higher gene expression was previously associated with ETEC K88 infection in the porcine cell line IPEC-J2 in several studies (Wu et al., 2016; Luo et al., 2019). We could hypothesize that the higher expression of claudin genes from enterocytes could be induced in order to repair disrupted tight junctions due to the presence of toxins or other virulence factors in the supernatants which, as reported by RT-qPCR, were indeed expressed in the bead medium of the MPigut-IVM. The MyD88-mediated innate immune response has been already proven to be primarily important for protection against microbial pathogen infection via the induction of inflammatory cytokine production (Scanga et al., 2002; Campos et al., 2004; von Bernuth et al., 2012; Issac et al., 2013, 2018). Indeed, MyD88 deficient mice showed to be profoundly susceptible to infection (Issac et al., 2013). In weaning piglets, an increased level of MyD88 was already reported in enterocytes both *in vivo* and *in vitro* by several studies after challenge with an ETEC K88 strain (Chytilová et al., 2014; Finamore et al., 2014; Xu et al., 2014). TNF $\alpha$  is one of the most widely studied proinflammatory cytokine involved in numerous bacterial, parasitic and viral infections and was suggested as a biomarker of digestive pathologies in weaned piglets due to its correlation with villi/crypt ratio damages (Van Reeth et al., 2002; Gustavo Hermes et al., 2013; Barba-Vidal et al., 2017; López-Colom et al., 2019). Indeed, increased concentration of TNF $\alpha$  or increased expression of the associated gene were previously reported in the intestine of piglets orally challenged with ETEC K88 (Pu et al., 2018; López-Colom et al., 2019) as well as in IPEC-J2 cells co-incubated with ETEC K88 (Xia et al., 2017a,b). Considering the matches between our results and literature, the incubation of MPigut-IVM bead medium supernatants with IPI-2I cells seemed to reproduce, at least in part, the effects of ETEC infection on piglet enterocytes. However, it is important to notice that significant differences were detected only with effluent collected at day 15. These findings could highlight that the introduction of a porcine ETEC strain in the MPigut-IVM led to modifications of microbial metabolites which could be secreted in sufficient quantity to induce differential inflammatory responses in porcine epithelial cells at day 15 only. The high concentration of tyramine and valerate or the low concentration of ethanol in the mucin bead medium after weaning simulation in the ETEC group could contribute to the transcriptomic regulation observed in epithelial cells *in vitro*.

To conclude, our studies reported that the reproduction of a weaning transition in the MPigut-IVM impacted the microbiota composition and functionality in a consistent manner compared to previous *in vivo* findings. The introduction of a porcine ETEC strain after the simulated weaning transition was positively correlated with an increase in several genera which should be considered in future investigations. If further research needs to be undertaken to fully understand the interactions, our results confirmed that members of *Prevotella*, *Escherichia*, and *Enterococcus* genera could play a role in the onset of post-weaning diarrhea in piglets. The incubation of the *in vitro* effluents with pig intestinal cell lines, which was performed for the first time, indicated that MPigut-IVM was able to report some effect of microbiota metabolites change on host cells. The MPigut-IVM seems to reproduce the effects of weaning transition and ETEC

colonization on the microbiota and will thus be used to evaluate preventive strategies against post-weaning intestinal dysbiosis.

## DATA AVAILABILITY STATEMENT

The datasets presented in this study can be found in online repositories. The names of the repository/repositories and accession number(s) can be found below: <https://www.ncbi.nlm.nih.gov/>, BioProject ID PRJNA703771.

## ETHICS STATEMENT

Ethical review and approval was not required for the animal study because we collected only fecal material.

## AUTHOR CONTRIBUTIONS

RG, FC-D, EF, and SB-D: conceptualization. RG, SD, FC-D, EF, TV, AJ-M, JGG, and SB-D: methodology. RG, AJ-M, and MB: formal analysis. RG: writing – original draft preparation. RG, FC-D, SD, EF, TV, MB, and SB-D: writing – review and editing. RG and MB: visualization. FC-D, EF, JGG, and SB-D: supervision. All authors read and approved the final manuscript.

## FUNDING

This research was funded by the Lallemand SAS.

## ACKNOWLEDGMENTS

We acknowledge Yacine Lebbaoui, Laurie Guillot, Sandrine Chalancon, and Aurélie Ameilbonne for technical assistance and The Farm “Porc Aubaines” where sampling was performed.

## SUPPLEMENTARY MATERIAL

The Supplementary Material for this article can be found online at: <https://www.frontiersin.org/articles/10.3389/fmicb.2021.703421/full#supplementary-material>

**Supplementary Figure 1** | Analyses of the pooled fecal inocula used for runs #1, 2 and 3: relative abundance of SCFAs measured by gas chromatography (A), relative abundances of the principal phyla (B), and families (C) measured by 16S Illumina sequencing.

**Supplementary Figure 2** | Relative abundances of the main bacterial phyla in the bioreactor medium (A) and the mucin beads (B) in MPigut-IVM during the runs 1, 2, and 3.

**Supplementary Figure 3** | Shannon (A) and observed (B) alpha diversity indexes MPigut-IVM samples collected from runs #1, 2 and 3 ( $n = 3$ ).

**Supplementary Figure 4** | Principal Component analysis (PCoA) plot with Bray-Curtis dissimilarity on the bacterial communities separated by the type of diet in the bioreactor medium, bead medium, and mucin beads of the MPigut-IVM.

## REFERENCES

- Adhikari, B., Kim, S. W., and Kwon, Y. M. (2019). Characterization of microbiota associated with digesta and mucosa in different regions of gastrointestinal tract of nursery pigs. *Int. J. Mol. Sci.* 20:1630. doi: 10.3390/ijms20071630
- Amezcu, R., Friendship, R. M., Dewey, C. E., Gyles, C., and Fairbrother, J. M. (2002). Presentation of postweaning *Escherichia coli* diarrhea in southern Ontario, prevalence of hemolytic *E. coli* serogroups involved, and their antimicrobial resistance patterns. *Can. J. Vet. Res.* 66, 73–78.
- Auer, L., Mariadassou, M., O'Donohue, M., Klopp, C., and Hernandez-Raquet, G. (2017). Analysis of large 16S rRNA Illumina data sets: Impact of singleton read filtering on microbial community description. *Mol. Ecol. Resour.* 17, e122–e132. doi: 10.1111/1755-0998.12700
- Barba-Vidal, E., Castillejos, L., López-Colom, P., Rivero Urgell, M., Moreno Muñoz, J. A., and Martín-Orúe, S. M. (2017). Evaluation of the probiotic strain *Bifidobacterium longum* subsp. *Infantis* CECT 7210 capacities to improve health status and fight digestive pathogens in a piglet model. *Front. Microbiol.* 8:533. doi: 10.3389/fmicb.2017.00533
- Beaumont, M., Paës, C., Mussard, E., Knudsen, C., Cauquil, L., Aymard, P., et al. (2020). Gut microbiota derived metabolites contribute to intestinal barrier maturation at the suckling-to-weaning transition. *Gut Microbes* 11, 1268–1286. doi: 10.1080/19490976.2020.1747335
- Bokulich, N. A., Subramanian, S., Faith, J. J., Gevers, D., Gordon, J. I., Knight, R., et al. (2013). Quality-filtering vastly improves diversity estimates from Illumina amplicon sequencing. *Nat. Methods* 10, 57–59. doi: 10.1038/nmeth.2276
- Bustin, S. A., Benes, V., Garson, J. A., Hellems, J., Huggett, J., Kubista, M., et al. (2009). The MIQE guidelines: minimum information for publication of quantitative real-time PCR experiments. *Clin. Chem.* 55, 611–622. doi: 10.1373/clinchem.2008.112797
- Campos, M. A., Closel, M., Valente, E. P., Cardoso, J. E., Akira, S., Alvarez-Leite, J. I., et al. (2004). Impaired production of proinflammatory cytokines and host resistance to acute infection with *Trypanosoma cruzi* in mice lacking functional myeloid differentiation factor 88. *J. Immunol.* 172, 1711–1718. doi: 10.4049/jimmunol.172.3.1711
- Castillo, M., Martín-Orúe, S. M., Roca, M., Manzanilla, E. G., Badiola, I., Perez, J. F., et al. (2006). The response of gastrointestinal microbiota to avilamycin, butyrate, and plant extracts in early-weaned pigs. *J. Anim. Sci.* 84, 2725–2734. doi: 10.2527/jas.2004-556
- Cheon, D. S., and Chae, C. (1996). Outbreak of diarrhea associated with *Enterococcus durans* in piglets. *J. Vet. Diagn. Invest.* 8, 123–124. doi: 10.1177/104063879600800123
- Chytilová, M., Nemcová, R., Gancarčíková, S., Mudroňová, D., and Tkáčiková, L. (2014). Flax-seed oil and *Lactobacillus plantarum* supplementation modulate TLR and NF- $\kappa$ B gene expression in enterotoxigenic *Escherichia coli* challenged gnotobiotic pigs. *Acta Vet. Hung.* 62, 463–472. doi: 10.1556/AVet.2014.024
- Comtet-Marre, S., Parisot, N., Lepercq, P., Chaucheyras-Durand, F., Mosoni, P., Peyretailade, E., et al. (2017). Metatranscriptomics reveals the active bacterial and eukaryotic fibrolytic communities in the rumen of dairy cow fed a mixed diet. *Front. Microbiol.* 8:67. doi: 10.3389/fmicb.2017.00067
- Defois, C., Ratel, J., Garrait, G., Denis, S., Le Goff, O., Talvas, J., et al. (2018). Food chemicals disrupt human gut microbiota activity and impact intestinal homeostasis as revealed by *in vitro* systems. *Sci. Rep.* 8, 1–12. doi: 10.1038/s41598-018-29376-9
- Dubreuil, J. D., Isaacson, R. E., and Schifferli, D. M. (2016). Animal enterotoxigenic *Escherichia coli*. *EcoSal Plus* 7, 1–47. doi: 10.1128/ecosalplus.ESP-0006-2016
- Dufourny, S., Everaert, N., Lebrun, S., Douny, C., Scippo, M.-L., Bing, L., et al. (2019). Baby-SPIME: A dynamic *in vitro* piglet model mimicking gut microbiota during the weaning process. *J. Microbiol. Methods* 167:105735. doi: 10.1016/j.mimet.2019.105735
- Escudé, F., Auer, L., Bernard, M., Mariadassou, M., Cauquil, L., Vidal, K., et al. (2018). FROGS: find, rapidly, OTUs with galaxy solution. *Bioinformatics* 34, 1287–1294. doi: 10.1093/bioinformatics/btx791
- Etienne-Mesmin, L., Chassaing, B., Desvaux, M., De Paepe, K., Gresse, R., Sauvatre, T., et al. (2019). Experimental models to study intestinal microbes-mucus interactions in health and disease. *FEMS Microbiol. Rev.* 43, 457–489. doi: 10.1093/femsre/fuz013
- Fairbrother, J. M., Nadeau, E., and Gyles, C. L. (2005). *Escherichia coli* in postweaning diarrhea in pigs: an update on bacterial types, pathogenesis, and prevention strategies. *Anim. Health Res. Rev.* 6, 17–39. doi: 10.1079/ahr2005105
- Feng, W., Wu, Y., Chen, G., Fu, S., Li, B., Huang, B., et al. (2018). Sodium butyrate attenuates diarrhea in weaned piglets and promotes tight junction protein expression in colon in a GPR109A-dependent manner. *Cell. Physiol. Biochem.* 47, 1617–1629. doi: 10.1159/000490981
- Finamore, A., Roselli, M., Imbinto, A., Seeboth, J., Oswald, I. P., and Mengheri, E. (2014). *Lactobacillus amylovorus* inhibits the TLR4 inflammatory signaling triggered by enterotoxigenic *Escherichia coli* via modulation of the negative regulators and involvement of TLR2 in intestinal Caco-2 cells and pig explants. *PLoS One* 9:e94891. doi: 10.1371/journal.pone.0094891
- Fleury, M. A., Le Goff, O., Denis, S., Chaucheyras-Durand, F., Jouy, E., Kempf, I., et al. (2017). Development and validation of a new dynamic *in vitro* model of the piglet colon (PigutIVM): application to the study of probiotics. *Appl. Microbiol. Biotechnol.* 101, 2533–2547. doi: 10.1007/s00253-017-8122-y
- Frese, S. A., Parker, K., Calvert, C. C., and Mills, D. A. (2015). Diet shapes the gut microbiome of pigs during nursing and weaning. *Microbiome* 3:28. doi: 10.1186/s40168-015-0091-8
- Germerodt, S., Bohl, K., Lück, A., Pande, S., Schröter, A., Kaleta, C., et al. (2016). Pervasive selection for cooperative cross-feeding in bacterial communities. *PLoS Comput. Biol.* 12:e1004986. doi: 10.1371/journal.pcbi.1004986
- González-Ortiz, G., Pérez, J. F., Hermes, R. G., Molist, F., Jiménez-Díaz, R., and Martín-Orúe, S. M. (2014). Screening the ability of natural feed ingredients to interfere with the adherence of enterotoxigenic *Escherichia coli* (ETEC) K88 to the porcine intestinal mucus. *Br. J. Nutr.* 111, 633–642. doi: 10.1017/S0007114513003024
- Gresse, R., Chaucheyras Durand, F., Denis, S., Beaumont, M., Van de Wiele, T., Forano, E., et al. (2021). Weaning-associated deprivation stress causes microbiota disruptions in a novel mucin-containing *in vitro* model of the piglet colon (MPigut-IVM). *J. Anim. Sci. Biotechnol.* 12:75. doi: 10.1186/s40104-021-00584-0
- Gresse, R., Chaucheyras Durand, F., Dunière, L., Blanquet-Diot, S., and Forano, E. (2019). Microbiota composition and functional profiling throughout the gastrointestinal tract of commercial weaning piglets. *Microorganisms* 7:343. doi: 10.3390/microorganisms7090343
- Gresse, R., Chaucheyras-Durand, F., Fleury, M. A., Van de Wiele, T., Forano, E., and Blanquet-Diot, S. (2017). Gut microbiota dysbiosis in postweaning piglets: understanding the keys to health. *Trends Microbiol.* 25, 851–873. doi: 10.1016/j.tim.2017.05.004
- Guevarra, R. B., Hong, S. H., Cho, J. H., Kim, B.-R., Shin, J., Lee, J. H., et al. (2018). The dynamics of the piglet gut microbiome during the weaning transition in association with health and nutrition. *J. Anim. Sci. Biotechnol.* 9:54. doi: 10.1186/s40104-018-0269-6
- Gustavo Hermes, R., Molist, F., Francisco Pérez, J., Gómez de Segura, A., Ywazaki, M., Davin, R., et al. (2013). Casein glycomacropeptide in the diet may reduce *Escherichia coli* attachment to the intestinal mucosa and increase the intestinal lactobacilli of early weaned piglets after an enterotoxigenic *E. coli* K88 challenge. *Br. J. Nutr.* 109, 1001–1012. doi: 10.1017/S0007114512002978
- Hendrickx, A. P. A., Top, J., Bayjanov, J. R., Kemperman, H., Rogers, M. R. C., Paganelli, F. L., et al. (2015). Antibiotic-Driven dysbiosis mediates intraluminal agglutination and alternative segregation of *Enterococcus faecium* from the intestinal epithelium. *mBio* 6:e01346-15. doi: 10.1128/mBio.01346-15
- Hermann-Bank, M. L., Skovgaard, K., Stockmarr, A., Strube, M. L., Larsen, N., Kongsted, H., et al. (2015). Characterization of the bacterial gut microbiota of piglets suffering from new neonatal porcine diarrhoea. *BMC Vet. Res.* 11:139. doi: 10.1186/s12917-015-0419-4
- Huijsdens, X. W., Linsens, R. K., Mak, M., Meuwissen, S. G. M., Vandenbroucke-Grauls, C. M. J. E., and Savelkoul, P. H. M. (2002). Quantification of bacteria adherent to gastrointestinal mucosa by Real-Time PCR. *J. Clin. Microbiol.* 40, 4423–4427. doi: 10.1128/JCM.40.12.4423-4427.2002
- Ikeobi, C. C., Ogunsanya, T. O., and Rotimi, V. O. (1996). Prevalence of pathogenic role of *Morganella-proteus-providencia*-group of bacteria in human faeces. *Afr. J. Med. Med. Sci.* 25, 7–12.
- Issac, J. M., Mohamed, Y. A., Bashir, G. H., Al-Sbiei, A., Conca, W., Khan, T. A., et al. (2018). Induction of hypergammaglobulinemia and autoantibodies by *Salmonella* infection in MyD88-deficient mice. *Front. Immunol.* 9:1384. doi: 10.3389/fimmu.2018.01384



- Issac, J. M., Sarawathiamma, D., Al-Ketbi, M. I., Azimullah, S., Al-Ojali, S. M., Mohamed, Y. A., et al. (2013). Differential outcome of infection with attenuated *Salmonella* in MyD88-deficient mice is dependent on the route of administration. *Immunobiology* 218, 52–63. doi: 10.1016/j.imbio.2012.02.001
- Ivarsson, E., Roos, S., Liu, H. Y., and Lindberg, J. E. (2014). Fermentable non-starch polysaccharides increases the abundance of *Bacteroides-Prevotella*-*Porphyromonas* in ileal microbial community of growing pigs. *Animal* 8, 1777–1787. doi: 10.1017/S1751731114001827
- Jertborn, M., and Svennerholm, A. M. (1991). Enterotoxin-producing bacteria isolated from Swedish travellers with diarrhoea. *Scand. J. Infect. Dis.* 23, 473–479. doi: 10.3109/00365549109075096
- Jonach, B., Boye, M., Stockmarr, A., and Jensen, T. K. (2014). Fluorescence in situ hybridization investigation of potentially pathogenic bacteria involved in neonatal porcine diarrhea. *BMC Vet. Res.* 10:68. doi: 10.1186/1746-6148-10-68
- Kaeffer, B., Botreau, E., Velge, P., and Pardon, P. (1993). Epithelioid and fibroblastic cell lines derived from the ileum of an adult histocompatible miniature boar (d/d haplotype) and immortalized by SV40 plasmid. *Eur. J. Cell Biol.* 62, 152–162.
- Kassinen, A., Krogius-Kurikka, L., Mäkiyuokko, H., Rinttilä, T., Paulin, L., Corander, J., et al. (2007). The fecal microbiota of irritable bowel syndrome patients differs significantly from that of healthy subjects. *Gastroenterology* 133, 24–33. doi: 10.1053/j.gastro.2007.04.005
- Kato, K., Hanss, A. D., Zemskova, M. A., Morgan, N. E., Kim, M., Knox, K. S., et al. (2017). *Pseudomonas aeruginosa* increases MUC1 expression in macrophages through the TLR4-p38 pathway. *Biochem. Biophys. Res. Commun.* 492, 231–235. doi: 10.1016/j.bbrc.2017.08.056
- Laine, T. M., Lyytikäinen, T., Yliaho, M., and Anttila, M. (2008). Risk factors for post-weaning diarrhoea on piglet producing farms in Finland. *Acta Vet. Scand.* 50:21. doi: 10.1186/1751-0147-50-21
- Lane, D. J., Pace, B., Olsen, G. J., Stahl, D. A., Sogin, M. L., and Pace, N. R. (1985). Rapid determination of 16S ribosomal RNA sequences for phylogenetic analyses. *Proc. Natl. Acad. Sci. U.S.A.* 82, 6955–6959. doi: 10.1073/pnas.82.20.6955
- Larsson, J., Lindberg, R., Aspán, A., Grandon, R., Westergren, E., and Jacobson, M. (2014). Neonatal piglet diarrhoea associated with enteroadherent *Enterococcus hirae*. *J. Comp. Pathol.* 151, 137–147. doi: 10.1016/j.jcpa.2014.04.003
- Le Dividich, J., and Sève, B. (2000). Effects of underfeeding during the weaning period on growth, metabolism, and hormonal adjustments in the piglet. *Domest. Anim. Endocrinol.* 19, 63–74. doi: 10.1016/s0739-7240(00)00067-9
- Leatham, M. P., Banerjee, S., Autieri, S. M., Mercado-Lubo, R., Conway, T., and Cohen, P. S. (2009). Precolonized human commensal *Escherichia coli* strains serve as a barrier to *E. coli* O157:H7 growth in the streptomycin-treated mouse intestine. *Infect. Immun.* 77, 2876–2886. doi: 10.1128/IAI.00059-09
- López-Colom, P., Castillejos, L., Barba-Vidal, E., Zhu, Y., Puyalto, M., Mallo, J. J., et al. (2019). Response of gastrointestinal fermentative activity and colonic microbiota to protected sodium butyrate and protected sodium heptanoate in weaned piglets challenged with ETEC F4+. *Arch. Anim. Nutr.* 73, 339–359. doi: 10.1080/1745039X.2019.1641376
- Lu, J. J., Zou, X. T., and Wang, Y. M. (2008). Effects of sodium butyrate on the growth performance, intestinal microflora and morphology of weanling pigs. *J. Anim. Feed Sci.* 17, 568–578. doi: 10.22358/jafs/66685/2008
- Luo, Y., Xu, J., Zhang, C., Jiang, C., Ma, Y., He, H., et al. (2019). Toll-like receptor 5-mediated IL-17C expression in intestinal epithelial cells enhances epithelial host defense against F4+ ETEC infection. *Vet. Res.* 50:48. doi: 10.1186/s13567-019-0665-8
- Luppi, A., Gibellini, M., Gin, T., Vangroenweghe, F., Vandenbroucke, V., Bauerfeind, R., et al. (2016). Prevalence of virulence factors in enterotoxigenic *Escherichia coli* isolated from pigs with post-weaning diarrhoea in Europe. *Porcine Health Manag.* 2:20. doi: 10.1186/s40813-016-0039-9
- Madec, F., Bridoux, N., Bounaix, S., and Jestin, A. (1998). Measurement of digestive disorders in the piglet at weaning and related risk factors. *Prev. Vet. Med.* 35, 53–72. doi: 10.1016/S0167-5877(97)00057-3
- Madoroba, E., Van Driessche, E., De Greve, H., Mast, J., Ncube, I., Read, J., et al. (2009). Prevalence of enterotoxigenic *Escherichia coli* virulence genes from scouring piglets in Zimbabwe. *Trop. Anim. Health Prod.* 41, 1539–1547. doi: 10.1007/s11250-009-9345-4
- Mahé, F., Rognes, T., Quince, C., de Vargas, C., and Dunthorn, M. (2014). Swarm: robust and fast clustering method for amplicon-based studies. *PeerJ* 2:e593. doi: 10.7717/peerj.593
- Main, R. G., Dritz, S. S., Tokach, M. D., Goodband, R. D., and Nelssen, J. L. (2004). Increasing weaning age improves pig performance in a multisite production system1. *J. Anim. Sci.* 82, 1499–1507. doi: 10.2527/2004.8251499x
- Mariani, V., Palermo, S., Fiorentini, S., Lanubile, A., and Giuffra, E. (2009). Gene expression study of two widely used pig intestinal epithelial cell lines: IPEC-J2 and IPI-2I. *Vet. Immunol. Immunopathol.* 131, 278–284. doi: 10.1016/j.vetimm.2009.04.006
- Marzorati, M., Vanhoecke, B., De Ryck, T., Sadaghian Sadabad, M., Pinheiro, I., Possemiers, S., et al. (2014). The HMITM module: a new tool to study the Host-Microbiota Interaction in the human gastrointestinal tract *in vitro*. *BMC Microbiol.* 14:133. doi: 10.1186/1471-2180-14-133
- McCracken, B. A., Spurlock, M. E., Roos, M. A., Zuckermann, F. A., and Gaskins, H. R. (1999). Weaning anorexia may contribute to local inflammation in the piglet small intestine. *J. Nutr.* 129, 613–619. doi: 10.1093/jn/129.3.613
- McGuckin, M. A., Every, A. L., Skene, C. D., Linden, S. K., Chionh, Y. T., Swierczak, A., et al. (2007). Muc1 mucin limits both *Helicobacter pylori* colonization of the murine gastric mucosa and associated gastritis. *Gastroenterology* 133, 1210–1218. doi: 10.1053/j.gastro.2007.07.003
- McMurdie, P. J., and Holmes, S. (2013). phyloseq: an R package for reproducible interactive analysis and graphics of microbiome census data. *PLoS One* 8:e61217. doi: 10.1371/journal.pone.0061217
- Melo, A. D. B., Silveira, H., Bortoluzzi, C., Lara, L. J., Garbossa, C. A. P., Preis, G., et al. (2016). Intestinal alkaline phosphatase and sodium butyrate may be beneficial in attenuating LPS-induced intestinal inflammation. *Genet. Mol. Res.* 15:gmr15048875. doi: 10.4238/gmr15048875
- Metzler-Zebeli, B. U., Lawlor, P. G., Magowan, E., and Zebeli, Q. (2016). Effect of freezing conditions on fecal bacterial composition in pigs. *Animals (Basel)* 6:18. doi: 10.3390/ani6030018
- Müller, H. E. (1986). Occurrence and pathogenic role of *Morganella-Proteus*-*Providencia* group bacteria in human feces. *J. Clin. Microbiol.* 23, 404–405.
- Ngeleka, M., Pritchard, J., Appleyard, G., Middleton, D. M., and Fairbrother, J. M. (2003). Isolation and association of *Escherichia coli* AIDA-I/STb, rather than EAST1 pathotype, with diarrhea in piglets and antibiotic sensitivity of isolates. *J. Vet. Diagn. Invest.* 15, 242–252. doi: 10.1177/104063870301500305
- Nicklasson, M., Sjöling, Å., von Mentzer, A., Qadri, F., and Svennerholm, A.-M. (2012). Expression of colonization factor CS5 of enterotoxigenic *Escherichia coli* (ETEC) is enhanced *in vivo* and by the bile component Na glycocholate hydrate. *PLoS One* 7:e35827. doi: 10.1371/journal.pone.0035827
- Ohene-Adjei, S., Chaves, A. V., McAllister, T. A., Benchaar, C., Teather, R. M., and Forster, R. J. (2008). Evidence of increased diversity of methanogenic archaea with plant extract supplementation. *Microb. Ecol.* 56, 234–242. doi: 10.1007/s00248-007-9340-0
- Pajarillo, E. A., Chae, J., Balolong, M., Kim, H. B., and Kang, D. (2014). Assessment of fecal bacterial diversity among healthy piglets during the weaning transition. *J. Gen. Appl. Microbiol.* 60, 140–146. doi: 10.2323/jgam.60.140
- Pasternak, J. A., Kent-Dennis, C., Van Kessel, A. G., and Wilson, H. L. (2015). Claudin-4 undergoes age-dependent change in cellular localization on pig jejunal villous epithelial cells, independent of bacterial colonization. *Mediators Inflamm.* 2015:263629. doi: 10.1155/2015/263629
- Payne, A. N., Zihler, A., Chassard, C., and Lacroix, C. (2012). Advances and perspectives in *in vitro* human gut fermentation modeling. *Trends Biotechnol.* 30, 17–25. doi: 10.1016/j.tibtech.2011.06.011
- Pfaffl, M. W., Tichopad, A., Prgomet, C., and Neuvians, T. P. (2004). Determination of stable housekeeping genes, differentially regulated target genes and sample integrity: BestKeeper–Excel-based tool using pair-wise correlations. *Biotechnol. Lett.* 26, 509–515. doi: 10.1023/b:biote.0000019559.84305.47
- Poehlein, A., Schneider, D., Soh, M., Daniel, R., and Seedorf, H. (2018). Comparative genomic analysis of members of the genera *methanospira* and *methanobrevibacter* reveals distinct clades with specific potential metabolic functions. *Archaea* 2018:7609847. doi: 10.1155/2018/7609847
- Pu, J., Chen, D., Tian, G., He, J., Zheng, P., Mao, X., et al. (2018). Protective effects of benzoic acid, bacillus coagulans, and oregano oil on intestinal injury caused by enterotoxigenic *Escherichia coli* in weaned piglets. *Biomed. Res. Int.* 2018:1829632. doi: 10.1155/2018/1829632



- Quast, C., Pruesse, E., Yilmaz, P., Gerken, J., Schweer, T., Yarza, P., et al. (2013). The SILVA ribosomal RNA gene database project: improved data processing and web-based tools. *Nucleic Acids Res.* 41, D590–D596. doi: 10.1093/nar/gks1219
- Rahman, M., Hasan, M. R., Oba, T., and Shimizu, K. (2006). Effect of rpoS gene knockout on the metabolism of *Escherichia coli* during exponential growth phase and early stationary phase based on gene expressions, enzyme activities and intracellular metabolite concentrations. *Biotechnol. Bioeng.* 94, 585–595. doi: 10.1002/bit.20858
- Rhouma, M., Beaudry, F., Thériault, W., Bergeron, N., Beauchamp, G., Laurent-Lewandowski, S., et al. (2016). *In vivo* therapeutic efficacy and pharmacokinetics of colistin sulfate in an experimental model of enterotoxigenic *Escherichia coli* infection in weaned pigs. *Vet. Res.* 47:58. doi: 10.1186/s13567-016-0344-y
- Rhouma, M., Fairbrother, J. M., Beaudry, F., and Letellier, A. (2017). Post weaning diarrhea in pigs: risk factors and non-colistin-based control strategies. *Acta Vet. Scand.* 59:31. doi: 10.1186/s13028-017-0299-7
- Rognes, T., Flouri, T., Nichols, B., Quince, C., and Mahé, F. (2016). VSEARCH: a versatile open source tool for metagenomics. *PeerJ* 4:e2584. doi: 10.7717/peerj.2584
- Rohart, F., Gautier, B., Singh, A., and Cao, K.-A. L. (2017). mixOmics: An R package for 'omics feature selection and multiple data integration. *PLoS Comput. Biol.* 13:e1005752. doi: 10.1371/journal.pcbi.1005752
- Roussel, C. (2019). Enterotoxigenic *Escherichia coli* (ETEC) physiopathology and probiotic modulation in human gastrointestinal systems. Spécialité: Biotechnologie, Microbiologie et Santé. Available online at: <http://www.theses.fr> (accessed September, 2021).
- Roussel, C., Galia, W., Leriche, F., Chalancon, S., Denis, S., Van de Wiele, T., et al. (2018). Comparison of conventional plating, PMA-qPCR, and flow cytometry for the determination of viable enterotoxigenic *Escherichia coli* along a gastrointestinal *in vitro* model. *Appl. Microbiol. Biotechnol.* 102, 9793–9802. doi: 10.1007/s00253-018-9380-z
- Sandberg, J., Kovatcheva-Datchary, P., Björck, I., Bäckhed, F., and Nilsson, A. (2019). Abundance of gut Prevotella at baseline and metabolic response to barley prebiotics. *Eur. J. Nutr.* 58, 2365–2376. doi: 10.1007/s00394-018-1788-9
- Scanga, C. A., Aliberti, J., Jankovic, D., Tilloy, F., Bennouna, S., Denkers, E. Y., et al. (2002). Cutting edge: MyD88 is required for resistance to *Toxoplasma gondii* infection and regulates parasite-induced IL-12 production by dendritic cells. *J. Immunol.* 168, 5997–6001. doi: 10.4049/jimmunol.168.12.5997
- Trckova, M., Lorencova, A., Babak, V., Neca, J., and Ciganek, M. (2018). The effect of leonardite and lignite on the health of weaned piglets. *Res. Vet. Sci.* 119, 134–142. doi: 10.1016/j.rvsc.2018.06.004
- Twitchell, E. L., Tin, C., Wen, K., Zhang, H., Becker-Dreps, S., Azcarate-Peril, M. A., et al. (2016). Modeling human enteric dysbiosis and rotavirus immunity in gnotobiotic pigs. *Gut Pathog.* 8:51. doi: 10.1186/s13099-016-0136-y
- Tytgat, H. L. P., Douillard, F. P., Reunanen, J., Rasinkangas, P., Hendrickx, A. P. A., Laine, P. K., et al. (2016). *Lactobacillus rhamnosus* GG outcompetes *Enterococcus faecium* via mucus-binding pili: evidence for a novel and heterospecific probiotic mechanism. *Appl. Environ. Microbiol.* 82, 5756–5762. doi: 10.1128/AEM.01243-16
- Van Reeth, K., Van Gucht, S., and Pensaert, M. (2002). *In vivo* studies on cytokine involvement during acute viral respiratory disease of swine: troublesome but rewarding. *Vet. Immunol. Immunopathol.* 87, 161–168. doi: 10.1016/S0165-2427(02)00047-8
- von Bernuth, H., Picard, C., Puel, A., and Casanova, J.-L. (2012). Experimental and natural infections in MyD88- and IRAK-4-deficient mice and humans. *Eur. J. Immunol.* 42, 3126–3135. doi: 10.1002/eji.201242683
- Wilson, R. H., and Leibholz, J. (1981). Digestion in the pig between 7 and 35 d of age. *Br. J. Nutr.* 45, 321–336. doi: 10.1079/BJN19810108
- Wu, Y., Zhu, C., Chen, Z., Chen, Z., Zhang, W., Ma, X., et al. (2016). Protective effects of *Lactobacillus plantarum* on epithelial barrier disruption caused by enterotoxigenic *Escherichia coli* in intestinal porcine epithelial cells. *Vet. Immunol. Immunopathol.* 172, 55–63. doi: 10.1016/j.vetimm.2016.03.005
- Xia, L., Dai, L., Yu, Q., and Yang, Q. (2017a). Persistent transmissible gastroenteritis virus infection enhances enterotoxigenic *Escherichia coli* K88 adhesion by promoting epithelial-mesenchymal transition in intestinal epithelial cells. *J. Virol.* 91:e01256-17. doi: 10.1128/JVI.01256-17
- Xia, L., Dai, L., Zhu, L., Hu, W., and Yang, Q. (2017b). Proteomic analysis of IPEC-J2 cells in response to coinfection by porcine transmissible gastroenteritis virus and enterotoxigenic *Escherichia coli* K88. *Proteomics Clin. Appl.* 11:1600137. doi: 10.1002/prca.201600137
- Xu, B., Yan, Y., Huang, J., Yin, B., Pan, Y., and Ma, L. (2020). Cortex Phellodendri extract's anti-diarrhea effect in mice related to its modification of gut microbiota. *Biomed. Pharmacother.* 123:109720. doi: 10.1016/j.biopha.2019.109720
- Xu, C., Wang, Y., Sun, R., Qiao, X., Shang, X., and Niu, W. (2014). Modulatory effects of vasoactive intestinal peptide on intestinal mucosal immunity and microbial community of weaned piglets challenged by an enterotoxigenic *Escherichia coli* (K88). *PLoS One* 9:e104183. doi: 10.1371/journal.pone.0104183
- Xu, J., Chen, X., Yu, S., Su, Y., and Zhu, W. (2016). Effects of early intervention with sodium butyrate on gut microbiota and the expression of inflammatory cytokines in neonatal piglets. *PLoS One* 11:0162461. doi: 10.1371/journal.pone.0162461
- Yang, Q., Huang, X., Wang, P., Yan, Z., Sun, W., Zhao, S., et al. (2019). Longitudinal development of the gut microbiota in healthy and diarrheic piglets induced by age-related dietary changes. *Microbiologyopen* 8:e923. doi: 10.1002/mbo3.923
- Yu, Y., Lee, C., Kim, J., and Hwang, S. (2005). Group-specific primer and probe sets to detect methanogenic communities using quantitative real-time polymerase chain reaction. *Biotechnol. Bioeng.* 89, 670–679. doi: 10.1002/bit.20347

**Conflict of Interest:** FC-D and RG are employees of Lallemand SAS. The authors declare that this study received funding from Lallemand SAS. The funder had the following involvement in the study: study design, data analysis, interpretation of the data and writing of the article.

The remaining authors declare that the research was conducted in the absence of any commercial or financial relationships that could be construed as a potential conflict of interest.

Copyright © 2021 Gresse, Chaucheyras-Durand, Garrido, Denis, Jiménez-Marín, Beaumont, Van de Wiele, Forano and Blanquet-Diot. This is an open-access article distributed under the terms of the Creative Commons Attribution License (CC BY). The use, distribution or reproduction in other forums is permitted, provided the original author(s) and the copyright owner(s) are credited and that the original publication in this journal is cited, in accordance with accepted academic practice. No use, distribution or reproduction is permitted which does not comply with these terms.



# New Insights From Transcriptomic Data Reveal Differential Effects of CO<sub>2</sub> Acidification Stress on Photosynthesis of an Endosymbiotic Dinoflagellate *in hospite*

## OPEN ACCESS

### Edited by:

David Kamanda Ngugi,  
German Collection of Microorganisms  
and Cell Cultures GmbH (DSMZ),  
Germany

### Reviewed by:

Lei Jiang,  
South China Sea Institute  
of Oceanology, Chinese Academy  
of Sciences, China  
Haruko Kurihara,  
University of the Ryukyus, Japan

### \*Correspondence:

Guoxin Cui  
guoxin.cui@kaust.edu.sa  
Manuel Aranda  
manuel.aranda@kaust.edu.sa

### † Present address:

Yi Jin Liew,  
CSIRO Health and Biosecurity, North  
Ryde, NSW, Australia

### Specialty section:

This article was submitted to  
Microbial Symbioses,  
a section of the journal  
Frontiers in Microbiology

**Received:** 10 February 2021

**Accepted:** 15 June 2021

**Published:** 19 July 2021

### Citation:

Herrera M, Liew YJ, Venn A,  
Tambutté E, Zoccola D, Tambutté S,  
Cui G and Aranda M (2021) New  
Insights From Transcriptomic Data  
Reveal Differential Effects of CO<sub>2</sub>  
Acidification Stress on Photosynthesis  
of an Endosymbiotic Dinoflagellate *in hospite*. *Front. Microbiol.* 12:666510.  
doi: 10.3389/fmicb.2021.666510

Marcela Herrera<sup>1</sup>, Yi Jin Liew<sup>1†</sup>, Alexander Venn<sup>2</sup>, Eric Tambutté<sup>2</sup>, Didier Zoccola<sup>2</sup>,  
Sylvie Tambutté<sup>2</sup>, Guoxin Cui<sup>1\*</sup> and Manuel Aranda<sup>1\*</sup>

<sup>1</sup> Red Sea Research Center (RSRC), Biological and Environmental Sciences and Engineering Division (BESE), King Abdullah University of Science and Technology (KAUST), Thuwal, Saudi Arabia, <sup>2</sup> Marine Department, Centre Scientifique de Monaco, Monaco, Monaco

Ocean acidification (OA) has both detrimental as well as beneficial effects on marine life; it negatively affects calcifiers while enhancing the productivity of photosynthetic organisms. To date, many studies have focused on the impacts of OA on calcification in reef-building corals, a process particularly susceptible to acidification. However, little is known about the effects of OA on their photosynthetic algal partners, with some studies suggesting potential benefits for symbiont productivity. Here, we investigated the transcriptomic response of the endosymbiont *Symbiodinium microadriaticum* (CCMP2467) in the Red Sea coral *Stylophora pistillata* subjected to different long-term (2 years) OA treatments (pH 8.0, 7.8, 7.4, 7.2). Transcriptomic analyses revealed that symbionts from corals under lower pH treatments responded to acidification by increasing the expression of genes related to photosynthesis and carbon-concentrating mechanisms. These processes were mostly up-regulated and associated metabolic pathways were significantly enriched, suggesting an overall positive effect of OA on the expression of photosynthesis-related genes. To test this conclusion on a physiological level, we analyzed the symbiont's photochemical performance across treatments. However, in contrast to the beneficial effects suggested by the observed gene expression changes, we found significant impairment of photosynthesis with increasing pCO<sub>2</sub>. Collectively, our data suggest that over-expression of photosynthesis-related genes is not a beneficial effect of OA but rather an acclimation response of the holobiont to different water chemistries. Our study highlights the complex effects of ocean acidification on these symbiotic organisms and the role of the host in determining symbiont productivity and performance.

**Keywords:** carbon-concentrating mechanism, coral-dinoflagellate symbiosis, ocean acidification, Symbiodiniaceae, F/Fm', pCO<sub>2</sub>, gene expression

## INTRODUCTION

Rising levels of anthropogenic carbon dioxide (CO<sub>2</sub>) are transforming the chemistry of our oceans; the average seawater pH has already decreased by 0.1 pH units (equivalent to almost 30% increase in acidity) since the Industrial Revolution and it is predicted to drop even further by the end of this century (Magnan et al., 2016; Hoegh-Guldberg et al., 2017). Thus, there is a great concern regarding the future of marine ecosystems and the ecological services they provide; particularly for coral reefs, as these depend entirely on the persistence of corals and other calcifiers (Hoegh-Guldberg et al., 2007, 2017; Pandolfi et al., 2011; Hughes et al., 2017). As CO<sub>2</sub> dissolves in water, carbonic acid (H<sub>2</sub>CO<sub>3</sub>) is formed and protons (H<sup>+</sup>) are released, which lowers the pH (i.e., more acidic) but also reacts with carbonate ions (CO<sub>3</sub><sup>2-</sup>), which in turn reduce carbonate concentrations and saturation state ( $\Omega$ ). Calcifying organisms are then unable to build skeletons, have slower growth and are more sensitive to disturbances (Doney et al., 2009).

Much attention has been focused on the detrimental effect of ocean acidification (OA) on calcification (Orr et al., 2005; Hofmann et al., 2010; Andersson and Gledhill, 2013), yet, it is unclear how it affects other physiological processes (Kroeker et al., 2010, 2013). Specifically, there is a growing interest in understanding how acidification will impact photosynthetic organisms (Mackey et al., 2015; Connell et al., 2018). For example, changes in diversity, structure, and productivity of phytoplankton communities are predicted to have profound consequences for marine food webs and biogeochemical processes (Dutkiewicz et al., 2015). Indeed, increased biomass of primary producers, such as sea grasses and algae, has been shown to alter the ecological functioning of benthic ecosystems by favoring the proliferation of some species and demise of others (Hall-Spencer et al., 2008; Connell et al., 2017). For symbiotic corals, OA may even have a greater impact on bleaching and productivity than on calcification (Anthony et al., 2008). Nonetheless, the effects are multi-faceted and complex. Like other aquatic photosynthetic organisms, the endosymbionts of corals (of the family Symbiodiniaceae) also have active CO<sub>2</sub>-concentrating mechanisms (CCMs) (Al-Moghrabi et al., 1996; Leggat et al., 1999) that allow them to cope with the challenges of living in a carbon-limited environment (Moroney and Ynalvez, 2007). To fuel photosynthesis, CO<sub>2</sub> must be converted to HCO<sub>3</sub><sup>-</sup> (and vice versa) so it can be transported inside the cell and ultimately reach RuBisCO, the enzyme that catalyzes the first step of CO<sub>2</sub> fixation. However, *in hospite*, this process is actively regulated by the host (Barott et al., 2015) through proteins like carbonic anhydrases and bicarbonate transporters that catalyze the interconversion of CO<sub>2</sub> and bicarbonate and mediate their transport. Certainly, this implies that the symbiont relies on the host to provide a suitable environment that supports its functioning (e.g., *in hospite* nutrient availability) so that if the physiological response of the latter is compromised, that of the symbiont will be too. Thus, even if productivity of the holobiont increases under elevated pCO<sub>2</sub> (Strahl et al., 2015; Biscéré et al., 2019), its performance and survival are ultimately limited by the physiological capabilities of the coral, which

can either be negatively impacted (e.g., reduced metabolism, increased oxidative stress, apoptosis, etc.) (Kaniewska et al., 2012) or (seemingly) unaffected (Wall et al., 2014; Tambutté et al., 2015; Davies et al., 2018).

Similar to the specific stress sensitivity of their cnidarian hosts (Anthony et al., 2008; Crawley et al., 2010; Edmunds, 2012; Kaniewska et al., 2012; Towanda and Thuesen, 2012; Jarrold et al., 2013; Gibbin and Davy, 2014; Hoadley et al., 2015b; Klein et al., 2017; Davies et al., 2018), differential responses to OA have also been observed among Symbiodiniaceae types (Buxton et al., 2009; Brading et al., 2011). This is not surprising considering the remarkable intra- and inter-specific functional diversity (Lajeunesse et al., 2018), including species-specific CCMs (Brading et al., 2013). For example, a recent study (Aranda et al., 2016) showed substantial differences in the number of bicarbonate transporters in the genomes of coral-associated endosymbionts; in particular, *Symbiodinium microadriaticum* appears to have significantly more compared to *Brevium minutum*, which likely has fundamental implications for carbon acquisition and (indirectly) productivity. Various combinations of host and symbiont genotypes may provide physiological (dis)advantages under changing ocean conditions. Hence, examining the response of different symbiotic associations to elevated pCO<sub>2</sub> can provide valuable understanding of OA effects on corals (Hoadley et al., 2015a).

Here, we investigated the global transcriptomic response of the endosymbiont *Symbiodinium microadriaticum* of the Red Sea coral *Stylophora pistillata* (Esper 1797) to long-term seawater acidification stress. This pocilloporid coral is not only one of the most abundant species and major contributor to reef structures in the Indo-Pacific (Veron, 2000) but has also been used as a model organism to study ecological, physiological, and evolutionary aspects of the cnidarian-dinoflagellate symbiosis (Ferrier-Pagès et al., 2003; Franklin et al., 2004; Putnam et al., 2008; Venn et al., 2013; Vidal-Dupiol et al., 2013; Maor-Landaw et al., 2014; Cohen and Dubinsky, 2015; Tambutté et al., 2015; Zoccola et al., 2015; Voolstra et al., 2017; Liew et al., 2018). Colonies of this coral have been successfully cultured under CO<sub>2</sub>-driven low pH conditions for almost 10 years, thus providing a unique opportunity to examine the effects of chronic exposure to high CO<sub>2</sub>. Further, most studies on OA represent data from short-term experiments that range from days to few weeks and focused on the physiological impact of coral calcification (Kaniewska et al., 2012; Chan and Connolly, 2013), however, little is known for the algal partner, especially with regard to responses on the molecular level. This study presents novel observations on the responses of a common coral symbiont to acidification stress.

## MATERIALS AND METHODS

### Experimental Incubations

Multiple colonies of a single clone of *S. pistillata* were subjected to long-term seawater acidification in an experimental setup at the Centre Scientifique de Monaco that has been maintained continuously from the early 2010s (Venn et al., 2013; Tambutté et al., 2015; Liew et al., 2018). Based on nuclear ITS and

mitochondrial COI, colonies were previously typed to be *S. pistillata* clade 4 (Voolstra et al., 2017), which is found throughout the northwest Indian Ocean including the Red Sea, the Persia/Arabian Gulf and Kenya (Keshavmurthy et al., 2013). Coral fragments were kept simultaneously in four aquaria, each supplied with Mediterranean seawater with an exchange rate of 70% per hour, salinity of 38 ppt, temperature of 25°C and irradiance of 170  $\mu\text{mol photons/m}^2\text{s}$  white light on a 12:12 h light:dark photoperiod provided by HQI-10000K metal halide lamps (BLV Nepturion), and fed with freshly hatched *Artemia* brine shrimps twice per week. Carbonate chemistry was manipulated by bubbling CO<sub>2</sub> to reduce pH to the reach values of pH 7.2, an extremely low value used to generate and study new phenotypes (Tambutté et al., 2015; Liew et al., 2018), pH 7.4, which represent extreme values observed today in some environments like volcanic CO<sub>2</sub> vents where mean pH can range between 7.4 and 7.6 (Hall-Spencer et al., 2008) and pH 7.8 or near future natural conditions as projected by the IPCC scenario RCP8.5 (Magnan et al., 2016), while a control aquarium was maintained at the current average seawater pH 8.0 (Doney et al., 2009). pH and temperature were constantly checked with a custom-made monitoring system (Enoleo, Monaco) so that similar conditions prevailed in each aquarium except for the carbonate chemistry. Details on chemistry parameters, pH and alkalinity measurements, and aquarium maintenance are provided in Tambutté et al. (2015) and Liew et al. (2018). For this experiment (same as Liew et al., 2018), coral fragments (three per tank) were added to the system in 2012 and taken out in 2014 (at the same time) after being subjected to the respective treatments for 2 years (Figure 1).

## Identification of Differentially Expressed Genes

High-quality total RNA was extracted from three replicate coral nubbins (one per colony, three colonies in each tank) that were kept in all different conditions for 2 years. Twelve strand-specific mRNA libraries were generated using the NEB Next Ultra Directional RNA Library Prep Kit for Illumina (New England Biolabs) and sequenced in six lanes of the HiSeq 2000 platform (Illumina) to retrieve a total of 674 million paired-end reads (101 bp). RNA-seq data was analyzed as implemented in Kallisto v0.44.0 (Bray et al., 2016) and its companion tool Sleuth v0.28.0 (Pimentel et al., 2017). Kallisto pseudo-aligns reads to a reference to produce a list of transcripts compatible with each read while avoiding alignment of individual bases, thus achieving much faster results compared to other approaches. Details on pseudo-alignment statistics are provided in **Supplementary Table 1**. Quantifications of gene expression in transcripts per million reads (TPM) resulting from the bootstrapping performed in Kallisto were then analyzed with Sleuth. Briefly, Sleuth builds a response error model that allows for the decoupling of biological variance from inferential variance to ultimately identify differentially expressed genes (DEGs). Significance of the differential expression levels is evaluated through a likelihood test (LRT), after which Sleuth returns a *q*-value per coding sequence (i.e., the corrected *p*-value following the Benjamini-Hochberg

correction for reducing the false discovery rate (FDR) due to multiple testing). Here, we chose a threshold of 0.05 for the *q*-value (corresponding to an FDR of 0.05), below which we considered the DEGs to be significant. Differential expression levels are outputted as a “beta” (*b*) value, which in order to get a differential expression level index similar to the classically used log<sub>2</sub> fold-change, we transformed by raising the number *e* to the *b*-th power (i.e.,  $e^b$ ).

While Liew et al. (2018) analyzed the transcriptomic response of *S. pistillata*, that study solely focused on the differential expression of methylated genes in the host, particularly those related to growth and biomineralization pathways. Thus, here we assessed the overall response of *S. pistillata*, along with the response of its endosymbiont *S. microadriaticum*. All analyses described above were carried out for both data sets. Reads were mapped to *S. microadriaticum* (Aranda et al., 2016) and *S. pistillata* (Voolstra et al., 2017) gene models (reference genomes can be found at<sup>1</sup>), and DEGs were identified by contrasting samples from all experimental conditions (pHs 7.2, 7.4, and 7.8) against the control (pH 8.0). Normalized expression values were log (*x* + 1) transformed and principal component analyses (based on Euclidean distances) were carried out after to assess the relationship between samples. Differences between treatments were tested using the function “Adonis” as implemented in the R (v3.5.1) (R Core Team, 2018) package “vegan” (Oksanen et al., 2019).

## Functional Enrichment Analyses

GO term enrichment analyses were performed with topGO (Alexa et al., 2006) using a self-developed R script<sup>2</sup> as described in Liew et al. (2018). Only GO terms with *p* < 0.05 and occurring at least five times were considered enriched. Furthermore, KEGG Orthology (KO) annotations were merged from the KEGG Automatic Annotation Server<sup>3</sup> (Moriya et al., 2007) (with the parameters “GHOSTZ,” “eukaryotes” and “bi-directional best hit”) and the results of the gene models of both *S. microadriaticum* and *S. pistillata*<sup>4</sup>. KEGG pathway enrichment analysis of DEGs were carried out using Fisher’s exact test and subsequent multiple testing correction via false discovery rate (FDR) estimation. Only pathways with *p* < 0.05 were considered significant. The R package “GOpot” (Walter et al., 2015) was used to visualize the relationship between genes and selected functional categories. This is presented as a circular plot where the inner ring shows the *z*-score and the outer ring scatterplots of the expression levels for the genes assigned to each GO term. The *z*-score is calculated as the number of up-regulated genes minus the number of down-regulated genes divided by the square root of the count (Walter et al., 2015).

## Symbiont “Typing”

In order to identify the main symbiont of the *S. pistillata* colonies kept in the aquaria system at the Centre Scientifique

<sup>1</sup><http://www.reefgenomics.org>

<sup>2</sup>[https://github.com/lyijin/topGO\\_pipeline](https://github.com/lyijin/topGO_pipeline)

<sup>3</sup>[www.genome.jp/tools/kaas/](http://www.genome.jp/tools/kaas/)

<sup>4</sup>[https://github.com/lyijin/common/blob/master/kegg\\_backgrounds/](https://github.com/lyijin/common/blob/master/kegg_backgrounds/)



de Monaco, RNA-seq data was mapped to SymPortal's (Hume et al., 2019) reference database. Briefly, SymPortal is a platform for phylogenetically resolving Symbiodiniaceae taxa using ITS2 rDNA amplicon data. Its reference database contains thousands of ITS2 sequences from taxa belonging to the seven named genera (formerly genus *Symbiodinium* containing "clades A–I"). Read counts were calculated using Kallisto and based on this, A1 (>97.5%) was determined to be the most abundant sequence in all samples (Supplementary Figure 1). Symbiodiniaceae taxa associated with a dominant ITS2 designated sequence A1 is, in turn, associated to the species definition of *S. microadriaticum* (LaJeunesse, 2001). Yet, it is noteworthy clarifying that, here, the binomial *S. microadriaticum* refers to the strain CCMP2467, which was originally isolated from *S. pistillata* from the Gulf of Aqaba and was the same symbiont strain used to sequence the genome (Aranda et al., 2016).

## Physiological Validation: Photochemical Efficiency Measurements

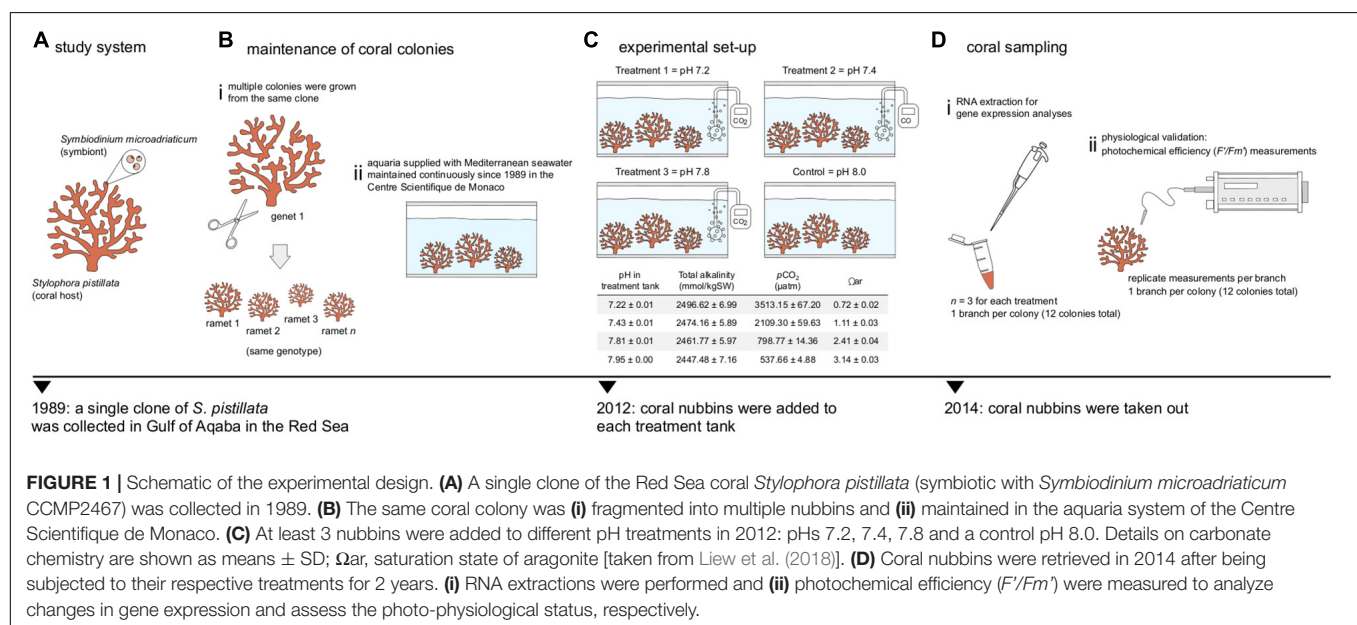
Light-acclimated yields ( $F'/F_m'$ ) were recorded in triplicate (one branch per colony and multiple measurements were taken for each branch at the same distance) with a Pulse Amplitude Modulated fluorometer (Junior-PAM, Walz, Germany) to assess the photo-physiological status of colonies at the different pH treatments (see raw data in Supplementary Table 2). Although measurements were not taken from the exact same fragments from which RNA was extracted, all colonies originated from the same coral genet (Figure 1) and phenotypes have been validated multiple times. A one-way analysis of variance (ANOVA) as implemented in R was conducted to assess the effect of pH in symbiont's photochemical efficiency. Differences were further identified through Student-Newman-Keuls (SNK) *post hoc* tests.

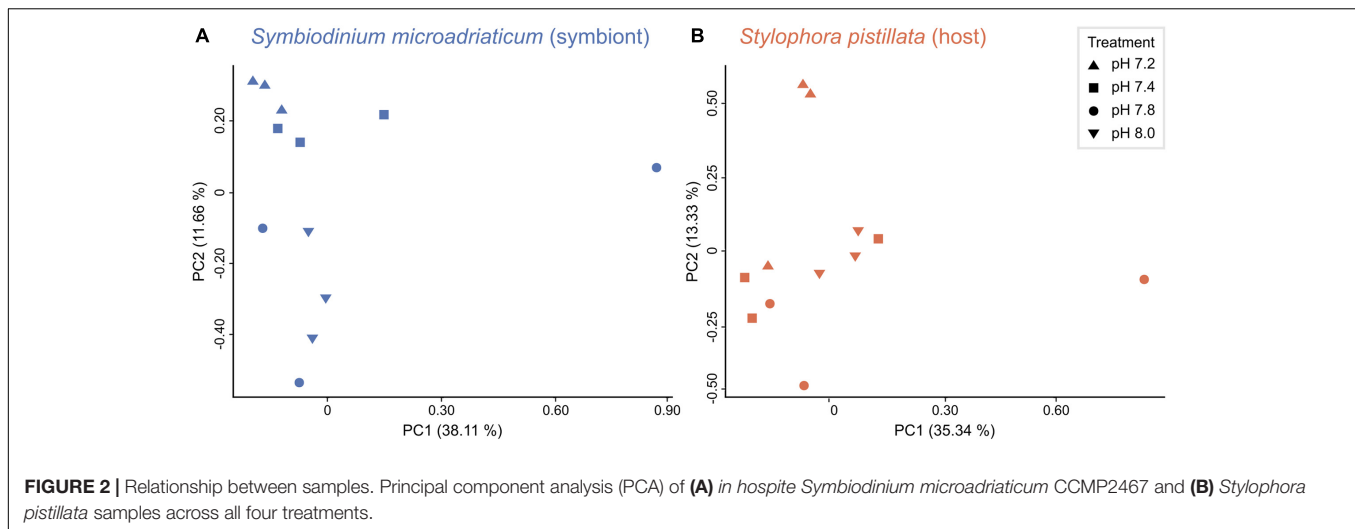
## RESULTS

Here, we investigated the *in hospite* transcriptomic response of *S. microadriaticum* in the Red Sea coral *S. pistillata* under long-term (2 years) acidification stress. Based on previous evidence showing beneficial effects from elevated  $p\text{CO}_2$  on productivity (Strahl et al., 2015; Biscéré et al., 2019), we focused on genes and processes involved in photosynthesis and carbon acquisition, which were also enriched in our differential gene expression analysis. Furthermore, we integrated the gene expression changes in the symbiont and host to assess the effect of low pH on both partners and overall response of the holobiont. Finally, we tested the conclusions from our transcriptomic analyses on the physiological level by measuring symbiont's light-acclimated photochemical yields and interpreting relevant molecular responses of the host.

## Differential Gene Expression Following Chronic Exposure to High $p\text{CO}_2$

Principal component analyses revealed that symbiont samples clustered according to treatment (Figure 2A), yet PERMANOVA tests did not show significant differences in gene expression between treatments ( $p = 0.08$ ). The opposite was true for the host (Figure 2B, PERMANOVA  $p = 0.01$ ), although no significant differences were observed among treatments (*post hoc* tests  $p > 0.05$ ). Overall, gene expression patterns revealed a weaker transcriptomic response (that is, a lower number of DEGs) to the experimental treatments for the symbiont (1,230 unique genes representing 2.50% of the transcriptome) compared to the coral host (986 unique genes corresponding to 3.80%). As expected, more differentially expressed genes (DEGs) were identified in response to the strongest treatment of pH 7.2 for both partners, followed by at least three times less DEGs in the other conditions. A total of 1,459 (964, 392 (249), and 1 (38)





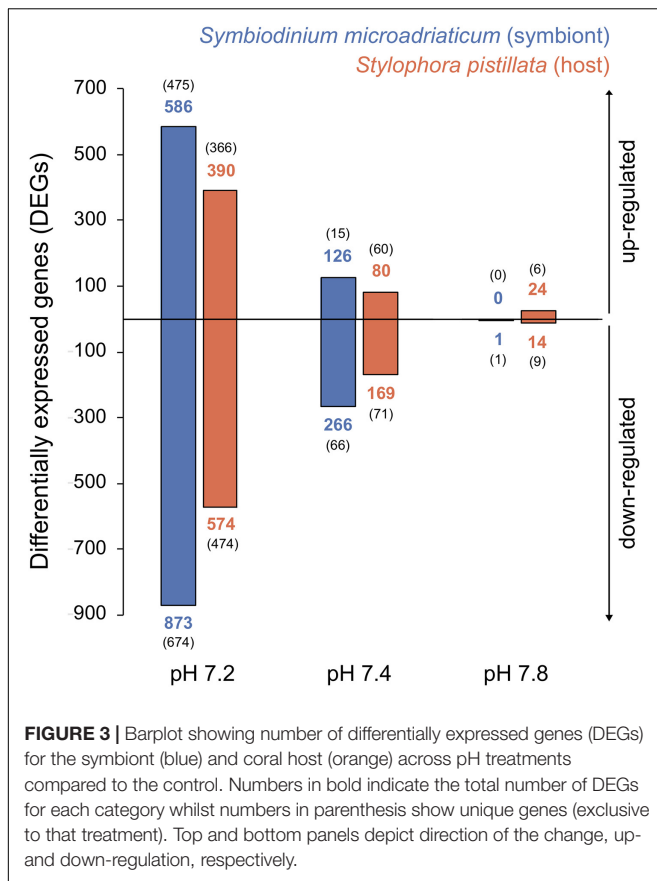
DEGs were identified for the symbiont (host) in pH 7.2, 7.4, and 7.8, respectively (Figure 3). In regard to *S. microadriaticum* CCMP2467 approximately 45% of the DEGs had  $\geq 2$ -fold change in expression (all of them up-regulated) and, again, most were observed in pH 7.2 (Figure 3). Only one DEG was identified at pH 7.8 (Smic24339), and it encoded for dimethylglycine dehydrogenase, a mitochondrial enzyme involved in pathways of degradation of amino acids and was only found in this treatment. Further, comparison of gene expression changes between pH 7.2 and 7.4 identified 310 shared DEGs, from which 111 and 199 were up- and down-regulated, respectively. Directionality of these changes was consistent across both treatments, although the magnitude of change was not. That is, 160 genes showed a higher fold change in expression in the pH 7.2 treatment whilst the remaining 150 had a lower expression compared to pH 7.4 (Supplementary Table 3). Patterns in expression for the *S. pistillata*, on the other hand (Figure 3), were similar to the symbiont's, with most genes being down-regulated (at least in pH treatments 7.2 and 7.4).

### Impact of Low pH on Specific Biological Functions: Enrichment of Genes Related to Photosynthesis and Carbon Acquisition Processes

We conducted GO and KEGG pathway enrichment analyses to further assess the functional impact of the previously identified DEGs. A total of 114 significantly enriched GO terms across all treatments were identified for *S. microadriaticum* CCMP2467 (81, 26, and 7 from pH 7.2, 7.4, and 7.8, respectively, see Supplementary Tables 4A–C). Particularly noteworthy terms (most of them underrepresented) were related to translation and transcription, regulation of metabolic processes, and cellular components (ribosome, cytoplasm and microtubule complexes, cilium, among others). We also identified a few DEGs (with  $\geq 2$ -fold change, all of them up-regulated) encoding for ion-transport activity; yet the associated GO terms were not significantly enriched.

We further focused on terms related to photosynthesis and carbon acquisition mechanisms as these have been previously reported to potentially benefit from increased CO<sub>2</sub>. Due to the lack of DEGs, we did not find any enriched GO terms for the pH 7.8 treatment, whilst at least 23 were identified for the other two conditions (Figure 4A, Supplementary Tables 4A–C). From these, most of them were predominant in pH 7.2 (21 compared to only 11 in pH 7.4) and related to photosynthesis light-harvesting proteins, the Calvin cycle and relevant enzymes (RuBisCO, transketolase and ferredoxin-NADP-reductase), as well as various cellular components and processes associated to photosystems I and II complexes. Fewer terms were associated with carbon acquisition mechanisms; most of them linked to genes encoding different subunits of the ATP synthase motor. Since pH 7.2 had the largest number of enriched GO terms, we investigated the expression changes of the genes associated with the corresponding processes (Figure 4B). A total of 172 DEGs were involved in these functional categories with most genes being over-expressed, thus suggesting an overall up-regulation of the process. Further, two of four significantly enriched KEGG pathways (Supplementary Table 5) in this treatment were related to photosynthesis (map00195) and carbon acquisition in photosynthetic organisms (map00710). DEGs involved in these pathways were mostly up-regulated with  $\geq 2$ -fold increase in expression (Supplementary Table 6).

To complement the analyses on the symbiont, we also performed a GO enrichment analyses for the transcriptional response of the host *S. pistillata*. This analysis revealed an overall enrichment of metabolic functions, RNA translational and transcriptional mechanisms, stress responses and cellular components (see Supplementary Tables 7A–C). Echoing the findings in the symbiont we also found more terms significantly enriched in the pH 7.2 treatment (167) compared to pH 7.4 (82) and pH 7.8 (94). Particularly relevant were terms related to ion activity and calcification across all treatments, but bicarbonate transport (GO:0015701) stood out (though it was only present in pH 7.2). We identified two genes (Spis16901 and Spis5056.t2) encoding for bicarbonate transporter like proteins,



and these were significantly up-regulated ( $\geq 2$ -fold change). Although not significant ( $\text{ANOVA}_{\text{Spis16901}} F = 3.023, p = 0.094$ ,  $\text{ANOVA}_{\text{Spis5056.t2}} F = 1.402, p = 0.311$ ), the absolute expression (TPM) of these genes followed the order pH 7.2 > 7.4 > 7.8 > 8.0 (Figure 5). Also interesting was the term symbiont-containing vacuole membrane (GO:0020005) present in pH 7.8, which was associated to Spis21140. This gene, which annotates for an interferon-induced guanylate-binding protein 2, was significantly over-expressed and had a 2.5-fold change in expression.

## Physiological Response to Acidification Stress

Our transcriptomic analyses showed enrichment of genes and processes involved in photosynthesis and carbon acquisition mechanisms, with most of the DEGs being significantly up-regulated. To test whether these transcriptomic changes were evident on the physiological level, we measured photosynthetic efficiency of the symbiont using Pulse-Amplitude-Modulation fluorometry. Seawater pH had a significant effect ( $\text{ANOVA } F = 7.503, p = 0.005$ ) on the photo-physiological performance ( $F'/F_m'$ ) of *S. microadriaticum* CCMP2467 (Figure 6). Specifically, lower  $F'/F_m'$  values were observed in colonies from the more acidic treatments (pH 7.2 and 7.4) compared to the control (pH 8.0) whereas no significant differences were detected for coral fragments from pH 7.8. Interestingly, however, is that photochemical yields dropped significantly from pH 7.8

to pH 7.4 (mean value  $\pm$  SD, from  $0.5 \pm 0.02$  to  $0.4 \pm 0.02$ ) but remained stable between pH 7.4 and pH 7.2 (mean  $\pm$  SD,  $0.4 \pm 0.02$  and  $0.4 \pm 0.03$ , respectively).

## DISCUSSION

### Responses of Coral Holobionts to OA Vary Greatly

Transcriptome sequencing has become a powerful tool for understanding the mechanistic underpinnings of coral resilience to environmental change by allowing the identification of genes and/or pathways that are specifically associated with stress responses (reviewed in Cziesselski et al., 2019; Strader et al., 2020). However, most studies have focused on the coral host and it was not until recently that changes in gene expression following exposure to high temperature and/or CO<sub>2</sub> levels have also been examined in their algal symbionts (Kenkel and Matz, 2016; González-Pech et al., 2017; Davies et al., 2018; Kenkel et al., 2018; Rivest et al., 2018), thus providing a more complete view of the holobiont responses. Indeed, both partners exhibit differential transcriptomic changes; some studies have shown that the host elicits a stronger response (up to five times) (Kaniewska et al., 2015; Kenkel and Matz, 2016; Davies et al., 2018) whereas others have found greater effects on the symbiont (Kenkel et al., 2018; Rivest et al., 2018). The magnitude of the response to different stressors also varies greatly. Generally speaking, warming, alone or in combination with acidification, has a larger effect on gene expression than just OA (Rocker et al., 2015; Davies et al., 2016, 2018; Rivest et al., 2018). For example, Davies et al. (2016) found almost 25% of the holobiont meta-transcriptome to be differentially expressed in response to temperature stress whilst less than 2% was attributed to elevated pCO<sub>2</sub>. Similarly, minimal (or no) transcriptomic responses to low seawater pH (close to RCP8.5 scenarios) have also been reported (Vidal-Dupiol et al., 2013; Kaniewska et al., 2015; González-Pech et al., 2017). Hence, it is not surprising that in our study, changes in expression only accounted for a small fraction of the transcriptome of both symbiont and host. Furthermore, the transcriptional responses to acute stress and chronic stress differ substantially (reviewed in Strader et al., 2020). An initial response to acute stress generally invokes greater changes in gene expression as a mean to regain homeostasis, whereas long-term chronic stress exposure implies that acclimation has already occurred and transcriptional changes are limited to processes necessary to maintain homeostasis (via up-/down-regulation of certain genes, for example).

Numerous studies have reported mixed findings on the effects of high pCO<sub>2</sub> on the photo-physiology of symbiotic cnidarians. For example, acidification stress has been shown to increase productivity, symbiont density and photochemical efficiency in non-calcifying anthozoans (Suggett et al., 2012; Towanda and Thuesen, 2012; Jarrold et al., 2013; Gibbin and Davy, 2014; Horwitz et al., 2015; Klein et al., 2017) but the opposite in corals (Anthony et al., 2008; Crawley et al., 2010; Edmunds, 2012; Kaniewska et al., 2012; Zhou et al., 2016), and in fewer cases, no significant effects have been observed

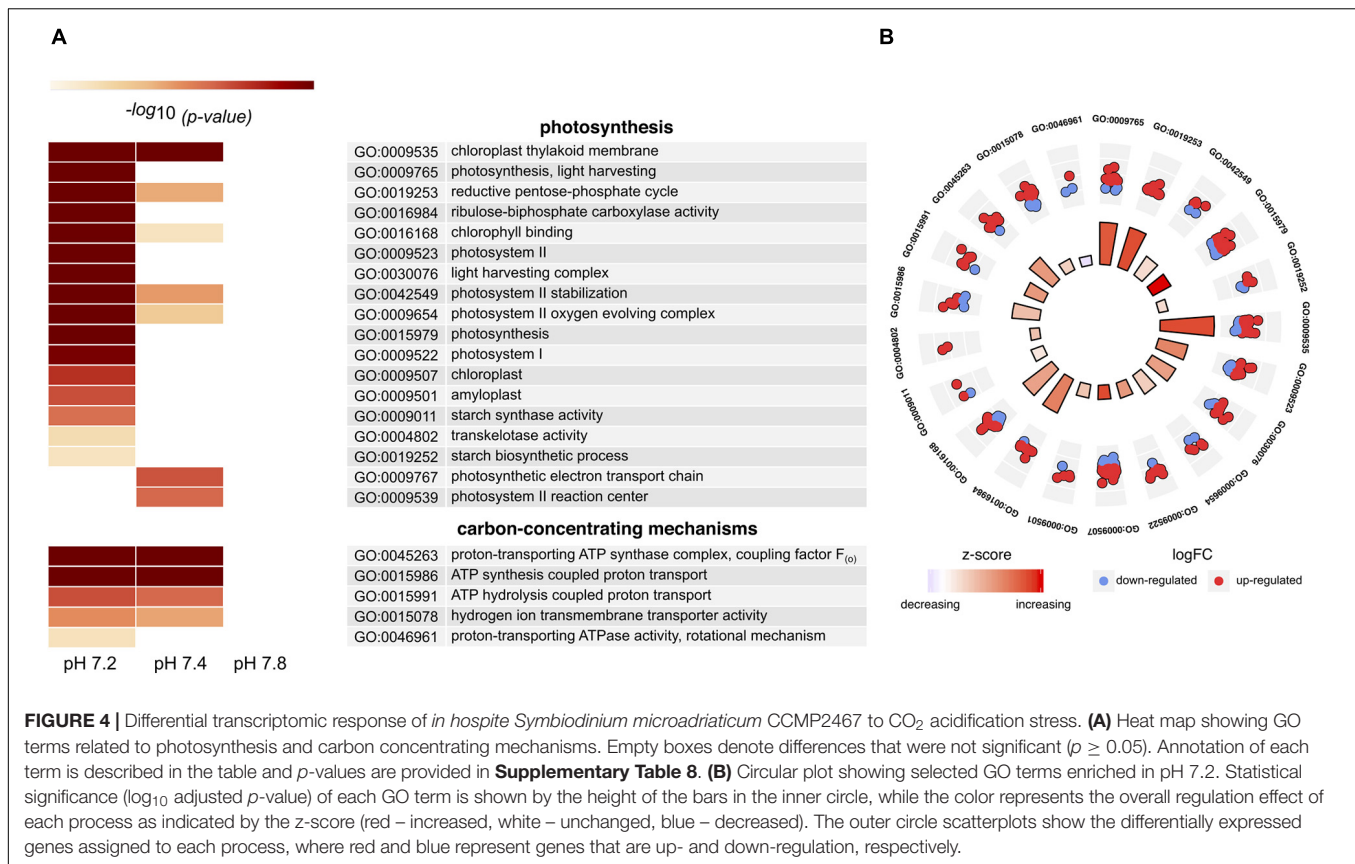


**FIGURE 4 |** Differential transcriptomic response of *in hospite* *Symbiodinium microadriaticum* CCMP2467 to CO<sub>2</sub> acidification stress. **(A)** Heat map showing GO terms related to photosynthesis and carbon concentrating mechanisms. Empty boxes denote differences that were not significant ( $p \geq 0.05$ ). Annotation of each term is described in the table and  $p$ -values are provided in **Supplementary Table 8**. **(B)** Circular plot showing selected GO terms enriched in pH 7.2. Statistical significance ( $\log_{10}$  adjusted  $p$ -value) of each GO term is shown by the height of the bars in the inner circle, while the color represents the overall regulation effect of each process as indicated by the Z-score (red – increased, white – unchanged, blue – decreased). The outer circle scatterplots show the differentially expressed genes assigned to each process, where red and blue represent genes that are up- and down-regulation, respectively.

(Wall et al., 2014; Tambutté et al., 2015; Davies et al., 2018). Certainly, the intertwined interaction between photosynthesis and calcification (Furla et al., 2000) might be key for determining how and to what extent OA will affect corals. Indeed, while OA has been shown to be detrimental to adult coral colonies (see above), contrasting responses have been observed in young recruits and larvae. For example, Jiang et al. (2019, 2020) found a positive photochemical response to OA along with enhanced symbiont CCMs in *Pocillopora* recruits and greater productivity in larvae. Finally, parabolic responses of photosynthetic processes to acidification stress have also been documented (Crawley et al., 2010; Castillo et al., 2014). Different  $p\text{CO}_2$  levels and the diverse CMMs of symbionts (Buxton et al., 2009; Brading et al., 2011) may contribute to these variable and contrasting responses. Finally, responses to acidification stress are not only symbiont strain-specific (Buxton et al., 2009; Brading et al., 2011) but may also differ depending on whether they are free-living or *in hospite* different hosts (see above).

## Coral Symbionts Acclimate to OA by Fine-Tuning Gene Expression and Photo-Physiology

This study provides novel insights into coral acclimation to OA by integrating the findings presented here with previously published data (Tambutté et al., 2015; Liew et al., 2018) that support our interpretation of the results. Although we did not

find significant differences in expression levels across treatments for the symbiont, there were still a number of genes that were significantly differentially expressed and biologically meaningful. Most of the changes in gene expression we observed here were associated with homeostasis and regulation of metabolic functions; yet we were particularly interested in those involved in photosynthesis and carbon-concentrating mechanisms (CCMs). These processes are essential for holobiont functioning but also different from the other biological processes in that they could potentially benefit from increased  $p\text{CO}_2$ . Over-expression of genes encoding for different cellular components critical for the photosynthetic machinery was common in both extreme treatments (pH 7.2 and pH 7.4); specifically, polypeptide subunits of photosystems, light-harvesting and oxygen-evolving complex proteins responsible for enhancing recruitment and functioning of PS II and several enzymes necessary for photosynthesis. Enrichment of  $\text{H}^+$  transporter genes were also observed; in particular, a vacuolar  $\text{H}^+$  ATPase (VHA) proton-pump essential to promote photosynthesis as it catalyzes ATP hydrolysis and lowers pH in the symbiosome (Barott et al., 2015). Indeed, inhibition of this transmembrane protein can result in reduced photosynthetic activity (Barott et al., 2015). Moreover, up-regulation of proton-pumps from the symbiont but also bicarbonate transporter-like proteins from the coral in response to acidification stress suggests that the holobiont might be trying to compensate and/or maintain the internal pH gradient necessary to support nutrient exchange



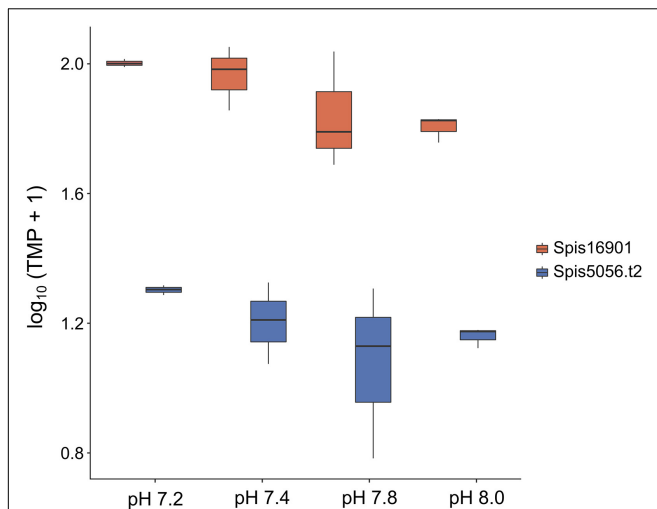


**FIGURE 5 |** Absolute gene expression (transcripts per million) of two *Stylophora pistillata* genes encoding for bicarbonate transporter-like proteins across pH treatments. Although expression of these genes was not significantly different among conditions (ANOVA<sub>Spis16901</sub>  $F = 3.023$ ,  $p = 0.094$ , ANOVA<sub>Spis5056.t2</sub>  $F = 1.402$ ,  $p = 0.311$ ), it followed the order pH 7.2 > 7.4 > 7.8 > 8.0.

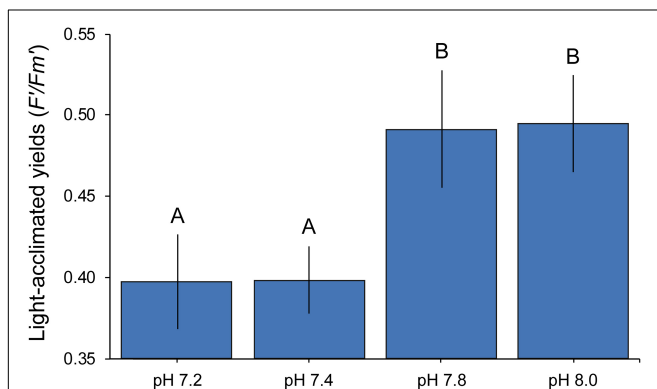


**FIGURE 6 |** Mean ( $\pm 1$  SE) photochemical efficiencies of *Symbiodinium microadriaticum* CCMP2467 across pH treatments. Letters indicate overall similarities (e.g., AA) or differences (e.g., AB) between treatments as determined by SNK *post hoc* tests.

between partners (Barott et al., 2015). Bicarbonate transporters are, in turn, important for the host as these not only play a role in biomineralization but also in homeostatic control of metabolic processes (Zoccola et al., 2015). Previous evidence even suggests that these transporters may play an important role in coral resilience to acidification (Zoccola et al., 2015), thus contributing to the notion that changes in their expression might be indeed an acclimation mechanism of the host to different water chemistries.

Neither host carbonic anhydrases nor solute carrier (specifically SLC4 and SLC26) genes were differentially expressed in any of the treatments, which was initially surprising because these have been shown to be significantly up-regulated in corals subjected to only few weeks of acidification stress (Vidal-Dupiol et al., 2013) (but see above for the effect of exposure time in

expression levels). Both play a major role in CCMs; carbonic anhydrases move carbon from the seawater environment across multiple layers into the symbiont cell whilst SLCs are responsible for transporting  $\text{HCO}_3^-$  and other ions, however, the main role of these specific transporters might be the provision of bicarbonate to the calcification process (Zoccola et al., 2015). Significant enrichment of symbiont-containing vacuole membrane (which here may refer to the host-derived symbiosome) further highlights the effect of elevated  $p\text{CO}_2$  on the holobiont CCMs. Acidification of this intracellular compartment is essential for promoting photosynthesis (Barott et al., 2015) and damage and/or disruption of its cellular components and functions could have a negative impact on host-symbiont communication and metabolic exchange. Indeed, a gene encoding for guanylate-binding proteins, previously associated with resistance to intracellular pathogenic microbes (Haldar et al., 2013), was significantly over-expressed. This might suggest the host's immune response is compromised and secretion of this protein increases as a compensation measure.

Despite previous evidence for beneficial effects from elevated  $p\text{CO}_2$ , often reflected by enhanced productivity (Strahl et al., 2015; Biscéré et al., 2019) and here seen as an enrichment of processes related to photosynthesis and carbon acquisition, our findings suggest that this might be instead an acclimation response of the holobiont to OA. For example, although here we observed significant declines in the operating efficiency of PS II ( $F'/Fm'$ ), gross photosynthesis rates (as previously reported in Tambutté et al., 2015 for the same coral genet used in this study) have been noted to remain unchanged. Discrepancy between these two measurements has been observed before (Briggs and Carpenter, 2019); multiple aspects of photo-physiology may indeed respond differently to acidification stress with potentially contrasting consequences for photosynthetic performance. The expression of specific proteins and/or maintenance of enzymes related to photo-physiology may be altered, and though this might not influence photosynthesis rates, it could have a significant effect at the cellular level. Protein turnover is particularly important for photosynthesis as it allows repairing damage to the PS II (Han, 2002; Briggs and Carpenter, 2019), thus changes in protein metabolism can eventually lead to a reduction in photochemical efficiency. Indeed, here we observed changes in expression of protein metabolism related functions (most of them depleted) such as protein transport (GO:0015031), intracellular protein transport (GO:0006886), ubiquitin protein ligase binding (GO:0031625) and protein autoubiquitination (GO:0051865), among others.

Other physiological measurements like respiration rates, symbiont densities and protein content were not affected either (also reported in Tambutté et al., 2015). Thus, suggesting that although the overall performance of the holobiont is not (seriously) compromised, the ability of this particular host-symbiont association to maintain carbon fluxes might be affected by OA. The latter because photosynthesis and respiration depend on the availability of dissolved inorganic carbon (Furla et al., 2000; Nakamura et al., 2013) so that

more substrate should theoretically enhance both processes; higher CO<sub>2</sub> fixation during photosynthesis results in increased oxygen production and thus stimulating respiration (Reece et al., 2015). Though this only holds true if the process is CO<sub>2</sub>-limited; otherwise, an increase in CO<sub>2</sub> will not affect oxygen fluxes as the system is already working at maximum capacity. Another possibility to consider is that CO<sub>2</sub> might not be efficiently acquired. This is surprising, however, since *S. microadriaticum* CCMP2467 in particular is known to have many more bicarbonate transporter domains than other symbiotic dinoflagellates (Aranda et al., 2016). As such, one would assume that it is more efficient in mobilizing HCO<sub>3</sub><sup>−</sup> across membranes. Nonetheless, it could also be that CCMs in this symbiont are mainly supported by the uptake of CO<sub>2</sub> and not HCO<sub>3</sub><sup>−</sup>, as it is the case for *S. necroappetens* (formally known as *Symbiodinium* A13; LaJeunesse et al., 2015) (Brading et al., 2013), for example. Thus, having more bicarbonate transporters might not necessarily improve carbon transport for photosynthesis. Further, CCMs are active, energy-consuming processes (Leggat et al., 1999) thus if the host is challenged in any way (see above), these can become less efficient and therefore limiting, independent of the symbionts ability to assimilate CO<sub>2</sub>.

## Methodological Considerations

We are cautious when interpreting the effect of pH on gene expression (i.e., PERMANOVA tests to assess differences between treatments) as low statistical power (because of low sample size) can negatively affect the likelihood that a statistically significant finding actually reflects a true effect. Ideally, more samples (i.e., coral nubbins) from different genotypes in each condition should be examined. Yet, this dataset was already published by Liew et al. (2018), who investigated the epigenetic mechanisms underlying OA stress responses (and thus used samples with the same genetic background in order to compare across treatments). Here, we simply provide initial transcriptomic observations of a coral endosymbiont to OA with respect to photosynthesis. This study adds to the growing body of work investigating how different marine organisms respond to OA. Similar efforts on this and other coral-Symbiodiniaceae pairings will eventually reveal the extent at which our findings can be generalized.

Finally, it is also worth noting that, as well as with other environmental factors (e.g., temperature and nutrients), light availability plays an important role in regulating calcification and photosynthetic processes under elevated *p*CO<sub>2</sub> (Suggett et al., 2013). Specifically, it has been shown that corals under low light growth conditions exhibit greater OA-induced calcification loss and lower gross photosynthesis rates. Since the light intensity used in this study (170 μmol photons/m<sup>2</sup>s) is similar to the one (100 μmol photons/m<sup>2</sup>s) tested by Suggett et al. (2013), it is fair to consider the possibility that even if *Symbiodinium* has the capacity to use CO<sub>2</sub> at lower pH, photosynthesis might have not been increased because of the low light. Under low light conditions, photo-acclimation processes that facilitate light harvesting also require protein production and maintenance which, as discussed

above, is negatively affected by OA (Briggs and Carpenter, 2019). This might explain the increasingly detrimental effects on photochemical efficiency as pH decreases. OA studies should then better account for the potential moderating role of light on elevated *p*CO<sub>2</sub> as together they clearly alter the energetic budgets and resource allocation among photosynthetic processes (Suggett et al., 2013; Briggs and Carpenter, 2019).

## CONCLUSION

Here, we present an overview of the *in hospite* transcriptomic response of a common coral symbiont exposed to different seawater pH conditions. This study together with Kenkel et al. (2018) are, to our knowledge, the only ones examining changes in expression patterns under long-term CO<sub>2</sub> acidification stress. Their contrasting findings, as they did not show differential expression of any gene related to photosynthesis nor carbon acquisition mechanisms, further highlight the importance of investigating different host-symbiont pairings to better understand the effects of OA on corals. Certainly, host and symbiont genetics (and the interaction between both) play a major role in gene expression in response to stress (Parkinson et al., 2015; Czieleski et al., 2019; Strader et al., 2020) such that conclusions based on this experiment may only be applicable to the host-symbiont combination in question and care should be taken in extrapolating this response to other coral-Symbiodiniaceae assemblages. In summary, our data suggest that, despite the existing hypothesis that elevated CO<sub>2</sub> benefits photosynthetic organisms, here, up-regulation of genes involved in photosynthesis processes might be an acclimation response to OA stress experienced by the host (and thus (indirectly) by the symbiont) and not a beneficial effect. Indeed, we show a significant drop in photochemical yields with increasing *p*CO<sub>2</sub>, which in turn demonstrates the extent of symbiont photo-acclimation that operates in response to a changing environment (reviewed in Nitschke et al., 2018). The implications of these changes under extended acidification stress and the effect this may have on symbiotic interactions is complex and thus warrants further study, especially since responses vary greatly among different host-symbiont combinations.

## DATA AVAILABILITY STATEMENT

All sequencing data from this study has been deposited in NCBI (<https://www.ncbi.nlm.nih.gov/bioproject/PRJNA386774>; Liew et al., 2018).

## AUTHOR CONTRIBUTIONS

MA and GC conceived and coordinated this project. MA, YL, AV, ET, DZ, and ST provided tools, reagents, and data.

AV and ET performed the experiments. MH and GC analyzed expression data. MH wrote the manuscript with help from MA. All authors read and approved the final manuscript.

## FUNDING

This study was based on work supported by the KAUST Office of Sponsored Research under award no. FCC/1/1973-22-01 and the Centre Scientifique de Monaco Research Program, which is supported by the Government of the Principality of Monaco.

## REFERENCES

- Alexa, A., Rahnenführer, J., and Lengauer, T. (2006). Improved scoring of functional groups from gene expression data by decorrelating GO graph structure. *Bioinformatics* 22, 1600–1607. doi: 10.1093/bioinformatics/btl140
- Al-Moghrabi, S., Goiran, C., Allemand, D., Speziale, N., and Jaubert, J. (1996). Inorganic carbon uptake for photosynthesis by the symbiotic coral-dinoflagellate association II. Mechanisms for bicarbonate uptake. *J. Exp. Mar. Biol. Ecol.* 199, 227–248. doi: 10.1016/0022-0981(95)00202-2
- Andersson, A. J., and Gledhill, D. (2013). Ocean acidification and coral reefs: effects on breakdown, dissolution, and net ecosystem calcification. *Annu. Rev. Mar. Sci.* 5, 321–348. doi: 10.1146/annurev-marine-121211-172241
- Anthony, K. R. N., Kline, D. I., Diaz-Pulido, G., Dove, S., and Hoegh-Guldberg, O. (2008). Ocean acidification causes bleaching and productivity loss in coral reef builders. *Proc. Natl. Acad. Sci. U.S.A.* 105:17442. doi: 10.1073/pnas.0804478105
- Aranda, M., Li, Y., Liew, Y. J., Baumgarten, S., Simakov, O., Wilson, M. C., et al. (2016). Genomes of coral dinoflagellate symbionts highlight evolutionary adaptations conducive to a symbiotic lifestyle. *Sci. Rep.* 6:39734.
- Barott, K. L., Venn, A. A., Perez, S. O., Tambutté, S., and Tresguerres, M. (2015). Coral host cells acidify symbiotic algal microenvironment to promote photosynthesis. *Proc. Natl. Acad. Sci. U.S.A.* 112, 607–612. doi: 10.1073/pnas.1413483112
- Biscéré, T., Zampighi, M., Lorrain, A., Jurriaans, S., Foggo, A., Houlbrèque, F., et al. (2019). High pCO<sub>2</sub> promotes coral primary production. *Biol. Lett.* 15:20180777. doi: 10.1098/rsbl.2018.0777
- Brading, P., Warner, M. E., Davey, P., Smith, D. J., Achterberg, E. P., and Suggett, D. J. (2011). Differential effects of ocean acidification on growth and photosynthesis among phylotypes of *Symbiodinium* (Dinophyceae). *Limnol. Oceanogr.* 56, 927–938. doi: 10.4319/lo.2011.56.3.0927
- Brading, P., Warner, M. E., Smith, D. J., and Suggett, D. J. (2013). Contrasting modes of inorganic carbon acquisition amongst *Symbiodinium* (Dinophyceae) phylotypes. *New Phytol.* 200, 432–442. doi: 10.1111/nph.12379
- Bray, N. L., Pimentel, H., Melsted, P., and Pachter, L. (2016). Near-optimal probabilistic RNA-seq quantification. *Nat. Biotechnol.* 34:525. doi: 10.1038/nbt.3525
- Briggs, A. A., and Carpenter, R. C. (2019). Contrasting responses of photosynthesis and photochemical efficiency to ocean acidification under different light environments in a calcifying alga. *Sci. Rep.* 9:3986. doi: 10.1038/s41598-019-40620-8
- Buxton, L., Badger, M., and Ralph, P. (2009). Effects of moderate heat stress and dissolved inorganic carbon concentration on photosynthesis and respiration of *Symbiodinium* sp. (Dinophyceae) in culture and in symbiosis. *J. Phycol.* 45, 357–365. doi: 10.1111/j.1529-8817.2009.00659.x
- Castillo, K. D., Ries, J. B., Bruno, J. F., and Westfield, I. T. (2014). The reef-building coral *Siderastrea siderea* exhibits parabolic responses to ocean acidification and warming. *Proc. R. Soc. B Biol. Sci.* 281:20141856. doi: 10.1098/rspb.2014.1856
- Chan, N. C., and Connolly, S. R. (2013). Sensitivity of coral calcification to ocean acidification: a meta-analysis. *Glob. Chang. Biol.* 19, 282–290.
- Cohen, I., and Dubinsky, Z. (2015). Long term photoacclimation responses of the coral *Stylophora pistillata* to reciprocal deep to shallow transplantation: photosynthesis and calcification. *Front. Mar. Sci.* 2:45. doi: 10.3389/fmars.2015.00045

## ACKNOWLEDGMENTS

We thank D. Desgre, N. Caminiti-Secondo, and N. Techer for assistance in coral husbandry as well as the KAUST Sequencing Core Facility for the sequencing of the libraries.

## SUPPLEMENTARY MATERIAL

The Supplementary Material for this article can be found online at: <https://www.frontiersin.org/articles/10.3389/fmars.2021.666510/full#supplementary-material>

- Connell, S. D., Doubleday, Z. A., Foster, N. R., Hamlyn, S. B., Harley, C. D. G., Helmuth, B., et al. (2018). The duality of ocean acidification as a resource and a stressor. *Ecology* 99, 1005–1010. doi: 10.1002/ecy.2209
- Connell, S. D., Doubleday, Z. A., Hamlyn, S. B., Foster, N. R., Harley, C. D. G., Helmuth, B., et al. (2017). How ocean acidification can benefit calcifiers. *Curr. Biol.* 27, R95–R96. doi: 10.1016/j.cub.2016.12.004
- Crawley, A., Kline, D. I., Dunn, S., Anthony, K., and Dove, S. (2010). The effect of ocean acidification on symbiont photorespiration and productivity in *Acropora formosa*. *Glob. Chang. Biol.* 16, 851–863. doi: 10.1111/j.1365-2486.2009.01943.x
- Cziesielski, M. J., Schmidt-Roach, S., and Aranda, M. (2019). The past, present, and future of coral heat stress studies. *Ecol. Evol.* 9, 10055–10066. doi: 10.1002/ece3.5576
- Davies, S. W., Marchetti, A., Ries, J. B., and Castillo, K. D. (2016). Thermal and pCO<sub>2</sub> stress elicit divergent transcriptomic responses in a resilient coral. *Front. Mar. Sci.* 3:112. doi: 10.3389/fmars.2016.00112
- Davies, S. W., Ries, J. B., Marchetti, A., and Castillo, K. D. (2018). *Symbiodinium* functional diversity in the Coral *Siderastrea siderea* is influenced by thermal stress and reef environment, but not ocean acidification. *Front. Mar. Sci.* 5:150. doi: 10.3389/fmars.2018.00150
- Doney, S. C., Fabry, V. J., Feely, R. A., and Kleypas, J. A. (2009). Ocean acidification: the other CO<sub>2</sub> problem. *Annu. Rev. Mar. Sci.* 1, 169–192. doi: 10.1146/annurev.marine.010908.163834
- Dutkiewicz, S., Morris, J. J., Follows, M. J., Scott, J., Levitan, O., Dyhrman, S. T., et al. (2015). Impact of ocean acidification on the structure of future phytoplankton communities. *Nat. Clim. Chang.* 5:1002.
- Edmunds, P. J. (2012). Effect of pCO<sub>2</sub> on the growth, respiration, and photophysiology of massive *Porites* spp. in Moorea, French Polynesia. *Mar. Biol.* 159, 2149–2160. doi: 10.1007/s00227-012-2001-y
- Ferrier-Pages, C., Witting, J., Tambutté, E., and Sebens, K. P. (2003). Effect of natural zooplankton feeding on the tissue and skeletal growth of the scleractinian coral *Stylophora pistillata*. *Coral Reefs* 22, 229–240. doi: 10.1007/s00338-003-0312-7
- Franklin, O. H. G., Jones, R. J., and Berges, J. A. (2004). Cell death and degeneration in the symbiotic dinoflagellates of the coral *Stylophora pistillata* during bleaching. *Mar. Ecol. Prog. Ser.* 272, 117–130.
- Furla, P., Galgani, I., Durand, I., and Allemand, D. (2000). Sources and mechanisms of inorganic carbon transport for coral calcification and photosynthesis. *J. Exp. Biol.* 203:3445.
- Gibbin, E. M., and Davy, S. K. (2014). The photo-physiological response of a model cnidarian–dinoflagellate symbiosis to CO<sub>2</sub>-induced acidification at the cellular level. *J. Exp. Mar. Biol. Ecol.* 457, 1–7. doi: 10.1016/j.jembe.2014.03.015
- González-Pech, R. A., Vargas, S., Francis, W. R., and Wörheide, G. (2017). Transcriptomic resilience of the *Montipora digitata* holobiont to low pH. *Front. Mar. Sci.* 4:403. doi: 10.3389/fmars.2017.00403
- Haldar, A. K., Saka, H. A., Piro, A. S., Dunn, J. D., Henry, S. C., Taylor, G. A., et al. (2013). IRG and GBP host resistance factors target aberrant, “Non-Self” vacuoles characterized by the missing of “Self” IRGM proteins. *PLoS Pathog.* 9:e1003414. doi: 10.1371/journal.ppat.1003414
- Hall-Spencer, J. M., Rodolfo-Metalpa, R., Martin, S., Ransome, E., Fine, M., Turner, S. M., et al. (2008). Volcanic carbon dioxide vents show ecosystem effects of ocean acidification. *Nature* 454, 96–99. doi: 10.1038/nature07051



- Han, B.-P. (2002). A mechanistic model of algal photoinhibition induced by photodamage to photosystem-II. *J. Theor. Biol.* 214, 519–527. doi: 10.1006/jtbi.2001.2468
- Hoadley, K. D., Pettay, D. T., Grottoli, A. G., Cai, W.-J., Melman, T. F., Schoepf, V., et al. (2015a). Physiological response to elevated temperature and pCO<sub>2</sub> varies across four Pacific coral species: understanding the unique host+symbiont response. *Sci. Rep.* 5:18371. doi: 10.1038/srep18371
- Hoadley, K. D., Rollison, D., Pettay, D. T., and Warner, M. E. (2015b). Differential carbon utilization and asexual reproduction under elevated pCO<sub>2</sub> conditions in the model anemone, *Exaiptasia pallida*, hosting different symbionts. *Limnol. Oceanogr.* 60, 2108–2120. doi: 10.1002/lno.10160
- Hoegh-Guldberg, O., Mumby, P. J., Hooten, A. J., Steneck, R. S., Greenfield, P., Gomez, E., et al. (2007). Coral reefs under rapid climate change and ocean acidification. *Science* 318:1737. doi: 10.1126/science.1152509
- Hoegh-Guldberg, O., Poloczanska, E. S., Skirving, W., and Dove, S. (2017). Coral reef ecosystems under climate change and ocean acidification. *Front. Mar. Sci.* 4:158. doi: 10.3389/fmars.2017.00158
- Hofmann, G. E., Barry, J. P., Edmunds, P. J., Gates, R. D., Hutchins, D. A., Klinger, T., et al. (2010). The effect of ocean acidification on calcifying organisms in marine ecosystems: an organism-to-ecosystem perspective. *Annu. Rev. Ecol. Syst.* 41, 127–147. doi: 10.1146/annurev.ecolsys.110308.120227
- Horwitz, R., Borell, E. M., Yam, R., Shemesh, A., and Fine, M. (2015). Natural high pCO<sub>2</sub> increases autotrophy in *Anemonia viridis* (Anthozoa) as revealed from stable isotope (C, N) analysis. *Sci. Rep.* 5:8779.
- Hughes, T. P., Barnes, M. L., Bellwood, D. R., Cinner, J. E., Cumming, G. S., Jackson, J. B. C., et al. (2017). Coral reefs in the Anthropocene. *Nature* 546:82.
- Hume, B. C. C., Smith, E. G., Ziegler, M., Warrington, H. J. M., Burt, J. A., LaJeunesse, T. C., et al. (2019). SymPortal: a novel analytical framework and platform for coral algal symbiont next-generation sequencing ITS2 profiling. *Mol. Ecol. Resour.* 19, 1063–1080. doi: 10.1111/1755-0998.13004
- Jarrod, M. D., Calosi, P., Verberk, W. C. E. P., Rastrick, S. P. S., Atfield, A., and Spicer, J. I. (2013). Physiological plasticity preserves the metabolic relationship of the intertidal non-calcifying anthozoan-*Symbiodinium* symbiosis under ocean acidification. *J. Exp. Mar. Biol. Ecol.* 449, 200–206. doi: 10.1016/j.jembe.2013.09.013
- Jiang, L., Guo, M.-L., Zhang, F., Zhang, Y.-Y., Zhou, G.-W., Lei, X.-M., et al. (2020). Impacts of elevated temperature and pCO<sub>2</sub> on the brooded larvae of *Pocillopora damicornis* from Luhuitou Reef, China: evidence for local acclimatization. *Coral Reefs* 39, 331–344. doi: 10.1007/s00338-020-01894-x
- Jiang, L., Guo, Y.-J., Zhang, F., Zhang, Y.-Y., McCook, L. J., Yuan, X.-C., et al. (2019). Diurnally fluctuating pCO<sub>2</sub> modifies the physiological responses of coral recruits under ocean acidification. *Front. Physiol.* 9:1952. doi: 10.3389/fphys.2018.01952
- Kaniewska, P., Campbell, P. R., Kline, D. I., Rodriguez-Lanetty, M., Miller, D. J., Dove, S., et al. (2012). Major cellular and physiological impacts of ocean acidification on a reef building coral. *PLoS One* 7:e34659. doi: 10.1371/journal.pone.0034659
- Kaniewska, P., Chan, C.-K. K., Kline, D., Ling, E. Y. S., Rosic, N., Edwards, D., et al. (2015). Transcriptomic changes in coral holobionts provide insights into physiological challenges of future climate and ocean change. *PLoS One* 10:e0139223. doi: 10.1371/journal.pone.0139223
- Kenkel, C. D., and Matz, M. V. (2016). Gene expression plasticity as a mechanism of coral adaptation to a variable environment. *Nat. Ecol. Evol.* 1:0014. doi: 10.1038/s41559-016-0014
- Kenkel, C. D., Moya, A., Strahl, J., Humphrey, C., and Bay, L. K. (2018). Functional genomic analysis of corals from natural CO<sub>2</sub>-seeps reveals core molecular responses involved in acclimatization to ocean acidification. *Glob. Chang. Biol.* 24, 158–171. doi: 10.1111/gcb.13833
- Keshavmurthy, S., Yang, S.-Y., Alamaru, A., Chuang, Y.-Y., Pichon, M., Obura, D., et al. (2013). DNA barcoding reveals the coral “laboratory-rat”, *Stylophora pistillata* encompasses multiple identities. *Sci. Rep.* 3:1520. doi: 10.1038/srep01520
- Klein, S. G., Pitt, K. A., Nitschke, M. R., Goyen, S., Welsh, D. T., Suggett, D. J., et al. (2017). *Symbiodinium* mitigate the combined effects of hypoxia and acidification on a noncalcifying cnidarian. *Glob. Chang. Biol.* 23, 3690–3703. doi: 10.1111/gcb.13718
- Kroeker, K. J., Kordas, R. L., Crim, R., Hendriks, I. E., Ramajo, L., Singh, G. S., et al. (2013). Impacts of ocean acidification on marine organisms: quantifying sensitivities and interaction with warming. *Glob. Chang. Biol.* 19, 1884–1896. doi: 10.1111/gcb.12179
- Kroeker, K. J., Kordas, R. L., Crim, R. N., and Singh, G. G. (2010). Meta-analysis reveals negative yet variable effects of ocean acidification on marine organisms. *Ecol. Lett.* 13, 1419–1434. doi: 10.1111/j.1461-0248.2010.01518.x
- LaJeunesse, T. C. (2001). Investigating the biodiversity, ecology, and phylogeny of endosymbiotic dinoflagellates in the genus *Symbiodinium* using the ITS region: in search of a “species” level marker. *J. Phycol.* 37, 866–880.
- LaJeunesse, T. C., Lee, S. Y., Gil-Agudelo, D. L., Knowlton, N., and Jeong, H. J. (2015). *Symbiodinium necroaappetens* sp. nov. (Dinophyceae): an opportunist ‘zooxanthella’ found in bleached and diseased tissues of Caribbean reef corals. *Eur. J. Phycol.* 50, 223–238. doi: 10.1080/09670262.2015.1025857
- LaJeunesse, T. C., Parkinson, J. E., Gabrielson, P. W., Jeong, H. J., Reimer, J. D., Woolstar, C. R., et al. (2018). Systematic revision of symbiodiniaceae highlights the antiquity and diversity of coral endosymbionts. *Curr. Biol.* 28, 2570.e6–2580.e6. doi: 10.1016/j.cub.2018.07.008
- Leggat, W., Badger, M. R., and Yellowlees, D. (1999). Evidence for an inorganic carbon-concentrating mechanism in the symbiotic dinoflagellate *Symbiodinium* sp. *Plant Physiol.* 121, 1247–1256. doi: 10.1104/pp.121.4.1247
- Liew, Y. J., Zoccola, D., Li, Y., Tambutti, E., Venn, A. A., Michell, C. T., et al. (2018). Epigenome-associated phenotypic acclimatization to ocean acidification in a reef-building coral. *Sci. Adv.* 4:eaar8028. doi: 10.1126/sciadv.aar8028
- Mackey, K. R. M., Morris, J. J., Morel, F. M. M., and Kranz, S. A. (2015). Response of photosynthesis to ocean acidification. *Oceanography* 28, 74–91.
- Magnan, A. K., Colombier, M., Billé, R., Joos, F., Hoegh-Guldberg, O., Pörtner, H.-O., et al. (2016). Implications of the Paris agreement for the ocean. *Nat. Clim. Chang.* 6:732.
- Maor-Landaw, K., Karako-Lampert, S., Ben-Asher, H. W., Goffredo, S., Falini, G., Dubinsky, Z., et al. (2014). Gene expression profiles during short-term heat stress in the red sea coral *Stylophora pistillata*. *Glob. Chang. Biol.* 20, 3026–3035. doi: 10.1111/gcb.12592
- Moriya, Y., Itoh, M., Okuda, S., Yoshizawa, A. C., and Kanehisa, M. (2007). KAAAS: an automatic genome annotation and pathway reconstruction server. *Nucleic Acids Res.* 35, W182–W185. doi: 10.1093/nar/gkm321
- Moroney, J. V., and Ynalvez, R. A. (2007). Proposed carbon dioxide concentrating mechanism in *Chlamydomonas reinhardtii*. *Eukaryot. Cell* 6:1251. doi: 10.1128/EC.00064-07
- Nakamura, T., Nadaoka, K., and Watanabe, A. (2013). A coral polyp model of photosynthesis, respiration and calcification incorporating a transcellular ion transport mechanism. *Coral Reefs* 32, 779–794. doi: 10.1007/s00338-013-1032-2
- Nitschke, M. R., Gardner, S. G., Goyen, S., Fujise, L., Camp, E. F., Ralph, P. J., et al. (2018). Utility of photochemical traits as diagnostics of thermal tolerance amongst great barrier reef corals. *Front. Mar. Sci.* 5:45. doi: 10.3389/fmars.2018.00045
- Oksanen, J., Blanchet, F. G., Friendly, M., Kindt, R., Legendre, P., McGlinn, D., et al. (2019). *Community Ecology Package*. Available online at: <https://cran.r-project.org/web/packages/vegan/vegan.pdf> (accessed June 22, 2021).
- Orr, J. C., Fabry, V. J., Aumont, O., Bopp, L., Doney, S. C., Feely, R. A., et al. (2005). Anthropogenic ocean acidification over the twenty-first century and its impact on calcifying organisms. *Nature* 437, 681–686. doi: 10.1038/nature04095
- Pandolfi, J. M., Connolly, S. R., Marshall, D. J., and Cohen, A. L. (2011). Projecting coral reef futures under global warming and ocean acidification. *Science* 333:418. doi: 10.1126/science.1204794
- Parkinson, J. E., Banaszak, A. T., Altman, N. S., LaJeunesse, T. C., and Baums, I. B. (2015). Intraspecific diversity among partners drives functional variation in coral symbioses. *Sci. Rep.* 5:15667. doi: 10.1038/srep15667
- Pimentel, H., Bray, N. L., Puente, S., Melsted, P., and Pachter, L. (2017). Differential analysis of RNA-seq incorporating quantification uncertainty. *Nat. Methods* 14:687.
- Putnam, H. M., Edmunds, P. J., and Fan, T.-Y. (2008). Effect of temperature on the settlement choice and photophysiology of larvae from the reef coral *Stylophora pistillata*. *Biol. Bull.* 215, 135–142.
- R Core Team (2018). *R: A Language and Environment for Statistical Computing*. Vienna: R Foundation for Statistical Computing.
- Reece, J. B., Urry, L. A., Cain, M. L., Wasserman, S. A., Minorsky, P. V., and Jackson, R. B. (2015). *Campbell Biology: Photosynthesis*. Boston, MA: Pearson, 199–201.



- Rivest, E. B., Kelly, M. W., DeBiasse, M. B., and Hofmann, G. E. (2018). Host and symbionts in *Pocillopora damicornis* larvae display different transcriptomic responses to ocean acidification and warming. *Front. Mar. Sci.* 5:186. doi: 10.3389/fmars.2018.00186
- Rocker, M. M., Noonan, S., Humphrey, C., Moya, A., Willis, B. L., and Bay, L. K. (2015). Expression of calcification and metabolism-related genes in response to elevated pCO<sub>2</sub> and temperature in the reef-building coral *Acropora millepora*. *Mar. Genomics* 24, 313–318. doi: 10.1016/j.margen.2015.08.001
- Strader, M. E., Wong, J. M., and Hofmann, G. E. (2020). Ocean acidification promotes broad transcriptomic responses in marine metazoans: a literature survey. *Front. Zool.* 17:7. doi: 10.1186/s12983-020-0350-9
- Strahl, J., Stolz, L., Uthicke, S., Vogel, N., Noonan, S. H. C., and Fabricius, K. E. (2015). Physiological and ecological performance differs in four coral taxa at a volcanic carbon dioxide seep. *Comp. Biochem. Physiol. A Mol. Integr. Physiol.* 184, 179–186. doi: 10.1016/j.cbpa.2015.02.018
- Suggett, D., Dong, L., Lawson, T., Lawrenz, E., Torres, L., and Smith, D. (2013). Light availability determines susceptibility of reef building corals to ocean acidification. *Coral Reefs* 32, 327–337.
- Suggett, D. J., Hall-Spencer, J. M., Rodolfo-Metalpa, R., Boatman, T. G., Payton, R., Tye Pettay, D., et al. (2012). Sea anemones may thrive in a high CO<sub>2</sub> world. *Glob. Chang. Biol.* 18, 3015–3025. doi: 10.1111/j.1365-2486.2012.02767.x
- Tambutté, E., Venn, A. A., Holcomb, M., Segonds, N., Techer, N., Zoccola, D., et al. (2015). Morphological plasticity of the coral skeleton under CO<sub>2</sub>-driven seawater acidification. *Nat. Commun.* 6:7368.
- Towanda, T., and Thuesen, E. V. (2012). Prolonged exposure to elevated CO<sub>2</sub> promotes growth of the algal symbiont *Symbiodinium muscatinei* in the intertidal sea anemone *Anthopleura elegantissima*. *Biol. Open* 1:615. doi: 10.1242/bio.2012521
- Venn, A. A., Tambutté, E., Holcomb, M., Laurent, J., Allemand, D., and Tambutté, S. (2013). Impact of seawater acidification on pH at the tissue–skeleton interface and calcification in reef corals. *Proc. Natl. Acad. Sci. U.S.A.* 110:1634. doi: 10.1073/pnas.1216153110
- Veron, J. E. N. (2000). *Corals of the World*. Monterey, CA: Sea Challengers.
- Vidal-Dupiol, J., Zoccola, D., Tambutté, E., Grunau, C., Cosseau, C., Smith, K. M., et al. (2013). Genes related to ion-transport and energy production are upregulated in response to CO<sub>2</sub>-driven pH decrease in corals: new insights from transcriptome analysis. *PLoS One* 8:e58652. doi: 10.1371/journal.pone.0058652
- Voolstra, C. R., Li, Y., Liew, Y. J., Baumgarten, S., Zoccola, D., Flot, J.-F., et al. (2017). Comparative analysis of the genomes of *Stylophora pistillata* and *Acropora digitifera* provides evidence for extensive differences between species of corals. *Sci. Rep.* 7:17583. doi: 10.1038/s41598-017-17484-x
- Wall, C. B., Fan, T.-Y., and Edmunds, P. J. (2014). Ocean acidification has no effect on thermal bleaching in the coral *Seriatopora caliendrum*. *Coral Reefs* 33, 119–130. doi: 10.1007/s00338-013-1085-2
- Walter, W., Sánchez-Cabo, F., and Ricote, M. (2015). GOplot: an R package for visually combining expression data with functional analysis. *Bioinformatics* 31, 2912–2914.
- Zhou, G., Yuan, T., Cai, L., Zhang, W., Tian, R., Tong, H., et al. (2016). Changes in microbial communities, photosynthesis and calcification of the coral *Acropora gemmifera* in response to ocean acidification. *Sci. Rep.* 6:35971.
- Zoccola, D., Ganot, P., Bertucci, A., Caminiti-Segonds, N., Techer, N., Voolstra, C. R., et al. (2015). Bicarbonate transporters in corals point towards a key step in the evolution of cnidarian calcification. *Sci. Rep.* 5:9983.

**Conflict of Interest:** The authors declare that the research was conducted in the absence of any commercial or financial relationships that could be construed as a potential conflict of interest.

Copyright © 2021 Herrera, Liew, Venn, Tambutté, Zoccola, Tambutté, Cui and Aranda. This is an open-access article distributed under the terms of the Creative Commons Attribution License (CC BY). The use, distribution or reproduction in other forums is permitted, provided the original author(s) and the copyright owner(s) are credited and that the original publication in this journal is cited, in accordance with accepted academic practice. No use, distribution or reproduction is permitted which does not comply with these terms.



# Differences in Gut Microbiome Composition Between Sympatric Wild and Allopatric Laboratory Populations of Omnivorous Cockroaches

Kara A. Tinker<sup>†</sup> and Elizabeth A. Ottesen<sup>\*</sup>

Department of Microbiology, University of Georgia, Athens, GA, United States

## OPEN ACCESS

### Edited by:

Aram Mikaelyan,  
North Carolina State University,  
United States

### Reviewed by:

Zakee L. Sabree,  
The Ohio State University,  
United States  
Jose Pietri,  
University of South Dakota,  
United States

### \*Correspondence:

Elizabeth A. Ottesen  
ottesen@uga.edu

### <sup>†</sup> Present address:

Kara A. Tinker,  
Department of Unconventional  
Resources, National Energy  
Technology Laboratory, Pittsburgh,  
PA, United States

### Specialty section:

This article was submitted to  
Microbial Symbioses,  
a section of the journal  
Frontiers in Microbiology

**Received:** 30 April 2021

**Accepted:** 07 July 2021

**Published:** 28 July 2021

### Citation:

Tinker KA and Ottesen EA (2021)  
Differences in Gut Microbiome  
Composition Between Sympatric Wild  
and Allopatric Laboratory Populations  
of Omnivorous Cockroaches.  
Front. Microbiol. 12:703785.  
doi: 10.3389/fmicb.2021.703785

Gut microbiome composition is determined by a complex interplay of host genetics, founder's effects, and host environment. We are using omnivorous cockroaches as a model to disentangle the relative contribution of these factors. Cockroaches are a useful model for host–gut microbiome interactions due to their rich hindgut microbial community, omnivorous diet, and gregarious lifestyle. In this study, we used 16S rRNA sequencing to compare the gut microbial community of allopatric laboratory populations of *Periplaneta americana* as well as sympatric, wild-caught populations of *P. americana* and *Periplaneta fuliginosa*, before and after a 14 day period of acclimatization to a common laboratory environment. Our results showed that the gut microbiome of cockroaches differed by both species and rearing environment. The gut microbiome from the sympatric population of wild-captured cockroaches showed strong separation based on host species. Laboratory-reared and wild-captured cockroaches from the same species also exhibited distinct gut microbiome profiles. Each group of cockroaches had a unique signature of differentially abundant uncharacterized taxa still present after laboratory cultivation. Transition to the laboratory environment resulted in decreased microbiome diversity for both species of wild-caught insects. Interestingly, although laboratory cultivation resulted in similar losses of microbial diversity for both species, it did not cause the gut microbiome of those species to become substantially more similar. These results demonstrate how competing factors impact the gut microbiome and highlight the need for a greater understanding of host–microbiome interactions.

**Keywords:** cockroach, gut microbiome, host–microbe, 16S rRNA amplicon sequencing, sympatric

## INTRODUCTION

The gut microbiome plays an important role in the health and fitness of most animals. Gut microorganisms assist with the breakdown of dietary substrates and play a role in nutritional absorption and energy regulation (Dillon and Dillon, 2003; Engel and Moran, 2013). The gut microbiome also protects against pathogens, both by inhibiting colonization by invading pathogenic microbes as well as by interacting with the host immune

(Engel and Moran, 2013). Certain toxins, including pesticides, can be metabolized by the gut microbiome (Engel and Moran, 2013; Brune and Dietrich, 2015; Claus, 2016). The presence of certain gut microbes is essential for the development of several types of insects, including the cockroach and mosquito (Bracke et al., 1978; Cruden and Markovetz, 1984; Gijzen and Barugahare, 1992; Coon et al., 2015; Jahnes and Sabree, 2020). Finally, recent work demonstrates that microbes can impact animal behavior across classes, from insects to mammals (Wada-Katsumata et al., 2015; Vuong et al., 2017). Examples include frequency of social interactions, mate choice, hyperactivity, anxiety, depression, and others (Wada-Katsumata et al., 2015; Delbare et al., 2020; Heys et al., 2020; Zhu et al., 2020). Therefore, identifying and understanding host–gut microbiome interactions is an important area of research.

Gut microbiome composition is determined by a complex interplay of host genetics, early environment, and immediate environment (Turnbaugh et al., 2009; Neu and Rushing, 2011; Ericsson and Franklin, 2015; Martinson et al., 2017; Ho et al., 2018; Kakumanu et al., 2018; Lee et al., 2020; Lim and Bordenstein, 2020; Sepulveda and Moeller, 2020; Tinker and Ottesen, 2020; Wolff et al., 2020). Host genetics has been shown to play the key role in the gut microbiome of certain species, including cockroaches, mosquitoes, and apes (Sanders et al., 2014; Novakova et al., 2017; Lim and Bordenstein, 2020; Tinker and Ottesen, 2020). In contrast, sympatric populations of *Drosophila* (Martinson et al., 2017) were shown to exhibit indistinguishable gut microbial communities, suggesting environment may be the primary factor in shaping the gut microbiome for certain species. Early environment and founder's effects are also thought to play a role in the gut microbiome, with studies in humans showing lasting signatures arising from mode of birth (vaginal vs. cesarean) and newborn diet (breastfeeding vs. formula feeding) (Neu and Rushing, 2011; Ho et al., 2018). Additionally, recent work suggests that the host's immediate environment can cause major impacts on the gut microbiome. For instance, temperature (Sepulveda and Moeller, 2020), diet (Turnbaugh et al., 2009), and/or housing conditions (isolated vs. co-housed) (Ericsson and Franklin, 2015; Caruso et al., 2019) can be manipulated in order to produce certain gut microbiome profiles in mice.

Cockroaches are an ideal organism for studying gut microbial community assembly and host–microbe interactions. Cockroaches represent an ancient lineage that emerged over 300 million years ago (Legendre et al., 2015; Wang et al., 2017) and have evolved to host a complex gut microbiome composed of hundreds of unique species of microbes (Bell et al., 2007; Engel and Moran, 2013; Dietrich et al., 2014). This gut microbiome is composed of insect-associated lineages, but is populated by microbial families and genera that are characteristic of the gut microbiomes of a wide range of omnivorous animals, including mice, and humans (Schauer et al., 2012; Dietrich et al., 2014; Tinker and Ottesen, 2016). The cockroach gut microbial community is not vertically transmitted, but indirectly acquired from other cockroaches in their immediate environment, a process aided by their typically gregarious lifestyle (Bell et al., 2007; Engel and Moran, 2013; Wada-Katsumata et al., 2015;

Kakumanu et al., 2018). Acquisition of a healthy gut microbial community is required for proper development (Bracke et al., 1978; Cruden and Markovetz, 1984; Gijzen and Barugahare, 1992; Jahnes and Sabree, 2020). Dysbiotic cockroaches are generally smaller than their healthy counterparts and rarely complete the final molt into adulthood (Bracke et al., 1978; Cruden and Markovetz, 1984; Gijzen and Barugahare, 1992; Jahnes and Sabree, 2020). Social behavior is also impacted by the gut microbiome, which produces volatile carboxylic acids (VCAs) which act as aggregation agents for the insect hosts (Wada-Katsumata et al., 2015). Axenic cockroaches produce no aggregation agents and thus have reduced social contact from other insects (Wada-Katsumata et al., 2015). Interestingly, once assembled, the cockroach gut microbiome appears to be robust to many environmental perturbations (Renelies-Hamilton et al., 2021). This may be due to regular conspecific inoculation events through social behaviors including coprophagy and trophallaxis (Renelies-Hamilton et al., 2021).

In this experiment, we used 16S rRNA gene sequencing to compare the hindgut microbiome of an in-house laboratory colony of *Periplaneta americana*, a second laboratory colony of *P. americana* obtained from the University of Florida, and sympatric wild-caught *P. americana* and *Periplaneta fuliginosa*. A subset of the transplanted laboratory colony and wild-caught cockroach populations were maintained under in-house laboratory conditions for a period of 14 days to observe changes in the hindgut microbiome following this transition. We were specifically interested in measuring changes in richness (alpha diversity) and dissimilarity (beta diversity) within and across the treatment groups after a transition into a laboratory environment. We were also interested in identifying which factors (treatment group, host species, and/or sample origin) most impacted the hindgut microbial community. Finally, we planned to identify and investigate any taxa that were uniquely associated with particular treatment groups.

## MATERIALS AND METHODS

### Insects

Our in-house laboratory colony of *P. americana* cockroaches was provided by the University of Georgia's entomology department from a colony that has been maintained in captivity for over 10 years. The cockroaches were maintained in mixed-age, mixed-sex colonies in aquarium tanks at room temperature on a diet of dog food (Kroger nutritionally complete bite-sized adult dog food, composed of 21% protein, 8% fat, and 6% fiber) *ad libitum*. Each tank was provided with corn cob bedding, cardboard tubes for nesting, and a cellulose sponge saturated with water. The laboratory colony from the University of Florida was generously obtained and provided by Brian Forschler, a colleague in the University of Georgia's entomology department.

For studies of wild-caught cockroaches, insects were collected in traps placed outside within a 135 m radius on the University of Georgia's campus. The traps were glass jars with petroleum jelly placed around the jar opening to prevent insects from escaping. Each trap contained glass wool saturated with beer as

a lure. Traps were checked daily, and any captured *P. americana* and *P. fuliginosa* adults were either sacrificed immediately or placed in an aquarium tank under laboratory culture conditions (as described above) for 14 days before being sacrificed. Wild *P. americana* and *P. fuliginosa* were visually identified by morphology. We confirmed our identifications by sequencing a representative sample from each insect species. For the *P. americana* sample we sequenced a modified A-tLeu/B-tLys and for the *P. fuliginosa* sample we sequenced the CO-II gene, both as previously described (Tinker and Ottesen, 2020). Ultimately, our experiment included a total number of 90 insect samples from the following groups: laboratory *P. americana* (12 samples), Florida laboratory *P. americana* at time 0 (8 samples), Florida laboratory *P. americana* at day 14 (20 samples), wild *P. americana* at time 0 (12 samples), wild *P. americana* at day 14 (11 samples), wild *P. fuliginosa* at time 0 (12 samples), and wild *P. fuliginosa* at day 14 (15 samples) (Supplementary Table 1). Each sample represented an individual dissected hindgut.

## Hindgut Collection and DNA Extraction

We opted to focus on the hindgut in this study due to its high bacterial density and diversity (Cruden and Markovetz, 1987). For this work, DNA was extracted from individual dissected hindguts; no hindguts were pooled. Each insect was placed on ice in a sterile culture plate until sufficiently torpid. The entire cockroach gut was dissected and any visible debris, including fat bodies or exoskeleton, was removed with forceps. The hindgut was then separated from the rest of the gut, placed on parafilm, and submerged in 100  $\mu$ L of RNeasy lysis buffer (Qiagen, Austin, TX, United States). A pipette tip was used to break open the hindgut and disperse the contents into the RNeasy lysis buffer before the suspended hindgut lumen was removed and stored at 80°C.

DNA was extracted from a 30  $\mu$ L aliquot of the preserved hindgut sample using a modified version of the EZNA Bacteria kit (Omega Biotek, Norcross, GA, United States). A 100  $\mu$ L of balanced salt solution (2.5 g K<sub>2</sub>HPO<sub>4</sub>, 1 g KH<sub>2</sub>PO<sub>4</sub>, 1.6 g KCl, 1.4 g NaCl, and 10 ml of 1 M NaHCO<sub>3</sub> per liter, pH 7.2) was added to each sample aliquot before mixing followed by centrifugation for 10 min at 5,000  $\times$  g. The supernatant was discarded and the pellet was resuspended in 100  $\mu$ L TE buffer [10 mM Tris, 1 mM EDTA (pH 8)] with 10  $\mu$ L lysozyme (as supplied by kit). The sample was incubated at 37°C for 30 min before adding approximately 25 mg of glass beads (as supplied by kit) and bead beating for 5 min at 3,000 rpm. Hundred microliters BTL buffer and 20  $\mu$ L proteinase K solution (as supplied by the kit) were added to each sample before incubation at 55°C while shaking at 600 rpm for 1 h. After this step, the manufacturer's protocol (June 2014 version) was followed beginning at step 11. Samples were eluted in 50  $\mu$ L preheated elution buffer after a 5-min incubation at 65°C. The final DNA concentrations (typically between 5 and 50 ng/ $\mu$ L) and A260/A280 were measured using a NanoDrop Lite spectrophotometer (Thermo Scientific, Wilmington, DE, United States).

## Library Preparation and Sequencing

The V4 region of the 16S rRNA gene from each hindgut sample was amplified using a two-step PCR method as previously

described (Tinker and Ottesen, 2016, 2018, 2020; Hassell et al., 2018). In brief, the initial PCR used Q5 Hot Start high-fidelity DNA polymerase (New England BioLabs, Ipswich, MA, United States) and 515F (GTGCCAGCMGCCGCGGTAA) and 806R (GGACTACHVGGGTWTCTAAT) primers in a 10  $\mu$ L PCR mixture [1 Q5 reaction buffer, 200 M deoxynucleoside triphosphates (dNTPs), 0.5 M 515F, 0.5 M 806R, 2 ng DNA, and 0.02 U/L Q5 polymerase] under the following conditions: 98°C for 30 s, followed by 15 cycles at 98°C for 10 s, 52°C for 30 s, and 72°C for 30 s, with a final extension step at 72°C for 2 min for the initial V4 region amplification. Immediately following the initial amplification, the resulting product was reamplified using double barcode primers (Tinker and Ottesen, 2016, 2018, 2020; Hassell et al., 2018). The secondary amplification mixture contained 1 Q5 reaction buffer, 200 M dNTPs, 0.5 M 515F, 0.5 M 806R, 2 ng DNA, and 0.02 U/L Q5 polymerase. From this mixture, 21  $\mu$ L was added to 9  $\mu$ L of the initial reaction product before cycling under the following conditions: 98°C for 30 s, followed by four cycles at 98°C for 10 s, 52°C for 10 s, and 72°C for 30 s, followed by six cycles at 98°C for 10 s and 72°C for 1 min, concluding with a final extension at 72°C for 2 min. The resulting PCR amplicons were purified using the EZNA Cycle Pure kit (Omega Bio-tek) before quantification with a NanoDrop Lite spectrophotometer (Thermo Scientific). Amplicons were then normalized to equal concentrations, pooled to a library concentration of 10 nM, and assessed for quality using the Agilent 2100 Bioanalyzer DNA-HS assay (Agilent Technologies, Santa Clara, CA, United States) before submission to the Georgia Genomics Facility for sequencing (Illumina MiSeq 250  $\times$  250 bp; Illumina Inc., San Diego, CA, United States).

## Data Analysis

16S rRNA gene sequences were analyzed using a modified version of the Mothur Miseq standard operating protocol (Schloss et al., 2009). In brief, after sequence assembly any sequence that had ambiguous bases or was longer than 275 bp was removed and remaining sequences were aligned to the Silva reference database (Release 132) (Pruess et al., 2007; Quast et al., 2012). Aligned sequences that contained homopolymers of 8 or more base pairs were removed before chimera identification and removal via VSEARCH (Rognes et al., 2016). Remaining sequences were classified using the Silva reference database (Release 138) (Pruess et al., 2007; Quast et al., 2012). Unclassified sequences or sequences identified as chloroplasts, mitochondria, Eukaryota, or *Blattabacterium* (cockroach endosymbiont found in fat body cells) were removed. The remaining sequences were clustered into OTUs based on 97% or greater sequence identity using OptiClust (Westcott and Schloss, 2017).

Data generated by Mothur was imported into R for further analysis (Schloss et al., 2009). The vegan (Oksanen et al., 2012) package was used to complete non-metric multidimensional scaling (NMDS) analyses and Analysis of Similarities (ANOSIM). Vegan (Oksanen et al., 2012) was also utilized to calculate Shannon diversity and Bray-Curtis dissimilarity values. Wilcoxon rank-sum tests were run using base R and differential abundance was measured with the DESeq2 (Love et al., 2014) package. Finally, we used base R,



ggplot (Wickham, 2016), and RColorBrewer (Neuwirth, 2014) to visualize the data.

## Data Mining

Our analysis utilizes previously published data as well as new, unpublished data. Please note that the 16S rRNA sequencing data from the laboratory *P. americana* (Tinker and Ottesen, 2016), wild *P. americana* at both timepoints (Tinker and Ottesen, 2016), and wild *P. fuliginosa* at time 0 (Tinker and Ottesen, 2020) were utilized in previous publications. These publications investigated the effect of diet on *P. americana* (Tinker and Ottesen, 2016) and measured the phyllosymbiotic signature in omnivorous cockroaches (Tinker and Ottesen, 2020). The 16S rRNA sequencing data from the wild *P. fuliginosa* at day 14 as well as the laboratory Florida *P. americana* at both time points is new, previously unpublished data. The methods described above were used to generate all data, both published and unpublished.

## RESULTS

### All Cockroaches Harbor a Hindgut Microbiome Dominated by Members of the Bacteroidota, Firmicutes, and Desulfobacterota Phyla

16S rRNA gene amplicon sequencing was completed for the hindguts of 90 unique cockroaches across the control and three treatment groups. A total of 6,969,201 sequences were generated, with 4,927,318 remaining after quality filtering and classification (Supplementary Table 1). Across all treatments, hindguts were dominated by members of the Bacteroidota, Firmicutes, and Desulfobacterota phyla. These three phyla comprised 32.84–92.04% of any one individual sample (Figure 1). Members of the Bacteroidota phyla were most abundant across all samples, comprising an average of 41.43% and a median of 42.51% (Figure 1). In contrast, the Firmicutes and Desulfobacterota phyla comprise an average of 30.16 and 10.22% across all samples (Figure 1).

The Bacteroidota observed in the cockroach guts represented a diverse array of families. An average of 2.74% of sequences across all samples belong to unclassified members of the Bacteroidia class with an additional 6.51% of sequences belonging to unclassified members of the Bacteroidales order (Figure 1). Nine other Bacteroidota families were especially abundant across all samples and comprised >5% of the total sequences from at least one sample. These include: Bacteroidaceae, COB P4-1 termite group, Dysgonomonadaceae, M2PB4-65 termite group, Marinifilaceae, Rikenellaceae, Parabacteroides, vadinHA21, and Williamwhitmaniaceae (Figure 1). All of these families except the M2PB4-65 termite group were present within all 90 samples and comprised anywhere from 0.005 to 17.22% of all sequences for any one sample (Figure 1). Of these families, Dysgonomonadaceae and Parabacteroides had the highest average relative abundance across all samples, at 6.11 and 5.37% (Figure 1). Members of the Dysgonomonadaceae and Parabacteroides families are commonly found in the gut

microbiome of animals and certain species of Parabacteroides have previously been associated with obesity and inflammation (Wang et al., 2019).

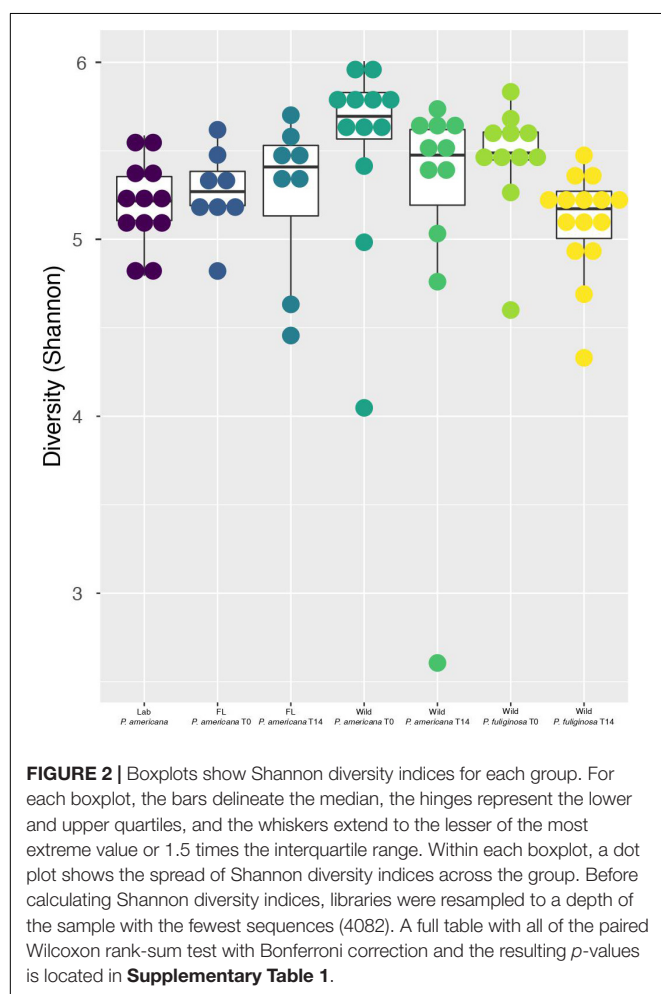
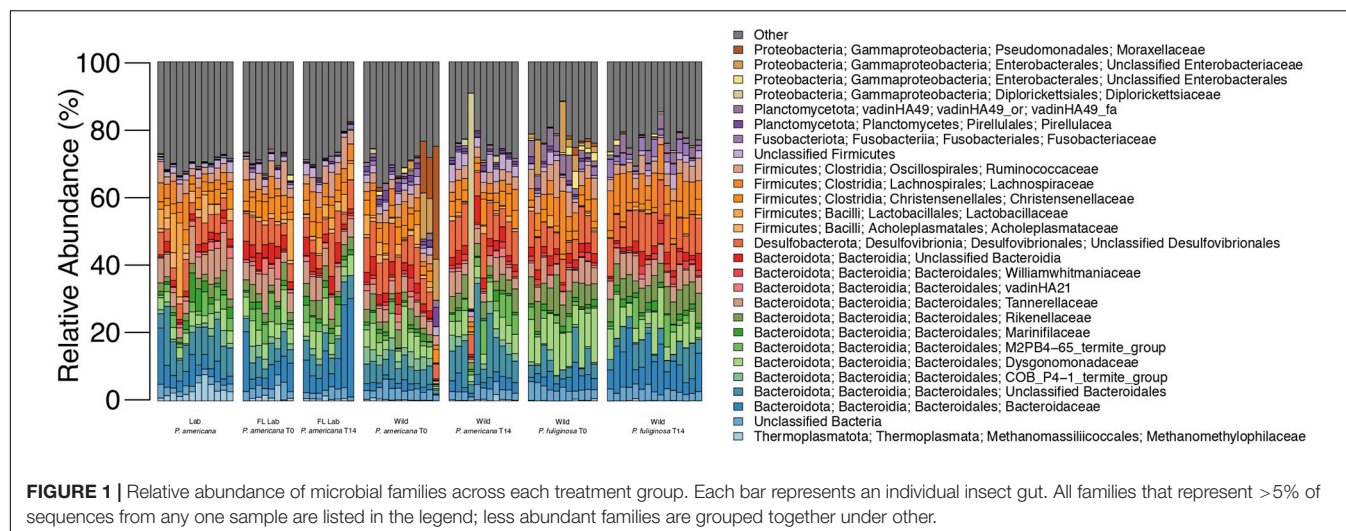
Most of the highly abundant Firmicutes families belonged to the Clostridia class (Figure 1). Members include the Christensenellaceae, Lachnospiraceae, and Ruminococcaceae families which composed an average of 3.38, 5.04, and 3.98% of sequences across all samples (Figure 1). Achleplasmataceae and Lactobacillaceae, both members of the Bacilli class, were also present with an average relative abundance of 1.08 and 1.51%. Finally, an average of 2.08% of sequences across all samples were unclassifiable members of the Firmicutes phylum (Figure 1).

The majority of the Desulfobacterota present in our experimental samples belonged to unclassified members of the Desulfovibrionales order, which comprised an average of 7.85% of sequences across all samples (Figure 1). Desulfovibrionales are commonly found in the gut microbiome of animals and have been associated with human diseases including obesity and type 2 diabetes (Rinninella et al., 2019). Eight Desulfobacterota families as well as sequences that belong to unclassified members of the Desulfobacterota phylum, Desulfuromonadia class, and the Desulfobacterales and Desulfobulbales orders were also present in select experimental samples at low abundances (Figure 1).

In addition to the three dominant phyla, bacteria from the Proteobacteria phylum was also present within all 90 experimental samples. Four families comprised the majority of these Proteobacteria: Diplorickettsiaceae, unclassified members of the Enterobacterales order, unclassified members of the Enterobacteriaceae order, and Moraxellaceae (Figure 1). These families were present at low abundance for most samples, composing an average of 0.38–1.03% (Figure 1). The maximum relative abundance for these families ranged from 5.03 to 62.62% and for each family, the individual sample with the maximum relative abundance belonged to the wild treatment group (Figure 1). Notably, the majority of the Diplorickettsiaceae present in our samples are members of the Rickettsiella genus, which is commonly thought to be an intracellular insect parasite (Leclerque and Kleespies, 2012). Interestingly, most samples contained <0.5% sequences from the Diplorickettsiaceae family (Figure 1). However, eight samples from the wild *P. americana* group had a high (>0.5%) abundance of Diplorickettsiaceae, with a maximum abundance of 63.62% in a wild *P. americana* day 14 sample (Figure 1).

### Wild-Collected Cockroaches Exhibit High Alpha Diversity That Decreases on Being Housed in Laboratory Conditions

Previous work demonstrates that the cockroach hindgut microbiome is highly diverse (Schauer et al., 2012, 2014; Bertino-Grimaldi et al., 2013; Dietrich et al., 2014; Wada-Katsumata et al., 2015; Tinker and Ottesen, 2016, 2020; Renelies-Hamilton et al., 2021). Congruent with this, all cockroach samples, except for one outlier from the day 14 wild *P. americana* treatment group, had a Shannon Diversity metric greater than 4.0 (Figure 2). Pielou's evenness was also high across all groups at each timepoint, with an average of 0.83 and a median of 0.84 across all samples.

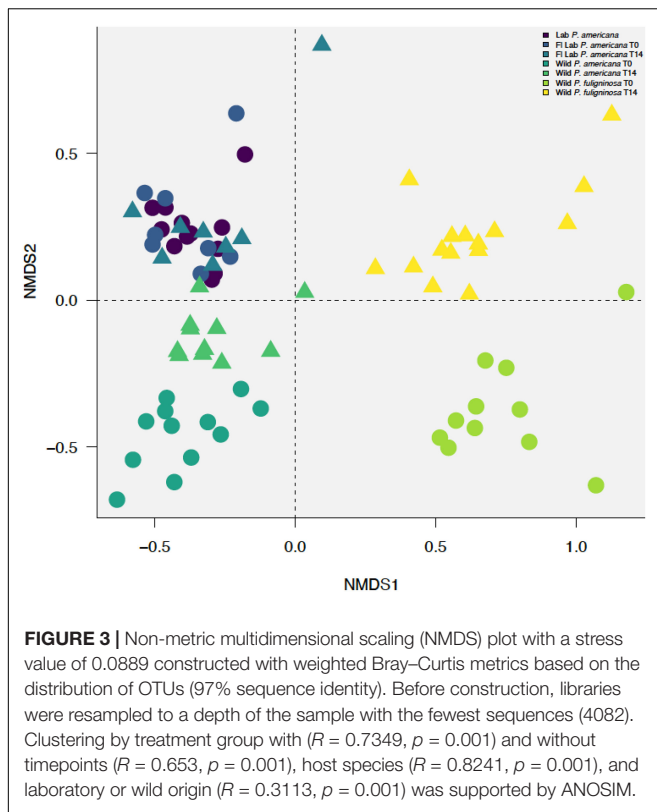


Overall, both laboratory populations had similar alpha diversity, but there were significant differences between the laboratory and wild cockroach groups (**Figure 2** and **Supplementary**

**Table 2**). Using the Wilcoxon rank-sum test with Bonferroni correction, we found that wild-collected *P. americana* exhibited significantly higher alpha diversity than both in-house and Florida laboratory *P. americana* populations as well as the wild-collected *P. fuliginosa* (**Supplementary Table 2**). This alpha diversity decreased on housing in the laboratory, and we found no significant difference ( $p > 0.05$ ) between the in-house laboratory or Florida laboratory *P. americana* and either day 14 wild *P. americana* or *P. fuliginosa* groups (**Supplementary Table 2**). In addition, we found no significant difference in alpha diversity between the two wild treatment groups at time 0. Interestingly, while there was a significant difference ( $p > 0.05$ ) between the time 0 *P. americana* and the day 14 *P. fuliginosa* groups and vice versa, there was no significant difference in alpha diversity between the two wild-collected groups after 14 days. This suggests that both species lost diversity at similar rates upon housing in the laboratory.

### Hindgut Microbial Communities Cluster by Treatment Group, Host Species, and Sample Origin

Previous research demonstrates that the cockroach hindgut microbiome is shaped by various compounding biological and environmental factors (Bracke et al., 1978; Bertino-Grimaldi et al., 2013; Dietrich et al., 2014; Schauer et al., 2014; Wada-Katsumata et al., 2015; Tinker and Ottesen, 2020). We used NMDS to visualize Bray–Curtis dissimilarities among our samples (**Figure 3** and **Supplementary Figure 1**). When plotting all samples, we identified a clear separation between the laboratory and wild groups (**Figure 3** and **Supplementary Figure 1**). Furthermore, we identified separation among the wild groups by both species and time point (**Figure 3** and **Supplementary Figure 1**). However, the in-house laboratory and the Florida laboratory group at both timepoints clustered together (**Figure 3** and **Supplementary Figure 1**). When we followed up with ANOSIM, we found there was no statistically significant difference between the in-house and



Florida laboratory cockroaches or the two timepoints for the Florida lab cockroaches. In contrast, there was significant separation between the wild *P. americana* ( $R = 0.4825$ ,  $p = 0.001$ ) and wild *P. fuliginosa* ( $R = 0.649$ ,  $p = 0.001$ ) at each timepoint. When the dataset was analyzed as a whole, we found that clustering by treatment group with ( $R = 0.7349$ ,  $p = 0.001$ ) and without timepoints ( $R = 0.653$ ,  $p = 0.001$ ), host species ( $R = 0.8241$ ,  $p = 0.001$ ), and laboratory or wild origin ( $R = 0.3113$ ,  $p = 0.001$ ) was supported by ANOSIM.

### Within- and Between-Group Comparisons Show Differences in Hindgut Microbiome Composition

We were interested in examining differences in within-group variability across populations (Figure 4 and Supplementary Table 3). We found that our in-house laboratory *P. americana* populations showed the lowest within-group variability by both weighted and unweighted Bray–Curtis metrics among the populations tested (Figure 4 and Supplementary Table 3). It was significantly lower than the Florida laboratory *P. americana* at day 14 and the wild *P. fuliginosa* at both time points using weighted measurements (Figure 4 and Supplementary Table 3). When using unweighted measurements, it was significantly lower than all of the treatments (Figure 4 and Supplementary Table 3). Within-group variability was highest for the wild-captured populations, with wild-collected *P. fuliginosa* showing significantly greater variability than wild-collected *P. americana* by weighted measurement (Figure 4 and Supplementary

Table 3). Both groups of wild-collected cockroaches showed slight decreases in within-group variability upon housing in the laboratory, but the only significant difference was in unweighted Bray–Curtis comparisons between T0 and T14 wild-captured *P. fuliginosa* (Figure 4 and Supplementary Table 3).

We also compared the between-group dissimilarity for the laboratory *P. americana* control with all other groups (Figure 4). Consistent with ANOSIM results, we found that the between-group dissimilarity for each treatment was significantly higher than the among group dissimilarity (Figure 4). For the Florida laboratory *P. americana*, between-group dissimilarity vs. in-house laboratory cockroaches remained consistent over both time points using both weighted and unweighted metrics. However, we saw a lower between-group dissimilarity vs. our in-house laboratory population after 14 days of laboratory cultivation for both the wild *P. americana* and *P. fuliginosa* groups. Interestingly, there was a greater difference in the unweighted metrics than the weighted metrics, suggesting that the decrease in dissimilarity is likely due to a loss of low-abundance, environmentally associated microbes.

### Differential Abundance Analysis Reveals Unique Taxa Associated With Each Group

In order to evaluate OTUs driving these between-group differences, we used DESeq2 to identify significantly enriched or depleted OTUs across groups (Supplementary Table 4). We found that there were 416 OTUs with a significant differential abundance between the laboratory *P. americana* and the Florida *P. americana* at time 0, 747 for the laboratory *P. americana* and the wild *P. americana* at time 0, and 996 for the laboratory *P. americana* and the wild *P. fuliginosa* at time 0 (Figure 5A). The number of OTUs with a significant differential abundance between the laboratory *P. americana* decreased to 351 for the Florida *P. americana*, 504 for the wild *P. americana*, and increased to 1,058 for the wild *P. fuliginosa* after 14 days in the laboratory environment (Figure 5A). When we compared the time 0 and day 14 samples within each group, we found that far fewer OTUs had significant compositional differences (Figure 5A). We found 18 between the Florida laboratory *P. americana* at each time point, 197 between the wild *P. americana* at each time point, and 274 between the wild *P. fuliginosa* at each time point (Figure 5A). Overall, this demonstrates that origin (laboratory v. wild) and species strongly impact the cockroach hindgut microbiome but that taxonomic differences are typically reduced when insects are housed in identical conditions.

We found that there were 602 OTUs with a significant differential abundance between the sympatrically collected wild populations of *P. americana* and *P. fuliginosa* (Figure 5A), suggesting that host species results in differences in hindgut microbiome composition among sympatric populations of closely related species. Interestingly, this value was comparable to that found when comparing the laboratory *P. americana* and the wild *P. americana* at time 0 (747) and the laboratory *P. americana* and the wild *P. fuliginosa* at time 0 (996), also



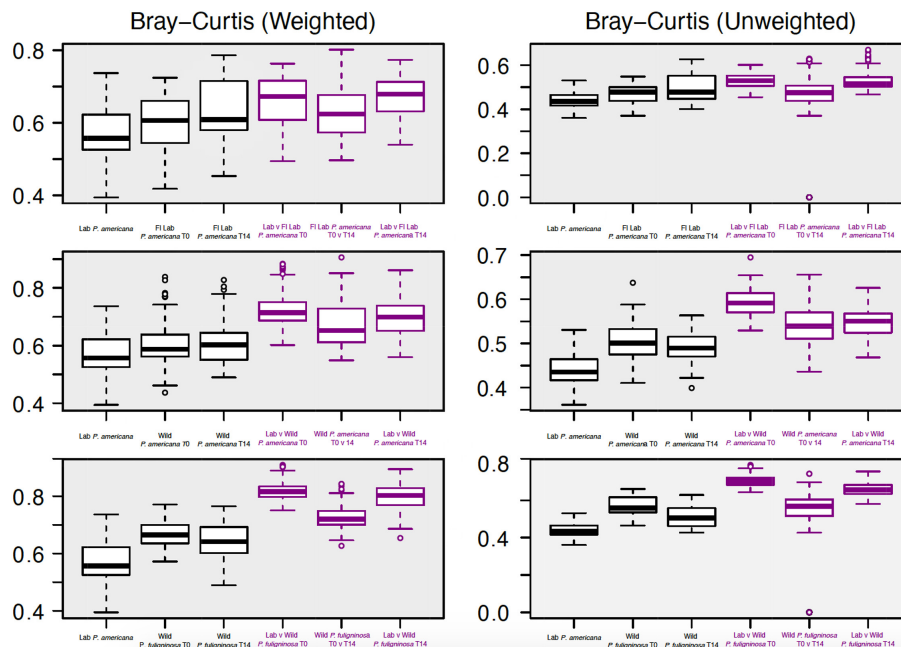


**FIGURE 4 |** Boxplots show weighted (right) and unweighted (left) pairwise Bray-Curtis dissimilarity metrics among (black) and between (purple) each group. For each boxplot, the bars delineate the median, the hinges represent the lower and upper quartiles, and the whiskers extend to the lesser of the most extreme value or 1.5 times the interquartile range. Before calculating Bray-Curtis dissimilarity metrics, libraries were resampled to a depth of the sample with the fewest sequences (4082). A table with all of the paired Wilcoxon rank-sum tests with Bonferroni correction and the resulting *p*-values is located in **Supplementary Table 3**.

confirming an important role for early environment in shaping the hindgut microbiome.

**Figure 5B** shows a heatmap illustrating OTUs that exhibit significant log<sub>2</sub>-fold changes across our four sets of three-way comparisons (**Supplementary Table 5**). We found 2, 20, and 74 OTUs with significant log<sub>2</sub>-fold changes across all three paired comparisons for the Florida *P. americana*, wild *P. americana*, and wild *P. fuliginosa* treatment groups, respectively (**Figure 5A**). We also found 89 OTUs with significant log<sub>2</sub>-fold changes found in the comparison of laboratory *P. americana* with the two wild-collected populations (**Figure 5A**). Removal of redundant sets resulted in a list of 158 OTUs which have exhibited significant log<sub>2</sub>-fold changes across all three pairwise comparisons of 1 or more treatment groups (**Supplementary Table 5**). When we visualize these 158 OTUs in an unscaled heatmap (**Figure 5B**), there are two notable trends. First, the majority of these OTUs have low taxonomic resolution and second, the majority of these OTUs have statistically significant, but minimal log<sub>2</sub>-fold changes (**Figure 5B** and **Supplementary Table 5**). Within the heatmap, there were 22 OTUs that had a large change across multiple treatment groups (**Figure 5B**). When we explicitly examine these OTUs they fall into four general categories (**Figure 5C**): those (1) associated only with the laboratory control *P. americana*; (2) associated with both the laboratory control *P. americana* and the Florida laboratory *P. americana*; (3) associated with wild *P. fuliginosa*; and (4) associated with wild *P. americana*. Fifteen out of 22 (and 57 out of the full 158) of these OTUs represent diverse Bacteroidota, including two *Dysgonomonas* genus OTUs as well as multiple OTUs that could not be classified beyond

the order or family level. Many of the Bacteroidota genera and families include multiple OTUs showing contrasting patterns in abundance across groups. A number of Firmicutes also show group-specific patterns, although they were more highly represented among organisms showing smaller fold changes between groups. As these groups are thought to play diverse roles in carbohydrate metabolism (Vera-Ponce de León et al., 2020), further studies are required to determine the functional implications of these OTU shifts. Another interesting taxon is *Arcobacter*, which was associated with wild *P. fuliginosa* and is thought to be an emerging pathogen (Collado and Figueras, 2011; Barboza et al., 2017).

## DISCUSSION

The cockroach is emerging as a common model organism for studying the gut microbiome due to their rich hindgut microbial community, omnivorous diet, and gut structure, which is analogous to the human stomach. Our goal was to better understand the factors that drive assembly and biodiversity in the cockroach gut microbiome. Previous work on the cockroach gut microbiome demonstrates that cockroaches have a gut microbiome which is more typical of omnivorous mammals than insects outside of the Blattodea order (Schauer et al., 2012; Tinker and Ottesen, 2016, 2020). Much like the mammalian gut microbiome, the cockroach gut microbiome is highly complex and primarily composed of bacterial lineages from the Bacteroidota and Firmicutes phyla (Schauer et al., 2012;



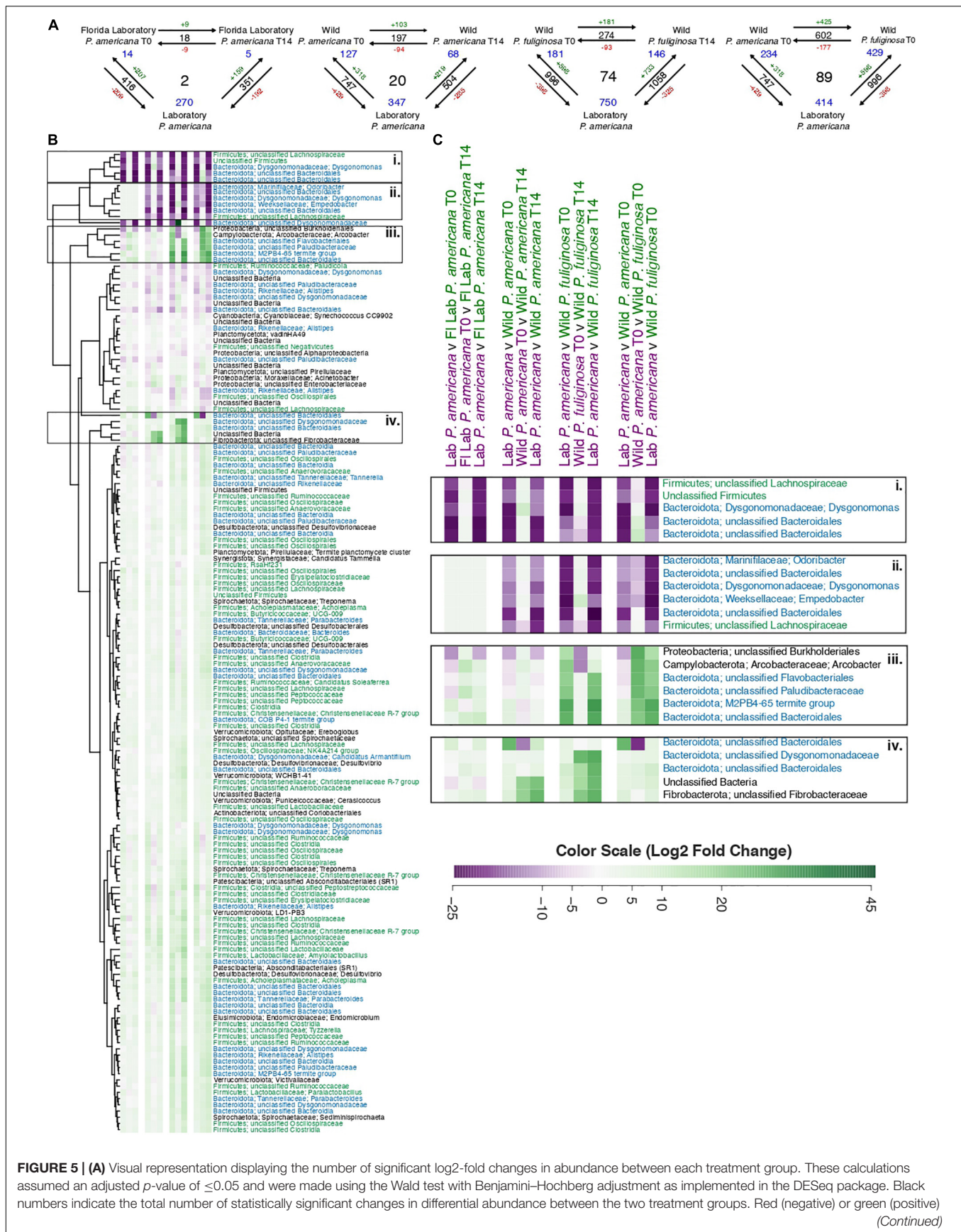


**FIGURE 5 | Continued**

numbers in conjunction with the arrows indicate the direction of the log<sub>2</sub>-fold change. Finally, blue numbers indicate the number of OTUs that have a significant change in differential abundance across either two groups (corners) or all groups (center). A table containing the raw data from DESeq for the significant log<sub>2</sub>-fold changes from all pairwise comparisons is located in **Supplementary Table 4**. **(B)** A heatmap of the 158 OTUs which have significant log<sub>2</sub>-fold changes across three or more treatment groups. Each row in the heatmap represents a unique OTU, with replicated labels representing multiple OTUs assigned to the same taxonomic group. For each pairwise comparison, the reference is the first pair listed. Each box in the heatmap represents unscaled log<sub>2</sub>-fold change and ranges from a minimum value of -26.31 (purple) to a maximum of 45.47 (green) with the color scale centered at white. To enable visualization of broader taxonomic patterns, row labels are color coded by phylum assignment, with members of the Bacteroidota phyla in blue, Firmicutes in green, and all others in black. A table containing the raw data and adjusted *p*-values from DESeq2 for these 158 OTUs is located in **Supplementary Table 5**. **(C)** A close-up of the highlighted sections of the heatmap presented in **B**.

Tinker and Ottesen, 2016, 2020). Our work was congruent with this and showed that all cockroaches contained a high abundance of uncharacterized, insect-associated microbial families.

Previous work showed that host species shapes the gut microbiome of cockroaches (Tinker and Ottesen, 2020). Consistent with this, we observed that sympatric populations of wild-collected cockroaches belonging to different species showed significantly different hindgut microbiome compositions, with over 602 microbial OTUs differing significantly in abundance between these two species. Upon housing in identical laboratory conditions, the wild-collected populations showed decreases in alpha and beta diversity. Wild-caught *Drosophila* gut microbiomes also decrease in diversity when brought into a laboratory setting (Martinson et al., 2017). This is interesting, as the *Drosophila* gut microbiome appears to be governed by different rules of assemblage, with local sampling environment shaping the gut microbiome rather than host species (Martinson et al., 2017). Renelies-Hamilton et al. (2021) have suggested that co-housing can, to some extent, overcome founder's effects in gut microbiome composition in cockroaches (Martinson et al., 2017). Therefore, it would be interesting to observe the extent to which these differences could be resolved by co-housing with laboratory-origin populations and/or rearing in the laboratory environment.

Interestingly, a comparable number of OTUs (747) were observed to exhibit significantly different abundances between laboratory and wild-caught *P. americana* as were differentially abundant between the sympatric wild populations of *P. americana* and *P. fuliginosa* (602). This is congruent with previous studies that have included wild-captured cockroaches (Bertino-Grimaldi et al., 2013; Pérez-Cobas et al., 2015; Tinker and Ottesen, 2016; Kakumanu et al., 2018), which have also typically found a distinct and more diverse gut microbiome. Housing in the laboratory resulted in decreases in alpha diversity, decreases in within-group beta diversity, and a significant change in abundance for 197 OTUs. However, the laboratory-housed *P. americana* of wild origin retained a distinct hindgut microbiome from the laboratory-raised *P. americana*, with 504 OTUs exhibiting significant differences between these two populations. Notably, 347 of these OTUs were also significantly different between the laboratory cockroaches and day 0 wild-captured cockroaches.

We found substantially greater similarities between the UGA and Florida laboratory populations of *P. americana*. In general, while our in-house laboratory populations of cockroach showed greater within-group similarity than the Florida-sourced

laboratory population (potentially as a result of disturbance resulting from the transport and altered housing of Florida-sourced cockroaches), both showed low within-group variability and similar levels of alpha diversity. The two laboratory populations clustered together to the exclusion of both wild-origin populations in our NMDS plot, although 270 OTUs were found to be significantly different between our in-house laboratory populations and both day 0 and day 14 Florida laboratory cockroaches. Interestingly, unlike the wild-captured cockroaches, the Florida-origin laboratory population showed significant changes in the abundance of only 18 microbial OTUs upon housing in our laboratory, suggesting substantially smaller shifts in microbiome composition upon transfer from one laboratory to another than that occurring during the transition to the wild to laboratory conditions.

We also found it notable that many of the group-specific OTUs belonged to the Bacteroidota phylum. Across all groups, 57 of the 158 significant OTUs, or 36.08%, were members of the Bacteroidota phylum. In contrast, Bacteroidota only represents 20.53% of the total number of OTUs. This increase in representation suggests that Bacteroidota strains may be particularly likely to vary across populations, perhaps since many are strict anaerobes without the ability to make endospores and therefore could be less easily transmitted through/acquired from the environment. Alternatively, they may be particularly responsive to dietary or environmental differences between groups.

We also found it notable that *Rickettsiella* and *Arcobacter* (Figure 5 and Supplementary Tables 4, 5) were highly abundant in wild *P. americana* and wild *P. fuliginosa*, respectively. *Rickettsiella* are most commonly known as intracellular insect pathogens (Leclercque and Kleespies, 2012), however, there is one symbiotic species found in aphids that can be found in extracellular tissues or in the hemolymph (Tsuchida et al., 2010). *Rickettsiella* can be transmitted both vertically and horizontally between insects (Iasur-Kruh et al., 2013; Marshall et al., 2017), and certain *Rickettsiella* species have been found to be transferred from insects to mammals via insect bites (Anstead and Chilton, 2014). Similarly, *Arcobacter* is an emerging animal and human pathogen with multiple roles of transmission (Collado and Figueras, 2011; Barboza et al., 2017). As cockroaches have previously been thought to act as a reservoir for pathogenic microbes (Pai, 2013; Menasria et al., 2014; Memona et al., 2016; Moges et al., 2016), it is unclear whether the insects harboring these taxa were in diseased states or acting as mechanical vectors. However, these findings highlight

the necessity of future work focused on the role of cockroaches in disease transmission.

This work provides new insight into the impact of prolonged cultivation in the laboratory on the gut microbiome of cockroaches. We found that culture in the laboratory consistently decreased hindgut microbiome diversity, and that laboratory-reared and wild-captured cockroaches belonging to the same species had distinct hindgut microbial communities, while long-separated laboratory populations of the same species were more similar in composition overall. Further, laboratory-reared populations showed smaller shifts in hindgut microbial community composition upon transfer to a new laboratory than wild-captured cockroaches did upon transfer to the same laboratory. Interestingly, differences between the hindgut microbial community of laboratory-reared and wild-caught cockroaches were similar in scale to the differences between sympatric populations of wild-captured cockroaches from different species, but while laboratory cultivation resulted in similar losses of microbial diversity between wild-captured populations of different species it did not cause them to become substantially more similar overall. Together, these illustrate strong effects of host biology, early environment, and recent environment on the gut microbiome of cockroaches, and underscores the potential of the cockroach as a model system for untangling the modes of action and interactions between these drivers in shaping host–microbiome interactions.

## DATA AVAILABILITY STATEMENT

The 16S rRNA sequences generated from this experiment were submitted to the NCBI Sequence Read Archive and are available under the accession numbers SRP075213, PRJNA726249, SRX1763652, and SRP132948. Insect host

sequences were deposited in GenBank under accession numbers MH360270 and MH360286.

## AUTHOR CONTRIBUTIONS

KT collected and processed the samples, prepared the sequencing libraries, analyzed the data, and wrote the manuscript. EO procured the funding, assisted in data analysis, and edited the manuscript. Both authors contributed to the article and approved the submitted version.

## FUNDING

This work was supported in part by the National Institute of General Medical Sciences of the National Institute of Health under award number R35GM133789.

## ACKNOWLEDGMENTS

We thank Brian Forschler for providing the laboratory strains of American cockroaches used in this work. We would also thank Brian Forschler and Tae-Young Lee for their help with insect identification. Finally, we would also like to thank Vickie Trinh for her assistance with field collection, dissection, and sequencing library preparation.

## SUPPLEMENTARY MATERIAL

The Supplementary Material for this article can be found online at: <https://www.frontiersin.org/articles/10.3389/fmicb.2021.703785/full#supplementary-material>

## REFERENCES

- Anstead, C. A., and Chilton, N. B. (2014). Discovery of novel *Rickettsiella* spp. in Ixodid Ticks from Western Canada. *Appl. Environ. Microbiol.* 80, 1403–1410. doi: 10.1128/AEM.03564-13
- Barboza, K., Cubillo, Z., Castro, E., Redondo-Solano, M., Fernández-Jaramillo, H., and Echandi, M. L. A. (2017). First isolation report of *Arcobacter cryaerophilus* from a human diarrhea sample in Costa Rica. *Rev. Inst. Med. trop. S. Paulo* 59:e72. doi: 10.1590/s1678-9946201759072
- Bell, W. J., Roth, L. M., and Nalepa, C. A. (2007). “Diets and foraging,” in *Cockroaches: Ecology, Behavior, and Natural History*, eds W. J. Bell, L. M. Roth, and C. A. Nalepa (Baltimore: The Johns Hopkins University Press), 61–75. doi: 10.1071/wr98050
- Bertino-Grimaldi, D., Medeiros, M. N., Vieira, R. P., Cardoso, A. M., Turque, A. S., Silveira, C. B., et al. (2013). Bacterial community composition shifts in the gut of *Periplaneta americana* fed on different lignocellulosic materials. *Springer Plus* 2:609. doi: 10.1186/2193-1801-2-609
- Bracke, J. W., Cruden, D. L., and Markovetz, A. J. (1978). Effect of metronidazole on the intestinal microflora of the American cockroach, *Periplaneta americana* L. *Antimicrob. Agents Chemother.* 13, 115–120. doi: 10.1128/aac.13.1.115
- Brune, A., and Dietrich, C. (2015). The gut microbiota of termites: digesting the diversity in the light of ecology and evolution. *Annu. Rev. Microbiol.* 69, 145–166. doi: 10.1146/annurev-micro-092412-155715
- Caruso, R., Ono, M., Bunker, M. E., Núñez, G., and Inohara, N. (2019). Dynamic and asymmetric changes of the microbial communities after cohousing in laboratory mice. *Cell Rep.* 27, 3401–3412.e3. doi: 10.1016/j.celrep.2019.05.042
- Claus, S. P. (2016). The gut microbiota: a major player in the toxicity of environmental pollutants? *NPJ Biofilms Microbiomes* 2:12. doi: 10.1038/npjbiofilms.2016.3
- Collado, L., and Figueras, M. J. (2011). Taxonomy, epidemiology, and clinical relevance of the genus *Arcobacter*. *Clin. Microbiol. Rev.* 24:19.
- Coon, K. L., Vogel, K. J., Brown, M. R., and Strand, M. R. (2015). Mosquitoes rely on their gut microbiota for development. *Mol. Ecol.* 23, 2727–2739. doi: 10.1111/mec.12771
- Cruden, D. L., and Markovetz, A. J. (1984). Microbial aspects of the cockroach hindgut. *Arch. Microbiol.* 138:9.
- Cruden, D. L., and Markovetz, A. J. (1987). Microbial ecology of the cockroach gut. *Annu. Rev. Microbiol.* 41, 617–643. doi: 10.1146/annurev.mi.41.100187.003153
- Delbare, S. Y. N., Ahmed-Braimah, Y. H., Wolfner, M. F., and Clark, A. G. (2020). Interactions between the microbiome and mating influence the female's transcriptional profile in *Drosophila melanogaster*. *Sci. Rep.* 10:18168. doi: 10.1038/s41598-020-75156-9
- Dietrich, C., Kohler, T., and Brune, A. (2014). The cockroach origin of the termite gut microbiota: patterns in bacterial community structure reflect major evolutionary events. *Appl. Environ. Micro.* 80, 2261–2269.



- Dillon, R., and Dillon, V. (2003). The gut bacteria of insects: nonpathogenic interactions. *Annu. Rev. Entomol.* 49:24. doi: 10.1146/annurev.ento.49.061802.123416
- Engel, P., and Moran, N. A. (2013). The gut microbiota of insects diversity in structure and function. *FEMS Microbiol. Rev.* 37, 699–735. doi: 10.1111/1574-6976.12025
- Ericsson, A. C., and Franklin, C. L. (2015). Manipulating the gut microbiota: methods and challenges: figure 1. *ILAR J.* 56, 205–217. doi: 10.1093/ilar/ilv021
- Gijzen, H. J., and Barugahare, M. (1992). Contribution of anaerobic protozoa and methanogens to hindgut metabolic activities of the American cockroach, *Periplaneta americana*. *Appl. Environ. Microbiol.* 58, 2565–2570. doi: 10.1128/aem.58.8.2565-2570.1992
- Hassell, N., Tinker, K. A., Moore, T., and Ottesen, E. A. (2018). Temporal and spatial dynamics in microbial community composition within a temperate stream network: microbial community assembly in streams. *Environ. Microbiol.* 20, 3560–3572. doi: 10.1111/1462-2920.14311
- Heys, C., Lizé, A., Lewis, Z., and Price, T. A. R. (2020). *Drosophila* sexual attractiveness in older males is mediated by their microbiota. *Microorganisms* 8:168. doi: 10.3390/microorganisms8020168
- Ho, N. T., Li, F., Lee-Sarwar, K. A., Tun, H. M., Brown, B. P., Pannaraj, P. S., et al. (2018). Meta-analysis of effects of exclusive breastfeeding on infant gut microbiota across populations. *Nat. Commun.* 9:4169. doi: 10.1038/s41467-018-06473-x
- Iasur-Kruh, L., Weintraub, P. G., Mozes-Daube, N., Robinson, W. E., Perlman, S. J., and Zchori-Fein, E. (2013). Novel *Rickettsiella* bacterium in the leafhopper *Orosius albicinctus* (Hemiptera: Cicadellidae). *Appl. Environ. Microbiol.* 79, 4246–4252. doi: 10.1128/AEM.00721-13
- Jahnes, B. C., and Sabree, Z. L. (2020). Nutritional symbiosis and ecology of host-gut microbe systems in the Blattodea. *Curr. Opin. Insect Sci.* 39, 35–41. doi: 10.1016/j.cois.2020.01.001
- Kakumanu, M. L., Maritz, J. M., Carlton, J. M., and Schal, C. (2018). Overlapping community compositions of gut and fecal microbiomes in lab-reared and field-collected german cockroaches. *Appl. Environ. Microbiol.* 84, e1037–18. doi: 10.1128/AEM.01037-18
- Leclercq, A., and Kleespies, R. G. (2012). A *Rickettsiella* bacterium from the hard tick, ixodes woodi: molecular taxonomy combining multilocus sequence typing (MLST) with significance testing. *PLoS One* 7:e38062. doi: 10.1371/journal.pone.0038062
- Lee, S., Kim, J. Y., Yi, M., Lee, I.-Y., Lee, W.-J., Moon, H. S., et al. (2020). Comparative Microbiome analysis of three species of laboratory-reared periplaneta cockroaches. *Korean J. Parasitol.* 58, 537–542. doi: 10.3347/kjp.2020.58.5.537
- Legendre, F., Nel, A., Svenson, G. J., Robillard, T., Pellens, R., and Grandcolas, P. (2015). Phylogeny of Dictyoptera: dating the origin of cockroaches, praying mantises and termites with molecular data and controlled fossil evidence. *PLoS One* 10:e0130127. doi: 10.1371/journal.pone.0130127
- Lim, S. J., and Bordenstein, S. R. (2020). An introduction to phyllosymbiosis. *Proc. Biol. Sci.* 287:20192900. doi: 10.1098/rspb.2019.2900
- Love, M. I., Huber, W., and Anders, S. (2014). Moderated estimation of fold change and dispersion for RNA-seq data with DESeq2. *Genome Biol.* 15:550. doi: 10.1186/s13059-014-0550-8
- Marshall, S. D. G., Townsend, R. J., van Koten, C., and Jackson, T. A. (2017). An epizootic of *Rickettsiella* infection emerges from an invasive scarab pest outbreak following land use change in New Zealand. *Ann. Clin. Cytol. Pathol.* 3:1058.
- Martinson, V. G., Douglas, A. E., and Jaenike, J. (2017). Community structure of the gut microbiota in sympatric species of wild *Drosophila*. *Ecol. Lett.* 20, 629–639. doi: 10.1111/ele.12761
- Memona, H., Manzoor, F., and Anjum, A. A. (2016). Cockroaches (*Blattodea: Blattellidae*): a reservoir of pathogenic microbes in human-dwelling localities in lahore. *J. Med. Entomol.* 54, 435–440. doi: 10.1093/jme/tjw168
- Menasria, T., Moussa, F., El-Hamza, S., Tine, S., Megri, R., and Chenchouni, H. (2014). Bacterial load of German cockroach (*Blattella germanica*) found in hospital environment. *Pathog. Global Health* 108, 141–147. doi: 10.1179/204773214Y.00000000136
- Moges, F., Eshetie, S., Endris, M., Huruy, K., Muluye, D., Feleke, T., et al. (2016). Cockroaches as a source of high bacterial pathogens with multidrug resistant strains in gondar town, Ethiopia. *BioMed Res. Int.* 2016:2825056. doi: 10.1155/2016/2825056
- Neu, J., and Rushing, J. (2011). Cesarean versus vaginal delivery: long-term infant outcomes and the hygiene hypothesis. *Clin. Perinatol.* 38, 321–331. doi: 10.1016/j.clp.2011.03.008
- Neuwirth, E. (2014). *RColorBrewer: ColorBrewer Palettes. R package version 1.1-2*. Available online at: <https://CRAN.R-project.org/package=RColorBrewer> (accessed January 6, 2021).
- Novakova, E., Woodhams, D. C., Rodríguez-Ruano, S. M., Brucker, R. M., Leff, J. W., Maharaj, A., et al. (2017). Mosquito Microbiome dynamics, a background for prevalence and seasonality of west nile virus. *Front. Microbiol.* 8:526. doi: 10.3389/fmicb.2017.00526
- Oksanen, J., Blanchet, F. G., Kindt, R., Legendre, P., Minchin, R., O'Hara, R. B., et al. (2012). *Vegan: Community Ecology Package. R Package Version 2.2-0*. Available online at: <http://CRAN.Rproject.org/package=vegan> (accessed January 6, 2021).
- Pai, H.-H. (2013). Multidrug resistant bacteria isolated from cockroaches in long-term care facilities and nursing homes. *Acta Tropica* 125, 18–22. doi: 10.1016/j.actatropica.2012.08.016
- Pérez-Cobas, A. E., Maiques, E., Angelova, A., Carrasco, P., Moya, A., and Latorre, A. (2015). Diet shapes the gut microbiota of the omnivorous cockroach *Blattella germanica*. *FEMS Microbiol. Ecol.* 91:fiv022. doi: 10.1093/femsec/fiv022
- Pruesse, E., Quast, C., Knittel, K., Fuchs, B. M., Ludwig, W., Peplies, J., et al. (2007). SILVA: a comprehensive online resource for quality checked and aligned ribosomal RNA sequence data compatible with ARB. *Nucleic Acids Res.* 35, 7188–7196. doi: 10.1093/nar/gkm864
- Quast, C., Pruesse, E., Yilmaz, P., Gerken, J., Schweer, T., Yarza, P., et al. (2012). The SILVA ribosomal RNA gene database project: improved data processing and web-based tools. *Nucleic Acids Res.* 41, D590–D596. doi: 10.1093/nar/gks1219
- Renelies-Hamilton, J., Germer, K., Sillam-Dussès, D., Bodawatta, K. H., and Poulsen, M. (2021). Disentangling the relative roles of vertical transmission, subsequent colonizations, and diet on cockroach Microbiome Assembly. *mSphere* 6:e1023–20. doi: 10.1128/mSphere.01023-20
- Rinninella, E., Raoul, P., Cintoni, M., Franceschi, F., Miggiano, G., Gasbarrini, A., et al. (2019). What is the healthy gut microbiota composition? a changing ecosystem across age, environment, diet, and diseases. *Microorganisms* 7:14. doi: 10.3390/microorganisms7010014
- Rognes, T., Flouri, T., Nichols, B., Quince, C., and Mahé, F. (2016). VSEARCH: a versatile open source tool for metagenomics. *PeerJ* 4:e2584. doi: 10.7717/peerj.2584
- Sanders, J. G., Powell, S., Kronauer, D. J. C., Vasconcelos, H. L., Frederickson, M. E., and Pierce, N. E. (2014). Stability and phylogenetic correlation in gut microbiota: lessons from ants and apes. *Mol. Ecol.* 23, 1268–1283. doi: 10.1111/mec.12611
- Schauer, C., Thompson, C., and Brune, A. (2014). Pyrotag sequencing of the gut microbiota of the cockroach *Shelfordella lateralis* reveals a highly dynamic core but only limited effects of diet on community structure. *PLoS One* 9:e85861. doi: 10.1371/journal.pone.0085861
- Schauer, C., Thompson, C. L., and Brune, A. (2012). The bacterial community in the gut of the cockroach *Shelfordella lateralis* reflects the close evolutionary relatedness of cockroaches and termites. *Appl. Environ. Microbiol.* 78, 2758–2767. doi: 10.1128/AEM.07788-11
- Schloss, P. D., Westcott, S. L., Ryabin, T., Hall, J. R., Hartmann, M., Hollister, E. B., et al. (2009). Introducing mothur: open-source, platform-independent, community-supported software for describing and comparing microbial communities. *Appl. Environ. Microbiol.* 75, 7537–7541. doi: 10.1128/AEM.01541-09
- Sepulveda, J., and Moeller, A. H. (2020). The effects of temperature on animal gut microbiomes. *Front. Microbiol.* 11:384. doi: 10.3389/fmicb.2020.00384
- Tinker, K. A., and Ottesen, E. A. (2016). The core gut microbiome of the american cockroach, *Periplaneta americana*, is stable and resilient to dietary shifts. *Appl. Environ. Microbiol.* 82, 6603–6610. doi: 10.1128/AEM.01837-16
- Tinker, K. A., and Ottesen, E. A. (2018). The hindgut microbiota of praying mantids is highly variable and includes both prey-associated and host-specific microbes. *PLoS One* 13:e0208917. doi: 10.1371/journal.pone.0208917
- Tinker, K. A., and Ottesen, E. A. (2020). Phyllosymbiosis across deeply diverging lineages of omnivorous cockroaches (Order Blattodea). *Appl. Environ. Microbiol.* 86:e2513–19. doi: 10.1128/AEM.02513-19



- Tsuchida, T., Koga, R., Horikawa, M., Tsunoda, T., Maoka, T., Matsumoto, S., et al. (2010). Symbiotic bacterium modifies aphid body color. *Science* 330, 1102–1104. doi: 10.1126/science.1195463
- Turnbaugh, P. J., Ridaura, V. K., Faith, J. J., Rey, F. E., Knight, R., and Gordon, J. I. (2009). The effect of diet on the human gut microbiome: a metagenomic analysis in humanized gnotobiotic mice. *Sci. Trans. Med.* 1:6ra14. doi: 10.1126/scitranslmed.3000322
- Vera-Ponce de León, A., Jahnes, B. C., Duan, J., Camuy-Vélez, L. A., and Sabree, Z. L. (2020). Cultivable, host-specific *Bacteroidetes* Symbionts exhibit diverse polysaccharolytic strategies. *Appl. Environ. Microbiol.* 86, e91–20. doi: 10.1128/AEM.00091-20
- Vuong, H. E., Yano, J. M., Fung, T. C., and Hsiao, E. Y. (2017). The microbiome and host behavior. *Annu. Rev. Neurosci.* 40, 21–49. doi: 10.1146/annurev-neuro-072116-031347
- Wada-Katsumata, A., Zurek, L., Nalyanya, G., Roelofs, W. L., Zhang, A., and Schal, C. (2015). Gut bacteria mediate aggregation in the German cockroach. *Proc. Natl. Acad. Sci. U.S.A.* 112:201504031. doi: 10.1073/pnas.1504031112
- Wang, K., Liao, M., Zhao, N., Wang, J., Liu, S.-J., and Liu, H. (2019). *Parabacteroides distasonis* alleviates obesity and metabolic dysfunctions via production of succinate and secondary bile acids. *Cell Rep* 26, 222–235.e5.
- Wang, Z., Shi, Y., Qiu, Z., Che, Y., and Lo, N. (2017). Reconstructing the phylogeny of *Blattodea*: robust support for interfamilial relationships and major clades. *Sci. Rep.* 7:3903. doi: 10.1038/s41598-017-04243-1
- Westcott, S. L., and Schloss, P. D. (2017). *OptiClust*, an improved method for assigning amplicon-based sequence data to operational taxonomic units. *mSphere* 2:e73–17. doi: 10.1128/mSphereDirect.00073-17
- Wickham, H. (2016). *ggplot2: Elegant Graphics for Data Analysis*. New York, NY: Springer-Verlag.
- Wolff, N. S., Jacobs, M. C., Haak, B. W., Roelofs, J. J. T. H., de Vos, A. F., Hugenholtz, F., et al. (2020). Vendor effects on murine gut microbiota and its influence on lipopolysaccharide-induced lung inflammation and Gram-negative pneumonia. *ICMx* 8:47. doi: 10.1186/s40635-020-00336-w
- Zhu, S., Jiang, Y., Xu, K., Cui, M., Ye, W., Zhao, G., et al. (2020). The progress of gut microbiome research related to brain disorders. *J. Neuroinflammation* 17:25. doi: 10.1186/s12974-020-1705-z
- Conflict of Interest:** The authors declare that the research was conducted in the absence of any commercial or financial relationships that could be construed as a potential conflict of interest.
- Publisher's Note:** All claims expressed in this article are solely those of the authors and do not necessarily represent those of their affiliated organizations, or those of the publisher, the editors and the reviewers. Any product that may be evaluated in this article, or claim that may be made by its manufacturer, is not guaranteed or endorsed by the publisher.

Copyright © 2021 Tinker and Ottesen. This is an open-access article distributed under the terms of the Creative Commons Attribution License (CC BY). The use, distribution or reproduction in other forums is permitted, provided the original author(s) and the copyright owner(s) are credited and that the original publication in this journal is cited, in accordance with accepted academic practice. No use, distribution or reproduction is permitted which does not comply with these terms.



# Decisive Effects of Life Stage on the Gut Microbiota Discrepancy Between Two Wild Populations of Hibernating Asiatic Toads (*Bufo gargarizans*)

Xiaowei Song<sup>1,2,3\*</sup>, Jingwei Zhang<sup>4</sup>, Jinghan Song<sup>1</sup> and Yuanyuan Zhai<sup>1</sup>

<sup>1</sup> College of Life Sciences, Xinyang Normal University, Xinyang, China, <sup>2</sup> Institute for Conservation and Utilization of Agro-Bioresources in Dabie Mountains, Xinyang Normal University, Xinyang, China, <sup>3</sup> Chengdu Institute of Biology, Chinese Academy of Sciences, Chengdu, China, <sup>4</sup> Hospital of Xinyang Normal University, Xinyang Normal University, Xinyang, China

## OPEN ACCESS

### Edited by:

Wakako Ikeda-Ohtsubo,  
Tohoku University, Japan

### Reviewed by:

Osiris Gaona,  
National Autonomous University  
of Mexico, Mexico  
Jean-François Brugère,  
Université Clermont Auvergne, France

### \*Correspondence:

Xiaowei Song  
shavisong@xynu.edu.cn

### Specialty section:

This article was submitted to  
Microbial Symbioses,  
a section of the journal  
Frontiers in Microbiology

Received: 09 February 2021

Accepted: 02 July 2021

Published: 03 August 2021

### Citation:

Song X, Zhang J, Song J and  
Zhai Y (2021) Decisive Effects of Life  
Stage on the Gut Microbiota  
Discrepancy Between Two Wild  
Populations of Hibernating Asiatic  
Toads (*Bufo gargarizans*).  
Front. Microbiol. 12:665849.  
doi: 10.3389/fmicb.2021.665849

Until now, the effects of driving factors on the gut microbiota of amphibians are still mostly confounded. Due to a long-term fasting, hibernating amphibians are ideal experimental materials to explore this question. In this study, we characterized the small intestine microbiota of adult hibernating Asiatic toads (*Bufo gargarizans*) collected from two geographical populations using 16S rRNA amplicon sequencing technique and evaluated the effects of non-dietary factors (e.g., sex and host genetic background). Proteobacteria (0.9196 ± 0.0892) was characterized as the most dominant phylum in the small gut microbiota of hibernating Asiatic toads, among which five core OTUs were identified and three were classified into *Pseudomonas*. In view of the coincidence between the dominant KEGG pathways (such as the two-component system) and *Pseudomonas*, *Pseudomonas* appeared to be a key adaptor for small gut microbiota during hibernation. Furthermore, we detected a greater discrepancy of gut microbiota between geographical populations than between sexes. Both sex and host genetic background showed a minor effect on the gut microbiota variation. Finally, life stage was determined to be the decisive factor driving the gut microbiota discrepancy between populations. However, a large proportion of the gut microbiota variation (~70%) could not be explained by the measured deterministic factors (i.e., sex, location, body length, and routine blood indices). Therefore, other factors and/or stochastic processes may play key roles in shaping gut bacterial community of hibernating amphibians.

**Keywords:** amphibian, driving factor, gut microbiota, hibernation, Proteobacteria, small intestine, 16S rRNA

## INTRODUCTION

Gut microbial community acts as a key regulator in host normal physiological activities and health maintenances (Sommer and Bäckhed, 2013; Feng et al., 2018; Simon et al., 2019). The structure and function of intestinal microbial community depend on both extrinsic factors (e.g., diet and habitat) and intrinsic factors (e.g., life stage and genetic background) (Sommer and Bäckhed, 2013; Jiménez and Sommer, 2017; Feng et al., 2018). The mutualistic symbionts coevolve with hosts at a long-term timescale, thereby they may exhibit a host phylogenetic signal, i.e., phyllosymbiosis (McFall-Ngai et al., 2013; Brooks et al., 2016; Amato et al., 2019). As cold-blooded vertebrates, amphibians

(such as frogs, toads, or salamanders) have gilled aquatic larvae and air-breathing adults, and they have intermediate characters between fishes and reptiles. The key intrinsic and extrinsic factors of amphibians assemble unique gut microbiota, i.e., gut microbial community. For instance, the gut microbiota of adult amphibians is more similar to that of mammals rather than fishes (Kohl et al., 2013; Colombo et al., 2015). By contrast, the gut bacterial community of amphibian tadpoles is more similar to that of fishes (Kohl et al., 2013; Vences et al., 2016; Chai et al., 2018).

Previous researches mainly focus on the effects of individual factors on the gut microbiota (i.e., bacterial community) of amphibians using culture-independent methods (Kohl et al., 2013; Bletz et al., 2016; Chang et al., 2016; Kohl and Yahn, 2016; Weng et al., 2016; Zhang et al., 2016). In recent years, more efforts were devoted to the compound effects of multiple factors on the gut microbiota of amphibians (Vences et al., 2016; Weng et al., 2016, 2017; Huang et al., 2017; Warne et al., 2017; Knutie et al., 2018; Tong et al., 2019b). For instance, the gut microbiota of amphibian larvae possesses a certain degree of species specificity, but the interspecific variation is probably subdominant (Vences et al., 2016; Warne et al., 2017). At the population scale, nevertheless, the relationship between host genetic background and the gut microbiota of amphibians is still not clear.

Amphibians generally enter a hibernation stage in winter to counteract the energy limitation in adverse circumstances, such as cold temperature and food shortage. The Asiatic toad (*Bufo gargarizans*), a widely distributed true toad in China, prefers overwintering in subaqueous or subterranean habitats of ponds, lakes, or rivers (Fei et al., 2012). Since higher-latitude regions generally maintain a longer cold temperature in winter than lower-latitude regions, the hibernation timespan of Asiatic toads shows a remarkable latitude-correlated variation (3–8 months), i.e., longer hibernation stage in higher-latitude regions. The structure of amphibian gut microbiota is significantly remodeled along with dramatic changes in physiological and metabolic activities during hibernation (Banas et al., 1988; Costanzo and Lee, 2013; Weng et al., 2016; Wiebler et al., 2018). Due to a long-term fasting, hibernating amphibians are ideal experimental materials to explore the effects of non-dietary factors (e.g., genetic background) on the gut microbiota (Tong et al., 2019a). In this study, we explored the gut microbiota of adult hibernating Asiatic toads collected from two geographical locations. The aim was to evaluate the relative effects of multiple intrinsic factors (i.e., sex, life stage, health condition, and genetic background) on the gut microbiota of amphibians.

## MATERIALS AND METHODS

### Preparation of Experimental Specimens

We acquired two wild populations of hibernating Asiatic toads (*B. gargarizans*) from fishermen, who collected these toads in Ji Canal of Tianjin City (TJ population,  $n = 22$ ) and Luoma Lake of Xuzhou City (XZ population,  $n = 23$ ) during the winter in 2014. The two populations located in a similar longitude possessed a geographical distance of about 600 km

(**Supplementary Figure 1**). The ecological systems of Ji Canal and Luoma Lake tend to be similarly affected by human activities, e.g., agriculture (Chen et al., 2000; Liu et al., 2021). These toads were placed into drinking water (5–10°C) before sacrificed by pithing the brain and spinal cord. After double pithing, we immediately sampled the experimental specimens (e.g., cardiac blood and small intestine) of each toad. Specifically, the cardiac blood was collected into anticoagulant tubes by using aseptic injectors. The small intestine cut off by sterile scissors was stored in a –80°C refrigerator until DNA extraction. For this research, we applied 25 sample individuals, among which 14 belonged to the TJ population and 11 belonged to the XZ population (**Supplementary Table 1**). All procedures used in this study were approved by the Animal Care and Use Committee of Xinyang Normal University.

### Measurement of Intrinsic Factors for Hibernating Asiatic Toads

The intrinsic factors measured for hibernating toads consisted of sex, life stage, health condition, and genetic background. Specifically, we identified the sex of toads by checking the sexual characteristics (i.e., nuptial pad and reproductive system). Although the body size of Asiatic toads presents a latitude- and sex-dependent variation, body size is an effective indicator for age (i.e., life stage) (Yu and Lu, 2013). We evaluated the life stage of toads by measuring five morphological traits, i.e., body length (i.e., snout–vent length), body mass, body mass/body length (BM:BL), eye space, and nasal space. Subsequently, the health condition was evaluated through routine blood test (RBT) for lactate dehydrogenase, creatine kinase, alanine aminotransferase, aspartate aminotransferase, total protein, albumin, globulin, and alkaline phosphatase. These RBT factors were measured using the autochemistry analyzer CS-600B and corresponding kits (Dirui Industrial Inc., Changchun, China). Finally, we evaluated the host genetic divergence by using mitochondrial DNA (mtDNA: cytb and D-loop) and microsatellite [i.e., simple sequence repeat (SSR)] markers. The mtDNA and SSR markers were amplified by using the primers designed in previous studies (**Supplementary Table 2**). The polymerase chain reaction (PCR) products of mtDNA were sequenced by using ABI 3730xl DNA analyzer (Applied Biosystems, Bedford, MA, United States) in a commercial company (GenScript Biotech Corporation, Nanjing, China). The sequences have been deposited into CNGB sequence archive (CNSA) of China National GeneBank DataBase (CNGBdb) with project number CNP0001473 (Guo et al., 2020). We genotyped the PCR samples of SSRs by means of polyacrylamide gel electrophoresis. We deduced the genetic relationship between sample individuals using mtDNA and SSRs, respectively. Steps for the mtDNA process were listed as follows: (i) multiple sequence alignment was executed on cytb and D-loop fragments with ClustalW (version 1.4) embedded in BioEdit (version 7.2.5), respectively (Thompson et al., 1994; Hall, 1999); (ii) haplotype sequences of concatenated cytb and D-loop fragments were generated by DnaSP (version 5.10) with gap consideration (Librado and Rozas, 2009); and (iii) maximum likelihood (ML) and Bayesian phylogenetic trees of

these haplotypes were reconstructed by using RAXML (version 8.2.10) and MrBayes (version 3.2), respectively (Ronquist et al., 2012; Stamatakis, 2014). In phylogenetic reconstructions, cytb and D-loop fragments were treated as separate partitions. A GTR + G model was applied to each partition in both ML and Bayesian tree reconstruction. The number of bootstrap runs was set to 1,000 in ML tree reconstruction. Two independent runs and four chains in each run were applied for the Bayesian inference. The posterior probability of Bayesian trees was calculated from tree spaces generated by 0.5 burnin fraction after 10,000,000 generations. As for SSRs, we used R package “vegan” (version 2.5-2) to calculate the between-individual Bray–Curtis dissimilarity.

## Metagenomic DNA Extraction, 16S rRNA Gene Amplicon Sequencing, and Operational Taxonomic Unit Clustering

We utilized liquid nitrogen to grind and homogenize the small intestine of each toad, and then applied the phenol–chloroform method (Song et al., 2018) to extract metagenomic DNA from each small intestine (**Supplementary Table 1**). The DNA quality was determined using agarose gel electrophoresis or NanoVue Plus Spectrophotometer (GE Healthcare Inc., Princeton, NJ, United States). DNA samples were stored in a  $-20^{\circ}\text{C}$  refrigerator for 16S rRNA gene amplification. The PCR conditions for 16S rRNA gene (hypervariable regions: V3–V4) and following MiSeq sequencing were performed in a commercial company (Biobit Biotech Inc., Chengdu, China). The detailed procedures were described previously (Xu et al., 2020). The V3–V4 regions of bacterial 16S rRNA genes were amplified using the universal primer pair 341F–CCTACGGGNGGCWGCAG and 805R–GACTACHVGGGTATCTAATCC (Klindworth et al., 2012). The raw reads of 16S rRNA genes can be found in the CNGBdb with project number CNP0001644 (Guo et al., 2020). The paired-end reads were merged by FLASH software (version 1.2.11) with a minimum overlap of 20 base pairs (bp) and a maximum overlap of 250 bp (Magoč and Salzberg, 2011). The quality control for primer-filtered reads was achieved using VSEARCH software (version 2.4.4) (Rognes et al., 2016). Specifically, those sequences with more than nine expected errors or zero ambiguous bases were discarded. Sequences with less than 300 bases were also discarded. In addition, the chimeras were detected using uchime\_denovo with the parameter “–abskew 1.” Subsequently, we clustered the dereplicated quality-controlled sequences into operational taxonomic units (OTUs) using the VSEARCH software with the identity threshold of 97% (Rognes et al., 2016). The chimeras were detected again with the above same procedure. The OTU table was generated with usearch\_global program with parameters “–id 0.97 –maxrejects 0 –maxaccepts 2.”

## Structural and Functional Annotation of Gut Microbiota

We profiled gut microbiota structures using the QIIME2 toolbox (version 2018.6) (Bolyen et al., 2019). Specifically, the core OTUs in a group were detected in each individual of this

group. Venn diagrams<sup>1</sup> were depicted to show the shared OTUs between groups. The MAFFT method in the alignment plugin was used to align OTU representative sequences (Kato and Standley, 2013), and then the phylogenetic tree of these sequences was reconstructed using the fasttree method in the phylogeny plugin (Price et al., 2010). Taxonomic classification of the OTU representative sequences was achieved using a scikit-learn classifier (confidence threshold = 0.8) in terms of Greengenes (version 13.8) (Pedregosa et al., 2011; McDonald et al., 2012). Stack bars were depicted to show taxonomic compositions of gut microbiota. To annotate the function of gut microbiota, we created a compatible OTU table for PICRUSt in terms of Greengenes (version 13.5) using usearch\_global program with parameters “–id 0.97 –maxrejects 0 –maxaccepts 2,” and then predicted KEGG (Kyoto Encyclopedia of Genes and Genomes) orthology (KO) and KEGG pathways by using PICRUSt (online Galaxy version 1.1.1<sup>2</sup>) (Langille et al., 2013).

To statistically analyze  $\alpha$  diversity (i.e., observed OTUs, Shannon, Pielou's evenness, and Faith's PD) and  $\beta$  diversity indices (i.e., Bray–Curtis, Jaccard, weighted UniFrac, and unweighted UniFrac), we rarefied the OTU table to the lowest sampling depth (i.e., 6,301). Moreover, we tested whether the sampling depth was appropriate by calculating Spearman correlations of  $\alpha$  and  $\beta$  diversity indices between 10 iteratively rarefied OTU tables. The  $\alpha$  and  $\beta$  diversity indices of the samples showed high Spearman correlation coefficients between iterative rarefied OTU tables at a sampling depth of 6,000 and 6,301, respectively (**Supplementary Figure 2**). The  $\alpha$  diversity and relative abundances of taxa or KEGG pathways in groups were shown as “mean  $\pm$  SD (standard deviation)” unless otherwise stated.

## Statistical Analysis for the Structure and Function of Gut Microbiota

First, we utilized two-way ANOVA (linear model and type III sum of squares) to test the effects of sex and location on  $\alpha$  diversity indices and intrinsic factors. Two-way PERMANOVA was carried out to test the effects of sex and location on Bray–Curtis and Jaccard distance matrices of the rarefied OTU table. The permutation number was set to be 9,999. These statistical analyses were executed using R project (version 3.6.1). We identified taxonomic markers of gut microbiota in two sexes or populations using the LefSe method (online Galaxy version 1.0<sup>3</sup>) (Segata et al., 2011). Per-sample sum was normalized to one million as the algorithm designers recommend. Both  $\alpha$  values for the factorial Kruskal–Wallis test among classes and the pairwise Wilcoxon test between subclasses were set to 0.01. The threshold on the logarithmic LDA score for discriminative features was set to 2.0. All-against-all strategy was executed for multiclass analysis. We used the STAMP software (version 2.1.3) to detect different KEGG pathways between populations and between sexes (Parks et al., 2014). Two-sided Welch's *t*-test method was utilized for the comparison of two groups.

<sup>1</sup><http://bioinformatics.psb.ugent.be/webtools/Venn/>

<sup>2</sup><http://galaxy.morganlangille.com/>

<sup>3</sup><http://huttenhower.sph.harvard.edu/galaxy/>



False discovery rate (FDR)-adjusted  $p$ -values were filtered at a significance level of 0.05.

To evaluate the effect of host genetic background on the gut microbial structure and function, we utilized the PASSaGE software (version 2.0.11.6) to perform Mantel tests on matrices (Rosenberg and Anderson, 2011), i.e., SSR-based Bray–Curtis distance, distances of ML and Bayesian trees, OTU-based distances (i.e., Bray–Curtis, Jaccard, weighted UniFrac, and unweighted UniFrac), and Bray–Curtis distances of KO and KEGG pathway tables. The R package “corrplot” (version 0.84) was taken to visualize these Mantel correlation values with FDR-adjusted  $p < 0.05$ .

To test whether life stage and health condition could produce a marked effect on the structure and function of gut microbiota, furthermore, we calculated Spearman correlations between life stage and RBT factors,  $\alpha$  diversity indices, and relative abundances of taxonomic (i.e., sex- or population-biased taxa) and functional markers (i.e., sex or population-biased KEGG pathways) detected above. The R package “corrplot” was taken to visualize these Spearman correlation values with FDR-adjusted  $p < 0.05$ .

Subsequently, we utilized the R packages “vegan” and “plspm” (version 0.4.9) to evaluate the explanatory power of intrinsic factors for structural variations of gut microbiota. Specifically, redundancy analysis (RDA) and variation partitioning analysis (VPA) were performed on the rarefied OTU table with Hellinger transformation. Since two sample individuals (i.e., S12 and S36) possessed incomplete RBT factors (i.e., alkaline phosphatase unavailable in S12 and lactate dehydrogenase and creatine kinase unavailable in S36), we removed these two samples in RDA and VPA. The life stage factors except for body length and RBT factor of total protein were excluded in terms of variance inflation factors. After detecting significant constraint axes in RDA by the “anova.cca” function, we applied the “envfit” function to identify the life stage and RBT factors significantly fitting to these axes. The OTUs associated to the significant constraint axes (i.e., RDA1 and RDA2) in RDA were screened in terms of Spearman correlations with FDR-adjusted  $p < 0.05$ . We applied partial least squares path modeling (PLSPM) for life stage, location, and  $\alpha$  diversity (or population-biased taxonomic compositions) to test whether life stage drove the structural divergence of gut microbiota between populations. As for location factors, we assigned “1” to “TJ” and “0” to “XZ.” The bootstrap method (number = 100) was utilized to evaluate the significance of direct path coefficients in PLSPM.

To test the effect of life stage on the topological properties of co-occurrence networks, we compared network parameters between younger (body length  $\leq 8.4$  cm,  $n = 10$ ) and older (body length  $\geq 9.8$  cm,  $n = 11$ ) samples. The co-occurrence networks were constructed using R package “igraph” in terms of Spearman correlations for 24 shared OTUs (existed in more than half of the samples in each group). Correlation coefficients were filtered at a minimum threshold of 0.6 with FDR-adjusted  $p < 0.05$ . Singleton nodes were removed in co-occurrence networks before calculation of network parameters. The keystone OTUs were predicted by using the criterion of both normalized degree and betweenness centrality  $> 0.1$ . To identify target OTUs of life

stage in co-occurrence network remodeling, we also constructed a co-occurrence network for body length, Shannon index, and 37 shared OTUs in all samples.

## RESULTS

### Gut Microbiota Structure and Function of Hibernating *Bufo gargarizans*

We got 457,632 quality-controlled 16S rRNA gene amplicons in total (**Supplementary Table 3**). The length of these sequences ranged from 300 to 492 bases (mean = 423 bases). From these sequences, 630 OTUs were picked to annotate 412,647 sequences (i.e., 90.17% of total sequences) (**Supplementary Material: raw\_otu\_table.txt** and **taxonomy\_assignment.tsv**). Specifically, the number of sequences matching OTUs ranged from 6,301 to 46,313 in 25 samples (mean = 16506). In total, we screened out an archaeal phylum (i.e., Crenarchaeota) and 18 bacterial phyla. The relative abundance of Proteobacteria ( $0.9196 \pm 0.0892$ ), which was the most dominant phylum in all samples, ranged from 60.78 to 99.60% (**Figure 1**). Five phyla, namely, Actinobacteria ( $0.0080 \pm 0.0100$ ), Bacteroidetes ( $0.0244 \pm 0.0587$ ), Firmicutes ( $0.0111 \pm 0.0190$ ), Fusobacteria ( $0.0019 \pm 0.0038$ ), and Spirochetes ( $0.0024 \pm 0.0101$ ), possessed a relative abundance more than 1% in at least one sample. The unassigned phylum taxa in gut microbiota occupied 0.16–18.64%. The top two dominant genera were assigned to be Pseudomonadaceae members, i.e., *Pseudomonas* ( $0.5023 \pm 0.2314$ ) and an unassigned genus ( $0.2662 \pm 0.1147$ ) (**Supplementary Figure 3**). The number of shared OTUs between populations and between sexes was 431 (68.41%) and 480 (76.19%), respectively (**Figure 1**). Neither location-specific (i.e., core OTUs unique for one location) nor sex-specific core OTUs (i.e., core OTUs unique for one sex) was detected. The counts of core OTUs in TJ and XZ populations were 8 and 9, but in male and female samples, these were 5 and 11 (**Supplementary Table 4**). The five core OTUs among all samples were classified into Proteobacteria comprising three families, i.e., Pseudomonadaceae (OTU1, OTU2, and OTU4), Enterobacteriaceae (OTU5), and Aeromonadaceae (OTU7). OTU1 (*Pseudomonas*), OTU2 (unassigned genus of Pseudomonadaceae), and OTU4 (*Pseudomonas*) were the three main members of the top two dominant genera among samples. Intriguingly, OTU2 was also classified (identity  $\geq 0.97$ ) as *Pseudomonas* by using SINA (version 1.2.11) in search of SILVA SSU Ref NR database (release 138.1<sup>4</sup>) (Pruesse et al., 2012). In addition, OTU5 and OTU7 without clear genus assignment based on Greengenes were classified by using the SINA tool as *Rahnella* (Yersiniaceae: a new family in Enterobacterales) and *Aeromonas*, respectively.

Due to method limitation, a lot of rare OTUs could not be successfully utilized in the PICRUSt analysis. Specifically, a small fraction of 630 OTUs (i.e., 30.63%) was identified as representative OTUs (based on 97% identity) of Greengenes (version 13.5). However, these dominant OTUs accounted for 83.61% of the quality-controlled sequences (i.e., 457,632).

<sup>4</sup><https://www.arb-silva.de/>

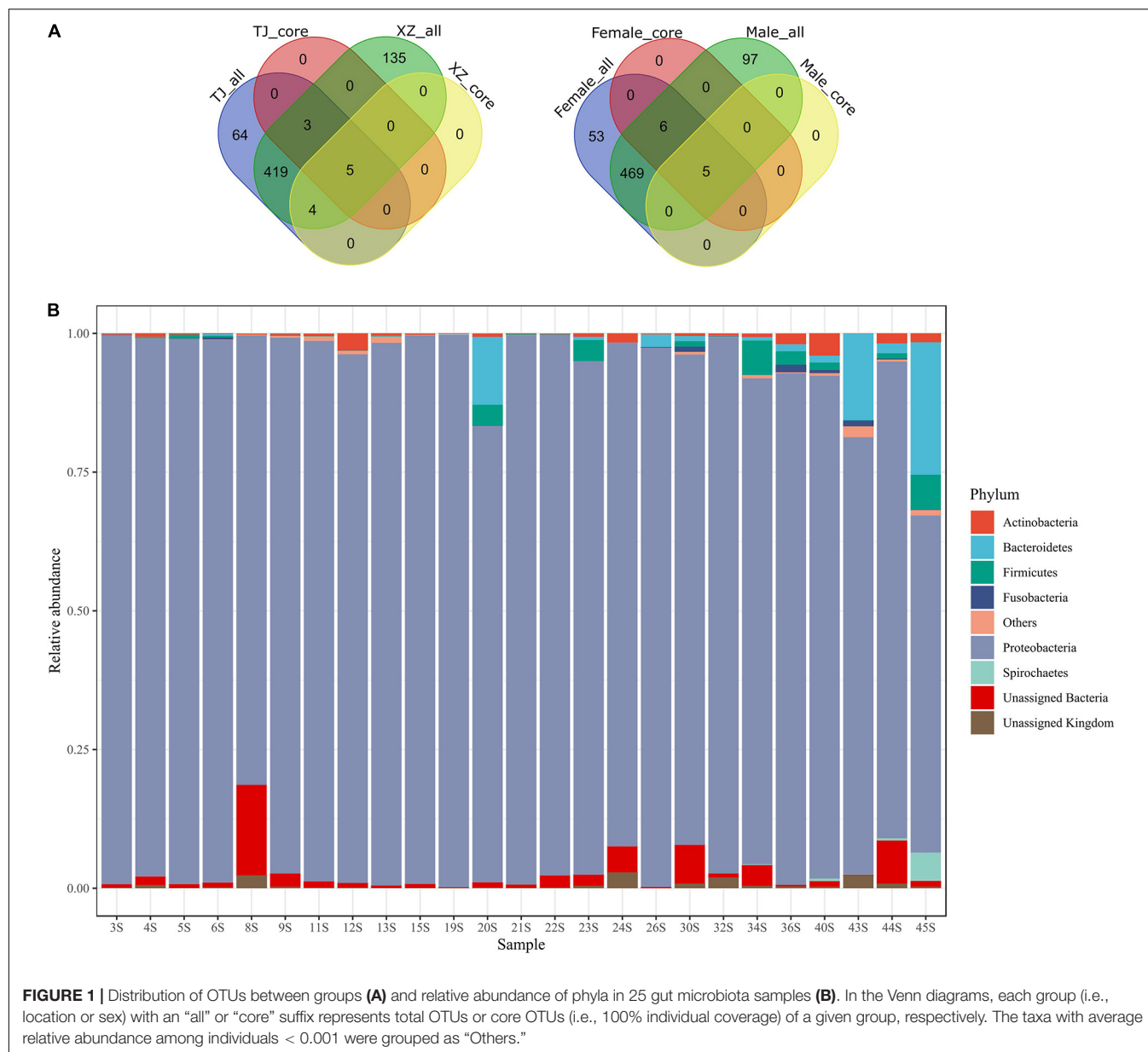


**FIGURE 1 |** Distribution of OTUs between groups (A) and relative abundance of phyla in 25 gut microbiota samples (B). In the Venn diagrams, each group (i.e., location or sex) with an “all” or “core” suffix represents total OTUs or core OTUs (i.e., 100% individual coverage) of a given group, respectively. The taxa with average relative abundance among individuals < 0.001 were grouped as “Others.”

The top five predicted KEGG pathways were transporters ( $0.0634 \pm 0.0046$ ), ABC transporters ( $0.0409 \pm 0.0026$ ), general function prediction only ( $0.0375 \pm 0.0012$ ), two-component system ( $0.0319 \pm 0.0018$ ), and secretion system ( $0.0261 \pm 0.0010$ ) (Supplementary Figure 4).

## Greater Divergence of Gut Microbiota Between Populations Than Between Sexes

After rarefaction to a sampling depth of 6,301, 588 (93.33% of 630) OTUs were retained. The average OTU number of 25 samples was 98 with a standard deviation of 53 (Supplementary Table 5). We detected significant differences in Shannon ( $p < 0.001$ ) and Pielou's evenness ( $p < 0.001$ ) but not in

observed OTUs ( $p = 0.140$ ) and Faith's PD ( $p = 0.610$ ) between two populations (Table 1). However, we did not detect any significant differences in  $\alpha$  diversity indices between sexes. In addition, a significant interactive effect on Faith's PD ( $p = 0.019$ ) appeared to exist in sex and location factors. The location factor had significant effects on Bray-Curtis ( $p = 0.001$ ) and Jaccard ( $p = 0.003$ ) distance matrices of rarefied OTU table (Table 1), but no significant effects of sex were observed on these  $\beta$  diversity indices. Furthermore, significant differences in relative abundances were detected in 29 taxa between populations and three taxa between sexes (Supplementary Figure 5). After excluding higher-level taxa with equal relative abundances to their daughter taxa, we got 17 taxa (e.g., *Pseudomonas*) between two populations and one taxon (i.e., Chlamydiales) between two sexes. However, none of the KEGG pathways showed a significant

**TABLE 1 |** Two-way (sex and location) ANOVA and PERMANOVA on  $\alpha$  and  $\beta$  diversity indices (i.e., Bray–Curtis and Jaccard distance matrices of rarefied OTU table, permutation number = 9,999).

	Source of variation	df	F	p
Observed OTUs	Sex	1	0.195	0.663
	Location	1	2.350	0.140
	Sex $\times$ location	1	3.879	0.062
Faith's PD	Sex	1	0.055	0.817
	Location	1	0.268	0.610
	Sex $\times$ location	1	6.503	<b>0.019</b>
Shannon	Sex	1	0.375	0.546
	Location	1	14.611	<b>&lt;0.001</b>
	Sex $\times$ location	1	0.084	0.775
Pielou's evenness	Sex	1	0.326	0.574
	Location	1	19.359	<b>&lt;0.001</b>
	Sex $\times$ location	1	0.892	0.356
Bray–Curtis distance	Sex	1	0.648	0.701
	Location	1	4.177	<b>0.001</b>
	Sex $\times$ location	1	2.056	0.070
Jaccard distance	Sex	1	0.722	0.661
	Location	1	3.548	<b>0.003</b>
	Sex $\times$ location	1	1.576	0.132

The *p* value in bold means  $<0.05$ .

difference between sexes or between populations. If unadjusted *p*-values were applied, a significant difference between two populations was detected in 81 KEGG pathways (**Supplementary Figure 6**). Thus, different populations owned greater divergence in gut microbiota than different sexes did.

## No Detectable Host Genetic Effects on Structural and Functional Variation of Gut Microbiotas

The mtDNA and SSR markers generated an inconsistent genetic divergence pattern among these individuals [ $r = 0.095$  (FDR-adjusted  $p = 0.309$ ) and  $r = 0.090$  (FDR-adjusted  $p = 0.309$ )] (**Supplementary Figure 7**, **Supplementary Material: genetic\_divergence.zip**). In addition, neither of the host genetic divergence patterns possessed a significant correlation with structural and functional variation of gut microbiotas.

## Dominant Effects of Life Stage on the Gut Microbiota Discrepancy Between Populations

Life stage possessed significant Spearman correlations with two  $\alpha$  diversity indices (i.e., Shannon and Pielou's evenness), 16 population-biased taxa, and nine of top 10 (in terms of differences between relative abundances) potential population-biased KEGG pathways (**Supplementary Figure 8**). Specifically, morphological traits of life stage showed negative correlations with  $\alpha$  diversity indices and XZ population-biased taxa and KEGG pathways but positive correlations with TJ population-biased ones. A few significant correlations were detected between population-biased taxa (and KEGG pathways) and five RBT factors (i.e., creatine kinase, aspartate aminotransferase, total

protein, globulin, and alkaline phosphatase), though only two of them (i.e., creatine kinase and alkaline phosphatase) manifested a significant correlation with  $\alpha$  diversity (**Supplementary Figure 8**). In addition, between-location difference was detected in creatine kinase and aspartate aminotransferase (**Supplementary Tables 1, 6**). No significant correlations were detected between RBT factors and life stage factors except creatine kinase (**Supplementary Figure 8**). Therefore, the gut microbiota discrepancy between populations might mainly result from the significant differences in life stage factors between populations.

In RDA analysis, we detected two significant constraint axes (i.e., RDA1 and RDA2) which interpreted 14.09 and 8.23% of gut microbiota variations (**Figure 2**). The TJ and XZ populations discriminated from each other in RDA1 and RDA2 dimensions. Body length, globulin, and creatine kinase were significantly associated with the gut microbiota variation based on RDA1 and RDA2. We identified three (i.e., OTU1, OTU3, and OTU4) and two OTUs (i.e., OTU6 and OTU68) significantly correlated with RDA1 and RDA2, respectively. However, the gut microbiota variation explained by constrained axes (i.e., 0.302) was much less than that explained by unconstrained axes. This phenomenon was confirmed by VPA results that sex, location, body length, and RBT accounted for 30.33% of gut microbiota variation (**Figure 2**). In addition to the dominant effect of body length on the variation associated with location, body length was the only one factor to singly explain the variation significantly.

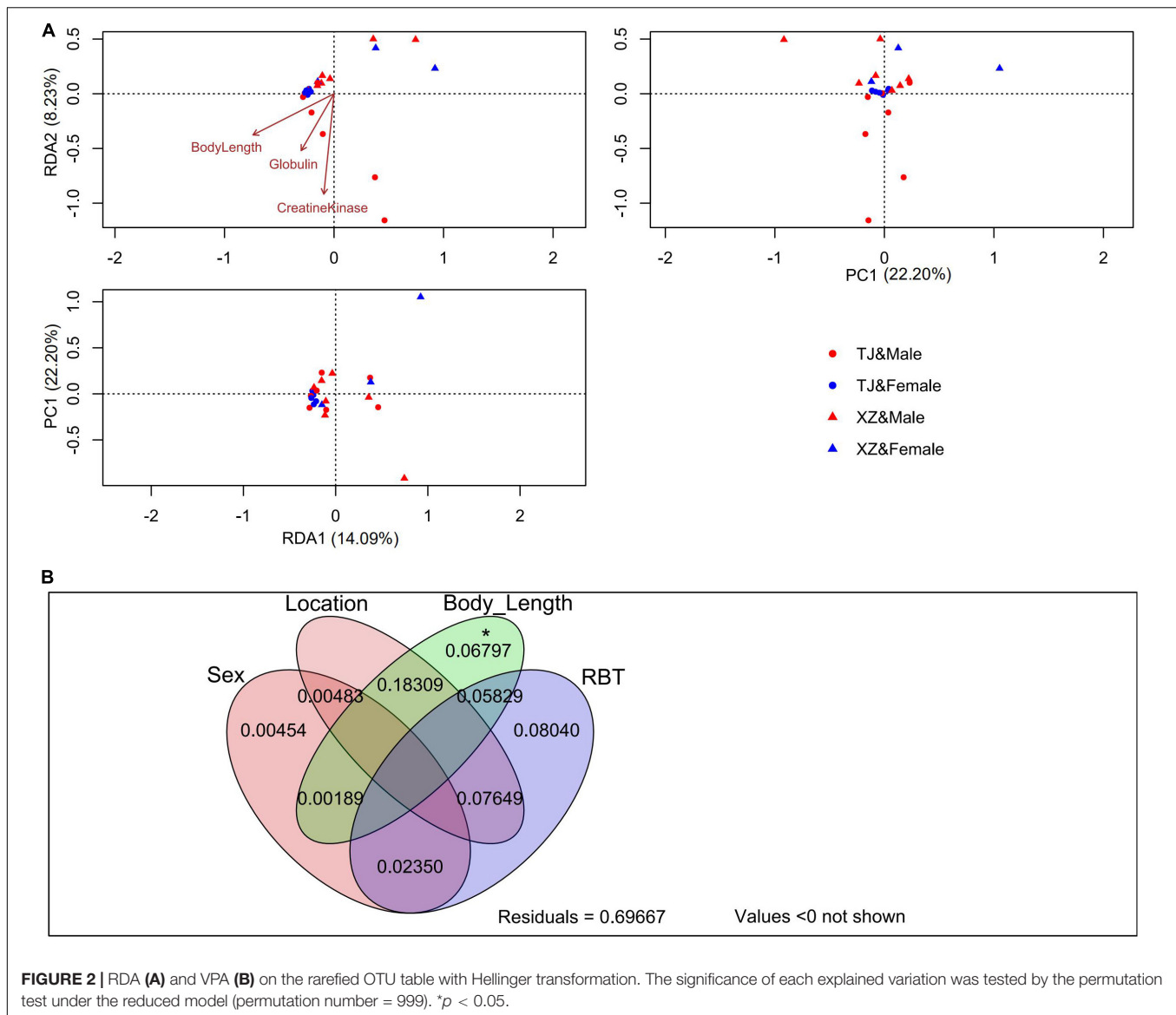
The PLSPM analyses confirmed the significant difference in life stage between two locations (**Figure 3**). No significant direct path coefficients were detected from location and life stage to  $\alpha$  diversity indices. However, a significant direct coefficient probably existed in paths from life stage to compositions of location-biased taxa.

## Discrepant Co-occurrence Networks of Gut Microbiota Between Younger and Older Toads

The OTU co-occurrence networks were significantly different between younger and older groups (**Figure 4** and **Table 2**). Specifically, six network parameters (i.e., edge count, node count, diameter, density, average path length, and normalized betweenness centrality) of the younger group were greater than those of the older group. Five keystone OTUs (i.e., OTU15, OTU33, OTU55, OTU63, and OTU70) were identified in the younger group but none in the older group. From the co-occurrence network of all samples (**Figure 4**), one keystone OTU (i.e., OTU8) was identified. In addition, we identified three target OTUs (i.e., OTU1, OTU4, and OTU8) associated with life stage (i.e., body length) in co-occurrence network remodeling.

## DISCUSSION

Here, we explored the small intestine microbiota of hibernating Asiatic toads (*B. gargarizans*) in two wild populations. Similar to the large or whole intestine microbiota in hibernating amphibians (e.g., *Rana amurensis*, *R. dybowskii*, *R. sylvatica*, and

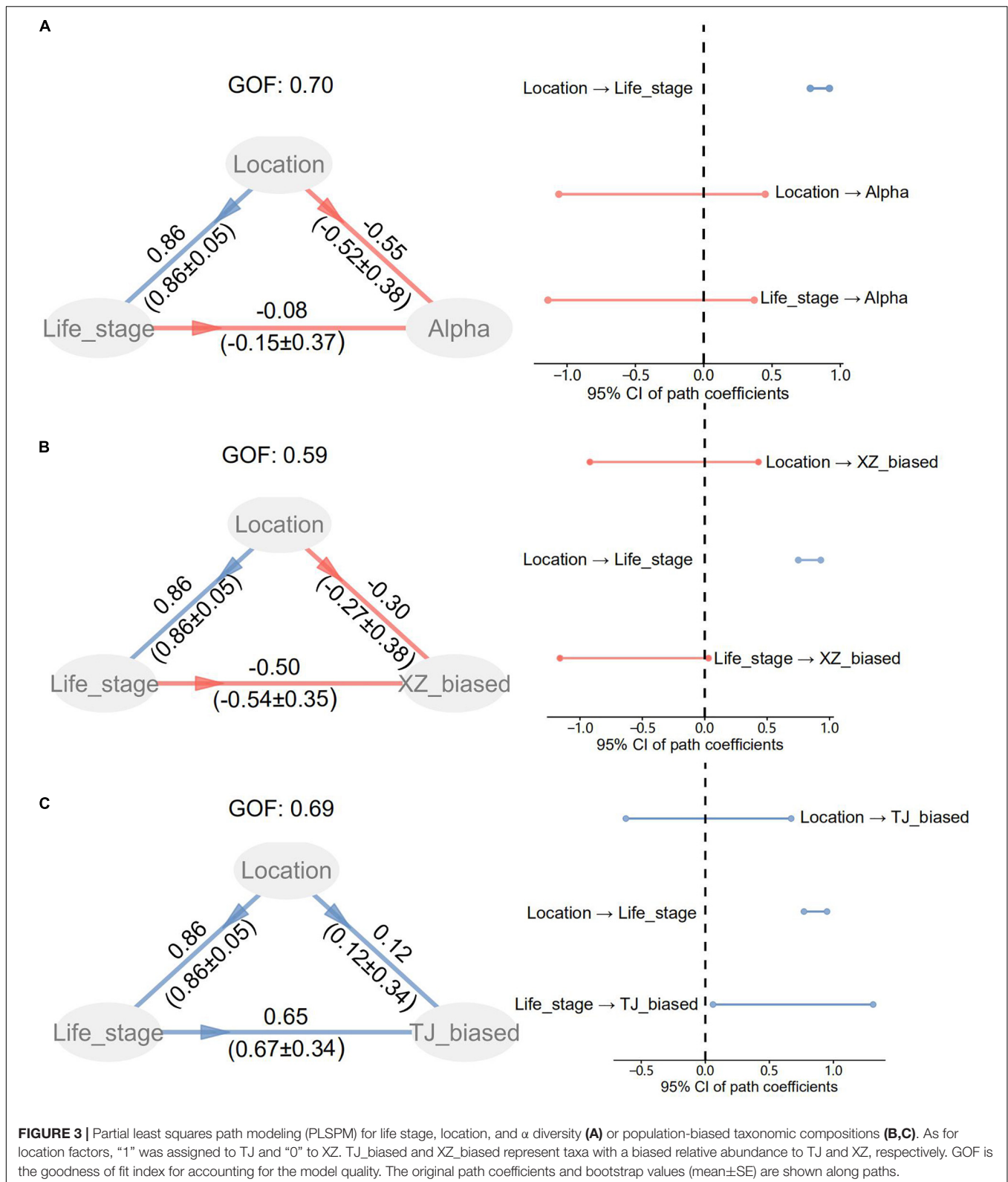


*Polypedates megacephalus*) (Weng et al., 2016; Wiebler et al., 2018; Tong et al., 2019a, 2020), Proteobacteria, Bacteroidetes, and Firmicutes dominate in the small intestine microbiota of hibernating *B. gargarizans* (Figure 1). However, the relative abundances of these three phyla in this study are dramatically different from those in previous studies on the large or whole intestine microbiota. For instance, Proteobacteria inhabits small intestine microbiota with the highest proportion ( $0.9196 \pm 0.0892$ ). In comparison with active individuals, the relative abundance of Proteobacteria tends to be higher in the large or whole gut microbiota of hibernators (Weng et al., 2016; Tong et al., 2020), which is not applicable for all amphibians (Wiebler et al., 2018). Given the comparable relative abundance of Proteobacteria in the small and large intestine microbiota of active amphibians (Zhang et al., 2018; Zhou et al., 2020), the increase rate of Proteobacteria in the small intestine seems to be greater than that in the large intestine during

hibernation. Since we have no data on the small gut microbiota of non-hibernating toads, nevertheless, and the hypothesis remains untested.

The depression of small intestinal performance with fasting (e.g., decreases in intestinal mass and length, enterocyte size, mucosal thickness, and digestive capacities) is evolutionarily prevailing in amphibians and more severe during estivation or hibernation (Cramp et al., 2005; Secor, 2005; Naya et al., 2009; Tamaoki et al., 2016; Wiebler et al., 2018). The dietary shift from external nutrition to intestinal mucus during hibernation is probably a key determinant factor in reshaping the gut microbiota of amphibians (e.g., reduction of bacterial number and increase of the Bacteroidetes/Firmicutes ratio) (Weng et al., 2016; Wiebler et al., 2018; Tong et al., 2020), though no data are about the small intestine microbiota. *Pseudomonas* is a facultative Gram-negative bacterial genus ubiquitously distributed in nature (e.g., drinking water) and host-associated





environments (e.g., intestines) (Vaz-Moreira et al., 2017; de la Maza et al., 2020b). Although *Pseudomonas* spp. are often treated as opportunistic pathogens for amphibians (Weng

et al., 2016; Tong et al., 2019b), moderate accumulation of *Pseudomonas* in the large intestine appears to be a trade-off between cold adaptation (e.g., urea-nitrogen recycling) and

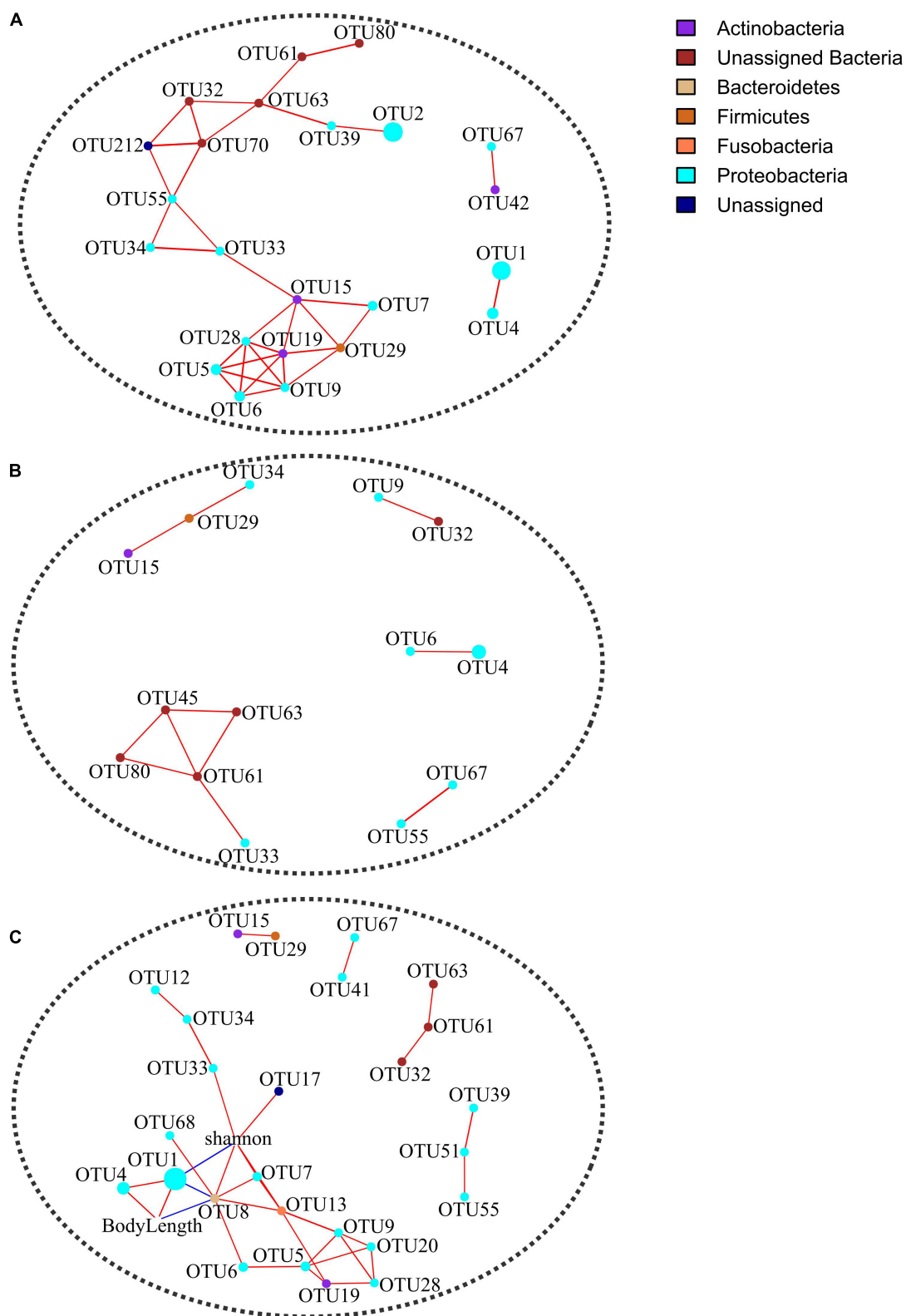


**FIGURE 4 |** Co-occurrence networks in terms of Spearman correlations for 24 shared OTUs in younger **(A)** and older **(B)** groups and for 37 shared OTUs in all samples **(C)**. Correlation coefficients were filtered at a minimum threshold of 0.6 with FDR-adjusted  $p < 0.05$ . Singleton nodes were removed. Node size is positively correlated with the relative abundance of an OTU.

**TABLE 2 |** Topological properties of the OTU co-occurrence networks in younger (body length  $\leq 8.4$  cm,  $n = 10$ ) and older (body length  $\geq 9.8$  cm,  $n = 11$ ) groups of hibernating *B. gargarizans*.

Parameters	Younger	Older	<i>p</i>
Edge count	34	11	–
Node count	23	14	–
Diameter	8	2	–
Density	0.134	0.121	–
Average path length	3.590	1.312	–
Normalized degree centrality (mean $\pm$ SD)	0.134 $\pm$ 0.072	0.121 $\pm$ 0.072	0.475
Normalized betweenness centrality (mean $\pm$ SD)	0.084 $\pm$ 0.128	0.004 $\pm$ 0.012	<b>0.016</b>

*p* shows the significance level of Mann–Whitney test on parameters between the younger and older groups. The *p* value in bold means  $<0.05$ .

immune costs (Wiebler et al., 2018). Intriguingly, we detected high accumulation of *Pseudomonas* in the small intestine of hibernating Asiatic toads (Supplementary Figure 3). One candidate reason for the phenomenon is more appropriate conditions (e.g., higher oxygen or easier accessibility for external *Pseudomonas*) in small intestines than large intestines (Martinez-Guryñ et al., 2019). Moreover, the predominant KEGG pathways predicted (e.g., ABC transporters) tend to be involved in environmental information processing (Supplementary Figure 4). According to significant correlations between *Pseudomonas* and the dominant KEGG pathways (e.g., two-component system), *Pseudomonas* appears to be a key adaptor for small gut microbiota during hibernation (Supplementary Figure 8). Here, we also identified two subdominant core OTUs (assigned as *Rahnella* and *Aeromonas*) widely distributed in aqueous environments (Kämpfer, 2015; de la Maza et al., 2020a), which could be related with the subaqueous hibernation style of Asiatic toads. In addition, the co-occurrence of psychrotolerant *Rahnella* and pathogenic *Aeromonas* appears to coincide with the trade-off hypothesis between cold adaptation and immune cost.

To effectively manipulate the gut microbiota and maintain the host health, we need to illuminate the association between driving factors and gut microbiota. However, it is a big challenge in the case that multiple driving factors play synergistic effects on gut microbiota. For instance, the gut microbiota discrepancy between geographical populations has been reported in many amphibian species, e.g., *B. gargarizans*, *Fejervarya limnocharis*, *Babina adenopleura*, and *Salamandra salamandra* (Bletz et al., 2016; Vences et al., 2016; Huang et al., 2017; Xu et al., 2020). In most cases, the interpopulation gut microbiota discrepancy can be attributed to the divergence of habitats (e.g., dietary structures and bacterial species pools) rather than genetic backgrounds. Even the species effect on the gut microbiota sometimes is subdominant to that of habitats. For instance, the habitat factor rather than the species factor explained significant structural and functional variation in gut microbiota of *F. limnocharis* and *B. adenopleura* (Huang et al., 2017). Due to a long-term fasting, hibernating amphibians provide an ideal experimental platform to evaluate the effects of non-dietary

factors on the gut microbiota. For example, an interspecific divergence was detected in the gut microbiota of two sympatric frogs (i.e., *R. amurensis* and *R. dybowskii*) during hibernation (Tong et al., 2019a).

The present study detected a significant discrepancy of small intestine microbiota between two geographical populations of hibernating Asiatic toads. However, the between-population discrepancy appears not to be decided by population-specific habitats. First, habitats during hibernation tend to be homogeneous between populations, such as long-term fasting and subaqueous hibernation. Second, Tianjian (Ji Canal) and Xuzhou (Luoma Lake) populations are located in similar ecological surroundings affected by human activities. Third, no location-specific core OTUs (i.e., 100% sample occurrence in a population) were identified for the two populations. Due to a geographical distance of about 600 km between two locations (Supplementary Figure 1), nevertheless, incongruent hibernation span in the two populations could be true and contributed to the gut microbiota discrepancy between populations (Fei et al., 2012). In addition, microhabitats of Asiatic toads during the active period might be heterogeneous in dietary structures and bacterial species pools. Location-specific OTUs accounting for 31.59% of total ones suggest a potential divergence of bacterial species pools between populations (Figure 1). However, the sample occurrence of these location-specific OTUs depicts a similar skewed distribution (e.g., 39.20% existence in a single individual) as that of location-shared OTUs. The phenomenon indicates that a high contingency of gut bacterial species exists among individuals and the contingency is similar between location-specific and location-shared OTUs. Since Asiatic toads (even in the same population) have a broad-spectrum diet (e.g., insects and earthworms) (Yu et al., 2009), the high heterogeneity in diet may contribute to the high contingency. Therefore, habitat (e.g., bacterial species pool) appears to play a weak role in the gut microbiota discrepancy between these two populations of hibernating Asiatic toads.

Although sex-specific effects may occur in the ecological adaptation of gut microbiota (Ling et al., 2020), here we did not detect significant between-sex differences in terms of  $\alpha$  and  $\beta$  diversity indices (Table 1), except for a female-biased taxon, i.e., pathogenic Chlamydiales (Borel et al., 2018). The VPA result indicates that sex is not an important driving factor for the gut microbiota variation among hibernating Asiatic toads ( $R^2 = 0.003$ ,  $p = 0.344$ ). As for the significant interactive effect on Faith's PD ( $p = 0.019$ ) between sex and location factors, a candidate reason is a by-product from the sampling bias on life stage (Supplementary Table 6). Specifically, life stage factors showed a significant between-location difference. In addition, life stage factors (e.g., body length) also manifested a significant interactive effect between sex and location factors. Anyway, it is just a bold deduction based on the driving effect of life stage on the gut microbiota (see following discussion in detail). The insignificant co-variation between genetic divergence patterns and  $\beta$  diversity of gut microbiota (Supplementary Figure 7) suggests that host genetic background may possess a minor explanatory capacity on the

gut microbial variation in hibernating Asiatic toads. Although we utilized two types of markers (nuclear and mitochondrial DNA) to deduce genetic divergence patterns, the kinship and relatedness could be biased. For instance, the inconsistent genetic divergence patterns probably result from the different inheritance rules for nuclear (biparental transmission) and mitochondrial DNA (maternal transmission). To identify the genetic materials filtering gut microbiota of Asiatic toads at the population scale, it is necessary to carry out an in-depth investigation from the genomic level (Lu et al., 2021). The life stage factors of the TJ population were significantly larger than those of the XZ population in this study (**Supplementary Tables 1, 6**). Although these factors (e.g., body length) cannot give the exact life stage (i.e., age) of Asiatic toads due to latitude- and sex-dependent variation (Yu and Lu, 2013), these two populations sampled are evidently different in life stage. In addition, the life stage factors possessed significant correlations with population-biased taxa and KEGG pathways (**Supplementary Figure 8**). The life stage has been identified an important determinant for the gut microbiota assembly of amphibians (Kohl et al., 2013; Knutie et al., 2017; Warne et al., 2017; Chai et al., 2018; Zhang et al., 2018). Therefore, it is reasonable to hypothesize that the sampling bias on life stage caused the between-population discrepancy in the gut microbiota. Even though the RBT factors also showed a certain degree of association with population-biased taxa and KEGG pathways, the association might be a by-product generated by the effects of life stage on the gut microbiota. For instance, creatine kinases play an essential role in creatine/phosphocreatine shuttle system to assist ATP hydrolysis and can be applied as an indicator of muscle degradation (Sumien et al., 2018). A positive correlation between creatine kinase and life stage suggests that older toads may possess greater muscle degradation than younger toads during hibernation. Nevertheless, we cannot exclude the possibility that some life stage-irrelevant RBT factors (e.g., aspartate aminotransferase) are able to explain a fraction of gut microbial variation, e.g., through blood metabolites (Wilmanski et al., 2019). The above hypothesis was supported by the subsequent analyses including RDA, VPA, and PLSPM (**Figures 2, 3**). Although body length and two RBT factors (i.e., creatine kinase and globulin) are significantly associated with the gut microbiota variation, the dominant factor for the gut microbiota variation is body length ( $R^2 = 0.128$ ,  $p = 0.001$ ) rather than RBT factors ( $R^2 = 0.056$ ,  $p = 0.255$ ). In addition, the VPA result also revealed that the fraction of variation explained by location ( $R^2 = 0.081$ ,  $p = 0.005$ ) is closely related with body length ( $R^2 = 0.183$ ). The PLSPM analyses further confirmed that life stage (i.e., body length) is the decisive factor for the gut microbiota discrepancy between two populations (**Figure 3**). In accordance with a previous study on pig gut microbiome (Ke et al., 2019), a life stage-linked discrepancy of OTU co-occurrence networks was detected in the hibernating Asiatic toads (**Figure 4**). The microbial network of the older group tends to be simpler than that of the younger group during hibernation. *Pseudomonas* (i.e., OTU1 and OTU4) and *Bacteroides* (i.e., OTU8) were identified as the effect targets of life stage in the co-occurrence network analysis.

Intriguingly, we also screened out *Pseudomonas* (i.e., OTU1 and OTU4), *Serratia* (i.e., OTU3), *Citrobacter* (i.e., OTU6), and *Shewanella* (i.e., OTU68) associated with the first two constraint axes in RDA. These opportunistic pathogens and/or cold-stress-related bacteria (e.g., *Pseudomonas* and *Citrobacter*) are significantly correlated with life stage (**Supplementary Figure 8**; Wiebler et al., 2018), suggesting that the responses to hibernation appear to be distinct in the gut microbiota across different adult stages.

To sum, the small intestine microbiota of adult hibernating Asiatic toads from two wild populations is characterized by a highest relative abundance of Proteobacteria, especially *Pseudomonas*. Sex and genetic background tend to play a minor role in the gut bacterial community of hibernating Asiatic toads. The significant discrepancy of gut microbiota between geographical locations mainly results from the life stage. However, most of the gut microbiota variation (~70%) in the two wild populations of hibernating Asiatic toads cannot be explained by the deterministic factors measured in this study, such as life stage. According to the significantly skewed distribution of location-specific OTUs, the gut microbiota of hibernating Asiatic toads seems to be driven by not only deterministic processes but also stochastic processes, e.g., historical contingency (Zhou and Ning, 2017). Finally, limitations do exist in our study based on wild populations of hibernating Asiatic toads, such as uncontrolled historical contingency in diets and habitats. Therefore, further studies on gut microbiota of hibernating amphibians need improvements with larger sample size and/or more precise control of untargeted factors.

## DATA AVAILABILITY STATEMENT

The datasets presented in this study can be found in online repositories. The names of the repository/repositories and accession number(s) can be found below: <https://db.cngb.org/search/project/CNP0001473/> and <https://db.cngb.org/search/project/CNP0001644/>.

## ETHICS STATEMENT

The animal study was reviewed and approved by Animal Care and Use Committee of Xinyang Normal University.

## AUTHOR CONTRIBUTIONS

XS designed the study, analyzed the data, and wrote the manuscript. XS, JZ, JS, and YZ performed the experiments and collected the data. All authors read and approved the final manuscript.

## FUNDING

This study was supported by the National Natural Science Foundation of China (NSFC 31600104), Key R&D and



Promotion Projects of Henan Province (192102110005), Ph.D. Research Startup Foundation of Xinyang Normal University (No. 0201424), and Nanhu Scholars Program for Young Scholars of Xinyang Normal University.

## ACKNOWLEDGMENTS

We are grateful to Qiyu Li, Rui Li, Shengli Jing, and Tonglei Yu for helping us in the experiments. In addition, we highly

appreciate for the constructive comments on the manuscript from Xiangzhen Li and reviewers.

## SUPPLEMENTARY MATERIAL

The Supplementary Material for this article can be found online at: <https://www.frontiersin.org/articles/10.3389/fmicb.2021.665849/full#supplementary-material>

## REFERENCES

- Amato, K. R., Sanders, J. G., Song, S. J., Nute, M., Metcalf, J. L., Thompson, L. R., et al. (2019). Evolutionary trends in host physiology outweigh dietary niche in structuring primate gut microbiomes. *ISME J.* 13, 576–587. doi: 10.1038/s41396-018-0175-0
- Banas, J. A., Loesche, W. J., and Nace, G. W. (1988). Classification and distribution of large intestinal bacteria in nonhibernating and hibernating leopard frogs (*Rana pipiens*). *Appl. Environ. Microbiol.* 54, 2305–2310. doi: 10.1128/AEM.54.9.2305-2310.1988
- Bletz, M. C., Goedbloed, D. J., Sanchez, E., Reinhardt, T., Tebbe, C. C., Bhujju, S., et al. (2016). Amphibian gut microbiota shifts differentially in community structure but converges on habitat-specific predicted functions. *Nat. Commun.* 7:13699. doi: 10.1038/ncomms13699
- Bolyen, E., Rideout, J. R., Dillon, M. R., Bokulich, N. A., Abnet, C. C., Al-Ghalith, G. A. et al. (2019). Reproducible, interactive, scalable and extensible microbiome data science using QIIME 2. *Nat. Biotechnol.* 37, 852–857. doi: 10.1038/s41587-019-0209-9
- Borel, N., Polkinghorne, A., and Pospischil, A. (2018). A review on chlamydial diseases in animals: still a challenge for pathologists? *Vet. Pathol.* 55, 374–390. doi: 10.1177/0300985817751218
- Brooks, A. W., Kohl, K. D., Brucker, R. M., van Opstal, E. J., and Bordenstein, S. R. (2016). Phyllosymbiosis: relationships and functional effects of microbial communities across host evolutionary history. *PLoS Biol.* 14:e2000225. doi: 10.1371/journal.pbio.2000225
- Chai, L., Dong, Z., Chen, A., and Wang, H. (2018). Changes in intestinal microbiota of *Bufo gargarizans* and its association with body weight during metamorphosis. *Arch. Microbiol.* 200, 1087–1099. doi: 10.1007/s00203-018-1523-1
- Chang, C.-W., Huang, B.-H., Lin, S.-M., Huang, C.-L., and Liao, P.-C. (2016). Changes of diet and dominant intestinal microbes in farmland frogs. *BMC Microbiol.* 16:33. doi: 10.1186/s12866-016-0660-4
- Chen, L., Li, J., Guo, X., Fu, B., and Li, G. (2000). Temporal and spatial characteristics of surface water quality in jiyun river. *Environ. Sci.* 6, 61–64. doi: 10.13227/j.hjlx.2000.06.014
- Colombo, B. M., Scalvenzi, T., Benlamara, S., and Pollet, N. (2015). Microbiota and mucosal immunity in amphibians. *Front. Immunol.* 6:111. doi: 10.3389/fimmu.2015.00111
- Costanzo, J. P., and Lee, R. E. (2013). Avoidance and tolerance of freezing in ectothermic vertebrates. *J. Exp. Biol.* 216, 1961–1967. doi: 10.1242/jeb.070268
- Cramp, R. L., Franklin, C. E., and Meyer, E. A. (2005). The impact of prolonged fasting during aestivation on the structure of the small intestine in the green-striped burrowing frog, *Cyclorana alboguttata*. *Acta Zool.* 86, 13–24. doi: 10.1111/j.0001-7272.2005.00180.x
- de la Maza, L. M., Pezzlo, M. T., Bittencourt, C. E., and Peterson, E. M. (eds). (2020a). “Aeromonas,” in *Color Atlas of Medical Bacteriology*, 141–144. doi: 10.1128/9781683671077.ch15
- de la Maza, L. M., Pezzlo, M. T., Bittencourt, C. E., and Peterson, E. M. (eds). (2020b). “Pseudomonas,” in *Color Atlas of Medical Bacteriology*, 145–149. doi: 10.1128/9781683671077.ch16
- Fei, L., Ye, C., and Jiang, J. (2012). *Colored Atlas of Chinese Amphibians and Their Distributions*. Chengdu: Sichuan Science and Technology Press.
- Feng, Q., Chen, W.-D., and Wang, Y.-D. (2018). Gut microbiota: an integral moderator in health and disease. *Front. Microbiol.* 9:151. doi: 10.3389/fmicb.2018.00151
- Guo, X., Chen, F., Gao, F., Li, L., Liu, K., You, L., et al. (2020). CNSA: a data repository for archiving omics data. *Database* 2020:55. doi: 10.1093/database/baaa055
- Hall, T. (1999). BioEdit: a user-friendly biological sequence alignment editor and analysis program for windows 95/98/NT. *Nucleic Acids Sympos. Ser.* 41, 95–98. doi: 10.1021/bk-1999-0734.ch008
- Huang, B.-H., Chang, C.-W., Huang, C.-W., Gao, J., and Liao, P.-C. (2017). Composition and functional specialists of the gut microbiota of frogs reflect habitat differences and agricultural activity. *Front. Microbiol.* 8:2670. doi: 10.3389/fmicb.2017.02670
- Jiménez, R. R., and Sommer, S. (2017). The amphibian microbiome: natural range of variation, pathogenic dysbiosis, and role in conservation. *Biodiver. Conserv.* 26, 763–786. doi: 10.1007/s10531-016-1272-x
- Kämpfer, P. (2015). “Rahnella,” in *Bergey's Manual of Systematics of Archaea and Bacteria*, eds M. E. Trujillo, S. Dedysh, P. DeVos, B. Hedlund, P. Kämpfer, F. A. Rainey, et al. 1–16. doi: 10.1002/9781118960608.gbm01164
- Katoh, K., and Standley, D. M. (2013). MAFFT multiple sequence alignment software version 7: improvements in performance and usability. *Mol. Biol. Evol.* 30, 772–780. doi: 10.1093/molbev/mst010
- Ke, S., Fang, S., He, M., Huang, X., Yang, H., Yang, B., et al. (2019). Age-based dynamic changes of phylogenetic composition and interaction networks of health pig gut microbiome feeding in a uniformed condition. *BMC Vet. Res.* 15:172. doi: 10.1186/s12917-019-1918-5
- Klindworth, A., Pruesse, E., Schweer, T., Peplies, J., Quast, C., Horn, M., et al. (2012). Evaluation of general 16S ribosomal RNA gene PCR primers for classical and next-generation sequencing-based diversity studies. *Nucleic Acids Res.* 41:e1. doi: 10.1093/nar/gks808
- Knutie, S. A., Gabor, C. R., Kohl, K. D., and Rohr, J. R. (2018). Do host-associated gut microbiota mediate the effect of an herbicide on disease risk in frogs? *J. Anim. Ecol.* 87, 489–499. doi: 10.1111/1365-2656.12769
- Knutie, S. A., Wilkinson, C. L., Kohl, K. D., and Rohr, J. R. (2017). Early-life disruption of amphibian microbiota decreases later-life resistance to parasites. *Nat. Commun.* 8:86. doi: 10.1038/s41467-017-00119-0
- Kohl, K. D., and Yahn, J. (2016). Effects of environmental temperature on the gut microbial communities of tadpoles. *Environ. Microbiol.* 18, 1561–1565. doi: 10.1111/1462-2920.13255
- Kohl, K. D., Cary, T. L., Karasov, W. H., and Dearing, M. D. (2013). Restructuring of the amphibian gut microbiota through metamorphosis. *Environ. Microbiol. Rep.* 5, 899–903. doi: 10.1111/1758-2229.12092
- Langille, M. G. I., Zaneveld, J., Caporaso, J. G., McDonald, D., Knights, D., Reyes, J. A., et al. (2013). Predictive functional profiling of microbial communities using 16S rRNA marker gene sequences. *Nat. Biotechnol.* 31:814. doi: 10.1038/nbt.2676

- Librado, P., and Rozas, J. (2009). DnaSP v5: a software for comprehensive analysis of DNA polymorphism data. *Bioinformatics* 25, 1451–1452. doi: 10.1093/bioinformatics/btp187
- Ling, F., Steinel, N., Weber, J., Ma, L., Smith, C., Correa, D., et al. (2020). The gut microbiota response to helminth infection depends on host sex and genotype. *ISME J.* 14, 1141–1153. doi: 10.1038/s41396-020-0589-3
- Liu, Q., Pang, Y., Xiang, S., and Wan, L. (2021). Distribution characteristics and source analysis of organic matter in surface sediments of Luoma Lake. *China Environ. Sci.* 1–7. doi: 10.19674/j.cnki.issn1000-6923.20210421.001 [Epub ahead of print].
- Lu, B., Jiang, J., Wu, H., Chen, X., Song, X., Liao, W., et al. (2021). A large genome with chromosome-scale assembly sheds light on the evolutionary success of a true toad (*Bufo gargarizans*). *Mol. Ecol. Resour.* 21, 1256–1273. doi: 10.1111/1755-0998.13319
- Magoč, T., and Salzberg, S. L. (2011). FLASH: fast length adjustment of short reads to improve genome assemblies. *Bioinformatics* 27, 2957–2963. doi: 10.1093/bioinformatics/btr507
- Martinez-Gurny, K., Leone, V., and Chang, E. B. (2019). Regional diversity of the gastrointestinal microbiome. *Cell Host Microbe* 26, 314–324. doi: 10.1016/j.chom.2019.08.011
- McDonald, D., Price, M. N., Goodrich, J., Nawrocki, E. P., DeSantis, T. Z., Probst, A., et al. (2012). An improved Greengenes taxonomy with explicit ranks for ecological and evolutionary analyses of bacteria and archaea. *ISME J.* 6, 610–618. doi: 10.1038/ismej.2011.139
- McFall-Ngai, M., Hadfield, M. G., Bosch, T. C. G., Carey, H. V., Domazet-Lošo, T., Douglas, A. E., et al. (2013). Animals in a bacterial world, a new imperative for the life sciences. *Proc. Natl. Acad. Sci. U.S.A.* 110, 3229–3236. doi: 10.1073/pnas.1218525110
- Naya, D. E., Veloso, C., Sabat, P., and Bozinovic, F. (2009). The effect of short- and long-term fasting on digestive and metabolic flexibility in the Andean toad *Bufo spinulosus*. *J. Exp. Biol.* 212, 2167–2175. doi: 10.1242/jeb.030650
- Parks, D. H., Tyson, G. W., Hugenholtz, P., and Beiko, R. G. (2014). STAMP: statistical analysis of taxonomic and functional profiles. *Bioinformatics* 30, 3123–3124. doi: 10.1093/bioinformatics/btu494
- Pedregosa, F., Varoquaux, G., Gramfort, A., Michel, V., Thirion, B., Grisel, O., et al. (2011). Scikit-Learn: machine learning in python. *J. Mach. Learn. Res.* 12, 2825–2830. doi: 10.1524/auto.2011.0951
- Price, M. N., Dehal, P. S., and Arkin, A. P. (2010). FastTree 2 – approximately maximum-likelihood trees for large alignments. *PLoS One* 5:e9490. doi: 10.1371/journal.pone.0009490
- Pruesse, E., Peplies, J., and Glöckner, F. O. (2012). SINA: Accurate high-throughput multiple sequence alignment of ribosomal RNA genes. *Bioinformatics* 28, 1823–1829. doi: 10.1093/bioinformatics/bts252
- Rognes, T., Flouri, T., Nichols, B., Quince, C., and Mahé, F. (2016). VSEARCH: a versatile open source tool for metagenomics. *PeerJ* 4:e2584. doi: 10.7717/peerj.2584
- Ronquist, F., Teslenko, M., van der Mark, P., Ayres, D. L., Darling, A., Höhna, S., et al. (2012). MrBayes 3.2: efficient bayesian phylogenetic inference and model choice across a large model space. *Syst. Biol.* 61, 539–542. doi: 10.1093/sysbio/sys029
- Rosenberg, M. S., and Anderson, C. D. (2011). PASSAGE: pattern analysis, spatial statistics and geographic exegesis. Version 2. *Methods Ecol. Evol.* 2, 229–232. doi: 10.1111/j.2041-210X.2010.00081.x
- Secor, S. M. (2005). Physiological responses to feeding, fasting and estivation for anurans. *J. Exp. Biol.* 208, 2595–2609. doi: 10.1242/jeb.01659
- Segata, N., Izard, J., Waldron, L., Gevers, D., Miropolsky, L., Garrett, W. S., et al. (2011). Metagenomic biomarker discovery and explanation. *Genome Biol.* 12:R60. doi: 10.1186/gb-2011-12-6-r60
- Simon, J.-C., Marchesi, J. R., Mougel, C., and Selosse, M.-A. (2019). Host-microbiota interactions: from holobiont theory to analysis. *Microbiome* 7:5. doi: 10.1186/s40168-019-0619-4
- Sommer, F., and Bäckhed, F. (2013). The gut microbiota — masters of host development and physiology. *Nat. Rev. Microbiol.* 11, 227–238. doi: 10.1038/nrmicro2974
- Song, X., Song, J., Song, H., Zeng, Q., and Shi, K. (2018). A robust noninvasive approach to study gut microbiota structure of amphibian tadpoles by feces. *Asian Herpetol. Res.* 9, 1–12. doi: 10.16373/j.cnki.ahr.170062
- Stamatakis, A. (2014). RAXML version 8: a tool for phylogenetic analysis and post-analysis of large phylogenies. *Bioinformatics* 30, 1312–1313. doi: 10.1093/bioinformatics/btu033
- Sumien, N., Shetty, R. A., and Gonzales, E. B. (2018). “Creatine, creatine kinase, and aging,” in *Biochemistry and Cell Biology of Ageing: Part I Biomedical Science*, eds J. R. Harris and V. I. Korolchuk (Singapore: Springer Singapore), 145–168.
- Tamaoki, K., Okada, R., Ishihara, A., Shiojiri, N., Mochizuki, K., Goda, T., et al. (2016). Morphological, biochemical, transcriptional and epigenetic responses to fasting and refeeding in intestine of *Xenopus laevis*. *Cell Biosci.* 6:2. doi: 10.1186/s13578-016-0067-9
- Thompson, J. D., Higgins, D. G., and Gibson, T. J. (1994). CLUSTAL W: improving the sensitivity of progressive multiple sequence alignment through sequence weighting, position-specific gap penalties and weight matrix choice. *Nucleic Acids Res.* 22, 4673–4680. doi: 10.1093/nar/22.22.4673
- Tong, Q., Du, X.-p., Hu, Z.-f., Cui, L.-y., Bie, J., Zhang, Q.-z., et al. (2019a). Comparison of the gut microbiota of *Rana amurensis* and *Rana dybowskii* under natural winter fasting conditions. *FEMS Microbiol. Lett.* 366:241. doi: 10.1093/femsle/fnz241
- Tong, Q., Hu, Z.-f., Du, X.-p., Bie, J., and Wang, H.-b. (2020). Effects of seasonal hibernation on the similarities between the skin microbiota and gut microbiota of an amphibian (*Rana dybowskii*). *Microb. Ecol.* 79, 898–909. doi: 10.1007/s00248-019-01466-9
- Tong, Q., Liu, X.-N., Hu, Z.-F., Ding, J.-F., Bie, J., Wang, H.-B., et al. (2019b). Effects of captivity and season on the gut microbiota of the brown frog (*Rana dybowskii*). *Front. in Microbiol.* 10:1912. doi: 10.3389/fmicb.2019.01912
- Vaz-Moreira, I., Nunes, O. C., and Manaia, C. M. (2017). Ubiquitous and persistent *Proteobacteria* and other Gram-negative bacteria in drinking water. *Sci. Total Environ.* 586, 1141–1149. doi: 10.1016/j.scitotenv.2017.02.104
- Vences, M., Lyra, M. L., Kueneman, J. G., Bletz, M. C., Archer, H. M., Canitz, J., et al. (2016). Gut bacterial communities across tadpole ecomorphs in two diverse tropical anuran faunas. *Sci. Nat.* 103:25. doi: 10.1007/s00114-016-1348-1
- Warne, R. W., Kirschman, L., and Zeglin, L. (2017). Manipulation of Gut microbiota reveals shifting community structure shaped by host developmental windows in amphibian larvae. *Integrat. Comparat. Biol.* 57, 786–794. doi: 10.1093/icb/ix100
- Weng, F. C.-H., Shaw, G. T.-W., Weng, C.-Y., Yang, Y.-J., and Wang, D. (2017). Inferring microbial interactions in the gut of the hong kong whipping frog (*Polypedates megacephalus*) and a validation using probiotics. *Front. Microbiol.* 8:525. doi: 10.3389/fmicb.2017.00525
- Weng, F. C.-H., Yang, Y.-J., and Wang, D. (2016). Functional analysis for gut microbes of the brown tree frog (*Polypedates megacephalus*) in artificial hibernation. *BMC Genom.* 17:1024. doi: 10.1186/s12864-016-3318-6
- Wiebler, J. M., Kohl, K. D., Lee, R. E., and Costanzo, J. P. (2018). Urea hydrolysis by gut bacteria in a hibernating frog: evidence for urea-nitrogen recycling in Amphibia. *Proc. R. Soc. B Biol. Sci.* 285:20180241. doi: 10.1098/rspb.2018.0241
- Wilmanski, T., Rappaport, N., Earls, J. C., Magis, A. T., Manor, O., Lovejoy, J., et al. (2019). Blood metabolome predicts gut microbiome  $\alpha$ -diversity in humans. *Nat. Biotechnol.* 37, 1217–1228. doi: 10.1038/s41587-019-0233-9
- Xu, L., Zhu, B., Li, C., Yao, M., Zhang, B., and Li, X. (2020). Development of biological soil crust prompts convergent succession of prokaryotic communities. *CATENA* 187:104360. doi: 10.1016/j.catena.2019.104360
- Xu, L. L., Chen, H., Zhang, M., Zhu, W., Chang, Q., Lu, G., et al. (2020). Changes in the community structure of the symbiotic microbes of wild amphibians from the eastern edge of the Tibetan Plateau. *Microbiol. Open* 9:e1004. doi: 10.1002/mbo3.1004
- Yu, T., and Lu, X. (2013). Body size variation of four latitudinally-separated populations of a toad species: age and growth rate as the proximate determinants. *Integr. Zool.* 8, 315–323. doi: 10.1111/j.1749-4877.2012.00294.x

- Yu, T., Gu, Y., Du, J., and Lu, X. (2009). Seasonal variation and ontogenetic change in the diet of a population of *Bufo gargarizans* from the farmland, Sichuan, China. *Bihar. Biol.* 3, 99–104.
- Zhang, M., Gaughan, S., Chang, Q., Chen, H., Lu, G., Wang, X., et al. (2018). Age-related changes in the gut microbiota of the Chinese giant salamander (*Andrias davidianus*). *Microbiol. Open* 8:e778. doi: 10.1002/mb.03.778
- Zhang, W., Guo, R., Yang, Y., Ding, J., and Zhang, Y. (2016). Long-term effect of heavy-metal pollution on diversity of gastrointestinal microbial community of *Bufo raddei*. *Toxicol. Lett.* 258, 192–197. doi: 10.1016/j.toxlet.2016.07.003
- Zhou, J., and Ning, D. (2017). Stochastic community assembly: does it matter in microbial ecology? *Microbiol. Mol. Biol. Rev.* 81:e00002-17. doi: 10.1128/mmbr.00002-17
- Zhou, J., Nelson, T. M., Rodriguez Lopez, C., Sarma, R. R., Zhou, S. J., and Rollins, L. A. (2020). A comparison of nonlethal sampling methods for amphibian gut microbiome analyses. *Mol. Ecol. Resour.* 20, 844–855. doi: 10.1111/1755-0998.13139

**Conflict of Interest:** The authors declare that the research was conducted in the absence of any commercial or financial relationships that could be construed as a potential conflict of interest.

**Publisher's Note:** All claims expressed in this article are solely those of the authors and do not necessarily represent those of their affiliated organizations, or those of the publisher, the editors and the reviewers. Any product that may be evaluated in this article, or claim that may be made by its manufacturer, is not guaranteed or endorsed by the publisher.

Copyright © 2021 Song, Zhang, Song and Zhai. This is an open-access article distributed under the terms of the Creative Commons Attribution License (CC BY). The use, distribution or reproduction in other forums is permitted, provided the original author(s) and the copyright owner(s) are credited and that the original publication in this journal is cited, in accordance with accepted academic practice. No use, distribution or reproduction is permitted which does not comply with these terms.



# The Effect of Ryegrass Silage Feeding on Equine Fecal Microbiota and Blood Metabolite Profile

Yiping Zhu<sup>1</sup>, Xuefan Wang<sup>1</sup>, Bo Liu<sup>1</sup>, Ziwen Yi<sup>1</sup>, Yufei Zhao<sup>1</sup>, Liang Deng<sup>2</sup>, Reed Holyoak<sup>3</sup> and Jing Li<sup>1\*</sup>

<sup>1</sup> Equine Clinical Diagnostic Center, College of Veterinary Medicine, China Agricultural University, Beijing, China, <sup>2</sup> College of Animal Husbandry and Veterinary Medicine, Shenyang Agricultural University, Shenyang, China, <sup>3</sup> College of Veterinary Medicine, Oklahoma State University, Stillwater, OK, United States

## OPEN ACCESS

### Edited by:

Aram Mikaelyan,  
North Carolina State University,  
United States

### Reviewed by:

Kimberly Ange-Van Heugten,  
North Carolina State University,  
United States  
Amy Sanders Biddle,  
University of Delaware, United States

### \*Correspondence:

Jing Li  
jjivet@cau.edu.cn

### Specialty section:

This article was submitted to  
Microbial Symbioses,  
a section of the journal  
Frontiers in Microbiology

Received: 27 May 2021

Accepted: 02 August 2021

Published: 23 August 2021

### Citation:

Zhu Y, Wang X, Liu B, Yi Z,  
Zhao Y, Deng L, Holyoak R and Li J  
(2021) The Effect of Ryegrass Silage  
Feeding on Equine Fecal Microbiota  
and Blood Metabolite Profile.  
Front. Microbiol. 12:715709.  
doi: 10.3389/fmicb.2021.715709

Silage is fed to horses in China and other areas in the world, however, knowledge about the impact of feeding silage on horse health is still limited. In the current study, 12 horses were assigned into two groups and fed ryegrass silage and ryegrass hay, respectively, for 8 weeks. High-throughput sequencing was applied to analyze fecal microbiota, while liquid chromatography–tandem mass spectrometry (LC–MS/MS) based metabolomics technique was used for blood metabolite profile to investigate the influence of feeding ryegrass silage (group S) compared to feeding ryegrass hay (group H) on equine intestinal and systemic health. Horses in group S had significantly different fecal microbiota and blood metabolomes from horses in group H. The results showed that Verrucomicrobia was significantly less abundant which plays important role in maintaining the mucus layer of the hindgut. *Rikenellaceae* and *Christensenellaceae* were markedly more abundant in group S and *Rikenellaceae* may be associated with some gut diseases and obesity. The metabolomics analysis demonstrated that ryegrass silage feeding significantly affected lipid metabolism and insulin resistance in horses, which might be associated with metabolic dysfunction. Furthermore, Pearson's correlation analysis revealed some correlations between bacterial taxa and blood metabolites, which added more evidence to diet-fecal microbiota-health relationship. Overall, ryegrass silage feeding impacted systemic metabolic pathways in horses, especially lipid metabolism. This study provides evidence of effects of feeding ryegrass silage on horses, which may affect fat metabolism and potentially increase risk of insulin resistance. Further investigation will be promoted to provide insight into the relationship of a silage-based diet and equine health.

**Keywords:** fecal microbiota, hay, horses, metabolome, silage

## INTRODUCTION

As a non-ruminant grazing herbivore, horses have undergone domestication and been adapted to eating forage-based diets with a mixed symbiotic microbiota (De Fombelle et al., 2003). Gut microbial flora plays critical roles in animal health by extracting energy from the diet for growth, guarding the gastrointestinal system as a commensal barrier and modulating gut mucosal immunity



(Shulman et al., 2008; Cox et al., 2014). Dietary composition undoubtedly impacts the intestinal ecosystem. Therefore, inappropriate diet management can also be a risk factor for intestinal diseases such as colic (Tinker et al., 1997). There is ever growing knowledge of the impact of different diets and feeding patterns on the microbial signatures of the horse gastrointestinal system (De Fombelle et al., 2001; Daly et al., 2012; Venable et al., 2017). Characterization of gut microbiota in horses fed forage, hay, high-starch diet, as well as different supplements such as cereal and oil have been reported (Dougal et al., 2014; Fernandes et al., 2014; Sorensen et al., 2021). Profound impact of the different diets on horse gut microbiota has been revealed.

Traditionally, horses were able to graze fresh pastures. However, nowadays many of them are fed preserved forages, including hay, haylage and silage, due to environmental limits on grazing and modern management systems (Glunk et al., 2015; Harris et al., 2017). Silage is a type of fermented forage preserved moist and airtight with more volatile products compared to hay (Han et al., 2006). In European countries, the use of silage as feed for horses is increasing since this type of diet is easier to store (Vandenput et al., 1997; Muhonen et al., 2008). Silage is also fed to horses in some areas of China, such as Xinjiang province, for economic reasons, convenience of harvesting, and some nutrition components, including volatile fatty acids (VFA) (Guo, 2014; Harris et al., 2017). Ryegrass was widely planted in Asia, Europe and America due to its high nutritional value (Parvin et al., 2010). It has been popular forage crop for large animals in China (Li et al., 2019), therefore, ryegrass was used as silage and hay source in this study. A few studies have reported effects of silage on the equine intestinal ecosystem, and it has been considered a cause of gut microbial flora disturbances, such as soft stools in horses (Holmquist and Müller, 2002). In Muhonen's study, the disturbance was explained as an abrupt change of diet, instead of silage feeding and only a small decrease in pH and an increase in VFA were observed (Muhonen et al., 2008). In a recent study, no significant impact was found on intestinal health of horses fed silage for 8 weeks, even though significant microbial differences were revealed between horses fed silage, hay and pasture grasses (Zhu et al., 2021). Nonetheless, the marked impact of diet induced gut microbial changes on horse general health remains unclear.

Gut microbiota is not only influenced by many host factors but also can modulate metabolic phenotypes (Armstrong et al., 2017). Microbial candidates strongly associated with host metabolic pathways are likely to be more relevant to host health, for example, *Faecalibacterium prausnitzii* population is associated with host energy metabolism and mucosal integrity indicating its critical role in host gastrointestinal health (Li et al., 2008). There is an increased effort to study diet-metabolite-health relationships in humans and other species including horses (Sun et al., 2016; Guasch-Ferré et al., 2018; Sanguinetti et al., 2018). Human based studies focusing on the multilevel dimensional complexity of diet-microbiome-host interactions have provided more insights into the impact of gut microbiota on systemic health via the production of metabolites (Marchesi et al., 2016). There is evidence that host gut microbiota is profoundly involved in many metabolic pathways, such as lipid metabolism and amino acid synthesis (Li et al., 2008). Nevertheless, the understanding on

the interactions among different dietary patterns, gut microbiota and health via metabolite production is still relatively new even in humans (Tindall et al., 2018).

In this study using high-throughput omics approaches, we investigated the interaction between the horse fecal microbiota and blood metabolite profile, when fed two diets (hay and ryegrass silage). Silage feeding to horses has been a hot topic in Chinese equine industry for years and this is the first study about the effect of silage diet on systemic metabolism and health in horses besides fecal microbiota. It is intended to facilitate understanding on health outcomes of horses fed different diets especially silage.

## MATERIALS AND METHODS

### Animal and Ethics Statement

All procedures involving animals in this study were carried out with welfare license (No. AW11101202-2-1) issued by Animal Care and Use Committee of the China Agriculture University.

### Experimental Design and Sample Collection

Twelve light breed (Guanzhong) horses located in the in Shanxi Province, including eight mares and four stallions with normal body condition scores (BCS 4–6, mean = 4.8), were selected for this study. Body weight of each horse was estimated using body weight formula developed by Carroll and Huntington (1988) and the average weight was 389 kg (SD  $\pm$  19 kg). A complete physical exam was performed on each animal before the initiation of the experiment. All were clinically healthy. Horses involved in this study had no history of illness or medical treatments in the 6 months prior to its initiation. The horses varied in age from 3 to 13 years, with a mean age of 6.9 (SD  $\pm$  2.7). Prior to this study, all horses were kept in individual stalls and fed with mainly commercial hay and a small amount of home-made corn-based concentrates formulated locally.

The diets involved in this study were either ryegrass hay (local pasture ryegrass, 15% dry matter [DM]) or ryegrass silage (26% DM). Hay used in this study was second cutting ryegrass from local pasture (September–October) and ryegrass silage was soft-dough-high stage cut from the pasture in the area. The nutritional analysis has been performed on both types of forages (Table 1), which was previously described (Zhu et al., 2021). The eight mares and the four stallions were randomly and equally divided into two groups, respectively. One group of mares and one group of stallions were combined in a random way as well with six horses (four mares and two stallions) in each group. One was fed ryegrass silage (group S) and one fed ryegrass hay (group H). Each group fed ryegrass silage or hay, respectively started at 0800 h on the same day, lasting for 8 weeks as previously described (Zhu et al., 2021). To minimize gut disturbances there was a gradual introduction and acclimatization of the new diets which was completed in 1 week. Each horse was fed a daily maintenance ration of 2% of body mass on a DM basis (Dugdale et al., 2010). Body weight estimation and physical exam were performed

weekly on each horse. All horses had access to water *ad libitum*, with no other dietary supplements throughout the experiment.

Fecal samples were collected manually from the rectum of all horses prior to the onset of the feed change and again at the end of the 8-week feeding phase as described previously (Zhu et al., 2021). Each fresh fecal sample was saved in a clean self-sealing bag and immediately placed on ice for transportation (approximately 2 h) to the lab. Upon arrival at the laboratory, the center of each fecal ball was collected sterily (Stewart et al., 2018) and transferred to a 2 mL sterile cryogenic vial (Corning, Corning, NY, United States). Each vial was marked and stored at  $-80^{\circ}\text{C}$  right after center collection for further analysis.

Meanwhile, one set of blood samples were collected from each horse at the end of the trial. Eight milliliter blood was drawn from the horse's jugular vein into a pro-coagulation tube (Sanli Medical and Technological Development Co., Ltd., Liuyang, China) and immediately placed upright in ice. The serum of each blood sample was centrifuged and stored at  $-80^{\circ}\text{C}$  right away until further analysis.

## Fecal Sample Processing and 16S rRNA High-Throughput Sequencing

Bacterial DNA from each fecal sample was extracted using a E.Z.N.A.<sup>®</sup> soil DNA Kit (Omega Bio-tek, Norcross, GA, United States) in accordance with manufacturer's instructions. DNA concentration and purity were assessed after extraction. High-throughput 16S rRNA sequencing was then performed to evaluate the composition and diversity of the bacterial community.

The V4 hypervariable region of the 16S rRNA genes was amplified using 515F (5'-GTGCCAGCMGCCGCGTAA-3') and 806R (5' GGACTACHVGGGTWTCTAAT-3') primer pairs. Positive template and negative control of distilled water were also employed. After PCR amplification, products were electrophoresed and purified using an AxyPrep DNA Gel Extraction Kit (Axygen Biosciences, Union City, CA, United States) following manufacturer's recommendations. PCR products were quantified using a Quantus Fluorometer (Promega, Madison, WI, United States). Purified amplicons pooling and paired-end sequencing were performed with Illumina MiSeq PE300 platform and NovaSeq PE250 platform

(Illumina, San Diego, CA, United States). Raw 16S gene sequence data was quality-filtered using FASTQ (v 0.20.0.) (Chen et al., 2018). The sequencing reads merge was performed with FLASH (v 1.2.7) (Magoč and Salzberg, 2011). Operational taxonomic units (OTUs) were clustered at a 97% similarity level (Stackebrandt and Goebel, 1994) using UPARSE (v 7.1) (Edgar, 2013). Each OTU taxon was evaluated for the most abundant sequences by QIIME (v 1.9.1) (Caporaso et al., 2010; Brandwein et al., 2019) and analyzed for the representative sequence against the Silva rRNA database (v 138) (Quast et al., 2013) with the Ribosomal Database Projection (RDP) Classifier (v 2.2.0) (Wang et al., 2007).

## Serum Sample Processing and Untargeted Metabolic Analysis

Untargeted metabolic analysis was performed on serum samples from each horse using liquid chromatography–tandem mass spectrometry (LC–MS/MS) system (Merware, Wuhan, China). To extract hydrophilic compounds, 50  $\mu\text{L}$  Serum samples were added to 300  $\mu\text{L}$  pure methanol after having been thawed on ice. The mixture was vortexed for 3 min, then centrifuged with 12,000 rpm at  $4^{\circ}\text{C}$  for 3 min. A 150  $\mu\text{L}$  sample of supernatant was taken for LC–MS/MS analysis. Hydrophobic compounds were extracted by homogenizing with 1 mL mixture (including methanol, MTBE and internal standard mixture), centrifuging with 12,000 rpm at  $4^{\circ}\text{C}$  for 10 min and supernatant dissolving with 200  $\mu\text{L}$  mobile phase B. Sample extracts were then analyzed using ultra performance liquid chromatography (UPLC) and tested for ion mode by electrospray ionization (ESI).

## Statistical Analysis

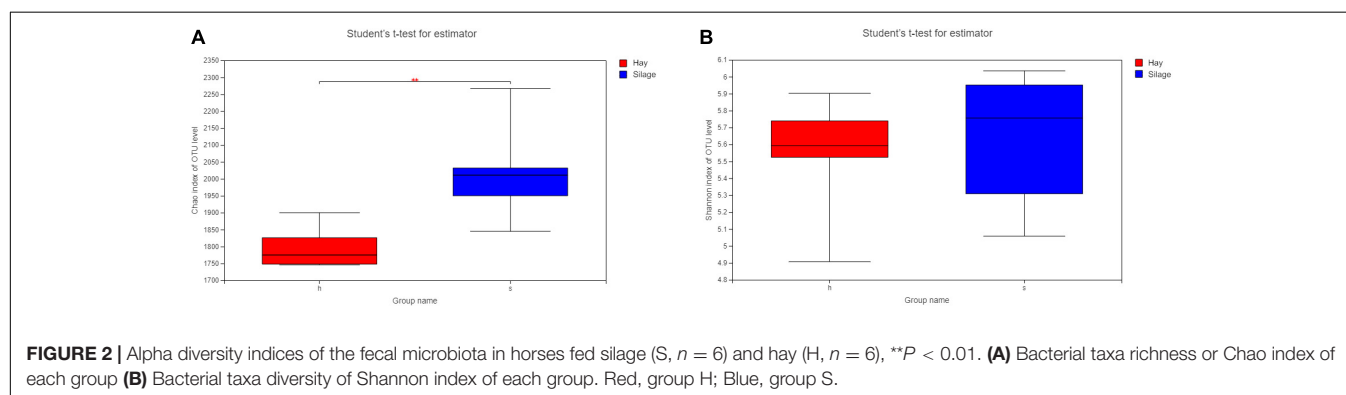
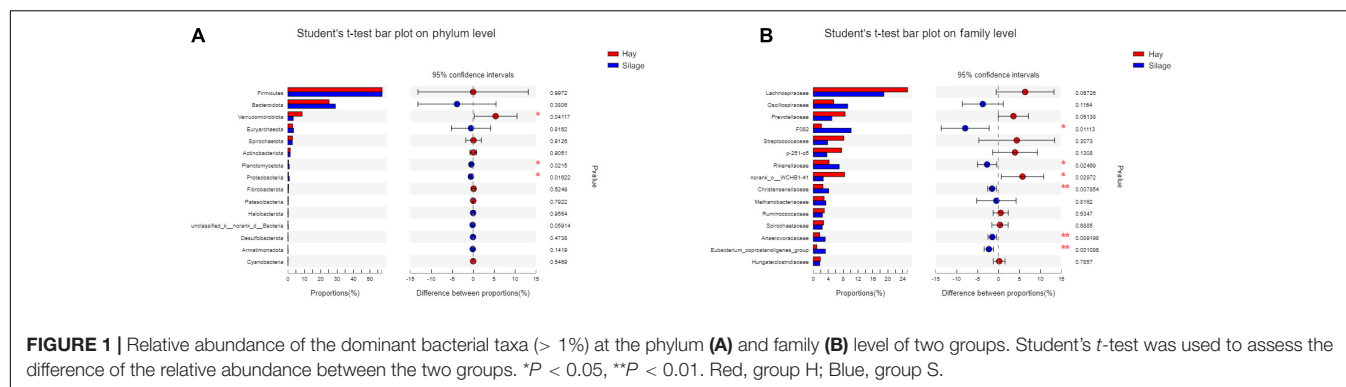
Alpha diversity analysis, including Chao index representing richness (number of taxonomic groups; Willis, 2019) and Shannon index illustrating diversity (the variety and abundance of taxonomic groups; Magurran, 2004), were conducted using MOTHUR (v 1.3.0). Subsampling was performed to normalize the dataset and pair-wise comparisons between groups were performed by the Student's *t*-test. Principal component analysis (PCA) and Principal coordinates analysis (PCoA) were carried out using QIIME (v 1.9.1). Linear discriminant analysis (LDA) effect size (LEfSe) (Segata et al., 2011) was performed by the Kruskal-Wallis sum-rank test to determine significant differences in abundance of the microbial community between the groups.

Significantly regulated metabolites between groups were detected by variable-importance-projection (VIP) values  $\geq 1.0$ , hypergeometric test's *p*-values  $< 0.05$  and absolute  $\text{Log}_2\text{FC}$  (fold change)  $\geq 1.0$ . VIP values were extracted from on orthogonal partial least squares discriminate analysis (OPLS-DA) result using MetaboAnalystR (v 1.0.1) (Edmonton, CA, United States). Metabolites set enrichment analysis (MSEA) was performed for pathways with significant regulated metabolites. Heatmaps were generated using Pearson's correlation coefficients (PCC) with ComplexHeatmap (v 3.5.0) (Gu et al., 2016). Identified metabolites were annotated by Kyoto Encyclopedia of Genes and Genomes (KEGG) compound database and mapped to the KEGG pathway database.

**TABLE 1** | Nutritional composition: ryegrass silage, hay (As fed).

	Ryegrass silage	Ryegrass hay
DM <sup>1</sup> (%NM <sup>2</sup> )	25.78	91.50
CP <sup>3</sup> (%DM)	8.54	9.36
CF <sup>4</sup> (%DM)	1.34	1.82
Ash (%DM)	9.91	5.04
NDF <sup>5</sup> (%DM)	66.62	59.89
ADF <sup>6</sup> (%DM)	46.94	34.71
Ca <sup>7</sup> (%DM)	0.28	0.16
P <sup>8</sup> (%DM)	0.22	0.06

1 dry matter; 2 natural matter; 3 crude protein; 4 crude fat; 5 neutral detergent fiber; 6 acid detergent fiber; 7 calcium; 8 phosphorus.



## RESULTS

Throughout the 8-week feeding phase the average body condition score and body weight of each horse did not change significantly. Weekly physical exam was unremarkable of each horse and no clinical abnormalities have been noted throughout the feeding trial.

### Summary of 16S rRNA Amplicon Sequencing Data

A total of 810,491 sequence reads were detected from all the samples. With 731,179 sequences, ranging from 44,873 to 71,449 per sample, remaining after quality control. After clustering at the 97% threshold level, 3,191 OTUs were retained and classified as bacteria within 25 phyla, 50 classes, 118 orders, 209 families, and 423 genera. The raw data were deposited into the NCBI Sequence Read Archive (SRA) database (Accession Number: PRJNA735708).

### Effects of Diet on Microbial Composition

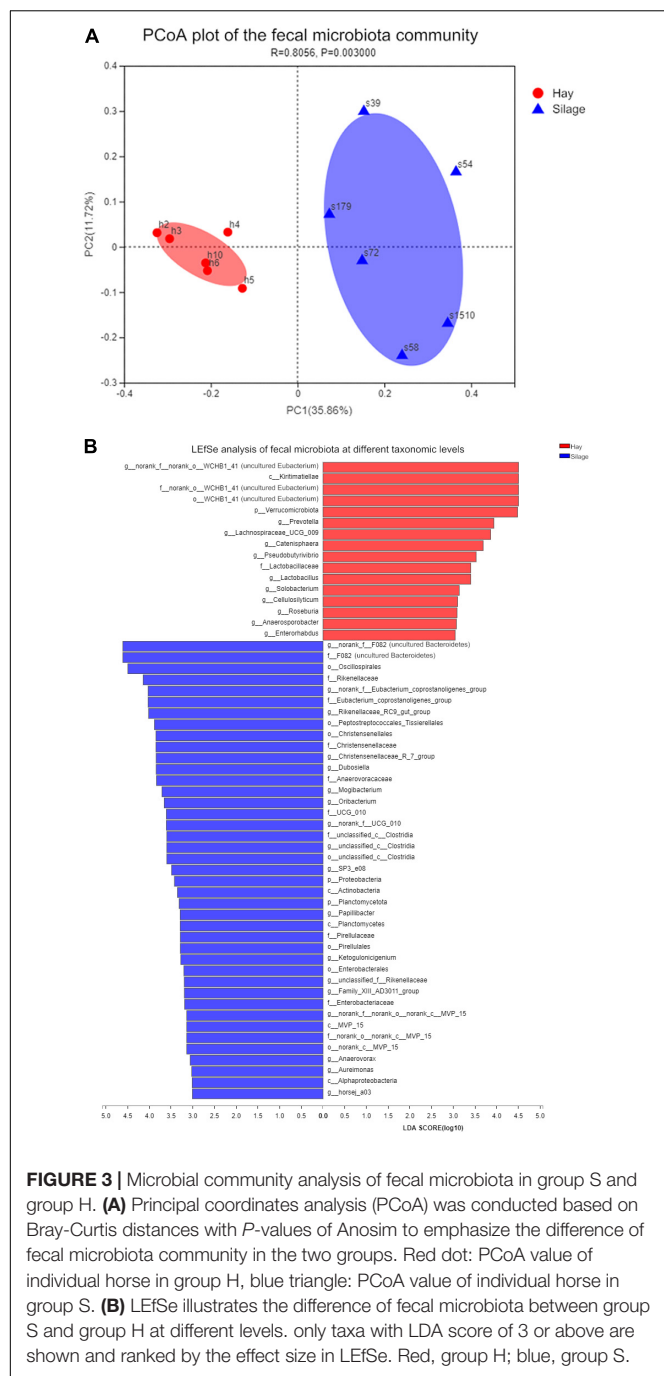
Six phyla and twenty-three families of bacterial taxa had relative abundance > 1%. The six most abundant phyla were Firmicutes, Bacteroidetes, Verrucomicrobia, Spirochaetes, Euryarchaeota, and Actinobacteria (Figure 1A). Only the relative abundance of Verrucomicrobia was significantly different between the two groups (*P* = 0.03943). The level of Verrucomicrobia was higher in group H than in group S. At the family level among the top 10 most abundant bacterial taxa, *Rikenellaceae* and

*Christensenellaceae* were notably affected by diet (*P* < 0.05), with both detected at a higher level in group S (Figure 1B).

Alpha diversity analysis including richness (Chao index) and diversity (Shannon index) of microbial species was conducted based on the Student's *t*-test. The Chao index showed the microbial composition of group S was significantly richer than that of group H (*P* < 0.01) (Figure 2A), while the Shannon index revealed no statistical difference in microbial diversity between the two groups (Figure 2B). The PCoA, based on the Bray-Curtis distance, demonstrated two separate clusters, representing group S and group H, respectively (Figure 3A). Additionally, to evaluate the variations of the microbial composition between two groups, LEfSe was performed with LDA score > 2.0. Sixteen taxa were most associated with group H, while forty-two were associated with group S (Figure 3B). In the samples from group S, excluding the undefined taxa, the most distinct bacterial taxa included *Oscillospirales*, *Rikenellaceae*, and *Eubacterium coprostanoligenes*. In group H, the two most associated bacterial taxa were *Kiritimatiellae* and *Verrucomicrobia*.

### Effects of Diet on Metabolite Profiles

To evaluate the effects of ryegrass silage and hay diets on the horse's metabolite production, untargeted metabolic analysis by LC-MS/MS was performed. Before differential analysis of the groups of metabolites, PCA analysis was conducted to illustrate the sample variation between groups and within groups (Figure 4A). Samples from group S and group H were well separated. Furthermore, the horses fed ryegrass



silage demonstrated larger metabolite composition variation as compared to horses on the hay diet.

Significant changes in metabolites between group S and H were detected according to the following criteria: VIP values > 1.0 based on OPLS-DA, fold change > 2 or < 0.5 or *P* < 0.05. In total, 206 discriminating metabolites were selected from the two groups. In group H, eighty-two compounds were up-regulated including estrone,  $\gamma$ - and  $\alpha$ -Linolenic acid, 7- and 12-ketolithocholic acid (Figure 4B). Whereas 124 metabolites were down-regulated in group H as compared

to group S, including 4-Hydroxy-3-methoxyphenylacetic acid, protocatechuic aldehyde, 4-methoxyphenylacetic acid, and most types of triglycerides belonging to glycerolipids (Supplementary Table 1). A heat map was produced to show the great variation in their distribution within each group (Figure 4C). Eighteen metabolites were shown to have significantly different distributions between group S and group H. Glycerolipids (mainly triglycerides) and fatty acids (mainly  $\gamma$ -linolenic acid, palmitoleic acid, stearidonic acid, and carnitine) were the most abundant metabolites in group S, while being notably lower in abundance in group H. Organic acids and derivatives, amino acids and metabolomics, benzene and substituted derivatives, as well as glycerophospholipids, were more abundant in group H than in group S.

To explore the biological functions of the metabolites in the two groups, KEGG enrichment analysis was conducted (Figure 4D). Seven significantly different enriched pathways (*P* < 0.05) were recognized including cholesterol metabolism, thermogenesis, regulation of lipolysis in adipocytes, insulin resistance, fat digestion and absorption, vitamin digestion and absorption and glycerolipid metabolism.

## Correlation Between Microbial Community and Blood Metabolites

To further explore the correlation between blood metabolites and the altered fecal microbiota as induced by the two diets, analyses based on the Pearson's correlation coefficients were conducted (Figure 5). Discriminating metabolites were selected based on a fold change of > 2 or < 0.5, while altered microbial taxa were identified using the *P*-value < 0.05. These analyses revealed high correlations between some bacterial taxa and typical metabolites. For instance, *Eubacterium coprostanoligenes* were positively correlated with triglycerides and fatty acids such as stearidonic acid,  $\alpha$ -linolenic acid and  $\gamma$ -linolenic acid, but negatively correlated with organic acids and phenolic acids, such as 4-methoxyphenylacetic acid, 3-hydroxyanthranilic acid and 2,4-dihydroxy benzoic acid. Triglycerides were positively correlated with *Sphingobacteriaceae*, *Eubacterium coprostanoligenes*, and *Paenibacillaceae*, however, negatively correlated with *Treponema*, *Roseburia* and *Lachnospiraceae*.

## DISCUSSION

Silage is often used as horse feed in China and other countries, especially in Europe (Muhonen et al., 2008; Domingues, 2009; Guo, 2014), however, occasional disturbances, such as soft or loose stool, have been reported when silage has been introduced as a feed stuff (Connysson et al., 2006). The available information about the influence of silage on equine gut and systemic health is limited. Therefore, the objectives of this study were to explore how the two different diets, including ryegrass silage and ryegrass hay, would modulate fecal microbiota and blood metabolomics, indicating the potential association of silage with intestinal and systemic level of health. Characterization of the blood metabolome, associated with fecal microbiota, highlights the effects of diet on systemic biological molecules and provides



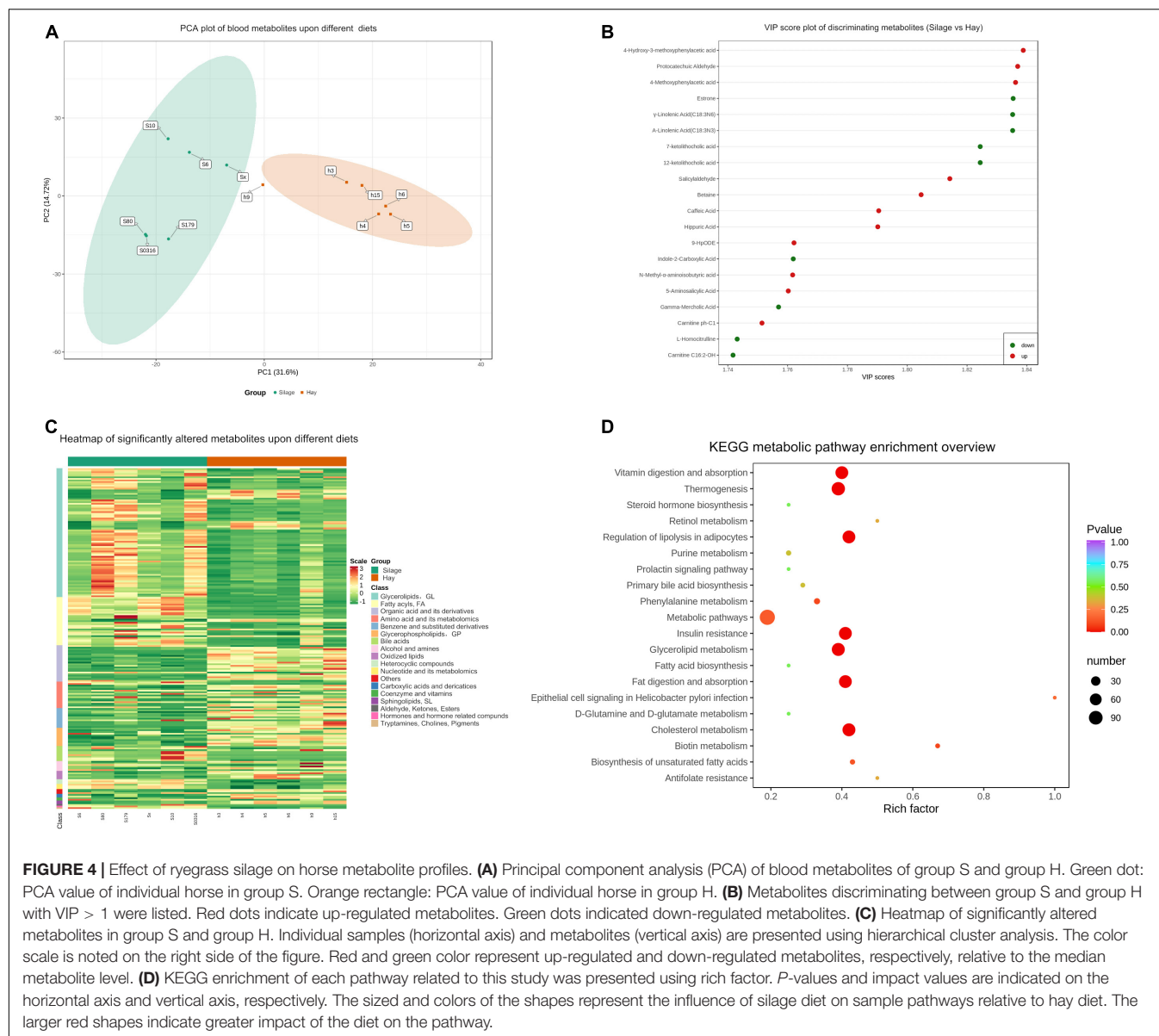
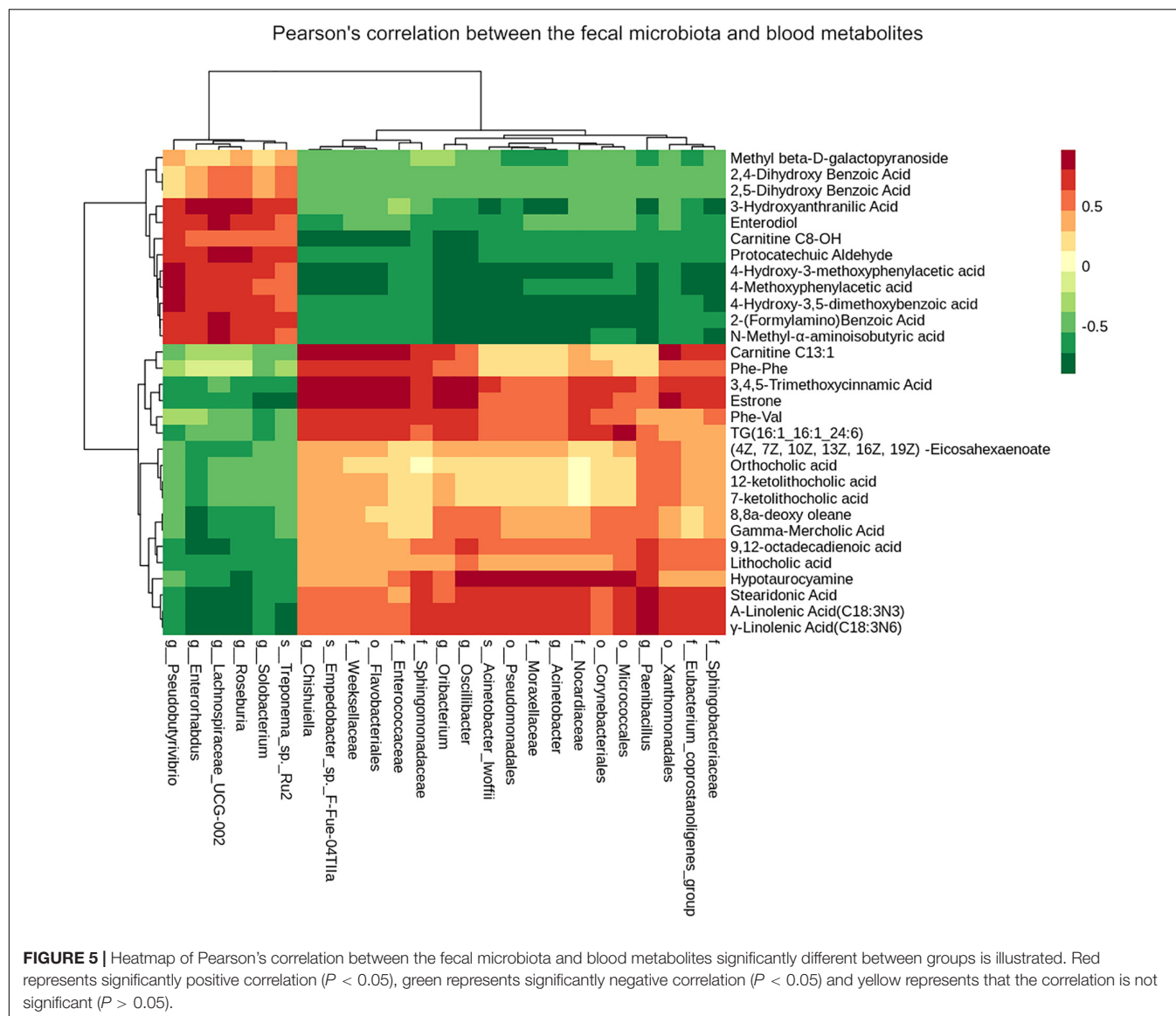


**FIGURE 4 |** Effect of ryegrass silage on horse metabolite profiles. **(A)** Principal component analysis (PCA) of blood metabolites of group S and group H. Green dot: PCA value of individual horse in group S. Orange rectangle: PCA value of individual horse in group H. **(B)** Metabolites discriminating between group S and group H with VIP > 1 were listed. Red dots indicate up-regulated metabolites. Green dots indicated down-regulated metabolites. **(C)** Heatmap of significantly altered metabolites in group S and group H. Individual samples (horizontal axis) and metabolites (vertical axis) are presented using hierarchical cluster analysis. The color scale is noted on the right side of the figure. Red and green color represent up-regulated and down-regulated metabolites, respectively, relative to the median metabolite level. **(D)** KEGG enrichment of each pathway related to this study was presented using rich factor. *P*-values and impact values are indicated on the horizontal axis and vertical axis, respectively. The sized and colors of the shapes represent the influence of silage diet on sample pathways relative to hay diet. The larger red shapes indicate greater impact of the diet on the pathway.

useful insights into the critical role of the gastrointestinal tract in maintaining general equine health. The results of fecal microbiota and blood metabolites have shown significant differences between horses fed ryegrass silage compared to being fed ryegrass hay. It will be more informative of the silage impact on horse gut and systemic health if larger number of horses and more types of silage or forages are involved in the future.

In horses, gut microbiota has been widely studied by high-throughput sequencing technique, therefore, the complexity of microbial communities can be demonstrated with the high depth of coverage of OTUs (Di Bella et al., 2013). However, since obtaining samples of intestinal ingesta is very difficult, fecal matter is used as a replacement for gut material (Julliand and Grimm, 2017). Fecal microbiota is sensitive to dietary variations and can be representative of the major hindgut sections (Julliand and Grimm, 2016). Therefore, this study used fecal samples to

investigate the influence of silage and hay on hindgut microbiota in horses. Silage and hay used in this study were both made out of ryegrass from local pasture which could be a representative of the most commonly used forage in China. Analysis on more types of silages will be helpful to better illustrate the impact of feeding silage on horse health. In the current study, we found that microbial richness in fecal samples from group S were significantly higher than that in group H. However, no difference in the diversity of fecal microbiota was identified. It has been reported that an increase in the concentration of total anaerobic bacteria was observed on day 14 and 22 after the onset of feeding silage to horses. However, this was attributed to variations of sampling time, instead of an impact from the diet (Muhonen et al., 2008). In this study, increased fecal microbial richness induced by silage-feeding is consistent with the previous research (Muhonen et al., 2008). Further investigations on the chemical



components in silage which may have contributed to our findings will facilitate a greater understanding of the association between silage diet and gut health in horses.

The relative abundance of Verrucomicrobia was higher in group H than in group S. Besides, it was also identified as the most discriminating phylum of group H based on LEfSe results. In previous studies, it is one of the most common and abundant phyla detected in the equine hindgut microbial ecosystem (Costa et al., 2012; Shepherd et al., 2012; Steelman et al., 2012). Verrucomicrobia is a phylum consisting mainly of strict anaerobes, considered to play an important role in hindgut function, for example, maintaining the mucus layer between the gut lumen and enterocytes (Arnold et al., 2020). Remarkably, a decreased abundance of Verrucomicrobia has been reported in horses with gastrointestinal disturbances after metronidazole administration (Arnold et al., 2020) and in horses with laminitis (Steelman et al., 2012). Therefore, Verrucomicrobia is a good

candidate to study for its impact on metabolic function. Further research will be necessary to investigate whether a lower abundance of Verrucomicrobia in ryegrass silage-fed horses is associated with a disruption of the gut ecosystem and associated systemic sequelae. Even though Kiritimatiellae was dominantly associated with horses on hay diet, there is not much information reported on its role or function in equine gut microbiota.

Statistically higher abundance levels of *Rikenellaceae* and *Christensenellaceae* were demonstrated in group S. *Rikenellaceae* has been reported in several studies of the equine microbiota (Biddle et al., 2018; Mach et al., 2020). *Rikenellaceae* is a mucin-degrading bacteria (Sivaprakasam et al., 2019) and mucin degradation has been shown to be a normal turnover process of the colon epithelium (Norin et al., 1985). In an investigation of gut flora modulation by the probiotic *Lactobacillus* in mice, *Rikenellaceae* was shown to decline along with an increase of *Lactobacillus* (Xing et al., 2018) and high

level of *Rikenellaceae* further associated with pathologic diseases, such as inflammatory bowel disease (Alkadhi et al., 2014) and obesity in other species (Kim et al., 2012). In accordance with LEfSe analysis, *Lactobacillus* was more associated with group H whilst *Rikenellaceae* was highly associated with group S. The relative abundances of *Rikenellaceae* in group S and group H were 7.0 and 4.2%, respectively, and *Lactobacillus* levels were 0.2 and 0.8% in group S and group H, which also presented a negative correlation between the two bacterial families in horse fecal microbiota. Even though biological function of *Rikenellaceae* and its relationship with *Lactobacillus* in horse gut are still not well defined, it might still be worth studying in silage-fed horses as one of the characteristic bacterial taxa. *Christensenellaceae* revealed the same trend as *Rikenellaceae*, however, its role in equine gut health requires more investigation.

*Eubacterium coprostanoligenes* is another bacterial family demonstrated significantly different relative abundance between two groups and more associated with group S according to LEfSe analysis. As a member of butyrate-producing bacteria, *Eubacterium coprostanoligenes* has been linked to mitochondrial gene expression involved in energy metabolism pathways including fatty acids (Mach et al., 2021) which was one of the most prominent metabolites in group S. Additionally, *Eubacterium coprostanoligenes* and fatty acids showed positive correlation in correlation analysis between fecal microbiota and blood metabolites. Even though not much investigation has been carried out on its specific role in equine gut microbiota, results in this study indicated that silage feeding could impact level of *Eubacterium coprostanoligenes* and fatty acids. Further study on the influence of silage feeding on gut microbial changes may help understand better about fat metabolism-silage relationship. According to LEfSe, *Oscillospiraceae* was shown associated with horses fed silage, however, further investigation will be necessary to learn more about its relationship with diet and gut health (Zhu et al., 2021).

Plasma and urine samples are considered the most appropriate biofluids for metabonomic analysis in horses due to lower variability in metabolomic results, compared to fecal samples (Escalona et al., 2015). In the current study, serum collected from each horse was used for metabolic analysis. There was a dramatic separation of metabolites between the two groups (Figure 4A), indicating a great influence of diet on systemic responses in horses. Triglycerides (belonging to group glycerolipids) and fatty acids were highly upregulated by ryegrass silage feeding (Figure 4C and Supplementary Table 1). As a critical diagnosis for hyperlipemia in horses, concentration of triglycerides is also used to predict metabolic dysregulation (Jacob et al., 2018). Increased concentrations of circulating fatty acids and triglycerides have been associated with insulin resistance in horses (Carter et al., 2009). In addition, the KEGG enrichment analysis (Figure 4D) identified that insulin resistance was one of the most differentiating pathways between the two groups, which further highlights the potential association of a silage diet and metabolic dysfunction. Fatty acids are also known to activate proinflammatory pathways leading to an increase of proinflammatory cytokines, including tumor necrosis factor alpha and interferon gamma, which interfere with the insulin

signaling cascade resulting in a negative impact on insulin sensitivity (Manning, 2004). One study also showed that high levels stearic acid and palmitoleic acid, which were also the two main fatty acids found significantly higher in group S, have been associated with high insulin resistance in humans (Kurotani et al., 2012). Therefore, silage may have negative impacts on metabolic function in the long term. More extensive research studying levels of inflammatory cytokines, inflammation-associated fatty acids, blood insulin as well as lipid level are warranted to provide more evidence on association of silage and equine metabolic disorders. There was another interesting finding in this study that the crude fat (CF) content in group S and group H was 1.34 DM and 1.83% DM, respectively, yet not positively correlated with the lipid-metabolism related metabolites. It could indicate that the impact of silage on lipid metabolism is not associated with the amount of dietary fat but metabolic pathways in the body.

By observing the VIP score plot (Figure 4B) bile acids, such as 7-ketolithocholic acid and 12-ketolithocholic acid, were significantly upregulated in group S horses as well. Bile acids are critical components of lipid metabolism, especially cholesterol, and function mainly in gut (Breuer et al., 1985). Higher bile acids may be a consequence of higher lipid biochemical matrices in horses fed ryegrass silage. It is characteristic in horses that bile acids are secreted continuously, therefore, interpretation of plasma concentrations requires additional relevant information (Toth et al., 2018), for example, a history of being on a silage-based diet, as highlighted by this study. The metabolites most associated with group H horses were relatively more diverse, including organic acids, amino acids and oxidized lipids, which were involved in different metabolic pathways. The biological significance of the many metabolite changes, including 4-Hydroxy-3-methoxyphenylacetic acid, protocatechuic aldehyde and 4-methoxyphenylacetic acid, were beyond the scope of this study. As a result, further controlled studies on the role of silage in horse health may provide deeper understanding of these metabolite functions.

We also investigated the correlation between fecal microbiota and blood metabolomes. Notably, triglycerides and some fatty acids, were positively correlated with the prevalence of the bacterial taxa which were statistically different between the two groups (Figure 5). Most of these bacteria were not very abundant in the horses within this study and only the *Eubacterium coprostanoligenes* group had a relative abundance of > 1%. It has been positively correlated with triglycerides and fatty acids such as stearidonic acid indicating its potential impact on these metabolites. There were also a few bacterial taxa negatively correlated with triglycerides and fatty acids, such as *Treponema* and *Roseburia*. Therefore, the lower levels of fatty acids and triglycerides were likely attributed to the presence of many bacterial floras at lower relative abundance, instead of just few influential bacterial taxa. The microbiome-metabolome correlation analysis can help recognize relationships between specific types of bacteria and metabolites, which in-turn may indicate a potential mechanism of a disease and their relative impacts on health (Zhao, 2013). However, this type of study alone is not able to determine the origin of the metabolite, as well as the causality between the bacteria and metabolites. As a result,

*in vitro* digestion models may be necessary to investigate the relationship between metabolites, diet, and health in horses.

In conclusion, 16S rRNA high-throughput sequencing and untargeted metabolomics helped reveal the fecal microbiota, blood metabolite profile and their correlation with ryegrass silage and hay diets. The major findings of this study are as follows: (a) ryegrass silage and hay lead to significant changes on fecal microbiota. (b) ryegrass silage and hay showed significant impact on blood metabolites composition. (c) ryegrass silage intake revealed association with lipid metabolism and might increase risk of insulin resistance; (d) some specific gut bacterial taxa-related metabolites were strongly correlated with altered gut microbes which indicated great impact of diet on gut and the body system of horses. These results suggest that silage could cause significant changes in the horse fecal microbiota and might be associated with metabolic dysfunctions, such as insulin resistance and lipid metabolic abnormality. Studies measuring level of blood insulin and lipid in horses fed silage will provide more evidence to the association. These findings may promote understanding on the impact of silage feeding on horse health and facilitate making more scientific diet plan for horses especially those with metabolic disorders such as insulin resistance and hypertriglyceridemia.

## DATA AVAILABILITY STATEMENT

The datasets presented in this study can be found in online repositories. The names of the repository/repositories and accession number(s) can be found below: [www.ncbi.nlm.nih.gov/PRJNA735708](http://www.ncbi.nlm.nih.gov/PRJNA735708).

## ETHICS STATEMENT

All procedures involving animals in this study were carried out with a welfare license (No. AW11101202-2-1) issued by the

Animal Care and Use Committee of the China Agricultural University.

## AUTHOR CONTRIBUTIONS

JL, YPZ, and RH designed the study. YPZ, XW, ZY, YFZ, LD, and JL participated in animal acquisition and sample collection. XW, LD, and BL helped conduct data analysis. YPZ and ZY contributed to the writing of the original draft. JL, BL, and RH helped review and edit the manuscript. All authors contributed to the article and approved the submitted version.

## FUNDING

This research was funded by the High Level Introduction of Talent Research Start-up Fund from the China Agricultural University (Grant No. 31051017).

## ACKNOWLEDGMENTS

The authors would like to thank all the staff members in Shanxi Horse Farm, especially Quansheng Guo and Xingyu Yong for their assistance in the horse management during this program.

## SUPPLEMENTARY MATERIAL

The Supplementary Material for this article can be found online at: <https://www.frontiersin.org/articles/10.3389/fmicb.2021.715709/full#supplementary-material>

The updated supplementary material has been deposited to FigShare: doi: 10.6084/m9.figshare.15128094

## REFERENCES

- Alkadhi, S., Kunde, D., Cheluvappa, R., Randall-Demllo, S., and Eri, R. (2014). The murine appendiceal microbiome is altered in spontaneous colitis and its pathological progression. *Gut Pathog.* 6:25. doi: 10.1186/1757-4749-6-25
- Armstrong, C. W., McGregor, N. R., Lewis, D. P., Butt, H. L., and Gooley, P. R. (2017). The association of fecal microbiota and fecal, blood serum and urine metabolites in myalgic encephalomyelitis/chronic fatigue syndrome. *Metabolomics* 13:8.
- Arnold, C. E., Isaiah, A., Pilla, R., Lidbury, J., Coverdale, J. S., Callaway, T. R., et al. (2020). The cecal and fecal microbiomes and metabolomes of horses before and after metronidazole administration. *PLoS One* 15:e0232905. doi: 10.1371/journal.pone.0232905
- Biddle, A. S., Tomb, J. F., and Fan, Z. (2018). Microbiome and blood analyte differences point to community and metabolic signatures in lean and obese horses. *Front. Vet. Sci.* 5:225. doi: 10.3389/fvets.2018.00225
- Brandwein, M., Katz, I., Katz, A., and Kohen, R. (2019). Beyond the gut: skin microbiome compositional changes are associated with bmi. *Hum. Microb. J.* 13:100063. doi: 10.1016/j.humic.2019.100063
- Breuer, N., Dommes, P., Jaekel, S., and Goebell, H. (1985). Fecal bile acid excretion pattern in colonic cancer patients. *Dig. Dis. Sci.* 30, 852–859. doi: 10.1007/bf01309516
- Caporaso, J. G., Kuczynski, J., Stombaugh, J., Bittinger, K., Bushman, F. D., Costello, E. K., et al. (2010). Qiime allows analysis of high-throughput community sequencing data. *Nat. Methods* 7, 335–336.
- Carroll, C., and Huntington, P. (1988). Body condition scoring and weight estimation of horses. *Equine Vet. J.* 20, 41–45. doi: 10.1111/j.2042-3306.1988.tb01451.x
- Carter, R. A., McCutcheon, L. J., George, L. A., Smith, T. L., Frank, N., and Geor, R. J. (2009). Effects of diet-induced weight gain on insulin sensitivity and plasma hormone and lipid concentrations in horses. *Am. J. Vet. Res.* 70, 1250–1258. doi: 10.2460/ajvr.70.10.1250
- Chen, S., Zhou, Y., Chen, Y., and Gu, J. (2018). Fastp: an ultra-fast all-in-one fastq preprocessor. *Bioinformatics* 34, i884–i890.
- Connors, M., Muhonen, S., Lindberg, J. E., Essén-Gustavsson, B., Nyman, G., Nostell, K., et al. (2006). Effects on exercise response, fluid and acid-base balance of protein intake from forage-only diets in standardbred horses. *Equine Vet. J. Suppl.* 36, 648–653. doi: 10.1111/j.2042-3306.2006.tb05620.x
- Costa, M. C., Arroyo, L. G., Allen-Vercos, E., Stämpfli, H. R., Kim, P. T., Sturgeon, A., et al. (2012). Comparison of the fecal microbiota of healthy horses and



- horses with colitis by high throughput sequencing of the v3-v5 region of the 16s rRNA gene. *PLoS One* 7:e41484. doi: 10.1371/journal.pone.0041484
- Cox, L. M., Yamanishi, S., Sohn, J., Alekseyenko, A. V., Leung, J. M., Cho, I., et al. (2014). Altering the intestinal microbiota during a critical developmental window has lasting metabolic consequences. *Cell* 158, 705–721. doi: 10.1016/j.cell.2014.05.052
- Daly, K., Proudman, C. J., Duncan, S. H., Flint, H. J., Dyer, J., and Shirazi-Beechey, S. P. (2012). Alterations in microbiota and fermentation products in equine large intestine in response to dietary variation and intestinal disease. *Br. J. Nutr.* 107, 989–995. doi: 10.1017/S0007114511003825
- De Fombelle, A., Julliand, V., Drogoul, C., and Jacotot, E. (2001). Feeding and microbial disorders in horses: 1-effects of an abrupt incorporation of two levels of barley in a hay diet on microbial profile and activities. *J. Equine Vet. Sci.* 21, 439–445. doi: 10.1016/S0737-0806(01)70018-4
- De Fombelle, A., Varloud, M., Goachet, A.-G., Jacotot, E., Philippeau, C., Drogoul, C., et al. (2003). Characterization of the microbial and biochemical profile of the different segments of the digestive tract in horses given two distinct diets. *Anim. Sci.* 77, 293–304. doi: 10.1017/S1357729800059038
- Di Bella, J. M., Bao, Y., Gloor, G. B., Burton, J. P., and Reid, G. (2013). High throughput sequencing methods and analysis for microbiome research. *J. Microbiol. Methods* 95, 401–414. doi: 10.1016/j.mimet.2013.08.011
- Domingues, J. L. (2009). Use of conserved roughage in the horse feeding. *Rev. Bras. Zootec.* 38, 259–269.
- Dougal, K., de la Fuente, G., Harris, P. A., Girdwood, S. E., Pinloche, E., and Geor, R. J. (2014). Characterisation of the faecal bacterial community in adult and elderly horses fed a high fibre, high oil or high starch diet using 454 pyrosequencing. *PLoS One* 9:e87424. doi: 10.1371/journal.pone.0087424
- Dugdale, A. H., Curtis, G. C., Cripps, P., Harris, P. A., and Argo, C. M. (2010). Effect of dietary restriction on body condition, composition and welfare of overweight and obese pony mares. *Equine Vet. J.* 42, 600–610. doi: 10.1111/j.2042-3306.2010.00110.x
- Edgar, R. C. (2013). Uparse: highly accurate OTU sequences from microbial amplicon reads. *Nat. Methods* 10, 996–998. doi: 10.1038/nmeth.2604
- Escalona, E. E., Leng, J., Dona, A. C., Merrifield, C. A., Holmes, E., Proudman, C. J., et al. (2015). Dominant components of the thoroughbred metabolome characterised by (1) h-nuclear magnetic resonance spectroscopy: a metabolite atlas of common biofluids. *Equine Vet. J.* 47, 721–730. doi: 10.1111/evj.12333
- Fernandes, K. A., Kittelmann, S., Rogers, C. W., Gee, E. K., Bolwell, C. F., Bermingham, E. N., et al. (2014). Faecal microbiota of forage-fed horses in New Zealand and the population dynamics of microbial communities following dietary change. *PLoS One* 9:e112846. doi: 10.1371/journal.pone.0112846
- Glunk, E. C., Hathaway, M. R., Grev, A. M., Lamprecht, E. D., Maher, M. C., and Martinson, K. L. (2015). The effect of a limit-fed diet and slow-feed hay nets on morphometric measurements and postprandial metabolite and hormone patterns in adult horses. *J. Anim. Sci.* 93, 4144–4152. doi: 10.2527/jas.2015-9150
- Gu, Z., Eils, R., and Schlesner, M. (2016). Complex heatmaps reveal patterns and correlations in multidimensional genomic data. *Bioinformatics* 32, 2847–2849. doi: 10.1093/bioinformatics/btw313
- Guasch-Ferré, M., Bhupathiraju, S. N., and Hu, F. B. (2018). Use of metabolomics in improving assessment of dietary intake. *Clin. Chem.* 64, 82–98. doi: 10.1373/clinchem.2017.272344
- Guo, Q. (2014). “Review of feeding silage to horses in northwest China for fifteen years,” in *Proceedings of the China Animal Science and Veterinary Medicine Convention*, (Beijing, China). Available at: <https://kns.cnki.net/kcms/detail/detail.aspx?dbcode=CPFD&dbname=CPFD0914&filename=ZGXJ201408001038&v=rdq46tNcyl%25mmd2F0D62AXTFW0KLN%25mmd2FA1HuRcxSptT%25mmd2BoSQgal1Ye%25mmd2F7M82fRELWpe7vwuQXmBZYGwA1xg%3d>
- Han, K., Collins, M., Vanzant, E., and Dougherty, C. (2006). Characteristics of baled silage made from first and second harvests of wilted and severely wilted forages. *Grass Forage Sci.* 61, 22–31. doi: 10.1111/j.1365-2494.2006.00501.x
- Harris, P. A., Ellis, A. D., Fradinho, M. J., Jansson, A., Julliand, V., Luthersson, N., et al. (2017). Review: feeding conserved forage to horses: recent advances and recommendations. *Animal* 11, 958–967. doi: 10.1017/S1751731116002469
- Holmquist, S., and Müller, C. E. (2002). “Problems related to feeding forages to horses,” in *13th International Silage Conference*, (Scotland: Auchincruive).
- Jacob, S. I., Murray, K. J., Rendahl, A. K., Geor, R. J., Schultz, N. E., and McCue, M. E. (2018). Metabolic perturbations in Welsh ponies with insulin dysregulation, obesity, and laminitis. *J. Vet. Intern. Med.* 32, 1215–1233. doi: 10.1111/jvim.15095
- Julliand, V., and Grimm, P. (2016). Horse species symposium: the microbiome of the horse hindgut: history and current knowledge. *Anim. Sci. J.* 94, 2262–2274. doi: 10.2527/jas.2015-0198
- Julliand, V., and Grimm, P. (2017). The impact of diet on the hindgut microbiome. *J. Equine Vet. Sci.* 52, 23–28. doi: 10.1016/j.jevs.2017.03.002
- Kim, K. A., Gu, W., Lee, I. A., Joh, E. H., and Kim, D. H. (2012). High fat diet-induced gut microbiota exacerbates inflammation and obesity in mice via the TLR4 signaling pathway. *PLoS One* 7:e47713. doi: 10.1371/journal.pone.0047713
- Kurotani, K., Sato, M., Ejima, Y., Nanri, A., Yi, S., Pham, N. M., et al. (2012). High levels of stearic acid, palmitoleic acid, and dihomo- $\gamma$ -linolenic acid and low levels of linoleic acid in serum cholesterol ester are associated with high insulin resistance. *Nutr. Res.* 32, 669–675.e3.
- Li, M., Wang, B., Zhang, M., Rantalainen, M., Wang, S., Zhou, H., et al. (2008). Symbiotic gut microbes modulate human metabolic phenotypes. *Proc. Natl. Acad. Sci. U. S. A.* 105, 2117–2122.
- Li, P., Zhang, Y., Gou, W., Cheng, Q., Bai, S., and Cai, Y. (2019). Silage fermentation and bacterial community of bur clover, annual ryegrass and their mixtures prepared with microbial inoculant and chemical additive. *Anim. Feed Sci. Tech.* 247, 285–293. doi: 10.1016/j.anifeedsci.2018.11.009
- Mach, N., Moroldo, M., Rau, A., Lecardonnell, J., Le Moyec, L., Robert, C., et al. (2021). Understanding the holobiont: crosstalk between gut microbiota and mitochondria during long exercise in horse. *Front. Mol. Biosci.* 8:656204. doi: 10.3389/fmolb.2021.656204
- Mach, N., Ruet, A., Clark, A., Bars-Cortina, D., Ramayo-Caldas, Y., Crisci, E., et al. (2020). Priming for welfare: gut microbiota is associated with equitation conditions and behavior in horse athletes. *Sci. Rep.* 10:8311.
- Magoč, T., and Salzberg, S. L. (2011). FLASH: fast length adjustment of short reads to improve genome assemblies. *Bioinformatics* 27, 2957–2963. doi: 10.1093/bioinformatics/btr507
- Magurran, A. E. (2004). *Measuring biological diversity*. Malden: Blackwell Science Ltd.
- Manning, B. D. (2004). Balancing Akt with S6K: implications for both metabolic diseases and tumorigenesis. *J. Cell Biol.* 167, 399–403. doi: 10.1083/jcb.200408161
- Marchesi, J. R., Adams, D. H., Fava, F., Hermes, G. D., Hirschfield, G. M., Hold, G., et al. (2016). The gut microbiota and host health: a new clinical frontier. *Gut* 65, 330–339. doi: 10.1136/gutjnl-2015-309990
- Muhonen, S., Connysson, M., Lindberg, J. E., Julliand, V., Bertilsson, J., and Jansson, A. (2008). Effects of crude protein intake from grass silage-only diets on the equine colon ecosystem after an abrupt feed change. *J. Anim. Sci.* 86, 3465–3472. doi: 10.2527/jas.2007-0374
- Norin, K. E., Gustafsson, B. E., Lindblad, B. S., and Midtvedt, T. (1985). The establishment of some microflora associated biochemical characteristics in feces from children during the first years of life. *Acta Paediatr. Scand.* 74, 207–212. doi: 10.1111/j.1651-2227.1985.tb10951.x
- Parvin, S., Wang, C., Li, Y., and Nishino, N. (2010). Effects of inoculation with lactic acid bacteria on the bacterial communities of Italian ryegrass, whole crop maize, guinea grass and Rhodes grass silages. *Anim. Feed Sci. Tech.* 160, 160–166. doi: 10.1016/j.anifeedsci.2010.07.010
- Quast, C., Pruesse, E., Yilmaz, P., Gerken, J., Schweer, T., Yarza, P., et al. (2013). The SILVA ribosomal RNA gene database project: improved data processing and web-based tools. *Nucleic Acids Res.* 41, D590–D596.
- Sanguinetti, E., Collado, M. C., Marrachelli, V. G., Monleon, D., Selma-Royo, M., Pardo-Tendero, M. M., et al. (2018). Microbiome-metabolome signatures in mice genetically prone to develop dementia, fed a normal or fatty diet. *Sci. Rep.* 8:4907.
- Segata, N., Izard, J., Waldron, L., Gevers, D., Miropolsky, L., Garrett, W. S., et al. (2011). Metagenomic biomarker discovery and explanation. *Genome Biol.* 12:R60.
- Shepherd, M. L., Swecker, W. S. Jr., Jensen, R. V., and Ponder, M. A. (2012). Characterization of the fecal bacteria communities of forage-fed horses by pyrosequencing of 16S rRNA V4 gene amplicons. *FEMS Microbiol. Lett.* 326, 62–68. doi: 10.1111/j.1574-6968.2011.02434.x

- Shulman, R. J., Eakin, M. N., Czyzewski, D. I., Jarrett, M., and Ou, C. N. (2008). Increased gastrointestinal permeability and gut inflammation in children with functional abdominal pain and irritable bowel syndrome. *J. Pediatr.* 153, 646–650. doi: 10.1016/j.jpeds.2008.04.062
- Sivaprakasam, S., Ganapathy, P. K., Sikder, M. O. F., Elmassry, M., Ramachandran, S., Kottapalli, K. R., et al. (2019). Deficiency of dietary fiber in slc5a8-null mice promotes bacterial dysbiosis and alters colonic epithelial transcriptome towards proinflammatory milieu. *Can. J. Gastroenterol. Hepatol.* 2019:2543082.
- Sorensen, R. J., Drouillard, J. S., Douthit, T. L., Ran, Q., Marthaler, D. G., Kang, Q., et al. (2021). Effect of hay type on cecal and fecal microbiome and fermentation parameters in horses. *J. Anim. Sci.* 99:skaa407.
- Stackebrandt, E., and Goebel, B. M. (1994). Taxonomic note: a place for DNA-DNA reassociation and 16s rRNA sequence analysis in the present species definition in bacteriology. *Int. J. Syst. Evol. Microbiol.* 44, 846–849. doi: 10.1099/00207713-44-4-846
- Steelman, S. M., Chowdhary, B. P., Dowd, S., Suchodolski, J., and Janečka, J. E. (2012). Pyrosequencing of 16s rRNA genes in fecal samples reveals high diversity of hindgut microflora in horses and potential links to chronic laminitis. *BMC Vet. Res.* 8:231. doi: 10.1186/1746-6148-8-231
- Stewart, H. L., Pitta, D., Indugu, N., Vecchiarelli, B., Engiles, J. B., and Southwood, L. L. (2018). Characterization of the fecal microbiota of healthy horses. *Am. J. Vet. Res.* 79, 811–819. doi: 10.2460/ajvr.79.8.811
- Sun, Y., Su, Y., and Zhu, W. (2016). Microbiome-metabolome responses in the cecum and colon of pig to a high resistant starch diet. *Front. Microbiol.* 7:779. doi: 10.3389/fmicb.2016.00779
- Tindall, A. M., Petersen, K. S., and Kris-Etherton, P. M. (2018). Dietary patterns affect the gut microbiome-the link to risk of cardiometabolic diseases. *J. Nutr.* 148, 1402–1407. doi: 10.1093/jn/nyx141
- Tinker, M. K., White, N. A., Lessard, P., Thatcher, C. D., Pelzer, K. D., Davis, B., et al. (1997). Prospective study of equine colic incidence and mortality. *Equine Vet. J.* 29, 448–453. doi: 10.1111/j.2042-3306.1997.tb03157.x
- Toth, B., Auth, A., Rompos, L., and Bakos, Z. (2018). Effect of feed deprivation on selected parameters of lipid mobilisation and hepatic function in healthy akhal teke horses. *Equine Vet. J.* 50, 98–103. doi: 10.1111/evj.12730
- Vandenput, S., Istasse, L., Nicks, B., and Lekeux, P. (1997). Airborne dust and aeroallergen concentrations in different sources of feed and bedding for horses. *Vet. Q.* 19, 154–158. doi: 10.1080/01652176.1997.9694762
- Venable, E. B., Fenton, K. A., Braner, V. M., Reddington, C. E., Halpin, M. J., Heitz, S. A., et al. (2017). Effects of feeding management on the equine cecal microbiota. *J. Equine Vet. Sci.* 49, 113–121. doi: 10.1016/j.jevs.2016.09.010
- Wang, Q., Garrity, G. M., Tiedje, J. M., and Cole, J. R. (2007). Naive bayesian classifier for rapid assignment of rRNA sequences into the new bacterial taxonomy. *Appl. Environ. Microbiol.* 73, 5261–5267. doi: 10.1128/aem.00062-07
- Willis, A. D. (2019). Rarefaction, alpha diversity, and statistics. *Front. Microbiol.* 10:2407. doi: 10.3389/fmicb.2019.0240710
- Xing, Z., Tang, W., Yang, Y., Geng, W., Rehman, R. U., and Wang, Y. (2018). Colonization and gut flora modulation of lactobacillus kefirano-faciens zw3 in the intestinal tract of mice. *Probiotics Antimicrob. Proteins* 10, 374–382. doi: 10.1007/s12602-017-9288-4
- Zhao, L. (2013). The gut microbiota and obesity: from correlation to causality. *Nat. Rev. Microbiol.* 11, 639–647. doi: 10.1038/nrmicro3089
- Zhu, Y., Wang, X., Deng, L., Chen, S., Zhu, C., and Li, J. (2021). Effects of pasture grass, silage, and hay diet on equine fecal microbiota. *Animals* 11:1330. doi: 10.3390/ani11051330

**Conflict of Interest:** The authors declare that the research was conducted in the absence of any commercial or financial relationships that could be construed as a potential conflict of interest.

**Publisher's Note:** All claims expressed in this article are solely those of the authors and do not necessarily represent those of their affiliated organizations, or those of the publisher, the editors and the reviewers. Any product that may be evaluated in this article, or claim that may be made by its manufacturer, is not guaranteed or endorsed by the publisher.

Copyright © 2021 Zhu, Wang, Liu, Yi, Zhao, Deng, Holyoak and Li. This is an open-access article distributed under the terms of the Creative Commons Attribution License (CC BY). The use, distribution or reproduction in other forums is permitted, provided the original author(s) and the copyright owner(s) are credited and that the original publication in this journal is cited, in accordance with accepted academic practice. No use, distribution or reproduction is permitted which does not comply with these terms.



# Controlled Complexity: Optimized Systems to Study the Role of the Gut Microbiome in Host Physiology

Robert W. P. Glowacki<sup>1†</sup>, Morgan J. Engelhart<sup>1,2†</sup> and Philip P. Ahern<sup>1,2,3\*</sup>

<sup>1</sup> Department of Cardiovascular and Metabolic Sciences, Lerner Research Institute, Cleveland Clinic, Cleveland, OH, United States, <sup>2</sup> Cleveland Clinic Lerner College of Medicine, Case Western Reserve University, Cleveland, OH, United States, <sup>3</sup> Center for Microbiome and Human Health, Cleveland Clinic, Cleveland, OH, United States

## OPEN ACCESS

### Edited by:

Jean-François Brugère,  
Université Clermont Auvergne, France

### Reviewed by:

Aaron Conrad Ericsson,  
University of Missouri, United States

Stephan Rosshart,  
University of Freiburg Medical Center,  
Germany

Preben Boysen,  
Norwegian University of Life Sciences,  
Norway

### \*Correspondence:

Philip P. Ahern  
ahernp@ccf.org

<sup>†</sup>These authors have contributed  
equally to this work

### Specialty section:

This article was submitted to  
Microbial Symbioses,  
a section of the journal  
Frontiers in Microbiology

Received: 02 July 2021

Accepted: 24 August 2021

Published: 27 September 2021

### Citation:

Glowacki RWP, Engelhart MJ and  
Ahern PP (2021) Controlled  
Complexity: Optimized Systems  
to Study the Role of the Gut  
Microbiome in Host Physiology.  
Front. Microbiol. 12:735562.  
doi: 10.3389/fmicb.2021.735562

The profound impact of the gut microbiome on host health has led to a revolution in biomedical research, motivating researchers from disparate fields to define the specific molecular mechanisms that mediate host-beneficial effects. The advent of genomic technologies allied to the use of model microbiomes in gnotobiotic mouse models has transformed our understanding of intestinal microbial ecology and the impact of the microbiome on the host. However, despite incredible advances, our understanding of the host-microbiome dialogue that shapes host physiology is still in its infancy. Progress has been limited by challenges associated with developing model systems that are both tractable enough to provide key mechanistic insights while also reflecting the enormous complexity of the gut ecosystem. Simplified model microbiomes have facilitated detailed interrogation of transcriptional and metabolic functions of the microbiome but do not recapitulate the interactions seen in complex communities. Conversely, intact complex communities from mice or humans provide a more physiologically relevant community type, but can limit our ability to uncover high-resolution insights into microbiome function. Moreover, complex microbiomes from lab-derived mice or humans often do not readily imprint human-like phenotypes. Therefore, improved model microbiomes that are highly defined and tractable, but that more accurately recapitulate human microbiome-induced phenotypic variation are required to improve understanding of fundamental processes governing host-microbiome mutualism. This improved understanding will enhance the translational relevance of studies that address how the microbiome promotes host health and influences disease states. Microbial exposures in wild mice, both symbiotic and infectious in nature, have recently been established to more readily recapitulate human-like phenotypes. The development of synthetic model communities from such “wild mice” therefore represents an attractive strategy to overcome the limitations of current approaches. Advances in microbial culturing approaches that allow for the generation of large and diverse libraries of isolates, coupled to ever more affordable large-scale genomic sequencing, mean that we are now ideally positioned to develop such systems. Furthermore, the development of sophisticated *in vitro* systems is allowing for detailed insights into host-microbiome interactions to be obtained. Here we discuss the need to leverage such approaches and highlight key challenges that remain to be addressed.

**Keywords:** microbiome, model system, synthetic communities, gnotobiotic, wild mice, translation, model microbial communities

## INTRODUCTION

As a species, humans are surrounded by and inhabited by trillions of microorganisms, encompassing bacteria, fungi, archaea, other eukaryotic organisms such as parasites and protists, as well as viruses (Gill et al., 2006; Parfrey et al., 2011; Hallen-Adams and Suhr, 2017; Koskinen et al., 2017; Nkamga et al., 2017; Gregory et al., 2020) that are collectively referred to as the microbiome. Decades of work have established the profound role of the microbiome in shaping host physiology and its capacity to regulate a wide variety of health and disease states. The rapid growth of microbiome research, spurred by technological innovations, has resulted in remarkable discoveries that have altered our conceptualization of the role played by this complex ecosystem in host health. Furthermore, these efforts have uncovered several features that highlight the therapeutic potential of the microbiome. First, dysfunction of the microbiome or host responses to the microbiome have been implicated in the pathogenesis of myriad human diseases, including, undernutrition and its associated maladies (Smith M. I. et al., 2013; Kau et al., 2015; Blanton et al., 2016; Charbonneau et al., 2016; Wagner et al., 2016; Cowardin et al., 2019), metabolic diseases such as obesity (Ley et al., 2005; Turnbaugh et al., 2006, 2008, 2009b; Hildebrandt et al., 2009; Ridaura et al., 2013), cardiovascular disease (Kelly et al., 2016), cancer and its susceptibility to treatment (Arthur et al., 2012; Buc et al., 2013; Sivan et al., 2015; Vétizou et al., 2015), food allergy (Feehley et al., 2019), multiple sclerosis (Berer et al., 2017; Cekanaviciute et al., 2017), and inflammatory bowel disease (IBD) (Manichanh et al., 2006; Frank et al., 2007; Gevers et al., 2014; Britton et al., 2019). Second, there is significant inter-personal variation in microbiome composition and/or function across individuals (Turnbaugh et al., 2009a; Qin et al., 2010; Schloissnig et al., 2013) that can impact host phenotypes, and thus, microbiome composition represents a personalized risk factor for the development of disease (Smith M. I. et al., 2013; Subramanian et al., 2014; Alavi et al., 2020). Third, microbiota repair, where specific microbial taxa or microbial consortia are introduced to communities lacking these microbes, has proven effective in restoration of beneficial microbiome-mediated effects (van Nood et al., 2013; Buffie et al., 2015; Blanton et al., 2016; Caballero et al., 2017; Di Luccia et al., 2020), underscoring the potential of microbiome manipulation for therapy.

This has prompted a flurry of exploration from researchers across a wide-array of disciplines to provide a systematic understanding of the microbiome and its interaction with the host, especially in defining the features that shape microbiome composition and function, as well as uncovering how the microbiome imparts its beneficial or deleterious effects on host physiology. Investigation of these processes has typically followed a trajectory beginning with identifying disruptions to microbiome composition, commonly referred to as dysbiosis, followed by *in vivo* animal studies whereby transplantation of microbiomes from donors exhibiting a phenotype of interest is used to assess how much, if any, of the donor phenotype can be transmitted by the microbiome. These studies are essential to establish a causal role for the microbiome and

microbe(s) in question. This process is exemplified by studies of malnutrition (obesity and undernutrition) and IBD. Obesity is associated with an altered gut microbiome composition (Ley et al., 2005; Turnbaugh et al., 2008, 2009b; Hildebrandt et al., 2009), and the gut microbiome from these individuals or obese mice promotes increased adiposity and metabolic dysfunction upon transplantation to germ-free recipient mice relative to healthy donor controls (Turnbaugh et al., 2006; Ridaura et al., 2013). Likewise, individuals suffering from undernutrition have disrupted gut microbiomes, and transplantation of fecal microbiomes from such donors recapitulates features of weight loss/cachexia in recipient mice relative to control donors (Smith M. I. et al., 2013; Kau et al., 2015; Blanton et al., 2016; Wagner et al., 2016). Although there remains some debate about whether or not IBD patients have distinct microbiome compositions, gut microbiomes from IBD patients elicit more severe intestinal inflammation in gnotobiotic IBD models than those from healthy controls (Gevers et al., 2014; Britton et al., 2019; Lloyd-Price et al., 2019). In addition to establishing a causal role for the microbiome in such diseases, model systems have also been leveraged to elucidate how specific microbiome members impact the progression or prevention of diseases. These efforts have yielded detailed insights that would have been likely impossible without a tractable model system. For example, particular strains of *E. coli* containing the pathogenicity island *pks* have been identified as being enriched in patients with colorectal cancer, and gnotobiotic mouse models have been utilized to demonstrate causality for these specific strains in the disease (Arthur et al., 2012; Buc et al., 2013). Enterotoxigenic strains of *B. fragilis* have also been linked to colorectal cancer development (Toprak et al., 2006; Wu et al., 2009), as well as aspects of undernutrition (Wagner et al., 2016). Species of *Clostridium* and the *Bacteroides* have also been implicated in limiting the severity of food allergy (Atarashi et al., 2011; Stefká et al., 2014; Abdel-Gadir et al., 2019). Animal model systems have thus proven essential in determining causal roles for the microbiome in shaping disease susceptibility and facilitating the precise delineation of host-microbiome interactions that mediate these effects on host physiology. As such, they remain an irreplaceable component of the microbiome researcher's toolkit.

While the advances to date have been captivating, there is still a dearth of information regarding the specific gut microbes that mediate the effects of the microbiome on the host. Moreover, despite the enormous progress that they have facilitated, current models have deficiencies that limit their translational relevance. As targeted and rational microbiome manipulation becomes an increasingly attractive approach for therapy, tractable and physiologically relevant model systems to interrogate host-microbiome interactions are needed. Here we will discuss current challenges and describe a path to addressing this need in microbiome research through the creation of new and improved model systems to interrogate host-microbiome interactions. We will focus our attention primarily on the effects of gut bacteria on host physiology. However, it is increasingly clear that intestinal fungi, viruses, archaea, and other eukaryotic species can profoundly impact host phenotypes, such as promoting intestinal immune system maturation and regulating disease susceptibility,



often able to imprint phenotypic responses equivalent to gut bacteria (Kernbauer et al., 2014; Chudnovskiy et al., 2016; Escalante et al., 2016; Lin et al., 2020; Yeung et al., 2020; Dallari et al., 2021). Moreover, these agents do not act in isolation, and their direct or indirect interactions may regulate host health as has been demonstrated in murine models of inflammatory bowel disease (IBD) and parasitic infection (Cadwell et al., 2010; Hayes et al., 2010). It would therefore be remiss to ignore the contributions of these oft-overlooked microbiome members in our conceptualization of the gut ecosystem and its effects on the host, as highlighted by others (Norman et al., 2014; Reynolds et al., 2015; Runge and Rosshart, 2021).

## Mouse Models for the Study of Host-Microbiome Interactions

Model systems have been widely employed by researchers going all the way back to the days of Gregor Mendel's use of pea plants to study inherited traits (Ellis et al., 2011). In order to define paradigms of host-microbiome mutualism, researchers have utilized a variety of organisms (Reyniers and Sacksteder, 1958; Smith et al., 2007; Ericsson, 2019), ranging from *Drosophila* (Lee and Brey, 2013), *Hydra* (Augustin et al., 2012), zebrafish (Kanter and Rawls, 2010; Stagaman et al., 2020) and squid (Nyholm and McFall-Ngai, 2004; McFall-Ngai, 2014) to mice and rats (Reyniers and Sacksteder, 1958; Smith et al., 2007), and pigs (Vlasova et al., 2018; Gehrig et al., 2019). This has enabled fundamental insights into the relationship between the host and the resident microbiome and the identification of features that typify these interactions, akin to Koch's postulates that describe the paradigm that defines microbial pathogenesis (Neville et al., 2018). Systems like *Drosophila*, *Hydra*, squid, and zebrafish offer numerous advantages including the relative ease of husbandry, the ability to study large numbers of offspring, less complex and more readily cultivated microbiomes for study than higher organisms, the availability of whole-organism imaging, etc. Pioneering studies in these systems have uncovered principles that govern host-microbiome interactions, including (but not limited to): (i) a role for gut symbionts in the coordination of tissue developmental programs and the microbial components responsible for these effects (particularly microbial cell wall products such as peptidoglycan and LPS, as well as microbial metabolites like acetate) (Koropatnick et al., 2004; Buchon et al., 2009; Shin et al., 2011; Troll et al., 2018), (ii) host adaptations to the microbiome that limit the inflammatory potential of microbiota-derived factors (Bates et al., 2007; Lhocine et al., 2008; Rader et al., 2012), (iii) host regulation of microbiome composition (Rawls et al., 2006; Ryu et al., 2008; Fraune et al., 2009), (iv) gut symbiont factors driving host adaptation (Rawls et al., 2007; Koehler et al., 2018), and (v) microbiome contributions to growth and nutrient acquisition (Storelli et al., 2011; Semova et al., 2012; Schwarzer et al., 2016). Gnotobiotic pigs have now become more widely utilized, which has allowed the study of these processes in an animal system with physiology more similar to that of humans than provided by commonly used murine models. While pig models present many challenges due to their size, they offer several advantages over more commonly

used model systems, including more human-like physiology, susceptibility to many human-relevant infectious agents, greater microbiome complexity, and therefore they offer important insights of more translational relevance (Vlasova et al., 2018; Ericsson, 2019; Gehrig et al., 2019). Although less commonly employed due to the more challenging and expensive nature of their husbandry, gnotobiotic pig models are proving to be a highly valuable component of microbiome research.

Despite the utility of these other model systems, the mouse has reigned supreme in biomedical research, especially for microbiome studies. The emergence of the mouse as a model organism can be traced to the early 1900s with the house mouse, *Mus musculus* being used to study Mendelian genetics (Castle and Little, 1910), followed shortly thereafter by the development of the first inbred *Mus musculus* strain in 1929 by C.C. Little at what is now known as Jackson labs (Phifer-Rixey and Nachman, 2015). Although models in other small animals have been widely used, including rats (Modlinska and Pisula, 2020), hamsters (Miao et al., 2019), and gerbils (Bleich et al., 2010), none are quite as adapted for the breadth of study possible with mice. Mice offer several advantages that include their relatively quick gestation period, their size, which allows for easier housing and manipulation, the plethora of tools for phenotypic assessment of the mouse, the availability of sophisticated tools for genetic modification to interrogate the role played by distinct genes and cell types, and most importantly the availability of approaches to raise mice in germ-free settings. Furthermore, the availability of inbred strains of mice and standardized, albeit imperfect, housing and husbandry that helps to minimize unwanted variation, allows for easier comparison of data from different researchers.

However, mirroring the interpersonal variation in human microbiomes, model organisms display significant variation in the composition of their microbiomes, which in turn contributes to phenotypic variation reported in mouse models, especially in studies associated with immune activation. Several notable examples highlight how microbiome variation can impact phenotypes in murine models: (i) microbiome mediated spontaneous colitis and metabolic dysfunction has been reported in TLR5-/- mice by some, but not by others (Vijay-Kumar et al., 2007, 2010; Letran et al., 2011); (ii) the aggravation of colitis and development of communicable disease in NLRP6-/- mice is critically dependent on the microbiome context in which it is studied (Elinav et al., 2011; Lemire et al., 2017; Mamantopoulos et al., 2017); (iii) IL-10-/- mice develop a spontaneous colitis in some animal facilities, yet they remain largely free of disease in others depending on the presence or absence of select microbes (Kuhn et al., 1993; Nagalingam et al., 2013; Seregin et al., 2017); (iv) DSS-induced colitis models display significantly varied kinetics and severity depending on microbiome composition (Forster et al., 2021); (v) diabetes in the Non-Obese Diabetic (NOD) type 1 diabetes model is regulated by various parameters, including the presence of specific gut microbes or infectious agents (Wilberz et al., 1991; Takei et al., 1992; Pozzilli et al., 1993; Kriegel et al., 2011; Markle et al., 2013; Yurkovetskiy et al., 2013). Although not an exhaustive list, these examples demonstrate that variation in the gut microbiome can lead to disparate phenotypic outcomes in mice. Experimental variation,

whether it be technical or biological in origin, has long been seen as a thorn in the side of researchers, contributing in part to issues of reproducibility in science (von Kortzfleisch et al., 2020). To limit the impact of overt pathogens, and the large-scale microbiome variation across different animal facilities, efforts were made to create a more standardized murine system that would limit issues of reproducibility. Thus, the concept of Specific Pathogen Free (SPF) mice was born. SPF mice are free of certain (but not all) pathogenic organisms or microorganisms capable of interfering with experimental outcomes (Lane-Petter, 1962). These mice provide the advantage of controlling the health status of the animal and allowing for better standardization between experiments, labs, and institutions. While the SPF mouse was adopted with the intention of allowing for more reproducible results, it has been shown that microbiome and phenotypic variability also exists between SPF mouse colonies from commercial vendors, as SPF only determines what is excluded, but not what should be present (Smith et al., 2007; Ivanov et al., 2009; Denning et al., 2011; Rosshart et al., 2017).

## Model Gut Microbiomes

To counteract the effects of microbiome variation researchers have turned to the use of defined reference communities. Beginning in the 1960s, Dubos et al. (1965), Schaedler et al. (1965), and Dewhirst et al. (1999) developed small model communities that were used to standardize the microbiome of animal models, mostly to be used in conventionally raised mice (Box 1). In an effort to move toward systems with greater control over community composition an ever-increasing number of researchers have begun to adopt germ-free/gnotobiotic models first established more than 60 years ago (Trexler and Reynolds, 1957; Gordon and Pesti, 1971). Such models allow the study of communities of interest without unwanted invasion by microbes

present in the environment. Pioneering studies using small communities, ranging from mono-associations (colonization with a single microbe) that establish the roles of individual genes and metabolic pathways in bacteria (Rey et al., 2010; Koppel et al., 2018; Glowacki et al., 2020) to more complex communities with up to 20 members (Mahowald et al., 2009; Faith et al., 2011, 2014; Geuking et al., 2011; Cahenzli et al., 2013; McNulty et al., 2013; Sefik et al., 2015; Brugiroux et al., 2016; Geva-Zatorsky et al., 2017; Becattini et al., 2021), reduced the complexity of the system (Figure 1). These simplified models have provided high-resolution insights into the ecological, transcriptional, and metabolic responses of microbes to environmental variations (e.g., diet, inflammation) (McNulty et al., 2013; Ridaura et al., 2013; Becattini et al., 2021), uncovered microbe-microbe interactions that shape community function (Mahowald et al., 2009; Caballero et al., 2017), and highlighted a role for microbiome members in host growth (Blanton et al., 2016; Charbonneau et al., 2016; Schwarzer et al., 2016), weight gain and metabolic health (Fei and Zhao, 2013; Ridaura et al., 2013), pathogen resistance (Fukuda et al., 2011; Hsiao et al., 2014; Alavi et al., 2020), as well as specific enzymatic functions that directly impact host health (Skye et al., 2018; Song et al., 2020). Thus, model communities studied in germ-free/gnotobiotic mice have provided key insights into the several facets of microbiome function and host-microbiome interactions.

The power of the germ-free mouse as a model system may be best exemplified by the advances they have facilitated in understanding immune-microbiome mutualism (reviewed extensively in Honda and Littman, 2016; Ost and Round, 2018; McCoy et al., 2019; Ahern and Maloy, 2020; Ansaldo et al., 2021). These studies have revealed the profound impact of the gut microbiome on immune function and provided detailed insights into the mechanisms that underlie these interactions. The absence of a microbiome leads to the development of a drastically altered intestinal immune system with striking defects in adaptive immune function including reductions in lymphocyte numbers and activation within the intestine and mesenteric lymph nodes, and an enhanced susceptibility to infection by certain pathogens (Abrams and Bishop, 1966; Thompson and Trexler, 1971; Imaoka et al., 1996; Macpherson and Harris, 2004). Notably, the microbiome has also been implicated in the shaping of the innate immune compartment, including aspects of trained immunity (reviewed in McCoy et al., 2019; Negi et al., 2019). Intensive efforts have subsequently identified specific microbial taxa/microbial consortia, and their derived molecules that influence the intestinal immune system of gnotobiotic mice, especially the intestinal T cell compartment. Colonizing germ-free mice with microbial consortia like the Altered Schaedler flora (ASF) and select *Clostridium* species, or mono-colonization with specific members of the *Bacteroides* genus (*Bacteroides thetaiotaomicron*, *Bacteroides caccae*, and *Bacteroides fragilis*) or *Bifidobacteria* (*B. bifidum*), coordinates the development of colonic regulatory T cells, an anti-inflammatory population of CD4<sup>+</sup> T cells that maintain intestinal homeostasis (Round and Mazmanian, 2010; Atarashi et al., 2011, 2013; Geuking et al., 2011; Faith et al., 2014; Sefik et al., 2015; Verma et al., 2018; Węgorzewska et al., 2019). Furthermore, cellular products

**BOX 1 |** Common terminology used to describe the colonization status/microbiome communities commonly found in murine model systems.

**Germ-free (GF)**-Mice that are raised devoid of all known microbes.

**Gnotobiotic**-Term used to denote GF mice that are now colonized with a defined community of microbes where all members are known such as the Altered Schaedler Flora and the use of synthetic bacterial communities.

**Specific Pathogen Free (SPF)**-Conventional mice that are devoid of particular known pathogens such as bacterial, viral, fungal, and parasitic inhabitants that could affect the health of the mouse colony and the validity of experimental outcomes.

**Conventional mice**-Laboratory mice that are raised in the presence of a gut microbiome, and are not necessarily considered free of pathogens (they may have inhabitants such as murine norovirus and *Helicobacter hepaticus*) but are generally considered healthy.

**Wild mice**-These are mice that have been captured in a non-lab environment (in the wild) and then transferred to a lab for study. Such mice can be mated with other wild-caught mice for study over several generations. Inbred lines of mice harboring wild-mouse microbiomes, often referred to as "WildR mice" (Rosshart et al., 2017), can be generated through microbial transfer from wild mice to inbred strains of lab mice to limit the effects of genetic variation.

**Synthetic communities**-Communities constructed from cultured isolates from naturally occurring complex microbiomes. These communities may represent isolates from a single donor, or isolates obtained from many different donors. Moreover, they may be constructed from subsets of all cultured isolates.

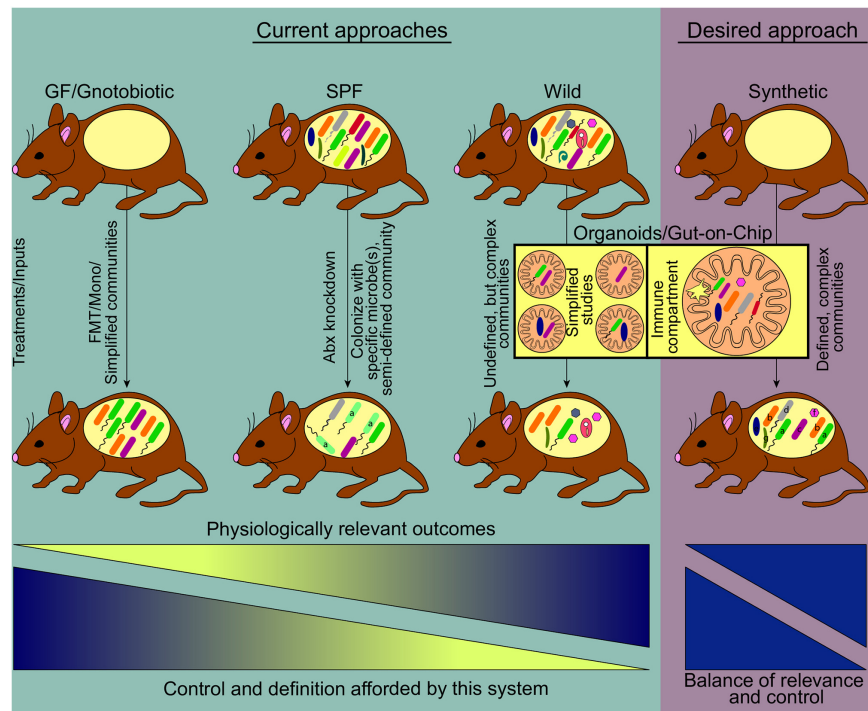


**FIGURE 1 |** Current and emerging systems to study host-gut microbiome interactions. Prevalent model systems in use to study physiological effects of gut microbiome-host interactions and representative community complexity within each model are shown (teal shaded area). The general usefulness of these systems based on physiologically relevant outcomes, increases left to right. At the same time, the ability to manipulate or define the community structure of these models decreases along the gradient, driving the need for a medium where physiologic relevance and tractability reach an optimum. Current technologies striving toward this desired model include the use of germ free mice where synthetic communities of known microorganisms are used for colonization, as well as the use of emerging lab-on-chip approaches (pink shaded area) (FMT, fecal microbiome transplant; Mono, monocolonization; Abx, antibiotics).

derived from these microbes, like polysaccharide A (PSA) (Round and Mazmanian, 2010) or  $\beta$ -glucan/galactan polysaccharides (Verma et al., 2018), short-chain fatty acids (SCFA; gut microbial fermentation products) (Arpaia et al., 2013; Furusawa et al., 2013; Smith P. M. et al., 2013) or microbially-transformed bile acids (Song et al., 2020) also regulate the size and function of colonic regulatory T cell pools. Likewise, Th17 cell differentiation can be coordinated by distinct microbes, most notably segmented filamentous bacteria (SFB) (Gaboriau-Routhiau et al., 2009; Ivanov et al., 2009) in addition to *Bifidobacterium adolescentis* (Tan et al., 2016) or particular strains of *E. coli* (Britton et al., 2020), which in turn can improve protective immunity against pathogens (Ivanov et al., 2009). Intraepithelial T cell populations are also impacted by gut microbes, with SFB able to shape the activation status of this immune compartment (Umesaki et al., 1999), while *Lactobacillus reuteri* promotes the development of  $CD4^+ CD8\alpha^+$  intraepithelial lymphocytes (IELs) by agonizing the aryl hydrocarbon pathway (Cervantes-Barragan et al., 2017).

Despite the enormous power of these systems, they have several limitations. First, the physiologic relevance of model communities can be hard to decipher. Second, due to their low diversity, they may fail to identify redundancy in effector functions that exist in larger communities, inappropriately attributing essential roles to particular microbes. Third, most groups study a limited number of strains of each species, which

ignores the enormous strain-level variation present in the gut microbiome. To overcome these limitations, models where mice are colonized with human gut microbiomes from healthy or diseased individuals ("humanized" mice) that could transmit features of their donor's health status (Raibaud et al., 1980; Turnbaugh et al., 2009b; Ridaura et al., 2013; Smith M. I. et al., 2013; Kau et al., 2015; Berer et al., 2017; Cekanaviciute et al., 2017; Britton et al., 2019; Feehley et al., 2019) have been widely adopted. The microbiomes of such humanized mice are typically more diverse than model communities and comprising distinct strains depending on the individual donor. Moreover, they represent a system with clear translational relevance, albeit with less defined community membership. For example, microbiome transplantation from individuals suffering from IBD (Britton et al., 2019), food allergy (Feehley et al., 2019), undernutrition (Smith M. I. et al., 2013; Kau et al., 2015; Wagner et al., 2016), obesity (Ridaura et al., 2013), and multiple sclerosis (Berer et al., 2017; Cekanaviciute et al., 2017), among other conditions, could enhance the susceptibility to such diseases in recipient gnotobiotic mice. However, despite all their advantages, significant caveats to the use of human-derived microbiomes exist that suggest a need for new and improved approaches. First, these communities are typically neither defined nor cultured (with exceptions; Wagner et al., 2016; Britton et al., 2019, 2020), limiting the establishment of causality for specific microbes



and/or microbial products. Second, while it is clear that microbes derived from humans can modulate particular facets of the murine immune system, host-specificity in such interactions (Atarashi et al., 2015) means that human-derived microbiota may not shape immune responses equivalent to murine-derived microbes (Gaboriau-Routhiau et al., 2009; Chung et al., 2012; Lundberg et al., 2020). Third, human-derived microbiomes are not as well adapted to the murine intestine as mouse-derived communities. Elegant studies using gnotobiotic mice colonized with either human or murine-derived microbiomes demonstrated that the murine microbiome exhibited superior fitness in the mouse intestine, and could displace many members of a human microbiome from a stably colonized mouse upon co-housing (Seedorf et al., 2014). Finally, the overall community composition and structure in the recipient mouse may vary significantly from the donor, both in terms of membership and microbial abundance, potentially over or understating the contributions of particular microbes (Turnbaugh et al., 2009b; Chung et al., 2012; Krych et al., 2013; Xiao et al., 2015; Lundberg et al., 2020). While there is obvious value to these approaches, and a wealth of information has been obtained from their use, it is important to consider that key elements of host-microbiome interactions may be missed by studying microbes outside of their natural environment (i.e., human microbes in the mouse).

While no single system is perfectly suited to address all goals, an optimized model to study host-microbiome interactions should encompass as many of the following features as possible: (i) Completely defined microbiome with high-quality reference genomes for each organism. Such systems allow high-resolution strain quantification and gene expression profiling with strain-level gene expression assessment; (ii) culturable and genetically manipulable strains. If all strains have been captured in culture in a clonally arrayed format, it allows for the construction of consortia of defined membership to determine how specific members impact the phenotype being studied (Goodman et al., 2011; Ahern et al., 2014; Faith et al., 2014), commonly referred to as synthetic communities. Moreover, the availability of tools for genetic modification allows for unambiguous assessment of the role for genes of interest, which has contributed to the significant insights afforded by members of the *Bacteroides*, for which sophisticated tools are available (Anderson and Salyers, 1989; Koropatkin et al., 2008; Goodman et al., 2009; Mimee et al., 2015; Wu et al., 2015; Lim et al., 2017); (iii) a genetically tractable host that allows for the interrogation of host pathways that mediate the effects of specific microbes/microbial products; (iv) a germ-free host that allows for high-level control over the composition of the community. The utility of germ-free mice for advancing microbiome studies is hard to overstate, and coupled with the ability to generate host mutants to dissect pathways of host-microbiome interactions is invaluable; and (v) microbiome whose members and imprinted host responses mirror the human population being modeled. Such a system would allow a high-resolution examination of complex communities that imprint human-like phenotypic variation, overcoming the shortcomings of the systems currently in vogue. An idealized system will capture all the advantages of the systems described above and is represented in **Figure 1**. While

a model that captures all these parameters remains aspirational, advances in microbial culturing and isolation, allied to genomic approaches that continue to decrease in cost while increasing in output mean that large libraries of cultured isolates can now be generated and characterized in wild-type and genetically modified gnotobiotic mice.

One of the primary challenges has been the identification of murine microbiomes that promote human-like phenotypes. Recent ground-breaking studies from a small number of labs have revealed that the microbial inhabitants of mice in the wild (or in pet stores) promote the acquisition of a human-like immune system in lab mice (**Figure 1**), recapitulating the activated and antigen-experienced phenotype found in humans (Beura et al., 2016; Rosshart et al., 2017, 2019; Lin et al., 2020; Yeung et al., 2020) by contrast with the typical immune system of lab mice that has a phenotype more akin to that of neonates (Beura et al., 2016). Wild mouse microbiomes lead to a profound reshaping of the host immune system, promoting a more human-like phenotype, most potently with respect to boosting T cells with effector/memory phenotypes. These alterations in immune phenotype are characterized by an expansion in systemic and tissue-resident memory CD8<sup>+</sup> T cell populations, increases in effector CD4<sup>+</sup> T cells (Th1, Th2, Th17, and Tregs), and innate immune populations such as innate-lymphoid cells and neutrophils (Beura et al., 2016; Lin et al., 2020; Yeung et al., 2020). Moreover, the levels of serum immunoglobulins and select cytokines are also increased (Beura et al., 2016). Consistent with this, these animals were found to be more resistant to viral infections (Influenza A), bacterial infections (*Listeria monocytogenes*), and colon cancer (DSS plus azoxymethane model) (Beura et al., 2016; Rosshart et al., 2017). Conversely, they are more susceptible to surgery-associated sepsis, likely due to increased inflammatory tone and/or increased reactivity to microbial products (Huggins et al., 2019). Thus, wild microbiome-driven enhancement of host immunity is associated with improved immune-mediated resistance to a variety of infectious diseases and cancer, and enhanced susceptibility to other inflammatory diseases, linking microbiome-mediated immunomodulation to organismal health.

Notably, the transcriptional responses that distinguish neonates and adults are reminiscent of those that differentiate SPF mice and those harboring a wild/pet store microbiome. These features are communicable to lab mice following co-housing, suggesting they are microbially-driven (Beura et al., 2016; Rosshart et al., 2017), although whether this is attributable to pathobionts, or the distinct strain composition of these communities is unknown. Moreover, the genomic diversity of wild mice, and its impact on host immune responses and disease susceptibility, may additionally contribute to distinct phenotypic features of wild mice, representing an area ripe for further exploration. Some of these features are likely attributable to infectious agents like pathogenic viruses (Reese et al., 2016), but notably, may also be due to specific endogenous bacterial or fungal members of the gut microbiome (Lin et al., 2020; Yeung et al., 2020). Indeed, wild mice that retained SPF status (i.e., free of all pathogens excluded under SPF guidelines) also induced distinct phenotypic variation relative to lab-raised SPF



counterparts, and this could be transmitted to lab mice through gut microbiome transplantation (Rosshart et al., 2017). These data suggest that differences in the specific strain composition of the gut microbiome of wild mice, rather than pathogen exposure, are responsible. More recently, a study revealed that wild mice more faithfully recapitulate the outcome of clinical trials targeting the immune system (Rosshart et al., 2019), by contrast with their conventional lab animals, reinforcing the notion that such models are of greater translational relevance. Thus, wild mice microbiomes provide an opportunity to improve the utility of mouse model systems.

However, while we and others (Hamilton et al., 2020; Graham, 2021; Kuypers et al., 2021) posit that wild microbiome-elicited phenotypes create a murine system with a more human-like phenotype, different approaches to wilding the microbiome including the specific donor material used, or the creation of environments that more accurately mimic the natural environment of the mouse (Arnesen et al., 2020; Lin et al., 2020; Yeung et al., 2020) vs. co-housing under controlled laboratory conditions (Beura et al., 2016; Rosshart et al., 2017), may lead to disparate phenotypic outcomes in recipients. The use of wild microbiomes thus may not fully humanize the murine response or be fully representative of human phenomena. For example, in the case of allergy development and the hygiene hypothesis, one study (Ottman et al., 2019) suggests that lack of microbe diversity drives such allergic states, while (Ma et al., 2021) contradicts these claims. Undoubtedly, the approach of using wild mice and/or their derived microbiomes does not fully address the nuances of *in vivo* mouse models vs. humans as discussed in depth elsewhere (Hamilton et al., 2020; Graham, 2021; Kuypers et al., 2021). To address these limitations, more studies are needed with comparative phenotyping of adult human and wild microbiome-exposed murine immune systems to determine whether these responses truly reflect the development of a more human-like response, as opposed to a response that is simply distinct from lab mice. With the advent of approaches that allow for detailed assessment of the non-lymphoid immune compartment in humans (Szabo et al., 2019), such studies are now possible. Moreover, as we discuss below, detailed knowledge of the microorganisms that coordinate the phenotypic features shared between mice harboring wild microbiomes and humans will advance efforts to generate improved murine model systems.

## Synthetic Wild Communities, an Optimized System to Study Immune-Microbiome Interactions

While wild microbiomes offer the potential to shed new light on host-microbiome interactions, currently there is limited information regarding the effector microbes within these communities. There is therefore a need to determine which microbes are responsible for mediating the human-like phenotypic variation that they induce. These efforts need not focus solely on non-pathogenic members of the microbiome but should include controlled pathogen as well as non-pathogen exposures. While defining these effector microbes is a daunting challenge, we and others have described effective strategies to

do so in a systematic and efficient manner (Goodman et al., 2011; Ahern et al., 2014; Faith et al., 2014; Palm et al., 2014; Kau et al., 2015; Surana and Kasper, 2017). The generation of culture libraries in arrayed format (i.e., where individual wells of multi-well plates contain distinct microbiome members) from human donor microbiomes that retain the effector functions of the donor community has allowed mechanistic insight into host-microbiome interactions of biological relevance (Ridaura et al., 2013; Faith et al., 2014; Wagner et al., 2016). Such strategies allow the precise delineation of the effects of individual community members, whether they operate in concert with other members or in isolation (Ahern et al., 2014; Faith et al., 2014). Similarly, the isolation in pure culture of the constituents of the wild mouse microbiome represents a key first step toward the generation of more complete synthetic communities that recapitulate wild microbiome imprinted functions and allow for greater manipulability. Likewise, in defining these wild microbiomes, it is important to appreciate that for the past several decades, non-bacterial residents of the gut (fungi, archaea, viruses, parasites, and other non-fungal eukaryotic members) have received scant attention, mostly attributable to technical challenges. Such impediments include the variability of internal transcribed spacer regions (ITS) within fungal ribosomal genes and a general lack of reference genomes to compare species prevalence in metagenomic samples (Paterson et al., 2017). Sequencing challenges have also dampened the ability to get a fully representative picture of the gut virome. Most techniques for nucleic acid isolation and sequencing are biased toward DNA viruses, largely missing RNA viruses, while isolation and propagation of gut viruses is also a challenge that needs to be overcome (Wang, 2020; Khan Mirzaei et al., 2021). This lack of cultivation methods extends to archaeal members as well, with archaea often requiring specific culture conditions (Borrel et al., 2020) which can hamper *in vivo* studies. The genesis of libraries of isolates of all microbiome-member types in arrayed format from wild-microbiomes that are known to impact host phenotypes, such that consortia of individual library members can be compiled to study their effects on the host will form an essential component moving forward in defining complex host-microbiome interactions (Goodman et al., 2011; Ahern et al., 2014; Faith et al., 2014; Palm et al., 2014). Moreover, this will facilitate the dissemination to other researchers for implementation in their studies. The use of a common library of microorganisms freely available to all researchers that can be leveraged to understand host-microbiome interactions at multiple scales will advance efforts to uncover mechanistic insights into the operations of large diverse communities that reflect the breadth of microbial taxa and viruses that characterize humans and their associated phenotypic effects.

Despite our call for more standardized gut microbiomes, it would be foolish to demand complete homogenization across institutions, or even within an institution. Microbiome variation can itself represent a form of “natural experiment” that can present a challenge to researchers, but that has also proved a rich source of information regarding how the microbiome can mediate interpersonal variation among a population. For example, the varied presence of Th17 cells in the small intestinal

lamina propria in C57BL/6 mice from different commercial vendors led to the identification of a single microbe, SFB, which was differentially represented in the microbiomes of these animals and was both required and sufficient for the development of intestinal Th17 cells (Ivanov et al., 2008, 2009; Gaboriau-Routhiau et al., 2009). Similarly, the varying presence of *Lactobacillus reuteri* in different animal facilities within the same institution led to its identification as a potent modulator of CD4<sup>+</sup> CD8 $\alpha$ <sup>+</sup> IEL development (Cervantes-Barragan et al., 2017). More recently, the fungus *Debaryomyces hansenii* was highlighted as a mediator of impaired intestinal healing, which again was differentially represented among different colonies of lab mice at the same institution and directly regulated the intestinal healing potential of mice (Jain et al., 2021). Others have also linked different microbiome composition to the phenotype of various animal models of infectious and autoimmune disease (Wu et al., 2010; Lee et al., 2014; Hilbert et al., 2017; Moskowitz et al., 2019; Velazquez et al., 2019). What these studies highlight is that phenotypic variance can be leveraged, even embraced (Ivanov et al., 2008, 2009; Cervantes-Barragan et al., 2017; Jain et al., 2021), to uncover novel host-microbiome interactions that shape host responses. Consequently, although variation poses challenges for microbiome research, total standardization is itself not without issue. Instead, the utility of such variance is linked to an ability to measure and define the causes of the variation, and the reporting of the microbiome composition that is associated with a phenotype will be of enormous value in linking specific microbes to phenotypes of interest. Such an approach will reveal contextualized roles for host phenotypes that may manifest only in the presence of particular community types. Thus, there remains a prominent place for non-standardized models in illuminating fundamentally important host-microbiome interactions.

## Alternatives to *in vivo* Mouse Models

In spite of all the advantages of the *in vivo* mouse models we describe, it is ultimately a system with limitations that demands alternative approaches that augment our understanding. Fundamental differences between mice and humans mean that key aspects of host-microbiome interactions may not be modeled in a murine system. Indeed, the specificity in molecular aspects of host-microbe interactions (Lecuit et al., 1999; Atarashi et al., 2015) demands systems to study human-derived microbes in the context of human cells. The advent of sophisticated *in vitro/ex vivo* approaches that use human-derived cells that can themselves be genetically manipulated represent attractive alternatives that can be used in parallel to murine models. In addition to overcoming shortfalls in murine systems, these approaches help with the continued efforts to replace, reduce, and refine animals in research.

## Organoids

Human intestinal organoids (HIOs) or enteroids (HIEs) remove the need for a live model organism, and instead rely on primary cells derived from human biopsies or stem cells. This technique was originally pioneered from the use of *ex vivo* tissue explants of human intestines (Browning and Trier, 1969). Growth

factors are used to drive differentiation of Lgr5<sup>+</sup> intestinal stem cells into intestinal cell types that mimic the 3D spatial and functional environment of the intestine, allowing for simultaneous differentiation into discrete cell types (Ootani et al., 2009; Sato et al., 2009). HIOs have some advantages over other *in vitro* systems as they maintain the crypt-villus architecture and allow for multiple columnar cell types to be generated (Hill and Spence, 2017). HIOs permit the study of phenomena that have proved challenging in other *in vivo* systems, including tight junctions of non-enterocyte cells of the small intestine (Pearce et al., 2018); IBD models of infection and inflammatory processes (Angus et al., 2019; Sarvestani et al., 2021); and models of infection such as human norovirus (Ettayebi et al., 2016) and rotavirus (Finkbeiner et al., 2012), for which no *in vivo* model organism exists, and *in vitro* culture efforts had not been successful at the time. Additionally, microinjection of bacterial and parasitic pathogens including *C. difficile* (Leslie et al., 2015), *S. enterica* Typhimurium (Forbester et al., 2015; Wilson et al., 2015), *E. coli* (In et al., 2016; Karve et al., 2017; Rajan et al., 2018), and *Cryptosporidium* (Heo et al., 2018) have all been performed. This platform has allowed for controlled studies into the interactions these pathogens have with the intestine, however, there are several key challenges that remain. Although bacteria can be injected into these structures, the process has drawbacks such that the specialized technique of microinjection is required to avoid compromising the organoid structure and the lumen within the organoid contains a growth-limiting concentration of nutrients that generally can only support the growth of bacteria for less than 24 h. This nutrient limitation also significantly hinders the diversity of microorganisms that can be cultured together in poly-microbial communities. Other constraints involve the physical structure of organoids, and the lack of immune cells, calling into question how well the system recapitulates *in vivo* biology with the absence of such features (Blutt et al., 2018). Despite the advantages that organoids provide, the noted limitations suggest that the organoid model is not yet advanced to the point of being able to replicate all aspects found *in vivo*. Instead, these systems are likely more useful as tools to study parameters such as the permeability of the mucosa, drug kinetics, and bacterial interactions in disease states using tissue derived from patients with IBD or related conditions.

## Gut-on-Chip Technologies

A relatively new approach to studying microbe-microbe and intestinal cell-microbe interactions are “lab-on-chip” technologies. Although systems such as Transwell plates (two-dimensional technology) and Ussing chambers (three-dimensional) have been used for decades (Ussing and Zerahn, 1951; Hidalgo et al., 1989) and have been used to study bacterial-host epithelium interactions and diseases of the intestine (Kurkchubasche et al., 1998; Thomson et al., 2019), both have known limitations. With respect to the microbiome, these technologies are not well-suited for maintenance of both aerobic and anaerobic compartments except in limited circumstances (Ulluwishewa et al., 2015; Jafari et al., 2016). This makes studying gut microbiome-host interactions with obligate anaerobes a challenge. Additional limitations involve the duration in which

bacteria can be co-cultured before either they or the epithelial cells die, with most ranging from hours to a few days due to the non-peristaltic nature of these devices (Sadaghian Sadabad et al., 2015). Although other devices, such as the mucosal simulator of the human intestinal microbial ecosystem (M-SHIME), or its derivative, the Host-Microbiota Interaction (HMI)-module, have shown promise in incorporating peristalsis-like flow; they suffer from similar problems of short co-culture incubation times and rely on artificial mucus layers (Van den Abbeele et al., 2012; Marzorati et al., 2014). The SHIME reactors are also large, expensive to produce, and not easily scalable.

Using technology pioneered by lithography of computer chip manufacturing (Bhatia and Ingber, 2014), microfluidic devices may be a happy medium that yields more information on bacterial-gut epithelial-immune system interactions. These devices allow for a 3-D spatial reconstruction of the *in vivo* environment. Specifically for bacteria, these platforms have been used to study bacterial quorum sensing (Osmekhina et al., 2018), the response to antibiotics, and other chemicals in a complex community (Hsu et al., 2019), and taxis and motility (Gurung et al., 2020). Adoption of these devices has led to the generation of new platforms that are being used to study the human gut ecosystem and the human gut microbiota (von Martels et al., 2017; Tan and Toh, 2020). These devices overcome a substantial amount of the need for using *in vivo* models and tissue explants to maintain an environment necessary to study long-duration, complex, multi-species, and multiple cell type interactions. Although there are at least 12 different microfluidic devices in use, the vast majority rely on the colorectal carcinoma cell line, Caco-2 cells, to establish an epithelium, and have only managed to culture one species of bacteria at a time; several of these devices have previously been reviewed for benefits and drawbacks (Bein et al., 2018; Tan and Toh, 2020). Recent advancements include the *nBioChip* which supports the co-culture of both bacteria (*Staphylococcus aureus* and *Pseudomonas aeruginosa*) together with the fungus, *Candida albicans* (Srinivasan et al., 2017). Perhaps the largest advancement is the Intestine Chip, with the ability to maintain over 200 operational taxonomic units (OTUs) of bacteria directly from human feces with both obligate anaerobes and aerobic bacteria established along a hypoxia gradient (Jalili-Firoozinezhad et al., 2019). The Intestine Chip can also support stable colonization periods of up to or beyond 1 week due to its peristalsis-like flow of media. However, like the platform of the two previous iterations of this specific device (Kim et al., 2012, 2016), Caco-2 cells are used to develop the epithelial compartment rather than primary cells, which limits some downstream applications due to these cells not being representative of the primary cells of the intestinal tract.

Recent advancements have merged organoid and gut-on-chip technologies. First described as an early version of the Intestine Chip, the use of matured organoids containing villus structures and multiple cell types were enzymatically broken down and used to seed extracellular matrix (ECM)-coated membranes of a microfluidic chip (Kasendra et al., 2018). The other half of the chip was then seeded with human intestinal microvascular endothelial cells to examine cell-cell interactions, thus creating a multi-system organ on a chip. Through RNA-sequencing, confocal microscopy, and tissue

staining it was shown that the Intestine Chip recapitulates key features of the signaling pathways, cellular differentiation, mucus production, and epithelial-endothelial interactions seen in the human duodenum. A similar platform termed the gut microbiome physiome (GuMI) has been developed, specifically for the culture of extremely oxygen-sensitive microbes such as *Faecalibacterium prausnitzii* (Zhang et al., 2021). Similar to the Intestine Chip, the gut microbiome (GuMI) ECM is impregnated with cells derived from organoids and the device has inlets for sampling and injection of bacteria. While many other chip-based devices are fabricated using polydimethylsiloxane (PDMS), the GuMI uses polysulfone, which can be autoclaved for sterility and is less permeable to oxygen, allowing for more strict control of oxygen gradients (Shin et al., 2019). Lastly, this chip allows for the independent culture of six different bacteria within the luminal portion. Using organoid-derived cells, this three-layer-chip contains an ECM seeded with both intestinal cells and monocyte-derived macrophages and recapitulates features observed in IBD patients (Beaurivage et al., 2020). While the presence of immune cells is an important advancement, the generation of systems that can maintain interaction with a complex immune system is essential to boost the translational relevance of these systems. Nevertheless, the combination of gut-on-chip and organoids is a promising step forward toward the goal of having a tunable system to interrogate complex interactions that are difficult to perform *in vivo* (Figure 1).

## DISCUSSION/PROSPECTUS

A wealth of knowledge about gut microbiome-host interactions has been gained through the use of the model systems discussed in this review. Conventionally raised mice (both SPF and non-SPF), and gnotobiotic mice, have been and continue to be essential tools to study interactions between the gut microbiome in host health and disease. While there is a continued use for these models, their limitations hinder efforts to gain the mechanistic insights required to target the microbiome for therapeutic purposes. Development of synthetic, wild mouse gut microbiome communities comprising cultured and genome-sequenced microbiome members derived from wild mice provides an opportunity to gain mechanistic understanding of specific microbe-host phenotypes that recapitulate the interactions of humans with their microbiomes and the associated microbiome imprinted phenotypes. Used in conjunction with ever-improving *in vitro/ex vivo* model systems that facilitate high-resolution studies of complex host-microbiome interactions, these technologies will advance our understanding of the range of microbiome members that shape host physiology and help define the nature of the interactions that underlie these phenomena.

## CONCLUSION

In conclusion, model systems to study gut microbiome-host interactions continue to evolve. The incorporation of synthetic, wild microbiomes into the suite of model systems provides an opportunity to increase mechanistic insight and translatability. The use of these advanced mouse models and ever-improving



alternative model systems to study gut microbiome-host interactions will increase our understanding of the functionality of specific microbes in human physiology and disease, advancing efforts to target the microbiome for therapeutic purposes.

## AUTHOR CONTRIBUTIONS

RWPG, MJE, and PPA performed relevant literature searches, critical appraisals of the literature, and wrote the review.

## REFERENCES

- Abdel-Gadir, A., Stephen-Victor, E., Gerber, G. K., Noval Rivas, M., Wang, S., Harb, H., et al. (2019). Microbiota therapy acts via a regulatory T cell MyD88/RORgammat pathway to suppress food allergy. *Nat. Med.* 25, 1164–1174. doi: 10.1038/s41591-019-0461-z
- Abrams, G. D., and Bishop, J. E. (1966). Effect of the normal microbial flora on the resistance of the small intestine to infection. *J. Bacteriol.* 92, 1604–1608. doi: 10.1128/jb.92.6.1604-1608.1966
- Ahern, P. P., Faith, J. J., and Gordon, J. I. (2014). Mining the human gut microbiota for effector strains that shape the immune system. *Immunity* 40, 815–823. doi: 10.1016/j.immuni.2014.05.012
- Ahern, P. P., and Maloy, K. J. (2020). Understanding immune-microbiota interactions in the intestine. *Immunology* 159, 4–14. doi: 10.1111/imm.13150
- Alavi, S., Mitchell, J. D., Cho, J. Y., Liu, R., Macbeth, J. C., and Hsiao, A. (2020). Interpersonal Gut Microbiome Variation Drives Susceptibility and Resistance to Cholera Infection. *Cell* 181, 1533–1546. doi: 10.1016/j.cell.2020.05.036
- Anderson, K. L., and Salyers, A. A. (1989). Genetic evidence that outer membrane binding of starch is required for starch utilization by *Bacteroides thetaiotaomicron*. *J. Bacteriol.* 171, 3199–3204. doi: 10.1128/jb.171.6.3199-3204.1989
- Angus, H. C. K., Butt, A. G., Schultz, M., and Kemp, R. A. (2019). Intestinal Organoids as a Tool for Inflammatory Bowel Disease Research. *Front. Med.* 6:334. doi: 10.3389/fmed.2019.00334
- Ansaldo, E., Farley, T. K., and Belkaid, Y. (2021). Control of Immunity by the Microbiota. *Annu. Rev. Immunol.* 39, 449–479. doi: 10.1146/annurev-immunol-093019-112348
- Arnesen, H., Knutsen, L. E., Hognestad, B. W., Johansen, G. M., Bemerk, M., Pabst, O., et al. (2020). A Model System for Feralizing Laboratory Mice in Large Farmyard-Like Pens. *Front. Microbiol.* 11:615661. doi: 10.3389/fmicb.2020.615661
- Arpaia, N., Campbell, C., Fan, X., Dikiy, S., van der Veeken, J., deRoos, P., et al. (2013). Metabolites produced by commensal bacteria promote peripheral regulatory T-cell generation. *Nature* 504, 451–455. doi: 10.1038/nature12726
- Arthur, J. C., Perez-Chanona, E., Mühlbauer, M., Tomkovich, S., Uronis, J. M., Fan, T. J., et al. (2012). Intestinal inflammation targets cancer-inducing activity of the microbiota. *Science* 338, 120–123. doi: 10.1126/science.1224820
- Atarashi, K., Tanoue, T., Ando, M., Kamada, N., Nagano, Y., Narushima, S., et al. (2015). Th17 Cell Induction by Adhesion of Microbes to Intestinal Epithelial Cells. *Cell* 163, 367–380. doi: 10.1016/j.cell.2015.08.058
- Atarashi, K., Tanoue, T., Oshima, K., Suda, W., Nagano, Y., Nishikawa, H., et al. (2013). Treg induction by a rationally selected mixture of Clostridia strains from the human microbiota. *Nature* 500, 232–236. doi: 10.1038/nature12331
- Atarashi, K., Tanoue, T., Shima, T., Imaoka, A., Kuwahara, T., Momose, Y., et al. (2011). Induction of colonic regulatory T cells by indigenous Clostridium species. *Science* 331, 337–341. doi: 10.1126/science.1198469
- Augustin, R., Fraune, S., Franzburg, S., and Bosch, T. C. (2012). Where simplicity meets complexity: hydra, a model for host-microbe interactions. *Adv. Exp. Med. Biol.* 710, 71–81. doi: 10.1007/978-1-4419-5638-5\_8
- Bates, J. M., Akerlund, J., Mitige, E., and Guillemin, K. (2007). Intestinal alkaline phosphatase detoxifies lipopolysaccharide and prevents inflammation in zebrafish in response to the gut microbiota. *Cell Host Microbe* 2, 371–382. doi: 10.1016/j.chom.2007.10.010
- Beaurivage, C., Kanapeckaite, A., Loomans, C., Erdmann, K. S., Stallen, J., and Janssen, R. A. J. (2020). Development of a human primary gut-on-a-chip to

All authors contributed to the article and approved the submitted version.

## FUNDING

The authors are supported by a grant from the National Institute of Diabetes and Digestive and Kidney Diseases, National Institutes of Health (R01DK126772).

- model inflammatory processes. *Sci. Rep.* 10:21475. doi: 10.1038/s41598-020-78359-2
- Beccattini, S., Sorbara, M. T., Kim, S. G., Littmann, E. L., Dong, Q., Walsh, G., et al. (2021). Rapid transcriptional and metabolic adaptation of intestinal microbes to host immune activation. *Cell Host Microbe* 29, 378–393e375. doi: 10.1016/j.chom.2021.01.003
- Bein, A., Shin, W., Jalili-Firoozinezhad, S., Park, M. H., Sontheimer-Phelps, A., Tovaglieri, A., et al. (2018). Microfluidic Organ-on-a-Chip Models of Human Intestine. *Cell Mol. Gastroenterol. Hepatol.* 5, 659–668. doi: 10.1016/j.jcmgh.2017.12.010
- Berer, K., Gerdes, L. A., Cekanaviciute, E., Jia, X., Xiao, L., Xia, Z., et al. (2017). Gut microbiota from multiple sclerosis patients enables spontaneous autoimmune encephalomyelitis in mice. *Proc. Natl. Acad. Sci. U S A* 114, 10719–10724. doi: 10.1073/pnas.1711233114
- Beura, L. K., Hamilton, S. E., Bi, K., Schenkel, J. M., Odumade, O. A., Casey, K. A., et al. (2016). Normalizing the environment recapitulates adult human immune traits in laboratory mice. *Nature* 532, 512–516. doi: 10.1038/nature17655
- Bhatia, S. N., and Ingber, D. E. (2014). Microfluidic organs-on-chips. *Nat. Biotechnol.* 32, 760–772. doi: 10.1038/nbt.2989
- Blanton, L. V., Charbonneau, M. R., Salih, T., Barratt, M. J., Venkatesh, S., Ilkaveya, O., et al. (2016). Gut bacteria that prevent growth impairments transmitted by microbiota from malnourished children. *Science* 351:6275. doi: 10.1126/science.aad3311
- Bleich, E. M., Martin, M., Bleich, A., and Klos, A. (2010). The Mongolian gerbil as a model for inflammatory bowel disease. *Int. J. Exp. Pathol.* 91, 281–287. doi: 10.1111/j.1365-2613.2009.00701.x
- Blutt, S. E., Crawford, S. E., Ramani, S., Zou, W. Y., and Estes, M. K. (2018). Engineered Human Gastrointestinal Cultures to Study the Microbiome and Infectious Diseases. *Cell Mol. Gastroenterol. Hepatol.* 5, 241–251. doi: 10.1016/j.jcmgh.2017.12.001
- Borrel, G., Brugère, J. F., Gribaldo, S., Schmitz, R. A., and Moissl-Eichinger, C. (2020). The host-associated archaeome. *Nat. Rev. Microbiol.* 18, 622–636. doi: 10.1038/s41579-020-0407-y
- Britton, G. J., Contijoch, E. J., Mogno, I., Vennaro, O. H., Llewellyn, S. R., Ng, R., et al. (2019). Microbiotas from Humans with Inflammatory Bowel Disease Alter the Balance of Gut Th17 and RORgammat(+) Regulatory T Cells and Exacerbate Colitis in Mice. *Immunity* 50, 212–224e214. doi: 10.1016/j.immuni.2018.12.015
- Britton, G. J., Contijoch, E. J., Spindler, M. P., Aggarwala, V., Dogan, B., Bongers, G., et al. (2020). Defined microbiota transplant restores Th17/RORgammat(+) regulatory T cell balance in mice colonized with inflammatory bowel disease microbiotas. *Proc. Natl. Acad. Sci. U S A* 117, 21536–21545. doi: 10.1073/pnas.1922189117
- Browning, T. H., and Trier, J. S. (1969). Organ culture of mucosal biopsies of human small intestine. *J. Clin. Invest.* 48, 1423–1432. doi: 10.1172/JCI106108
- Brugiroux, S., Beutler, M., Pfann, C., Garzetti, D., Ruscheweyh, H. J., Ring, D., et al. (2016). Genome-guided design of a defined mouse microbiota that confers colonization resistance against *Salmonella enterica* serovar Typhimurium. *Nat. Microbiol.* 2:16215. doi: 10.1038/nmicrobiol.2016.215
- Buc, E., Dubois, D., Sauvanet, P., Raich, J., Delmas, J., Darfeuille-Michaud, A., et al. (2013). High prevalence of mucosa-associated *E. coli* producing cyclomodulin and genotoxin in colon cancer. *PLoS One* 8:e56964. doi: 10.1371/journal.pone.0056964
- Buchon, N., Broderick, N. A., Chakrabarti, S., and Lemaitre, B. (2009). Invasive and indigenous microbiota impact intestinal stem cell activity through



- multiple pathways in *Drosophila*. *Genes Dev.* 23, 2333–2344. doi: 10.1101/gad.1827009
- Buffie, C. G., Bucci, V., Stein, R. R., McKenney, P. T., Ling, L., Gouberne, A., et al. (2015). Precision microbiome reconstitution restores bile acid mediated resistance to *Clostridium difficile*. *Nature* 517, 205–208. doi: 10.1038/nature13828
- Caballero, S., Kim, S., Carter, R. A., Leiner, I. M., Susac, B., Miller, L., et al. (2017). Cooperating Commensals Restore Colonization Resistance to Vancomycin-Resistant *Enterococcus faecium*. *Cell Host Microbe* 21, 592–602e594. doi: 10.1016/j.chom.2017.04.002
- Cadwell, K., Patel, K. K., Maloney, N. S., Liu, T. C., Ng, A. C., Storer, C. E., et al. (2010). Virus-plus-susceptibility gene interaction determines Crohn's disease gene Atg16L1 phenotypes in intestine. *Cell* 141, 1135–1145. doi: 10.1016/j.cell.2010.05.009
- Cahenzli, J., Koller, Y., Wyss, M., Geuking, M. B., and McCoy, K. D. (2013). Intestinal microbial diversity during early-life colonization shapes long-term IgE levels. *Cell Host Microbe* 14, 559–570. doi: 10.1016/j.chom.2013.10.004
- Castle, W. E., and Little, C. C. (1910). On a Modified Mendelian Ratio among Yellow Mice. *Science* 32, 868–870. doi: 10.1126/science.32.833.868
- Cekanaviciute, E., Yoo, B. B., Runia, T. F., Debelius, J. W., Singh, S., Nelson, C. A., et al. (2017). Gut bacteria from multiple sclerosis patients modulate human T cells and exacerbate symptoms in mouse models. *Proc. Natl. Acad. Sci. U S A* 114, 10713–10718. doi: 10.1073/pnas.1711235114
- Cervantes-Barragan, L., Chai, J. N., Tianero, M. D., Di Luccia, B., Ahern, P. P., Merriman, J., et al. (2017). *Lactobacillus reuteri* induces gut intraepithelial CD4(+)CD8alphaalpha(+) T cells. *Science* 357, 806–810. doi: 10.1126/science.aah5825
- Charbonneau, M. R., O'Donnell, D., Blanton, L. V., Totten, S. M., Davis, J. C., Barratt, M. J., et al. (2016). Sialylated Milk Oligosaccharides Promote Microbiota-Dependent Growth in Models of Infant Undernutrition. *Cell* 164, 859–871. doi: 10.1016/j.cell.2016.01.024
- Chudnovskiy, A., Mortha, A., Kana, V., Kennard, A., Ramirez, J. D., Rahman, A., et al. (2016). Host-Protozoan Interactions Protect from Mucosal Infections through Activation of the Inflammasome. *Cell* 167, 444–456e414. doi: 10.1016/j.cell.2016.08.076
- Chung, H., Pamp, S. J., Hill, J. A., Surana, N. K., Edelman, S. M., Troy, E. B., et al. (2012). Gut immune maturation depends on colonization with a host-specific microbiota. *Cell* 149, 1578–1593. doi: 10.1016/j.cell.2012.04.037
- Cowardin, C. A., Ahern, P. P., Kung, V. L., Hibberd, M. C., Cheng, J., Guruge, J. L., et al. (2019). Mechanisms by which sialylated milk oligosaccharides impact bone biology in a gnotobiotic mouse model of infant undernutrition. *Proc. Natl. Acad. Sci. U S A* 116, 11988–11996. doi: 10.1073/pnas.1821770116
- Dallari, S., Heaney, T., Rosas-Villegas, A., Neil, J. A., Wong, S. Y., Brown, J. J., et al. (2021). Enteric viruses evoke broad host immune responses resembling those elicited by the bacterial microbiome. *Cell Host Microbe* 29, 1014–1029e1018. doi: 10.1016/j.chom.2021.03.015
- Denning, T. L., Norris, B. A., Medina-Contreras, O., Manicassamy, S., Geem, D., Madan, R., et al. (2011). Functional specializations of intestinal dendritic cell and macrophage subsets that control Th17 and regulatory T cell responses are dependent on the T cell/APC ratio, source of mouse strain, and regional localization. *J. Immunol.* 187, 733–747. doi: 10.4049/jimmunol.1002701
- Dewhirst, F. E., Chien, C. C., Paster, B. J., Ericson, R. L., Orcutt, R. P., Schauer, D. B., et al. (1999). Phylogeny of the defined murine microbiota: altered Schaedler flora. *Appl. Environ. Microbiol.* 65, 3287–3292. doi: 10.1128/aem.65.8.3287-3292.1999
- Di Luccia, B., Ahern, P. P., Griffin, N. W., Cheng, J., Guruge, J. L., Byrne, A. E., et al. (2020). Combined Prebiotic and Microbial Intervention Improves Oral Cholera Vaccination Responses in a Mouse Model of Childhood Undernutrition. *Cell Host Microbe* 27, 899–908e895. doi: 10.1016/j.chom.2020.04.008
- Dubos, R., Schaedler, R. W., Costello, R., and Hoet, P. (1965). Indigenous, normal, and autochthonous flora of the gastrointestinal tract. *J. Exp. Med.* 122, 67–76. doi: 10.1084/jem.122.1.67
- Elinav, E., Strowig, T., Kau, A. L., Henao-Mejia, J., Thaiss, C. A., Booth, C. J., et al. (2011). NLRP6 inflammasome regulates colonic microbial ecology and risk for colitis. *Cell* 145, 745–757. doi: 10.1016/j.cell.2011.04.022
- Ellis, T. H., Hofer, J. M., Timmerman-Vaughan, G. M., Coyne, C. J., and Hellens, R. P. (2011). Mendel, 150 years on. *Trends Plant Sci.* 16, 590–596. doi: 10.1016/j.tplants.2011.06.006
- Ericsson, A. C. (2019). The use of non-rodent model species in microbiota studies. *Lab. Anim.* 53, 259–270. doi: 10.1177/0023677219834593
- Escalante, N. K., Lemire, P., Cruz Tleugabulova, M., Prescott, D., Mortha, A., Streutker, C. J., et al. (2016). The common mouse protozoa *Tritrichomonas muris* alters mucosal T cell homeostasis and colitis susceptibility. *J. Exp. Med.* 213, 2841–2850. doi: 10.1084/jem.20161776
- Ettayebi, K., Crawford, S. E., Murakami, K., Broughman, J. R., Karandikar, U., Tenge, V. R., et al. (2016). Replication of human noroviruses in stem cell-derived human enteroids. *Science* 353, 1387–1393. doi: 10.1126/science.aaf5211
- Faith, J. J., Ahern, P. P., Ridaura, V. K., Cheng, J., and Gordon, J. I. (2014). Identifying gut microbe-host phenotype relationships using combinatorial communities in gnotobiotic mice. *Sci. Transl. Med.* 6:220ra211. doi: 10.1126/scitranslmed.3008051
- Faith, J. J., McNulty, N. P., Rey, F. E., and Gordon, J. I. (2011). Predicting a human gut microbiota's response to diet in gnotobiotic mice. *Science* 333, 101–104. doi: 10.1126/science.1206025
- Feehley, T., Plunkett, C. H., Bao, R., Choi Hong, S. M., Culleen, E., Belda-Ferre, P., et al. (2019). Healthy infants harbor intestinal bacteria that protect against food allergy. *Nat. Med.* 25, 448–453. doi: 10.1038/s41591-018-0324-z
- Fei, N., and Zhao, L. (2013). An opportunistic pathogen isolated from the gut of an obese human causes obesity in germfree mice. *ISME J.* 7, 880–884. doi: 10.1038/ismej.2012.153
- Finkbeiner, S. R., Zeng, X. L., Utama, B., Atmar, R. L., Shroyer, N. F., and Estes, M. K. (2012). Stem cell-derived human intestinal organoids as an infection model for rotaviruses. *mBio* 3, e159–e112. doi: 10.1128/mBio.00159-12
- Forbester, J. L., Goulding, D., Vallier, L., Hannan, N., Hale, C., Pickard, D., et al. (2015). Interaction of *Salmonella enterica* Serovar Typhimurium with Intestinal Organoids Derived from Human Induced Pluripotent Stem Cells. *Infect. Immun.* 83, 2926–2934. doi: 10.1128/IAI.00161-15
- Forster, S. C. S., Beresford-Jones, B. S., Harcourt, K., Notley, G., Stares, M., Kumar, N., et al. (2021). Novel gut pathobionts confound results in a widely used mouse model of human inflammatory disease. *bioRxiv* 2021:430393. doi: 10.1101/2021.02.09.430393
- Frank, D. N., St Amand, A. L., Feldman, R. A., Boedeker, E. C., Harpaz, N., and Pace, N. R. (2007). Molecular-phylogenetic characterization of microbial community imbalances in human inflammatory bowel diseases. *Proc. Natl. Acad. Sci. U S A* 104, 13780–13785. doi: 10.1073/pnas.0706625104
- Fraune, S., Abe, Y., and Bosch, T. C. (2009). Disturbing epithelial homeostasis in the metazoan Hydra leads to drastic changes in associated microbiota. *Environ. Microbiol.* 11, 2361–2369. doi: 10.1111/j.1462-2920.2009.01963.x
- Fukuda, S., Toh, H., Hase, K., Oshima, K., Nakanishi, Y., Yoshimura, K., et al. (2011). Bifidobacteria can protect from enteropathogenic infection through production of acetate. *Nature* 469, 543–547. doi: 10.1038/nature09646
- Furusawa, Y., Obata, Y., Fukuda, S., Endo, T. A., Nakato, G., Takahashi, D., et al. (2013). Commensal microbe-derived butyrate induces the differentiation of colonic regulatory T cells. *Nature* 504, 446–450. doi: 10.1038/nature12721
- Gaboriau-Routhiau, V., Rakotobe, S., Lecuyer, E., Mulder, I., Lan, A., Bridonneau, C., et al. (2009). The key role of segmented filamentous bacteria in the coordinated maturation of gut helper T cell responses. *Immunity* 31, 677–689. doi: 10.1016/j.immuni.2009.08.020
- Gehrig, J. L., Venkatesh, S., Chang, H. W., Hibberd, M. C., Kung, V. L., Cheng, J., et al. (2019). Effects of microbiota-directed foods in gnotobiotic animals and undernourished children. *Science* 365. doi: 10.1126/science.aau4732
- Geuking, M. B., Cahenzli, J., Lawson, M. A., Ng, D. C., Slack, E., Hapfelmeier, S., et al. (2011). Intestinal bacterial colonization induces mutualistic regulatory T cell responses. *Immunity* 34, 794–806. doi: 10.1016/j.immuni.2011.03.021
- Geva-Zatorsky, N., Sefik, E., Kua, L., Pasman, L., Tan, T. G., Ortiz-Lopez, A., et al. (2017). Mining the Human Gut Microbiota for Immunomodulatory Organisms. *Cell* 168, 928–943e911. doi: 10.1016/j.cell.2017.01.022
- Gevers, D., Kugathasan, S., Denson, L. A., Vazquez-Baeza, Y., Van Treuren, W., Ren, B., et al. (2014). The treatment-naïve microbiome in new-onset Crohn's disease. *Cell Host Microbe* 15, 382–392. doi: 10.1016/j.chom.2014.02.005
- Gill, S. R., Pop, M., Deboy, R. T., Eckburg, P. B., Turnbaugh, P. J., Samuel, B. S., et al. (2006). Metagenomic analysis of the human distal gut microbiome. *Science* 312, 1355–1359. doi: 10.1126/science.1124234
- Glowacki, R. W. P., Pudlo, N. A., Tuncil, Y., Luis, A. S., Sajjakulnukit, P., Terekhov, A. I., et al. (2020). A Ribose-Scavenging System Confers Colonization Fitness

- on the Human Gut Symbiont *Bacteroides thetaiotaomicron* in a Diet-Specific Manner. *Cell Host Microbe* 27, 79–92e79. doi: 10.1016/j.chom.2019.11.009
- Goodman, A. L., Kallstrom, G., Faith, J. J., Reyes, A., Moore, A., Dantas, G., et al. (2011). Extensive personal human gut microbiota culture collections characterized and manipulated in gnotobiotic mice. *Proc. Natl. Acad. Sci. U S A* 108, 6252–6257. doi: 10.1073/pnas.1102938108
- Goodman, A. L., McNulty, N. P., Zhao, Y., Leip, D., Mitra, R. D., Lozupone, C. A., et al. (2009). Identifying genetic determinants needed to establish a human gut symbiont in its habitat. *Cell Host Microbe* 6, 279–289. doi: 10.1016/j.chom.2009.08.003
- Gordon, H. A., and Pesti, L. (1971). The gnotobiotic animal as a tool in the study of host microbial relationships. *Bacteriol. Rev.* 35, 390–429. doi: 10.1128/br.35.4.390-429.1971
- Graham, A. L. (2021). Naturalizing mouse models for immunology. *Nat. Immunol.* 22, 111–117. doi: 10.1038/s41590-020-00857-2
- Gregory, A. C., Zablocki, O., Zayed, A. A., Howell, A., Bolduc, B., and Sullivan, M. B. (2020). The Gut Virome Database Reveals Age-Dependent Patterns of Virome Diversity in the Human Gut. *Cell Host Microbe* 28, 724–740e728. doi: 10.1016/j.chom.2020.08.003
- Gurung, J. P., Gel, M., and Baker, M. A. B. (2020). Microfluidic techniques for separation of bacterial cells via taxis. *Microb. Cell* 7, 66–79. doi: 10.15698/mic2020.03.710
- Hallen-Adams, H. E., and Suhr, M. J. (2017). Fungi in the healthy human gastrointestinal tract. *Virulence* 8, 352–358. doi: 10.1080/21505594.2016.1247140
- Hamilton, S. E., Badovinac, V. P., Beura, L. K., Pierson, M., Jameson, S. C., Masopust, D., et al. (2020). New Insights into the Immune System Using Dirty Mice. *J. Immunol.* 205, 3–11. doi: 10.4049/jimmunol.2000171
- Hayes, K. S., Bancroft, A. J., Goldrick, M., Portsmouth, C., Roberts, I. S., and Grencis, R. K. (2010). Exploitation of the intestinal microflora by the parasitic nematode *Trichuris muris*. *Science* 328, 1391–1394. doi: 10.1126/science.1187703
- Heo, I., Dutta, D., Schaefer, D. A., Iakobachvili, N., Artegiani, B., Sachs, N., et al. (2018). Modelling Cryptosporidium infection in human small intestinal and lung organoids. *Nat. Microbiol.* 3, 814–823. doi: 10.1038/s41564-018-0177-8
- Hidalgo, I. J., Raub, T. J., and Borchardt, R. T. (1989). Characterization of the Human Colon Carcinoma Cell Line (Caco-2) as a Model System for Intestinal Epithelial Permeability. *Gastroenterology* 96, 736–748.
- Hilbert, T., Steinhagen, F., Senzig, S., Cramer, N., Bekereldjian-Ding, I., Parcina, M., et al. (2017). Vendor effects on murine gut microbiota influence experimental abdominal sepsis. *J. Surg. Res.* 211, 126–136. doi: 10.1016/j.jss.2016.12.008
- Hildebrandt, M. A., Hoffmann, C., Sherrill-Mix, S. A., Keilbaugh, S. A., Hamady, M., Chen, Y. Y., et al. (2009). High-fat diet determines the composition of the murine gut microbiome independently of obesity. *Gastroenterology* 137, e1711–e1712. doi: 10.1053/j.gastro.2009.08.042
- Hill, D. R., and Spence, J. R. (2017). Gastrointestinal Organoids: Understanding the Molecular Basis of the Host-Microbe Interface. *Cell Mol. Gastroenterol. Hepatol.* 3, 138–149. doi: 10.1016/j.jcmgh.2016.11.007
- Honda, K., and Littman, D. R. (2016). The microbiota in adaptive immune homeostasis and disease. *Nature* 535, 75–84. doi: 10.1038/nature18848
- Hsiao, A., Ahmed, A. M., Subramanian, S., Griffin, N. W., Drewry, L. L., Petri, W. A. Jr., et al. (2014). Members of the human gut microbiota involved in recovery from *Vibrio cholerae* infection. *Nature* 515, 423–426. doi: 10.1038/nature13738
- Hsu, R. H., Clark, R. L., Tan, J. W., Ahn, J. C., Gupta, S., Romero, P. A., et al. (2019). Microbial Interaction Network Inference in Microfluidic Droplets. *Cell Syst.* 9, 229–242e224. doi: 10.1016/j.cels.2019.06.008
- Huggins, M. A., Sjaastad, F. V., Pierson, M., Kucaba, T. A., Swanson, W., Staley, C., et al. (2019). Microbial Exposure Enhances Immunity to Pathogens Recognized by TLR2 but Increases Susceptibility to Cytokine Storm through TLR4 Sensitization. *Cell Rep.* 28, 1729–1743e1725. doi: 10.1016/j.celrep.2019.07.028
- Imaoka, A., Matsumoto, S., Setoyama, H., Okada, Y., and Umesaki, Y. (1996). Proliferative recruitment of intestinal intraepithelial lymphocytes after microbial colonization of germ-free mice. *Eur. J. Immunol.* 26, 945–948. doi: 10.1002/eji.1830260434
- In, J., Foulke-Abel, J., Zachos, N. C., Hansen, A. M., Kaper, J. B., Bernstein, H. D., et al. (2016). Enterohemorrhagic *Escherichia coli* reduce mucus and intermicrovillar bridges in human stem cell-derived colonoids. *Cell Mol. Gastroenterol. Hepatol.* 2, 48–62e43. doi: 10.1016/j.jcmgh.2015.10.001
- Ivanov, I. I., Atarashi, K., Manel, N., Brodie, E. L., Shima, T., Karaoz, U., et al. (2009). Induction of intestinal Th17 cells by segmented filamentous bacteria. *Cell* 139, 485–498. doi: 10.1016/j.cell.2009.09.033
- Ivanov, I. I., Frutos Rde, L., Manel, N., Yoshinaga, K., Rifkin, D. B., Sartor, R. B., et al. (2008). Specific microbiota direct the differentiation of IL-17-producing T-helper cells in the mucosa of the small intestine. *Cell Host Microbe* 4, 337–349. doi: 10.1016/j.chom.2008.09.009
- Jafari, N. V., Kuehne, S. A., Minton, N. P., Allan, E., and Bajaj-Elliott, M. (2016). Clostridium difficile-mediated effects on human intestinal epithelia: Modelling host-pathogen interactions in a vertical diffusion chamber. *Anaerobe* 37, 96–102. doi: 10.1016/j.anaerobe.2015.12.007
- Jain, U., Ver Heul, A. M., Xiong, S., Gregory, M. H., Demers, E. G., Kern, J. T., et al. (2021). Debaryomyces is enriched in Crohn's disease intestinal tissue and impairs healing in mice. *Science* 371, 1154–1159. doi: 10.1126/science.abd0919
- Jalili-Firoozinezhad, S., Gazzaniga, F. S., Calamari, E. L., Camacho, D. M., Fadel, C. W., Bein, A., et al. (2019). A complex human gut microbiome cultured in an anaerobic intestine-on-a-chip. *Nat. Biomed. Eng.* 3, 520–531. doi: 10.1038/s41551-019-0397-0
- Kanther, M., and Rawls, J. F. (2010). Host-microbe interactions in the developing zebrafish. *Curr. Opin. Immunol.* 22, 10–19. doi: 10.1016/j.coi.2010.01.006
- Karve, S. S., Pradhan, S., Ward, D. V., and Weiss, A. A. (2017). Intestinal organoids model human responses to infection by commensal and Shiga toxin producing *Escherichia coli*. *PLoS One* 12:e0178966. doi: 10.1371/journal.pone.0178966
- Kasendra, M., Tovaglieri, A., Sontheimer-Phelps, A., Jalili-Firoozinezhad, S., Bein, A., Chalkiadaki, A., et al. (2018). Development of a primary human Small Intestine-on-a-Chip using biopsy-derived organoids. *Sci. Rep.* 8:2871. doi: 10.1038/s41598-018-21201-7
- Kau, A. L., Planer, J. D., Liu, J., Rao, S., Yatsunenko, T., Trehan, I., et al. (2015). Functional characterization of IgA-targeted bacterial taxa from undernourished Malawian children that produce diet-dependent enteropathy. *Sci. Transl. Med.* 7:276ra224. doi: 10.1126/scitranslmed.aaa4877
- Kelly, T. N., Bazzano, L. A., Ajami, N. J., He, H., Zhao, J., Petrosino, J. F., et al. (2016). Gut Microbiome Associates With Lifetime Cardiovascular Disease Risk Profile Among Bogalusa Heart Study Participants. *Circ. Res.* 119, 956–964. doi: 10.1161/CIRCRESAHA.116.309219
- Kernbauer, E., Ding, Y., and Cadwell, K. (2014). An enteric virus can replace the beneficial function of commensal bacteria. *Nature* 516, 94–98. doi: 10.1038/nature13960
- Khan Mirzaei, M., Xue, J., Costa, R., Ru, J., Schulz, S., Taranu, Z. E., et al. (2021). Challenges of Studying the Human Virome - Relevant Emerging Technologies. *Trends Microbiol.* 29, 171–181. doi: 10.1016/j.tim.2020.05.021
- Kim, H. J., Huh, D., Hamilton, G., and Ingber, D. E. (2012). Human gut-on-a-chip inhabited by microbial flora that experiences intestinal peristalsis-like motions and flow. *Lab. Chip* 12, 2165–2174. doi: 10.1039/c2lc40074j
- Kim, H. J., Li, H., Collins, J. J., and Ingber, D. E. (2016). Contributions of microbiome and mechanical deformation to intestinal bacterial overgrowth and inflammation in a human gut-on-a-chip. *Proc. Natl. Acad. Sci. U S A* 113, E7–E15. doi: 10.1073/pnas.1522193112
- Koehler, S., Gaedeke, R., Thompson, C., Bongrand, C., Visick, K. L., Ruby, E., et al. (2018). The model squid-vibrio symbiosis provides a window into the impact of strain- and species-level differences during the initial stages of symbiont engagement. *Environ. Microbiol.* 2018:14392. doi: 10.1111/1462-2920.14392
- Koppel, N., Bisanz, J. E., Pandelia, M. E., Turnbaugh, P. J., and Balskus, E. P. (2018). Discovery and characterization of a prevalent human gut bacterial enzyme sufficient for the inactivation of a family of plant toxins. *Elife* 7:33953. doi: 10.7554/eLife.33953
- Koropatkin, N. M., Martens, E. C., Gordon, J. I., and Smith, T. J. (2008). Starch catabolism by a prominent human gut symbiont is directed by the recognition of amylose helices. *Structure* 16, 1105–1115. doi: 10.1016/j.str.2008.03.017
- Koropatnick, T. A., Engle, J. T., Apicella, M. A., Stabb, E. V., Goldman, W. E., and McFall-Ngai, M. J. (2004). Microbial factor-mediated development in a host-bacterial mutualism. *Science* 306, 1186–1188. doi: 10.1126/science.1102218
- Koskinen, K., Pausan, M. R., Perras, A. K., Beck, M., Bang, C., Mora, M., et al. (2017). First Insights into the Diverse Human Archaeome: Specific Detection of

- Archaea in the Gastrointestinal Tract, Lung, and Nose and on Skin. *mBio* 8:6. doi: 10.1128/mBio.00824-17
- Kriegel, M. A., Sefik, E., Hill, J. A., Wu, H. J., Benoist, C., and Mathis, D. (2011). Naturally transmitted segmented filamentous bacteria segregate with diabetes protection in nonobese diabetic mice. *Proc. Natl. Acad. Sci. U S A* 108, 11548–11553. doi: 10.1073/pnas.1108924108
- Krych, L., Hansen, C. H., Hansen, A. K., van den Berg, F. W., and Nielsen, D. S. (2013). Quantitatively different, yet qualitatively alike: a meta-analysis of the mouse core gut microbiome with a view towards the human gut microbiome. *PLoS One* 8:e62578. doi: 10.1371/journal.pone.0062578
- Kuhn, R., Lohler, J., Rennick, D., Rajewsky, K., and Muller, W. (1993). Interleukin-10-deficient mice develop chronic enterocolitis. *Cell* 75, 263–274. doi: 10.1016/0092-8674(93)80068-p
- Kurkchubasche, A. G., Cardona, M., Watkins, S. C., Smith, S. D., Albanese, C. T., Simmons, R. L., et al. (1998). Transmucosal passage of bacteria across rat intestinal epithelium in the Ussing chamber: effect of nutritional factors and bacterial virulence. *Shock* 9, 121–127. doi: 10.1097/00024382-199802000-00008
- Kuypers, M., Despot, T., and Mallevaey, T. (2021). Dirty mice join the immunologist's toolkit. *Microbes Infect.* 23:104817. doi: 10.1016/j.micinf.2021.104817
- Lane-Petter, W. (1962). The Provision and Use of Pathogen-free Laboratory Animals. *Proc. R. Soc. Med.* 55, 253–263.
- Lecuit, M., Dramsi, S., Gottardi, C., Fedor-Chaikin, M., Gumbiner, B., and Cossart, P. (1999). A single amino acid in E-cadherin responsible for host specificity towards the human pathogen *Listeria monocytogenes*. *EMBO J.* 18, 3956–3963. doi: 10.1093/emboj/18.14.3956
- Lee, H., Jin, B. E., Jang, E., Lee, A. R., Han, D. S., Kim, H. Y., et al. (2014). Gut-residing Microbes Alter the Host Susceptibility to Autoantibody-mediated Arthritis. *Immune Netw.* 14, 38–44. doi: 10.4110/in.2014.14.1.38
- Lee, W. J., and Brey, P. T. (2013). How microbiomes influence metazoan development: insights from history and Drosophila modeling of gut-microbe interactions. *Annu. Rev. Cell Dev. Biol.* 29, 571–592. doi: 10.1146/annurev-cellbio-101512-122333
- Lemire, P., Robertson, S. J., Maughan, H., Tattoli, I., Streutker, C. J., Platnich, J. M., et al. (2017). The NLR Protein NLRP6 Does Not Impact Gut Microbiota Composition. *Cell Rep.* 21, 3653–3661. doi: 10.1016/j.celrep.2017.12.026
- Leslie, J. L., Huang, S., Opp, J. S., Nagy, M. S., Kobayashi, M., Young, V. B., et al. (2015). Persistence and toxin production by *Clostridium difficile* within human intestinal organoids result in disruption of epithelial paracellular barrier function. *Infect. Immun.* 83, 138–145. doi: 10.1128/IAI.02561-14
- Letran, S. E., Lee, S. J., Atif, S. M., Flores-Langarica, A., Uematsu, S., Akira, S., et al. (2011). TLR5-deficient mice lack basal inflammatory and metabolic defects but exhibit impaired CD4 T cell responses to a flagellated pathogen. *J. Immunol.* 186, 5406–5412. doi: 10.4049/jimmunol.1003576
- Ley, R. E., Bäckhed, F., Turnbaugh, P., Lozupone, C. A., Knight, R. D., and Gordon, J. I. (2005). Obesity alters gut microbial ecology. *Proc. Natl. Acad. Sci. U S A* 102, 11070–11075. doi: 10.1073/pnas.0504978102
- Lhocine, N., Ribeiro, P. S., Buchon, N., Wepf, A., Wilson, R., Tenev, T., et al. (2008). PIMS modulates immune tolerance by negatively regulating Drosophila innate immune signaling. *Cell Host Microbe* 4, 147–158. doi: 10.1016/j.chom.2008.07.004
- Lim, B., Zimmermann, M., Barry, N. A., and Goodman, A. L. (2017). Engineered Regulatory Systems Modulate Gene Expression of Human Commensals in the Gut. *Cell* 169, 547–558.e515. doi: 10.1016/j.cell.2017.03.045
- Lin, J. D., Devlin, J. C., Yeung, F., McCauley, C., Leung, J. M., Chen, Y. H., et al. (2020). Rewilding Nod2 and Atg16l1 Mutant Mice Uncovers Genetic and Environmental Contributions to Microbial Responses and Immune Cell Composition. *Cell Host Microbe* 27, 830–840.e834. doi: 10.1016/j.chom.2020.03.001
- Lloyd-Price, J., Arze, C., Ananthakrishnan, A. N., Schirmer, M., Avila-Pacheco, J., Poon, T. W., et al. (2019). Multi-omics of the gut microbial ecosystem in inflammatory bowel diseases. *Nature* 569, 655–662. doi: 10.1038/s41586-019-1237-9
- Lundberg, R., Toft, M. F., Metzdrorff, S. B., Hansen, C. H. F., Licht, T. R., Bahl, M. I., et al. (2020). Human microbiota-transplanted C57BL/6 mice and offspring display reduced establishment of key bacteria and reduced immune stimulation compared to mouse microbiota-transplantation. *Sci. Rep.* 10:7805. doi: 10.1038/s41598-020-64703-z
- Ma, J., Classon, C. H., Stark, J. M., Li, M., Huang, H. J., Vrtala, S., et al. (2021). Laboratory mice with a wild microbiota generate strong allergic immune responses. *bioRxiv* doi: 10.1101/2021.03.28.437143
- Macpherson, A. J., and Harris, N. L. (2004). Interactions between commensal intestinal bacteria and the immune system. *Nat. Rev. Immunol.* 4, 478–485. doi: 10.1038/nri1373
- Mahowald, M. A., Rey, F. E., Seedorf, H., Turnbaugh, P. J., Fulton, R. S., Wollam, A., et al. (2009). Characterizing a model human gut microbiota composed of members of its two dominant bacterial phyla. *Proc. Natl. Acad. Sci. U S A* 106, 5859–5864. doi: 10.1073/pnas.0901529106
- Mamantopoulos, M., Ronchi, F., Van Hauwermeiren, F., Vieira-Silva, S., Yilmaz, B., Martens, L., et al. (2017). Nlrp6- and ASC-Dependent Inflammasomes Do Not Shape the Commensal Gut Microbiota Composition. *Immunity* 47, 339–348.e334. doi: 10.1016/j.immuni.2017.07.011
- Manichanh, C., Rigottier-Gois, L., Bonnaud, E., Gloux, K., Pelletier, E., Frangeul, L., et al. (2006). Reduced diversity of faecal microbiota in Crohn's disease revealed by a metagenomic approach. *Gut* 55, 205–211. doi: 10.1136/gut.2005.073817
- Markle, J. G., Frank, D. N., Mortin-Toth, S., Robertson, C. E., Feazel, L. M., Rolle-Kampczyk, U., et al. (2013). Sex differences in the gut microbiome drive hormone-dependent regulation of autoimmunity. *Science* 339, 1084–1088. doi: 10.1126/science.1233521
- Marzotati, M., Vanhoecke, B., De Ryck, T., Sadaghian Sadabad, M., Pinheiro, I., Possemiers, S., et al. (2014). The HMI module: a new tool to study the Host-Microbiota Interaction in the human gastrointestinal tract in vitro. *BMC Microbiol.* 14:133. doi: 10.1186/1471-2180-14-133
- McCoy, K. D., Burkhard, R., and Geuking, M. B. (2019). The microbiome and immune memory formation. *Immunol. Cell Biol.* 97, 625–635. doi: 10.1111/imcb.12273
- McFall-Ngai, M. J. (2014). The importance of microbes in animal development: lessons from the squid-vibrio symbiosis. *Annu. Rev. Microbiol.* 68, 177–194. doi: 10.1146/annurev-micro-091313-103654
- McNulty, N. P., Wu, M., Erickson, A. R., Pan, C., Erickson, B. K., Martens, E. C., et al. (2013). Effects of diet on resource utilization by a model human gut microbiota containing *Bacteroides cellulosilyticus* WH2, a symbiont with an extensive glycobiome. *PLoS Biol.* 11:e1001637. doi: 10.1371/journal.pbio.1001637
- Miao, J., Chard, L. S., Wang, Z., and Wang, Y. (2019). Syrian Hamster as an Animal Model for the Study on Infectious Diseases. *Front. Immunol.* 10:2329. doi: 10.3389/fimmu.2019.02329
- Mimee, M., Tucker, A. C., Voigt, C. A., and Lu, T. K. (2015). Programming a Human Commensal Bacterium, *Bacteroides thetaiotaomicron*, to Sense and Respond to Stimuli in the Murine Gut Microbiota. *Cell Syst.* 1, 62–71. doi: 10.1016/j.cels.2015.06.001
- Modlinska, K., and Pisula, W. (2020). The Norway rat, from an obnoxious pest to a laboratory pet. *Elife* 9:50651. doi: 10.7554/eLife.50651
- Moskowitz, J. E., Andreatta, F., and Amos-Landgraf, J. (2019). The gut microbiota modulates differential adenoma suppression by B6/J and B6/N genetic backgrounds in Apc(Min) mice. *Mamm. Genome* 30, 237–244. doi: 10.1007/s00335-019-09814-3
- Nagalingam, N. A., Robinson, C. J., Bergin, I. L., Eaton, K. A., Huffnagle, G. B., and Young, V. B. (2013). The effects of intestinal microbial community structure on disease manifestation in IL-10<sup>-/-</sup> mice infected with *Helicobacter hepaticus*. *Microbiome* 1:15. doi: 10.1186/2049-2618-1-15
- Negi, S., Das, D. K., Pahari, S., Nadeem, S., and Agrewala, J. N. (2019). Potential Role of Gut Microbiota in Induction and Regulation of Innate Immune Memory. *Front. Immunol.* 10:2441. doi: 10.3389/fimmu.2019.02441
- Neville, B. A., Forster, S. C., and Lawley, T. D. (2018). Commensal Koch's postulates: establishing causation in human microbiota research. *Curr. Opin. Microbiol.* 42, 47–52. doi: 10.1016/j.mib.2017.10.001
- Nkama, V. D., Henrissat, B., and Drancourt, M. (2017). Archaea: Essential inhabitants of the human digestive microbiota. *Hum. Microb. J.* 3, 1–8.
- Norman, J. M., Handley, S. A., and Virgin, H. W. (2014). Kingdom-agnostic metagenomics and the importance of complete characterization of enteric microbial communities. *Gastroenterology* 146, 1459–1469. doi: 10.1053/j.gastro.2014.02.001



- Nyholm, S. V., and McFall-Ngai, M. J. (2004). The winnowing: establishing the squid-vibrio symbiosis. *Nat. Rev. Microbiol.* 2, 632–642. doi: 10.1038/nrmicro957
- Ootani, A., Li, X., Sangiorgi, E., Ho, Q. T., Ueno, H., Toda, S., et al. (2009). Sustained in vitro intestinal epithelial culture within a Wnt-dependent stem cell niche. *Nat. Med.* 15, 701–706. doi: 10.1038/nm.1951
- Osmekhina, E., Jonkerougou, C., Schmidt, G., Jahangiri, F., Jokinen, V., Franssila, S., et al. (2018). Controlled communication between physically separated bacterial populations in a microfluidic device. *Commun. Biol.* 1:97. doi: 10.1038/s42003-018-0102-y
- Ost, K. S., and Round, J. L. (2018). Communication Between the Microbiota and Mammalian Immunity. *Annu. Rev. Microbiol.* 72, 399–422. doi: 10.1146/annurev-micro-090817-062307
- Ottman, N., Ruokolainen, L., Suomalainen, A., Sinkko, H., Karisola, P., Lehtimäki, J., et al. (2019). Soil exposure modifies the gut microbiota and supports immune tolerance in a mouse model. *J. Allergy Clin. Immunol.* 143, 1198–1206e1112. doi: 10.1016/j.jaci.2018.06.024
- Palm, N. W., de Zoete, M. R., Cullen, T. W., Barry, N. A., Stefanowski, J., Hao, L., et al. (2014). Immunoglobulin A coating identifies colitogenic bacteria in inflammatory bowel disease. *Cell* 158, 1000–1010. doi: 10.1016/j.cell.2014.08.006
- Parfrey, L. W., Walters, W. A., and Knight, R. (2011). Microbial eukaryotes in the human microbiome: ecology, evolution, and future directions. *Front. Microbiol.* 2:153. doi: 10.3389/fmicb.2011.00153
- Paterson, M. J., Oh, S., and Underhill, D. M. (2017). Host-microbe interactions: commensal fungi in the gut. *Curr. Opin. Microbiol.* 40, 131–137. doi: 10.1016/j.mib.2017.11.012
- Pearce, S. C., Al-Jawadi, A., Kishida, K., Yu, S., Hu, M., Fritzky, L. F., et al. (2018). Marked differences in tight junction composition and macromolecular permeability among different intestinal cell types. *BMC Biol.* 16:19. doi: 10.1186/s12915-018-0481-z
- Phifer-Rixey, M., and Nachman, M. W. (2015). Insights into mammalian biology from the wild house mouse *Mus musculus*. *Elife* 4:5959. doi: 10.7554/eLife.05959
- Pozzilli, P., Signore, A., Williams, A. J., and Beales, P. E. (1993). NOD mouse colonies around the world—recent facts and figures. *Immunol. Today* 14, 193–196. doi: 10.1016/0167-5699(93)90160-M
- Qin, J., Li, R., Raes, J., Arumugam, M., Burgdorf, K. S., Manichanh, C., et al. (2010). A human gut microbial gene catalogue established by metagenomic sequencing. *Nature* 464, 59–65. doi: 10.1038/nature08821
- Rader, B. A., Kremer, N., Apicella, M. A., Goldman, W. E., and McFall-Ngai, M. J. (2012). Modulation of symbiont lipid A signaling by host alkaline phosphatases in the squid-vibrio symbiosis. *mBio* 3:3. doi: 10.1128/mBio.00093-12
- Raibaud, P., Ducluzeau, R., Dubos, F., Hudault, S., Bewa, H., and Muller, M. C. (1980). Implantation of bacteria from the digestive tract of man and various animals into gnotobiotic mice. *Am. J. Clin. Nutr.* 33, 2440–2447. doi: 10.1093/ajcn/33.11.2440
- Rajan, A., Vela, L., Zeng, X. L., Yu, X., Shroyer, N., Blutt, S. E., et al. (2018). Novel Segment- and Host-Specific Patterns of Enteroregulatory *Escherichia coli* Adherence to Human Intestinal Enteroids. *mBio* 9:1. doi: 10.1128/mBio.02419-17
- Rawls, J. F., Mahowald, M. A., Goodman, A. L., Trent, C. M., and Gordon, J. I. (2007). In vivo imaging and genetic analysis link bacterial motility and symbiosis in the zebrafish gut. *Proc. Natl. Acad. Sci. U S A* 104, 7622–7627. doi: 10.1073/pnas.0702386104
- Rawls, J. F., Mahowald, M. A., Ley, R. E., and Gordon, J. I. (2006). Reciprocal gut microbiota transplants from zebrafish and mice to germ-free recipients reveal host habitat selection. *Cell* 127, 423–433. doi: 10.1016/j.cell.2006.08.043
- Reese, T. A., Bi, K., Kambal, A., Filali-Mouhim, A., Beura, L. K., Burger, M. C., et al. (2016). Sequential Infection with Common Pathogens Promotes Human-like Immune Gene Expression and Altered Vaccine Response. *Cell Host Microbe* 19, 713–719. doi: 10.1016/j.chom.2016.04.003
- Rey, F. E., Faith, J. J., Bain, J., Muehlbauer, M. J., Stevens, R. D., Newgard, C. B., et al. (2010). Dissecting the in vivo metabolic potential of two human gut acetogens. *J. Biol. Chem.* 285, 22082–22090. doi: 10.1074/jbc.M110.117713
- Reyniers, J. A., and Sacksteder, M. R. (1958). The use of germfree animals and techniques in the search for unknown etiological agents. *Ann. N. Y. Acad. Sci.* 73, 344–356.
- Reynolds, L. A., Finlay, B. B., and Maizels, R. M. (2015). Cohabitation in the Intestine: Interactions among Helminth Parasites, Bacterial Microbiota, and Host Immunity. *J. Immunol.* 195, 4059–4066. doi: 10.1049/jimmunol.1501432
- Ridaura, V. K., Faith, J. J., Rey, F. E., Cheng, J., Duncan, A. E., Kau, A. L., et al. (2013). Gut microbiota from twins discordant for obesity modulate metabolism in mice. *Science* 341:1241214. doi: 10.1126/science.1241214
- Rosshart, S. P., Herz, J., Vassallo, B. G., Hunter, A., Wall, M. K., Badger, J. H., et al. (2019). Laboratory mice born to wild mice have natural microbiota and model human immune responses. *Science* 365:6452. doi: 10.1126/science.aaw4361
- Rosshart, S. P., Vassallo, B. G., Angeletti, D., Hutchinson, D. S., Morgan, A. P., Takeda, K., et al. (2017). Wild Mouse Gut Microbiota Promotes Host Fitness and Improves Disease Resistance. *Cell* 171, 1015–1028e1013. doi: 10.1016/j.cell.2017.09.016
- Round, J. L., and Mazmanian, S. K. (2010). Inducible Foxp3+ regulatory T-cell development by a commensal bacterium of the intestinal microbiota. *Proc. Natl. Acad. Sci. U S A* 107, 12204–12209. doi: 10.1073/pnas.0909122107
- Runge, S., and Rosshart, S. P. (2021). The Mammalian Metaorganism: A Holistic View on How Microbes of All Kingdoms and Niches Shape Local and Systemic Immunity. *Front. Immunol.* 12:702378. doi: 10.3389/fimmu.2021.702378
- Ryu, J. H., Kim, S. H., Lee, H. Y., Bai, J. Y., Nam, Y. D., Bae, J. W., et al. (2008). Innate immune homeostasis by the homeobox gene caudal and commensal-gut mutualism in *Drosophila*. *Science* 319, 777–782. doi: 10.1126/science.1149357
- Sadaghian Sadabad, M., von Martels, J. Z., Khan, M. T., Blokzijl, T., Paglia, G., Dijkstra, G., et al. (2015). A simple coculture system shows mutualism between anaerobic faecalibacteria and epithelial Caco-2 cells. *Sci. Rep.* 5:17906. doi: 10.1038/srep17906
- Sarvestani, S. K., Signs, S., Hu, B., Yeu, Y., Feng, H., Ni, Y., et al. (2021). Induced organoids derived from patients with ulcerative colitis recapitulate colitic reactivity. *Nat. Commun.* 12:262. doi: 10.1038/s41467-020-20351-5
- Sato, T., Vries, R. G., Snippert, H. J., van de Wetering, M., Barker, N., Stange, D. E., et al. (2009). Single Lgr5 stem cells build crypt-villus structures in vitro without a mesenchymal niche. *Nature* 459, 262–265. doi: 10.1038/nature07935
- Schaedler, R. W., Dubs, R., and Costello, R. (1965). Association of germfree mice with bacteria isolated from normal mice. *J. Exp. Med.* 122, 77–82. doi: 10.1084/jem.122.1.77
- Schloissnig, S., Arumugam, M., Sunagawa, S., Mitreva, M., Tap, J., Zhu, A., et al. (2013). Genomic variation landscape of the human gut microbiome. *Nature* 493, 45–50. doi: 10.1038/nature11711
- Schwarzer, M., Makki, K., Storelli, G., Machuca-Gayet, I., Srutkova, D., Hermanova, P., et al. (2016). *Lactobacillus plantarum* strain maintains growth of infant mice during chronic undernutrition. *Science* 351, 854–857. doi: 10.1126/science.aad8588
- Seedorf, H., Griffin, N. W., Ridaura, V. K., Reyes, A., Cheng, J., Rey, F. E., et al. (2014). Bacteria from diverse habitats colonize and compete in the mouse gut. *Cell* 159, 253–266. doi: 10.1016/j.cell.2014.09.008
- Sefik, E., Geva-Zatorsky, N., Oh, S., Konnikova, L., Zemmour, D., McGuire, A. M., et al. (2015). Mucosal immunology. Individual intestinal symbionts induce a distinct population of RORgamma(+) regulatory T cells. *Science* 349, 993–997. doi: 10.1126/science.aaa9420
- Semova, I., Carten, J. D., Stombaugh, J., Mackey, L. C., Knight, R., Farber, S. A., et al. (2012). Microbiota regulate intestinal absorption and metabolism of fatty acids in the zebrafish. *Cell Host Microbe* 12, 277–288. doi: 10.1016/j.chom.2012.08.003
- Seregin, S. S., Golovchenko, N., Schaf, B., Chen, J., Pudlo, N. A., Mitchell, J., et al. (2017). NLRP6 Protects Il10(-/-) Mice from Colitis by Limiting Colonization of Akkermansia muciniphila. *Cell Rep.* 19, 733–745. doi: 10.1016/j.celrep.2017.03.080
- Shin, S. C., Kim, S. H., You, H., Kim, B., Kim, A. C., Lee, K. A., et al. (2011). *Drosophila* microbiome modulates host developmental and metabolic homeostasis via insulin signaling. *Science* 334, 670–674. doi: 10.1126/science.1212782
- Shin, W., Wu, A., Massidda, M. W., Foster, C., Thomas, N., Lee, D. W., et al. (2019). A Robust Longitudinal Co-culture of Obligate Anaerobic Gut Microbiome With Human Intestinal Epithelium in an Anoxic-Oxic Interface-on-a-Chip. *Front. Bioeng. Biotechnol.* 7:13. doi: 10.3389/fbioe.2019.00013
- Sivan, A., Corrales, L., Hubert, N., Williams, J. B., Aquino-Michaels, K., Earley, Z. M., et al. (2015). Commensal *Bifidobacterium* promotes antitumor immunity



- and facilitates anti-PD-L1 efficacy. *Science* 350, 1084–1089. doi: 10.1126/science.aac4255
- Skye, S. M., Zhu, W., Romano, K. A., Guo, C. J., Wang, Z., Jia, X., et al. (2018). Microbial Transplantation With Human Gut Commensals Containing CutC Is Sufficient to Transmit Enhanced Platelet Reactivity and Thrombosis Potential. *Circ. Res.* 123, 1164–1176. doi: 10.1161/CIRCRESAHA.118.313142
- Smith, K., McCoy, K. D., and Macpherson, A. J. (2007). Use of axenic animals in studying the adaptation of mammals to their commensal intestinal microbiota. *Semin. Immunol.* 19, 59–69. doi: 10.1016/j.smim.2006.10.002
- Smith, M. I., Yatsunenken, T., Manary, M. J., Trehan, I., Mkakosya, R., Cheng, J., et al. (2013). Gut microbiomes of Malawian twin pairs discordant for kwashiorkor. *Science* 339, 548–554. doi: 10.1126/science.1229000
- Smith, P. M., Howitt, M. R., Panikov, N., Michaud, M., Gallini, C. A., Bohlooly, Y. M., et al. (2013). The microbial metabolites, short-chain fatty acids, regulate colonic Treg cell homeostasis. *Science* 341, 569–573. doi: 10.1126/science.1241165
- Song, X., Sun, X., Oh, S. F., Wu, M., Zhang, Y., Zheng, W., et al. (2020). Microbial bile acid metabolites modulate gut RORgamma(+) regulatory T cell homeostasis. *Nature* 577, 410–415. doi: 10.1038/s41586-019-1865-0
- Srinivasan, A., Torres, N. S., Leung, K. P., Lopez-Ribot, J. L., and Ramasubramanian, A. K. (2017). nBioChip, a Lab-on-a-Chip Platform of Mono- and Polymicrobial Biofilms for High-Throughput Downstream Applications. *mSphere* 2:3. doi: 10.1128/mSphere.00247-17
- Stagaman, K., Sharpton, T. J., and Guillemin, K. (2020). Zebrafish microbiome studies make waves. *Lab. Anim.* 49, 201–207. doi: 10.1038/s41684-020-0573-6
- Stefka, A. T., Feehley, T., Tripathi, P., Qiu, J., McCoy, K., Mazmanian, S. K., et al. (2014). Commensal bacteria protect against food allergen sensitization. *Proc. Natl. Acad. Sci. U S A* 111, 13145–13150. doi: 10.1073/pnas.1412008111
- Storelli, G., Defaye, A., Erkosar, B., Hols, P., Royet, J., and Leulier, F. (2011). Lactobacillus plantarum promotes Drosophila systemic growth by modulating hormonal signals through TOR-dependent nutrient sensing. *Cell Metab.* 14, 403–414. doi: 10.1016/j.cmet.2011.07.012
- Subramanian, S., Huq, S., Yatsunenken, T., Haque, R., Mahfuz, M., Alam, M. A., et al. (2014). Persistent gut microbiota immaturity in malnourished Bangladeshi children. *Nature* 510, 417–421. doi: 10.1038/nature13421
- Surana, N. K., and Kasper, D. L. (2017). Moving beyond microbiome-wide associations to causal microbe identification. *Nature* 552, 244–247. doi: 10.1038/nature25019
- Szabo, P. A., Miron, M., and Farber, D. L. (2019). Location, location, location: Tissue resident memory T cells in mice and humans. *Sci. Immunol.* 4:34. doi: 10.1126/sciimmunol.aas9673
- Takei, I., Asaba, Y., Kasatani, T., Maruyama, T., Watanabe, K., Yanagawa, T., et al. (1992). Suppression of development of diabetes in NOD mice by lactate dehydrogenase virus infection. *J. Autoimmun.* 5, 665–673. doi: 10.1016/0896-8411(92)90184-r
- Tan, H. Y., and Toh, Y. C. (2020). What can microfluidics do for human microbiome research? *Biomicrofluidics* 14:051303. doi: 10.1063/5.0012185
- Tan, T. G., Sefik, E., Geva-Zatorsky, N., Kua, L., Naskar, D., Teng, F., et al. (2016). Identifying species of symbiont bacteria from the human gut that, alone, can induce intestinal Th17 cells in mice. *Proc. Natl. Acad. Sci. U S A* 113, E8141–E8150. doi: 10.1073/pnas.1617460113
- Thompson, G. R., and Trexler, P. C. (1971). Gastrointestinal structure and function in germ-free or gnotobiotic animals. *Gut* 12, 230–235. doi: 10.1136/gut.12.3.230
- Thomson, A., Smart, K., Somerville, M. S., Lauder, S. N., Appanna, G., Horwood, J., et al. (2019). The Ussing chamber system for measuring intestinal permeability in health and disease. *BMC Gastroenterol.* 19:98. doi: 10.1186/s12876-019-1002-4
- Toprak, N. U., Yagci, A., Gulluoglu, B. M., Akin, M. L., Demirkalem, P., Celenk, T., et al. (2006). A possible role of *Bacteroides fragilis* enterotoxin in the aetiology of colorectal cancer. *Clin. Microbiol. Infect.* 12, 782–786. doi: 10.1111/j.1469-0691.2006.01494.x
- Trexler, P. C., and Reynolds, L. I. (1957). Flexible film apparatus for the rearing and use of germfree animals. *Appl. Microbiol.* 5, 406–412. doi: 10.1128/am.5.6.406-412.1957
- Troll, J. V., Hamilton, M. K., Abel, M. L., Ganz, J., Bates, J. M., Stephens, W. Z., et al. (2018). Microbiota promote secretory cell determination in the intestinal epithelium by modulating host Notch signaling. *Development* 145:4. doi: 10.1242/dev.155317
- Turnbaugh, P. J., Backhed, F., Fulton, L., and Gordon, J. I. (2008). Diet-induced obesity is linked to marked but reversible alterations in the mouse distal gut microbiome. *Cell Host Microbe* 3, 213–223. doi: 10.1016/j.chom.2008.02.015
- Turnbaugh, P. J., Hamady, M., Yatsunenken, T., Cantarel, B. L., Duncan, A., Ley, R. E., et al. (2009a). A core gut microbiome in obese and lean twins. *Nature* 457, 480–484. doi: 10.1038/nature07540
- Turnbaugh, P. J., Ley, R. E., Mahowald, M. A., Magrini, V., Mardis, E. R., and Gordon, J. I. (2006). An obesity-associated gut microbiome with increased capacity for energy harvest. *Nature* 444, 1027–1031. doi: 10.1038/nature05414
- Turnbaugh, P. J., Ridaura, V. K., Faith, J. J., Rey, F. E., Knight, R., and Gordon, J. I. (2009b). The effect of diet on the human gut microbiome: a metagenomic analysis in humanized gnotobiotic mice. *Sci. Transl. Med.* 1:6ra14. doi: 10.1126/scitranslmed.3000322
- Ulluwishewa, D., Anderson, R. C., Young, W., McNabb, W. C., van Baarlen, P., Moughan, P. J., et al. (2015). Live Faecalibacterium prausnitzii in an apical anaerobic model of the intestinal epithelial barrier. *Cell Microbiol.* 17, 226–240. doi: 10.1111/cmi.12360
- Umesaki, Y., Setoyama, H., Matsumoto, S., Imaoka, A., and Itoh, K. (1999). Differential roles of segmented filamentous bacteria and clostridia in development of the intestinal immune system. *Infect. Immun.* 67, 3504–3511. doi: 10.1128/IAI.67.7.3504-3511.1999
- Ussing, H. H., and Zerahn, K. (1951). Active transport of sodium as the source of electric current in the short-circuited isolated frog skin. *Acta Physiol. Scand.* 23, 110–127. doi: 10.1111/j.1748-1716.1951.tb00800.x
- Van den Abbeele, P., Roos, S., Eeckhaut, V., MacKenzie, D. A., Derde, M., Verstraete, W., et al. (2012). Incorporating a mucosal environment in a dynamic gut model results in a more representative colonization by lactobacilli. *Microb. Biotechnol.* 5, 106–115. doi: 10.1111/j.1751-7915.2011.00308.x
- van Nood, E., Vrieze, A., Nieuwdorp, M., Fuentes, S., Zoetendal, E. G., de Vos, W. M., et al. (2013). Duodenal infusion of donor feces for recurrent Clostridium difficile. *N. Engl. J. Med.* 368, 407–415. doi: 10.1056/NEJMoa1205037
- Velazquez, E. M., Nguyen, H., Heasley, K. T., Saechao, C. H., Gil, L. M., Rogers, A. W. L., et al. (2019). Endogenous Enterobacteriaceae underlie variation in susceptibility to Salmonella infection. *Nat. Microbiol.* 4, 1057–1064. doi: 10.1038/s41564-019-0407-8
- Verma, R., Lee, C., Jeun, E. J., Yi, J., Kim, K. S., Ghosh, A., et al. (2018). Cell surface polysaccharides of Bifidobacterium bifidum induce the generation of Foxp3(+) regulatory T cells. *Sci. Immunol.* 3:28. doi: 10.1126/sciimmunol.aat6975
- Vétizou, M., Pitt, J. M., Daillère, R., Lepage, P., Waldschmitt, N., Flament, C., et al. (2015). Anticancer immunotherapy by CTLA-4 blockade relies on the gut microbiota. *Science* 350, 1079–1084. doi: 10.1126/science.aad1329
- Vijay-Kumar, M., Aitken, J. D., Carvalho, F. A., Cullender, T. C., Mwangi, S., Srinivasan, S., et al. (2010). Metabolic syndrome and altered gut microbiota in mice lacking Toll-like receptor 5. *Science* 328, 228–231. doi: 10.1126/science.1179721
- Vlasova, A. N., Rajashekara, G., and Saif, L. J. (2018). Interactions between human microbiome, diet, enteric viruses and immune system: novel insights from gnotobiotic pig research. *Drug Discov. Today Dis. Models.* 28, 95–103. doi: 10.1016/j.ddmod.2019.08.006
- Vijay-Kumar, M., Sanders, C. J., Taylor, R. T., Kumar, A., Aitken, J. D., Sitaraman, S. V., et al. (2007). Deletion of TLR5 results in spontaneous colitis in mice. *J. Clin. Invest.* 117, 3909–3921. doi: 10.1172/JCI33084
- von Kortzfleisch, V. T., Karp, N. A., Palme, R., Kaiser, S., Sachser, N., and Richter, S. H. (2020). Improving reproducibility in animal research by splitting the study population into several 'mini-experiments'. *Sci. Rep.* 10:16579. doi: 10.1038/s41598-020-73503-4
- von Martels, J. Z. H., Sadaghian Sadabad, M., Bourgonje, A. R., Blokzijl, T., Dijkstra, G., Faber, K. N., et al. (2017). The role of gut microbiota in health and disease: In vitro modeling of host-microbe interactions at the aerobe-anaerobe interphase of the human gut. *Anaerobe* 44, 3–12. doi: 10.1016/j.anaerobe.2017.01.001
- Wagner, V. E., Dey, N., Guruge, J., Hsiao, A., Ahern, P. P., Semenkovich, N. P., et al. (2016). Effects of a gut pathobiont in a gnotobiotic mouse model of childhood undernutrition. *Sci. Transl. Med.* 8:366ra164. doi: 10.1126/scitranslmed.aah4669
- Wang, D. (2020). 5 challenges in understanding the role of the virome in health and disease. *PLoS Pathog.* 16:e1008318. doi: 10.1371/journal.ppat.1008318

- Wegorzewska, M. M., Glowacki, R. W. P., Hsieh, S. A., Donermeyer, D. L., Hickey, C. A., Horvath, S. C., et al. (2019). Diet modulates colonic T cell responses by regulating the expression of a *Bacteroides* thetaiotaomicron antigen. *Sci. Immunol.* 4:32. doi: 10.1126/sciimmunol.aau9079
- Wilberz, S., Partke, H. J., Dagnaes-Hansen, F., and Herberg, L. (1991). Persistent MHV (mouse hepatitis virus) infection reduces the incidence of diabetes mellitus in non-obese diabetic mice. *Diabetologia* 34, 2–5. doi: 10.1007/BF00404016
- Wilson, S. S., Tocchi, A., Holly, M. K., Parks, W. C., and Smith, J. G. (2015). A small intestinal organoid model of non-invasive enteric pathogen-epithelial cell interactions. *Mucosal Immunol.* 8, 352–361. doi: 10.1038/mi.2014.72
- Wu, H. J., Ivanov, I. I., Darce, J., Hattori, K., Shima, T., Umesaki, Y., et al. (2010). Gut-residing segmented filamentous bacteria drive autoimmune arthritis via T helper 17 cells. *Immunity* 32, 815–827. doi: 10.1016/j.immuni.2010.06.001
- Wu, M., McNulty, N. P., Rodionov, D. A., Khoroshkin, M. S., Griffin, N. W., Cheng, J., et al. (2015). Genetic determinants of in vivo fitness and diet responsiveness in multiple human gut *Bacteroides*. *Science* 350:aac5992. doi: 10.1126/science.aac5992
- Wu, S., Rhee, K. J., Albesiano, E., Rabizadeh, S., Wu, X., Yen, H. R., et al. (2009). A human colonic commensal promotes colon tumorigenesis via activation of T helper type 17 T cell responses. *Nat. Med.* 15, 1016–1022. doi: 10.1038/nm.2015
- Xiao, L., Feng, Q., Liang, S., Sonne, S. B., Xia, Z., Qiu, X., et al. (2015). A catalog of the mouse gut metagenome. *Nat. Biotechnol.* 33, 1103–1108. doi: 10.1038/nbt.3353
- Yeung, F., Chen, Y. H., Lin, J. D., Leung, J. M., McCauley, C., Devlin, J. C., et al. (2020). Altered Immunity of Laboratory Mice in the Natural Environment Is Associated with Fungal Colonization. *Cell Host Microbe* 27, 809–822e806. doi: 10.1016/j.chom.2020.02.015
- Yurkovetskiy, L., Burrows, M., Khan, A. A., Graham, L., Volchkov, P., Becker, L., et al. (2013). Gender bias in autoimmunity is influenced by microbiota. *Immunity* 39, 400–412. doi: 10.1016/j.immuni.2013.08.013
- Zhang, J., Huang, Y. J., Yoon, J. Y., Kemmitt, J., Wright, C., Schneider, K., et al. (2021). Primary human colonic mucosal barrier crosstalk with super oxygen-sensitive *Faecalibacterium prausnitzii* in continuous culture. *Med* 2, 74–98e79. doi: 10.1016/j.medj.2020.07.001

**Conflict of Interest:** The authors declare that the research was conducted in the absence of any commercial or financial relationships that could be construed as a potential conflict of interest.

**Publisher's Note:** All claims expressed in this article are solely those of the authors and do not necessarily represent those of their affiliated organizations, or those of the publisher, the editors and the reviewers. Any product that may be evaluated in this article, or claim that may be made by its manufacturer, is not guaranteed or endorsed by the publisher.

Copyright © 2021 Glowacki, Engelhart and Ahern. This is an open-access article distributed under the terms of the Creative Commons Attribution License (CC BY). The use, distribution or reproduction in other forums is permitted, provided the original author(s) and the copyright owner(s) are credited and that the original publication in this journal is cited, in accordance with accepted academic practice. No use, distribution or reproduction is permitted which does not comply with these terms.



# Microbiome Heritability and Its Role in Adaptation of Hosts to Novel Resources

Karen Bisschop<sup>1,2,3,4\*</sup>, Hylke H. Kortenbosch<sup>1†</sup>, Timo J. B. van Eldijk<sup>1</sup>, Cyrus A. Mallon<sup>1</sup>, Joana F. Salles<sup>1</sup>, Dries Bonte<sup>2‡</sup> and Rampal S. Etienne<sup>1‡</sup>

<sup>1</sup>Groningen Institute for Evolutionary Life Sciences, University of Groningen, Groningen, Netherlands, <sup>2</sup>Terrestrial Ecology Unit (TEREC), Department of Biology, Ghent University, Ghent, Belgium, <sup>3</sup>Institute for Biodiversity and Ecosystem Dynamics, University of Amsterdam, Amsterdam, Netherlands, <sup>4</sup>Laboratory of Aquatic Biology, Department of Biology, KU Leuven, Kortrijk, Belgium

## OPEN ACCESS

### Edited by:

Wakako Ikeda-Ohtsubo,  
Tohoku University, Japan

### Reviewed by:

Karin E. Groten,  
Max Planck Institute for Chemical  
Ecology, Germany  
Alejandro Frank,  
National Autonomous University of  
Mexico, Mexico

### \*Correspondence:

Karen Bisschop  
kbisschop.evo@gmail.com

<sup>†</sup>These authors have contributed  
equally to this work and share first  
authorship

<sup>‡</sup>These authors have contributed  
equally to this work and share last  
authorship

### Specialty section:

This article was submitted to  
Microbial Symbioses,  
a section of the journal  
Frontiers in Microbiology

Received: 30 April 2021

Accepted: 06 June 2022

Published: 05 July 2022

### Citation:

Bisschop K, Kortenbosch HH, van  
Eldijk TJB, Mallon CA, Salles JF,  
Bonte D and Etienne RS (2022)  
Microbiome Heritability and Its Role in  
Adaptation of Hosts to Novel  
Resources.  
Front. Microbiol. 13:703183.  
doi: 10.3389/fmicb.2022.703183

Microbiomes are involved in most vital processes, such as immune response, detoxification, and digestion and are thereby elementary to organismal functioning and ultimately the host's fitness. In turn, the microbiome may be influenced by the host and by the host's environment. To understand microbiome dynamics during the process of adaptation to new resources, we performed an evolutionary experiment with the two-spotted spider mite, *Tetranychus urticae*. We generated genetically depleted strains of the two-spotted spider mite and reared them on their ancestral host plant and two novel host plants for approximately 12 generations. The use of genetically depleted strains reduced the magnitude of genetic adaptation of the spider mite host to the new resource and, hence, allowed for better detection of signals of adaptation *via* the microbiome. During the course of adaptation, we tested spider mite performance (number of eggs laid and longevity) and characterized the bacterial component of its microbiome (16S rRNA gene sequencing) to determine: (1) whether the bacterial communities were shaped by mite ancestry or plant environment and (2) whether the spider mites' performance and microbiome composition were related. We found that spider mite performance on the novel host plants was clearly correlated with microbiome composition. Because our results show that only little of the total variation in the microbiome can be explained by the properties of the host (spider mite) and the environment (plant species) we studied, we argue that the bacterial community within hosts could be valuable for understanding a species' performance on multiple resources.

**Keywords:** local adaptation, bacterial communities, endosymbionts, spider mites, *Tetranychus urticae*

## INTRODUCTION

Microbiomes are communities of microorganisms and their associated gene expression in a particular environment (Berg et al., 2020). Hence, the microbiome of a certain host species includes all microorganisms on the inside and outside of an organism with no distinction between microbes with beneficial, neutral, or detrimental effects on their host. Over the last decade, research on host-microbiome interactions has revealed that microbial communities can

influence host immunity, digestion and detoxification (Stecher and Hardt, 2008; Berendsen et al., 2012; Huttenhower et al., 2012; David et al., 2014; Kohl et al., 2014; Kohl and Dearing, 2016). These complex, often beneficial host-microbiome interactions illustrate the importance of microbiota in their ability to affect the performance of their hosts. For instance, Zhu et al. (2019) showed that lower fecundity was associated with lower bacterial diversity in the cassava mite, *Tetranychus truncatus*. The importance of the microbiome for host phenotype has led some to suggest the concept of the “holobiont” (i.e., the host with its microorganisms) as a unit of selection (Zilber-Rosenberg and Rosenberg, 2008; Theis et al., 2016). A single unit of selection implies, however, one interconnected fate of the host and his microbiome which has led to a lot of criticism as microbiomes are rarely entirely inherited (Moran and Sloan, 2015; Henry et al., 2021). The transmission occurs *via* vertical transfer from parent to offspring, horizontal transfer from the environment, or both (Ebert, 2013; Henry et al., 2021). Therefore, some prefer the “extended genotype” where the microorganisms are having extended effects on the host phenotype and may shift the mean host phenotype or change the phenotypic variance in a population (Henry et al., 2021).

Because microbiomes are usually diverse, the versatility of different bacteria may help for better functioning of the host and assist in optimal adaptation to changing conditions (Zilber-Rosenberg and Rosenberg, 2008). It has been found that the bacterial communities need to be specialized to improve the adaptive fitness of the host, the influence of more homogeneous communities is often negligible (Huitzil et al., 2018). For herbivores adapting to novel resources, the microbiome may assist in the digestion of cellulose or lignin and the detoxification of potential poisonous substances (David et al., 2014; Franchini et al., 2014; Kohl et al., 2014; Kohl and Dearing, 2016; Staudacher et al., 2017). Microbial symbionts may even contribute to the synthesis of essential nutrients as seen in aphids where the obligate symbiont *Buchnera aphidicola* provides missing amino acids (Baumann, 2005; Oliver et al., 2010). Novel resources often cause other challenges such as parasitoids or fungi, however, a diverse community of facultative symbionts may provide protection against those challenges (Oliver et al., 2010; Vorburger and Perlman, 2018; Hafer and Vorburger, 2019). For instance, some aphid populations showed improved fecundity when feeding on clover if they were infected with *Regiella insecticola* (Leonardo and Muir, 2003; Oliver et al., 2010; Zélé et al., 2018a). Besides beneficial host-microbiome interactions, some facultative symbionts are also known to interfere with reproduction, such as *Wolbachia*, *Cardinium*, and *Spiroplasma* spp. (Breeuwer and Jacobs, 1996; Gotoh et al., 2003, 2007; Enigl and Schausberger, 2007; Xie et al., 2016). These endosymbionts use cytoplasmic incompatibility, feminization, parthenogenesis or male killing to secure their persistence (Staudacher et al., 2017). However, it remains unclear whether only these endosymbionts rather than the microbiome as a whole are responsible for these effects (Brinker et al., 2019).

Host-microbiome interactions are not unidirectional and microbiomes themselves are known to be affected by host diet, host taxonomy and host genetics (Santo Domingo et al., 1998;

Broderick et al., 2004; Spor et al., 2011; Colman et al., 2012; Jandhyala et al., 2015). A study on whiteflies suggested that the host's genome influences the potential fitness benefits of *Rickettsia* (Cass et al., 2016), as *Rickettsia* decreased the developmental time and increased the fecundity in one but not another genetic line of whiteflies. Another example was provided by Chaplinska et al., 2016 who showed the importance of the population background (i.e., genotype, geographic origin, and founder effects) of the host. They discovered differences in microbiome composition between different *Drosophila melanogaster* populations that had been maintained on the same food source and laboratory conditions for several years. However, because these populations had never been mixed, it was difficult to disentangle founder effects and drift from selection. Nonetheless, the fact that different microbiomes could persist and were transgenerationally transmitted shows that some components of the microbiome are heritable (Chaplinska et al., 2016).

The host-microbiome concepts (Bourtzis et al., 1996; Bordenstein et al., 2001; Shin et al., 2011; Sommer and Bäckhed, 2013; Lizé et al., 2014; Chaplinska et al., 2016) developed for insects can be extended to other arthropods such as the two-spotted spider mite or *Tetranychus urticae*, the focal species in this study. It has, for instance, been found in aphids that endosymbionts can offer protection against fungi or parasitoids (Oliver et al., 2005, 2010; Scarborough et al., 2005; Łukasik et al., 2013; Weldon et al., 2013; Guidolin et al., 2018; King, 2019), suggesting that endosymbionts may play a role in host immunity for other arthropods as well. So far, mainly behavioral adaptation such as avoidance of contaminated food has been found in the two-spotted spider mite, but no resistance or tolerance mechanisms against pathogenic bacteria (Santos-Matos et al., 2017; Zélé et al., 2019), although the latter may be due to the fact that the most common endosymbionts in spider mites (*Wolbachia*, *Rickettsia*, *Cardinium*, and *Arsenophonus*) were not present in the studied spider mite populations (Santos-Matos et al., 2017). Additionally, many microbial genes have been discovered within the *T. urticae* genome. These genes have different biochemical functions, such as the potential biosynthesis of pantothenate or vitamin B<sub>5</sub> (Wybouw et al., 2018). Given that this vitamin is essential for the biosynthesis of for instance fatty acids and peptides (Kleinkauf, 2000), this hints at a deep evolutionary significance of endosymbionts in *T. urticae* adaptation.

We here aimed to elucidate the role of the bacterial component of the microbiome of *T. urticae* in the host's adaptation to novel resources (i.e., host plants) using experimental evolution. More precisely, we (1) investigate the heritability of the spider mite-associated bacterial communities by looking at the relative effects of host plant and spider mite line on the bacterial communities and (2) study the relationship between the performance of the spider mite host on the different plant species and the bacterial composition. Adaptation of the spider mite host in our study does not refer to genetic adaptation, but to an overall improvement in host performance, which could be explained by the host-associated bacterial communities as well. The use of the microbiome as a fast-response mechanisms to changes in the environment has also recently been suggested (Voolstra and Ziegler, 2020).



From a single ancestral population, we created genetically depleted lines of *T. urticae*. These lines originated from one generation of mother-son mating and were therefore not homozygous inbred lines. We also created mixed lines by placing individuals from different genetically depleted lines together. On the one hand, the use of genetically depleted lines minimizes the chance for genetic adaptation (due to lower genetic variation) and increases the possibility to detect signals of adaptation *via* the microbiome, while on the other hand, the increase in genetic variation in the mixed lines will enhance the opportunity for genetic adaptation. These lines were transferred onto their initial host plant and two challenging novel resources for 150 days (about 12 mite generations). Performance on the host plants was recorded at several time points and the bacterial component of the mite microbiome was assessed after 150 days *via* high throughput sequencing of the V3-V4 region of the 16S rRNA gene.

While we only found a minor role for spider mite ancestry and host plant in determining the bacterial component of the mite microbiome, we report a substantial correlation between the total performance (i.e., fecundity and longevity) of the spider mite lines on the novel resources and the composition of bacterial communities associated with these lines.

## MATERIALS AND METHODS

### Model System: Spider Mites and Plants

The two-spotted spider mite *Tetranychus urticae* Koch, 1836, is a model organism that is widely used in evolutionary experiments due to its well-known biology, small body size, high fecundity and short generation time (Bitume et al., 2013; Magalhães et al., 2014; Rodrigues et al., 2016; Alzate et al., 2017, 2019; Bisschop et al., 2019). Here, we used a stock population that was created by assembling different inbred lines that were created by Bitume et al. (2013) in August 2015. The initial collection of the stock population dates back to October 2000 when mites were collected from roses near Ghent, Belgium. The stock population has always been maintained on bean plants, *Phaseolus vulgaris* Prelude, at 18:6 L:D (light dark cycle) and 25°C. We here tested adaptation to novel host plants, cucumber *Cucumis sativus* Marketmaker, and tomato *Solanum lycopersicum* Moneymaker. We used two-week-old bean plants, four-week-old cucumber plants and six-week-old tomato plants. The ages of the host plants were chosen based on a previously performed pilot study to provide similar amounts of resource per plant species to the spider mite populations. Plants were grown in controlled greenhouse conditions at 28°C under 12:12 L:D and watered three times a week.

### Creating Genetically Depleted Lines to Allow for Testing the Effect of Host Ancestry

We sampled 20 deutonymph females from the stock population in January 2017 and created genetically depleted spider mite lines by placing each deutonymph female separately on bean leaf cuts and fertilizing her with her own sons resulting in

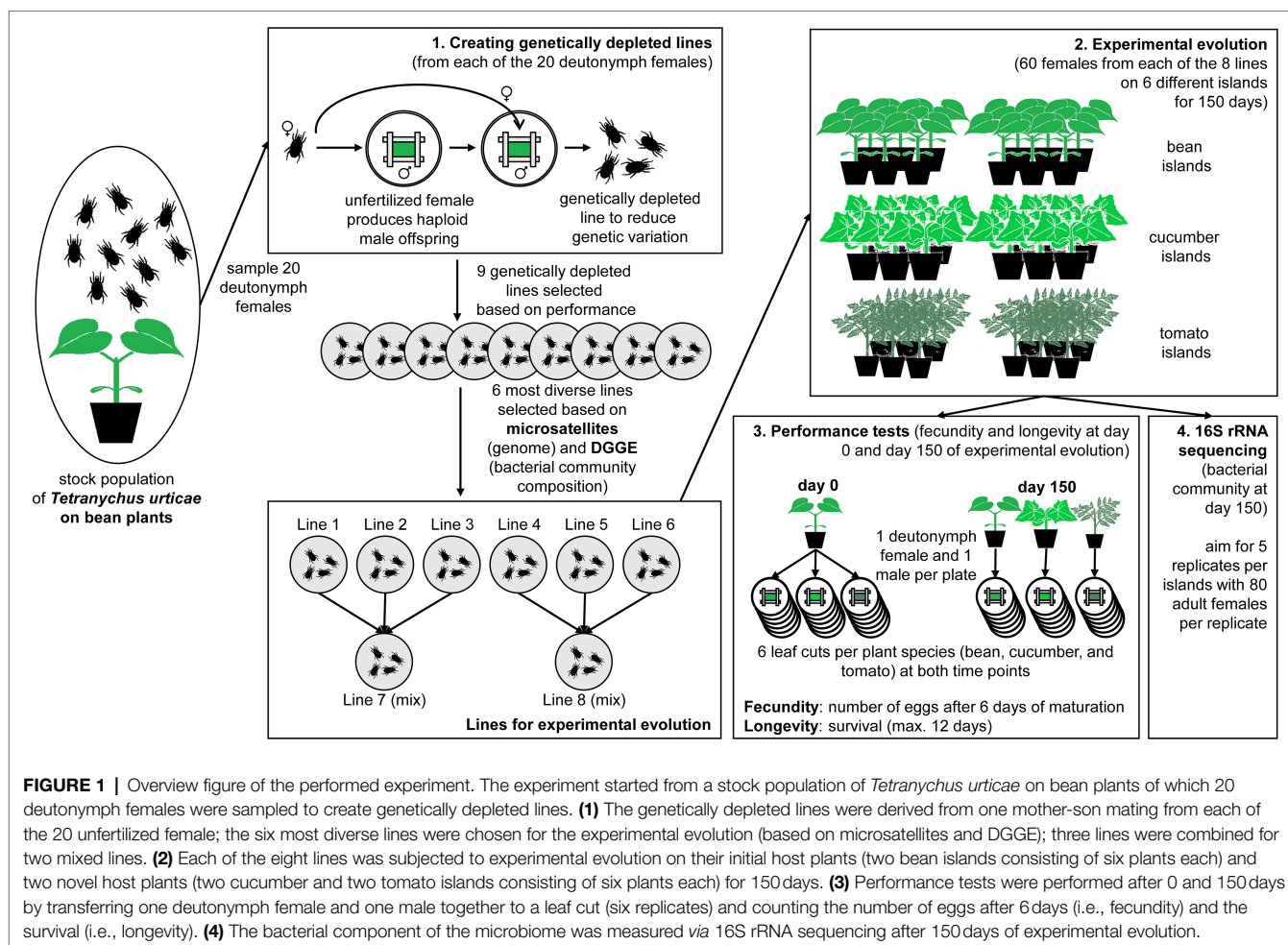
one mother-son mating (*T. urticae* only produced haploid male offspring as they did not mate before; **Figure 1.1**). We want to emphasize that this procedure was followed to reduce the impact of genetic variation on adaptation, and not to create entirely homozygous inbred lines. Out of these 20 lines, we selected the nine lines that were best growing after two generations and maintained them on bean plants at 25°C and 18:6 L:D. These nine lines were subjected to microsatellite analysis and bacterial community analysis using denaturing gradient gel electrophoresis (DGGE, Pereira Silva et al., 2012). The six most different lines, both in terms of their genome and bacterial community composition (see **Supplementary Materials and Methods S1**) were then selected to ensure sufficient genetic and microbial variation across lines (from here-on the different genetically depleted lines are numbered as lines 1 to 6).

### Design of Experiment: A Scenario for Local Adaptation

Each genetically depleted spider mite line was transferred to two bean “islands,” two cucumber “islands” and two tomato “islands” with an initial population size of 60 adult females on each island (**Figure 1.2**). These islands were groups of six plants maintained in separate open boxes with sticky paper at the bottom and Vaseline at the sides to prevent contamination between the populations. Besides the six original lines, two additional lines were created by mixing 20 adult females from lines 1, 2 and 3, and lines 4, 5 and 6, respectively (hereafter referred to as lines 7 and 8). This allowed us to study the effect of the level of standing genetic variation, because these mixed lines were genetically more diverse. For logistical reasons, the experiment was divided into two batches that were run 1 month apart from each other. The first batch contained lines 1, 2 and 3 and its mixed line 7; the second contained lines 4, 5 and 6 and its mixed line 8. This resulted in a total of 48 islands or 24 islands per batch (six islands per spider mite line and another six islands per mixed line) that were divided among three climate rooms under the same conditions (25°C under an 18:6 L:D photoperiod). Every week, two fresh plants were placed in the middle of the island, while the two oldest plants were removed. We chose this refreshment method to minimize selection for dispersive phenotypes and make sure that all older plants were touching the fresh ones.

### Testing Performance on Different Hosts Plants

The performance tests (measurement of the two fitness proxies: fecundity and longevity) were at the start (day 0) and at the end of the experiment (day 150; **Figure 1.3**). At the start, 18 quiescent female deutonymphs and 18 adult males per genetically depleted line were sampled from bean plants. Pairs consisting of one quiescent female deutonymph and one adult male were separately placed on six leaf cuts (2×3 cm; within a Petri dish with wet cotton and bordered by paper strips) from each of the three different plant species (bean, cucumber, and tomato plants). At the end of the experiment, the same procedure



was followed, but pairs of quiescent female deutonymphs and adult males were only placed on leaf cuts from the same plant species as the experimental island they were collected from. These Petri dishes were kept under the same climatic conditions as the experimental islands (25°C and 18:6 L:D).

Fecundity was measured by counting the total number of eggs and larvae 6 days after maturation of the female (Alzate et al., 2017, 2019). In case the quiescent deutonymph female did not reach maturity, she was replaced by another quiescent deutonymph with a maximum of three replacements. Longevity was counted as the number of days the female was alive with a maximum of 12 days. This maximum was imposed because after 12 days the influence of the decay of the leaves on longevity might be too large. The adult females were checked daily and, when possible, saved from unnatural deaths such as drowning in the cotton. In the case of an unnatural death or the individual was still alive after 12 days, it was censored from the survival data: when this happened before the sixth day, the data points were excluded from the fecundity data (because fecundity was measured on the sixth day, later drowning did not affect the outcome). Due to the possibility of unnatural deaths or quiescent deutonymph females not reaching maturation, the number of replicates per time point and plant species was not equal among

all genetically depleted lines. The largest discrepancy in number of replicates for performance was between plant species, for instance less replicates on tomato plants than on bean plants, which matched the difficulties of the novel host plants (overview in **Supplementary Figure S1**).

In many studies investigating genetic adaptation juvenile and maternal effects are standardized by placing the individuals for two generations under common garden (Magalhães et al., 2011; Kawecki et al., 2012). We deliberately did not do this, because two additional mite generations on a benign host plant (as is usually done, see Alzate et al., 2017, 2019; Bisschop et al., 2019) might disrupt the signal of the microbiome due to the very short microbial generation times. This makes it impossible, however, to distinguish maternal effects from microbiome effects.

### Investigating the Internal Microbiome (Sampling, DNA Extraction, Sequencing, and Data Processing)

At the end of the experiment (after 150 days), we sampled 80 adult females per replicate for the microbiome (which was necessary to get sufficient DNA), and we aimed to take five replicates per island (**Figure 1.4**). Sampling was done by sucking

adult females from the plants onto a filter using a small vacuum pump. The mites were then transferred into an Eppendorf tube. The samples were directly frozen at  $-25^{\circ}\text{C}$ . We intended to also collect samples at the start, but only have data from four genetically depleted lines, due to failed sampling (i.e., too small population sizes), DNA extractions, or low numbers of sequencing reads. A comparison between the initial and final samples for those four lines can be found in **Supplementary Figure S2**.

After sampling, the mites were surface-sterilized with ethanol: we submerged the mites in 0.5 ml 90% ethanol for 20 min, removed the ethanol, washed four times with 0.2 ml sterile distilled water (centrifuge in between washes for 1 min at 1,000 g). Then, the mites were crushed in the 0.1 ml of sterile distilled water leftover from the last washing step. The crushing was performed using sterile pestles, powered with a cordless pellet mixing motor. The crushed mites were then transferred into powerbead tubes from the DNeasy PowerSoil kit (Qiagen). DNA was extracted according to the manufacturer's protocol with two additional steps: (1) to enhance crushing of bacterial cell walls, 0.25 gr of 0.1 mm glass beads were added to the powerbead tubes, and (2) the bead beating face was elongated to two times 10 min instead of two times 5 min.

The resulting DNA was quantified using the Quant-iT<sup>TM</sup> PicoGreen<sup>TM</sup> dsDNA Assay kit following the manufacturer's protocol, in order to standardize the amount of DNA used in the following PCR protocol. From each sample, bacterial community composition was determined by using 2.5 ng DNA as the template in a PCR reaction targeting the V3-V4 region of the 16S rRNA gene; PCR protocol and primer sequences for the first PCR are given in **Supplementary Materials and Methods S2**. After the first PCR, the quantity of the DNA was estimated using the Eurogentec SmartLadder MW-1700-10 during gel electrophoresis (1% agarose gel at 100 V for 40 min); it was necessary to keep track of the quantity to ensure enough DNA for sequencing (35  $\mu\text{l}$  of 30 ng/ $\mu\text{l}$ ). In most cases, the requirements were not met after a first PCR and hence additional PCRs from the same initial sample were performed starting with the same initial amount of DNA (average was three PCRs per sample). We did not start the second PCR from the previous PCR product as that would amplify errors introduced by PCR. The samples of the different PCRs were pooled per sample and purified using the QIAquick PCR Purification kit (QIAGEN). Library preparation, Illumina MiSeq (2x250bp) sequencing and demultiplexing were performed by INRA Science and Impact (GeT-PlaGe platform of GenoToul, INRA Auzeville).

After demultiplexing, the data were preprocessed using QIIME2 version 2017.12, denoised, amplicon sequence variants (ASVs) determined with DADA2 (Callahan et al., 2016) and primers were trimmed (max. sequence lengths for forward and reverse reads were set at 300 bp). A MAFFT alignment (Katoh et al., 2017) of the ASV sequences was made, which was used for constructing a phylogenetic tree using FastTree (Price et al., 2009, 2010). We used the 97% identity GreenGenes 13\_8 reference database (DeSantis et al., 2006) for 16S rRNA for a taxonomy table. The resulting sequence table, phylogenetic

tree, and taxonomy table were merged into a phyloseq object in R. Singletons were removed from the samples and all datasets were rarefied before analyzing to an even depth of minimum 24,712 (based on the number of reads per sample and the rarefaction curves; **Supplementary Figure S3**). We used five different random seeds for the rarefaction to limit influences from sampling bias. This was especially necessary as many of the reads were absorbed by a single family, which created a long tail of rare diversity in our microbial community, and hence a potential sampling bias during rarefaction. At this point, 148 samples were present with ASV numbers between 1,126 and 1,148. More microbiome samples were available in the rarefied datasets for bean, than for cucumber and tomato, the numbers were 73, 46, and 29, respectively (an overview of the number of samples per line and plant species is given in **Supplementary Table S1**). The main reason for this discrepancy is the smaller population sizes on cucumber and tomato as well as the fact that certain lines did not survive on cucumber (line 1) and tomato (lines 1 and 3).

## Data Analysis

The analyses below are divided in three sections: (1) the exploration of the bacterial communities within the spider mites, i.e., host-associated bacterial communities (the influence of the spider mite line and plant species on the alpha and beta diversity of the bacterial communities), (2) the investigation of the performance tests which include fecundity and longevity of the spider mites themselves, and (3) the relation between the bacterial communities (both alpha and beta diversity) and the performance of the spider mites.

### Host-Associated Bacterial Communities

#### *Alpha Diversity of Bacterial Communities*

To investigate whether alpha diversity of the bacterial communities differed per host spider mite line and plant species, we first calculated three different metrics of alpha diversity for each community: Faith's phylogenetic diversity, Shannon diversity index, and species richness. We used GLMMs with a lognormal distribution for Faith's phylogenetic diversity and the Shannon diversity index, and with a negative binomial distribution for species richness. The distribution was chosen based on a goodness-of-fit test using Akaike's Information Criterion (AIC). The metric for alpha diversity was used as the dependent variable, while the host plant species, host spider mite line, and their interaction were the explanatory variables. The different islands nested within their respective batches were treated as a random variable for the Shannon diversity index and species richness. For Faith's phylogenetic diversity, the nested random variable induced an overfitting of the model, as the variance was estimated to be zero (Magnusson et al., 2018). Hence, we only considered the island as a random variable for phylogenetic diversity. We performed model selection with stepwise removal of the non-significant variables. The pairwise comparisons were corrected for multiple comparisons with the Tukey method.

### Bacterial Community Composition

We used permutational analysis of variance (PERMANOVA; Anderson, 2017; Anderson et al., 2017) to investigate which variable had the largest influence on the beta diversity of the bacterial communities; the host ancestry (different spider mite lines) or the environment (different host plants). To comply with the requirement of homogeneity of multivariate dispersions for each potential grouping variable (tested with betadisper), we were not able to use the abundance-weighted statistics (weighted UniFrac and Bray-Curtis distance) and we only used the unweighted UniFrac distance metric as input in the PERMANOVAs (Bray and Curtis, 1957; Lozupone et al., 2011).

The independent variables were the different spider mite lines, the host plants, and their interaction. The different islands were added as groups within which permutations were constrained (total of 1,000 permutations). We used PCoA plots to visualize the ordination. We furthermore calculated average microbiome dissimilarity values from this ordination by taking the average of the values in the distance matrix.

Furthermore, we investigated the similarities in community structure between the separate and mixed spider mite lines on the different plant species with the Cramer-von Mises test statistic using the libshuff method in mothur v. 1.45.0 (Schloss et al., 2009). This test statistic explores the likelihood of randomly obtaining the same structure. The distance matrices were constructed per batch and per island using the unweighted UniFrac distance metric. We used Bonferroni's correction for multiple pairwise comparisons.

### Performance, i.e., Fecundity and Longevity of the Spider Mites

To investigate differences in fitness proxies per host plant species and host spider mite line, the fecundity and longevity were analyzed with GLMMs (with Gaussian distribution) and Mixed Effects Cox Models, respectively. In both cases, the maximal model consisted of all combinations with the host plant species and host spider mite line. The random variables were the different islands nested within the batches. We selected the model *via* stepwise removal of non-significant variables. Pairwise comparisons were adjusted for multiple comparisons by using the Tukey method for fecundity and the Benjamini and Hochberg method for longevity.

### Relation Between Performance and Microbiome Composition

The link between the performance and bacterial community composition was tested using a Procrustes and a Mantel test (with Pearson correlation method and 9,999 permutations). Distances between mite performance and the distance matrix generated for the bacterial communities per spider mite line (using the unweighted UniFrac metric) were used. This was done for each host plant species separately (i.e., bean, cucumber, and tomato) to rule out major differences based on host plant species. Two different distance metrics were used for the Procrustes and Mantel test: Euclidean distance and Manhattan distance. We performed the tests for the effect on fecundity and longevity

simultaneously and for each of them separately (only fecundity or only longevity). For the performance, the mean fecundity and/or longevity was taken per spider mite line. For the matrix based on the bacterial component of the microbiome, the data was merged per line and rarefied based on the number of reads per sample and host plant species; in this way each sample received equal weight in the analyses. We additionally performed the analyses on island level (see results in **Supplementary Table S2**), but for seven islands we only had one or two samples from the bacterial community (six out of seven on tomato islands) which could create a bias in the results. Hence, we only present results on the level of spider mite line.

We also tested whether the different alpha diversity metrics were related to fecundity and longevity (no direct measurements were possible from the same individuals for bacterial communities and performance measurements). We used GLMMs with Gaussian distribution after transforming the data to obtain a normal distribution (an arc-sine, logarithmic, and Box-Cox transformation on the mean Faith's phylogenetic diversity, Shannon diversity index, and species richness, respectively). The alpha metric was the dependent variable and the plant species, fecundity/longevity and their interaction as independent variables. The different spider mite lines were used as a random variable.

Statistical analyses were performed in R version 4.1.2 (2021-05-18) and the following R packages: phyloseq version 1.36.0 (McMurdie and Holmes, 2013), vegan version 2.5-7 (Oksanen et al., 2020), glmmTMB 1.1.1 (Brooks et al., 2017), emmeans 1.6.1 (Lenth, 2021), fitdistrplus 1.1-5 (Delignette-Muller, 2015), coxme 2.2-16 (Therneau, 2020), bestNormalize 1.8.0 (Peterson, 2019). The R code is made available as **Supplementary Material**.

## RESULTS

### Host-Associated Bacterial Communities General Overview

Out of the six spider mite lines created for this study, one line did not survive on tomato, and another line did not survive on both cucumber and tomato. For the surviving lines, we found between 1,126 and 1,148 ASVs with an average of 1,141 ASVs depending on the seed used during rarefaction. Most of this microbial diversity was found exclusively in the spider mite lines that had been put on bean plants, the ancestral host plant of the spider mite stock population. After correcting for the sampling bias (the number of samples from spider mite populations on bean, cucumber, and tomato were 73, 46, and 29, respectively; **Supplementary Table S1**) by selecting 29 samples per host plant species at random (and repeating this for 2,000 times), the average percentage of ASVs unique to bean, cucumber, and tomato were 41.7%, 27.2%, and 17.2%, respectively, while the average standardized percentage of ASVs common to all host plants was 6.0%. We provide an overview of the different host plants and their unique and shared ASVs in absolute and standardized numbers in **Figure 2** (a complete



overview of all ASVs per line and plant species is provided in **Supplementary Table S3**).

### Alpha Diversity of Bacterial Communities

We used three diversity indices to quantify the alpha microbial diversity: Faith's phylogenetic diversity, Shannon diversity, and species richness (**Supplementary Figure S4**; **Supplementary Tables S4–S9**). The results were consistent across the different random seeds used in rarefaction for microbial diversity. In general, spider mite line 5 had a higher alpha diversity than spider mite lines 1, 2, and 7 for Faith's phylogenetic diversity and species richness. The spider mites' host plant species could not explain the microbial variance found in alpha diversity and was not included in the most parsimonious model. Although the number of ASVs varied strongly between host plants, as reported above, we did not observe significant differences in the bacterial diversity between the samples from the different host plant species. We visualized this in **Figure 3**; where a large difference in species richness was found between host plant species when reads from all samples were pooled together, but, if individual samples were compared, the diversity did not differ among plant species. The mixed lines (line 7 and line 8) did not show a higher or lower microbial diversity than the genetically depleted lines, except for the significantly lower alpha diversity of line 7 compared to spider mite line 5 (**Supplementary Figure S4**).

### Bacterial Community Composition

Analyses of bacterial community composition revealed a high abundance of Rickettsiales, mostly those belonging to genera *Wolbachia* and *Rickettsia* (**Supplementary Figure S5**). The significantly lower abundant orders that followed were the Xanthomonadales, Saprospirales, Enterobacteriales, Burkholderiales, and Actinomycetales (**Figure 4**). Despite the vast abundance of the Rickettsiales, they only comprised between 86 and 89 ASVs or between 7.6 and 7.8% (depending on the seed) of the total number of ASVs after rarefaction, indicating low genetic variability among Rickettsiales.

The relatively low R-squared values from the PERMANOVA analyses indicated that a large amount of variation in the microbiomes of the spider mites remains unexplained by the tested variables (on average only 7.8%, 1.9%, and 6.7% for host ancestry, plant species, and their interaction, respectively, was explained, **Table 1**), which may explain the absence of clustering in the PCoA plot (**Figure 5**; **Supplementary Figure S6**). While for all data sets the host-associated bacterial communities were significantly determined by host ancestry, only one out of five seeds revealed significant results for plant species (**Table 1**).

The average community dissimilarities showed the largest variation in composition across plant species for spider mite line 3, followed by lines 8 and 5 (on average 0.691, 0.634, and 0.628, respectively), whereas the lowest variation was

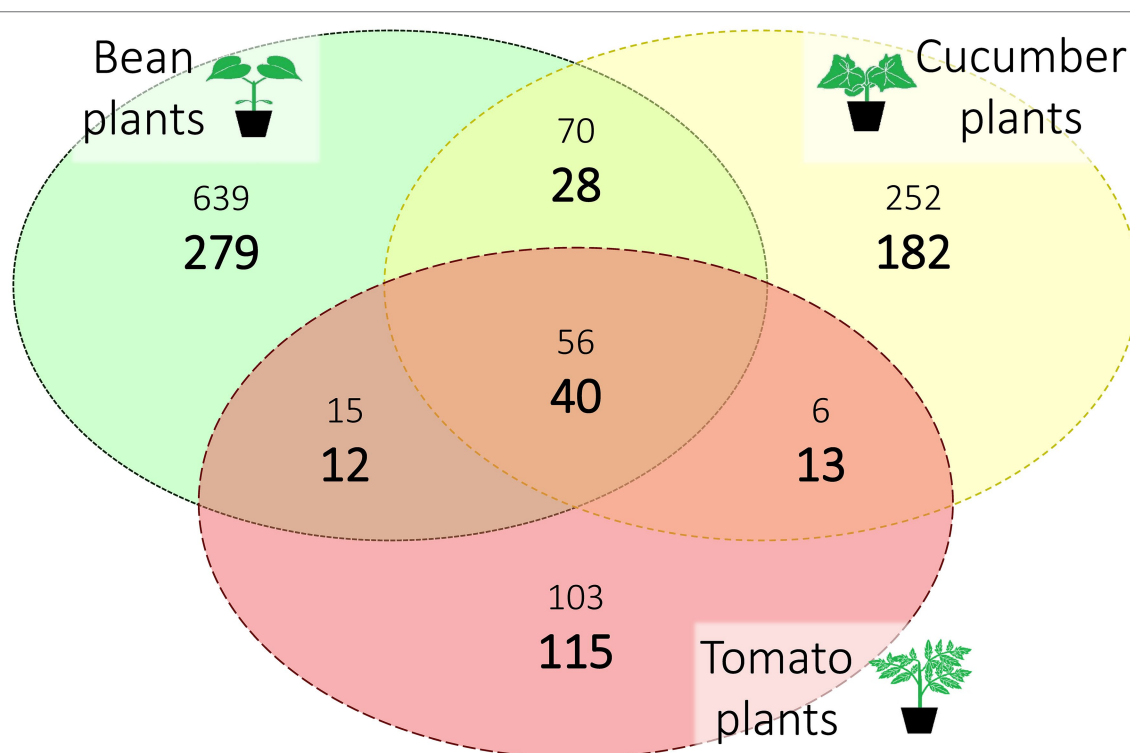
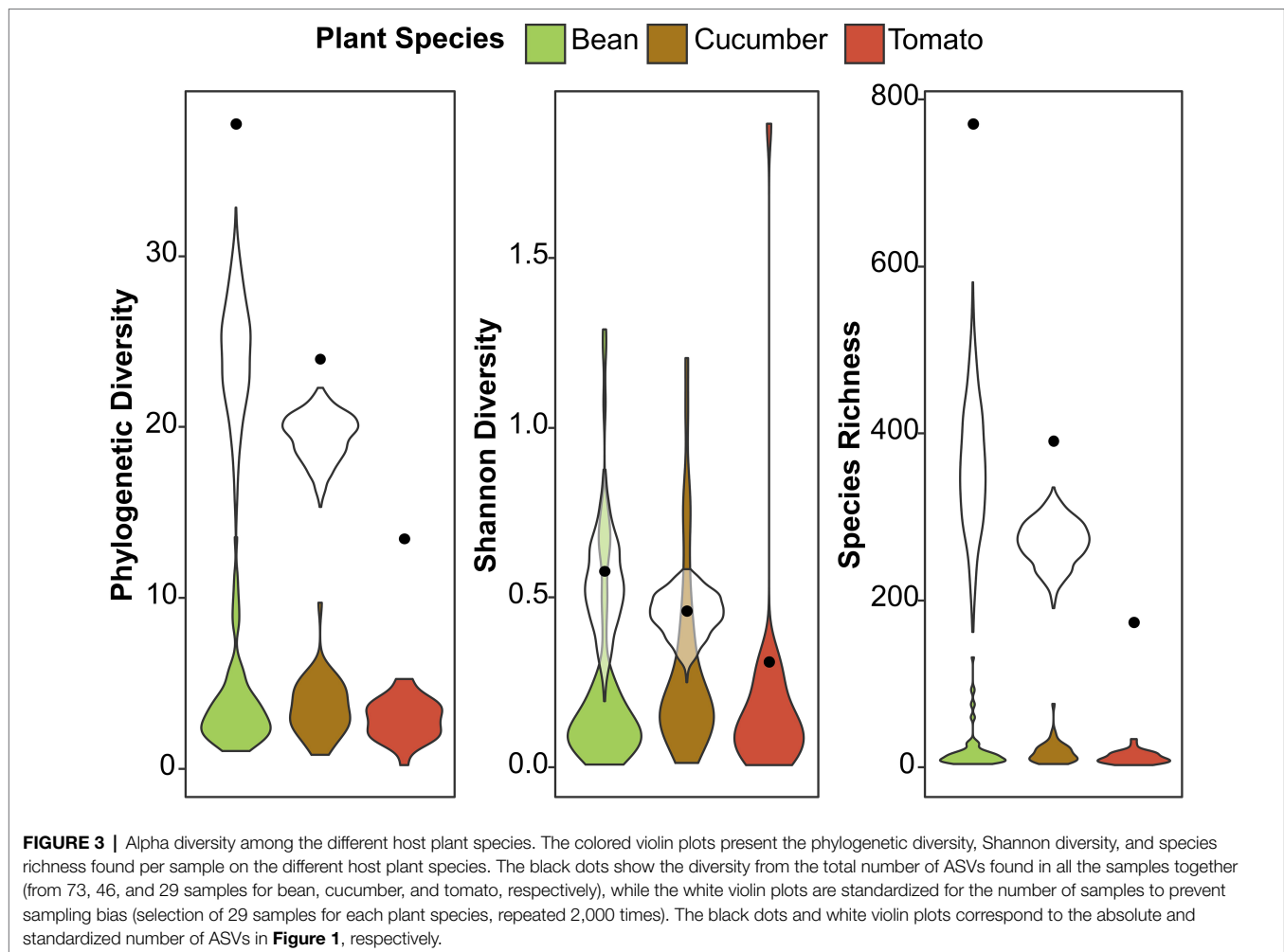


**FIGURE 2 |** Distribution of the amplicon sequence variants (ASVs) over host plant species after rarefaction. The three different host plant species (bean, cucumber, and tomato) are represented with their unique and shared ASVs. Sample sizes per host plant were 73, 46, and 29 (for bean, cucumber, and tomato, respectively); the large, bold numbers are standardized for this sampling bias by selecting at random 29 samples (repeated 2,000 times) for each plant species. The smaller numbers are the absolute numbers of ASVs. All numbers are averaged over the seeds.



found for spider mite line 1, followed by lines 4 and 6 (average microbiome dissimilarity of 0.548, 0.572, and 0.572, respectively). Although the average microbiome dissimilarity for the samples from the mixed line 8 was rather large, we did not see strong differences between the genetically depleted lines and the mixed lines. In general, the variation in bacterial communities associated with the spider mites living on cucumber plants was smaller (average microbiome dissimilarity of 0.598) than with those living on the other two plant species (0.609 and 0.640 for tomato and bean, respectively; **Figure 5**).

The Cramer-von Mises statistic revealed no consistent significant results (**Supplementary Table S10**) among the different rarefied datasets, indicating that none of the microbial communities were more similar to each other than could be explained by chance. Hence, the mixed lines were not more similar to a single spider mite line.

## Spider Mite Performance

The fecundity assessed on bean plants was initially significantly higher than the fecundity on tomato plants for all the different spider mite lines (**Figure 6**; **Supplementary Figures S7, S8**; **Supplementary Table S11**). This changed

at day 150 when mites living on bean and those living on tomato for lines 2, 3, and 4 showed a similar performance (**Supplementary Figure S7**). These particular spider mite lines thus achieved the same fecundity on tomato plants as on the ancestral bean plants. Fecundity on cucumber was initially intermediate between bean and tomato; only individuals from line 1 ( $t=3.861$  and  $p=0.0233$ ) had a significantly lower fecundity on cucumber than on bean plants. After 150 days lower fecundity on cucumber than on bean was observed for line 4 ( $t=4.285$  and  $p=0.0054$ ), line 5 ( $t=8.133$  and  $p<0.0001$ ), and line 6 ( $t=3.951$  and  $p=0.0182$ ). Different replicates from the same spider mite line obtained similar fecundity after 150 days (**Supplementary Figure S8**). Regarding longevity, the longest living individuals were from the populations living on cucumber, while the shortest survival probabilities were observed in the tomato populations (**Figure 6**; **Supplementary Figure S9**; **Supplementary Table S12**). Individuals from lines 2 and 7 had a low survival probability overall. Different replicates for the same lines showed the same trend for longevity (**Supplementary Figure S8**). The mixed lines did not perform better than the genetically depleted lines in terms of longevity or fecundity.

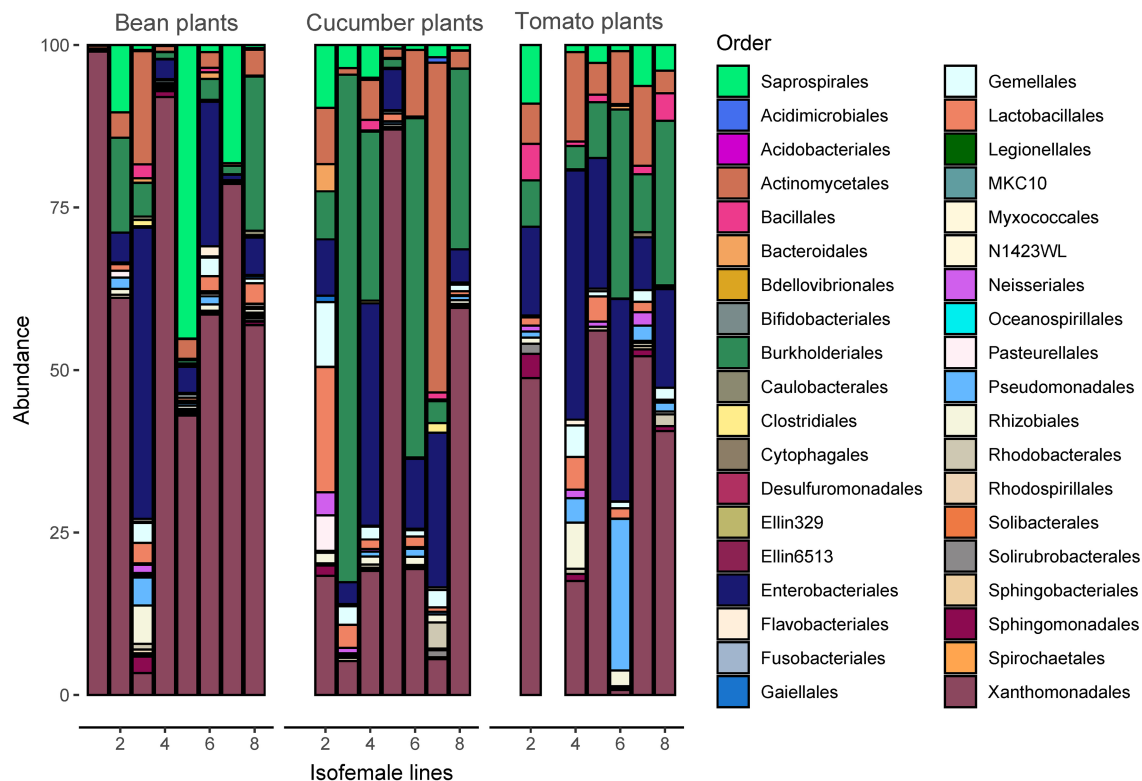


**FIGURE 4 |** Taxonomy of the microbiome at the order level (the Rickettsiales are excluded from the figure for better visualization) per spider mite line and plant species. The most abundant taxonomic orders are Actinomycetales, Burkholderiales, Enterobacteriales, Saprospirales, and Xanthomonadales. A figure including Rickettsiales is provided in **Supplementary Figure S5**.

## Relation Between Performance and Microbiome Composition

All results were consistent across the different random seeds used in rarefaction, except the results where the performance matrix was created only from longevity; only for some seeds significant correlations were found on tomato. We found a strong correlation between the difference in performance of the spider mite lines and the difference in their microbiome on the two novel host plants (cucumber and tomato) based on the fecundity and longevity data combined (**Table 2**). This relation was not found on their initial host plant (bean) alone. A significant relation on both novel host plants was also found if only fecundity was considered. However, if only longevity was considered, the relation with the microbiome composition on cucumber plants disappeared. The significance for longevity on tomato plants depended on the ASVs that were sampled during rarefaction (i.e., the used seed).

On the one hand, we discovered a significant positive correlation between mean fecundity and Faith's phylogenetic diversity (trend =  $0.1370 \pm 0.0485$ ,  $t$  ratio = 2.826, and  $p = 0.0083$ ) and between fecundity and species richness (trend =  $0.1289 \pm 0.0484$ ,  $t$  ratio = 2.665, and  $p = 0.0123$ ) on bean. On the other hand, we found a significant negative correlation on cucumber for Shannon diversity index (trend =  $-0.1242 \pm 0.0572$ ,  $t$  ratio = -2.172, and  $p = 0.0379$ ) and species richness (trend =  $-0.1166 \pm 0.0559$ ,  $t$  ratio = -2.084, and  $p = 0.0457$ ). No significant interactions were found between alpha diversity and longevity (**Supplementary Figure S10**).

## DISCUSSION

We used experimental evolution to gain insights into the role of the microbiome in adaptation of the host to new resources. We here studied adaptation to host plants from the perspective of fitness maximization, including genetics and plasticity through interaction with microbiomes. Our results show a potential importance of the microbiome for adaptation of spider mites to novel food sources, and suggest that while both host ancestry and plant host environment may contribute to shaping the microbiome, these factors only explain a small part of the variation in the microbiome composition. In general, we did not discover large discrepancies between the mixed and genetically depleted lines. On the one hand, this might be because the genetic diversity provided in the mixed lines was still rather low for a good comparison: the genetically depleted lines were made from a population that had been maintained for many generations in the lab, meaning that the genetic diversity among spider mite lines was potentially low. On the other hand, this could be due to outbreeding depression. The genetically depleted lines were preselected to obtain the most different lines based on the bacterial part of their microbiome and genome. Mating these lines could potentially lead to heterozygote disadvantage and the break-up of coadapted gene complexes and epistatic interactions (Price and Price and Waser, 1979; Peer and Taborsky, 2005).

**TABLE 1** | PERMANOVA output for the unweighted UniFrac.

Model: unweighted UniFrac ~ spider mite line * plant species (strata=batch)							
		Df	Sum of sqs	F.model	R <sup>2</sup>	Pr(>F)	
Seed 1	<b>Line</b>	7	2.260	1.655	0.077	<b>0.001</b>	***
	Plant Species	2	0.571	1.465	0.019	0.063	
	Line: Plant	11	1.905	0.888	0.065	0.822	
	Species						
	Residuals	127	24.765		0.839		
Seed 2	<b>Line</b>	7	2.370	1.719	0.079	<b>0.001</b>	***
	Plant Species	2	0.597	1.513	0.020	<b>0.045</b>	*
	Line: Plant	11	2.058	0.949	0.068	0.650	
	Species						
	Residuals	127	25.025		0.833		
Seed 3	<b>Line</b>	7	2.345	1.723	0.079	<b>0.001</b>	***
	Plant Species	2	0.540	1.388	0.018	0.077	.
	Line: Plant	11	2.006	0.938	0.068	0.679	
	Species						
	Residuals	127	24.701		0.835		
Seed 4	<b>Line</b>	7	2.416	1.774	0.081	<b>0.001</b>	***
	Plant Species	2	0.550	1.413	0.019	0.073	.
	Line: Plant	11	1.981	0.925	0.067	0.747	
	Species						
	Residuals	127	24.713		0.833		
Seed 5	<b>Line</b>	7	2.251	1.652	0.076	<b>0.001</b>	***
	Plant Species	2	0.553	1.419	0.019	0.076	.
	Line: Plant	11	1.980	0.925	0.067	0.765	
	Species						
	Residuals	127	24.729		0.838		
	Total	147	29.513		1.000		

A–E: the different results are from the five different random seeds for rarefaction to prevent sampling bias of the ASVs. Depending on the selected ASVs, ancestral line and host plant significantly influence the microbiome. Overall, only a small amount of the total variation is explained ( $R^2 \approx 0.17$ ) and most of each is explained by the ancestral spider mite line ( $R^2 \approx 0.08$ ). Values in bold are considered significant as they are lower than the conventional  $p$ -value of 0.05. The asterisks indicate the level of significance (':  $p$ -value  $\leq 0.10$  and  $> 0.05$ , \*\*:  $p$ -value  $\leq 0.05$  and  $> 0.01$ , \*\*\*:  $p$ -value  $\leq 0.01$  and  $> 0.001$ , and \*\*\*\*:  $p$ -value  $\leq 0.001$ ).

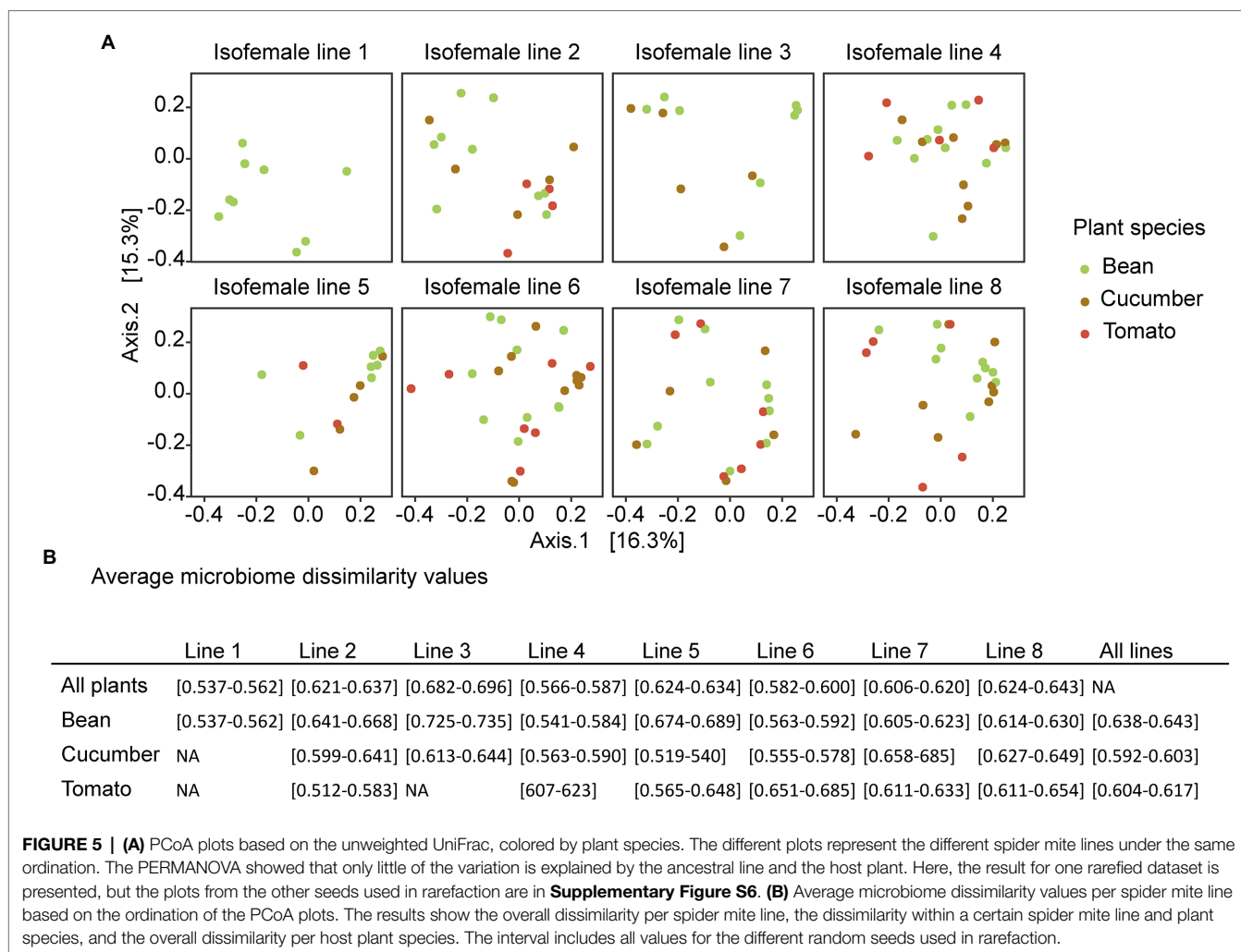
## Influence of Experimental Evolution on Performance

Before the evolutionary experiment, the fecundity of the spider mites on tomato leaves was significantly lower for all genetically depleted lines compared to their fecundity on bean leaves (**Supplementary Figure S7**). After 150 days of evolution, some lines (lines 2, 3, and 4) managed to obtain an equal fecundity on tomato and on bean, even though all lines were genetically depleted. Interestingly, this was not found for the mixed lines; the performance on tomato was still significantly lower than on bean. We expected that mixing or outbreeding of lines would lead to an increase in fitness. However, under certain conditions, an outbreeding depression resulting in lower fecundity, is likely (Price and Waser, 1979; Peer and Taborsky, 2005). Indeed, the two-spotted spider mite is a haplodiploid species with fast exponential growth followed by population collapses, indicating higher chances for sibling mating and prolonged inbreeding. It is therefore probable that the species is better protected against inbreeding depression than outbreeding depression (e.g., *via* purifying selection on recessive

deleterious alleles). In fact, a study of Tien et al. (2015) found no negative effect of inbreeding on oviposition rate in *T. urticae* anymore at an inbreeding coefficient,  $F$ , of 0.5 (i.e., selfing).

Adaptation of *T. urticae*, which was maintained on a single host plant for many generations in the lab, to tomato plants has been observed in previous research as well (Magalhães et al., 2007; Alzate et al., 2017). We expected tomato plants to be challenging host plants due to their induced responses and glandular trichomes (Lucini et al., 2015; Godinho et al., 2016). The differences among lines was not surprising as intraspecific variation within *T. urticae* has been found to result in different responses to plant defenses; some lines may induce defenses to which they are susceptible, others induce but are not susceptible, while certain lines may suppress defenses (Kant et al., 2008). The fecundity on cucumber plants was initially intermediate between the fecundity on bean and tomato, but not significantly different from the bean leaves. Only line 1 had a significant lower fecundity on both novel host plants and did not survive the evolutionary experiment on the novel host plants.





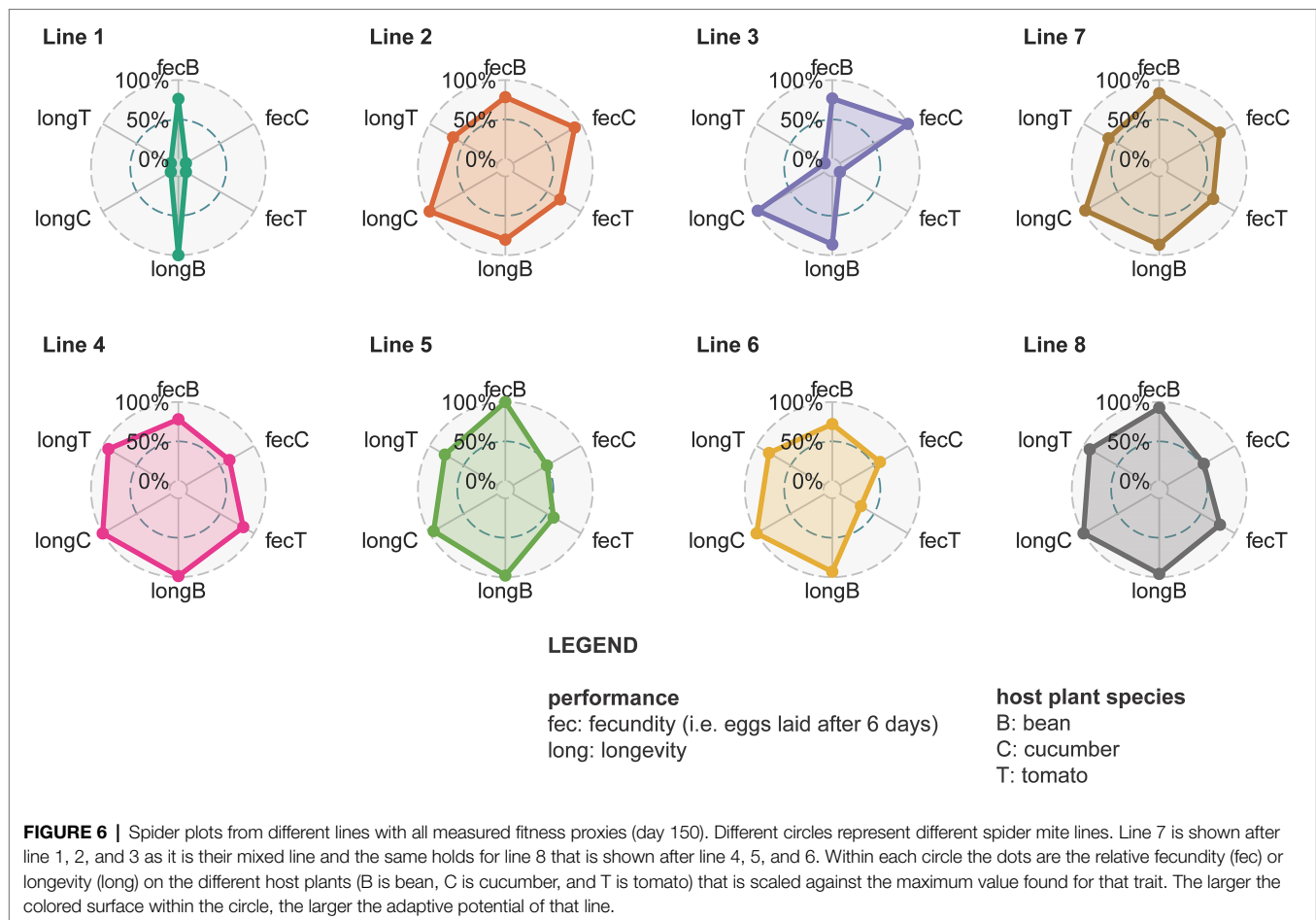
Longevity was highest on cucumber plants, followed by bean and tomato (Fig. S9). The higher mortality on the hostile tomato plants was expected, but longer lifetimes on cucumber were unanticipated. Also, no interaction effects between spider mite line and host plant species were found, which indicates that certain spider mite lines survived longer but independently of their host plant species.

## Effect of Host Ancestry on the Bacterial Communities

The bacterial communities associated with our focal species are partly horizontally transmitted from the plant environment, but also inherited from parents to offspring, given the significant effect of the spider mite line on microbiome composition in the PERMANOVA. Heritability of microbiomes ranges from entirely faithful as seen in intracellular infection of oocytes to completely unfaithful in for instance marine sponges (Bruijning et al., 2022). This flexibility could be beneficial to create variable microbiomes for rapidly changing environments or for different life stages (Henry et al., 2021; Bruijning et al., 2022).

Many microorganisms, such as *Wolbachia* spp. and *Rickettsia* spp., are intracellularly transmitted in the egg cytoplasm (Hong et al., 2002; Veneti et al., 2005; Zilber-Rosenberg and Rosenberg, 2008). We found a high abundance of these commonly found bacteria in our populations of *T. urticae*, which could explain the importance of host ancestry to microbiome composition. It is, however, possible that also other ASVs were vertically transmitted, particularly because the distance metric we used (unweighted UniFrac) does not take abundance into account and only on average 7.7% of all ASVs belonged to the Rickettsiales family. While spider mites reproduce by laying eggs, it is unknown whether the surface of the eggs is a transgenerational carrier of bacteria. This is known for some, yet unsupported for other species (Romero and Navarrete, 2006; van Veelen et al., 2018).

Although the contribution of host ancestry to microbiome composition was significant, it was very small, which may be due to the fact that individual lines were created from the same population. The used mite strains already persisted for more than 40 generations and had been feeding on the same host plant species for more than 400 generations. Such co-feeding does not necessarily lead to transfection or homogenization



of the microbiome (Oliver et al., 2010). The (albeit small) contribution of ancestry indicates that certain microorganisms may have been vertically transmitted, but another option is a strong filter of the genetically depleted spider mite line creating microbial differences between individuals.

We aimed to provide results from the initial bacterial communities of the different lines, but only have data from four spider mite lines due to low population sizes and failed DNA extractions. On the one hand, two spider mite lines (lines 1 and 6) seem to be less affected by the host plant species or the measured time point (**Supplementary Figure S2**), which could indicate a more stable bacterial community. On the other hand, the other two lines show a small shift due to host plant species (line 2) or both time and host plant species (line 4; **Supplementary Figure S2**). Interestingly, these latter two lines obtained a similar fecundity on tomato compared to their initial host plant after the experimental evolution, while this did not happen in lines 1 and 6 (**Supplementary Figure S7**).

## Effect of Host Environment (Host Plant Species) on the Bacterial Communities

The standardized number of ASVs found in bean plants was higher than the ASVs in the novel host plants, cucumber and

tomato (**Figure 3**). Especially the small number of shared ASVs may indicate a strong environmental filter for each host plant (Diamond, 1975; Takeuchi et al., 2015). Besides, an indirect influence of the host plant species on the microbiome variation is likely due to differences in spider mite population sizes and inbreeding. Indeed, lower numbers of ASVs on tomato plants could be linked to the smaller population sizes on these host plant species.

In our study, the plant species plays a minor role in shaping the microbiome: as, on average, only 2% of the total variation was explained by host plant species in the PERMANOVA. Acquiring bacteria through the environment from other members in the community is known to occur frequently (Oliver et al., 2010; Henry et al., 2013) and is a potential advantage for adaptation. In contrast to genetic adaptation, acquiring microorganisms might even happen throughout an individual's life (Zilber-Rosenberg and Rosenberg, 2008). An example of such horizontal transmission can be found in aphids, where horizontally transmission occurred by feeding on a diet including symbionts, potentially aided by the sugar-rich liquid or honeydew (Darby and Douglas, 2003). A similar horizontal transmission is possible in spider mites through foraging close to fecal pellets or co-feeding from plant tissues (Chrostek et al., 2017). An example of this plant-mediated transfer has for instance been found for *Cardinium* in aphids (Gonella et al., 2015).

**TABLE 2 |** Relationship between spider mite fitness proxies and microbiome community structure, using Procrustes and Mantel tests.

	Fecundity						Longevity						Fecundity and longevity					
	Bean		Cucumber		Tomato		Bean		Cucumber		Tomato		Bean		Cucumber		Tomato	
	st.	p-v.	st.	p-v.	st.	p-v.	st.	p-v.	st.	p-v.	st.	p-v.	st.	p-v.	st.	p-v.	st.	p-v.
Euclidian	0.62	0.118	0.46	<b>0.006</b>	0.47	<b>0.031</b>	0.741	0.798	0.73	0.462	0.52	0.074	0.58	0.125	0.46	<b>0.006</b>	0.42	<b>0.024</b>
	0.61	0.080	0.45	<b>0.001</b>	0.48	<b>0.028</b>	0.721	0.686	0.70	0.196	0.46	<b>0.013</b>	0.57	0.104	0.44	<b>0.001</b>	0.41	<b>0.007</b>
	0.62	0.087	0.49	<b>0.003</b>	0.49	<b>0.014</b>	0.734	0.849	0.71	0.278	0.48	<b>0.021</b>	0.57	0.095	0.49	<b>0.003</b>	0.43	<b>0.001</b>
	0.63	0.092	0.51	<b>0.005</b>	0.48	<b>0.013</b>	0.735	0.880	0.70	0.225	0.49	<b>0.029</b>	0.58	0.102	0.51	<b>0.004</b>	0.42	<b>0.007</b>
	0.62	0.088	0.54	<b>0.017</b>	0.45	<b>0.004</b>	0.711	0.596	0.71	0.265	0.49	<b>0.026</b>	0.58	0.106	0.53	<b>0.017</b>	0.39	<b>0.007</b>
Manhattan	0.62	0.118	0.46	<b>0.006</b>	0.47	<b>0.031</b>	0.741	0.798	0.73	0.462	0.52	0.074	0.55	0.143	0.44	<b>0.007</b>	0.37	<b>0.017</b>
	0.61	0.080	0.45	<b>0.001</b>	0.48	<b>0.028</b>	0.721	0.686	0.70	0.196	0.46	<b>0.013</b>	0.54	0.115	0.42	<b>0.001</b>	0.36	<b>0.007</b>
	0.62	0.087	0.49	<b>0.003</b>	0.49	<b>0.014</b>	0.734	0.849	0.71	0.278	0.48	<b>0.021</b>	0.54	0.120	0.47	<b>0.003</b>	0.37	<b>0.001</b>
	0.63	0.092	0.51	<b>0.005</b>	0.48	<b>0.013</b>	0.735	0.880	0.70	0.225	0.49	<b>0.029</b>	0.55	0.120	0.49	<b>0.003</b>	0.36	<b>0.007</b>
	0.62	0.088	0.54	<b>0.017</b>	0.45	<b>0.004</b>	0.711	0.596	0.71	0.265	0.49	<b>0.026</b>	0.54	0.109	0.51	<b>0.015</b>	0.33	<b>0.007</b>
Euclidian	0.28	0.105	0.57	<b>0.014</b>	0.56	<b>0.019</b>	−0.133	0.758	0.03	0.462	0.31	0.146	0.27	0.106	0.57	<b>0.014</b>	0.60	<b>0.010</b>
	0.34	0.072	0.73	<b>0.002</b>	0.45	<b>0.026</b>	−0.118	0.719	0.22	0.110	0.64	<b>0.025</b>	0.34	0.081	0.73	<b>0.002</b>	0.53	<b>0.007</b>
	0.32	0.077	0.71	<b>0.004</b>	0.41	<b>0.018</b>	−0.089	0.662	0.17	0.205	0.43	0.081	0.34	0.071	0.71	<b>0.004</b>	0.45	<b>0.001</b>
	0.31	0.076	0.64	<b>0.008</b>	0.51	<b>0.015</b>	−0.185	0.849	0.24	0.114	0.49	0.058	0.30	0.084	0.64	<b>0.008</b>	0.57	<b>0.004</b>
	0.29	0.090	0.49	<b>0.029</b>	0.61	<b>0.008</b>	−0.084	0.640	0.17	0.224	0.42	0.100	0.28	0.098	0.49	<b>0.028</b>	0.66	<b>0.008</b>
Manhattan	0.28	0.105	0.57	<b>0.014</b>	0.56	<b>0.019</b>	−0.133	0.758	0.03	0.462	0.31	0.146	0.26	0.115	0.57	<b>0.014</b>	0.64	<b>0.010</b>
	0.34	0.072	0.73	<b>0.002</b>	0.45	<b>0.026</b>	−0.118	0.719	0.22	0.110	0.64	<b>0.025</b>	0.33	0.085	0.74	<b>0.002</b>	0.60	<b>0.004</b>
	0.32	0.077	0.71	<b>0.004</b>	0.41	<b>0.018</b>	−0.089	0.662	0.17	0.205	0.43	0.081	0.31	0.088	0.72	<b>0.003</b>	0.52	<b>0.001</b>
	0.31	0.076	0.64	<b>0.008</b>	0.51	<b>0.015</b>	−0.185	0.849	0.24	0.114	0.49	0.058	0.28	0.091	0.65	<b>0.006</b>	0.63	<b>0.004</b>
	0.29	0.090	0.49	<b>0.029</b>	0.61	<b>0.008</b>	−0.084	0.640	0.17	0.224	0.42	0.100	0.28	0.099	0.50	<b>0.026</b>	0.71	<b>0.008</b>

The distance matrices used for both the Procrustes and the Mantel test measure the differences between the microbiome composition of the different spider mite lines on their host plant (bean, cucumber, or tomato) and the differences between the fecundity, longevity, or both fecundity and longevity at the last time point (150 days). The significant results (p-value lower than 0.05) are visualized in bold. For the microbiome distance table, the unweighted UniFrac was chosen, while for the performance table two different distance measures were used (i.e., Euclidean and Manhattan). The Mantel test was done with 9,999 permutations based on the Pearson method.

## Bacterial Communities Correlate With Spider Mite Performance

The difference in bacterial diversity between lines was clearly associated with the difference in mite fecundity and their overall performance (fecundity and longevity) on the two novel host plants. Fecundity and alpha bacterial diversity also showed to be related. We therefore dare to suggest that the microbial community is not just transient, but that it could play a role in the life history traits of the host. More importantly, as there was no correlation between the genetic distances and differences in performance between spider mite lines (**Supplementary Table S13**), this result may be independent of the genetic background of the mites. Alternatively, it is also possible that both the microbiome and the performance of the mites respond to parts of the host genome that were not screened with the microsatellites. More research is necessary to further unravel the influence of the genetic background and microbiome on spider mite adaptation. Despite the fact that we obtained similar results for fecundity and longevity for the different replicates within the same spider mite line (see **Supplementary Figure S8**), we cannot rule out drift effects. However, drift may lead to evolution, but rarely to adaptation. We therefore believe that the correlation between the microbial composition and performance is not the result of drift.

The large abundance of Rickettsiales in our samples may partly explain the relation between performance and the microbiome composition. Endosymbionts such as *Wolbachia* (belonging to the Rickettsiales), *Cardinium*, and *Spiroplasma* have been found to inconsistently alter mite performance and plant resistance (Staudacher et al., 2017). Also, *Wolbachia* might help or hinder mite performance which strongly depends on the host plant (Zélé et al., 2018b). Interestingly, *Wolbachia* has been observed to be most prevalent on bean and to hamper performance on Solanaceous plants (Zélé et al., 2018b). This could explain why we found such high *Wolbachia* abundances in our populations, which had been maintained on bean for more than 400 generations, and also why two spider mite lines failed to survive on the tomato plants. To further determine the role of the Rickettsiales, we redid the analysis including only the reads from this specific order. We found no consistent correlation between performance and this subset of the bacterial composition (**Supplementary Table S14**), which shows the potential importance of the other orders in the microbiome. Identifying which specific genera or species play a role in spider mite performance on novel host plants will be a fascinating area of exploration, and future studies should investigate this research topic.

Besides Rickettsiales, Enterobacteriales might also affect the performance of the host. This was the fourth most abundant order in our samples. In aphids some bacteria from this order seem to be important for defense against fungi (e.g., *Regiella insecticola*) or parasitoids (e.g., *Hamiltonella defensa*; Oliver et al., 2005, 2010; Scarborough et al., 2005; Łukasik et al., 2013; Weldon et al., 2013; Dykstra et al., 2014; Oliver and Higashi, 2019). Facultative symbionts are known to both interfere with and promote reproduction, and boost survival (Oliver et al., 2010). For instance, some *Wolbachia* strains have been

reported to decrease fecundity in *T. urticae* (Vala et al., 2003), but in the same study no influence on longevity was found. However, we did find some influence of the microbiome on longevity of *T. urticae*, what leads to three potential alternatives for this discrepancy: (i) *Wolbachia* may not be causing the described effect, (ii) the influence of the host plant species as we mainly saw an effect on tomato plants and the former study was conducted on cucumber plants, or (iii) the tetracycline and heat treatments used (Vala et al., 2003) for clearing the mites of *Wolbachia* infection might have partly affected other components of the microbiome.

It is interesting that we find relationships between difference in performance (fecundity and longevity) between lines and difference in microbiome composition on the novel host plants, but not on the ancestral plant species. Because these spider mite populations have been reared on bean plants for over 400 generations, the most drastic improvements to their fitness and performance on bean plants have likely already occurred. This can explain why no relationship between performance and microbial composition was found on bean plants. Also, the amount of variation in performance found between the lines on bean plants was rather minor compared to the differences in fecundity and longevity found on the other host plants, which makes it difficult to reveal clear signals. Although the overall variation in the bacterial community was larger in bean compared to the novel host plants (as seen in the average microbiome dissimilarities), slight differences in the microbiome may have been beneficial for the adaptation to novel host plants. This suggests that the microbiome could be mainly of importance when adapting to a new environment. Adaptation through the microbiome could potentially provide a rapid response to novel environments when genetic adaptation would be too slow, similarly to how phenotypic plasticity can aid adaptation through “plastic rescue” (Snell-Rood et al., 2018; Fox et al., 2019).

The microbial variation is only partly explained by host genetics and diet, but is to a large extent influenced by other unknown factors. Environmental factors such as temperature and altitude are for instance known to be crucial for the prevalence of endosymbionts in *Tetranychus* spp. (tested in *T. truncatus*, Zhu et al., 2018), to standardize many factors, we performed our experiments under the same climate-controlled conditions. However, we cannot control for random processes such as drift that may influence assembly processes (Vellend, 2010).

We decreased potential biases in contaminants from host plant species (e.g., phyllosphere microbial communities) by only comparing bacterial communities of spider mite lines reared on the same host plant species. We neither compared the fecundity and longevity of spider mite populations reared on novel host plant species with their performance on the ancestral host plant species. Such a comparison would likely lead to an overestimation of the performance on the novel host plant species, because juvenile and maternal effects could not be standardized in our experiments (i.e., we did not have a two generations common garden given that this would indicate many bacterial generations). Moreover, maternal effects may be stronger in certain populations compared to others which



would complicate the interpretation of the results. Hence, we only compare spider mite lines on the same host plants at the same time points.

In conclusion, although the evolutionary interests of the microorganisms might not be entirely in line with those from their host, our results suggest that the microbiome could play a role in the performance of spider mites on novel host plants. The potential effect of the microbiome on its host phenotype linked with the significant influence of host genetics on the bacterial community composition, implies a possible advantage of including microbiome data in heritability studies (Douglas et al., 2020). Furthermore, we found that the composition of the spider mite bacterial communities depends partly on host genetics and on the host's environment (i.e., the plant it feeds on), but mostly on other, yet unknown, factors. We speculate that founder and priority effects may be important, where the specific bacterial species or even the order of uptake of the bacterial community members influences the final community (Fukami, 2015; Debray et al., 2022); future studies using axenic lines could provide insights. Multiple bacteria could perform similar functions or work together forming functional groups or guilds, hence, guild-based analyses could be meaningful (Wu et al., 2021). Another possibility is the existence of a core group while the other members of the bacterial communities are the result of stochastic or neutral sampling processes. As our study is only correlative, we do not want to take strong conclusions, but advocate that the microbiome should be considered when studying adaptation. Adaptation through the microbiome could be a fast solution under rapidly changing conditions (Snell-Rood et al., 2018).

## DATA AVAILABILITY STATEMENT

The datasets presented in this study can be found in online repositories. The names of the repository/repositories and accession number(s) can be found at: <http://www.ncbi.nlm.nih.gov/bioproject/596721>, NCBI GenBank Sequence Read Archive (SRA) database as project PRJNA596721. The script and data for the manuscript are available on DataVerseNL (<https://doi.org/10.34894/AMTPZS>).

## REFERENCES

- Alzate, A., Bisschop, K., Etienne, R. S., and Bonte, D. (2017). Interspecific competition counteracts negative effects of dispersal on adaptation of an arthropod herbivore to a new host. *J. Evol. Biol.* 30, 1966–1977. doi: 10.1111/jeb.13123
- Alzate, A., Etienne, R. S., and Bonte, D. (2019). Experimental island biogeography demonstrates the importance of island size and dispersal for the adaptation to novel habitats. *Glob. Ecol. Biogeogr.* 28, 238–247. doi: 10.1111/geb.12846
- Anderson, M. J. (2017). “Permutational multivariate analysis of variance (PERMANOVA)” in *Wiley StatsRef Stat. Ref. Online*. (John Wiley & Sons, Ltd.), 1–15.
- Anderson, M. J., Walsh, D. C. I., Robert Clarke, K., Gorley, R. N., and Guerra-Castro, E. (2017). Some solutions to the multivariate Behrens–Fisher problem for dissimilarity-based analyses. *Aust. New Zeal. J. Stat.* 59, 57–79. doi: 10.1111/anzs.12176

## AUTHOR CONTRIBUTIONS

All authors contributed to the idea of the experiment, discussions, and revisions. KB and CM did the pilot study. KB, HK, and TE performed the final experiments. KB and HK did the statistical analysis. KB wrote the draft of the manuscript. All authors contributed to the article and approved the submitted version.

## FUNDING

RE and KB thank the Netherlands Organization for Scientific Research (NWO) for financial support through a VICI grant (VICI grant number 865.13.00) and an NWA-ORC grant (grant number 400.17.606/4175). KB thanks the Special Research Fund (BOF) of Ghent University and the Ubbo Emmius sandwich program of the University of Groningen. KB, DB, and RE thank the FWO for the obtained funding from the research community “An eco-evolutionary network of biotic interactions,” project G018017N and junior FWO fellowship 12T5622N. TE thanks the Erasmus Mundus Master Programme in Evolutionary Biology (MEME) for the opportunities and funding provided.

## ACKNOWLEDGMENTS

We thank Akashi Negi, Kasper J. Meijer, Laura E. M. Arends, Viki Vandomme, Jacob J. Hogendorf, Richel J. C. Bilderbeek, Leonel Herrera Alsina, Giovanni Laudanno, Paul van Els, G. Jan van den Burg, and Carmen Ijsebaart for assisting during the experiments. We thank the Genomic Platform of Genopole Toulouse Midi-Pyrénées of INRA Auzeville for the Illumina MiSeq and Andy Vierstraete for the sequencing of the microsatellites.

## SUPPLEMENTARY MATERIAL

The Supplementary Material for this article can be found online at: <https://www.frontiersin.org/articles/10.3389/fmicb.2022.703183/full#supplementary-material>

- Baumann, P. (2005). Biology of bacteriocyte-associated endosymbionts of plant sap-sucking insects. *Annu. Rev. Microbiol.* 59, 155–189. doi: 10.1146/annurev.micro.59.030804.121041
- Berendsen, R. L., Pieterse, C. M. J., and Bakker, P. A. H. M. (2012). The rhizosphere microbiome and plant health. *Trends Plant Sci.* 17, 478–486. doi: 10.1016/j.tplants.2012.04.001
- Berg, G., Rybakova, D., Fischer, D., Cernava, T., Vergès, M. C. C., Charles, T., et al. (2020). Microbiome definition re-visited: old concepts and new challenges. *Microbiome* 8:103. doi: 10.1186/s40168-020-00875-0
- Bisschop, K., Mortier, F., Etienne, R. S., and Bonte, D. (2019). Transient local adaptation and source–sink dynamics in experimental populations experiencing spatially heterogeneous environments. *Proc. R. Soc. B Biol. Sci.* 286:20190738. doi: 10.1098/rspb.2019.0738
- Bitume, E. V., Bonte, D., Ronce, O., Bach, F., Flaven, E., Olivieri, I., et al. (2013). Density and genetic relatedness increase dispersal distance in a subsocial organism. *Ecol. Lett.* 16, 430–437. doi: 10.1111/ele.12057

- Bordenstein, S. R., O'Hara, F. P., and Werren, J. H. (2001). Wolbachia-induced incompatibility precedes other hybrid incompatibilities in *Nasonia*. *Nature* 409, 707–710. doi: 10.1038/35055543
- Bourtzis, K., Nirgianaki, A., Markakis, G., and Savakis, C. (1996). Wolbachia infection and cytoplasmic incompatibility in *Drosophila* species. *Genetics* 144, 1063–1073. doi: 10.1093/genetics/144.3.1063
- Bray, J. R., and Curtis, J. T. (1957). An ordination of the upland forest communities of southern Wisconsin. *Ecol. Monogr.* 27, 325–349. doi: 10.2307/1942268
- Breeuwer, J. A. J., and Jacobs, G. (1996). Wolbachia: intercellular manipulators of mite reproduction. *Exp. Appl. Acarol.* 20, 421–434. doi: 10.1007/BF00053306
- Brinker, P., Fointaine, M. C., Beukeboom, L. W., and Salles, J. F. (2019). Host, symbionts, and the microbiome: the missing tripartite interaction. *Trends Microbiol.* 27, 480–488. doi: 10.1016/j.tim.2019.02.002
- Broderick, N. A., Raffa, K. F., Goodman, R. M., and Handelsman, J. (2004). Census of the bacterial community of the gypsy moth larval midgut by using culturing and culture-independent methods. *Appl. Environ. Microbiol.* 70, 293–300. doi: 10.1128/AEM.70.1.293-300.2004
- Brooks, M. E., Kristensen, K., van Benthem, K. J., Magnusson, A., Berg, C. W., Nielsen, A., et al. (2017). glmmTMB balances speed and flexibility among packages for zero-inflated generalized linear mixed modeling. *R J.* 9, 378–400. doi: 10.3929/ETHZ-B-000240890
- Bruijning, M., Henry, L. P., Forsberg, S. K. G., Metcalf, C. J. E., and Ayroles, J. F. (2022). Natural selection for imprecise vertical transmission in host–microbiota systems. *Nat. Ecol. Evol.* 6, 77–87. doi: 10.1038/s41559-021-01593-y
- Callahan, B. J., McMurdie, P. J., Rosen, M. J., Han, A. W., Johnson, A. J. A., and Holmes, S. P. (2016). DADA2: High-resolution sample inference from Illumina amplicon data. *Nat. Methods* 13, 581–583. doi: 10.1038/nmeth.3869
- Cass, B. N., Himler, A. G., Bondy, E. C., Bergen, J. E., Sierra, F. K., Kelly, S. E., et al. (2016). Conditional fitness benefits of the Rickettsia bacterial symbiont in an insect pest. *Oecologia* 180, 169–179. doi: 10.1007/s00442-015-3436-x
- Chaplinka, M., Gerritsma, S., Dini-Andreote, F., Salles, J. F., and Wertheim, B. (2016). Bacterial communities differ among *Drosophila melanogaster* populations and affect host resistance against parasitoids. *PLoS One* 11:e167726. doi: 10.1371/journal.pone.0167726
- Chrostek, E., Pelz-Stelinski, K., Hurst, G. D. D., and Hughes, G. L. (2017). Horizontal transmission of intracellular insect symbionts via plants. *Front. Microbiol.* 8:28. doi: 10.3389/fmicb.2017.02237
- Colman, D. R., Toolson, E. C., and Takacs-Vesbach, C. D. (2012). Do diet and taxonomy influence insect gut bacterial communities? *Mol. Ecol.* 21, 5124–5137. doi: 10.1111/j.1365-294X.2012.05752.x
- Darby, A. C., and Douglas, A. E. (2003). Elucidation of the transmission patterns of an insect-borne bacterium. *Appl. Environ. Microbiol.* 69, 4403–4407. doi: 10.1128/AEM.69.8.4403-4407.2003
- David, L. A., Maurice, C. F., Carmody, R. N., Gootenberg, D. B., Button, J. E., Wolfe, B. E., et al. (2014). Diet rapidly and reproducibly alters the human gut microbiome. *Nature* 505, 559–563. doi: 10.1038/nature12820
- Debray, R., Herbert, R. A., Jaffe, A. L., Crits-Christoph, A., Power, M. E., and Koskella, B. (2022). Priority effects in microbiome assembly. *Nat. Rev. Microbiol.* 20, 109–121. doi: 10.1038/s41579-021-00604-w
- Delignette-Muller, M. L. (2015). fitdistrplus: an R package for fitting distributions. *J. Stat. Softw.* 64, 1–34. doi: 10.18637/jss.v064.i04
- DeSantis, T. Z., Hugenholtz, P., Larsen, N., Rojas, M., Brodie, E. L., Keller, K., et al. (2006). Greengenes, a chimera-checked 16S rRNA gene database and workbench compatible with ARB. *Appl. Environ. Microbiol.* 72, 5069–5072. doi: 10.1128/AEM.03006-05
- Diamond, J. M. (1975). "Assembly of species communities" in *Ecology and Evolution of Communities*. eds. J. M. Diamond and M. L. Cody (Boston: Harvard University Press), 342–344.
- Douglas, G. M., Bielawski, J. P., and Langille, M. G. I. (2020). Re-evaluating the relationship between missing heritability and the microbiome. *Microbiome* 8:87. doi: 10.1186/s40168-020-00839-4
- Dykstra, H. R., Weldon, S. R., Martinez, A. J., White, J. A., Hopper, K. R., Heimpel, G. E., et al. (2014). Factors limiting the spread of the protective symbiont *Hamiltonella defensa* in *Aphis craccivora* aphids. *Appl. Environ. Microbiol.* 80, 5818–5827. doi: 10.1128/AEM.01775-14
- Ebert, D. (2013). The epidemiology and evolution of symbionts with mixed-mode transmission. *Annu. Rev. Ecol. Evol. Syst.* 44, 623–643. doi: 10.1146/annurev-ecolsys-032513-100555
- Enigl, M., and Schausberger, P. (2007). Incidence of the endosymbionts *Wolbachia*, *Cardinium* and *Spiroplasma* in phytoseiid mites and associated prey. *Exp. Appl. Acarol.* 42, 75–85. doi: 10.1007/s10493-007-9080-3
- Fox, R. J., Donelson, J. M., Schunter, C., Ravasi, T., and Gaitán-Espitia, J. D. (2019). Beyond buying time: the role of plasticity in phenotypic adaptation to rapid environmental change. *Philos. Trans. R. Soc. B* 374:20180174. doi: 10.1098/rstb.2018.0174
- Franchini, P., Fruciano, C., Frickey, T., Jones, J. C., and Meyer, A. (2014). The gut microbial community of Midas cichlid fish in repeatedly evolved limnetic-benthic species pairs. *PLoS One* 9:e95027. doi: 10.1371/journal.pone.0095027
- Fukami, T. (2015). Historical contingency in community assembly: integrating niches, species pools, and priority effects. *Annu. Rev. Ecol. Evol. Syst.* 46, 1–23. doi: 10.1146/annurev-ecolsys-110411-160340
- Godinho, D. P., Janssen, A., Dias, T., Cruz, C., and Magalhães, S. (2016). Down-regulation of plant defence in a resident spider mite species and its effect upon con- and heterospecifics. *Oecologia* 180, 161–167. doi: 10.1007/s00442-015-3434-z
- Gonella, E., Pajoro, M., Marzorati, M., Crotti, E., Mandrioli, M., Pontini, M., et al. (2015). Plant-mediated interspecific horizontal transmission of an intracellular symbiont in insects. *Sci. Rep.* 5, 1–10. doi: 10.1038/srep15811
- Gotoh, T., Noda, H., and Hong, X.-Y. (2003). Wolbachia distribution and cytoplasmic incompatibility based on a survey of 42 spider mite species (Acari: Tetranychidae) in Japan. *Heredity* 91, 208–216. doi: 10.1038/sj.hdy.6800329
- Gotoh, T., Noda, H., and Ito, S. (2007). Cardinium symbionts cause cytoplasmic incompatibility in spider mites. *Heredity* 98, 13–20. doi: 10.1038/sj.hdy.6800881
- Guidolin, A. S., Cataldi, T. R., Labate, C. A., Francis, F., and Cónsoli, F. L. (2018). *Spiroplasma* affects host aphid proteomics feeding on two nutritional resources. *Nat. Sci. Rep.* 8, 2466–2413. doi: 10.1038/s41598-018-20497-9
- Hafer, N., and Vorburger, C. (2019). Diversity begets diversity: do parasites promote variation in protective symbionts? *Curr. Opin. Insect Sci.* 32, 8–14. doi: 10.1016/j.cois.2018.08.008
- Henry, L. P., Bruijning, M., Forsberg, S. K. G., and Ayroles, J. F. (2021). The microbiome extends host evolutionary potential. *Nat. Commun.* 12, 5141–5113. doi: 10.1038/s41467-021-25315-x
- Henry, L. M., Peccoud, J., Simon, J.-C., Hadfield, J. D., Maiden, M. J. C., Ferrari, J., et al. (2013). Horizontally transmitted symbionts and host colonization of ecological niches. *Curr. Biol.* 23, 1713–1717. doi: 10.1016/j.cub.2013.07.029
- Hong, X. Y., Gotoh, T., and Nagata, T. (2002). Vertical transmission of Wolbachia in *Tetranychus kanzawai* Kishida and *Panonychus mori* Yokoyama (Acari: Tetranychidae). *Heredity* 88, 190–196. doi: 10.1038/sj.hdy.6800026
- Huitzil, S., Sandoval-Motta, S., Frank, A., and Aldana, M. (2018). Modeling the role of the microbiome in evolution. *Front. Physiol.* 9:1836. doi: 10.3389/fphys.2018.01836/BIBTEX
- Huttenhower, C., Gevers, D., Knight, R., Abubucker, S., Badger, J. H., Chinwalla, A. T., et al. (2012). Structure, function and diversity of the healthy human microbiome. *Nature* 486, 207–214. doi: 10.1038/nature11234
- Jandhyala, S. M., Talukdar, R., Subramanyam, C., Vuyyuru, H., Sasikala, M., and Reddy, D. N. (2015). Role of the normal gut microbiota. *World J. Gastroenterol.* 21, 8787–8803. doi: 10.3748/wjg.v21.i29.8787
- Kant, M. R., Sabelis, M. W., Haring, M. A., and Schuurink, R. C. (2008). Intraspecific variation in a generalist herbivore accounts for differential induction and impact of host plant defences. *Proc. Biol. Sci.* 275, 443–452. doi: 10.1098/rspb.2007.1277
- Katoh, K., Rozewicki, J., and Yamada, K. D. (2017). MAFFT online service: multiple sequence alignment, interactive sequence choice and visualization. *Brief. Bioinform.* 20, 1160–1166. doi: 10.1093/bib/bbx108
- Kawecki, T. J., Lenski, R. E., Ebert, D., Hollis, B., Olivieri, I., and Whitlock, M. C. (2012). Experimental evolution. *Trends Ecol. Evol.* 27, 547–560. doi: 10.1016/j.tree.2012.06.001
- King, K. C. (2019). Defensive symbionts. *Curr. Biol.* 29, R78–R80. doi: 10.1016/j.cub.2018.11.028
- Kleinkauf, H. (2000). The role of 4'-phosphopantetheine in the biosynthesis of fatty acids, polyketides and peptides. *Biofactors* 11, 91–92. doi: 10.1002/biof.5520110126
- Kohl, K. D., and Dearing, M. D. (2016). The woodrat gut microbiota as an experimental system for understanding microbial metabolism of dietary toxins. *Front. Microbiol.* 7:1165. doi: 10.3389/fmicb.2016.01165

- Kohl, K. D., Weiss, R. B., Cox, J., Dale, C., and Dearing, M. D. (2014). Gut microbes of mammalian herbivores facilitate intake of plant toxins. *Ecol. Lett.* 17, 1238–1246. doi: 10.1111/ele.12329
- Lenth, R. (2021). emmeans: estimated marginal means, aka least-squares means. R package version 1.6.1. Available at: <https://cran.r-project.org/package=emmeans> (Accessed June 6, 2022).
- Leonardo, T. E., and Muir, G. T. (2003). Facultative symbionts are associated with host plant specialization in pea aphid populations. *Proc. R. Soc. B* 270, S209–S212. doi: 10.1098/rsbl.2003.0064
- Lizé, A., McKay, R., and Lewis, Z. (2014). Kin recognition in *Drosophila*: the importance of ecology and gut microbiota. *ISME J.* 8, 469–477. doi: 10.1038/ismej.2013.157
- Lopez, C. A., Lladser, M. E., Knights, D., Stombaugh, J., and Knight, R. (2011). UniFrac: An effective distance metric for microbial community comparison. *ISME J.* 5, 169–172. doi: 10.1038/ismej.2010.133
- Lucini, T., Faria, M. V., Rohde, C., Resende, J. T. V., and de Oliveira, J. R. F. (2015). Acylsugar and the role of trichomes in tomato genotypes resistance to *Tetranychus urticae*. *Arthropod Plant Interact.* 9, 45–53. doi: 10.1007/s11829-014-9347-7
- Lukasik, P., Guo, H., Van Asch, M., Ferrari, J., and Godfray, H. C. J. (2013). Protection against a fungal pathogen conferred by the aphid facultative endosymbionts *Rickettsia* and *Spiroplasma* is expressed in multiple host genotypes and species and is not influenced by co-infection with another symbiont. *J. Evol. Biol.* 26, 2654–2661. doi: 10.1111/jeb.12260
- Magalhães, S., Blanchet, E., Egas, M., and Olivieri, I. (2011). Environmental effects on the detection of adaptation. *J. Evol. Biol.* 24, 2653–2662. doi: 10.1111/j.1420-9101.2011.02388.x
- Magalhães, S., Cailleau, A., Blanchet, E., and Olivieri, I. (2014). Do mites evolving in alternating host plants adapt to host switch? *J. Evol. Biol.* 27, 1956–1964. doi: 10.1111/jeb.12453
- Magalhães, S., Fayard, J., Janssen, A., Carbonell, D., and Olivieri, I. (2007). Adaptation in a spider mite population after long-term evolution on a single host plant. *J. Evol. Biol.* 20, 2016–2027. doi: 10.1111/j.1420-9101.2007.01365.x
- Magnusson, A., Skaug, H., Nielsen, A., Berg, C. W., Kristensen, K., Maechler, M., et al. (2018). Troubleshooting with glmmTMB. Available at: <https://cran.r-project.org/web/packages/glmmTMB/vignettes/troubleshooting.html> (Accessed June 6, 2022).
- McMurdie, P. J., and Holmes, S. P. (2013). phyloseq: An R package for reproducible interactive analysis and graphics of microbiome census data. *PLoS One* 8:e61217. doi: 10.1371/journal.pone.0061217
- Moran, N. A., and Sloan, D. B. (2015). The hologenome concept: helpful or hollow? *PLoS Biol.* 13:e1002311. doi: 10.1371/journal.pbio.1002311
- Oksanen, J., Blanchet, F. G., Friendly, M., Kindt, R., Legendre, P., Minchin, P. R., et al. (2020). Vegan: community ecology package. R package version 2.5-7. Available at: <https://cran.r-project.org/package=vegan%0A> (Accessed June 6, 2022).
- Oliver, K. M., Degnan, P. H., Burke, G. R., and Moran, N. A. (2010). Facultative symbionts in aphids and the horizontal transfer of ecologically important traits. *Annu. Rev. Entomol.* 55, 247–266. doi: 10.1146/annurev-ento-112408-085305
- Oliver, K. M., and Higashi, C. H. (2019). Variations on a protective theme: *Hamiltonella* defense infections in aphids variably impact parasitoid success. *Curr. Opin. Insect Sci.* 32, 1–7. doi: 10.1016/j.cois.2018.08.009
- Oliver, K. M., Moran, N. A., and Hunter, M. S. (2005). Variation in resistance to parasitism in aphids is due to symbionts not host genotype. *Proc. Natl. Acad. Sci.* 102, 12795–12800. doi: 10.1073/pnas.0506131102
- Peer, K., and Taborsky, M. (2005). Outbreeding depression, but no inbreeding depression in haplodiploid *Ambrosia* beetles with regular sibling mating. *Evolution* 59, 317–323. doi: 10.1111/J.0014-3820.2005.TB00992.X
- Pereira Silva, M. C., Cavalcante Franco Dias, A., Dirk van Elsas, J., and Salles, J. F. (2012). Spatial and temporal variation of archaeal, bacterial and fungal communities in agricultural soils. *PLoS One* 7:e51554. doi: 10.1371/journal.pone.0051554
- Peterson, R. A. (2019). Ordered quantile normalization: a semiparametric transformation built for the cross-validation era. *J. Appl. Stat.* 47, 2312–2327. doi: 10.1080/02664763.2019.1630372
- Price, M. N., Dehal, P. S., and Arkin, A. P. (2009). FastTree: computing large minimum evolution trees with profiles instead of a distance matrix. *Mol. Biol. Evol.* 26, 1641–1650. doi: 10.1093/molbev/msp077
- Price, M. N., Dehal, P. S., and Arkin, A. P. (2010). FastTree 2—approximately maximum-likelihood trees for large alignments. *PLoS One* 5:e9490. doi: 10.1371/journal.pone.0009490
- Price, M. V., and Waser, N. M. (1979). Pollen dispersal and optimal outcrossing in *Delphinium nelsoni*. *Nature* 277, 294–297.
- Rodrigues, L. R., Duncan, A. B., Clemente, S. H., Moya-Laraño, J., and Magalhães, S. (2016). Integrating competition for food, hosts, or mates via experimental evolution. *Trends Ecol. Evol.* 31, 158–170. doi: 10.1016/j.tree.2015.12.011
- Romero, J., and Navarrete, P. (2006). 16S rDNA-based analysis of dominant bacterial populations associated with early life stages of Coho salmon (*Oncorhynchus kisutch*). *Microb. Ecol.* 51, 422–430. doi: 10.1007/s00248-006-9037-9
- Santo Domingo, J. W., Kaufman, M. G., Klug, M. J., Holben, W. E., Harris, D., and Tiedje, J. M. (1998). Influence of diet on the structure and function of the bacterial hindgut community of crickets. *Mol. Ecol.* 7, 761–767. doi: 10.1046/j.1365-294x.1998.00390.x
- Santos-Matos, G., Wybouw, N., Martins, N. E., Zélé, F., Riga, M., Leitão, A. B., et al. (2017). *Tetranychus urticae* mites do not mount an induced immune response against bacteria. *Proc. R. Soc. B* 284, 1–8. doi: 10.1098/rspb.2017.0401
- Scarborough, C. L., Ferrari, J., and Godfray, H. C. J. (2005). Aphid protected from pathogen by endosymbiont. *Science* 310:1781. doi: 10.1126/science.1120180
- Schloss, P. D., Westcott, S. L., Ryabin, T., Hall, J. R., Hartmann, M., Hollister, E. B., et al. (2009). Introducing mothur: open-source, platform-independent, community-supported software for describing and comparing microbial communities. *Appl. Environ. Microbiol.* 75, 7537–7541. doi: 10.1128/AEM.01541-09
- Shin, S. C., Kim, S.-H., You, H., Kim, B., Kim, A. C., Lee, K.-A., et al. (2011). *Drosophila* microbiome modulates host developmental and metabolic homeostasis via insulin signaling. *Science* 334, 666–670. doi: 10.1126/science.1209867
- Snell-Rood, E. C., Kobiela, M. E., Sikkink, K. L., and Shephard, A. M. (2018). Mechanisms of plastic rescue in novel environments. *Annu. Rev. Ecol. Syst.* 49, 331–354. doi: 10.1146/annurev-ecolsys-110617-062622
- Sommer, F., and Bäckhed, F. (2013). The gut microbiota-masters of host development and physiology. *Nat. Rev. Microbiol.* 11, 227–238. doi: 10.1038/nrmicro2974
- Spor, A., Koren, O., and Ley, R. (2011). Unravelling the effects of the environment and host genotype on the gut microbiome. *Nat. Rev. Microbiol.* 9, 279–290. doi: 10.1038/nrmicro2540
- Staudacher, H., Schimmel, B. C. J., Lamers, M. M., Wybouw, N., Groot, A. T., and Kant, M. R. (2017). Independent effects of a herbivore's bacterial symbionts on its performance and induced plant defences. *Int. J. Mol. Sci.* 18, 1–26. doi: 10.3390/ijms18010182
- Stecher, B., and Hardt, W. D. (2008). The role of microbiota in infectious disease. *Trends Microbiol.* 16, 107–114. doi: 10.1016/j.tim.2007.12.008
- Takeuchi, Y., Chaffron, S., Salcher, M. M., Shimizu-Inatsugi, R., Kobayashi, M. J., Diway, B., et al. (2015). Bacterial diversity and composition in the fluid of pitcher plants of the genus *Nepenthes*. *Syst. Appl. Microbiol.* 38, 330–339. doi: 10.1016/j.syapm.2015.05.006
- Theis, K. R., Dheilly, N. M., Klassen, J. L., Brucker, R. M., Baines, J. F., Bosch, T. C. G., et al. (2016). Getting the hologenome concept right: an eco-evolutionary framework for hosts and their microbiomes. *mSystems* 1, e00028–e00016. doi: 10.1128/mSystems.00028-16
- Therneau, T. M. (2020). coxme: mixed effects cox models. R package version 2.2-16. Available at: <https://cran.r-project.org/package=coxme> (Accessed June 6, 2022).
- Tien, N. S. H., Sabelis, M. W., and Egas, M. (2015). Inbreeding depression and purging in a haplodiploid: gender-related effects. *Heredity* 114, 327–332. doi: 10.1038/hdy.2014.106
- Vala, F., Breeuwer, J. A. J., and Sabelis, M. W. (2003). Sorting out the effects of *Wolbachia*, genotype and inbreeding on life-history traits of a spider mite. *Exp. Appl. Acarol.* 29, 253–264. doi: 10.1023/A:1025810414956
- van Veelen, H. P. J., Salles, J. F., and Tieleman, B. I. (2018). Microbiome assembly of avian eggshells and their potential as transgenerational carriers of maternal microbiota. *ISME J.* 12, 1375–1388. doi: 10.1038/s41396-018-0067-3
- Vellend, M. (2010). Conceptual synthesis in community ecology. *Q. Rev. Biol.* 85, 183–206. doi: 10.1086/652373

- Veneti, Z. L., Reuter, M., Montenegro, H., Hornett, E. A., Charlat, S., and Hurst, G. D. (2005). "Interactions between inherited bacteria and their hosts: The *Wolbachia* paradigm" in *The Influence of Cooperative Bacteria on Animal Host Biology*. eds. M.-J. McFall-Ngai, B. Henderson and E.-G. Ruby (New York: Cambridge University Press), 119–142.
- Voolstra, C. R., and Ziegler, M. (2020). Adapting with microbial help: microbiome flexibility facilitates rapid responses to environmental change. *Bioessays* 42, 2000004. doi: 10.1002/bies.202000004
- Vorburger, C., and Perlman, S. J. (2018). The role of defensive symbionts in host-parasite coevolution. *Biol. Rev. Camb. Philos. Soc.* 93, 1747–1764. doi: 10.1111/brv.12417
- Weldon, S. R., Strand, M. R., and Oliver, K. M. (2013). Phage loss and the breakdown of a defensive symbiosis in aphids. *Proc. R. Soc. B* 280, 20122103–20122107. doi: 10.1098/rspb.2012.2103
- Wu, G., Zhao, N., Zhang, C., Lam, Y. Y., and Zhao, L. (2021). Guild-based analysis for understanding gut microbiome in human health and diseases. *Genome Med.* 13:22. doi: 10.1186/S13073-021-00840-Y
- Wybouw, N., Van Leeuwen, T., and Dermauw, W. (2018). A massive incorporation of microbial genes into the genome of *Tetranychus urticae*, a polyphagous arthropod herbivore. *Insect Mol. Biol.* 27, 333–351. doi: 10.1111/imb.12374
- Xie, R. R., Sun, J. T., Xue, X. F., and Hong, X. Y. (2016). Cytoplasmic incompatibility and fitness benefits in the two-spotted spider mite *Tetranychus urticae* (red form) doubly infected with *Wolbachia* and *Cardinium*. *Syst. Appl. Acarol.* 21, 1161–1173. doi: 10.11158/saa.21.9.1
- Zélé, F., Santos, J. L., Godinho, D. P., and Magalhães, S. (2018b). *Wolbachia* both aids and hampers the performance of spider mites on different host plants. *FEMS Microbiol. Ecol.* 94, 187. doi: 10.1093/femsec/fiy187
- Zélé, F., Santos, I., Olivieri, I., Weill, M., Duron, O., and Magalhães, S. (2018a). Endosymbiont diversity and prevalence in herbivorous spider mite populations in South-Western Europe. *FEMS Microbiol. Ecol.* 94, fiy015. doi: 10.1093/femsec/fiy015
- Zélé, F., Santos-Matos, G., Figueiredo, A. R. T., Eira, C., Pinto, C., Laurentino, T. G., et al. (2019). Spider mites escape bacterial infection by avoiding contaminated food. *Oecologia* 189, 111–122. doi: 10.1007/s00442-018-4316-y
- Zhu, Y., Song, Y., Hoffmann, A. A., Jin, P., Huo, S., and Hong, X. (2019). A change in the bacterial community of spider mites decreases fecundity on multiple host plants. *Microbiology* 8:e00743. doi: 10.1002/mbo3.743
- Zhu, Y.-X., Song, Y.-L., Zhang, Y.-K., Hoffmann, A. A., Zhou, J.-C., Sun, J.-T., et al. (2018). Incidence of facultative bacterial endosymbionts in spider mites associated with local environments and host plants. *Appl. Environ. Microbiol.* 84, e02546–e02517. doi: 10.1128/AEM.02546-17
- Zilber-Rosenberg, I., and Rosenberg, E. (2008). Role of microorganisms in the evolution of animals and plants: the hologenome theory of evolution. *FEMS Microbiol. Rev.* 32, 723–735. doi: 10.1111/j.1574-6976.2008.00123.x
- Conflict of Interest:** The authors declare that the research was conducted in the absence of any commercial or financial relationships that could be construed as a potential conflict of interest.
- Publisher's Note:** All claims expressed in this article are solely those of the authors and do not necessarily represent those of their affiliated organizations, or those of the publisher, the editors and the reviewers. Any product that may be evaluated in this article, or claim that may be made by its manufacturer, is not guaranteed or endorsed by the publisher.

Copyright © 2022 Bisschop, Kortenbosch, van Eldijk, Mallon, Salles, Bonte and Etienne. This is an open-access article distributed under the terms of the Creative Commons Attribution License (CC BY). The use, distribution or reproduction in other forums is permitted, provided the original author(s) and the copyright owner(s) are credited and that the original publication in this journal is cited, in accordance with accepted academic practice. No use, distribution or reproduction is permitted which does not comply with these terms.



# Advantages of publishing in Frontiers



## OPEN ACCESS

Articles are free to read  
for greatest visibility  
and readership



## FAST PUBLICATION

Around 90 days  
from submission  
to decision



## HIGH QUALITY PEER-REVIEW

Rigorous, collaborative,  
and constructive  
peer-review



## TRANSPARENT PEER-REVIEW

Editors and reviewers  
acknowledged by name  
on published articles

## Frontiers

Avenue du Tribunal-Fédéral 34  
1005 Lausanne | Switzerland

Visit us: [www.frontiersin.org](http://www.frontiersin.org)

Contact us: [frontiersin.org/about/contact](http://frontiersin.org/about/contact)



## REPRODUCIBILITY OF RESEARCH

Support open data  
and methods to enhance  
research reproducibility



## DIGITAL PUBLISHING

Articles designed  
for optimal readership  
across devices



## FOLLOW US

@frontiersin



## IMPACT METRICS

Advanced article metrics  
track visibility across  
digital media



## EXTENSIVE PROMOTION

Marketing  
and promotion  
of impactful research



## LOOP RESEARCH NETWORK

Our network  
increases your  
article's readership